Commissariat à l'énergie atomique et aux énergies alternatives

e-den

A Nuclear Energy Division
Monograph

Neutronics

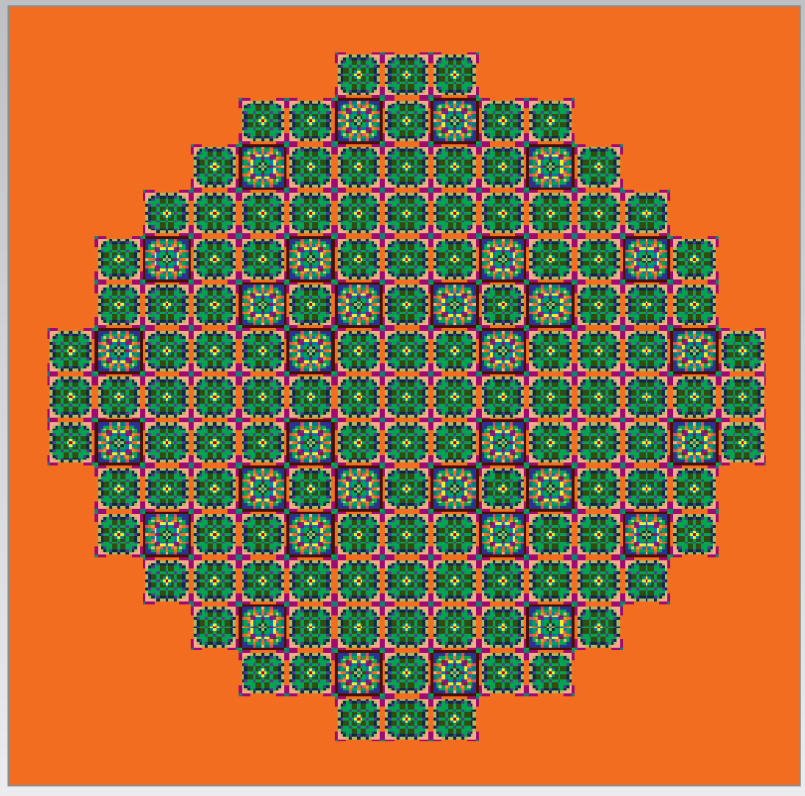

EDITIONS LE MONITEUR

DE LA RECHERCHE À L'INDUSTRIE
cea

DEN Monographs

A Nuclear Energy Division Monograph
Commissariat à l'énergie atomique et aux énergies alternatives
91191 Gif-sur-Yvette Cedex (France)
Tel: +33 (0)1 64 50 10 00

Correspondence: all correspondence should be addressed to the Editor or to CEA/DEN Direction scientifique, CEA Saclay 91191 Gif-sur-Yvette Cedex (France).
Tel: +33 (0)1 69 08 16 75

ISBN 978-2-281-11372-3
ISSN 1950-2672

Front cover: Geometry of a nuclear pressurized water reactor core as modeled by the APOLLO3® transport code.

Commissariat à l'énergie atomique et aux énergies alternatives

e-den

A Nuclear Energy Division
Monograph

Neutronics

EDITIONS LE MONITEUR

DE LA RECHERCHE À L'INDUSTRIE
cea

Foreword

After a dazzling start in the 1950's when, for many, it stood as the hope of an inexhaustible, economically competitive energy source, nuclear energy experienced in the 1980's and 1990's a rejection by majority public opinion in several Western countries, which suddenly brought its development to a halt.

Although the 1973 and 1979 oil crises marked the launch of massive equipment programs in a few countries heavily penalized by oil imports, in particular France and Japan, they were paradoxically followed by a gap in nuclear investments, first, in the United States, and then in Western Europe. However, repeated oil market tensions and emerging concerns over the possible depletion of natural resources, as well as expectable effects on climate and the environment due to their large-scale burning should have, by contrast, enhanced such investments.

There are surely many reasons for this pause, which can in part be explained by the accidents at Three Mile Island in 1979, and Chernobyl in 1986, deeply impacting public opinion. Fukushima recent accident legitimately raises again the same questions, although the context is quite different.The pending issue is not so much whether reactors are technically able to withstand the most improbable events: Fukushima focuses renewed attention, indeed, on how to train operators and members of the decision-making line in charge of tackling a severe dysfunction of engineered safety systems in the case of equipment failure.

In France, whereas the siting of nuclear power plants had never - except for one case - aroused a true debate in the population, a negative attitude emerged in the late 1980's concerning the nuclear waste issue. Given the growing difficulties of the French national agency for radioactive waste management (ANDRA) in its search for an underground laboratory site, the Government of the time decided to suspend work, set a one-year moratorium, and submitted the issue to the French parliamentary office for evaluation of scientific and technological options (OPECST).

By adopting most of the OPECST's recommendations, in particular its definition of a diversified research program, and also the basis for a democratic debate with the populations concerned, the French Act of December 30, 1991 on nuclear waste management thus greatly contributed to calm the debate. Following a fifteen-year period, in which various options for long-term radioactive waste management were investigated, the Act of June 28, 2006 made it possible to set out the basic framework for this management, to be recognized as a necessity from now on.

In addition, the starting century is marked by collective awareness that our generation's energy needs cannot be met without concern for the environment, and without preserving future generations' right to satisfy these same needs. This is the concept of sustainable development which our society will inevitably face, indeed.

Today, it goes unquestioned that global warming due to increasing greenhouse gas emissions is a human-caused problem. Only the extent and consequences of of this warming are still debated. Industrialized countries, who are for the most part the origin of the current situation, should hold a particular responsibility, which should induce them to voluntarily

reduce emissions of these gases. By its very nature, nuclear energy is not concerned by this type of emissions, while being able to produce a relatively abundant, reliable, and economically competitive energy source. Quite naturally, it is therefore expected to be the predominant energy source.

Even if the worldwide situation is still contrasted, more especially in Europe, several countries (China, South Korea, Finland, India, South Africa, Poland, the United Arab Emirates…) have already decided to make huge investments in developing this energy, and do keep this option after Fukushima accident. Others are very close to taking this step, in particular Great Britain and the United States, who seem to be determined to launch programs for the construction of new nuclear power plants by the end of the decade, picking up a process that had been on hold for thirty years.

Following France's national energy debate that took place in the first half of 2003, the Strategic Orientation Act on energy passed in June 2005 established the decision to build an EPR demonstrator reactor, to pave the way for the replacement of currently operating power plants.

A number of signs thus lead us to believe that a worldwide revival of nuclear energy is taking place. Nevertheless, the future of nuclear energy in our country, as in many others, will largely depend on its capacity to properly address the following two concerns:

- The first concern has to do with its social acceptability, for it is crucial that nuclear energy be deployed under optimum safety and security conditions, generating a minimum amount of ultimate waste, and the latter be fully controlled with regard to its possible impact on health and the environment.The shock caused by Fukushima accident can but enhance this safety requirement as an absolute priority.

- The second concern relates to the availability of its resources: it is important to guarantee a long-term supply of fuel, by preparing to resort to systems which are more economical in terms of natural fissile materials and, above all, less dependent on market fluctuations.

These topics are a key part of the CEA Nuclear Energy Division's work. Indeed, this Division is a major player in the research work aimed at supporting the nuclear industry in improving reactor safety and competitiveness, providing the Public Authorities with the elements necessary to make choices on long-term nuclear waste management, and, finally, developing the nuclear systems of the future. These systems, mainly fast neutron reactors, exhibit highly promising improvements with regard to waste management and raw materials use.

As a fervent partisan of the broadest possible dissemination of scientific and technical knowledge, it seems to me of the utmost importance that this research work, which calls upon a wide range of scientific disciplines, and often ranks as among the best in the world, should be presented and explained to all those who would like to form their own opinion on nuclear energy. This is the reason why I welcome the publication of these DEN Monographs with deep satisfaction, indeed. No doubt that close reading of these works will afford an invaluable source of information to the, I hope, many readers.

I would like to thank all the researchers and engineers who, by contributing to this project, willingly shared their experience and knowledge.

Bernard Bigot,
CEA Chairman

Introduction

What is neutronics?

The neutron, which was assumed to be one of the constituents of the atomic nucleus, together with the proton, was first identified by the British scientist James Chadwick in 1932. He observed the radiation of the neutrons released by the nuclear reaction ${}^{4}_{2}He + {}^{9}_{4}Be \Rightarrow {}^{1}_{0}n + {}^{12}_{6}C$ through bombarding a beryllium target with the α particles of a radioactive emitter.

In some specific materials, these particles are likely to undergo **scattering***, and slow down until they are absorbed. For, as indicated by their name, neutrons are electrically neutral, and can therefore interact only with atomic nuclei, ten thousand to a hundred thousand times smaller than atoms themselves, and can so move almost in vacuum. Their paths are one centimeter long or so, - which means going through a hundred million atoms -, and can even extend, along a straight line, over decimeters in materials in which they can properly scatter, such as water, heavy water or graphite. This is why neutron physics, also referred to as "**neutronics***", which was born with Chadwick's experiment, can be defined as the ***study of neutrons travelling through matter***.

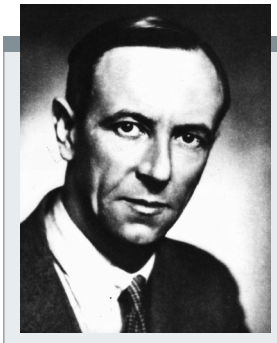

Sir **James Chadwick** (1891-1974), a British physicist, who discovered the neutron by investigating the following reaction, still used for neutron sources today:
$^{4}He + {}^{9}Be \Rightarrow {}^{1}n + {}^{12}C$

"As he was pursuing the study of light element bombardment by α particles undertaken by Rutherford, the German physicist Bothe discovered (1931) that beryllium, so bombarded, emitted a radiation far more penetrating than the γ radiation. Frédéric Joliot and Irène Joliot-Curie discovered (1932) that this Bothe radiation going through hydrogenated structures, such as paraffin, projected highly energetic protons forward. Finally, the English physicist Chadwick, as he reproduced those experiments with a Wilson chamber full of hydrogen, helium or nitrogen, showed that the atomic nuclei of these various elements were projected by the Bothe radiation as if this radiation consisted of neutral projectiles (not leaving any trace in the gases they went through), of a diameter comparable to that of nuclei, and with a mass close to that of the proton. He named that new nuclear particle "neutron" (of symbol n), and stated that it was torn out of the atomic nucleus of beryllium by the reaction $^{4}He + {}^{9}Be \Rightarrow {}^{12}C + n$."

Extract from **Francis Perrin**'s appendix (1970) to *Les Atomes* (1913), a book by his father **Jean Perrin**.

In 1938, in Germany, neutron-induced fission was discovered by **Otto Hahn** (left, 1879-1968), **Fritz Strassmann** (1902-1980), and **Lise Meitner** (right, 1878-1968).

A few years later, in 1938, **fission*** induced by a neutron was discovered by Otto Hahn, Fritz Strassmann and Lise Meitner in Germany. In 1939, in France, Frédéric Joliot-Curie observed the emission of two or three secondary neutrons during fission.

Physicists soon understood that a nuclear chain reaction could so be expected, *i.e.* neutrons => fissions => neutrons => fissions => etc. (Fig. 1). This reaction releases a significant amount of energy: 200 MeV per fission, *i.e.* typically one million times more than a chemical reaction if it can be self-sustained. So the previous definition had to be completed as follows: … ***and the study of the conditions for a chain reaction***, especially of the multiplication factor, *i.e.* the ratio between the neutron (or fission) population at a given generation, and the population at the previous generation.

In a nuclear reactor, the nuclear chain reaction is controlled through suitable devices (control rods, burnable poisons…) so as to keep the neutron population constant. In this case, the neutron multiplication factor is equal to 1, and the reactor is referred to as "**critical***". If this factor is over 1, the neutron population grows exponentially as a function of time, and the reactor is referred to as "**supercritical***". Last, if it is lower than 1, the neutron population disappears: the reactor is then referred to as "**subcritical***".

Nuclear fission

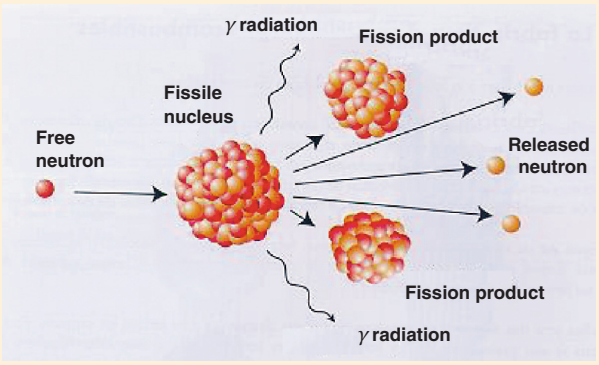

Nuclear chain reaction

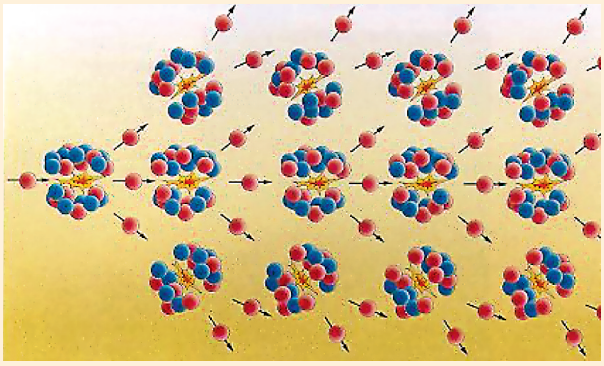

Fig. 1. Nuclear fission and nuclear chain reaction.

A few characteristics of the fission process

Energy balance of fission

Fission reaction releases an energy corresponding to the energy difference between initial and final states, *i.e.* about 200 MeV, which mainly corresponds to the difference between the binding energies of the initial heavy nucleus and fission products. This energy is mainly released as kinetic energy of fission fragments (Table 1). As the latter are excited and radioactive, they in turn release energy as *beta* and *gamma* radiation, as well as neutrinos, which themselves carry away a small part of the reaction energy. As fission products have a very small path in matter, their kinetic energy can be assumed to be locally released in fuel as heat. Such is not the case for neutron, *gamma*, and neutrino contributions, which may be both delayed in time (the decay of fission products results in the release of the so-called "residual" power), and deposited far away from the area where fission takes place (radiation shielding).

Two families of neutrons released by fission: prompt and delayed neutrons

The fission of a heavy nucleus can occur in many different ways, and more than a thousand or so fission fragments can be identified. Some of them, called "precursors", are out of the stability valley of nuclei, and therefore undergo one or several *beta* decays. In a few cases, the separation energy of a neutron from the daughter nucleus is relatively low, and the excitation energy of this nucleus is higher than this separation energy. The nucleus can then emit a neutron. Neutrons arising from this second emission are "delayed", in contrast with fission neutrons: the time interval between fission and delayed neutron emission is governed by the "decay law", in relation to the *beta* decay of precursor nuclei. The order of magnitude of the time lag ranges from a fraction of second to a few dozens of seconds.

Delayed neutrons are not numerous, in contrast with **prompt neutrons*** instantaneously emitted during fission: in the case of uranium-235, the emission of only 0.66% (660 **pcm***) of all of the neutrons generated by fission is delayed. These neutrons' time delay versus fission is significant, *i.e.* an average of 11 seconds or so. It is worth to mention that, despite their low percentage, these neutrons do alter the kinetic behavior of the overall population, through significantly increasing the average time between two neutron generations. This physical phenomenon allows to control the chain reaction in nuclear reactors.

Table 1.

MeV energy balance of neutron-induced fission in various heavy nuclei

(From M.F. James, "Energy Released in Fission", *Journal of Nuclear Energy*, vol. 23, p. 529, 1969).

	U 235	U 238	Pu 239	Pu 241
Fission fragments	166.2	166.9	172.8	172.2
Neutrons	4.8	5.5	5.9	5.9
Prompt *gammas*	8.0	7.5	7.7	7.6
***Gammas* released by fission products**	7.2	8.4	6.1	7.4
***Betas* released by fission products**	7.0	8.9	6.1	7.4
Neutrinos/antineutrinos	9.6	11.9	8.6	10.2
Total energy released by fission	202.7	205.9	207.2	210.6

As early as 1942 was the first self-sustained and controlled reaction generated by Enrico Fermi in the first atomic pile, the so-called Chicago pile (CP1), within the framework of the Manhattan project. Although the pile power did not exceed a few watts in that experiment, reactors likely to deliver a high power were very soon built, first dedicated to plutonium generation for early atomic bombs, and then for electric power generation. As a consequence, a third component had to be added to the definition of neutronics: … ***and the study of changes in matter's temperature and composition due to nuclear reactions"***.

Neutronics: from the microscopic phenomenon to the macroscopic quantities

Fundamentally, neutronics, a branch of nuclear physics, is a science devoted to the microscopic, *i.e.* the study of interactions between neutrons and atomic nuclei, the most important of which are described in Table 2.

The occurrence of these neutron-induced nuclear reactions is characterized by microscopic cross sections (see inset).

Space and time scales in neutronics

On account of its twofold - microscopic and macroscopic - profile, and its multiple goals, neutronics involves extremely broad space and time scales, as shown in the table below.

Space scales of neutronics	
10^{-15} m	Neutron-nucleus interaction distance.
10^{-3} to 10^{-2} m	**Mean free path*** of neutrons (before interaction).
10^{-1} to 1 m	Straight-line path travelled by neutrons (before absorption).
1 to several dozens of meters	Dimension of a **nuclear reactor***.
Time scales of neutronics	
0 to 10^{-14} s	Neutron-nucleus interaction.
10^{-9} s	Time for an elementary path of a **fast neutron***.
10^{-7} s	Nuclear explosion in a weapon.
10^{-5} s	Time for an elementary path of a **thermal neutron***.
10^{-6} to 10^{-3} s	Neutron lifetime in reactors.
10^{-2} s	Transient in a **criticality accident***.
10 s	Mean delayed emission of **delayed neutrons***.
10^{2} s	Transient in thermal equilibrium.
1 day	**Xenon*** 135-induced transient.
1 to 4 years	Irradiation of a **nuclear fuel***.
50 years	Order of magnitude of nuclear reactor lifetime.
300 years	Radioactive extinction of most **fission products***.
10^{3} to 10^{6} years	Radioactive extinction of artificial **actinides***.
2.10^{9} years	Age of the **Oklo*** natural reactor.

The two main quantities that neutronics tends to determine in a reactor, are the neutron population and the isotopic composition. These quantities have to be known in detail at any moment, and in any point of the reactor, whether in normal or accidental operating conditions.

The variables these quantities depend on, are described in Table 3.

Neutronics is a discipline whose specific feature is to use microscopic data arising from the quantum world (microscopic cross sections…) to calculate macroscopic quantities (power density of a reactor…). So it can also, and above all, be seen as a science of the macroscopic: referring to a modeling very similar to that of fluid mechanics, the neutron population is characterized by its density in any point – number of particles per unit volume –, and is considered as a continuous fluid evolving in the system.

Neutronics objectives and stakes

The main purpose of neutronics is the design and follow-up of reactors, especially nuclear power reactors. However, neutron physicists also bring their contribution to other branches of science or industry:

- Criticality risk assessment in the facilities where fissile materials are handled, especially reactor fuel cycle plants;
- the study of blankets for (future) fusion reactors;
- radiation protection studies (in the case of neutron radiation, and in the very similar case of *gamma* photon radiation);
- assessment of reactor vessel **fluence***;
- the study of activation of structures by neutrons;
- the assessment of radiation levels before dismantling nuclear facility;
- nuclear waste transmutation;
- neutron use in imaging, for molecular or crystalline structure examination, and in medicine;
- neutron use in activation analysis …

So, in its broader meaning, neutronics can be subdivided into the following fields:

- Reactor core physics under normal or accidental operation,
- criticality of the fissile materials processed in fuel cycle operations;
- radiation shielding in nuclear facilities;
- *in-core* or *ex-core* nuclear instrumentation.

Table 2.

Main nuclear processes taking place in a reactor

The photonuclear processes [(γ, n), (γ,f), …] are not described here.

${}^{A}_{Z}X$ refers to a target nucleus with atomic number Z and mass number A.

Interaction without formation of a compound nucleus			**Usual notation of the reaction type**
Potential (elastic) **scattering***	$n + {}^{A}_{Z}X \rightarrow n + {}^{A}_{Z}X$	Always possible.	(n, n)
Interactions through formation of a compound nucleus			
Resonant elastic scattering	$n + {}^{A}_{Z}X \rightarrow n + {}^{A}_{Z}X$	Always possible.	(n, n)
Resonant inelastic scattering	$n + {}^{A}_{Z}X \rightarrow n' + {}^{A}_{Z}X^{*}$ ${}^{A}_{Z}X^{*} \rightarrow \gamma + {}^{A}_{Z}X$	Threshold: first energy level of ${}^{A}_{Z}X$.	(n, n')
(n, 2n) scattering	$n + {}^{A}_{Z}X \rightarrow n_1 + n_2 + {}^{A-1}_{Z}X$	Threshold: energy for separating a neutron from ${}^{A}_{Z}X$.	(n, 2n)
Radiative **capture***	$n + {}^{A}_{Z}X \rightarrow \gamma + {}^{A+1}_{Z}X$	Always possible.	(n, γ)
Capture releasing a light charged particule	$n + {}^{A}_{Z}X \rightarrow p + {}^{A}_{Z-1}Y$ $n + {}^{A}_{Z}X \rightarrow \alpha + {}^{A-3}_{Z-2}Y$ etc.	Generally with a threshold; sometimes without threshold.	(n, p) (n,α)
Fission* (binary)	$n + {}^{A}_{Z}X \rightarrow PF_1 + PF_2 + \nu n$ (ν between 0 and 7, generally 2 or 3)	With no threshold for odd heavy nuclei; otherwise with threshold (excepting "tunnel effect").	(n, f)

Main radioactive phenomena taking place in a nuclear fuel			**Usual notation of the phenomenon type**
Alpha decay	${}^{A}_{Z}X \rightarrow {}^{A-4}_{Z-2}Y + {}^{4}_{2}He$	${}^{4}_{2}He$ is a helium-4 nucleus, also called "***alpha**** particle".	(α)
Beta minus decay	${}^{A}_{Z}X \rightarrow {}^{A}_{Z+1}Y + e^{-} + \bar{\nu}$	e^{-} is an electron also called "***beta**** minus particle" $\bar{\nu}$ is an **antineutrino*.**	(β^{-})
Beta plus decay	${}^{A}_{Z}X \rightarrow {}^{A}_{Z-1}Y + e^{+} + \nu$	e^{+} is a positron also called "***beta**** plus particle" ν is a **neutrino***.	(β^{+})
Electron capture	$e^{-}_{atomic} + {}^{A}_{Z}X \rightarrow {}^{A}_{Z-1}Y$	e^{-}_{atomic} is an electron belonging to the electron cloud of the ${}^{A}_{Z}X$ atom.	(E.C.)
Isomeric transition	${}^{A}_{Z}X^{*} \rightarrow {}^{A}_{Z}X + \gamma$	${}^{A}_{Z}X^{*}$ is an isomer which decays by emitting a ***gamma* radiation*** denoted "γ".	(I.T.)
Delayed neutron emission	${}^{A}_{Z}X^{*} \rightarrow {}^{A-1}_{Z}X + n$	${}^{A}_{Z}X^{*}$ is a fission product called "delayed neutron precursor".	
Spontaneous fission	${}^{A}_{Z}X \rightarrow PF_1 + PF_2 + \nu n$	${}^{A}_{Z}X$ is a **heavy nucleus*** (ν : number of emitted neutrons).	(sf)

Neutronics equations

Neutronics equations describe neutron transport through matter, and alterations in the latter's composition due to induced nuclear processes. Simplifications can be introduced.

Neutron-electron interactions are fully negligible, for they can only take place as a result of weak interaction. Neutron-neutron interactions, too, are negligible. It is a matter of density: in a power reactor there is about 1 neutron for 10^{14} atomic nuclei. Neutrons in a free state disappear through radioactivity, but this, too, is fully negligible in reactors, for radioactive half-life (~1,000 s) is very long versus neutron path time (less than one millisecond).

Important basic data in neutronics: microscopic cross sections

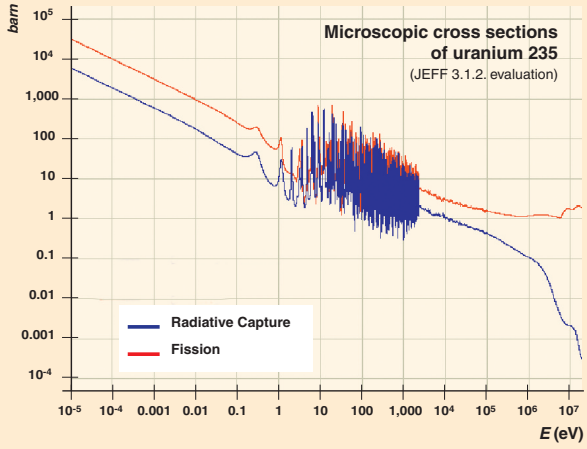

Fig. 2. Uranium 235 capture and fission microscopic cross sections as a function of the incident neutron's energy.

The microscopic cross section σ of a nucleus characterizes the probability of a neutron to interact with the latter: a cross section can be seen as the cross sectional area presented by the target nucleus to the incident neutron. But this image is too simple, for it cannot explain the often numerous, and quite significant, variations in cross sections as a function of the incident neutron's velocity - resonances -, due to the energetic levels of nuclei and the quantum character of the interaction.

The microscopic cross section is expressed in barns (1 barn = 10^{-24} cm^2), and is used to relate the reaction rate R to the neutron flux ϕ and to the number of target nuclei per unit volume N :

$$R = N\sigma\phi$$

Neutrons inside the reactor do not only induce fissions (otherwise, the chain reaction would not be steady), but also a whole series of more or less probable **nuclear reactions***.

There exist as many cross sections as nuclear reactions likely to take place between the incident neutron and the target nucleus.
Concerning the incident energies of neutrons related to reactor physics, two types of possible reactions can be distinguished:

1. The **potential elastic scattering***, which is the mere reflexion of the neutron by the potential barrier of the nucleus. The collision is of the same type as that of two billiard balls. This is the most probable mechanism of neutron slowing-down.

2. Nearly all the other reactions result from a single mechanism: the formation of a **compound nucleus***, consisting of the initial nucleus and the incident neutron. This compound nucleus is excited, for the neutron provides it with its binding energy and its kinetic energy.

The compound nucleus then selects its decay channel independently from its formation mode, among the following:
- Resonant elastic scattering: which leaves the impinged nucleus in its fundamental state (the compound nucleus goes back to the system which gave rise to it);
- resonant inelastic scattering: in which the identity of the impinged nucleus remains unchanged, this nucleus being however brought to one of its excited states;
- radiative capture: in which the compound nucleus undergoes decay only through the emission of one or several photons;
- fission: in which the compound nucleus undergoes decay by splitting into two or three fission fragments of average masses, with emission of a few neutrons;
- and other, less usual reactions.

One of the difficulties in neutronics lies in accurately taking account of the very complex variations in microscopic cross sections as a function of the neutron's velocity (or energy) [see Fig. 2].

Despite low density, neutron population is numerous, *i.e.* about 10^8 neutrons per cm^3, and can so be described statistically.

This statistical treatment can be performed using the Monte-Carlo method. The latter, referred to as stochastic, was initially designed by Fermi, and is currently implemented through the powerful computers available to us. It consists in a sampling of neutron histories – often from several millions to several billions – reproduced as accurately as possible by computer simulation (the events being sampled according to relevant probability laws during the neutron's path that is a Markovian process).

Yet, "deterministic" treatment, the only one which could be considered in the earlier age of neutronics, is still the processing most frequently implemented today, due to its high performance in terms of cost/accuracy ratio. Neutron population in a system is much similar to that of an ideal gas. This is why neutron physicists could use, through adaptation, the equation written for gases by Boltzmann in 1879, that is half a century prior to neutron discovery.

In a nuclear reactor, neutron population is governed by the Boltzmann equation, also called "transport equation", while isotopic composition (which neutron population depends on) is governed by the Bateman equations, also called "generation/depletion equations" ("burnup equations").

Boltzmann equation

The Boltzmann equation makes the neutron population balance as a function of the variables – *i.e.* space, velocity vector (or energy and direction), and time – the neutron population depends on, taking into account the various types of nuclear reactions likely to create neutrons or to make them disappear (see *infra*, the chapter titled "Neutronics methods", pp. 43 *et sq.*).

The data required for solving the Boltzmann equation are the nuclear data of the various nuclides present in the reactor and their concentrations, as well as external neutron sources (if any). These quantities are summarized in Table 4.

The solution of the Boltzmann equation provides the neutron flux, a quantity which characterizes neutron population. Derived quantities such as reaction rates can be deduced from neutron flux. All of these physical quantities are displayed in Table 5.

It is worth noting that *gamma* photon propagation, a key item in radiation shielding, is governed by a Boltzmann equation similar to that of neutrons.

Bateman equations

Nuclear reactions not only have an influence on neutron population; they also induce variations in the population of atomic nuclei. The evolution in concentrations of the various nuclides is governed by the Bateman equations, a set of space and time balance equations, taking into account atomic nuclei generations and disappearances through nuclear reactions and radioactive decay process (see *infra*, the chapter titled "Neutronics methods", pp. 43 *et sq.*).

The data required for solving the Bateman equations are those relating to the decay of the various nuclides present in the reactor, and the reaction rates issued from the solution of the Boltzmann equation. These quantities are summarized in Table 6.

Solving the Bateman equations provides the concentrations of the various nuclides present in the reactor (also needed among the data of the Boltzmann equation), as well as related activities.

All of these physical quantities are displayed in Table 7 (p. 13). Derived quantities, such as residual powers (α, β, γ and neutron), radiation sources, and radiotoxicities, can be directly deduced from them.

Table 3.

Usual variables in neutronics

Quantity	Usual notation	Definition	Usual unit
Point	$\vec{r}$	Position in the system.	cm
Velocity	v	Neutron velocity.	cm.s^{-1}
Phase	$\vec{\Omega}$	Neutron direction.	sr
Time	t	Instant of interest, time.	s
Phase space	$P \equiv (\vec{r}, E, \vec{\Omega})$	Point in phase space.	–
Energy	E	Neutron's energy.	eV, keV, MeV
Lethargy	$u = ln\frac{E_0}{E}$	Dimensionless quantity characterizing neutron's energy versus an arbitrary energy E_0.	–

Table 4.

Data for solving the Boltzmann neutron transport equation

Quantity	Usual notation	Definition	Usual unit
Concentration	$N_i(\vec{r}, t)$	Number of atoms of species i per unit volume in $\vec{r}$, at a given instant t.	cm^{-3}
Microscopic cross section	$\sigma(E)$	Cross sectional area of the "target" (*i.e.* the atomic nucleus "seen" by a neutron).	barn (b)
Macroscopic cross section	$\Sigma(\vec{r}, E, t) = N(\vec{r}, t)\sigma(E)$	Collision probability by unit length.	cm^{-1}
Mean free path	$\frac{1}{\Sigma(\vec{r}, E, t)}$	Average distance before the next collision.	cm
Fission kerma	κ	Energy deposited in the reactor per fission.	MeV
Neutron multiplication by fission	ν	Average number of neutrons emitted per fission.	–
Fission spectrum	$\chi(E, E')$	Proportion of neutrons emitted at the E' energy, due to a fission induced by a neutron of energy E.	MeV^{-1}
Source	$S(\vec{r}, E, \vec{\Omega}, t)$	Neutron emission per unit volume in $\vec{r}$, per unit energy in E, per unit of solid angle in the $\vec{\Omega}$ direction, and per unit time in t.	cm^{-3}. MeV^{-1}. sr^{-1}.s^{-1}

Table 5.

Basic physical quantities deduced from solving the Boltzmann neutron transport equation

Quantity	Usual notation	Definition	Usual unit
Neutrons density	$n\,(\vec{r}, E, \vec{\Omega}, t)$	Number of neutrons per unit volume in $\vec{r}$, per unit energy in E, per unit of solid angle in the $\vec{\Omega}$ direction, at a given instant t.	$cm^{-3}.MeV^{-1}.sr^{-1}$
Angular flux	$\psi\,(\vec{r}, E, \vec{\Omega}, t) = n\,(\vec{r}, E, \vec{\Omega}, t)\,\upsilon$	Number of neutrons of velocity υ perpendicularly going through a unit surface located in $\vec{r}$, perpendicular to $\vec{\Omega}$, per unit energy in E, per unit of solid angle in the $\vec{\Omega}$ direction, and per unit time in t.	$cm^{-2}.MeV^{-1}.sr^{-1}.s^{-1}$
Scalar flux	$\phi\,(\vec{r}, E, t)$	Integral over angles of angular flux.	$cm^{-2}.MeV^{-1}.\,s^{-1}$
Total flux	$\Phi\,(\vec{r}, t)$	Integral over energy of scalar flux.	$cm^{-2}.s^{-1}$
Current	$\vec{J}(\vec{r}, E, \vec{\Omega}, t) = \vec{\Omega}\,\psi(\vec{r}, E, \vec{\Omega}, t)$	$\vec{J}(\vec{r}, E, \vec{\Omega}, t).\vec{N}$ Number of neutrons going through a unit surface located in $\vec{r}$ perpendicular to $\vec{N}$, per unit energy in E, per unit of solid angle in the $\vec{\Omega}$ direction, and per unit time in t.	$cm^{-2}.MeV^{-1}.sr^{-1}.s^{-1}$
Reaction rate	$\tau_i(\vec{r}, E, t) = \Sigma_i(\vec{r}, E, t)\phi(\vec{r}, E, t)$	Number of reactions of type i per unit volume in $\vec{r}$, per unit energy in E, and per unit time in t.	$cm^{-3}.\,MeV^{-1}.\,s^{-1}$
Energy-integrated reaction rate	$\tau_i\,(\vec{r}, t)$	Number of reactions of type i per unit volume in $\vec{r}$, and per unit time in t.	$cm^{-3}.\,s^{-1}$
Fluence	$F(\vec{r}, t) = \int_0^t \Phi(\vec{r}, t')dt'$	Time-integrated total flux, number of neutrons received per unit surface in $\vec{r}$, after time t.	cm^{-2} ou $kilobarn^{-1}$
Burn-up	$Bu = \int \frac{\kappa}{\varrho}\Sigma_f(\vec{r}, E, t)\phi(\vec{r}, E, t)d^3rdEdt$	Amount of thermal energy generated per unit mass, in which ϱ is the specific mass of fuel (only for heavy atoms).	MWd/t
Multiplication factor	k	Population of a generation versus population of the previous generation.	–
Reactivity	$\rho = \frac{k-1}{k}$	Deviation with respect to the critical state: $\rho < 0$ subcritical state $\rho = 0$ critical state $\rho > 0$ supercritical state	pcm *(pour cent mille: 10^{-5})*

Table 6.

Data of the Bateman equations

Quantity	Usual notation	Definition	Usual unit
Partial decay constants	$\lambda_{\alpha,i}, \lambda_{\beta^-,i}, \cdots$	Probability of disintegration per unit time of nuclide i, according to a given radioactive process.	s^{-1}
Energy-integrated microscopic reaction rates	$\int_E \sigma_{q,k\leftarrow m}\,(E)\phi(\vec{r}, E, t)dE$	Microscopic rate of generation (or disappearance) of a k nuclide (or m).	s^{-1}
Fission yields	$Y_{i\leftarrow f}\,(E)$	Fission yield of nuclide i for a fission induced by a neutron of energy E on a fissile nucleus f.	–

Table 7.

Basic physical quantities deduced from solving the Bateman equations

Quantity	Usual notation	Definition	Usual unit
Concentration	$N_i\,(\vec{r}, t)$	Number of atoms of nuclide i per unit volume in $\vec{r}$ at a given instant t.	cm^{-3}
Activity	$A_i\,(\vec{r}, t) = \lambda N_i\,(\vec{r}, t)$	Number of disintegrations of nuclide i per unit volume in $\vec{r}$ and per unit time in t, relating to the radioactive process of constant λ.	$Bq.cm^{-3}$

Equation coupling

It is worth to mention that the **Boltzmann and Bateman equations*** form a coupled system, since reaction rates depend on the neutron flux, the latter being itself dependent on the system's composition. In practice, however, these equations can be decoupled by solving them separately over successive time intervals, short enough to allow variations in isotopic composition in the Boltzmann equation, and variations in flux in the Bateman equations to be neglected over each of these intervals.

In addition to the Boltzmann and Bateman equations, it is necessary to use equations that describe the temperature and thermal hydraulics feedback effects.

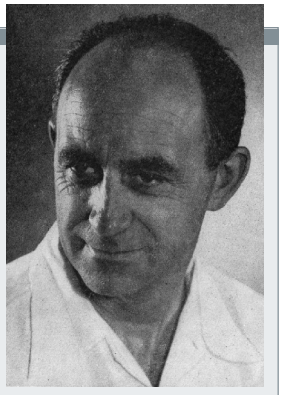

Enrico Fermi (1901-1954) received the Nobel Prize (1938) for his works about, not neutronics, but *beta* radioactivity. **Enrico Fermi** and his team built and operated the very first atomic pile in man's history in the basement of the Chicago University's football ground.
He established the "four-factor formula", still used today, and roughly laid the foundations of the resonance self-shielding theory. It is remarkable that, from the very beginning, Fermi thought about all the basic features of nuclear reactors: *i.e.* reactor control, radiation protection and safety (emergency shutdown), as well as the necessary dialogue between the members of the staff assuming these various functions.

From left to right: **Frédéric Joliot-Curie** (1900-1958), Nobel Prize of Chemistry in 1935 jointly with his wife **Irène Joliot-Curie** (1897-1956) for the "synthesis of new radioactive elements" (discovery of artificial radioactivity), **Hans von Halban** (1908-1964), and **Lew Kowarski** (1907-1979). In 1939, they reported the emission of two or three secondary neutrons during fission.

Neutronics development in France: research, industry and teaching

In early 1939, in a letter sent to **Frédéric Joliot-Curie**, **Leó Szilárd**, a Hungarian-born American scientist, had predicted that several neutrons could be generated following the splitting of an uranium nucleus induced by a neutron. In April of the same year, in his laboratory of *Collège de France*, **Frédéric Joliot-Curie** and his collaborators **Hans Halban** and **Lew Kowarski**, to be joined by **Francis Perrin**, evidenced this very phenomenon originating the emission of 2 or 3 neutrons, that is one week before **Leó Szilárd**'s and **Enrico Fermi**'s American team. They very quickly understood the practical interest to be drawn from this nuclear fission phenomenon - *i.e.* power generation -, and determined the conditions in which this process could be enhanced (*i.e.* slowing down neutrons which can then interact with uranium 235 nuclei). That is tes-

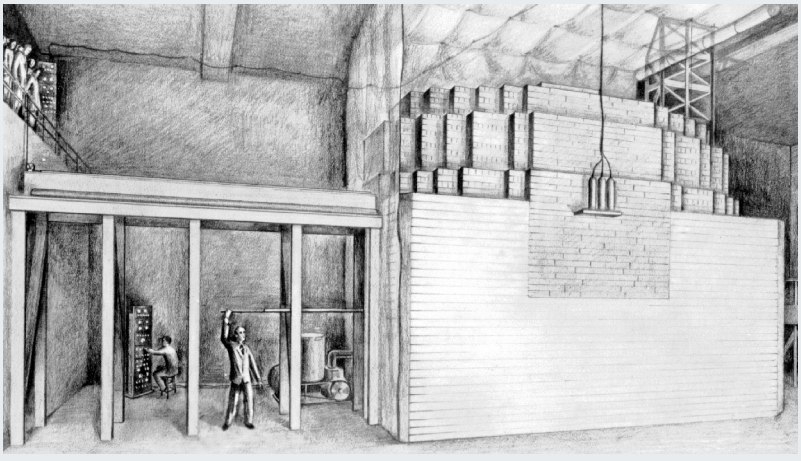

Chicago atomic pile.
Though photographs of the first layers of the pile can still be found, there is nothing left but a drawing and a painting of the Chicago pile made several months later by recollection. It diverged on December 2, 1942, generating about 0.5 watt. In the following days, Enrico Fermi pushed it to a few hundred watts, and finally had it dismantled.

tified by the three patents filled in on May 1st, 2nd, and 4th, 1939, on account of French *Caisse Nationale de la Recherche Scientifique* (CNRS). In the patent of May 4th, **Francis Perrin** stated a formula of critical mass. The French team immediately focused on getting heavy water (deuterium had also been discovered by an American, **Harold Urey**, in 1932), with the purpose of building an atomic pile (at that time the expression "nuclear reactor" was not yet used).

That project came to an end when World War II started, so that **Enrico Fermi** and his team finally built and operated the first atomic pile in human history, in the basement of the Chicago University's football ground. **Enrico Fermi** had previously stated the so-called ***"four-factor formula"***, *i.e.* the famous neutronics formula expressing the neutron multiplication factor in a fissile medium, which was to enable him to predict the *critical mass* of that first atomic pile. Consisting of 6 tons of metal uranium, 50 tons of oxide, and 400 tons of graphite, a neutron slowing-down, little-absorbing material, it diverged on December 2nd, 1942. Controlled by rods of cadmium, a thermal neutron-absorbing material, it delivered no more than one watt of power at its first divergence, which was a deliberate choice for reasons of radiation protection.

As soon as World War II ended, the French Atomic Energy Commission (CEA: *Commissariat à l'Énergie Atomique*), created by Ordinance of October 18, 1945, built the first French atomic pile, **ZOE** (this French acronym stands for *"puissance Zéro, Oxyde d'uranium, Eau lourde"*: zero power, uranium oxide, heavy water), which diverged on December 15th, 1948 at 12.12pm.

The ZOE team, in December 1948; from top to bottom, and from left to right: André Ertaud, Bertrand Goldschmidt, Maurice Surdin, Lew Kowarski, Frédéric Joliot-Curie, Eugène le Meur, Jules Guéron, Jacques Stohr, Roland Echard, José Foglia, Hubert de Laboulaye, Roger Martin, Henry Fauquez, Edmond Jaly, Roger Beauge, Jacky Weill, Jacques Pottier, Jules Chimot, André Berthelot, Jacques Cordeaux, Anatole Rogozinski, Victor Raievski, Georges Valladas, Gaston Clairet, Maurice Nel and Robert Bonnerue.

On the CEA's 50th Anniversary a colloquium titled ***"Birth of a scientific discipline: neutronics"***, opened by **Georges Vendryes**, was held at Paris on February 12, 1996: six papers were then successively presented, that recalled the main steps of neutronics development in France, as well as the conceptual and prospective vision assumed by its actors: **Jean Bussac**, with "CEA's Role in the Early Developments of Neutronics", **Paul Reuss**, with "The Evolution of Paradigms in Neutronics", **Daniel Paya**, with "Nuclear Physics and Neutronics", **Jean-Baptiste Thomas**, with "Neutronics Applications. Thermal Neutron Reactors", **Massimo Salvatores**, with "Neutronics Applications. Fast Neutron Reactors", and **Pierre Bacher**, with "Training Problems in the Neutronics Area".

After the pioneers' age (**Frédéric Joliot-Curie**, **Hans Halban**, **Lew Kowarski**, **Francis Perrin**, **Irène Joliot-Curie**, **Bertrand Goldschmidt**…), the development of theoretical neutronics, on the one hand, and experimental neutronics, on the other hand, took place under the incentive and supervision of **Jacques Yvon**, a theoretical physics professor in the Strasbourg University and a specialist in statistical mechanics. One of the prominent figures among the new generation's theoreticians was **Jules Horowitz**, often presented as the founder of the French School of neutronics: the experimental reactor JHR was named after him.

In 1952, **Jacques Yvon**, who had been Head of the Mathematical Physics Section (SPM: *Service de Physique Mathématique*) since its creation at the CEA in 1949, left this supervision to **Jules Horowitz**, in order to take up the supervision of a new entity, the Pile Research Department (DEP: *Département des Études de Piles*). The CEA/DEN units whose activities are focused on computational method and code development and experimental neutronics, are the daughters of DEP and SPM.

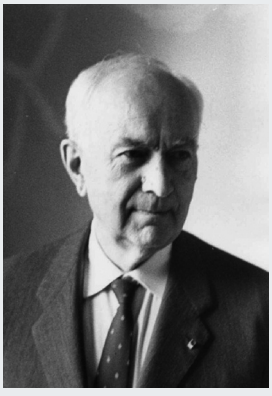

Jacques Yvon (1901-1979) was Head of the Mathematical Physics Section, and then High-Commissioner (1970-1975).

Jules Horowitz (1921-1995) is often considered as the founder of the so-called "French School of neutronics", at the Mathematical Physics Section; he was then Head of the Atomic Pile Division, and then of the Fundamental Research Division at the CEA.

Jules Horowitz then inaugurated the age devoted to building physical-mathematical models for nuclear reactor physics. Two examples are the neutron thermalization model built by **Jules Horowitz** and **Michel Cadilhac**, and the ABH (Amouyal-Benoist-Horowitz) *formula* giving the *thermal utilization factor*.

Georges Vendryes, on his own part, was in charge of endowing neutronics with a broad, robust experimental basis, especially with the cross section measurements which the EL2 heavy-water reactor built at the Saclay site was chiefly dedicated to. "Critical mockups" (AQUILON, ALIZÉ, PROSERPINE, MASURCA, MINERVE, MARIUS, CÉSAR, ÉOLE…) were to be built and operated at the various CEA sites, Fontenay-aux-Roses, Saclay, and Cadarache, taking an active part in this outlook.

In the early sixties, a third generation of neutron physicists emerged, who still used to work on numerical tables and power-actuated mechanical machines, such as the noisy *Frieden* (named after the place where it was manufactured).

The first neutronics Ph. D. were then defended, such as **Pierre Benoist**'s thesis on the "theory of neutron diffusion coefficient in a lattice displaying cavities" *("Théorie du coefficient de diffusion des neutrons dans un réseau comportant des cavités")* [1964]. The first ***neutronics codes*** appeared, specific of a given reactor type: COREGRAF for the *natural uranium-graphite-gas* reactor type, CRUEL for the *heavy-water* reactor type, COPPÉLIA and, then, EVEREST for the *ordinary water* reactor type, and, finally, HETAÏRE for the *fast neutron* reactor type.

Nevertheless, these codes did not yet solve the *Boltzmann equation* which governs neutron transport. Thanks to computers, this challenge could be taken up successfully towards the late sixties, discarding the too problem-dependent phenomenological models, which were however kept in academic education for their pedagogical value.

The APOLLO neutronics code, initially developed by **Alain Hoffmann**, **Françoise Jeanpierre**, **Alain Kavenoky**, **Michel Livolant** and **Henri Lorain**, was first dedicated to the pressurized water reactor (PWR) type. It belongs to this new sequence of nuclear reactor physics history where neutronics, numerical techniques, and computer engineering are intimately connected.

While some models were found to become obsolete, new issues raised, or older ones had to be formulated again in order to solve the Boltzmann equation with a calculation time/accuracy ratio acceptable for industrial use. Let us mention, for example, the indeed fundamental issue of *homogenization*, which was reviewed by **Richard Sanchez** in a thorough article titled *"Assembly homogenization techniques for core calculations"*.

The increasing power of computers made it possible to develop, not only *deterministic* neutronics codes , as those previously mentioned, but also, in the same time, codes using a probabilistic method, the *Monte-Carlo method*, to solve the Boltzmann equation. In the latter case, the individual history of neutrons in the nuclear reactor is simulated "without approximations", which means a computing time much higher than with deterministic codes. The very first neutron transport softwares using the Monte-Carlo method - ZEUS, POKER - were written at the CEA in the sixties. Their successor, TRIPOLI, whose development was initiated by **Jean-Claude Nimal**, was edited in its first version in the mid-seventies.

The French National Institute for Nuclear Science and Technology (INSTN: *Institut National des Sciences et Techniques Nucléaires*), set up in 1956: the initial building. A teaching-dedicated reactor, ULYSSE, was installed in this place: it has allowed the training of future nuclear technicians and engineers for a number of years (1961-2007).

INSTN: view of the new building, built up against the former building.

In *Neutron Physics*, a handbook by **Paul Reuss**, a commented bibliography provides a number of references especially relating to scientific production in France in the neutronics field: theses, articles, and books.

The R&D activity and the deployment of the various industrial nuclear reactor types for power generation have been accompanied by nuclear or atomic engineering training. "Atomic Engineering Courses" were taught from 1954, and were to be held from 1956 at the French National Institute for Nuclear Science and Technology (INSTN), where **Jean Debiesse** was the first head. They were published in 1963 by *Presses Universitaires de France*, with a foreword by **Francis Perrin**. The INSTN then spread to Cherbourg, Grenoble and Cadarache. In 1961, in agreement with **Jean Teillac**, who was then a professor at the Paris University, Head of the Orsay Nuclear Physics Institute *(Institut de Physique Nucléaire d'Orsay)*, **Jules Horowitz** created a master's degree (DEA: *Diplôme d'Études Approfondies*) in nuclear reactor physics. This course is going on today as part of the *International Master in Nuclear Energy* co-organized by CEA/INSTN, Paris-Sud University, ParisTech – the consortium of French top engineering schools *(Grandes Écoles)* –, and EDF, AREVA and GDF Suez industries. It is held every year for students from over a dozen countries. Besides, neutronics education modules have been gradually integrated in the curricula of some Universities and *Grandes Écoles*.

New atomic engineering collections have been published, the latest being that supervised by **Joseph Safieh** and edited by INSTN and EDP Sciences.

Monograph presentation

This Monograph has been purposely focused on **core physics**, which aims at characterizing the state of a reactor core, and understanding its behavior under normal and accidental conditions. This requires, in particular, the determination of its power distribution, as well as its nuclide composition at each of its points and at any time. The Monograph highlights the neutron physicist's approach, which consists in designing optimized computational schemes for specific configurations. These computational schemes implement nuclear data libraries as well as computer codes solving the Boltzmann and Bateman equations. The content of this Monograph has however been extended to a few applications relating to the fields mentioned above.

This Monograph gives an overview of what is neutronics, emphasizing its multidisciplinary character. Insets have been inserted, some of them recalling fundamental notions (on orange or green background), others reporting historical and/or conceptual information (on light grey background). This book should be understood as a new insight into neutronics in addition to long-existing or more recent books, such as *Neutron Physics (Précis de neutronique)* by P. Reuss (CEA), *Applied Reactor Physics* by A. Hébert (École Polytechnique of Montréal), *La physique des réacteurs nucléaires* by S. Marguet (EDF), *Nuclear Computational Science: A Century in Review* co-edited by E. Sartori and Y. Azmy, or the *Handbook of Nuclear Engineering - Nuclear Engineering Fundamentals* by D. Cacuci.

Should the reader wish to study a special point more attentively, he could refer to the bibliographical information provided all along his text reading. These references will also give him further information about other contributions to neutronics development, from a number of persons whose names could not be mentioned in the Monograph's available space.

The sections of this Monograph are successively devoted to nuclear data and their processing, general neutronics equations, and some emblematic resolution methods, the major neutronics codes and the benefits of high-performance computing with the advent of supercomputers, experimental neutronics and qualification, and last, the various applications of neutronics.

Bibliography

Azmy (Y.) and Sartori (E.) [editors], *Nuclear Computational Science: A Century in Review*, Springer Science+Business Media B.V., 2010.

Bussac (J.), Reuss (P.), *Traité de Neutronique - Physique et calcul des réacteurs nucléaires avec application aux réacteurs à eau pressurisée et aux réacteurs à neutrons rapides*, Paris, Hermann, 1978, 1985 (2e édition).

Cacuci (D.) [editor], *Handbook of Nuclear Engineering – Nuclear Engineering Fundamentals*, (5 volumes), Springer, 2010.

Goldschmidt (B.), *Le Complexe atomique – Histoire politique de l'énergie nucléaire*, Paris, Fayard, 1980.

Hébert (A.), *Applied Reactor Physics*, Montréal, Presses internationales Polytechnique, 2009.

Hoffmann (A.), Jeanpierre (F.), Kavenoky (A.), Livolant (M.), Lorain (H.), *APOLLO : code multigroupe de résolution de l'équation du transport pour les neutrons thermiques et rapides*, note CEA-N-1610, mars 1973.

Khairallah (A.) et Recolin (J.), « Calcul de l'Autoprotection Résonnante dans les Cellules Complexes par la Méthode des Sous-Groupes » (code HETAÏRE), *Proc. Seminar Numerical Reactor Calculations*, IAEA-SM-154/37, Vienna, January 17-21,1972.

Marguet (S.), *La Physique des réacteurs nucléaires*, Éditions Lavoisier TEX & DOC, Paris, 2011.

Pinault (M.), *Frédéric Joliot-Curie*, Odile Jacob, Paris, 2000.

Reuss (P.), Coste-Delclaux (M.), « Development of Computational Models used in France for Neutron Resonance Absorption in Light Water Lattices », *Progress in Nuclear Energy*, vol. 42, n° 3, pp. 237-282, 2003.

Reuss (P.), *Précis de neutronique*, Les Ulis - France, EDP Sciences / INSTN, 2003 ; Traduction anglaise : *Neutron Physics*, EDP Sciences / ENEN /INSTN, 2008.

Reuss (P.), « Saga française de la neutronique », Leçon inaugurale donnée au *Génie atomique*, INSTN/Saclay, 25 octobre 2010.

Reuss (P.), *Du noyau atomique au réacteur nucléaire – La saga de la neutronique française*, Les Ulis, France, EDP Sciences, 2013.

Salvatores (M.), « *Naissance d'une discipline scientifique : la neutronique* » (un colloque présenté par), 50 ans du CEA, Paris, 12 février 1996.

Sanchez (R.), « Assembly homogenization techniques for core calculations », *Progress in Nuclear Energy*, 51, pp. 14-31, 2009.

Segrè (E.), *Les Physiciens modernes et leurs découvertes – Des rayons X aux Quarks*, Paris, Fayard, Coll. Le temps des Sciences, 1984.

Lefebvre (V.), *Au cœur de la matière : 50 ans de recherches au CEA de Saclay*, Paris, Le Cherche-Midi, 2002.

Paul Reuss
French National Institute for Nuclear Science and Technology (INSTN)
and Cheikh M. Diop
Department for Systems and Structures Modeling

Nuclear Data

In order to describe neutron transport through matter, **nuclear chain reactions***, and modifications in matter composition due to nuclear reactions, neutronics needs basic data: **microscopic cross sections*** characterizing the interaction probabilities between neutrons and matter, post-fission observables (spectrum and multiplicity of neutrons emitted by **fission***, **fission yields***), **radioactive decay*** data relating to the radionuclides formed by the nuclear reactions involved, nature and energy of emitted radiations. These data are determined through experiments and theoretical models of nuclear physics. The complex work of analyzing all of these data is conducted by **evaluation* experts**. It results in the production of international nuclear databases.

From Measurement to Evaluation of Nuclear Data

Needs in evaluated nuclear data for nuclear reactor physics are expressed not only through studies relating to current reactors, but also through innovating concepts of Generation III (*e.g.* **EPR***) and IV (**ASTRID***) reactors. The **computational code package*** and calculation tool **qualification*** documents based on the JEFF (Joint Evaluated Fission and Fusion file) evaluated nuclear data library enable target accuracies to be determined on neutronics parameters, and biases arising from nuclear data to be pinpointed. Several actions have therefore to be conducted simultaneously: (i) taking part in /initiating/ supporting the microscopic measurements of cross sections at existing or new facilities, (ii) developing new nuclear data evaluation tools and codes in order to improve mastery in physical modeling and uncertainty assessment (CONRAD code), (iii) evaluating related nuclear data, and (iv) processing these nuclear data so as to use them in neutronics computer codes (GALILÉE code system).

The implementation takes place in a background of close partnership within the CEA (DAM-DEN-DSM), as well as with national and international organizations. The whole of these works is promoted through the OECD's JEFF [1] group.

Cross sections in the resolved and unresolved resonance ranges, and in the continuum

The modeling of neutron cross sections is based on nuclear reaction models, the parameters of which (*e.g.* **resonance*** characteristics) are not currently predicted with enough accuracy by microscopic physical theories. This is why they are fitted to a set of observations (measurements). Three types of experiments are analyzed then, *i.e.* microscopic experiments, integral analytical experiments focused on the influence of a specific nuclide, and mockup experiments which are representative of reactor concepts. That third type will be detailed in the paragraph dealing with nuclear data qualification (see *infra*, pp. 162-182).

"Time-of-flight" microscopic experiments

Cross sections play a key role among the basic data required for neutronics calculations. Cross sections as a function of the incident neutron's energy are called "microscopic", in contrast, here, with integral cross sections, which result in quantities integrated over the energy spectrum of incident neutrons. In Europe, only two facilities enable this type of measurements to be achieved: the linear accelerator GELINA (GEel LINear Accelerator) of the Institute for Reference Materials and Measurements (IRMM) located at Geel (Belgium), and the n-TOF facility located at the European Organization for nuclear research (CERN), Geneva (Switzerland). Both of them use the "time-of-flight" technique, which consists in accurately measuring the duration between the time of neutron generation and the time when the neutron interacts with a target. Neutron energy can be deduced from the knowledge of this neutron time-of-flight and of the distance traveled by the neutron. We are going to give a brief description of the Geel facility with which the CEA has been maintaining a very fruitful co-operation for a number of years.

GELINA Facility

This facility is one of the more powerful neutron sources in the world, featuring both a very high energy resolution, but also a very broad energy spectrum (from a few milli electronvolts to several millions of electronvolts). Its operating principle (see Fig. 1) lies in the acceleration of a very intense pulsed electron beam, which hits a rotating target of uranium. Typically, these electron bursts (lasting a few nanoseconds) are emitted 800 times per second. As they penetrate into a rotating target of natural uranium, electrons lose their energy, generating the so-called "bremsstrahlung" radiation, which induces reactions producing a neutron [the so-called (γ,n) reactions], or inducing a fission [photofission reaction referred to as (γ,f)]. (γ,n) reactions generate a neutron spectrum that can reach up to several dozens of MeV, while (γ,f) reactions provide a fission spectrum with an average energy of about 2 MeV. In order to generate neutrons of lower energy (especially to cover the thermal range), neutrons are slowed down in two beryllium-made water containers, put above and under the rotating target. Once emitted, then slowed down, neutrons are transferred to the time-of-flight bases where beam collimation is ensured by lead-, copper- and paraffin-made devices. About 4.3×10^{10} neutrons per electron burst are generated [2].

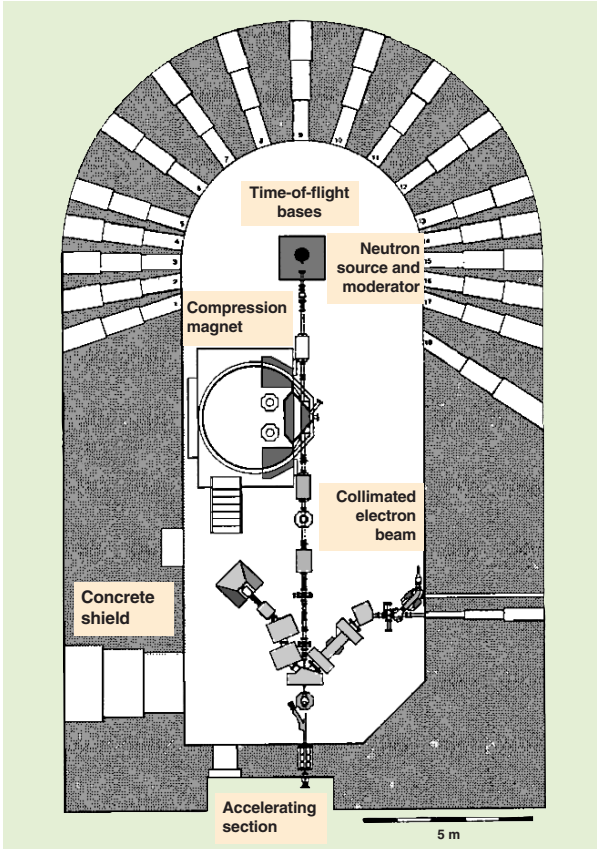

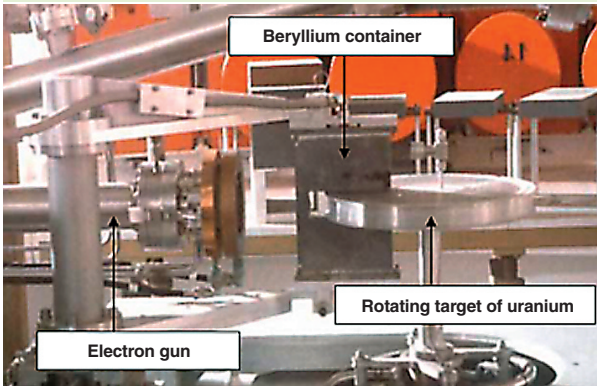

Fig. 3. General view of the electron-accelerating device (top) of GELINA Facility at Geel (Belgium). The target room, where neutrons are generated (bottom), gives access to the time-of-flight bases, which are 8 - 400 m long. (Photo courtesy of IRMM).

Among the time-of-flight measurements achieved, the so-called "transmission measurements", dedicated to measuring the fraction of neutrons transmitted through a sample put on the neutron beam's trajectory, are essential for the evaluation of neutron-induced cross sections. Figure 4 displays an example of such a measurement, performed with samples of natural hafnium of three various thicknesses [3]. The analysis of the resonances quite visible on this figure consists in modeling the observed structures, using the *R matrix theory* (see the paragraph below), taking into account many experimental corrections.

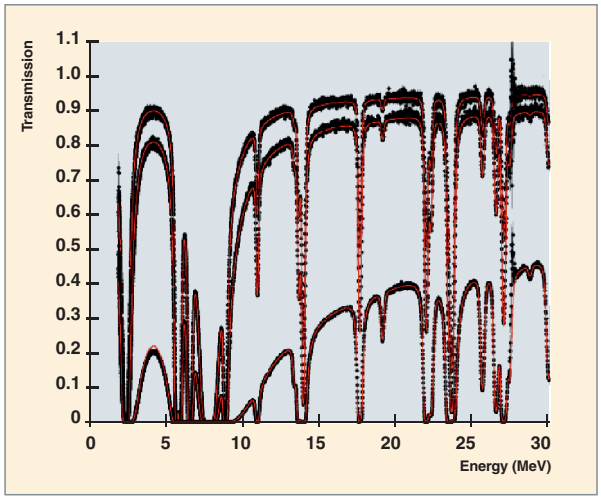

Fig. 4. Transmission measurements achieved with three samples of natural hafnium 15 mm, 2 mm and 1 mm thick [3]. The observed structures correspond to the resonances of the six isotopes of hafnium.

Integral analytical measurements of cross sections

The Mini-Inca Project at the Laue Langevin Institute (ILL), Grenoble

As part of the feasibility study relating to the **transmutation*** of a certain number of **minor actinides***, and in cooperation with the Laue Langevin Institute (ILL: *Institut Laue Langevin*) of Grenoble (France), the CEA installed a device able to measure capture and fission cross sections integrated over various neutron spectra [4]. This experimental project "Mini-Inca" was conducted at the Laue Langevin Institute's reactor, which delivers a neutron flux which is one the highest in the world (1.5×10^{15} n/s/cm^2). These cross section measurements referred to as "integral", that is averaged on an energy spectrum of the incident neutron, use various irradiation channels placed in the reactor core. According to the position of the sample inside these channels, the intensity and spectrum of incident neutrons can be made to vary as illustrated on Figure 5.

Thus, in Channel V4, a sample located at a 100 cm height is irradiated by a flux of strictly **thermal neutrons***, whereas an **epithermal neutron*** component (about 15%) can be observed at a 0 cm distance (*i.e.* very close to reactor fuel).

After irradiation, the **capture rate*** of the specimen can be measured by *alpha* and/or *gamma* spectroscopy in order to deduce the capture cross section. Similarly, the use of miniature fission chambers fabricated by the CEA's Experimental Physics Section (SPEX: *Service de Physique Expérimentale*) makes it possible to determine the **reaction rate*** from which the fission cross section can be calculated.

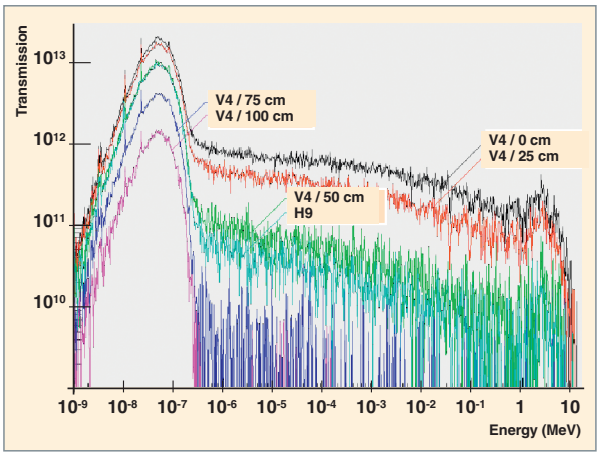

Fig. 5. Variation of the intensity and spectrum of neutrons used for irradiating a sample whose cross section is to be measured. Various irradiation fluxes can be obtained according to the channel (V4 or H9), and to the sample position within the channel. (Figure from O. Bringer's publication [5]).

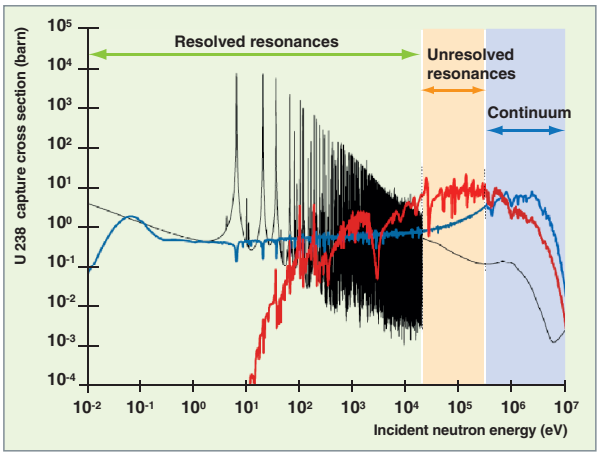

Fig. 6. Representation of the U 238 capture cross section (JEFF-3.1.1) and of the neutron fluxes representative of a sodium-cooled fast reactor (SFR) (red curve) or of a pressurized water reactor (PWR) (blue curve). The three major energy ranges (resolved resonances, unresolved resonances, and continuum) are also displayed.

Nuclear reaction models

In the energy ranges between 0 eV and 20 MeV, *i.e.* the energy range of Reactor Physics, the calculation of neutron cross sections is based on the compound-nucleus model, which assumes the neutron-nucleus interaction to take place in two distinct steps: first, the formation of the compound nucleus consisting of the target nucleus and of the incident neutron, and then its decay, which is assumed to be independent of the formation mode.

The neutron cross section of a nucleus characterizes the probability of a neutron to interact with this nucleus. This probability may get very high when the energy of the incident neutron is such that the energy received by the compound nucleus is close to the energy of one of its excitation levels. That results in a sharp rise of the neutron-nucleus interaction cross section in the neighboring of these energies. The nucleus is then said to exhibit resonances, or to be resonant, for these energies. These resonances are strictly separated in energy at low levels of excitation energy (resolved resonance range). In contrast, when the excitation energy level increases (unresolved resonance range), their spacing decreases to zero (range of continuum).

One of the major difficulties in evaluating nuclear data comes from this resonant character of neutron-nucleus cross sections, which gives them a both complex and very strong energy dependence (Fig. 6).

The work of evaluating neutron cross-sections consists in using the CONRAD [6], **ECIS*** [7], and **TALYS*** [8] codes to establish a coherent set of parameters for nuclear reaction models likely to describe the range of (resolved and unresolved) resonances and the "continuum" up to a few dozens of MeV.

Figure 6 shows the boundaries of each range in the case of the uranium 238 capture cross section.

CONRAD, a tool for cross section evaluation

The development of Code CONRAD ("COde for Nuclear Reaction Analysis and Data assimilation") corresponds to the endeavors within the CEA to endow it with a modern tool for nuclear reaction modeling, taking into account the propagation of related uncertainties. This code enables evaluations useful to reactor physics to be produced. More precisely, it makes it possible to analyze and evaluate total and partial neutron-nucleus cross sections (radiative capture, fission…) in the energy range between the electronvolt and the mega-electronvolt. The parameters of nuclear reaction models (R matrix, optical models) are assessed by adjustment of calculation results to microscopic (transmission, capture yield…) and integral experiments. In addition CONRAD provides a framework to improve fission-related models. Last, it makes it possible to assess uncertainties relating to the parameters of nuclear reaction models, taking into account the whole of experimental uncertainties, and then assess cross section covariances.

The nuclear reaction models mentioned above were either developed in the tool (R matrix), or integrated through interfaces (ECIS and TALYS codes). CONRAD's major aim is to allow the integration of various nuclear physics models into a generic framework.

Collision matrix and cross sections

The two steps of compound nucleus formation and decay can be defined by the concept of reaction channel [9], named c and characterized by:

- Particle pairs before or after the reaction;
- their **spins*** (i et I);
- their orbital relative angular momentum (ℓ) and its projection (m);
- the channel spin ($s = i + I$) and its projection (m_s);
- the total angular momentum (J).

Cross section calculation involves the use of collision matrix U, which describes the transition between entrance and exit wave functions.

The partial cross section of an entrance channel c towards an exit channel c' is then expressed as follows:

$$\sigma_{cc'} = \pi\bar{\lambda}_c^2 g_J |\delta_{cc'} - U_{cc'}|^2 \quad (1)$$

with $g_J = \dfrac{2J+1}{(2I+1)(2i+1)}$

$\bar{\lambda}_c$ being the reduced wavelength relating to channel c.
The total cross section of channel c is a linear function of the collision matrix:

$$\sigma_c = 2\pi\bar{\lambda}_c^2 \sum_{c'} g_J (1 - Re(U_{cc'})) \quad (2)$$

Nuclear reaction models then provide the form and energy-dependent behavior of this collision matrix.

Resolved resonance range

The formalism of the R matrix [9] allows to determine the form of the collision matrix components in the range of resolved resonances.
For neutrons, this matrix is expressed as follows:

$$U_{cc'} = e^{-i(\varphi_c + \varphi_{c'})} \left\{ \delta_{cc'} + 2iP_c^{\frac{1}{2}} [(1 - RL^0)^{-1} R]_{cc'} P_{c'}^{\frac{1}{2}} \right\}$$

with $L^0_{cc'} = (S_c + iP_c - B_c)\delta_{cc'}$ (3)

where φ_c is the hard-sphere phase shift, P_c and S_c respectively are the penetrability and shift factors of the potential barrier, and B_c is a boundary condition. At last, the components of the R matrix are defined by:

$$R_{cc'} = \sum_{\lambda} \frac{\gamma_{\lambda c}\gamma_{\lambda c'}}{E_\lambda - E} \quad (4)$$

where $\gamma_{\lambda c}$ stands for the channel amplitudes, E_λ the energy of level λ, and E the kinetic energy (in the laboratory system) of the incident particle.

Channel amplitudes and the energies of levels (the latter being taken as real and energy-independent through a relevant choice of boundary conditions values B_c) are fitted by comparison with cross section measurements. Channel widths $\Gamma_{\lambda c}$ are given by: $\Gamma_{\lambda c} = 2\gamma_{\lambda c}^2 P_c$.

The resonant structure explicitly appears in terms $(E_\lambda - E)$ which are present at the R matrix denominator.

Unresolved resonance range and continuum

The unresolved resonance energy range is an intermediate range between the resolved resonance range and the "continuum". As the spacing between resonances as well as the time resolution of time-of-flight spectrometers no longer allow the individual analysis of resonances, the evaluation work then lies in describing the behavior of cross sections as a function of several parameters called "average parameters". At a higher energy, calculations are based on the resolution of the **Schrödinger equation*** by using a complex potential, $V + iW$ (contrary to the R matrix, which uses a real square potential), representing the interaction of the incident neutron with all of the target **nucleons***. These potentials are called "optical potentials", by analogy with Quantum Optics. This direct resolution of the Schrödinger equation is implemented in codes CONRAD (concerning spherical nuclei) and ECIS.

The evaluator has to make sure that the averaged formulation of the R matrix and the use of optical model calculations allow a continuity of cross sections at the fronteer between these two energy ranges.

Mean total cross section

In the unresolved resonance range, the total mean cross section can be obtained with the help of the averaged collision matrix ($\overline{U_{cc'}}$):

$$\bar{\sigma_c} = 2\pi\bar{\lambda}_c^2 g_J (1 - Re(\overline{U_{cc}})) \quad (5)$$

The components of the average collision matrix within the framework of the R matrix theory are obtained as a function of average parameters, such as the average level spacing $<D_\ell>$, the density function $<S_\ell>$, and the average reduced neutron width $<g\Gamma_n^\ell>$. A first assessment of these parameters can be achieved through a statistical analysis of resonances. This analysis also makes it possible to evidence missing levels, miss-attributed resonance spins, or resonances due to sample impurities.

At a higher energy, calculations of optical models directly provide a collision matrix value as a function of the energy $U_{cc'}(E)$, and this only for an entrance channel c of the nuclear reaction (*e.g.* the neutron channel). The total cross section of the entrance channel c can then be written as follows:

$$\bar{\sigma_c} = 2\pi\bar{\lambda}_c^2 g_J (1 - Re(U_{cc})) \quad (6)$$

Mean partial cross sections

The statistical Hauser-Feshbach model is used to describe the decay process of the compound nucleus (radiative capture cross section; fission cross section, elastic and inelastic scattering cross section). It uses the concept of reaction channel penetrability T_c.

Within the framework of the Hauser-Feshbach theory, partial cross sections are written as a function of transmission coefficients as follows:

$$\bar{\sigma}_{cc'} = \sigma_p \delta_{cc'} + \pi \bar{\lambda}_c^2 g_J \frac{T_c T_{c'}}{\sum_c T_c} W_{cc'} \quad (7)$$

The first term $\sigma_p \delta_{cc'}$ is related with (shape elastic scattering) direct reaction, $\pi \bar{\lambda}_c^2 g_J \frac{T_c T_{c'}}{\sum_c T_c}$ originates in the compound nucleus component, and $W_{cc'}$ is a term corresponding to fluctuations and interferences between channels.

For each reaction channel, transmissions are calculated starting from nuclear models. For instance, for the neutron channel, we get: $T_c(E) = 1 - |U_{cc}|^2$ (or $T_c(E) = 1 - |\overline{U_{cc}}|^2$ for the unresolved resonance range).

Concerning fission, these coefficients can be calculated using the concept of fission barrier penetrability (see paragraph 1.3.5), with a more or less fine approach: a rough Hill-Wheeler type formalism, or a more elaborate formalism (**WKB*** or Cramer-Nix approximation).

Modeling fission cross sections

The current research effort is focused on using in evaluations [10] the Lynn theory relating to the average R matrix, which allows mean cross sections of actinides to be calculated more accurately in the unresolved resonance range (average parameters more adapted, and more representative of the fission channel). On the other hand, in CONRAD and TALYS, the trend is increased use of microscopic data (collective levels, individual level orbitals, continuum level density) associated with an either phenomenological or more fundamental modeling of fission barriers as a function of the application. The fundamental approach is based on equipotential, possibly multidimensional surface calculations.

The calculation of a double-humped barrier (see Fig. 7) using a Cramer-Nix type formalism [11] evidences the occurrence of nucleus states in the second potential well, which appear as (experimentally visible) resonances in the fission probability. This probability, usually near zero for fertile nuclei having excitation energy lower than the fission threshold, is then locally amplified (in energy). Fission channel transmissions can so be calculated with higher accuracy through these approaches.

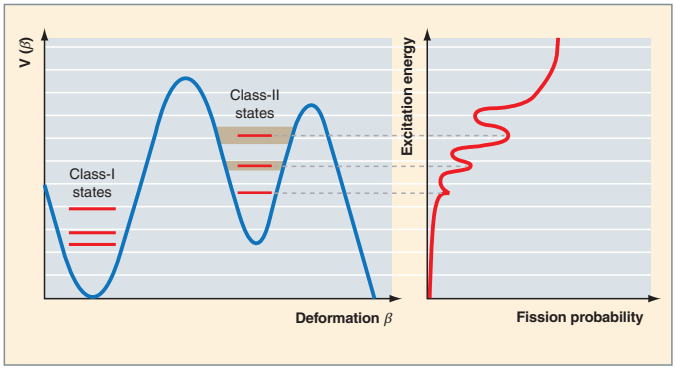

Fig. 7. Double-humped fission barrier as a function of fissioning nucleus deformation (left), and related fission probability (right).

Nuclear data uncertainties

The major part of the uncertainty on neutronics calculation results originates in the uncertainty on basic nuclear data. Consequently, validating margins taken on the design parameters of future reactors, or ensuring uncertainty propagation on the neutronics parameters of current reactors, requires an "a priori" control of uncertainties on nuclear data. In order to include variance/covariance matrices explicating correlations between diverse nuclear data in coming evaluations, a significant work is pending, that consists in re-analyzing microscopic measurements, and developing mathematical methods to evaluate all uncertainty components, whether arising from experiments or from models. Concrete results of this work are expected for future nuclear databases.

CONRAD: a tool for analyzing uncertainties

Within CONRAD, model parameters assessment is based on the concept of Bayes inference. Assuming that the aim is finding the probability to get the parameters $\vec{x}$, that U is the preliminary knowledge about these parameters, and that $\vec{y}$ is a new set of measurements, the Bayes theorem generalized for continuous variables gives the relationship between the following $[p(.)]$ probability densities:

$$p\left(\vec{x}|\vec{y},U\right) = \frac{p\left(\vec{x}|U\right) p(\vec{y}|\vec{x},U)}{\int d\vec{x'}\, p\left(\vec{x'}|U\right) p(\vec{y}|\vec{x'},U)} \quad (8)$$

The probability density $p\,(\vec{x}|U)$ is named *a priori*. The quantity $p\,(\vec{y}|\vec{x},\,U)$ stands for the likelihood function, which indicates the likelihood of measurements knowing U if the parameters $\vec{x}$ are unknown. The quantity $p\,(\vec{x}|\vec{y},U)$ is the *a posteriori* probability density of $\vec{x}$. So this relationship (8) can be understood as the update of an *a priori* knowledge by a likelihood function relating to new measurements.

$$posterior\left[p\left(\vec{x}|\vec{y},U\right)\right] \propto prior\left[p\left(\vec{x}|U\right)\right] likelihood\left[p(\vec{y}|\vec{x},U)\right] \quad (9)$$

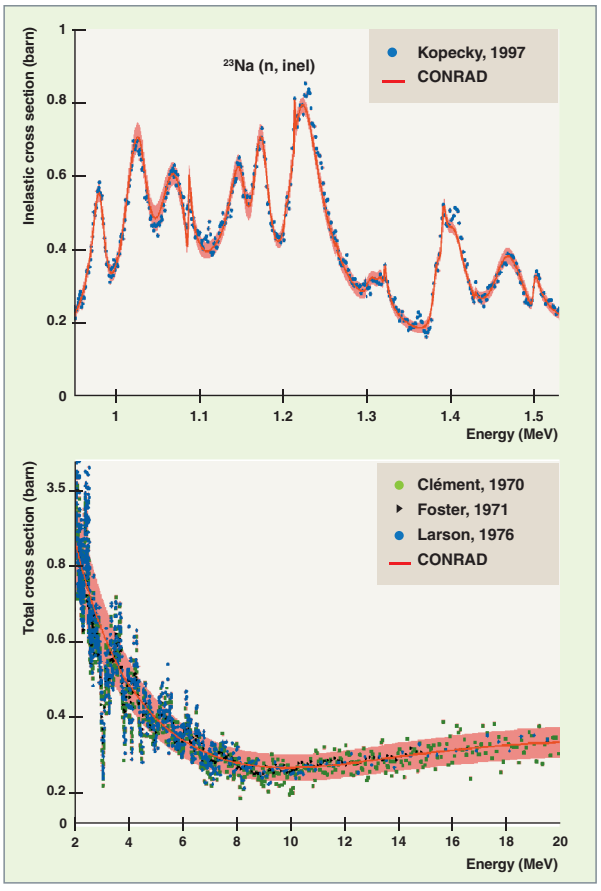

Fig. 8. Analysis of the inelastic and total cross sections of sodium [14].

The objective of nuclear model parameter assessment is getting their *a posteriori* distribution (average values, or values of the covariance matrix in the case of an analytic resolution).

In the evaluation of these data, measurements also bring their set of own parameters (normalization, resolution, etc.). The latter are useful to simulate the experiment, thereby allowing adjustment. Parameters of this type are named "nuisance parameters". The influence of uncertainties relating to nuisance parameters on the covariance matrix of model parameters (resulting from the adjustment) is significant. This is why original mathematical methods of marginalization [12][13] were developed in CONRAD.

Figure 8 shows an example of marginalization of an experimental normalization achieved during an analysis of sodium [14]. The uncertainties obtained for this analysis without using marginalization methods would have been fully unrealistic, that is lower than the %.

Post-fission observables

Prompt fission neutron spectrum and multiplicity

The characteristics of the prompt fission neutrons emitted during fission fragment decay are among the basic data used in neutronics calculations. So these characteristics are recorded in international nuclear data libraries. Significant efforts are still being deployed, both experimentally and theoretically, to improve our knowledge of the spectrum of prompt neutron emission. The photograph on Figure 9 (top) shows a very simple device recently used within the framework of a CEA/IRMM cooperation [15].

This device consists of an ionization chamber (dedicated to the detection of the two fission fragments), as well as a NE213-type scintillator dedicated to fission neutron detection. A thin target of Cf 252 (*i.e.* a few nanograms per cm^2) was deposited at the center of the chamber. Coincidence measurement of the two fragments resulting from the spontaneous fission of californium and of a prompt fission neutron enabled correlations to be determined between the properties of the

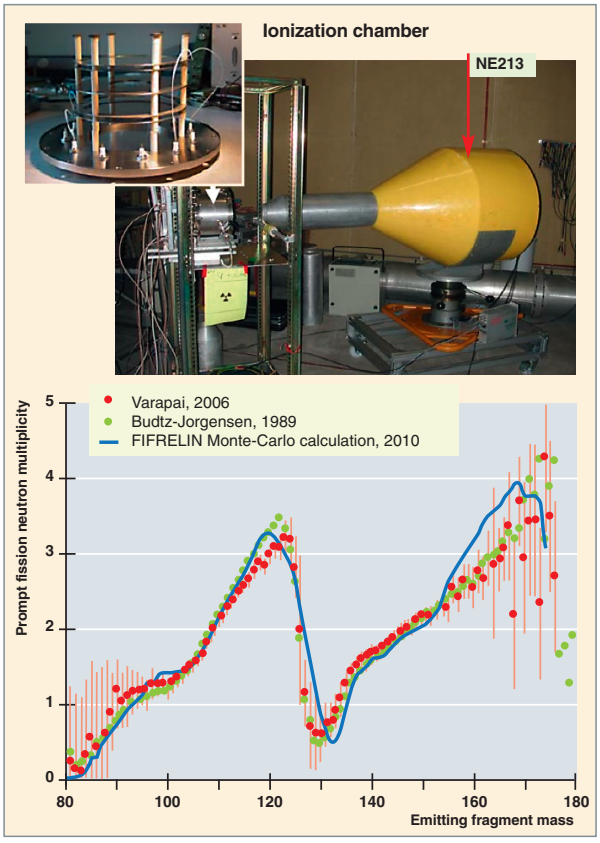

Fig. 9. Experimental device for measuring prompt neutrons in coincidence with fission fragments [15]. The bottom figure shows the measured multiplicity [15, 16] of neutrons versus the emitting fragment's mass (the so-called "sawtooth" curve), which FIFRELIN simulation of fission product decay (blue curve [17]) reproduces.

emitting fragment (mass, kinetic energy…) and the neutron's characteristics (multiplicity, spectrum…).

In addition, the CEA also initiated a Monte-Carlo type approach [17] which allows fragment decay through neutron and *gamma* ray emission to be followed in detail, particularly over the whole of mass and kinetic energy distribution. This approach makes it possible to go beyond the Madland-Nix [18] model (the basis of most of evaluations recorded in data libraries), the latter only providing an overview of the fragment decay process without explicitly taking account of the whole decay chain. The first results of the Monte-Carlo code FIFRELIN developed at CEA are very stimulating, as shown on Figure 9 (bottom), where the average number of prompt neutrons (multiplicity) emitted as a function of the emitting fragment mass was calculated, and compared with experimental data. In addition, simulating the whole decay cascade of the fragments emitted during the fission process gives access to other observables of interest for applications: prompt *gamma* radiation spectra, their average multiplicity [19], as well as the distribution of the number of emitted quanta, the fission yields, or the prompt component of released energies.

Fission yields

Knowing the **primary** and **cumulated fission yields*** of some fission products emitted during neutron-induced fission reactions is of prime interest to reactor physics (residual power calculations, summation method calculation of delayed neutron production, fission rate normalization in a reactor through measuring the *gamma* emission of a fission product…). In nuclear data libraries (JEFF, ENDF/B-VII or JENDL), these yields exhibit significant differences, together with, in some cases, often too high uncertainties in view of current requirements, and of advances in relation to other nuclear data (cross sections). In such a background, new measuring surveys have been initiated at the mass spectrometer "Lohengrin" of the Laue Langevin Institute (ILL) at Grenoble, as the result of a broad cooperation between the ILL, the Laboratory for Subatomic Physics and Cosmology (LPSC), and the CEA [20, 21].

The mass spectrometer "Lohengrin" (schematically represented on the left part of Figure 10) is an instrument particularly well adapted to investigating fission products yields, especially thanks to its excellent mass resolution. Under the combined action of a magnetic field and an electrostatic field, this instrument enables fission products to be selected as a function of their mass and their kinetic energy. The nuclear charge of the selected fission product can be known using an ionization chamber added at the end of the spectrometer. So it is possible to investigate the isotopic and isobaric yields, as well as the kinetic energy distributions of the fission products emitted during a fission reaction induced by thermal neutrons. An example of mass distribution of fission products arising from the U 235 (n_{th},f) reaction is displayed on Figure 10 (right).

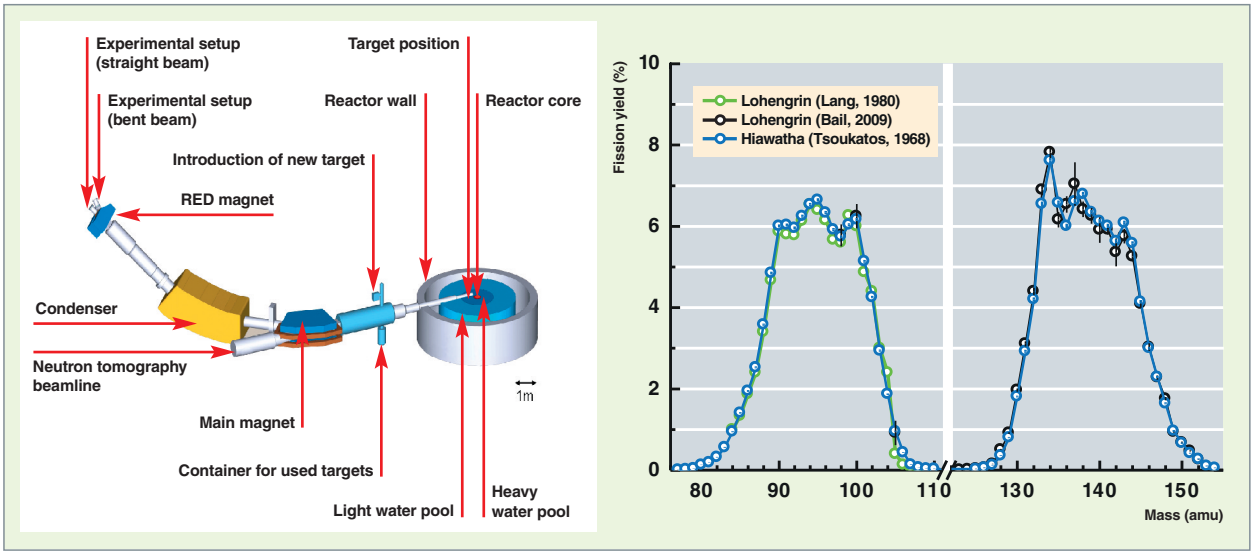

Fig. 10. Schematic view of the "Lohengrin" mass spectrometer located at the Laue Langevin Institute, Grenoble (left). Mass distribution of the fission products released during reaction U 235 (n_{th},f) (right).

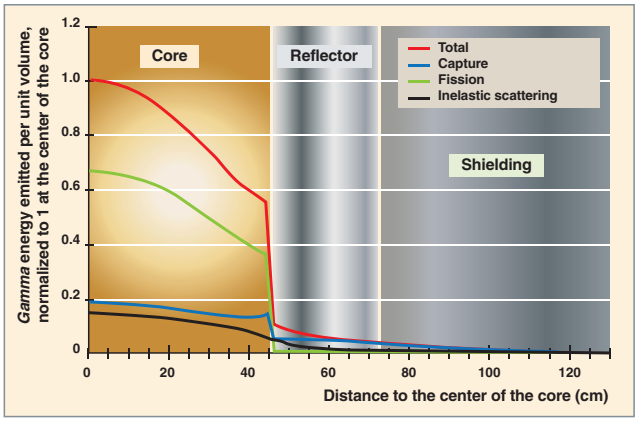

Fig. 11. Source of photon heating in a nuclear reactor.

Improving evaluation of nuclear heating

Materials heating in reactors (B_4C, Hf… control rods, fuels, heavy baffle, experimental devices) is one of the parameters used in the design of the EPR, the materials irradiation reactor Jules Horowitz (**JHR***), and the Generation IV reactor concepts. The term "nuclear heating", in its broader meaning, refers to the energy deposition of charged particles following the nuclear processes. Various deposition types can thus be distinguished: local energy deposition due to neutron reactions (fission fragments, α from (n, α) reactions, recoil nuclei...), photon energy deposition, and energy deposition of radioactive disintegrations (α, β). Three integral quantities are to be considered: **dose*** and **dose rate*** for heating, **dpa*** and gas generation through (n, p) and (n, α) reactions, fissions and α and β radioactive decays of actinides for assessing radiation damage in reactor materials.

Figure 11 shows the various primary generation sources of photon heating in reactor components (core, reflector). Fission *gammas* are responsible for over 60% of in-core photon heating (20% for captures, and a little less for inelastic scatterings). Evaluation of *gamma* production nuclear data is a preliminary step to any interpretation of integral experiments, and is to be chiefly based on nuclear structure data and models, and level electromagnetic decay data and models (whether energy levels are discrete or in the continuum).

Conclusion

Nuclear data for reactor physics are dedicated to the fine characterization (qualified data and reduced uncertainties) of the physical quantities in power nuclear systems (GEN. II, III and IV reactors and fuel cycle), research reactors (JHR, ÉOLE, MINERVE, MASURCA, CABRI…), and naval propulsion reactors. That requires pursuing an activity of both integral and differential measurement, evaluation (for the JEFF database), modeling, and validation. The collaboration between the CEA's divisions has proved to be a key factor to allow skill sharing. The future nuclear library JEFF-4 will mean challenges dealing with nuclear reaction models, which will include more and more microscopic components, evaluation of post-fission observables data, nuclear-heating data, and uncertainty evaluation.

References

[1] A.J. Koning *et al.* « *Status of the JEFF Nuclear Data Library* », Proceedings of the International Conference on Nuclear Data for Science and Technology, Nice, France, 2007.

[2] http://www.irmm.jrc.be/about_IRMM/laboratories/Pages/gelina_neutron_time_of_flight_facility.aspx

[3] G. Noguère, E. Rich, C. de Saint-Jean, O. Litaize, P. Siegler and V. Avrigeanu, "Average neutron parameters for hafnium", *Nucl. Phys.* A831, pp.106-136, 2009.

[4] G. Fioni *et al.*, « *The Mini-Inca project: Experimental study of the transmutation of actinides in high intensity neutron fluxes* », Proceedings of the International Conference on Nuclear Data for Science and Technology, Tsukuba, Japan, 2001.

[5] O. Bringer, *Mesure des sections efficaces de capture et potentiels d'incinération des actinides mineurs dans les haut-flux de neutrons. Impact sur la transmutations des déchets*, thèse INP Grenoble, 2007.

[6] C. de Saint-Jean *et al.*, "Uncertainly Evaluation of Nuclear Reaction Model Parameters using Integral and Microscopic Measurements with the Conrad Code", *Proceedings of International Conference on Nuclear Data for Science and Technology (ND-2010)*, Jeju Island (Korea), April 2010.

[7] J. Raynal, *code ECIS95*, Note CEA-N-2772, 1994.

[8] A.J. Koning, S. Hilaire, M.C. Duijvestijn, "TALYS : Comprehensive nuclear reaction modeling", *Procceedings of the International Conference on Nuclear Data for Science and Technology*, Santa Fe, New Mexico, USA, 2004.

[9] A.M. Lane et R.G. Thomas, R-Matrix Theory of Nuclear Reactions, *Rev. Mod. Phys.*, 30,2, pp. 257-353, 1958.

[10] O. Bouland *et al.*, "Recent Advances in Modeling Fission Cross Section over Intermediate Structures", *Compound Nucleus Reactions,* 2009, Workshop (Bordeaux), *European Physical Journal*, 08001, p. 6, V2, 2010.

[11] J.D. Cramer et J.R. Nix, "Exact Calculation of the Penetrability Through Two-Peaked Fission Barriers", *Phys. Rev.* C 2, pp. 1048-1057, 1970.

The JEFF project for building an international reference nuclear database

The basic nuclear data (cross sections, spectra of emitted particles…) initially used in **Nuclear Reactor Physics** arise from various compilations, among which the English compilation **UKNDL** (United Kingdom Nuclear Data Library) [1]. The U.S. **ENDF/B-IV** evaluation, issued in 1975 by the **Nuclear Data Center** of the **Brookaven National Laboratory**, has also been widely used until the mid-eighties [2]. It includes cross sections for 90 nuclides from hydrogen to curium-244.

In 1981, the "**Joint Evaluated File Project" (JEF)** was initiated, under the aegis of the **OECD's Nuclear Energy Agency (NEA)**, issued from the combined efforts of Europe and Japan to set up a reference nuclear database in the field of nuclear fission applications. The target areas were core physics, radiation protection, fuel cycle, and nuclear reactor dismantling.

The first "**Joint Evaluated File**", "**JEF-1**", was produced in 1985. It stored basic nuclear data for 300 nuclides. It was issued from a co-operation between Austria, France, the Federal Republic of Germany, Italy, Japan, the Netherlands, the United Kingdom, Sweden, and Switzerland. The JEF-1 data were put in the ENDF-5 US format. The JEF-1 beneficiaries were the NEA Data Bank Members [3] exclusively.

The **CEA**, especially under the initial impulse of **Massimo Salvatores**, actively worked on the successive evaluations: **JEF-1**, **JEF-2** [4], **JEFF-3** [5]. Evaluation **JEFF-3** – **Joint Evaluated Fission and Fusion File** – results from gathering evaluations **JEF** and **EFF** – **European Fusion File** – into only one "file", the latter's setting-up being conducted by **Harm Gruppelaar**, from the **Energy Research Center of the Netherlands (ECN)**, Petten (Netherlands) from 1985. More recently, the **European Activation File (EAF)**, that contains cross section values for over 15,000 neutron-induced activation reactions,and whose building was initiated by **EURATOM/UKAEA**, has also been integrated in JEFF-3. This evaluation complies with the US ENDF-6 format.

The CEA contributions, its strong relationship with nuclear power applications, and its physics test capacities stand as one of the JEFF project assets. In the future, the main goals of the project will be to preserve or improve the database performance for current and planned reactors (EPR, **JHR***), as well as for fast reactor applications, especially **ASTRID***, to propose realistic covariance matrices encompassing the above mentioned applications, and to make significant advances in the physical knowledge of the main nuclei (Actinides, Fission Products), hence files of ever increasing quality. Recently, as an initiative of the Lawrence Livermore National Laboratory, an international study has been undertaken to define a new updated, worldwide shared format of basic nuclear data [6].

Bibliography

[1] K. Parker, "The Aldermaston Nuclear Data Library", AWRE Report No. O-70/63 (September 1963); J. S. Story, R. W. Smith, "The 1981 Edition of the United Kingdom Nuclear Data Library: A Status Summary", September 1981.

[2] ENDF/B-IV General purpose file (Ed.) D. Garber: "ENDF/B Summary Documentation", BNL-17541, 2nd Edition, 1975.

[3] JEF Report 1, *Index of the JEF-1 Nuclear Data Library, Volume I, General Purpose File*, OECD NEA Data Bank, July 1985 ; http://www.oecd-nea.org/dbdata/nds_jefreports/

[4] JEFF Report 17, *The JEF-2.2 Nuclear Data Library*; OECD NEA Data Bank (April 2000).

[5] JEFF Report 22, *The JEFF-3.1.1 Nuclear Data Library*; OECD NEA Data Bank (May 2009).

[6] Working Party on International Nuclear Data Evaluation Co-operation (WPEC) Subgroup 38, *Beyond the ENDF format: A modern nuclear database structure:* http://www.oecd-nea.org/science/wpec/sg38/

[12] C. de Saint-Jean *et al.*, "A Monte-Carlo Approach to Nuclear Model Parameter Uncertainties Propagation", *Nucl. Sci. Eng.* 161, 363, 2009.

[13] B. Habert *et al.*, "Retroactive Generation of Covariance Matrix of Nuclear Model Parameters Using Marginalization Techniques", *Nucl. Sci. Eng.* 166, p. 276, 2010.

[14] P. Archier *et al.*, "Modeling and Evaluation of Na 23 Cross Sections" *GEDEPEON Workshop on Nuclear Data Evaluation*, OECD/NEA databank, 2010.

[15] N. Varapai, *Développement d'un dispositif expérimental basé sur la digitalisation des signaux et dédié à la caractérisation des fragments de fission et des neutrons prompts émis*, Thèse Université de Bordeaux I, 2006.

[16] C. Budtz-Jorgensen *et al.*, "Simultaneous Investigation of Fission Fragments and Neutrons in Cf 252 (sf)", *Nucl. Phys.* A 490, 307, 1988.

[17] O. Litaize and O. Serot, "Investigation of phenomenological models for the Monte-Carlo simulation of the prompt fission neutron and *gamma* emission", *Phys. Rev. C 82*, 054616, 2010.

[18] D.G. Madland et R.J. Nix, "New calculation of prompt fission neutron spectra and average prompt neutron multiplicities", *Nucl. Sci. Eng. 81*, p. 213, 1982.

[19] D. Régnier, O. Litaize, O. Sérot, *Preliminary Results of a Full Hauser-Feshbach Simulation of the Prompt Neutron and Gamma Emission from Fission Fragments*, Scientific Workshop on Nuclear Fission Dynamics and the Emission of Prompt Neutrons and *Gamma* Rays, Biarritz, France, 28-30 November 2012.

[20] A. Bail, *Mesures de rendements isobariques et isotopiques des produits de fission lourds sur le spectromètre de masse Lohengrin*, Thèse Université de Bordeaux I, 2009.

[21] A. Bail, O. Serot, L. Mathieu, O. Litaize, T. Materna, U. Koster, H. Faust, A. Letourneau, S. Panebianco, "Isotopic yield measurement in the heavy mass region for Pu 239 thermal neutron induced fission" *Phys. Rev. C 84*, 034605, 2011.

Cyrille de Saint-Jean, Olivier Sérot, Pascal Archier, David Bernard, Olivier Bouland, Olivier Litaize and Gilles Noguère
Reactor Study Department

Nuclear Data Processing

The outcome of the previously described measuring and analysis work is to generate evaluated nuclear data files, more simply called "**evaluations***". These files contain, in a form as compact as possible, information likely to help reconstruct all nuclear data required for the modeling of a nuclear system. These evaluations generally share a same U.S. computer format, which was internationally adopted: this is the ENDF-n format, in which n is a digit specifying the format version. The current evaluations are produced in the format ENDF-6 (Evaluated Nuclear Data Format, version 6) [1].

Data available in evaluations

Data available in evaluations deal with the following items:

- Neutron-induced nuclear reactions;
- photon-induced nuclear reactions;
- photon-induced electromagnetic interactions, the so-called "photo-atomic reactions";
- decay data;
- fission products yields for a spontaneous or neutron-induced fission;
- data relating to transport of charged particles (protons, deuterons, tritium, helium-3);
- related uncertainties.

Neutron-induced nuclear reactions

Most of the data describing neutron-induced nuclear reactions are recorded in sublibraries of international evaluated nuclear data files. These data are described in Table 8. They are provided for about 400 nuclides in an energy range between 10^{-5} eV and at least 20 MeV. The latest evaluations are the following: ENDF/B-VII [2], JEFF-3.1.1 [3], JENDL-4.0 [4], CENDL-3.1 [5], ROSFOND [6].

Description of neutron capture-induced fission products requires further data *i.e.* **fission yields***, for each fissile nucleus. These yields can be found in the so-called "Fission Yields" (FY) files of the evaluated nuclear data files mentioned above.

Figure 12 (next page) displays a comparison between mass number yields of fission products for a fission induced by a thermal neutron on an uranium 235 or plutonium 239 nucleus.

In order to process the chemical bonds of some nuclei bound in a molecular structure (hydrogen in water, hydrogen in zirconium hydride, zirconium in zirconium hydride…) in the thermal field, thermalization data can be provided in specific files. All these data are chiefly used to calculate **particle** (**neutron**, **photon**…) **propagation**, and **secondary particle sources**.

Table 8.

Nature of the information stored in the sublibrary "Neutron-induced nuclear reactions"

"File" number (MF)	Nature of stored information
1	General information.
2	**Resonance*** parameter data.
3	Reaction **cross sections***.
4	Angular distributions for emitted particles.
5	Energy distributions for emitted particles.
6	Energy/angle distributions for emitted particles.
7	Thermal neutron scattering law data.
8	Radioactivity and fission-product yield data.
12	Multiplicities for photon production.
14	Angular distributions for photon production.
15	Energy distributions for photon production.

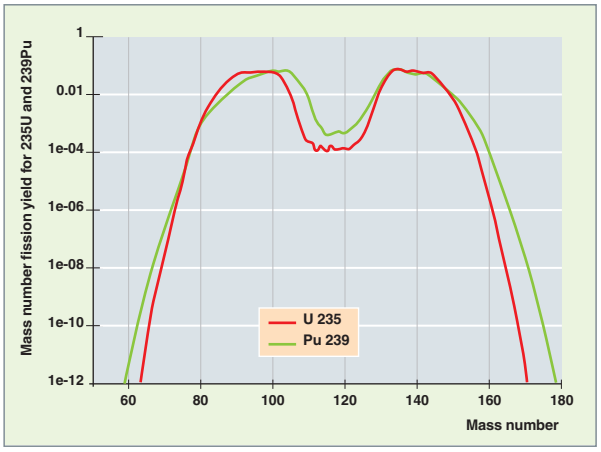

Fig. 12. Mass number fission yield for U 235 and Pu 239.

Remark

There exist special evaluations, which only contain cross sections dedicated to specific fields of application.

- **Structure activation under neutron flux.** Let us quote the EAF 2010 evaluation [7], which, for 816 target nuclei, mentions the cross sections of almost 66,000 activation reactions (partial cross sections) for an energy range between 10^{-5} eV and 60 MeV.

- **Dosimetry.** In the IRDF-2002 evaluation (IRDF: International Reactor Dosimetry File) [8] are grouped specific activation cross sections used, for instance, to evaluate the neutron fluence received by structures under irradiation.

Photon-induced nuclear reactions

Photons can interact with the atom (photo-atomic interactions [9]), or with the nucleus (photo-nuclear interactions [10]). In the energy range going up to 20 MeV, only photo-atomic interactions are taken into account to solve the **transport*** equation (photo-electric effect, coherent and incoherent scatterings, and creation of e^+, e^- pairs). But photo-nuclear interactions are the origin of secondary neutron sources which have to be evaluated.

These data are mainly used to calculate photon propagation and secondary neutron sources.

Radioactive decay data

Matter may contain natural radionuclides or become radioactive because of nuclear reactions.

The data relating to radioactive nuclei are the following:

- Cross sections of radioactive nuclei, distinguishing the fundamental state and isomeric states;
- decay modes (β^-, β^+, E.C., I.T., α, …);
- radioactive half-lives;
- branching ratios between several possible decay channels;
- spontaneous fission yields;
- neutron multiplicities of spontaneous fission;
- the average energies involved in radioactive transitions;
- the intensities and energy spectra of emitted particles.

These quantities can be found in various sublibraries. It is worth mentioning the setting-up in Europe of the NUBASE database [11], "*A Database of Nuclear and Decay Properties*" which includes structure data (spin, mass, parity…) for over 3,000 nuclei. Another reference book is "*Atomic Mass Evaluation*" [12].

These data are essential to calculate fuel's **isotopic depletion over time**.

Charged-particle transport data

Charged particles appear following nuclear or photo-atomic interaction processes. These particles are, for example, *alphas* and *betas* in relation to radioactive processes, recoil electrons of the Compton or photoelectric effect, or the (electron-positron) pairs arising from *gamma* rays that materialize. These phenomena induce what is called an "**electromagnetic cascade shower**", *i.e.* a kind of tree propagation of electrons, positrons, and *gamma* particles.

Main data are the following:

- Cross sections of nuclear reactions induced by charged particles;
- bremsstrahlung cross sections;
- cross sections of electron/positron scattering in matter;
- stopping powers of electrons/positrons and ions in matter.

These data are available either as tabulated values (EEDL evaluations [13] for electron-induced cross sections), or are determined by computer programs able to calculate them (ESTAR, PSTAR, ASTAR [14] for stopping powers and paths of electrons, positrons, and *alphas*).

Nuclear data uncertainties

The aim is to attribute an uncertainty to the calculated value of a physical quantity, in as much as it is possible. This uncertainty results from uncertainties of various natures: uncertainties on basic physical data, uncertainties due to the calculation method, uncertainties on technological data, etc. Knowing these uncertainties is crucial for safety, especially to optimize design basis. They also have an economical impact. In most neutronics calculations, basic nuclear data uncertainties are predominant, hence the interest of knowing them well, and getting methods likely to help evaluate their effect on the uncertainty associated with the physical quantity of interest.

These calculations of uncertainties are the purpose of making "sublibraries" 30 to 40 of ENDF-format evaluations. These files contain covariance data (*i.e.* relating to uncertainties with correlations, if any) corresponding to the nuclear data described in "files" 1 to 10 of Table 8 (see *supra*, p. 31).

Nuclear data processing

In order to be usable in codes devoted to nuclear systems modeling (transport and depletion codes), nuclear data available in evaluations generally have to undergo a **physical**, **numerical**, and **computer processing**. The latter depends on the nature of information stored in evaluations, the nature of the physical problem investigated, and the computational methods implemented in the codes used. The final product of the processing is a **physical data library** (or **application library**) which can be used by a given modeling code.

Nuclear data representation

Generally speaking, nuclear data characterizing the interaction of a neutron or photon with a nuclide or an element depend on the incident particle's energy E, and on the target's temperature T. In application libraries, energy dependence can be displayed in a continuous (pointwise) or discrete (multigroup) mode, whereas temperature dependence is generally displayed in a continuous mode.

Pointwise representation

The nuclear datum D is displayed by a set of value couples $(x_i, D(x_i))$, where x_i characterizes the parameter which the datum D is dependent on, and $D(x_i)$ is the value of the datum for this parameter. An interpolation law is associated with this description, so that the datum can be recalculated for any value of the x parameter (incident energy or temperature).

Multigroup representation

This representation is associated with the (incident particle's) energy-dependence of a datum D. The energy range is subdivided into intervals called **groups***, the energy bounds of these intervals constituting a **multigroup meshing***. On each of these groups g, the pointwise nuclear datum D is described by an average value D^g called "multigroup value".

In the case of cross sections, another representation is also currently used: the multigroup probability table representation.

Multigroup probability table representation

This representation [15] also requires the definition of a multigroup meshing. On each group, the pointwise cross section is displayed by a given number of couples (p_i, σ_i), where σ_i describes the characteristic values (or steps) likely to be attained by the cross section in this group, and p_i the probability of attaining the value σ_i.

Figure 13 displays the three representations of the cross section for uranium 238.

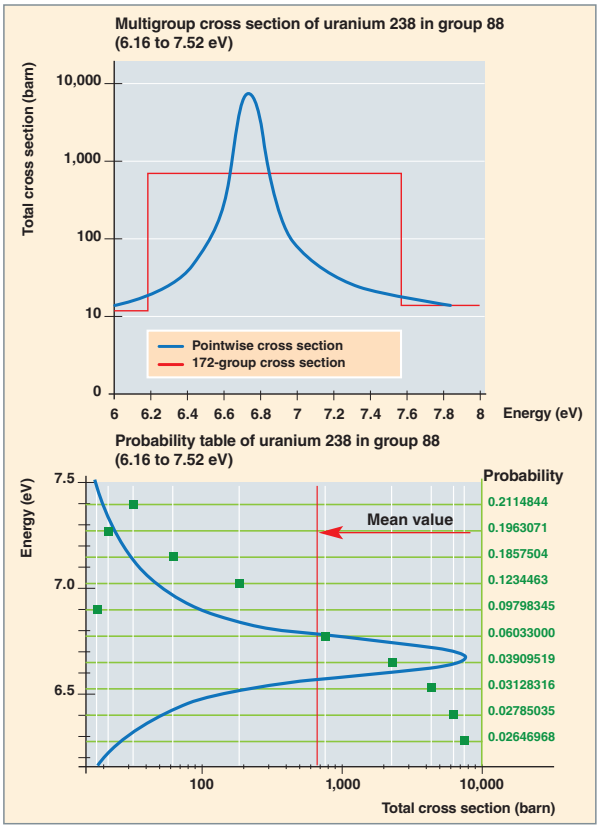

Fig. 13. Various representations of a cross section: pointwise and multigroup representations (top), pointwise representation and representation by probability table (bottom).

Main steps of nuclear data processing

Two main steps can be distinguished in data processing: the generation of pointwise data at a given temperature, and the generation of multigroup data. Concerning cross sections, an additional step required will be the generation of probability tables.

In the following pages are detailed the processing steps for two types of data, cross sections and angular and energy distributions of secondary neutrons.

Cross section processing

Pointwise cross sections

Whatever the final representation of cross sections in a modeling code, the first processing step is always the reconstruction of pointwise nuclear cross sections as a function of the incident neutron's energy E in the laboratory system for a target nucleus at rest, *i.e.* for T = 0 Kelvin. This reconstruction is carried out using various nuclear formalisms. The most used are the single- or multi-level Breit and Wigner formalism, and the Reich-Moore formalism, approximations derived from the general formalism of the "R matrix" [16]. The data of these formalisms are the resonance parameters stored in evaluations. The energy grid on which the cross section is reconstructed, is coupled with a linear interpolation which allows reconstructing at any energy E, in compliance with a given accuracy criterion (relative discrepancy between the interpolated value and the exact value).

The pointwise cross section, at the temperature of interest T Kelvin, is then calculated, taking account of the **Doppler effect*** through a convolution of the pointwise cross section at 0 Kelvin with the velocity distribution of the target nucleus.

This description, the most accurate indeed, is that used in neutron transport codes based on the "continuous-energy" Monte-Carlo method, to describe the **resolved resonance*** range of nuclides.

Figure 14 displays the Doppler effect on uranium 238 cross section, as a function of temperature.

Multigroup cross sections

The mean value on each group g of a cross section is obtained by weighting the pointwise cross section on the group g with a weighting flux Φ_w "representative" of the neutron spectrum of the nuclear system to be modelled, and only energy-dependent. For instance, in the case of a thermal neutron reactor, the weighting flux is a fission spectrum above 1 MeV, a slowing-down spectrum between 1 MeV and a few eV, and a thermal spectrum (Maxwellian) at lower values.

$$\sigma^g = \frac{\int_g \sigma(E)\Phi_w(E)dE}{\int_g \Phi_w(E)dE}$$

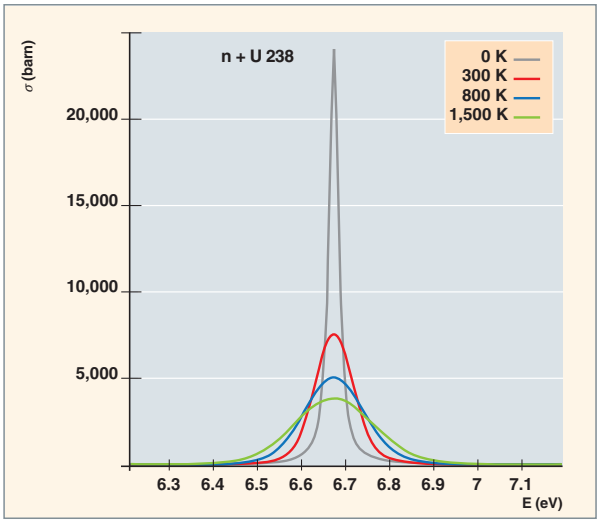

Fig. 14. Total pointwise cross section of uranium 238 at different temperatures.

This description is used by both the Monte-Carlo and the deterministic multigroup transport codes. This very simple technique of grouping may prove not sufficiently accurate for resonant nuclides when the energy mesh is rather broad. In this case, multigroup cross sections are recalculated in the transport code with a weighting function (the so-called "fine structure factor") which takes into account the resonances of all the nuclei present in the specific case to be dealt with. This problem will be considered again in the paragraph related to the self-shielding phenomenon, the modeling of which will require further data to be described then.

Probability tables

The steps (ladders) of probability tables (PTs) on a group g can be seen as the points of a quadrature formula on group g, in which the weights are proportional to the related probabilities. So there exist various ways to establish these tables according to the choice of the functions for which the quadrature formula is required to be accurate. When it is chosen to preserve the momenta of the total cross section function, the probability tables result in Gauss quadrature formulae, which assigns them very interesting mathematical properties.

This third representation can be used in "continuous-energy" Monte-Carlo codes to describe the **unresolved resonance*** range of nuclides, and in Monte-Carlo and deterministic multigroup codes to describe the whole energy range.

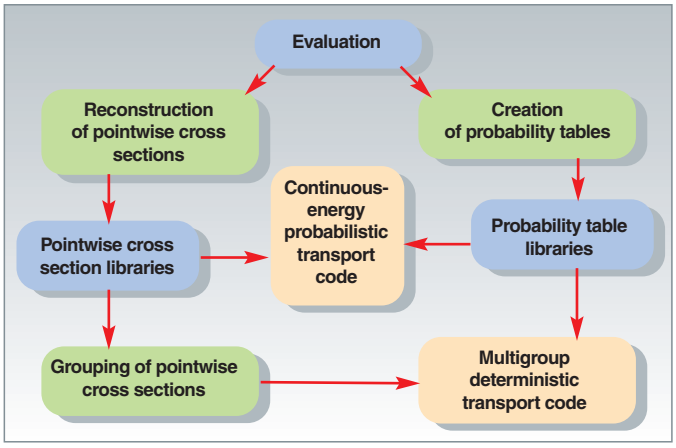

Fig. 15. Simplified scheme for building libraries for Monte-Carlo and deterministic transport codes.

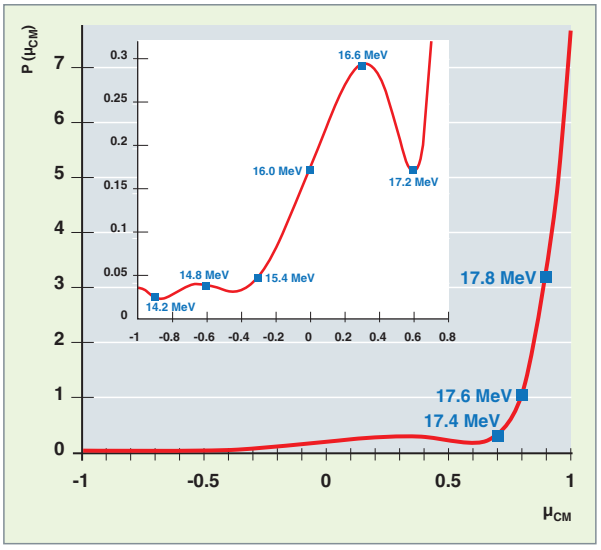

Fig. 16. Angular distribution of an elastic collision of an 18-MeV neutron on oxygen 16.

Figure 15 shows the simplified scheme for the building of cross section libraries for Monte-Carlo and deterministic transport codes.

Angular and energy distributions treatment of secondary neutrons

After an elastic or inelastic collision, corresponding to a discrete excitation level of the residual nuclide, between a neutron and a target nuclide, the energy distribution of secondary neutrons in the laboratory system can be deduced from their angular distribution in the center-of-mass system. These distributions are given in nuclear evaluations for several values of incident energy, and are associated with an interpolation law.

They are used as they are, or turned into equiprobable ranges of deviation cosine μ by the Monte-Carlo transport codes. Figure 16 describes the angle distribution of the neutron scattered by elastic collision on an oxygen-16 nucleus, for an energy of the incident neutron in the laboratory system of 18 MeV. The x-axis displays the cosine of the deviation angle in the center-of-mass system (CM). The energies mentioned are the corresponding energies of the emerging neutron in the laboratory system.

Concerning deterministic transport codes, the most usual representation is the Legendre polynomial expansion of matrices describing energy transfer from one group to another.

Decay data treatment

Decay data treatment results in establishing radioactive **decay*** chains. For example, Figure 17 on the next page displays the U 238 decay chain that leads to the stable lead isotope of mass number 206. The durations indicated on the left-hand side of nuclides, refer to their half-lives.

Nuclear data processing systems

Several code systems able to partially or fully achieve this neutron and *gamma* nuclear data processing are reported to exist in the world. Let us quote:

- The NJOY system [17] designed at the Los Alamos Center, distributed by the RSICC (Radiation Shielding Information and Computational Center) at Oak Ridge (USA) and by the OECD/NEA;
- the CALENDF code [18] developed at the CEA and distributed, too, by the OECD/NEA;
- the AMPX system [19], developed at the Oak Ridge Center and distributed by the RSICC (Radiation Shielding Information and Computational Center) at Oak Ridge (USA);
- the PREPRO system [20], maintained and distributed by the International Agency for Atomic Energy (IAEA) at Vienna (Austria).

The development of GALILÉE [21], the nuclear data processing system for transport, depletion, and radiation shielding codes, completes the efforts deployed at the CEA (with the development of the CONRAD system) to have a set of efficient tools aimed at evaluating and processing nuclear data and their uncertainties, which are the foundation of any neutronics modeling. The basis of the GALILÉE system is the new code TREND (Treatment and Representation of Evaluated Nuclear Data), the physical models of which are mainly issued from the CALENDF code.

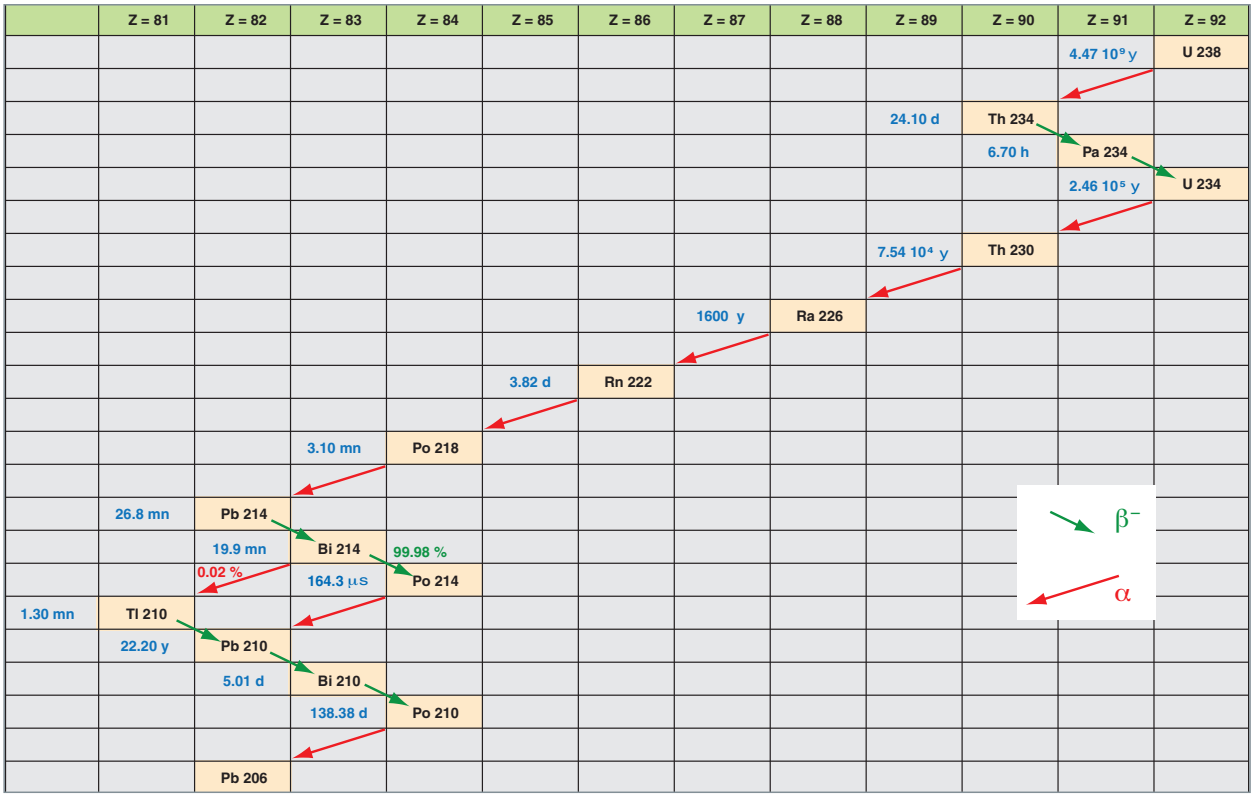

Fig. 17. Simplified scheme of uranium 238 decay chain.

The CONRAD and GALILÉE tools endow the CEA with a full, consistent device likely to both generate and process nuclear data, which turns it into a key player in the field.

References

[1] *ENDF-6 Formats Manual*, Edited by A. Trkov, M. Herman and D.A. Brown, BNL-90365-2009 Rev.2, 2011.

[2] M. B. Chadwick *et al.*, « ENDF/B-VII.0: Next Generation of Evaluated Nuclear Data Library for Nuclear Science and. Technology », Nuclear Data Sheets, 107, 2931-3060, 2006.

[3] A. Santamarina *et al.*, *The JEFF-3.1.1 Nuclear Data Library - Validation Results from JEF-2.2 to JEFF-3.1.1*, JEFF Report 22, OECD 2009 NEA No 6807, 2009.

[4] K. Shibata *et al.*, « JENDL-4.0: A New Library for Nuclear Science and Engineering », *J. Nucl. Sci. Technol.* 48(1), 1-30, 2011. http://www.jstage.jst.go.jp/article/jnst/48/1/48_1/_article/

[5] R. Xu *et al.*, « The Updated Version of Chinese Evaluated Nuclear Data Library (CENDL-3.1) », *International Conference on Nuclear Data for Science and Technology*, Jeju Island, Korea, April 26-30, 2010.

[6] http://www-nds.iaea.org/ndspub/download-endf/ROSFOND-2010/backup/

http://www.ippe.ru/podr/abbn/english/libr/rosfond.php

[7] J.C. Sublet *et al.*, *The European Activaion File : EAF-2010 neutron-induced cross section library*, EASY documentation Series CCFE-R (10) 05.

[8] http://www-nds.iaea.org/irdf2002/

[9] http://www-nds.iaea.org/indg_phat.html

[10] http://www-nds.iaea.or.at/photonuclear/

[11] G. Audi, O. Bersillon, J. Blachot, A.H. Wapstra, « The NUBASE evaluation of nuclear and decay properties », *Nuclear Physics A*, vol. 729, 2003, pp. 3-128.
http://csnwww.in2p3.fr/amdc/web/nubase_fr.html

[12] G. Audi, A.H. Wapstra et C. Thibault, « The AME2003 Atomic Mass Evaluation », *Nucl. Phys.* Vol. 729, Issue 1, pp. 129-676, 2003.

[13] http://www.oecd-nea.org/dbdata/data/manual-endf/nds_eval_eedl.pdf

[14] http://physics.nist.gov/PhysRefData/Star/Text/contents.html

[15] P. Ribon, J. M. Maillard, *Les Tables de probabilité. Application au traitement des sections efficaces pour la neutronique*, Note CEA-N-2485, CEA/Saclay, France, 1986.

[16] A.M. Lane and R.G. Thomas, « R-Matrix Theory of Nuclear Reactions », *Rev. Mod. Phys.*, 30, 2, pp. 257-353, 1958.

Cross section processing for nuclear reactor physics codes at the CEA

For the purposes of its early neutronics computer codes the CEA has developed cross section processing tools. Among them it is worth to mention the following codes [1]:

- **MICRAL** and **CELADON**, which produce multigroup cross sections from basic data compilations;
- **AUTOSECOL**, which gathers two previously written codes, **CARLRÉSONNE** and **SECOL**, dedicated to cross section processing in the resonance range;
- **SEFAC**, derived from **CARLRÉSONNE**, which computes self-shielding factors in the resonance range, and is used for fast neutron reactor calculation.
- **SEMUL** and **MODERATO**, in charge of working out matrices for thermalization or for functions used in thermalization models.

In the early eighties the **NJOY** [2] system for cross section processing, produced by **Robert E. MacFarlane** from Los Alamos National Laboratory (LANL) (USA), and distributed by the **Radiation Shielding Information Center** (RSIC, nowadays knows as RSICC: Radiation Safety Information Computational Center) of Oak Ridge (ORNL), was introduced at the CEA. Under the impulse of **Jean Gonnord**, the NJOY system was the basis on which the CEA developed and maintained the cross section processing system named **THÉMIS** [3] till the nineties, with the following two benefits: first, ensuring the consistency of cross sections (origin, processing: reconstructing, Doppler broadening, grouping…) between the deterministic and Monte-Carlo probabilistic transport calculation routes for both neutronics (Pressurized Water Reactors and Fast Neutron Reactors) and radiation shielding applications, and, secondly, providing new functionalities to consult, handle, convert the storage format, and display the processed nuclear data on screen.

In the same period was created **CALENDF** [4], the French code for nuclear evaluation processing. This code, developed at the CEA by **Pierre Ribon**, is mainly dedicated to producing cross section probability tables in the resolved and unresolved resonance ranges. The originality of this code lies in processing the unresolved range through reconstructing one or several samples of "pointwise pseudo-cross sections", and in the method for setting up probability tables by conservation of cross section momenta. That code is still under development, and has been distributed by **OECD/NEA** in France since 2002 [5]. The first transport codes using **CALENDF** were the deterministic code **ECCO** [6], due to its subgroup method, and the Monte-Carlo code **TRIPOLI-3** [7], in order to treat the resonance range.

Today, the NJOY system and the CALENDF code are still the tools used for producing the CEA transport and depletion code libraries.

However, due to computer environment evolution and increased requirements in mastering tools for basic nuclear data evaluation and processing, consistency, traceability, and flexibility of use of these tools, the CEA has to reorganize its system for processing nuclear data dedicated to nuclear reactor calculation: **GALILÉE** is the name of this new system based on the **TREND** code which is under development.

References

[1] P. Reuss, *Traité de Neutronique*, p. 648, Paris, Hermann, 1985.

[2] R. E. MacFarlane, D. W. Muir, R. M. Boicourt, *The NJOY Nuclear Data Processing System*, LA-9303-M / ENDF-324, LANL, May 1982.

[3] G. Dejonghe, J. Gonnord, A. Monnier, J. C. Nimal, "THEMIS-4: A Coherent Punctual and Multigroup Cross Section Library for Monte-Carlo and SN Codes from ENDF/B4", May 1983 ; Seminar on *NJOY-91 and THEMIS for the processing of Evaluated Nuclear Data Files*, OCDE/AEN, Saclay, April 7-8, 1992.

[4] P. Ribon, J. M. Maillard, *Les tables probabilité. Application au traitement des sections efficaces pour la neutronique*, Note CEA-N-2485, CEA/Saclay, France, 1986.

[5] J.C. Sublet, P. Ribon, M. Coste-Delclaux, CALENDF-2010: *User Manual*, Rapport CEA-R-6277, 2011.

[6] G. Rimpault *et al.*, "Algorithmic Features of the ECCO Cell Code for Treating Heterogeneous Fast Reactor Subassemblies", *International Topical Meeting on Reactor Physics and Computations*, Portland, Oregon, May 1-5, 1995.

[7] S. H. Zheng, T. Vergnaud, J.C. Nimal, "Neutron cross section probability tables in TRIPOLI-3 Monte-Carlo code", *Nuclear Science and Engineering*, 128, pp. 321-328, 1998.

[17] R.E. MacFarlane, D.W. Muir, D.C. George, *NJOY99.0 : Code System for Producing Pointwise and Multigroup Neutron and Photon Cross-Sections from ENDF/B Data*, PSR-480/NJOY99.0 – *RSICC Peripheral Shielding Routine Collection* – Contributed by Los Alamos National Laboratory - 2000.

[18] J.C. Sublet, P. Ribon, M. Coste-Delclaux, *CALENDF-2010: User Manual*, CEA-R-6277, 2011.

[19] M. E. Dunn and N. M. Greene, "AMPX-2000: A Cross-Section Processing System for Generating Nuclear Data for Criticality Safety Applications", *Trans. Am. Nucl. Soc.* 86, pp. 118 and 119, 2002.

[20] D. E. Cullen, "PREPRO2012: 2012 ENDF/B Pre-processing Codes", IAEA-NDS-39, Rev. 15, octobre 2012.

[21] M. Coste-Delclaux, « GALILÉE: A nuclear data processing system for transport, depletion and shielding codes », *International Conference on the Physics of Reactors "Nuclear Power: A Sustainable Resource"*, Casino-Kursaal Conference Center, Interlaken, Switzerland, September 14-19, 2008.

Mireille Coste-Delclaux, Cheikh M. Diop, Cédric Jouanne and Claude Mounier
Department for Systems and Structures Modeling

High-Energy Nuclear Data: Spallation

In a fission reactor or even in a fusion reactor, nuclear reactions mainly involve neutrons which display an energy extending up to twenty MeV or so at the utmost. This is why until recently, these nuclear reactions alone were taken into account in nuclear data libraries.

However, there exist other applications which involve nuclear reactions of higher-energy, or other types of particles. Such is the case, for example, of subcritical accelerator-driven systems (**ADS***), considered for nuclear waste transmutation, or as irradiation tools, and of spallation sources which provide neutrons for materials research needs. These systems use a beam of protons accelerated to an energy of about one GeV, which bombard a target made of a heavy element (tungsten, mercury, lead-bismuth). A process referred to as **spallation*** then takes place, during which a number of particles, chiefly neutrons, are ejected, thereby leaving a smaller nucleus than the initial nucleus. Some of the particles emitted exhibit an energy sufficiently high to induce a new reaction with the neighboring nucleus (Fig. 18). In a thick target, this cascade of reactions leads to the generation of a high number of neutrons, most of which will escape from the target. This allows the generation of intense fluxes of neutrons directly usable, after slowing down, as a spallation source, or to compensate for subcriticality in an ADS.

These systems also face specific problems due to high-energy reactions that take place, not only in the target, but also in the neighboring materials. In the target, each incident proton leads, either directly or during secondary reactions, to the generation through spallation of almost 25 neutrons and 3 residual nuclei on the average, most of the latter being radioactive. Short-lived nuclei raise a radiation protection issue in the case of an intervention or an accident: this is especially true of volatile elements in the case of a liquid target. As regards long-lived nuclei, they have to be taken into account in assessing long-term radiotoxicity. Finally, neutrons generated in spallation reactions exhibit an energy spectrum reaching to values far higher than those to be found in reactors, even in fusion. Although they are not numerous in proportion to the overall number of neutrons, high-energy neutrons are liable to raise shielding problems.

All these aspects have to be assessed accurately as early as the design step. For this purpose, simulation codes called "high-energy transport codes" are generally used, which describe the propagation, slowing-down, and interactions of all the incident and secondary particles in the whole of the system. For nuclear interaction treatment, the transport code uses reaction probabilities (**cross sections***) and the characteristics (nature, energy, angle) of all the particles and nuclei generated in these reactions. Two different energy ranges have to be distinguished: intermediate energies, between 20 and 200 MeV and higher energies beyond this range. At intermediate energies, as in the case of lower energies, codes use evaluated data libraries which contain tabulated data for cross sections, energy spectra and angle distributions of light particles, as well as residual nuclei generation rates, and this for the whole range of energies and nuclei considered. In fact, the database production is based on the use of codes containing a whole collection of nuclear reactions models, the parameters of which are adjusted to well selected experiments. Those code are then used to produce all the data related to the whole energy range and for all the reaction channels. In contrast, at

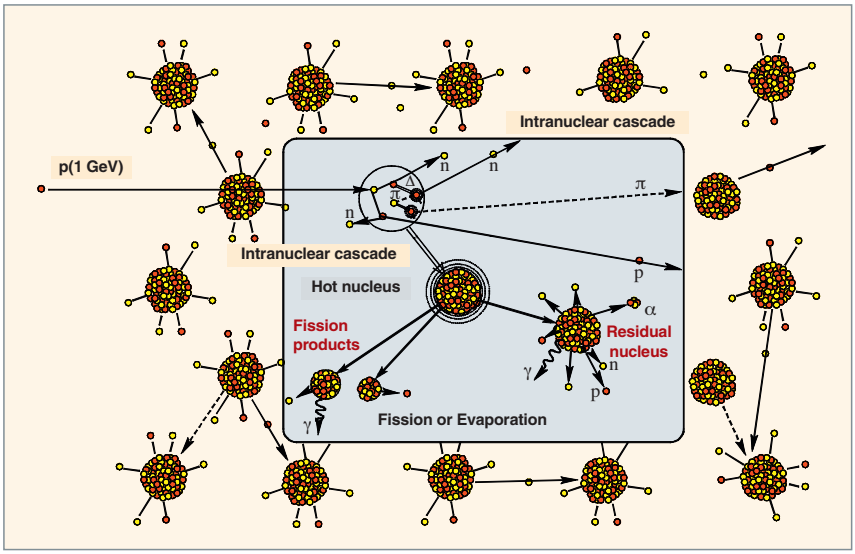

Fig. 18. Spallation mechanism in a thick target.

energies higher than 200 MeV, the number of possible reaction channels is much too high to allow the use of libraries: the cross sections and characteristics of the emitted particles are then calculated at each interaction by nuclear physics models directly integrated in the transport code. Improving the quality and reliability of simulation codes requires, in both cases, experimental measurements of quality likely to put constraints in the physics models describing reactions, theoretical developments likely to improve these models, and validations through integral measurements (*cf. supra*, p. 22 and *infra*, p. 166).

Spallation modeling

Spallation is generally described as a two-step process: the first one is a quick step (a few 10^{-22}s), which consists in successive collisions between the projectile and the nuclear constituents (nucleons), similarly to shocks between billiard balls. It is referred to as an "intranuclear cascade". These collisions lead to the ejection of a certain number of energetic particles (nucleons, **pions***). At the end of this process, the incident energy is distributed over all of the nuclear constituents (nucleons), the nucleus being left in an excited state. The second step, much slower, is de-excitation, which usually takes place with the emission of low-energy particles (neutrons above all, but also protons, *alphas*, or even much heavier fragments). In the case of heavy nuclei, fission into two smaller nuclei also competes with particle emission. At the end of de-excitation, *(gamma)* photons are also emitted.

Therefore modeling most often consists in coupling two models, a model of intranuclear cascade and a de-excitation model. In the first one, the main ingredients are the well-known nucleon-nucleon interaction, the potential enclosing nucleons within the nucleus, and the semi-classical Pauli principle treatment. De-excitation is treated with a statistical model which assesses the probability of emission of a particle starting from the available states and the probability of reverse reaction (capture of the particle by the nucleus). In the case of fission are also involved fission barriers, and the way the two fragments separate. These ingredients can be phenomenological parametrizations, or can be obtained from more microscopic models.

The objective is to arrive to a couple of models, whose ingredients and parameters have been determined based on experimental data analysis and then validated with all of available data, in order to establish them once and for all.

Elementary measurements

This objective cannot be reached without a good understanding of the spallation reaction mechanisms. That requires basic experimental data of quality which cover the whole of the energy and mass range. At the energies of interest, contrary to what occurs at lower energies, when the structure effects play a more significant role, variations depending on the nucleus nature or the reaction energy are low. It is therefore possible to carry out a mere exploration of a few areas in the periodic table of elements, with relatively broad energy steps. At the opposite, if the aim is a good control of the various steps of the mechanism, it is necessary to get the data relating to the production rates, and the characteristics of all the reaction products (neutrons, charged particles, nuclei). In fact, the ideal would be to measure all these products simultaneously, event by event. A number of experiments were carried out within the framework of European programs allowing a coordination of results. The CEA's teams more especially took part in obtaining the data related to neutron production on the SATURNE accelerator (shut down today) and to residual nuclei measurements at the GSI accelerator (Germany) (Fig.19). Concerning the residual nuclei production, significant progress could be achieved thanks to the reverse kinematics technique, which enabled all of the isotopes generated in a reaction and their recoil velocity to be measured simultaneously. This method uses a heavy ion beam which bombards a proton target, i.e. liquid hydrogen. The advantage is that the nuclei so generated are strongly focused in the forward direction, due to the fact that the center of mass almost identifies with the projectile. This simplifies the reaction products identification thanks to a succession of magnets and detectors. Isotope distributions measured at the GSI particularly helped test the behavior of nuclear models as regards the competition between neutron and charged particle emission, and fission. A second generation of experiments has followed, still in reverse kinematics at the GSI, which consists in simultaneously measuring the various reaction products, *e.g.* residues and light particles: it has given access to nuclear characteristics prior to de-excitation, and has so helped put separate constraints on the cascade and de-excitation models.

More generally, the quality of experimental data has allowed better understanding of the reaction mechanism and the origin of the flaws in existing models. New models have been then developed in cooperation with theoreticians, especially the intranuclear cascade model of Liège, INCL4, and the de-excitation model ABLA, from the GSI group at Darmstadt. This INCL4-ABLA combination was introduced in high-energy transport codes currently used for ADS design, and is now available for the whole of the community. Recently, an intercomparison of the spallation models used in transport codes, organized by the IAEA, has shown that INCL4-ABLA is the model in best agreement with the whole of available data, especially as regards residual nuclei generation rates.

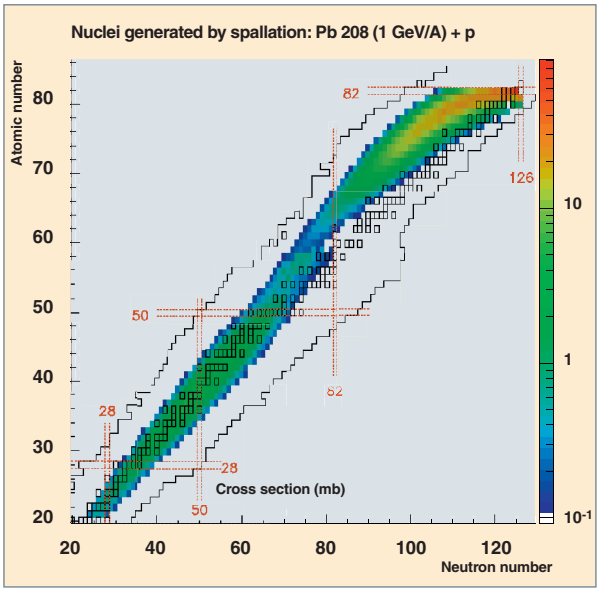

Fig. 19. Generation rate of numerous nuclides measured in a spallation experiment using a lead beam of 1 GeV per nucleon at the GSI, Darmstadt. The squares stand for stable nuclei.

Integral measurements

Once the physics models are integrated in the transport codes, it is required to test the latter on integral experiments in order to assess their degree of predictability of physical quantities useful for applications. Measurements are then made on targets, referred to as "thick targets", representative of a spallation target. For example, an experiment of measurement of volatile fission products on a thick lead-bismuth target, generated at the CERN, confirmed that the new models are able to reproduce much the observed generation rates. Similarly, the energy spectra of the neutrons escaping from a thick target are relatively well reproduced by models. This shows that the calculations of high-energy neutron losses, of high interest for shielding and radiation protection problems, can be considered as sufficiently reliable. The lead-bismuth spallation target MEGAPIE, which was successfully irradiated during 4 months by the intense proton beam of the SINQ source at the Paul Scherrer Institute at Zürich, was the first full-scale test of liquid-metal target such as those considered for ADS. After a period of decay, a number of specimens have been collected, and are under analysis, which will help bring an answer to questions related to the residual nuclei generated and consequently to material damage.

The whole of these studies, first initiated by accelerator-driven systems (ADS) and spallation sources, is expected to pave the way to reliable simulation codes likely to be used in numerous other fields: space, in relation to astronauts' radiation protection, and to damage to electronic components (as a matter of fact cosmic radiation mainly consists of light particles, the spectrum of which exhibits a maximum value around one GeV), medicine, in relation to hadron therapy treatments or isotope production, astrophysics, radiation protection near particle accelerators, etc.

Bibliography

Filges (D.) and Goldenbaum (F.), *Handbook of Spallation Research Theory, Experiments and Applications*, Wiley VCH, Berlin, 2010.

Gudowski (W.), "Accelerator-driven Transmutation Projects. The importance of Nuclear Physics Research for Waste Transmutation", *Nuclear Physics A* 654, pp. 436c-457c,1999.

Aït Abderrahim (H.), Baeten (P.), De Bruyn (D.), Heyse (J.), Schuurmans (P.) and Wagemans (J.), "MYRRHA, a Multi-purpose Hybrid Research Reactor for High-end Applications", *Nuclear Physics News*, vol. 20, Issue 1, pp. 24-28, 2010.

Bauer (G.S), Salvatores (M.) and Heusener (G.), "MEGAPIE, a 1 MW pilot experiment for a liquid metal spallation target", *Journal of Nuclear Materials*, 296, pp. 17-33, 2001.

Boudard (A.), Cugnon (J.), Leray (S.) and Volant (C.), "Intranuclear cascade model for a comprehensive description of spallation reaction data", *Physical Review* C 66, 044615 -1 to 28, 2002.

Leray (S.) *et al.*, "Results from the IAEA Benchmark of Spallation Models", *Journal of the Korean Physical Society*, 59(2), pp. 791-796, 2011.

Zanini (L.) *et al.*, "Experience from the post-test analysis of MEGAPIE", *Journal of Nuclear Materials*, 415(3): pp. 367-377, 2011.

Leray (S.), "Specific features of particle/matter interaction for accelerator-driven sub-critical reactors", *Materials Issues for Generation IV Systems: Status, Open Questions and Challenges*, (Editors: V. Ghetta, D. Gorse, D. Mazière and V. Pontikis), pp. 559-573, 2008.

Sylvie Leray
Institute for Research on the Fundamental Laws of the Universe

Neutronics Methods

About the foundations of the transport equation

Neutron propagation in a given medium belongs to a family of transport processes gathering phenomena as varied as light (photon) propagation in stellar matter or in the Earth's atmosphere, dynamics of rarefied gases, plasma physics, macromolecular orientation in space, car traffic…, as put forth by **J. J. Duderstadt** and **W. R. Martin** in their ***Transport Theory*** [1]. These processes are governed by the kinetic theory equations (not to be confused here with nuclear reactor kinetics equations). In the following we mention the broad lines of these two authors' presentation about the relationship between the transport theory and the kinetic theory for it displays the interest of reconnecting the transport equation with a more general background, and apprehends its foundations. Moreover, it shows the relationship between the stochastic and deterministic formulations of the transport problem, connecting them with the measurements of a physical quantity of interest achieved during an experiment.

The **Boltzmann equation** and the **neutron transport equation** are two examples of kinetic theory equations. As a matter of fact, the **neutron transport equation** is a specific case of the **Boltzmann equation** in which a neutron "gas" is diffused in a nuclide "gas". Neutron transport processes are characterized by the fact that particles (*i.e.* gas molecules or neutrons) have **mean free paths*** much larger than the range of the interaction potential between particles (nuclear reaction, see *supra*, p. 9), the latter being then assumed to be pointwise.

The Boltzmann equation, often directly established, can be derived in several manners from the **Liouville equation**, a more general partial differential equation, relating to Statistical Mechanics. This equation is itself established from the **Hamilton's equations**. So is achieved the transition from microscopic equations, which govern the motion of each of a given physical system's particles, to the kinetic theory equations, which give access to "mean" and experimentally measurable macroscopic quantities.

The discipline which is the theoretical frame of this microscopic-to-macroscopic transition is the so-called **Nonequilibrium Statistical Mechanics**.

In order to precisely define the link between these two levels of description of a physical system's state, let us consider a system consisting of N particles. Each particle i of this set is characterized at a given instant t by its position $\vec{r}_i(t)$ and its velocity $\vec{v}_i(t)$. The ensemble of positions and velocities of N particles at the instant t is denoted $\Gamma_N(t)$, that is: $\Gamma_N(t) \equiv \{\vec{r}_i(t), \vec{v}_i(t)\}_{i=1,N}$, where $\vec{r}_i(t)$ and $\vec{v}_i(t)$ are governed by mechanics laws. Let us state that G is a physical macroscopic quantity characterizing the system and, so, dependent on its state: at a given instant t, quantity G takes the value $G(\Gamma_N(t))$. Measuring G consists in calculating the average $<G>$ over an observation time T:

$$< G >_T = \frac{1}{T}\int_0^T G(\Gamma_N(t))dt \; ; \; < G > = \lim_{T\to\infty} < G >_T$$

Now, let us no longer consider a unique system of N particles, but a set of macroscopically identical systems of N particles. Let us state Γ_N a possible configuration in the phase space of these systems. A probability density function $\rho(\Gamma_N)$ can then be associated to Γ_N; the mean value of G, $< G >$, is then obtained through:

$$< G > = \int \rho(\Gamma_N) G(\Gamma_N)\, d\Gamma_N$$

The fundamental postulate of Statistical Mechanics is that averages $< G >$ are identified as the measurements of the macroscopic quantity G, which are but the time averages $< G >_T$. Consequently, the following equality can be stated:

$$\int \rho(\Gamma_N) G(\Gamma_N)\, d\Gamma_N = \lim_{T\to\infty} \frac{1}{T} \int_0^T G(\Gamma_N\,(t))\, dt = < G >$$

Quite schematically, this equality stands for the **ergodicity assumption** introduced by **W. Gibbs** (though Boltzmann [2,3] was apparently the first to introduce the **ergodicity concept**.) This assumption states that the study of a unique system can be replaced by that of a set of macroscopically identical systems having different arbitrary initial conditions.

The probability density $\rho(\Gamma_N)$ is obtained through the **Liouville equation** mentioned above.

Thus we passed from the **6 × N dimension** space of the **microscopic** level to the **6-dimension** space (*i.e.* a space with an "average" configuration) of the "**kinetic level**".

In fact, in the case of a neutron population, which displays a Markovian behavior, and a certain number of which may disappear, *e.g.* by absorption, the probability density function $\rho(\Gamma_N)$ is deduced from the **Chapman-Kolmogorov equations**.

"Shrinking" the dimensions once more so as to only retain the three space dimensions makes it possible to reach the "**hydrodynamic level**", which the **Navier-Stokes** equations and the **neutron diffusion equation** belong to.

So this is a **mean quantity** (the angular flux), which fulfills the **Boltzmann equation** or the **transport equation**. **Deterministic methods** implemented to solve this equation no longer give access to the individual history of each particle of the system being investigated.

The **Monte-Carlo probabilistic method** applied to the resolution of the transport equation explicitly simulates the set of equivalent physical systems considered above as part of the ergodic assumption, then concludes the simulation with a statistical average of all the results produced by each of these simulations, alike a set of measurements which would be achieved and averaged within a strictly experimental framework. This average is a statistical assessment of the result of interest. The microscopic level is preserved in that the characteristics (positions, energies, events) of the simulated history of each of systems particles can be stored, analyzed, and retreated.

It shall be noticed that the deterministic approach *a priori* gives the (mean) value of the physical quantity of interest **in any point of the phase space**. This cannot be the case in practice with a natural probabilistic simulation, due to a mere statistical reason: the probability for two simulated particles to go across a same point in space is almost null.

References

[1] J. J. Duderstadt, W. R. Martin, *Transport Theory*, New York, John Wiley & Sons, USA, 1979.

[2] L. Boltzmann, « Weitere Studien über das Wärmegleicgewicht unter Gasmolekülen », *Wiener Berichte*, 66, pp. 275-370, 1872.

[3] L. Boltzmann, *Théorie cinétique des gaz*, trad. française, Ed. Jacques Gabay, 1987.

Neutronics Fundamental Equations

In the core of a nuclear reactor, neutron propagation is coupled with the transmutation of the media in which they propagate. As a matter of fact, the neutron irradiation and the temperature of fuel, moderator, and of the whole of existing structures, exhibit significant space and time variations. Consequently, the nuclide composition of irradiated media varies in space and time. This explains why neutronics focuses on two coupled basic equations which govern in space and time, the one, neutron motion, and the other, the evolution of isotopic compositions.

Integro-differential Boltzmann equation: neutron transport

The solution of the Boltzmann equation gives the neutron population's density as a function of time and space. This equation also applies to the transport of photons, which are involved in reactor studies, especially in radiation shielding and materials heating calculations.

The quantum behavior of neutrons is displayed during collisions with nuclei, but to the neutron physicist, these collisions can be considered as punctual and instantaneous events, of which the consequences alone are of interest. According to the incident neutron's energy, and to the nucleus with which it interacts, various types of reactions may take place: the neutron may be **absorbed***, or **scattered***, or it may induce nuclear **fission***. It is to be recalled that the probability of each reaction is characterized by a quantity named **microscopic cross section***. Between two collisions, neutrons behave as classical particles, described by their position and velocity. Uncharged (as neutral particles), they move along a straight line, at least on short distances for which the gravitational effect can be neglected.

The establishment of the Boltzmann equation in neutronics is based on the following assumptions and simplifications:

- The neutron number in the considered system is sufficiently high for a neutron density to be defined. The conditions in a nuclear reactor, with an order or magnitude of 10^8 neutrons per cm^3, comply with this assumption;
- neutron-neutron interactions can be neglected versus neutron-matter interactions. The ratio between neutron density and atom density in the propagation medium (water, uranium oxide…) is of about 10^{-15}, which justifies this approximation. This assumption is of major importance, for it leads to a linear formulation of the Boltzmann equation, much simpler that the nonlinear version used in the gas kinetics theory;
- relativistic effects are neglected. In a reactor, neutrons generated by fission exhibit a maximum kinetic energy of about 20 MeV, corresponding to 2% of their mass at rest;
- the decay of the neutron into a proton ($n \rightarrow p + e^- + \bar{\nu}_e$) can be neglected in that its lifetime in the reactor prior to being absorbed is much shorter that its decay time. As a matter of fact, its lifetime is between 10^{-5} and 10^{-3} seconds, depending on reactor types, and its radioactive decay half-life is about 10 minutes.

The Boltzmann equation expresses the balance of the number of neutrons in an elementary volume $D \equiv d\vec{r}\,.\,dE.\,d\vec{\Omega}$ around point $P \equiv (\vec{r}\,,\, E,\, \vec{\Omega}\,)$ of the phase space, during the elementary time interval dt around instant t.

Six terms are involved in this balance:

a) The algebraic disappearance of neutrons of domain D escaping across the surfaces which bound the elementary volume around point $\vec{r}$ (net balance of entering and exiting neutrons) within the elementary time interval dt.

$$-\vec{\Omega}.\vec{\nabla}\psi(\vec{r},E,\vec{\Omega},t)d\vec{r}.\,dE.\,d\vec{\Omega}.\,dt$$

- $\psi(\vec{r}\,,\, E,\, \vec{\Omega}\,,\, t)$ angular flux in $(\vec{r}\,,\, E,\, \vec{\Omega}\,,\, t)$ [see introduction].

b) Neutron disappearance in domain D, by absorption and scattering, the absorptions inducing neutron disappearances, and the scatterings bringing them to another energy, and sending them in another direction, within the elementary time interval dt:

$$-\sum_k N_k(\vec{r},t)\,\sigma_k(E)\psi(\vec{r},E,\vec{\Omega},t)d\vec{r}.\,dE.\,d\vec{\Omega}.\,dt$$

- $N_k(\vec{r},t)$: concentration of nuclides k at point $\vec{r}$ and instant t,
- $\sigma_k(E)$: total microscopic cross section of nuclide k for an incident neutron of energy E.

Phase space, neutron density, and neutron flux

In reactor physics, neutron populations undergo a statistical treatment. They are described using the notion of **neutron density***, which stands for the average number of neutrons observed per unit volume. However, this neutron density is a more general notion than the usual notion of density, for the elementary volume to be considered is not only a volume in physical space.

As a matter of fact, neutrons have to be counted, not only in space, but also according to their velocity, which is not the same for all, and plays a fundamental role in their future. Generally, this density is also time-dependent. So, to sum up it all, a full description of a neutron population requires three space variables, three velocity variables, and the time variable. In practice, materials used in reactors are isotropic. Their properties (especially, their cross sections) then only depend on the speed (or energy) of incident neutrons, and not on their direction. This is why the speed (or, directly, neutrons' kinetic energy) and neutron direction are often distinguished. This distinction is achieved introducing the unit vector built on the velocity vector:

$$\vec{\Omega} = \frac{\vec{v}}{v}.$$

Finally, density (referred to as phase density) is denoted $n(\vec{r}, E, \vec{\Omega}, t)$. It can express the average number of neutrons included, at instant t, in an elementary volume of a six-dimension space called the "**phase space***".

Moreover, it is often easier to work with the quantity $\psi(\vec{r}, E, \vec{\Omega}, t) = vn(\vec{r}, E, \vec{\Omega}, t)$, named the **angular flux**, which represents the number of neutrons of energy E, that, at instant t and at point $\vec{r}$, go across a unit surface perpendicular to the propagation direction $\vec{\Omega}$. The **scalar flux** $\phi(\vec{r}, E, t)$ is also defined as the integral over all the directions of the angular flux: $\phi(\vec{r}, E, t) = \int_{4\pi} \psi(\vec{r}, E, \vec{\Omega}, t) d\vec{\Omega}$. The interest of knowing the scalar flux lies in that the number of nuclear reactions generated per unit volume and time, the so-called **reaction rate**, denoted $\tau(\vec{r}, E, t)$, is calculated as the product of the scalar flux and the **macroscopic cross section*** corresponding to the nuclear reaction under consideration, of microscopic cross section $\sigma(E)$:

$$\tau(\vec{r}, E, t) = N(\vec{r}, t)\sigma(E)\phi(\vec{r}, E, t) = \Sigma(\vec{r}, E, t)\phi(\vec{r}, E, t)$$

where $N(\vec{r}, t)$ stands for the concentration of the nuclide target of neutrons at point $\vec{r}$ and at time t.

c) Neutron arrival in domain D as a result of scatterings. These are neutrons which, before collision, had another energy, and moved in another direction, and which emerge from collision at energy E and in direction $\vec{\Omega}$, within the elementary time interval dt :

$$\sum_k N_k(\vec{r}, t) \int_0^\infty dE' \int_{4\pi} d\vec{\Omega}' \, \sigma_{s,k}(E' \to E, \vec{\Omega}' \to \vec{\Omega}) \psi(\vec{r}, E', \vec{\Omega}', t) d\vec{r}. dE. d\vec{\Omega}. dt$$

- $\sigma_{s,k}(E' \to E, \vec{\Omega}' \to \vec{\Omega})$: microscopic transfer cross section which moves the neutron from energy E' to energy E and from direction $\vec{\Omega}'$ to direction $\vec{\Omega}$, upon scattering on nuclide k. The isotropic nature of materials with respect to neutrons means that in the scattering process, for a given deflecting angle following collision, all emergence directions forming a revolution cone around the axis defined by the incidence direction are equiprobable. This is why differential scattering cross sections can be reformulated with a scalar product as follows:

$$\sigma_{s,k}(E' \to E, \vec{\Omega}' \to \vec{\Omega}) = \sigma_{s,k}(E' \to E, \vec{\Omega}'. \vec{\Omega}).$$

When dealing with the transport equation, these differential scattering cross sections are generally represented by an expansion on the Legendre polynomial basis $P_n(\mu)$:

$$\sigma_{s,k}(E' \to E, \vec{\Omega}'. \vec{\Omega}) = \sigma_{s,k}(E' \to E, \mu) = \sum_{n=0}^{\infty} (2n+1) \, \sigma_{sn,k}(E' \to E) P_n(\mu)$$

d) The source of **prompt neutrons*** emitted by induced or spontaneous fission within domain D and during the elementary time interval dt:

$$\frac{1}{4\pi} \sum_k N_k(\vec{r}, t) \int_0^\infty dE' \, \nu_{p,k}(E') \sigma_{f,k}(E') \chi_{p,k}(E' \to E) \phi(\vec{r}, E', t) \, d\vec{r}. dE. d\vec{\Omega}. dt$$
$$+ \frac{1}{4\pi} \sum_k \nu_{p,fs,k} \lambda_{fs,k} N_k(\vec{r}, t) \chi_{p,fs,k}(E) \, d\vec{r}. dE. d\vec{\Omega}. dt$$

- $\sigma_{f,k}(E')$: fission microscopic cross section relating to nuclide k, for an incident neutron at the energy E';
- $\nu_{p,k}(E')$: average number of prompt neutrons emitted following an induced fission on a nucleus k by an incident neutron of energy E';
- $\chi_{p,k}(E' \to E)$: energy spectrum of the prompt neutrons isotropically emitted following an induced fission on a nucleus k by an incident neutron of energy E';
- $\phi(\vec{r}, E', t)$: scalar flux in $(\vec{r}, E', t)$ [see introduction];
- $\nu_{p,fs,k}$: average number of prompt neutrons emitted by spontaneous fission of nuclide k;
- $\lambda_{fs,k}$: spontaneous fission decay constant of the nuclide k;
- $\chi_{p,fs,k}(E)$: spectrum of the prompt neutrons isotropically emitted by spontaneous fission of nuclide k.

e) The source of delayed neutrons emitted by induced or spontaneous fission within domain D and within the elementary time interval dt. These neutrons arise from particular radioactive **fission products***, **assumed to be emitted at the moment of fission**, and referred to as **precursors***. These nuclei have the property to be able to decay through the (β^-, n), channel, *i.e.* a β^- decay followed by the immediate emission of a neutron.

As the decay of a precursor nucleus according to this channel results in the emission of a single neutron, the delayed neutron source can be written as follows:

$$\frac{1}{4\pi}\sum_k \lambda_{d,k} N_k(\vec{r},t)\chi_{d,k}(E)\ d\vec{r}.\,dE.\,d\vec{\Omega}.\,dt$$

• $\lambda_{d,k}$: partial decay constant of nuclide k, corresponding to channel (β^-, n);
• $\chi_{d,k}(E)$: energy spectrum of delayed neutrons isotropically emitted by nuclide k.

f) External neutron sources:

$$S_{ext}(\vec{r},E,\vec{\Omega},t)d\vec{r}.\,dE.\,d\vec{\Omega}.\,dt$$

The time variation of angular flux:

$$\frac{1}{v}\frac{\partial\psi(\vec{r},E,\vec{\Omega},t)}{\partial t}d\vec{r}.\,dE.\,d\vec{\Omega}.\,dt$$

is equal to the algebraic sum of the six quantities previously recorded. This equality leads to the integro-differential Boltzmann equation, fulfilled by the angular neutron flux $\psi(\vec{r},\ E,\ \vec{\Omega},\ t)$:

$$\frac{1}{v}\frac{\partial\psi(\vec{r},E,\vec{\Omega},t)}{\partial t} = -\vec{\Omega}.\vec{\nabla}\psi(\vec{r},E,\vec{\Omega},t) - \sum_k N_k(\vec{r},t)\,\sigma_k(E)\psi(\vec{r},E,\vec{\Omega},t) \tag{1}$$
$$+\sum_k N_k(\vec{r},t)\int_0^\infty dE'\int_{4\pi} d\vec{\Omega}'\,\sigma_{s,k}(E'\to E,\vec{\Omega}'\to\vec{\Omega})\psi(\vec{r},E',\vec{\Omega}',t)$$
$$+\frac{1}{4\pi}\sum_k N_k(\vec{r},t)\int_0^\infty dE'\,\nu_{p,k}(E')\sigma_{f,k}(E')\chi_{p,k}(E'\to E)\phi(\vec{r},E',t)$$
$$+\frac{1}{4\pi}\sum_k \nu_{p,fs,k}\lambda_{fs,k}N_k(\vec{r},t)\chi_{p,fs,k}(E) + \frac{1}{4\pi}\sum_k \lambda_{d,k}N_k(\vec{r},t)\chi_{d,k}(E) + S_{ext}(\vec{r},E,\vec{\Omega},t)$$

This formulation of the Boltzmann equation is general because it does not make any assumption on the nuclide nature. Thus, when applied to a given physical configuration, the fission cross section $\sigma_{f,k}(E')$, for example, will take a null value if nuclide k is not fissile, or the partial decay constant $\lambda_{d,k}$ will take a null value if nuclide k is not a precursor of delayed neutrons.

A time-dependence corresponding to variation in temperature could be written for microscopic cross sections, but it is not mentioned here.

The Boltzmann equation also exists in an integral form, which is the starting point for some numerical methods, especially the Monte-Carlo-type methods (see the subchapter dealing with the derived forms of basic equations).

In particular situations (criticality and radiation shielding studies conducted, *e.g.* within the framework of fuel cycle), other neutron sources are taken into account, among which:

a) the neutron sources resulting from nuclear reactions of type (α, n) :

$$\frac{1}{4\pi}\sum_k \zeta^{(k)}_{(\alpha,n)}(E)\,\lambda_{\alpha,k}N_k(\vec{r},t)\,d\vec{r}.\,dE.\,d\vec{\Omega}.\,dt$$

where:

• $\zeta^{(k)}_{(\alpha,n)}(E)$: yield of neutrons of energy E, by reactions (α, n) induced by *alpha* particles emitted by the decay of the nucleus k,
• $\lambda_{\alpha,k}$: α decay constant of the nucleus k.

b) the neutron source resulting from the photonuclear reactions (γ, n), $(\gamma, 2n)$, (γ, f), etc. :

$$\sum_k N_k(\vec{r},t)\int_0^\infty dE'_\gamma\int_{4\pi} d\vec{\Omega}'_\gamma\sum_q \sigma_{\gamma,q,k}(E'_\gamma\to E,\vec{\Omega}'_\gamma\to\vec{\Omega})\,\psi_\gamma(\vec{r},E'_\gamma,\vec{\Omega}'_\gamma,t)d\vec{r}.\,dE.\,d\vec{\Omega}.\,dt$$

where:

• $\sigma_{\gamma,q,k}(E'_\gamma\to E,\vec{\Omega}'_\gamma\to\vec{\Omega})$: differential cross section of production of neutrons at energy E, in direction $\vec{\Omega}$ by the q type photonuclear reaction of nuclide k,
• $\psi_\gamma(\vec{r}, E'_\gamma, \vec{\Omega}'_\gamma, t)$: flux of *gammas* (neutral particles) which can also be obtained by solving a propagation equation similar to that established for neutrons. It is worth to mention that:

- in the energy range of nuclear reactors, the emitted *gammas* exhibit energies in the (0 - 20 MeV) range, and so their propagation in matter is mainly governed by the Compton effect, the photoelectric effect, the pair effect (electron-positrons) and the coherent scattering;
- this neutron source term couples neutron and *gamma* propagations.

Ludwig Eduard Boltzmann (1844-1906)

He taught experimental physics, theoretical physics, and mathematics in several universities: Munich, Leipzig, Graz, Vienna. As he was an excellent professor, his audience also came from England, the United States, and Japan.

Ludwig Eduard Boltzmann was born in Vienna on February 20, 1844. His PhD's degree, awarded in 1866, concluded his thesis works devoted to the **kinetic theory of gases**. This thesis had been supervised by **Jožef Stefan**, a famous Slovenian-culture physicist and writer, who was the father of the **blackbody radiation law**, the so-called ***Stefan-Boltzmann Law***. As a matter of fact, the theoretical justification of that law was brought by L. E. Boltzmann himself. Both an experimentalist and a theoretician, **L. E. Boltzmann** indeed contributed to developing most of physics fields in his age.

However, his most significant contribution lies in the revolution he brought in **matter's atomistic theory**. One of the major pending issues was the following: *how to predict the macroscopic properties of a given physical system starting from the myriad of atoms it consists of?* In order to give an answer, **L. E. Boltzmann** laid the foundations of **Statistical Mechanics**, starting from a genial, bold and brave idea: combining **Analytical Mechanics**, issued from the former works by **Newton, d'Alembert**, **Lagrange**, **Hamilton**… to **Probability Calculation** which theoretical foundations were to be established later on by mathematicians such as **Émile Borel** and **Henri Lebesgue**, in the frame of the **Measure Theory** [1,2].

Today it may seem strange that **Boltzmann's Statistical Mechanics** then appeared as a trend attached to the past, not to say retrograde, to his physicist contemporaries. Perhaps that may be explained by two factors:

- The prominent philosophic climate of positivism promoted by **Ernst Mach** and **Auguste Comte**, among others, and characterized by an attitude of distrust towards **Probability Calculation** [3];
- the notion of **energy** itself, at that age, was the object of a true conceptual revolution, to such an extent that, to someone like **Wilhelm Ostwald**, a renowned chemist and physician, and **Ludwig Boltzmann**'s close friend, everything was **energy**. This entity had become a synonym of modernity, and had thus succeeded to the "archaic" entity **Matter**. Continuum physics was supposed to win over discontinuum physics.

In his work ***Lessons on the gas theory***, several pages bear obvious traces of the tragic scientific and epistemological fight experienced by **Ludwig Boltzmann** to set up the new research paradigm associated with **Statistical Mechanics** within the European scientific community, in the late 19th century.

Almost paradoxically, being an intellectual outsider, prone to fits of melancholia and anxiety and in bad health, **L. Boltzmann** did not know how, or was not able, to seize the opportunity brought by the two new emerging physics, **Nuclear Physics** and **Quantum Mechanics**, which could have helped him defend his vision of Nature in front of the scientific world.

Ludwig Boltzmann committed suicide on September 5, 1906 at Duino, near Trieste, where he was spending holidays. His work was to be fully recognized by posterity later on, probably beyond what he was then able to imagine.

A few references

[1] L. Boltzmann, « Weitere Studien über das Wärmegleichgewicht unter Gasmoilekülen », *Wiener Berichte*, 66, pp. 275-370, 1872.

[2] L. Boltzmann, *Leçons sur la théorie des gaz, Parties I et II*, édition française : Éditions Jacques Gabay, 1987, réimpression de l'édition originale de la traduction française publiée en 1902 pour la partie I et 1905 pour la partie II par Gauthier-Villars.

[3] S. Callens, *Les Maîtres de l'erreur – Mesure et probabilité au XIXe siècle*, Paris, Presses Universitaires de France, 1997.

http://www.ipnl.in2p3.fr/delphi/laktineh/monitorat/public_html/boltzmann/boltzmann.htm

Ludwig Boltzmann's tomb in the Central Cemetery (Zentralfriedhof) at Vienna (Austria). Source: http://fr.wikipedia.org/wiki/Ludwig_Boltzmann#Biographie

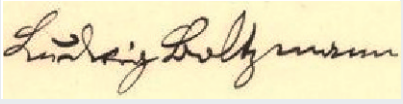

L. E. Boltzmann established the equation bearing his name, thereby generalizing the Maxwell's velocity distribution law. He gave a statistical interpretation of entropy which is summarized by the law $S = k\,Log\,W$, written as an epitaph on the top of his tomb-stone, thereby unifying mechanics and thermodynamics, and connecting the little probable to the most probable.

Generalized Bateman equations: nuclide depletion / generation

General equations which govern the time evolution in the concentration $N_k(\vec{r},t)$ of the atomic nuclei of the nuclides k, during irradiation, are derived from the balance at point $\vec{r}$, and within the elementary time interval dt around instant t, of the nuclides k which:

a) appear through nuclear reactions:

$$\sum_{m\neq k} \varsigma_{k\leftarrow m}(\vec{r},t)N_m(\vec{r},t)dt$$

- $\varsigma_{k\leftarrow m}(\vec{r},t)$: microscopic reaction rate relating to the formation of nuclide k from nuclide m:

$$\varsigma_{k\leftarrow m}(\vec{r},t) = \sum_q \int_0^\infty \sigma_{q,k\leftarrow m}(E)\phi(\vec{r},E,t)dE$$

- $\sigma_{q,k\leftarrow m}(E)$: microscopic cross section of the reaction q induced by a neutron of energy E on nuclide m, resulting in the formation of nuclide k,

b) appear through radioactive decay:

$$\sum_{m\neq k} \lambda_{k\leftarrow m}N_m(\vec{r},t)dt$$

- $\lambda_{k\leftarrow m}$: decay constant of a nuclide of type m towards nuclide k under consideration,

c) disappear through nuclear reactions:

$$-\varsigma_k(\vec{r},t)N_k(\vec{r},t)dt$$

- $\varsigma_k(\vec{r},t)$: microscopic reaction rate relating to the disappearance of nuclide k :

$$\varsigma_k(\vec{r},t) = \sum_q \int_0^\infty \sigma_{q,k}(E)\phi(\vec{r},E,t)dE$$

- $\sigma_{q,k}(E)$: microscopic cross section of the reaction q induced by a neutron of energy E on nuclide k, resulting in the disappearance of nuclide k,

d) disappear through radioactive decay:

$$-\lambda_k N_k(\vec{r},t)dt$$

- λ_k : total decay constant of nuclide of type k (with all resulting nuclei undistinguished)

The expression of the variation per unit time of the number of nuclides $N_k(\vec{r},t)$, at point $\vec{r}$ and time t, leads to a system of coupled differential equations called « generation/depletion equations » or « burnup equations »:

$$\frac{dN_k(\vec{r},t)}{dt} = \sum_{m\neq k} \varsigma_{k\leftarrow m}(\vec{r},t)N_m(\vec{r},t) + \sum_{m\neq k} \lambda_{k\leftarrow m}N_m(\vec{r},t) - \lambda_k N_k(\vec{r},t) - \varsigma_k(\vec{r},t)N_k(\vec{r},t) \quad (2)$$

They are also known as the **generalized Bateman equations**, after the name of **Harry Bateman** [1], an English mathematician who made his career in the United States, and brought a general solution to the radioactive decay differential equations.

The above mentioned setting-up of the Boltzmann equation (1), and of the Bateman equations (2) shows that they are coupled, thereby constituting a well posed system.

Bibliography

[1] Bateman (H.), "The solution of a system of differential equations occurring in the theory of radioactive transformations", *Proceedings Cambridge Philosophical Society*, vol. 15, pp. 423-427, 1910.

Mireille Coste-Delclaux, Cheikh M. Diop, Fausto Malvagi and Anne Nicolas
Department for Systems and Structures Modeling

The Nuclear Reactor Physicist's Approach

Reactor design and operation studies are based on numerical simulation. It is therefore crucial to make computational methods which combine accurateness, speed, and robustness.

In order to solve the Boltzmann equation and the generalized Bateman equations, the nuclear reactor physicist has to select the computational routes most suitable for the reactor under study.

Three factors go against an easy, straight resolution of the Boltzmann and Bateman equations:

- Technological (dimensions, structures, …) and operational complexity of a nuclear reactor core;
- the high number of variables which equations are dependent on, *i.e.* seven variables;
- the evolutionary feature, highlighted above, of macroscopic cross sections, $\Sigma(\vec{r}, E, t) = N(\vec{r}, t)\,\sigma(E, t)$, which vary in time, with very different scales:
  - when the system's temperature undergoes an evolution (*e.g.* through a power excursion), the density of the medium varies, as well as microscopic cross sections (by **Doppler effect***); its geometry, too, may be altered;
  - when fuel is irradiated, its nuclide composition is altered as a result.

In addition, time scales vary significantly according to the phenomena investigated:

- About one microsecond for the Doppler feedback;
- ranging from about a few dozen minutes to a few hours for core **poisoning*** (by **xenon*** 135 or **samarium*** 149);
- about a few years for fuel residence time in the reactor core.

When the reactor is finely described in energy, angle, and space, the Boltzmann equation entails taking into account almost 1,000 billion unknowns (see *infra*, p. 62 and 63 "Phase space discretization"). Now, today's computer power is not always able to solve problems of such a dimension. So it is indispensable to introduce simplifications and decouplings in relation to the specific physics of the reactor type under calculation. The choice of these simplifications and decouplings lies in the definition of what reactor physicists call the **computational** (or **calculation**) **scheme***.

The nuclear reactor physicist derives a benefit from the following fundamental observations:

1) Neutron density in a reactor is sufficiently low to assume that there is no neutron-neutron interaction. So, the Boltzmann equation is linear for the flux, providing macroscopic cross sections are assumed to be flux-independent, which is quite a valid approximation in so far as the evolution of core situation can be modeled by a succession of steady states.

2) When the reactor is critical, or near criticality, the balance equation (steady-state Boltzmann equation) expresses that, in any point, neutron production is equal to neutron losses (leakage + absorption).

3) In the resolution of the neutron balance equation, a heterogeneous medium can be replaced by an equivalent homogeneous medium if the latter does not upset the calculation of its environment.

4) The solution of the Boltzmann equation on the heterogeneous, finely discretized configuration can be used to obtain space and energy averaged neutron quantities; these quantities themselves can be used in a new homogeneous formulation of the Boltzmann equation, which will comply with each of the balance terms: production, losses, and absorption.

As a result, a reactor deterministic calculation can be achieved within two main steps. The first one is devoted to the fine calculation of fuel assemblies, assumed to be infinitely replicated. It provides the neutron quantities representative of the assembly which will be used in the second step. The latter is dedicated to calculations of neutron exchange between assemblies, taking account of the core's real boundary conditions.

In a more detailed manner:

- The first step, the so-called "**assembly calculation***", consists in a detailed calculation (in both space and energy) of a basic pattern of the core (a fuel assembly, a control assembly…). This calculation of an object, on the scale of the **mean free path*** of a neutron (a few centimeters) is performed by solving the transport equation on a horizontal (*i.e.* 2-D) section of the assembly, and assuming that this pattern is infinitely repeated, or that it occupies the whole space (calculation in an "infinite medium"). So most of the heterogeneity is taken into account, provided the heterogeneities be less strong axially than radially (as is generally the case). This fine calculation allows a "data reduction", which provides the neutron characteristics (macroscopic cross sections) of a homogeneous equivalent medium, either to the full assembly (total homogenization), or to each type of constitutive assembly portion, *e.g.* fuel rod and surrounding moderator/coolant (partial homogenization). This space "**homogenization***" is accompanied by an energy "**condensation***": the number of **groups*** used to describe the variation in energy of these "homogenized" cross sections is strongly reduced versus the number of groups in the input multigroup library. The reduction factor depends on the reactor type, especially the space variations of the neutron **spectrum***;

- the second step (the calculation of the core itself) consists in the 2-D or 3-D solving of an exact or approximate transport equation (*e.g.* the diffusion equation) by replacing each assembly or cell type, in the core by the homogeneous medium defined in the first step. Thus an object of large size can be treated, but with a coarser description in both space and energy. This calculation is the basis for providing the various useful quantities (reactivity, absorber efficiency, feedback coefficients, reaction rate distribution, isotope balance…).

In these two steps, the nuclear reactor physicist details what models, solvers, and discretizations will be the most suitable for an efficient, accurate solution of the problem to be tackled. Advances in computer engineering and computational methods regularly pave the way to further progress.

However, this type of scheme suffers from limitations, among which we can mention, on the one hand, the assumption of infinite-lattice calculation of an assembly's constants – which allows to separate fine calculation in the assembly and calculation of neutron exchange between assemblies –, and, on the other hand, approximations to the transport equation (diffusion, simplified transport) possibly retained in the second step. Due to differences in the modeling used during the two core calculation steps, it is most often indispensable to consider the so-called "**equivalence**" step, which allows for reducing discrepancies due to a mere **homogenization/condensation*** [1], [2].

Yet, this is currently the only operational type of scheme qualified to treat a three-dimensional core taking account of fuel burnup and feedbacks. As a matter of fact:

- As mentioned above, "straightforward" calculation by three-dimensional (3-D) resolution of the transport equation on the whole core of a large-sized reactor is still out of reach without simplifying the space and/or energy model. The only straightforward calculations ever possible (and already achieved) are two-dimensional, and are related to small reactors (experimental reactors), or part of a large-sized reactor (*e.g.* 1/8th of the EPR core). Even not taking fuel depletion (or burnup) into account, these calculations are still very long;

- "straightforward" calculation by three-dimensional (3-D) resolution of the transport equation using the Monte-Carlo method coupled with a deterministic depletion code is achievable, indeed. Nevertheless, this method requires to calculate the reaction rates with a statistical uncertainty that be acceptable everywhere, and raises the issue of the uncertainty propagation treatment in transport/depletion coupled calculations.

The nuclear reactor physicist's work thus consists in designing models and computational schemes likely to obtain the physical quantities of interest while optimizing the accuracy / calculation cost ratio.

Practically, according to the timescales considered to describe a reactor's neutronic state, the nuclear reactor physicist usually distinguishes the three following items:

- The "static" behavior of the physical system studied, for which the Boltzmann equation is solved in steady state (time-independent) conditions (see *infra*, pp. 56-59);

- the "slow" time evolution of nuclear fuel composition, which is governed by the Bateman equations (see *infra*, pp. 107-113);

- the "fast" transient phases governed by the kinetic equations, during which delayed neutrons play a prominent role (see *infra* pp. 59-60 and pp. 115-124).

Distinguishing these different time scales makes it possible to set the relevant assumptions likely to help solve the equations of interest.

Industrial calculation of nuclear reactors: modeling paradigms

(after R. Sanchez and P. Reuss)

Solving the transport equation in its (energy, space, angle, and time) continuous form is not compatible with the requirements of routine or project industrial studies, to be achieved within a reasonable amount of time. Some calculations have to deliver results within a few seconds. In order to take up this challenge, the **nuclear reactor physicist** has developed diverse techniques for solving the transport equation, all of them being based on the discretization of the phase space and sophisticated numerical methods [1], [2] relating to the deterministic modeling paradigms briefly mentioned below. These paradigms especially relate to the energy treatment of neutron propagation, the treatment of the reactor's geometry/composition heterogeneity, the energy and space treatment coupling, the reconstructing of the fine distribution of the power released by the reactor core. They use the **basic concept of equivalence**, which specifies the **requirement to preserve reaction rates when going from the nuclear reactor's actual configuration to its modeled configuration**.

- **Multigroup treatment of the transport equation.** This is the transition from the continuous-energy equation to the energy discretized equation. The continuous-energy equation is replaced by a set of so-called "multigroup equations", the number of which is that of the energy groups subdividing the 0-20 MeV neutron energy range. As a matter of fact, multigroup equations are obtained by integrating the continuous-energy equation over each of the energy groups. The continuous-energy physical quantities are then replaced by corresponding multigroup quantities. This continuous / discrete transition particularly leads to replace continuous-energy cross sections by constant cross sections in each energy group: these are the **multigroup cross sections** [3],[4]. The issue raised here is **how to determine these multigroup cross sections** so that the multigroup reaction rates preserve the reaction rates predicted by the continuous-energy equation. This issue is referred to by the term **energy condensation of cross sections**. The difficulty here lies in that to determine the multigroup cross sections enabling the reaction rates issued from the continuous-energy equation resolution to be preserved, assumes to know the angular neutron flux, the latter precisely being the unknown of the problem to be solved. Consequently, multigroup cross sections which would thus be defined, would no longer correspond to those of isotropic media, for they would depend on angle and space.

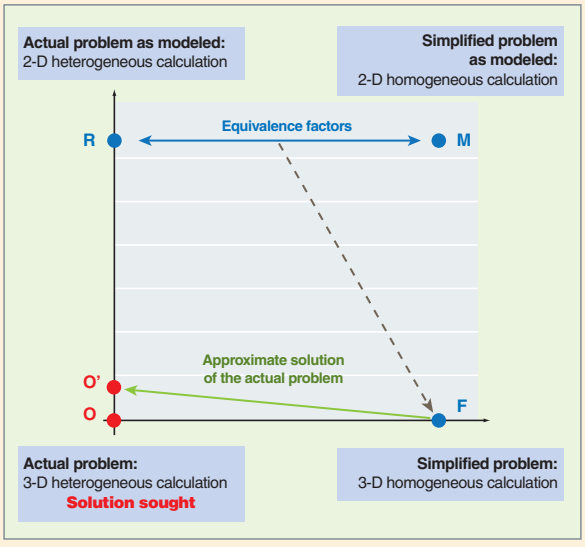

Principle scheme of equivalence for the example of a 3-D core calculation

IIn the present state of computational capabilities, the O point cannot yet be calculated directly (this is an objective to be reached in a few years). The use of an equivalence makes it possible to approach the exact solution (O point). The points R, M and F are first calculated, the latter being already achievable. Then "equivalence factors" are computed between the R and M points and are applied to the F point in order to obtain the point O', approximation of the point O.

Grouping also impacts the laws of transfer of one neutron from one group to another, through elastic and inelastic discrete scatterings, for which post-scattering energy and direction are fully correlated: its effect is to create an **artificial anisotropy of the intergroup transfer** [5], the latter being all the more marked as the multigroup energy meshing is fine.

Modeling the **resonance self-shielding phenomenon** plays a key role in the general problem of calculating multigroup cross sections. In the resonance range, multigroup cross section calculation can be achieved through various methods, among which the ***Livolant-Jeanpierre method*** [6] and the ***subgroup method*** [7], [8]. They make it possible to generate "self-shielded" multigroup cross sections for a multigroup energy meshing with few (100-500) groups relatively broad, suitable for transport calculations in homogeneous and heterogeneous bidimensional geometries (see *infra*, pp. 64-67).

- **Homogenization techniques for core calculations** [9 to 18]. The tridimensional, deterministic calculation of a nuclear power reactor core requires to design new modelings convenient for big-sized complex systems, including a high number of heterogeneous components, for which direct calculation is hardly possible, or needs a time and/ or calculation resources (power and number of computer processors…), prohibitive for routine or project studies. The aim of **homogeneization** is **to replace heterogeneous components** by **homogeneous components** so that the calculation of the homogeneized system results in accurate mean values. The solution to the homogeneized problem cannot preserve in detail the solution to the initial heterogeneous problem. It follows that the homogeneization process is accompanied with information loss, and that only the mean values of the solution can be preserved.

Homogenization techniques are implemented on assemblies. They are based on:

- the definition and achievement of the **heterogeneous reference calculation(s)** which specifies(y) the values to be preserved by the homogenization operation,
- the joint use of the **fundamental mode theory** and the **critical leakage** concept,
- the equivalence methods involving neutron **current discontinuity factors** (CDF), or **flux discontinuity factors** (FDF), between homogenized assemblies.

• **Heterogeneous flux reconstruction.** The aim of core calculation is to get detailed reaction rates with respect to space and power distribution, and, in particular, to predict the power peak in the core. As a consequence, once the core calculation has been performed, a reconstruction method has to be used in order to get the detailed results of interest. This is a problem, to be solved with one of the following techniques:
  - The *factorization technique*;
  - the reconstructing *by transport*;
  - the *multiscale technique*.

  which, each of them in a different way, combine the results from core calculation with those from reference transport calculation.

There exists a much better, but more expensive method, the so-called **dynamical homogenization**, which determines the neutron flux of the detailed transport by iteratively homogenizing the assemblies, so as to take account of average inter-assembly exchange of core calculation. So this method, in which core calculation and assembly calculation in transport are made to converge simultaneously, does not need reconstructing.

For the latest few years, the Monte-Carlo calculations have brought reference results which allow a "computational validation" of the above mentioned methods. This is detailed *infra*, pp. 165-170.

References

[1] R. Sanchez, J. Mondot, Z. Stankovski, A, Cossic, I. Zmijarevic, "APOLLO2: a user oriented, portable, modular code for multigroup transport assembly calculations", *Nuclear Science and Engineering*, 100, pp. 352-362, 1988.

[2] R. Sanchez, I. Zmijarevic, M. Coste-Delclaux, E. Masiello, S. Santandrea, E. Martinolli, L. Villatte, N. Schwartz, N. Guler, "APOLLO2 Year 2010", *Nuclear Engineering and Technology*, vol. 42, n° 5, pp. 474-499, October 2010.

[3] N. Hfaiedh, *Nouvelle Méthodologie de Calcul de l'Absorption Résonnante*. Thèse de doctorat, Université Louis Pasteur Strasbourg I, 2006.

[4] P. Mosca, *Conception et développement d'un mailleur énergétique adaptatif pour la génération des bibliothèques multigroupes des codes de transport*, Thèse de Doctorat, Université Paris Sud 11, Orsay, France, 2009.

[5] A. Calloo, *Développement d'une nouvelle modélisation de la loi du choc dans les codes de transport multigroupes : application au calcul des réacteurs de Génération III et IV*, Thèse de Doctorat de l'Université de Grenoble, France 2012.

[6] M. Livolant, F. Jeanpierre, *Autoprotection des résonances dans les réacteurs nucléaires*, Rapport CEA-R-4533- 1974.

[7] G. Rimpault et *al.*, "The ERANOS Code and Data System for Fast Reactor Neutronic Analysis", *Proc. Int. Conf. PHYSOR 2002*, Seoul, Korea, October 7-10, 2002.

[8] M. Coste, S. Mengelle, "Implementation of a sub-group method for self-shielding calculations in APOLLO2 code", *International Conference on the Physics of Reactors, PHYSOR 96*, Vol I, pp. 323-331, Mito, Ibaraki, Japan,1996.

[9] D.S. Selengut, "Diffusion coefficients for heterogeneous systems", *Transactions of the American Nuclear Society*, 3, 398, 1960.

[10] E.W. Larsen, "Neutron transport and diffusion in inhomogeneous media", I. J. Math. Phys. 16 (7), pp. 1421-1427, 1975.

[11] A. Kavenoky, "The SPH Homogenization Method", AIEA, Comité technique en physique des réacteurs, Würenlingen, Suisse, 1978 ; *Proc. Specialists Meeting on Homogenization Methods in Reactor Physics*, AIEA, Lugano, 1978.

[12] A. Hébert, *Développement de la méthode SPH : Homogénéisation de cellules dans un réseau non uniforme et calcul des paramètres de réflecteur*, Thèse de Doctorat, Université Paris Sud XI, Orsay, 1980, Note CEA-N-2209, 1981.

[13] P. Benoist, *Homogenization, Theory in Reactor Lattices*, Note CEA-N-2471, février 1986.

[14] K.S. Smith, "Assembly homogenization techniques for light water reactor analysis", *Progress in Nuclear Energy*, 17 (3), pp. 303-335, 1986.

[15] R. Sekkouri, *Analyse des techniques d'homogénéisation et des schémas de calcul pour les réacteurs à eau*, Thèse de Doctorat, Université Paris Sud XI, Orsay, 1994.

[16] Ph. Magat, *Analyse des techniques d'homogénéisation spatiale et énergétiques dans la résolution de l'équation du transport des neutrons dans les réacteurs nucléaires*, Thèse de Doctorat, Université Aix-Marseille I, 1997.

[17] R. Sanchez, "Assembly homogenization techniques for core calculations", *Progress in Nuclear Energy*, 51, pp. 14-31, 2009.

[18] P. Reuss, *Neutron Physics*, EDP Sciences/ENEN, 2008.

Richard Lenain and Anne Nicolas
Department for Systems and Structures Modeling

Derived Forms of Fundamental Equations

In a system under flux, the neutron emission process related to the spontaneous fission of nuclides is quite negligible. So it will be discarded here.

Steady-state transport calculations

Most of the time, a reactor operates under a steady state, i.e. at constant power. As a result, its neutron population is constant: at each generation, the number of neutrons is the same as for the previous generation. The reactor is then referred to as **critical***.

In a supercritical reactor, the number of neutrons increases with time, and, *a contrario*, in a subcritical reactor, the neutron number decreases with time.

Describing a critical reactor requires to find a stationary solution of the Boltzmann equation, in which neutron sources are limited to induced fission sources. In the description of this source are involved the total number of neutrons emitted (**prompt neutrons*** and **delayed neutrons***), and the emission spectrum of prompt neutrons alone, the latter accounting for nearly all the neutrons emitted by fission. So, once the relevance of this assumption is ascertained, the impact of the emission spectrum of delayed neutrons can be discarded.

Integro-differential form of the steady-state Boltzmann equation

So this leads to solve the following equation:

$$\vec{\Omega}.\vec{\nabla}\psi(\vec{r},E,\vec{\Omega}) + \sum_k N_k(\vec{r})\,\sigma_k(E)\psi(\vec{r},E,\vec{\Omega}) \qquad (1)$$

$$= \sum_k N_k(\vec{r}) \int_0^\infty dE' \int_{4\pi} d\vec{\Omega}'\,\sigma_{s,k}(E' \to E, \vec{\Omega}' \to \vec{\Omega})\psi(\vec{r},E',\vec{\Omega}')$$

$$+ \frac{1}{4\pi}\sum_k N_k(\vec{r}) \int_0^\infty dE'\,\nu_{t,k}(E')\sigma_{f,k}(E')\chi_{p,k}(E' \to E)\phi(\vec{r},E')$$

- $\nu_{t,k}(E')$: average neutron number (prompts and delayed) isotropically emitted following an induced fission on a k nucleus, by an incident neutron of energy E'.

Equation (1) describes the perfect equilibrium between neutron productions and losses that leads the system to a steady state.

Integral form of the steady-state Boltzmann equation

The steady-state Boltzmann equation can be written in such a form that all the variables of the phase space appear in integral operators. This integral form of the Boltzmann equation is used in two types of neutron transport treatment: the collision probability method, and the Monte-Carlo method.

The integral form of the Boltzmann equation can be either deduced from the Equation (1) established in the chapter dealing with the basic equations of neutronics, or be directly established.

As shown on Figure 20 (next page), the angular flux $\psi(\vec{r}, E, \vec{\Omega})$ at the point of phase space $(\vec{r}, E, \vec{\Omega})$ results from two terms:

- Neutrons emitted in $\vec{r}\,' = \vec{r} - s\vec{\Omega}$ at energy E and in direction $\vec{\Omega}$, $S(\vec{r} - s\vec{\Omega}, E, \vec{\Omega})$. These neutrons have a probability $\exp(-\int_0^s \Sigma(\vec{r} - s'\vec{\Omega}, E)\,ds')$ to arrive at $(\vec{r}, E, \vec{\Omega})$ without undergoing any collision. By integrating over all the distances s separating the emission point $\vec{r}\,'$ and the considered arrival point $\vec{r}$ of neutrons, the first term contributing to the angular flux $\psi(\vec{r}, E, \vec{\Omega})$ can be obtained:

$$\int_0^\infty ds\, exp(-\int_0^s \Sigma(\vec{r} - s'\vec{\Omega}, E)\,ds')\, S(\vec{r} - s\vec{\Omega}, E, \vec{\Omega})$$

- Neutrons of energy E' and direction $\vec{\Omega}'$ undergoing a scattering in $\vec{r}\,' = \vec{r} - s\vec{\Omega}$ which gives them energy E and direction $\vec{\Omega}$:

$$\int_0^\infty dE' \int_{4\pi} d\vec{\Omega}'\,\Sigma_s(\vec{r} - s\vec{\Omega}, E' \to E, \vec{\Omega}' \to \vec{\Omega})\psi(\vec{r} - s\vec{\Omega}, E', \vec{\Omega}')$$

Using the same reasoning as previously, the second term contributing to the angular flux $\psi(\vec{r},\ E,\ \vec{\Omega})$ can be obtained:

$$\int_0^{\infty} ds\ exp\left(-\int_0^{s}\Sigma\left(\vec{r}-s'\vec{\Omega},E\right)ds'\right)\int_0^{\infty}dE'\int_{4\pi}d\vec{\Omega}'\,\Sigma_s\left(\vec{r}-s\vec{\Omega},E'\rightarrow E,\vec{\Omega}'\rightarrow\vec{\Omega}\right)\psi\left(\vec{r}-s\vec{\Omega},E',\vec{\Omega}'\right)$$

So, in steady-state conditions, the integral transport equation is written as follows:

$$\psi(\vec{r},E,\vec{\Omega})=\int_0^{\infty}ds\ exp\left(-\int_0^{s}\Sigma\left(\vec{r}-s'\vec{\Omega},E\right)ds'\right)\ S\left(\vec{r}-s\vec{\Omega},E,\vec{\Omega}\right) \tag{2}$$
$$+\int_0^{\infty}ds\ exp\left(-\int_0^{s}\Sigma\left(\vec{r}-s'\vec{\Omega},E\right)ds'\right)\int_0^{\infty}dE'\int_{4\pi}d\vec{\Omega}'\,\Sigma_s\left(\vec{r}-s\vec{\Omega},E'\rightarrow E,\vec{\Omega}'\rightarrow\vec{\Omega}\right)\psi\left(\vec{r}-s\vec{\Omega},E',\vec{\Omega}'\right)$$

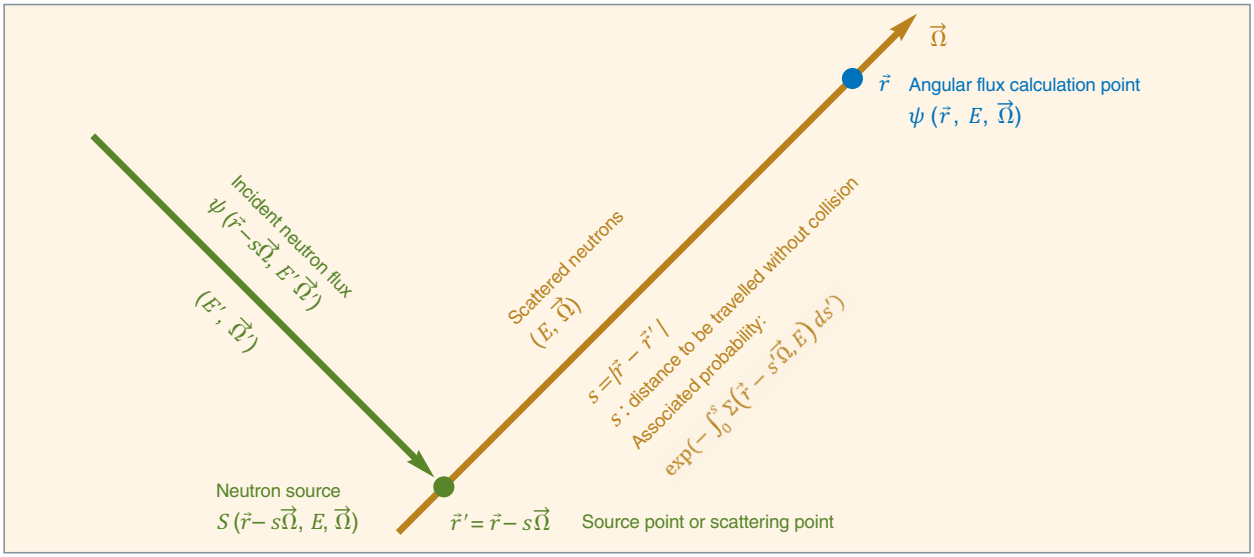

Fig. 20. Establishment of the Boltzmann integral equation in steady state. The angular flux $\psi\ (\vec{r},\ E,\ \vec{\Omega})$ results from the neutrons arising from source $S\ (\vec{r}-s\vec{\Omega},\ E,\ \vec{\Omega})$ and from the scattering source $\Sigma_s\ (\vec{r}-s\vec{\Omega},\ E'\rightarrow E,\ \vec{\Omega}'\rightarrow\vec{\Omega})\ \psi\ (\vec{r}-s\vec{\Omega}',\ E',\ \vec{\Omega}')$.

Critical equation - Introduction of the effective multiplication factor

In order to get a steady-state solution of the equation, whatever the actual state of the system (critical, supercritical, or subcritical), equation (1) is modified dividing fission sources by a factor which enables the equilibrium between productions and losses to be re-established. This factor is named "effective multiplication factor*", or k_{eff}. Equation (1) then becomes

$$\vec{\Omega}.\vec{\nabla}\psi\left(\vec{r},E,\vec{\Omega}\right)+\sum_k N_k(\vec{r})\,\sigma_k(E)\psi\left(\vec{r},E,\vec{\Omega}\right) \tag{3}$$
$$=\sum_k N_k(\vec{r})\int_0^{\infty}dE'\int_{4\pi}d\vec{\Omega}'\,\sigma_{s,k}\left(E'\rightarrow E,\vec{\Omega}'\rightarrow\vec{\Omega}\right)\psi\left(\vec{r},E',\vec{\Omega}'\right)$$
$$+\frac{1}{k_{eff}}\frac{1}{4\pi}\sum_k N_k(\vec{r})\int_0^{\infty}dE'\,\nu_{t,k}\left(E'\right)\sigma_{f,k}(E')\chi_{p,k}(E'\rightarrow E)\phi(\vec{r},E')$$

Equation (3), which is an eigenvalue equation. It can be shown that k_{eff} is the highest eigenvalue, and that $\psi\ (\vec{r},\ E,\ \vec{\Omega})$ is the related eigenfunction.

The related critical problem is described by Equation (3). The solution $\psi\ (\vec{r},\ E,\ \vec{\Omega})$ is named critical flux. It can also be shown that the k_{eff} introduced in the equation, is in agreement with the definition of the multiplication factor, *i.e.* the ratio between neutrons of generation $(i+1)$ and neutrons of generation i.

The eigenvalue problem (3) is solved by a method known as "power iteration": the first step is an arbitrary distribution of the source (usually a constant in space and a Watt spectrum in energy), and the resulting fixed-source problem can then be solved. The distribution of fission sources is updated with the flux resulting from this computation, and so on, according to the iterative scheme:

$$\vec{\Omega}.\vec{\nabla}\psi^{(n)}\left(\vec{r},E,\vec{\Omega}\right)+\sum_k N_k(\vec{r})\,\sigma_k(E)\psi^{(n)}\left(\vec{r},E,\vec{\Omega}\right)=\sum_k N_k(\vec{r})\int_0^{\infty}dE'\int_{4\pi}d\vec{\Omega}'\,\sigma_{s,k}\left(E'\rightarrow E,\vec{\Omega}'\rightarrow\vec{\Omega}\right)\psi^{(n)}\left(\vec{r},E',\vec{\Omega}'\right) \tag{4}$$
$$+\frac{1}{k_{eff}^{(n-1)}}\frac{1}{4\pi}\sum_k N_k(\vec{r})\int_0^{\infty}dE'\,\nu_{t,k}\left(E'\right)\sigma_{f,k}(E')\chi_{p,k}(E'\rightarrow E)\phi^{(n-1)}(\vec{r},E')$$

Formal analogy between the integral Boltzmann and Bateman equations

Introducing the collision density $\zeta(\vec{r},\ E,\ \vec{\Omega}) = \Sigma(\vec{r},\ E)\ \psi(\vec{r},\ E,\ \vec{\Omega})$, the integral Boltzmann equation in a steady state for a problem involving a fixed source in a non-multiplying medium is written as follows:

$$\zeta(\vec{r},E,\vec{\Omega}) = \Sigma(\vec{r},E)\int_0^{\infty} ds\ exp(-\int_0^{s}\Sigma(\vec{r}-s'\vec{\Omega},E)\,ds')\ S(\vec{r}-s\vec{\Omega},E,\vec{\Omega})$$
$$+\ \Sigma(\vec{r},E)\int_0^{\infty} ds\ exp(-\int_0^{s}\Sigma(\vec{r}-s'\vec{\Omega},E)\,ds')\ \int_0^{\infty} dE'\int_{4\pi} d\vec{\Omega}'\frac{\Sigma_s(\vec{r}-s\vec{\Omega},\ E'\to E,\vec{\Omega}'\to\vec{\Omega})}{\Sigma(\vec{r}-s\vec{\Omega},E')}\ \zeta(\vec{r}-s\vec{\Omega},E',\vec{\Omega}')$$

In the case when the flux inducing nuclide transmutation is time-independent, the Bateman equations can be rewritten under the following integral form:

$$N_k(\vec{r},t) = \int_0^t \sum_{m\neq k}\mu_{k\leftarrow m}(\vec{r},t')N_m(\vec{r},t')e^{-\mu_k(\vec{r})(t-t')}dt' + \int_0^t U_k(\vec{r},t')e^{-\mu_k(\vec{r})(t-t')}dt'$$

where:

- $\mu_k(\vec{r}) = \lambda_k + \varsigma_k(\vec{r})$
- $\mu_{k\leftarrow m}(\vec{r}) = \lambda_{k\leftarrow m} + \varsigma_{k\leftarrow m}(\vec{r})$
- $U_k(\vec{r},t')$: generation rate of nuclide k at point $\vec{r}$ and at instant t'.

The "generalized activitiy" of all of the nuclides is defined as a vector, the k component of which is given by the following relationship:

$$A_k(\vec{r},t) = \mu_k(\vec{r})N_k(\vec{r},t)$$

The generalized activity fulfills the following integral equation:

$$\forall k\quad A_k(\vec{r},t) = \mu_k(\vec{r})\int_0^t\sum_{m\neq k}\frac{\mu_{k\leftarrow m}(\vec{r})}{\mu_m(\vec{r})}A_m(\vec{r},t')e^{-\mu_k(\vec{r})(t-t')}dt' + \mu_k(\vec{r})\int_0^t U_k(\vec{r},t')e^{-\mu_k(\vec{r})(t-t')}dt'$$

The formal analogy between steady state transport and transmutation in a given point $\vec{r}$ is made explicit in the table below:

Table 9.

Formal analogy between transport in steady state conditions and transmutation

Steady-state transport	Depletion / Generation at a given point
Space: $\vec{r}$	Time: t
Energy: E (continuous variable)	Nuclide species: k (discrete variable)
Direction: $\vec{\Omega}$	Time non-reversibility: $t > 0$
Angular flux: $\psi(\vec{r},\ E,\ \vec{\Omega})$	Radionuclide concentration: $N_k(\vec{r},\ t)$
Total macroscopic cross section: $\Sigma(\vec{r},\ E)$	Total microscopic rate of transmutation: $\mu_k(\vec{r})$
Collision density: $\zeta(\vec{r},\ E,\ \vec{\Omega}) = \Sigma(\vec{r},\ E)\ \psi(\vec{r},\ E,\ \vec{\Omega})$	Generalized activity: $A_k(\vec{r},\ t) = \mu_k(\vec{r})\ N_k(\vec{r},\ t)$
Neutron source: $S(\vec{r},\ E,\ \vec{\Omega})$	Source activity: $S = U_k(\vec{r},\ t)$
Integral transport equation: $\zeta = TC\zeta + TS$	Integral equation of transmutation: $A = TCA + TS$
T integral operator of displacement in space: $TS(\vec{r},E,\vec{\Omega}) = \Sigma(\vec{r},E)\int_0^{\infty} ds\ S(\vec{r}-s\vec{\Omega},E,\vec{\Omega})\ exp(-\int_0^{s}\Sigma(\vec{r}-s'\vec{\Omega},E)\,ds')$	T integral operator of displacement in time: $TU_k(\vec{r},t) = \mu_k(\vec{r})\int_0^t U_k(\vec{r},t')e^{-\mu_k(\vec{r})(t-t')}dt'$
C scattering operator: $C\zeta(\vec{r},E,\vec{\Omega}) = \int_0^{\infty}dE'\int_{4\pi}d\vec{\Omega}'\frac{\Sigma_s(\vec{r},E'\to E,\vec{\Omega}'\to\vec{\Omega})\zeta(\vec{r},E',\vec{\Omega}')}{\Sigma(\vec{r},E')}$	C transmutation operator: CA is a vector whose k^{th} component is given as follows: $[CA]_k(\vec{r},t) = \sum_{m\neq k}\frac{\mu_{k\leftarrow m}(\vec{r})}{\mu_k(\vec{r})}A_m(\vec{r},t)$

References

P. H. Wilson, "Analog Monte-Carlo Methods for Simulating Isotopic Inventories in Complex Systems", *Nuclear Science and Engineering*, 152, 3, pp. 243-255, March 2006.

C. M. Diop, "Integral form of nuclide generation and depletion equations for Monte-Carlo simulation. Application to perturbation calculations", *Annals of Nuclear Energy*, 35, pp. 2156-2159, 2008.

Adjoint flux, importance, and Green function

The adjoint equation* of the Boltzmann equation is also often used in neutronics. The **adjoint flux*** is the solution of this equation. It is interpreted as the average number of neutrons issued from the history of an initial neutron of fixed energy, put in a given point of space. In a subcritical state, this number is finite. In contrast, in a critical or supercritical state, the sum of successive generations' daughters is infinite, hence a problem of interpretation. This leads "*to drop the adjoint flux concept for a supercritical system, and to consider the adjoint flux of a critical case as the limit of the adjoint flux of the subcritical case when its (negative) reactivity tends to zero… In a critical system, an infinitesimal fraction of neutrons has an infinite daughter population: evaluating the limit therefore raises a problem of the* " $0 \times \infty$ " *type.* » [1]

This mean number of daughters is a measure of the **importance*** [2] of the initial neutron considered to sustain chain reaction. Hence the name "**importance**" often used for this concept. Contrary to the flux, its mathematical nature is a function, and not a density.

The adjoint flux is used to tackle different neutronics problems, for example:

- In kinetics, where it helps define effective kinetic coefficients used for the kinetics of a point reactor;
- in kinetics and experimental neutronics, to carry out perturbation calculations, and design/interpret reactivity measurements [3];
- in transport and depletion, to calculate the sensitivity profiles allowing uncertainty calculations to be performed on physical quantities of interest, by propagation of the uncertainties coupled with the physical data of the problem to be solved (cross sections…);
- in Monte-Carlo transport, to speed up the simulation, and significantly increase its figure of merit;
- in transport, to achieve parametric studies, such as those relating to the determination of detector response as a function of reactor core power distribution, as is shown below:

Let us consider a detector k occupying a phase space domain Z, characterized by a response or sensitivity function s_k (*e.g.* a macroscopic cross section). The response associated with the scalar flux of neutrons $\phi(P)$, where P stands for the couple of variables $(\vec{r}, E)$, is written as follows:

$$R_k(Z) = \int_Z s_k(P)\,\phi(P)dP \qquad (1)$$

The flux $\phi(P)$ results from a neutron source $S(P')$ circumscribed within phase space domain Z'. Let us assume that the behavior of the $R_k(Z)$ response is to be investigated as a function of diverse distributions of sources $S(P')$. It is always possible to perform a transport calculation for each of the source distributions to be considered. Another calculation route consists in solving the adjoint transport equation, taking as the source term the sensitivity of the $s_k(P)$ detector for $P \in Z$. The solution of this equation provides the adjoint flux $\psi^+(P)$ and it can be shown that $R_k(Z)$ is also given by:

$$R_k(Z) = \int_{Z'} S(P')\,\psi^+(P')dP' \qquad (2)$$

The interest of this expression for parametric calculations is obvious, since it is only required to carry out a single adjoint transport calculation, and to convolute the resulting adjoint flux with the various source distributions considered to determine the corresponding $R_k(Z)$ response.

By the way, it is worth mentioning the relationship between the adjoint flux and the Green function $G(P' \to P)$:

$$R_k(Z) = \int_Z s_k(P)\,dP \int_{Z'} S(P')\,G(P' \to P)dP'$$
$$= \int_{Z'} S(P')\,dP' \int_Z s_k(P)G(P' \to P)dP$$

hence the following relationship after comparing with (2):

$$\psi^+(P') = \int_Z s_k(P)G(P' \to P)dP \qquad (3)$$

References

[1] P. Reuss, *Précis de neutronique*, p. 370, Les Ulis, EDP Sciences/INSTN, 2003.

[2] J. Lewins, *Importance – The Adjoint Function*, Pergamon Press, 1965.

[3] J. Bussac, P. Reuss, *Traité de Neutronique*, chapitre XXV : "Théorie des perturbations", pp. 403-415, Paris, Hermann, 1985.

The multiplication factor at step (n) is calculated as the ratio between the flux at step (n) and the flux at step $(n-1)$. So the eigenvalue problem is solved as a succession of fixed-source problems until reaching numerical convergence.

Equation (3) requires numerical resolution, often complex owing to the high number of unknowns, due to dimension 6 of the phase space $(\vec{r},\ E,\ \vec{\Omega})$. Its solution is the angular flux $\psi\ (\vec{r},\ E,\ \vec{\Omega})$, while the fission rate calculation only needs the knowledge of the scalar flux.

Space-dependent kinetics equations

The overall treatment of a time-dependent problem requires starting from the coupled equation system established in the chapter dealing with the fundamental equations of neutronics.

One often distinguishes the time evolution of the reactor core over a range from a second's fraction to a few minutes (power changes, reactor startup and shutdown phases, accidental situations), and fuel depletion through changes in its isotopic composition over timescales ranging from a few hours to several months. The latter feature is partially dealt within the chapter "Methods for solving generalized Bateman equations" (see *infra*, pp. 107-113).

Kinetics consists in predicting how the neutron population evolves at timescales in which the delayed neutron emission phenomenon plays a determining role in reactivity evolution. It is crucial for fine reactor control in normal and accidental situations.

As the delayed neutron source is expressed as a function of concentrations of precursor nuclei, the time evolution of these specific nuclides must be known. In contrast, as the timescale is relatively short, the time evolution of nuclide concentrations can be neglected regarding neutron transport.

The set of delayed neutron precursor nuclei is noted P. It is worth mentioning that these nuclei have the property **to be able** to decay through the $(\beta^-,\ n)$, channel, *i.e.* the β^- decay followed by the immediate emission of a neutron. Yet this channel is not their unique decay mode. In the specific case of bromine-87, one of the main precursors of delayed neutrons, its decay through the $(\beta^-,\ n)$ channel takes place in only 0.02% of cases.

Let us state that the ensemble of all the fissile nuclides that is disconnected from the P set, is denoted F. The precursor concentration depletion equation can be then written, relatively to the phenomenon of delayed neutron emission alone. In order to distinguish this equation from that derived from the Bateman equation, where all the transmutation processes would be taken into account, the concentration of a precursor p is noted C_p.

The main contribution to precursor generation is induced fission. The main contribution to precursor losses, relatively to the delayed neutron emission phenomenon alone, is their decay through the $(\beta^-,\ n)$ channel. By discarding the other causes of variation, the following equation can be obtained for a p precursor of the P set:

$$\frac{dC_p(\vec{r},t)}{dt} = -\lambda_{d,p}C_p(\vec{r},t) + \sum_{k\epsilon F} N_k(\vec{r})\beta_p^{(k)}\int_0^\infty dE'\,\nu_{t,k}(E')\sigma_{f,k}(E')\phi(\vec{r},E',t) \quad (5)$$

This is a balance, at point $\vec{r}$ and at instant t, of any precursor nuclide p. In this equation we note:

- $\lambda_{d,p}$: partial decay constant of nuclide p, corresponding to the $(\beta^-,\ n)$ channel;
- $\nu_{t,k}\ (E')$: mean total number of neutrons emitted during a fission induced by an incident neutron of energy E' on nuclide k;
- $\beta_p^{(k)}\,\nu_{t,k}\ (E')$: number of delayed neutrons arising from a p precursor, which originates in the fission induced at energy E' on nuclide k;
- $N_k\ (\vec{r})\ \beta_p^{(k)}\ \int_0^\infty dE'\ \nu_{t,k}\ (E')\ \sigma_{f,k}\ (E')\ \phi\ (\vec{r}\,,E',\ t)$: production of a p precursor by fission induced on nuclide k, knowing that, for one delayed neutron emitted, there is one precursor nucleus formed.

Usually, the **time emission of delayed neutrons** is parameterized, for each fissile nucleus $k \in F$, by grouping the emission processes due to precursor nuclei (about 150) into six or eight families denoted by the index couple $(k,\ i)$. To each family is associated a mean decay constant $\lambda_i^{(k)}$, which takes into account the production rate of the delayed neutrons arising from this family (so it corresponds to weighted partial decay constants $\lambda_{d,p}$ of the various precursor nuclei grouped in the family), as well as a proportion of delayed neutrons $\beta_i^{(k)}$. The concentration of "precursors" in the $(k,\ i)$ family is denoted $C_i^{(k)}$. It is given by the following equation:

$$\frac{dC_i^{(k)}(\vec{r},t)}{dt} = -\lambda_i^{(k)}C_i^{(k)}(\vec{r},t) + N_k(\vec{r})\beta_i^{(k)}\int_0^\infty dE'\,\nu_{t,k}(E')\sigma_{f,k}(E')\phi(\vec{r},E',t) \quad (6)$$

Using the parameterization of precursors makes it possible to write the delayed neutron source of the transport equation as follows:

$$\frac{1}{4\pi}\sum_{k\in F}\sum_i \lambda_i^{(k)}C_i^{(k)}(\vec{r},t)\chi_{d,i}^{(k)}(E)$$

where $\chi_{d,i}^{(k)}(E)$ is the delayed neutron proportion of the $(k,\ i)$ family emitted at energy E.

The transport equation is then rewritten as follows:

$$\frac{1}{v}\frac{\partial\psi(\vec{r},E,\vec{\Omega},t)}{\partial t} = -\vec{\Omega}.\vec{\nabla}\psi(\vec{r},E,\vec{\Omega},t) - \sum_k N_k(\vec{r})\,\sigma_k(E)\psi(\vec{r},E,\vec{\Omega},t) + \sum_k N_k(\vec{r})\int_0^\infty dE'\int_{4\pi} d\vec{\Omega}'\,\sigma_{s,k}(E'\to E,\vec{\Omega}'\to\vec{\Omega})\psi\left(\vec{r},E',\vec{\Omega}',t\right) + \frac{1}{4\pi}\sum_{k\in F} N_k(\vec{r})\int_0^\infty dE'\,\nu_{p,k}(E')\sigma_{f,k}(E')\chi_{p,k}(E'\to E)\phi(\vec{r},E',t) + \frac{1}{4\pi}\sum_{k\in F}\sum_i \lambda_i^{(k)} C_i^{(k)}(\vec{r},t)\chi_{d,i}^{(k)}(E) + S_{ext}(\vec{r},E,\vec{\Omega},t) \tag{7}$$

Coupled Equations (6) and (7) are called « **space-dependent kinetics equations** ».

Mireille Coste-Delclaux, Cheikh M. Diop, Fausto Malvagi and Anne Nicolas
Department for Systems and Structures Modeling

Deterministic Methods for Solving the Steady-State Boltzmann Equation

As mentioned by **B. Davison** and **J. B. Skypes** [1] in their pioneering work *Neutron Transport Theory*, published in 1957, if problems raised by the neutral particle transport theory have been identified, and partly solved, even before the neutron discovery, by astrophysicists such as **K. Schwarzschild** and **E. A. Milne**, and then, later on, by **S. Chandrasekhar**, who investigated radiative transfers, a *boomerang effect* was that methods developed later on in relation to neutron transport have benefited in radiative transfer treatment. The numerous methods developed within the framework of the neutron transport theory originate in the variety of situations to be investigated in reactor physics (multiplicity of forms, of materials, of dimensions, heterogeneities, steady and unsteady states conditions…). An examination of all of these methods evidences various computational strategies listed by **J. J. Duderstadt** and **W. R. Martin** [2] and summarized in Table 10 according to the degree of complexity of the transport problem to be solved:

- Simple analytical models that aim at analyzing a specific feature of the neutron population behavior. For example, the slowing-down theory makes it possible to understand the neutron energy spectrum profile, as well as the behavior characteristics of neutrons entering a resonance.

Table 10.

Types of neutron transport problems and computational strategies

A : possible analytical resolution N : numerical resolution

	Geometries					
	One-dimensional			Two-dimensional		Three-dimensional
Nature of the problem	**Infinite**	**Semi-infinite**	**Finite**	**x-y and r-z**		**General**
Energy						
Monokinetic	A	A	A	N	N	N
Multigroup	A	A, N	N	N	N	N
Continuous	A	A, N	N	N	N	N
Direction						
Isotropic	A	A	A	N	N	N
Anisotropic	A	A	N	N	N	N
Medium						
Vacuum	A	A	A	A	A	A
Purely absorbing	A	A	A	A	A	A
Homogeneous	A	A	A	N	N	N
Heterogeneous	N	A	N	N	N	N
Sources						
Localized: point, line, plane	A	A	A	N	N	N
Green function	A	A	A	N	N	N
Pulsed or oscillating	A	A	A	N	N	N
With or without boundary conditions	-	A	N	N	N	N
Any	N	N	N	N	N	N
Time dependence						
Steady-state conditions with fixed source	A	A	A	N	N	N
Steady-state conditions and critical state	A	A	A	N	N	N
Pulsed or oscillating source	A	A	A	N	N	N

- Approximations that "alter" the original form of the transport equation. The diffusion equation is one example.

- Deterministic numerical methods – *e.g.* S_N method, or method of characteristics (MOC) – or stochastic methods, such as the Monte-Carlo method, in order to treat complex configurations.

The **deterministic*** approach chosen to bring a computer solution to the Boltzmann equation in a steady state is based on a discretization of the phase space. Several types of discretization exist for a same variable, and modeling can be simultaneously introduced. All these possible options of related discretization and modeling, result in the development of as many numerical methods to solve the Boltzmann equation, each of them displaying advantages and drawbacks.

This section first gives a brief description of the transition from the continuous transport equation to a discretized form. Then the major principles of a few methods, among the deterministic numerical methods which are most typical of neutronics, are successively presented.

Phase space discretization

The knowledge of the angular flux $\psi(\vec{r}, E, \vec{\Omega})$, defined in the previous section, gives access to other quantities of interest to be evaluated. Among them, the scalar flux $\phi(\vec{r}, E)$ plays a prominent role, because the various reaction rates, the knowledge of which is indispensable for reactor physics studies, are computed starting from this quantity.

The deterministic resolution of the steady state Boltzmann equation lies in discretizing all the variables of the phase space, *i.e.* space $\vec{r}$, energy E, and direction $\vec{\Omega}$. The variable first discretized is usually energy and, then, the direction and space variables.

The 0-20 MeV energy range of neutrons is split into intervals conventionally called "energy groups" or, even more concisely, "**groups***" (see *supra*, p. 33). For instance, the APOLLO neutronics code solves the transport equation for 172 or 281 groups, or even 12,000 groups, according to the specificity of the physical configuration investigated and of the modelings adopted to represent the strong variation of neutrons cross sections in resonances. In the following pages, any group of the energy range will be denoted g.

The angular discretization ($\vec{\Omega}$ variable) generally exhibits about 100 to 1,000 directions, so as to get a fine description of the angular flux. The n^{th} direction of angular discretization is denoted $\vec{\Omega}_n$.

In a nuclear reactor, the system size is in the order of the meter, and the size of local heterogeneities (*e.g.* fuel clad thickness, characteristic length of flux gradient in rod, etc.) is in the order of the millimeter. So the space (variable $\vec{r}$) has to be divided into 10^3 meshes per dimension, which results in 10^9 space meshes. Any mesh of the space range is denoted i.

Applying such a discretization to the transport equation results in replacing the derivatives by, *e.g.* finite differences, and the integrals by discrete sums, or quadrature formulae. The angular flux $\psi(\vec{r}, E, \vec{\Omega})$ is replaced by the discretized forms $\psi_i^g(\vec{\Omega}_n)$, $\psi^g{}_{i-1/2}(\vec{\Omega}_n)$ et $\psi^g{}_{i+1/2}(\vec{\Omega}_n)$ which represent the angular neutron flux in the g energy group, in mid-interval i and at the latter's bounds denoted $(i - 1/2)$ and $(i + 1/2)$, and in direction $\vec{\Omega}_n$. Given the linear character of the transport equation, its discretization results in a linear equation system in which the quantities $\psi_i^g(\vec{\Omega}_n)$, $\psi^g{}_{i-1/2}(\vec{\Omega}_n)$ and $\psi^g{}_{i+1/2}(\vec{\Omega}_n)$ are the unknowns to be determined. An effective resolution of this system needs to get as many equations as unknowns. Hence the addition, on the one hand, of boundary conditions (*e.g.* the angular flux values at the boundaries of the reactor core), and, on the other hand, of relations modeling the space variation of the flux between mid-space intervals and their respective ends. As it allows compact writing, matrix formalism is often used to describe the system of equations to be solved.

Taking the above mentioned highest orders of magnitude for the various discretizations results in $10^9 \times 10^3 \times 10^5 = 10^{17}$ elementary volumes of the phase space. Consequently, that means solving, for each time step, linear systems with 10^{17} degrees of freedom!

Historically, it can be understood why analytical or semi-analytical models have initially prevailed in nuclear reactor physics, thereby allowing to significantly reduce the number of degrees of freedom, while being efficient. Gradually, some of these models have been hybrided with increasingly sophisticated numerical techniques, that the availability of electronic calculators and, then, of computers has caused to emerge.

Figure 21 below displays a few of the main methods used in neutronics to solve the transport equation:

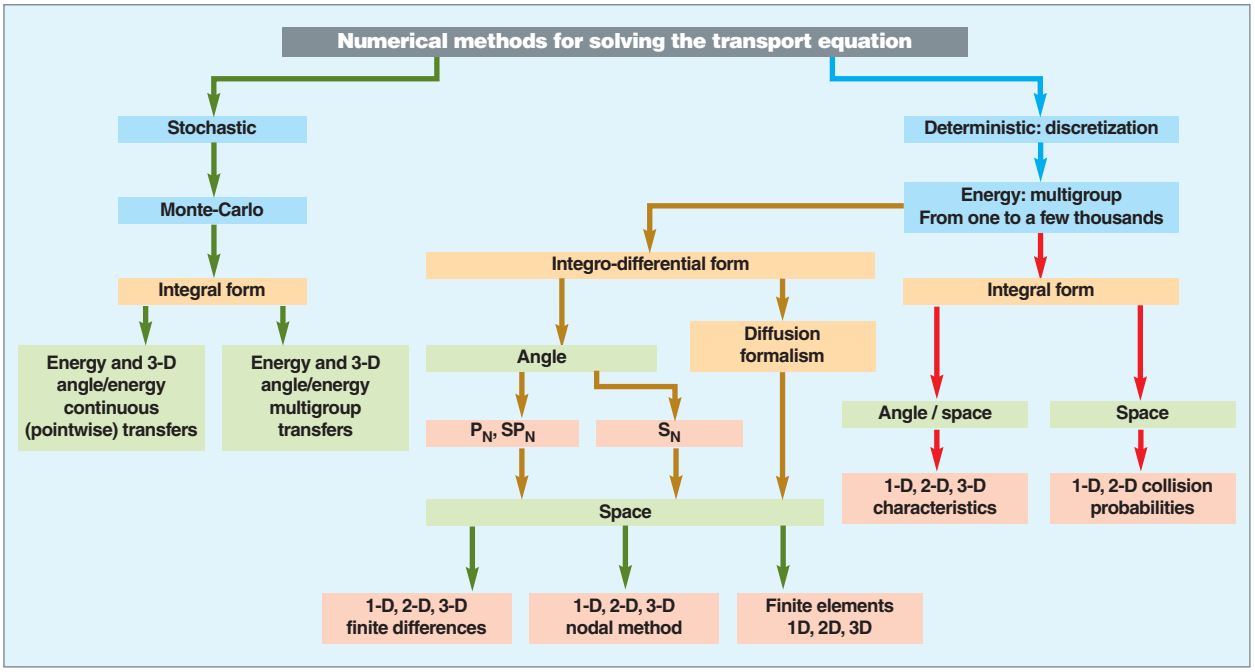

Fig. 21. Classification of the various numerical methods for solving the neutron transport equation (see also Y. Azmy, *International School in Nuclear Engineering*, Saclay, 2010).

The minimum number of unknowns associated with the calculation of a power nuclear reactor core

The discretization required by the numerical resolution of the Boltzmann equation results in the following minimum orders of magnitude for a 900-Mwe PWR:

- Assembly number: 150, 4 m high;
- rod/cell number (fuel, clad, moderator) per assembly: 17 x 17 = 289;
- total cell number: 150 x 289 = 43,350;
- number of concentric regions in fuel: 3;
- number of regions per cell: 3 + 2 = 5;
- number of axial regions: 40. One rod is 4 m long. As the axial flux gradient is *a priori* smaller than its radial gradient, the region is taken 10 cm high;
- number of regions per cell: 5 x 40 = 200;
- number of cells in the whole core: 8.6 10^6;
- Number of energy groups: 100;
- total number of scalar flux values (unknowns) in the whole core: 8.6 10^6 x 100 = 8.6 10^8.

If the scalar flux is built starting from the angular flux (*e.g.* in the case of the S_N method), the latter, too, has to be calculated. So about 250 angular directions have still to be defined, hence a number of unknowns – *i.e.* the angular flux values of interest – of about:

8.6 10^8 x 250 ~ 2 10^{11}.

The corresponding linear equation system is to be solved through iterations on the fission source, and on the thermal energy groups, and uses acceleration techniques.

Needs in computer memory coupled with such a resolution are assessed to be a few Gigaoctets.

It has been mentioned above that solving the transport equation with computational methods requires replacing continuous integrals by quadrature formulae. This is a numerical approximation with an associated error that depends on how fine the discretization of the variables of interest is.

Considering as an illustration a trapezoidal quadrature, and calling d the dimension of the problem under consideration (*e.g.* the 3 dimensions of space), and n the total number of discretization nodes, it is shown that the resulting error is proportional to:

$$1/n^{\frac{2}{d}}$$

This expression stands for the convergence rate of the quadrature selected as a function of the discretization fineness. So it can be observed that getting a target convergence (the given value of the error) is all the more costly in computational time as the d dimension of the problem to be solved is high.

The mean free path, and space and energy discretizations

The mean free path of a neutron in matter is the average distance it travels before interacting. The latter depends on the density of target nuclei $N(\vec{r})$, and on the total microscopic cross section $\sigma(E)$:

$$\lambda(\vec{r},E) = \frac{1}{N(\vec{r})\sigma(E)} = \frac{1}{\Sigma(\vec{r},E)}$$

The mean free path is the inverse of the total macroscopic cross section, and so depends, in a given point, of neutron energy. As many mean free paths can be defined as interaction types: in the previous definition, the total microscopic (resp. macroscopic) cross section is to be then replaced by the partial microscopic (resp. macroscopic) cross section under consideration.

Let us give a few orders of magnitude: in the 5%-enriched uranium dioxide UO_2, for slow neutrons of a few hundredths of eV, the fission mean free path is about 1 centimeter (*i.e.* the diameter of a fuel rod), and the capture mean free path is about 20 centimeters (*i.e.* the transverse dimension of an assembly). Yet, the cross section of the first U 238 capture resonances is neighboring 10,000 barns, which corresponds to a mean free path of about 50 micrometers.

In order to get an accurate neutronics calculation, the space discretization of the neutronics system to be investigated has to be of the same order of magnitude as the mean free path.

For comparison, the convergence of the stochastic Monte-Carlo method is controlled by a statistical error varying as $1/\sqrt{n}$ where n here stands for the number of neutron histories simulated in the physical system investigated. This expression shows that the statistical error behavior is independent of the dimension d of the problem considered.

The comparison between the convergence behaviors of both deterministic and stochastic approaches explains why the Monte-Carlo method becomes attractive when the dimension of the problem to be solved is increased.

Energy discretization

The solving of the transport equation is made especially complex by the energy variation of some data, such as the neutron cross sections of the nuclei present in a reactor.

It is worth to mention that the microscopic cross section of a nucleus characterizes the probability of a neutron to interact with this nucleus. This probability may get very high when the energy of the incident neutron is such that the energy conferred to the compound nucleus is close to the energy of one of its excitation levels. That corresponds to a sharp rise in the neutron-nucleus interaction cross section in the neighboring of these energies. The nucleus displays resonances for these energies and is said to be **resonant*** (see Fig. 22).

The transport equation can be solved, either in an energy pointwise approach (pointwise Boltzmann equation), or in an energy multigroup approach. In the first approach, the "accurate" energy variation of data is treated, and the pointwise distribution of neutrons as a function of energy is calculated. In the second approach, the energy range is discretized into a certain number of intervals, referred to as "groups", and only an average distribution of neutrons within each group is evaluated. Here, conventionally, the first group is that exhibiting the maximum energy and the last one is that displaying the minimum energy. As a matter of fact, most of neutrons arising from

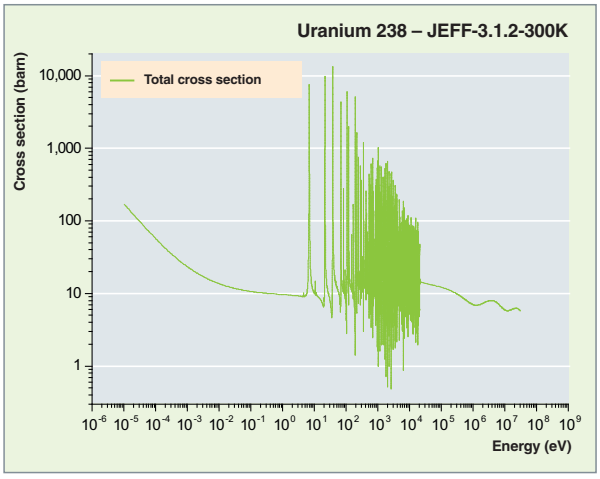

Fig. 22. Total microscopic cross section of uranium 238.

fission are generated at high energy (~ 2 MeV), and slow down to thermal energies (< ~ 1eV). Generally, the energy range is split into a "reasonable" number of groups, i.e. about a few hundreds to a few thousands. This number of groups is to be compared with the number of points used to represent the pointwise energy variation in cross sections in reference Monte-Carlo calculations (*i.e.* several dozens, or even several hundreds of thousands of points).

The integral of the pointwise angular flux $\psi(\vec{r}, E, \vec{\Omega})$ in the group is called the **multigroup angular flux** $\psi^g(\vec{r}, \vec{\Omega})$, that is:

$$\psi^g(\vec{r},\vec{\Omega}) = \int_g \psi(\vec{r},E,\vec{\Omega})\, dE$$

Similarly, the integral of the pointwise scalar flux $\phi(\vec{r}, E)$ is called the **multigroup scalar flux** $\phi^g(\vec{r})$, that is:

$$\phi^g(\vec{r}) = \int_g \phi(\vec{r},E)\, dE$$

In order to get the equations giving access to multigroup fluxes, the Boltzmann equation is integrated over each of the groups. These equations are named “multigroup equations”.

As an example, in the case of a steady state problem with an external source, the following multigroup equations can be obtained for the angular flux:

$$\vec{\Omega}.\vec{\nabla}\psi^{g}(\vec{r},\vec{\Omega}) + \sum_{k} N_{k}(\vec{r})\,\sigma_{k}^{g}\,\psi^{g}(\vec{r},\vec{\Omega}) = \sum_{k} N_{k}(\vec{r}) \sum_{g'} \int_{4\pi} d\vec{\Omega}'\,\sigma_{s,k}\left(g' \to g, \vec{\Omega}' \to \vec{\Omega}\right)\psi^{g'}(\vec{r},\vec{\Omega}') + S_{ext}^{g}(\vec{r},\vec{\Omega}) \quad (1)$$

These equations would contain no approximation if the multigroup cross sections $\sigma^{g}(\vec{r},\vec{\Omega})$ and the transfer **cross sections*** $\sigma^{g'\to g}(\vec{r},\vec{\Omega}'\to\vec{\Omega})$ were defined as averages weighted by the energy pointwise angular flux $\psi(\vec{r},E,\vec{\Omega})$, which would mean that these microscopic multigroup cross sections would be space- and angle-dependent. In practice, to avoid angular dependence, these cross sections are weighted by the scalar flux $\phi(\vec{r},E)$, which leads to multigroup cross sections depending only on space. For example, the total cross section is defined by:

$$\sigma^{g}(\vec{r}) = \frac{\int_{g} \sigma(E)\phi(\vec{r},E)\,dE}{\int_{g} \phi(\vec{r},E)\,dE} \quad (2)$$

Despite this approximation, getting multigroup nuclear data still remains one of the most delicate problems of neutronics that today still requires complex modeling known as “self-shielding formalism”. As an example, we shall describe in the following paragraph the **self-shielding*** formalism used in the APOLLO2 code.

Self-shielding formalism

Definition of multigroup cross sections

The data of the multigroup equation are multigroup cross sections. These cross sections are defined in such a way that, for each group g, the multigroup reaction rate (*i.e.* the product of the multigroup cross section by the multigroup scalar flux, which is the solution of the Boltzmann multigroup equation) be equal to the value, integrated on group g of the pointwise reaction rate (the product of the pointwise cross section by the scalar flux, which is the solution of the Boltzmann pointwise equation). So the aim is to preserve, in each group g, the number of reactions observed between a neutron and a nucleus, per unit time and volume.

For simplicity, equations in this paragraph are written as a function of the variable “**lethargy***”, and not as a function of the variable “energy”.

So the multigroup cross section in group g, for the nuclear reaction of type q induced by a neutron, σ_{q}^{g}, is obtained by writing reaction rates conservation:

$$\sigma_{q}^{g}(\vec{r})\,\phi^{g}(\vec{r}) = \int_{g} \sigma_{q}(u)\phi(\vec{r},u)du \quad (3)$$

In equation (3), $\phi(\vec{r},u)$ stands for the scalar flux at point $\vec{r}$ and at lethargy u, and $\phi^{g}(\vec{r})$ for the multigroup scalar flux at point $\vec{r}$, in group g.

Reaction rates are quantities which depend on space, through the flux (except in the case of an infinite homogeneous medium). So is it for multigroup cross sections $\sigma_{q}^{g}(\vec{r})$.

Consequently, strictly speaking, it is not possible to define multigroup cross sections of nuclei once for all, and build libraries of non-geometry-dependent multigroup cross sections.

Equation (3) shows how complex it is to get these sections:

- The pointwise reaction rates to be preserved (right hand term of Equation (3)) are unknown, since the pointwise flux is unknown;
- the multigroup flux $\phi^{g}(\vec{r})$ is the solution of the Boltzmann multigroup equation, the data of which are to be calculated (multigroup cross sections $\sigma_{q}^{g}(\vec{r})$) ;
- the pointwise cross sections $\sigma_{q}(u)$ may have a resonant behavior as a function of lethargy.

It is natural to try to simplify Equation (3) using instead of the actual unknown flux $\phi(\vec{r},u)$, a known weighting spectrum (representative of the reactor to be treated), independent of space: $\phi_{w}(u)$. Such is the process applied when building multigroup data libraries (see *supra*, pp. 33-35).

As a conclusion, two methods for getting multigroup cross sections can be distinguished:

- Those using the actual flux $\phi(\vec{r},u)$.
  - The multigroup cross sections are called **self-shielded multigroup cross sections**.
  - They are given by Equation (3).
  - They are space-dependent, and can be obtained only when the actual flux is known.

- Those using a known weighting spectrum $\phi_{w}(u)$.
  - The multigroup cross sections are called “infinite-dilution” multigroup cross sections. The terminology used will be explained in the following pages.

- They are denoted $\sigma^{g}_{q,\infty}$, and are given by Equation (4);
- They are space-independent, and can be calculated once and for all prior to transport calculation, during the building of multigroup libraries.

$$\sigma^{g}_{q,\infty} = \frac{\int_g \sigma_q(u)\phi_W(u)du}{\int_g \phi_W(u)du} \qquad (4)$$

It is worth to investigate "infinite-dilution" multigroup cross sections from the relevance point of view. Apart from their resonance range, nuclei have cross sections which vary slowly and regularly with lethargy. In this case, the influence of the weighting spectrum used to average their cross sections is weak, and the simplified weighting described by Equation (4) is relevant.

Yet, as regards resonant nuclei, in the resonance range, this simplification is generally unacceptable (coarse multigroup energy meshing). As a matter of fact, cross sections may vary several times and by several decades, inside a group of the multigroup meshing (see Fig. 23). So self-shielded multigroup cross sections have to be calculated with Equation (3) in the specific geometry of the case to be dealt with.

The physical self-shielding phenomenon

The physical self-shielding phenomenon can be described as follows. In a given medium, the neutron flux dips, as a function of energy, all the more sharply as the macroscopic cross section of this medium is high. So reaction rates exhibit energy-dependent variations much slower than those experienced by cross sections and flux. This compensation of effects in reaction rate calculation is referred to as **self-shielding**.

Calculation of multigroup cross sections, when performed using the actual flux that dips at the level of resonances, takes account of the self-shielding phenomenon, and thus leads to **self-shielded multigroup cross sections**.

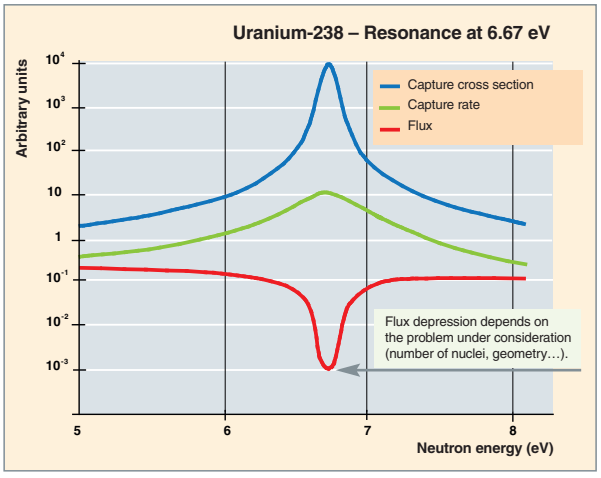

Fig. 23. The self-shielding phenomenon.

The self-shielding phenomenon exhibits both an energy and a space aspect. As a matter of fact, it takes place at nuclide **resonance*** energies, and in materials containing resonant nuclides.

In order to illustrate the space aspect of self-shielding, let us take the example of a 6.67 eV neutron (*i.e.* at the energy of the first uranium 238 resonance). In uranium dioxide, this neutron mean free path is only 80 µm, which means that it cannot penetrate deeply inside the fuel rod of a thermal neutron reactor. As a result, the peripheral part of the fuel rod will be differently irradiated from the rod center. Neutronics calculations are to be able to describe this phenomenon, which will require a very fine space meshing on the peripheral part of the rod, in the case when a meshed calculation is used.

The energetic feature of the self-shielding phenomenon is schematized in Fig. 23.

Concerning uranium 238, in the case of a 6.67 eV resonance, the capture cross section varies by four decades approximately, and the flux, by a little less than three decades in the reverse way, while the reaction rate only varies by about one decade.

Stakes of self-shielding phenomenon modeling

Taking into account the self-shielding phenomenon as part of a multigroup transport code is indispensable. Let us take the example of the calculation of a cell that contains a fuel rod consisting of uranium 238 and uranium 235, with an energy meshing of a hundred groups. If calculation is carried out using infinite-dilution multigroup cross sections of uranium 238, instead of its self-shielded multigroup cross sections, the uranium 238 absorption rate within its resonance range is over-estimated by a factor 2, and the value of the effective multiplication coefficient, which characterizes the balance of the chain reaction taking place in a nuclear system, is under-estimated by 25%. The orders of magnitude of these calculated quantities are lost.

So the self-shielding phenomenon has to be modeled in deterministic multigroup codes before any flux calculation. For these codes, such a modeling can thus be seen as the last step of cross section treatment.

In thermal neutron reactors, the major resonances to be treated are heavy nucleus absorption resonances. But for fast neutron reactors, or for specific calculations (*e.g.* reflector calculations), scattering resonances of lighter nuclei such as sodium or iron have also to be taken into account.

Principles of self-shielding phenomenon modeling

As shown by Equation (3), a necessary step in calculating the self-shielded multigroup cross sections of a resonant nucleus is assessing the actual flux $\phi(\vec{r}, u)$ which depends on space and energy variables. In fact, the main energy range for which nuclei display resonances, is the slowing-down energy range (from a few hundreds of keV to a few eV). The flux used to calculate self-shielded multigroup cross sections is thus obtained solving a slowing-down equation. The space distribution of the flux is calculated through a discretization of the media containing the resonant nucleus in various self-shielding regions denoted α. It is assumed that, in each self-shielding region α, the flux is pointwise in lethargy, and is constant in space. It is denoted $\varphi_\alpha(u)$, and is used to calculate self-shielded multigroup cross sections in the region α.

Through this modeling a set of multigroup cross sections specific of each self-shielding region α can be associated with a resonant nucleus. For a reaction of type q, they are given, in each energy group g, by Equation (5):

$$\sigma_{q,\alpha}^{g} = \frac{\int_g \sigma_q(u)\varphi_\alpha(u)du}{\varphi_\alpha^g} \qquad (5)$$

where φ_α^g is the multigroup flux in the group g and the region α.

There exist two families of methods allowing self-shielded multigroup cross sections to be calculated for resonant nuclei.

Methods using an equivalence with an infinite homogeneous medium

An equation called "fine structure equation" can be derived from the slowing-down equation. This equation is established in an infinite homogeneous medium in the inset below (p. 68).

As regards methods using an equivalence with an infinite homogeneous medium, the fine structure factor, the solution of the fine structure equation in the self-shielding region α, is selected to be used for $\varphi_\alpha(u)$ [in Equation (5)]. The self-shielding calculation can then be performed in the two following steps:

- As the pointwise reaction rates associated with this fine structure factor cannot be directly calculated in the frame of the self-shielding phenomenon modeling (the fine description of energy transfers is "lost" in a multigroup calculation), the self-shielding calculation assesses them by establishing an equivalence with an infinite homogeneous medium, for which these reaction rates are known thanks to tabulations performed prior to the transport code, at the step of library construction (*cf.* insert, p. 68).
- Once obtained the pointwise reaction rates, the self-shielding calculation achieves a second equivalence called "multigroup equivalence", which calculates multigroup cross sections preserving these reaction rates for the multigroup Boltzmann equation.

The tricky part of such a calculation is how to get the reaction rates to be preserved. As a matter of fact, this part requires a physical modeling of the resonant slowing-down operator. The "multigroup equivalence" part corresponds to the solving of a nonlinear system.

The methods of this type, initially dedicated to thermal neutron reactors, are implemented in several multigroup transport codes, such as APOLLO, WIMS, HELIOS, CASMO, LANCER02, and DRAGON (*cf.* neutronics code table, p.138-139).

"Subgroup"-type methods

The "subgroup"-type methods were initially dedicated to fast neutron reactors.

They rely on the fundamental assumption that resonant cross sections and collision densities (slowing-down sources) are not correlated. This assumption is checked in the unresolved resonance range of nuclei (a prevailing range in the case of fast neutron reactors) or in any energy range, provided that the multigroup meshing be sufficiently fine. These methods are reference methods in their scope. They are part of the ECCO code and the APOLLO code.

Thanks to these methods, which do not require any modeling of the resonant slowing-down operator, self-shielded multigroup cross sections can be obtained through a direct solution of the slowing-down equation in every self-shielding region α. These cross sections are then given by Equation (6).

$$\sigma_{q,\alpha}^{g} = \frac{\int_g \sigma_q(u)\,\varphi_\alpha(u)du}{\int_g \varphi_\alpha(u)du} \qquad (6)$$

The "subgroup"-type methods can also be "extended" so that their scope may include thermal neutron reactors even with a coarse multigroup meshing. This is done in the WIMS code or the DRAGON code. The resulting methods can no longer then be considered as reference methods.

Flux factorization - Fine structure notion

Due to the resonant character of cross sections, the flux, too, has a resonant character. Usually, the scalar flux ϕ is factorized in a macroscopic flux Υ, which is the flux prevailing outside the resonances, and which so exhibits a very slow variation as a function of lethargy, and in a fine structure factor φ, which characterizes the resonant behavior of the flux in the resonance. This factor is dimensionless. The equation allowing this calculation is referred to as the "fine structure equation". It results from factorizing the scalar flux in the slowing-down equation.

For an infinite homogeneous medium containing a resonant nucleus, the data of which have a 0 index, and moderating nuclei, the data of which have a 1 index, the slowing-down equation can be written as follows:

$$\left(N_0\sigma_0(u) + \Sigma_1(u)\right)\phi(u) = N_0 r_0\phi(u) + \mathrm{R}_1\phi(u)$$

- N_0: number of resonant nuclei per unit volume;
- $\sigma_0(u)$: total microscopic cross section of the resonant nucleus at lethargy u;
- $\Sigma_1(u)$: total macroscopic cross section of moderating nuclei at lethargy u;
- $r_0\phi(u)$: microscopic slowing-down operator for resonant nucleus;
- $R_1\phi(u)$: macroscopic slowing-down operator for moderating nuclei.

This balance equation expresses the fact that there are as many neutrons disappearing by collisions as there are neutrons produced through slowing-down at a given lethargy u.

The macroscopic flux and the fine structure factor are respectively given by:

$$\begin{cases} \Upsilon(\mathrm{u}) = \dfrac{\mathrm{R}_1\phi(u)}{\Sigma_1(u)} \\ \varphi(\mathrm{u}) = \dfrac{\phi(u)}{\Upsilon(u)} \end{cases}$$

The microscopic operator of slowing-down on the resonant nucleus is expressed by:

$$r_0\phi(u) = \int_{u-\varepsilon_0}^{u} \sigma_{s0}\left(u' \to u\right)\phi\left(u'\right)du'$$

where ε_0 is the maximum gain in lethargy on the resonant nucleus (about $\frac{4}{a}$ for a heavy nucleus, a being the ratio between nucleus mass and neutron mass).

By substituting the product of the fine structure factor and the macroscopic flux for the real flux in the slowing-down equation, and performing the approximation $r_0(\varphi\Upsilon)(u) \approx \Upsilon(u) r_0\varphi(u)$, the latter being justified by the fact that the integration range of the operator r_0 is very small, and the macroscopic flux $\Upsilon(u)$ undergoes a very low variation versus lethargy, it can be obtained:

$$\left(\sigma_0(u) + \frac{\Sigma_1(u)}{N_0}\right)\varphi(u) = r_0\varphi(u) + \frac{\Sigma_1(u)}{N_0}$$

The parameter σ_b, *i.e.* the ratio between the total macroscopic cross section of moderating nuclei and the number of resonant nuclei per unit volume:

$$\sigma_b = \frac{\Sigma_1(u)}{N_0}$$

characterizes the resonant nucleus dilution in moderating nuclei. It is referred to as the "dilution cross section". This leads to the so-called **fine structure equation**:

$$(\sigma_0(u) + \sigma_b)\varphi(u) = r_0\varphi(u) + \sigma_b$$

When the number of resonant nuclei equals zero, the dilution cross section becomes infinite. Then there is no longer a self-shielding phenomenon, since there are no more resonances. This is what explains the terminology "infinite dilution multigroup cross sections" in relation to the multigroup cross sections calculated without taking the self-shielding phenomenon into account (see Equation [4]).

In the case of an infinite homogeneous medium which contains a single resonant nucleus, the fine structure equation is solved, for a series of temperatures and dilutions, by codes using pointwise nuclear data. These calculations are generally done by nuclear data processing systems at the multigroup library construction step.

The results are kept as tabulations, as a function of temperature and dilution, of the different reaction rates (absorption, scattering and production) of the resonant nucleus on a given multigroup meshing. These reaction rates are named "effective reaction rates", and are part of the basic data of the self-shielding methods proceeding by equivalence with an infinite homogeneous medium.

Treatment of a mixture of resonant nuclei

One particularly tricky point of self-shielding phenomenon modeling is the treatment of a mixture of resonant nuclei. This treatment is often carried out through simplified methods, among which:

- Iterative methods: each resonant nucleus is separately computed, while other resonant nuclei are considered as moderating nuclei with constant cross sections for each group. These calculations can be iterated.

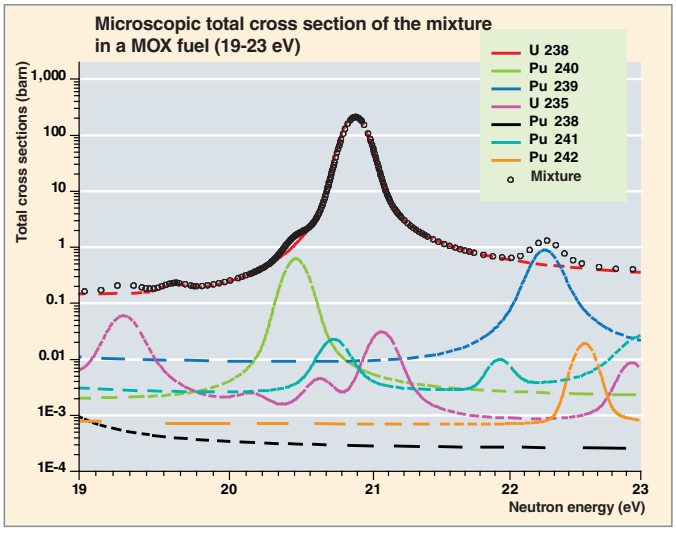

Fig. 24. MOX fuel: resonance overlapping and microscopic total cross section of the mixture.

- "Williams" type methods: the nuclear reaction rates in the mixture are calculated from the reaction rates of the nucleus alone (when other resonant nuclei are replaced by their potential cross sections), and from a corrective factor (characterizing the resonant mixture) evaluated with the help of a fine multigroup calculation.

These simplified methods do not correctly take into account the flux depression due to all of the resonances of all the present nuclei. So a difficulty emerges when nuclei constituting the resonant mixture display resonance overlapping. This problem is shown on Fig. 24, in which are plotted the cross sections of the resonant nuclei present in a mixed uranium and plutonium oxide (MOX) fuel, in a 19-23 eV energy range.

The fundamental idea of the treatment developed in the APOLLO2 code is to consider the resonant mixture as a unique resonant entity which has the same cross section as the mixture. This cross section is displayed with black circles on Fig. 24.

Resonant mixture treatment is presented as part of the method using an equivalence with an infinite homogeneous medium, the so-called "Livolant-Jeanpierre" method, after the name of its two authors who devised it in the APOLLO-1 code in the late sixties.

What is of interest, here, is only the calculation of the reaction rates to be preserved in the self-shielded multigroup cross section calculation, for, as already mentioned, this very part is what needs to be modeled. These rates result from the solving of the fine structure equation in each self-shielding region. This equation is established, using the collision probability method (see p. 84) to deal with the space variable.

In order to set up this equation in a given geometry, it shall be assumed that the macroscopic flux is flat with respect to space, an assumption which has not been disproved till now.

For a mixture of M resonant nuclei, the fine structure equation can be written as follows:

$$\begin{cases} \varphi_\alpha(u) = \sum_\beta C_{\alpha\beta}(u) R_{0\beta}\varphi_\beta(u) + S_\alpha(u) \\ R_{0\beta}\varphi_\beta(u) = \sum_{m=1}^{M} a_{0m\beta} r_{0m\beta}\varphi_\beta(u) \end{cases} \quad (7)$$

- $\varphi_\alpha(u)$: fine structure factor in region α
- $r_{0m\beta}\ \varphi_\beta(u)$: slowing-down operator of the m *component of the resonant mixture in region* β
- $a_{0m\beta}$: proportion in the resonant mixture of component m in region β

In this equation, the C, matrix, deduced from the probability collision matrix, gives the space coupling between the different self-shielding regions and the vector S, the sources resulting from non-resonant nuclei.

Modeling of the resonant slowing-down operator

Within the framework of a multigroup calculation on a coarse meshing, any fine piece of information on energy transfers has been lost. So it is no longer possible to accurately take into account the energy coupling resulting from resonant slowing-down operators. This is why Equation (7) is simplified through introducing a modeling of these operators. There exist several slowing-down models, either "physical", i.e. relating to a shape or a resonance distribution, or "mathematical", *i.e.* general. The following models can be mentioned:

- NR : "Narrow Resonance", which treats an isolated narrow resonance within a group,
- WR : "Wide Resonance", which treats an isolated broad resonance within a group,
- ST : which treats a "STatistical" distribution of narrow resonances within a group,
- TR : *"Toute Résonance"* (*i.e.* any resonance), which treats any resonance distribution.

In the case of mixture treatment, the model used was the TR model that approximates operator r_{0m} through:

$$\forall u \in g \quad r_{0m}\varphi^{TR}(u) = \sum_{g' \le g} \pi_m(g', g) \langle\ \sigma_{s0m}\varphi\rangle^{g'} \quad (8)$$

In this formulation, $\pi_m(g', g)$ is the average probability for the neutron to be scattered by the resonant nucleus m from group g' to group g and $\langle\sigma_{s0m}\varphi\rangle^{g'}$ is the average scattering reaction rate of the resonant nucleus m within group g'.

The "TR" modeling exhibits a fundamental property used in the following: the finer the multigroup meshing, the more accurate the TR modeling relating to this meshing.

The "TR" modeling of heavy slowing-down operators helps solve Equation (7) in a numerically approximated manner, and so deduce from it an approximate flux denoted $\varphi_{\alpha}^{TR}(u)$ in each self-shielding region. Thanks to the specific quadrature formulae deduced from the probability tables of each nucleus in the resonant mixture, approximated reaction rates are computed in group g, for each mixture component m and each self-shielding region α. For reaction q, they are written as follows:

$$T_{q0m\alpha}^{g,TR} = \int_{g} \sigma_{q0m}(u)\varphi_{\alpha}^{TR}(u)du \qquad (9)$$

Equivalence with an infinite homogeneous medium

The reaction rates obtained by Equation (9) contain the modeling error on the resonant slowing-down operators. In order to eliminate this error, for each resonant group g, each self-shielding region α, and each mixture component m, an equivalence is established with an infinite homogeneous medium containing the resonant nucleus mixture at a certain dilution to be defined.

This equivalence is made explicit through the fine structure equation written for the mixture in an infinite homogeneous medium, modeling the slowing-down operators with the "TR" model previously described in Equation (8):

$$\left(\sum_{m=1}^{M} a_{0m}\sigma_{0m}(u)+\sigma_b\right)\varphi(u)=\sum_{m=1}^{M} a_{0m}\sum_{g'\le g}\pi_m(g',g)\langle\sigma_{s0m}\varphi\rangle^{g'}+\sigma_b \qquad (10)$$

This equation helps obtain an analytical formulation of the fine structure factor, which is parameterized versus the dilution σ_b.

The equivalence principle is the following:

- For each resonant group g, each self-shielding region α, and each mixture component m, an infinite homogeneous medium characterized by its dilution (so-called the "equivalent dilution") is sought, so that the absorption rate computed with the "TR model" be the same for component m in the infinite medium and in the self-shielding region α;

- according to whether the resonant mixture consists of a single nucleus or several nuclei, the treatment will vary as follows:
  - In the specific case when the resonant mixture consists of a single nucleus, an interpolation is performed, at the equivalent dilution, in the tabulated exact reaction rates of the nucleus, computed in an infinite homogeneous medium (see inset "Flux factorization - Fine structure notion", p. 68) ;
  - in the case of an infinite homogeneous medium containing a resonant nucleus mixture, the fine structure equation can no longer be solved once for all prior to the transport calculation, since the proportions of the mixture's different nuclei are unknown. Therefore, the "exact" solving of the fine structure equation in an infinite homogeneous medium has to be carried out during the self-shielding calculation. This is achieved by approximating the resonant slowing-down operators through their "TR" models performed on an extremely fine multigroup meshing consisting of over a dozen thousand groups. This modeling is then almost exact as explained above;

- finally, the "corrected" reaction rates are deduced in each resonant group g and each self-shielding region α.

This equivalence is summarized in Fig. 25 below:

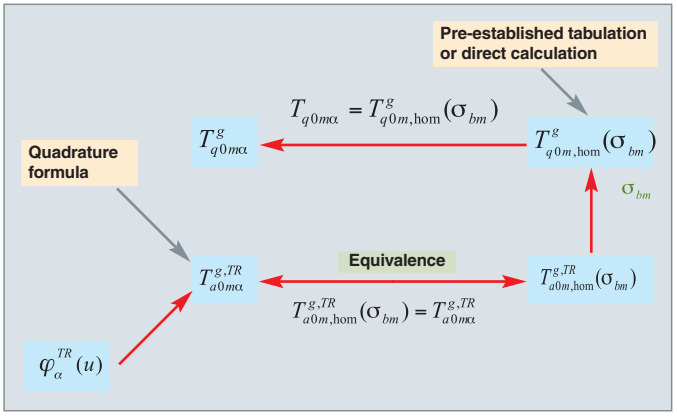

Fig. 25. Equivalence between homogeneous and heterogeneous reaction rates for a mixture of resonant nuclei.

During the calculation for one nucleus, quadrature formulae can be established once for all, and stored in multigroup data libraries, whereas they have to be computed "on the fly" for a mixture of resonant nuclei, as relative proportions are not known.

Modeling a mixture of resonant nuclei: example of validation on a boiling water reactor (BWR) assembly calculation

The illustration presented here is drawn from the study of the international benchmark ATRIUM-10 MOX. The aim is to compute a BWR assembly. The physical quantities calculated are the effective neutron multiplication factor, k_{eff}, and the absorption reaction rates on various resonant nuclides: uranium 238, plutonium 239, plutonium 240, and plutonium 241. The validation route relies on comparing the results drawn from three types of calculation:

- A reference calculation using the Monte-Carlo transport code TRIPOLI-4® (one hundred million neutron histories were simulated);
- an APOLLO2 calculation, denoted ITER, which uses the iterative method to calculate self-shielded multigroup cross sections;
- an APOLLO2 calculation, denoted MEL, which uses the resonant mixture treatment method.

The two APOLLO2 calculations have been carried out on a 172-group energy meshing, and the self-shielding calculation was achieved between 13.71 eV and 203.995 eV, energy range corresponding to groups 64 to 82.

The ATRIUM-10 assembly is a 10 x 10 assembly containing:

- "MOX" fuel rods in which fuel consists of PuO_2/UO_2 mixed oxide, with six different plutonium enrichments (MOX1 to MOX6 cells);
- absorbing rods consisting of uranium oxide and gadolinium (UOXG cells).

"MOX" fuel rods basically consist of depleted uranium (0.2% mass enrichment in uranium 235). Absorbing rods consist of enriched uranium (3.95% mass enrichment in uranium 235). The treated assembly does not contain any inserted control cross.

Figure 26 represents the geometry of an ATRIUM-10 assembly eighth.

The comparison of the effective multiplication factors between the two APOLLO2 calculations and the TRIPOLI-4® calculation is given in Table 11:

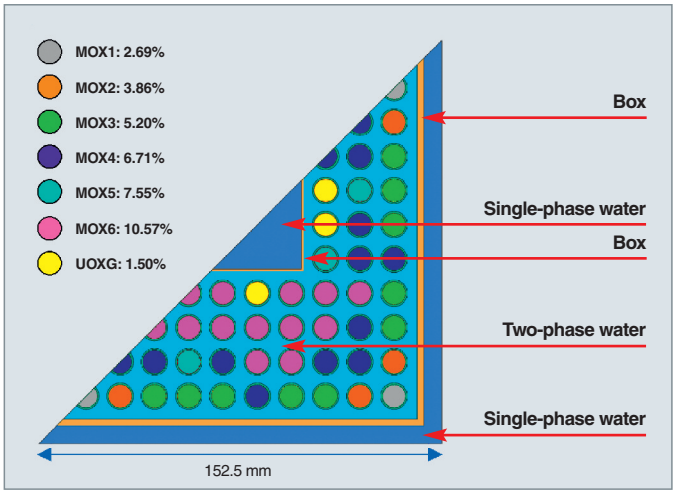

Fig. 26. Geometry of an ATRIUM-10 assembly eighth.

Table 11.

Effective multiplication factors from TRIPOLI-4® and APOLLO2 calculations for an ATRIUM-10 MOX fuel assembly

	k_{eff}	σ TRIPOLI-4®	Discrepancy in **pcm***
TRIPOLI-4®	1.14016	11 pcm	
ITER calculation	1.13637		-379 ± 33
MEL calculation	1.13795		-221 ± 33

Although none of the two APOLLO2 calculation results is in the three standard deviation bars of TRIPOLI-4®, it can be observed that using the resonant mixture direct treatment model enables the calculation result to be significantly improved, by about 160 pcm. This conclusion is corroborated by the detailed (group by group, and nucleus by nucleus comparison of deterministic and stochastic calculations.

As an illustration, Figure 27 shows resonant absorption in "MOX-6"-type fuel rods, which display the highest plutonium content, and are so the most sensitive to the resonance overlapping phenomenon (see Fig. 28). The lower graph represents the reference reaction rates (expressed in pcm) calculated by TRIPOLI-4®. The higher graph represents the relative discrepancies, expressed in %, between the APOLLO2 and TRIPOLI-4® calculations. With the MEL method, in "MOX-6"-type fuel rods, the resonant absorption integrated between groups 64 and 82 is computed very accurately, since the relative discrepancy is 0.16%, whereas it was 4.27% when using the iterative method. Moreover, relative discrepancies in all groups are reduced from 16.4 to 2.3%, which is an excellent result. The most visible improvements are brought in groups 69, 73, and 82, in which resonance overlapping can be respec-

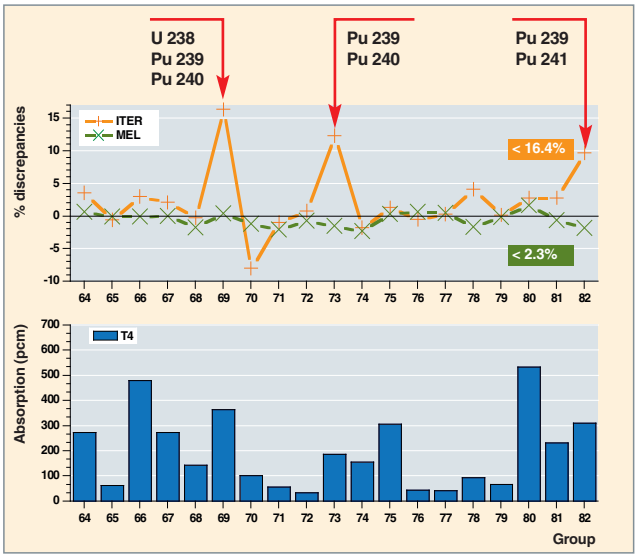

Fig. 27. Resonant absorption in "MOX-6" fuel rods: comparison of self-shielding models in the case of resonance overlapping, versus the Monte-Carlo reference code TRIPOLI-4® (referred to as T4). It is worth to mention the contribution of the mixture treatment model.

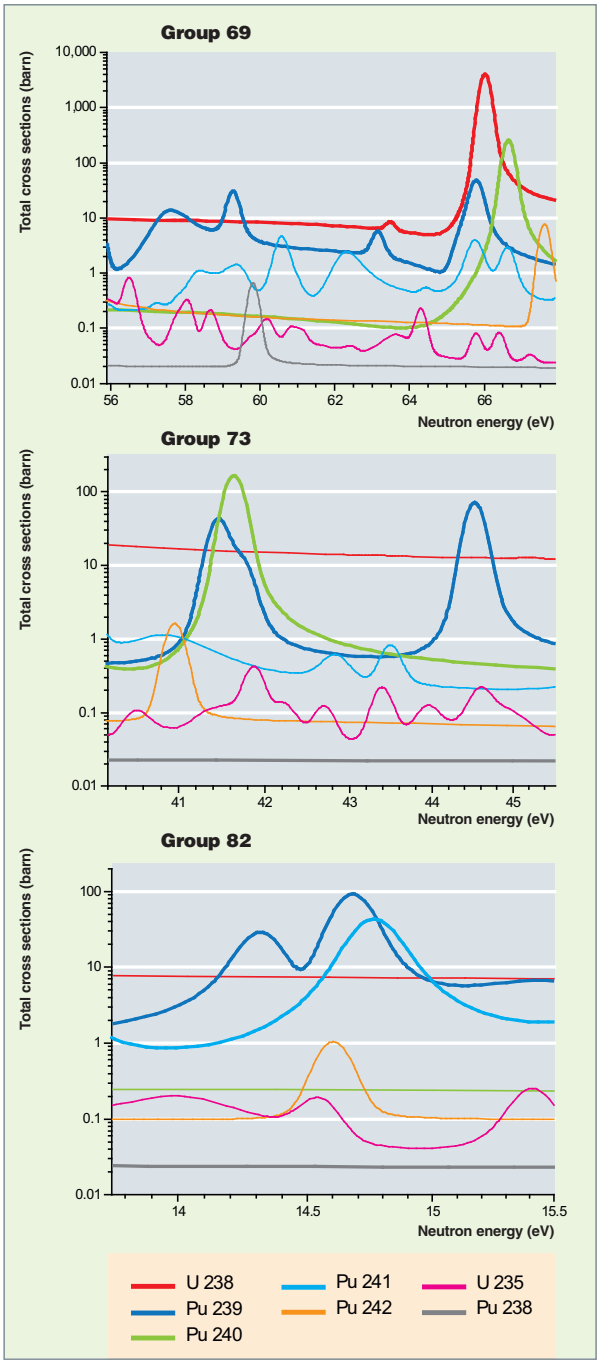

Fig. 28. Resonance overlapping in "MOX-6" fuel rods.

tively observed between uranium 238, plutonium 239, and plutonium 240, between plutonium 239 and plutonium 240, and between plutonium 239 and plutonium 241. This overlapping can be seen in Figure 28.

Outlooks

The modeling of the self-shielding phenomenon is one of the trickiest steps of a deterministic multigroup transport code, but it has now reached some maturity.

Methods based on equivalence with an infinite homogeneous medium have been refined to the utmost in order to take into account complex geometries, temperature profiles in fuel, resonance overlapping…

"Subgroup"-type methods, that are by nature much simpler and more accurate as they do not require any modeling of the slowing-down operator, are only adapted to the unresolved resonance range or to a fine multigroup meshing. As computer power is always increasing, these methods are bound to be used in the future. Of course that will mean a cost, that is the use of a sufficiently fine energy meshing, but the self-shielding calculation can be carried out on a multigroup meshing different from that of the flux calculation.

Angle discretization for a given energy group

The discretization related to the direction variable $\vec{\Omega}$ of the phase space is called "angle discretization". It benefits from the above mentioned isotropy of the materials crossed by neutrons.

There are two methods mainly used to treat the angular variable: one is a *collocation method*, known as the *discrete ordinates method* or S_N method; the other is an angular flux expansion method based on spherical harmonics, known as the P_N method, or *spherical harmonics method*.

S_N method

The **S_N method** consists in selecting a set of discrete directions in 4π steradians: $\{\vec{\Omega}_n; n = 1, N\}$, and writing the transport equation for these directions. The source steady-state transport equation, for one group g, is:

$$\vec{\Omega}_n.\vec{\nabla}\psi^g(\vec{r},\vec{\Omega}_n) + \Sigma^g(\vec{r})\psi^g(\vec{r},\vec{\Omega}_n) = \int_{4\pi} d\vec{\Omega}'\,\Sigma_s(\vec{r}, g\to g, \vec{\Omega}'\to\vec{\Omega}_n)\psi^g(\vec{r},\vec{\Omega}') + S_n^g(\vec{r},\vec{\Omega}_n) \quad (11)$$

In order to assess the integral over the angles, the following quadrature formula can be used:

$$\int_{4\pi} d\vec{\Omega} f(\vec{\Omega}) = \sum_{n=1}^{N} w_n\, f(\vec{\Omega}_n) \quad (12)$$

Once selected the N directions $\vec{\Omega}_n$ and the N weights w_n, Equation (11) can be written N times for n =1,…N, and a source coupled equation system which unknowns are $\psi_n^g = \psi^g(\vec{r},\vec{\Omega}_n)$ has to be solved. These space differential equations have to be discretized with respect to space variable.

To the origins of the discrete ordinates method, or S_N method

G. C. Wick was an Italian theoretical physicist who brought major contributions in the Quantum Field Theory. In his works he was led to approximate an integro-differential equation by a system of differential equations, replacing the integral term by a **quadrature formula** [1]:

$$\int_{-1}^{+1} f(\mu)d\mu \approx \sum_{j=1}^{n} a_j f\left(\mu_j\right)$$

Wick quadrature formula allowing to approximate integral of an arbitrary function $f(\mu)$ defined in interval [-1, +1].

There are several ways to compute the constants a_j and μ_j. **G. C. Wick** suggested Gaussian quadrature as the best one because it makes exact the above relation for (2n-1) degree polynomial in μ.

Gian Carlo Wick
(1909-1992)

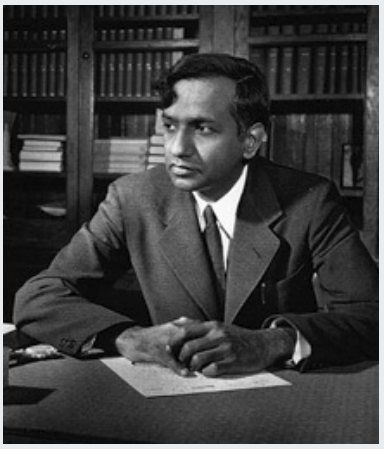

Subrahmanyan Chandrasekhar
(1910-1995)

S. Chandrasekhar was an Indian-born American astrophysicist and mathematician, co-laureate of the Nobel Prize of Physics in 1983. S. Chandrasekhar re-used the numerical scheme proposed before by **G. C. Wick**, developing it for a wide utilization [2].

This method will be popularized under the "***Wick-Chandrasekhar discrete ordinate method***". The mathematical demonstration of its convergence was established only in 1958 by the mathematician **P. M. Anselone** [3].

Since the fifties, this method is applied to neutron transport equation by **B. G. Carslon**, **C. E. Lee** and **K. D. Lathrop** [4] at *Los Alamos Scientific Laboratory* (USA). It is often called "*S_N method*" (*S* for angular segmentation and *N* for angular quadrature order). The first calculation codes solving the neutron transport equation using deterministic method appear. In a paper published at *Oak Ridge National Laboratory* [5], **P. M. Anselone** studied again the S_N method convergence in the frame of numerical resolution of the neutron transport equation. K. D. Lathrop studied its ray effect that is a kind of Achilles' heel of this method in lacunar configuration for instance. Several historical families of one –, two –, and three-dimensional S_N codes are produced by the American national laboratories, from **ANISN** to **TORT**, through **TWOTRAN** and **TWODANT**. They will be widely used in world nuclear community *via* their **RSICC** and **OECD/NEA** distribution for both neutronics/criticality and radiation shielding calculations. The CEA developed the **BISTRO *S_N*** code [6] that was to be integrated in the lattice code **APOLLO2** and **SN1D** code [7] dedicated to radiation shielding studies. One original development was to introduce in the SN1D code cross sections represented by **probability tables**, thereby bringing significant improvement in calculating neutron propagation as a function of their energy [8] in configurations with strong neutron-flux attenuation.

A few historical references

[1] G. C. Wick, "Über ebene Diffusionsproblem", Zs. f. Phys., 121, 702, 1943.

[2] S. Chandrasekhar, *Radiative Transfer*, Oxford, Clarendon Press, 1950; réédition: New York, Dover, 1960.

[3] P. M. Anselone, "Convergence of the Wick-Chandrasekhar Approximation Technique in Radiative Transfer" *Astrophys. J.*, 128, 124; 130, 881, 1958.

[4] K. D. Lathrop, "The Early Days of the S_N method", SLAC-PUB 5829, December 1992; B. G. Carlson, "A solution of the transport equation by S_N approximations", LA- 1599, Los Alamos Scientific Laboratory, 1953, revised version, LA 1891, 1955 ; B. G. Carlson, C. E. Lee, "Mechanical Quadrature and Transport Equations", LAMS-2573, *Physics*, TID-4500, June 1961.

[5] P. M. Anselone, A. G. Gibbs, "Convergence of the Discrete Ordinates Method for the Transport Equation", ORNL-4984, UC-32, *Mathematics and Computers*, July 1974.

[6] G. Palmiotti, J.M. Rieunier, C. Gho, M. Salatores, "BISTRO Optimized Two Dimensional S_N Transport Code", *Nucl. Sc. Eng.* 104, 26, 1990.

[7] G. Dejonghe, L. Luneville, SN1D : "Code de protection nucléaire à une dimension", Rapport interne CEA, 1983.

[8] L. Luneville, *Méthode multibande aux ordonnées discrètes. Formalisme et résultats*, Note CEA-N-2832, 1998.

There exists an infinity of choices as regards directions and weights. For instance, in an unidimensional plane geometry, the angle being only reduced to the variable $\mu = cos\theta$ (with θ, the angle between the propagation direction and the reference axis), it is usual to choose the $\{\mu_n, w_n\}$ corresponding to a **Gaussian quadrature***.

The S_N method is widely used despite its inner weakness *i.e.* the "**ray effect**": in presence of a neutron source locally concentrated in a little diffusive medium, some of the selected directions may completely "miss" a straight view of the source, and so lead to almost null nonphysical fluxes. This defect can be counterbalanced through refining the angular meshing.

P_N method

The P_N method consists in using an expansion of the angular flux dependence into spherical harmonics $Y_m^\ell(\vec{\Omega})$ (for one space dimension, the latter become the **Legendre polynomials**, hence the name of the method) according to the following expression:

$$\psi(\vec{r},\vec{\Omega}) = \sum_{m=0}^{\infty} \sum_{\ell=-m}^{m} \psi_m^\ell(\vec{r})\, Y_m^\ell(\vec{\Omega}) \qquad (13)$$

As the spherical harmonics constitute an orthonormal complete set, Equation (13) is known to be always true, even if the expansion has to be cut after the first terms in practice. In order to obtain equations for the unknowns $\psi_m^\ell(\vec{r})$, the expansion (13) is introduced into the transport equation giving a system of coupled space differential equations.

It is rather difficult to analytically express P_N equation coefficients (except in the case of one dimension). In addition, the equations obtained through projection of the transport equation on spherical harmonics, are strongly coupled and consequently need specific solving algorithms. At the opposite, the P_N method does not exhibit notable problems such as the ray effect of the S_N method.

The difficulties to implement the three-dimensional P_N method explain why few industrial codes use this approach.

Simplified transport (SP_N) method

In the sixties, in order to reduce the high complexity of P_N equations for multidimensional problems, and allow them to be solved, E.M. Gelbard [3] proposed a new approximation named "simplified P_N method" or "SP_N". The principle of the method was to build an operator generalizing the diffusion operator, and taking most of transport effects into account. Gelbard's idea was to assume that locally the transport solution was equivalent to the solution to a plane geometry equation, and so could be found through a 1-D P_N method. That reduces the number of harmonics to be taken into account which then grows in N instead of N^2. In the proposed method, going from local to 3-D equations was obtained through an empirical, formal method. After a thirty years' period of oblivion due to computer lack of power to solve these equations, as well as to a lack of theoretical justification, a renewed interest emerged in the nineties, when Pomraning [4] and Larsen, Morel and McGhee [5] independently presented asymptotical analyses justifying Gelbard's empirical method.

SP_N equations can also be obtained through a variational principle. That principle was first proposed by Pomraning for the infinite medium and the anisotropic scattering in the monokinetic theory, and was then extended to a finite medium by Brantley and Larsen [6], as part of SP3 equations, taking account of items such as boundary conditions, isotropic scattering, and multigroup description of the energy variable.

The analysis performed by Pomraning is presented below. It starts from the following consideration: if the transport equation locally is in a plane geometry, then the SP_N solution also is a solution to the transport equation. For instance, this assumption may be justified for a homogeneous calculation when being far from the interfaces between the different media.

Let us consider a **local system of coordinates** $(\vec{i}, \vec{j}, \vec{k})$. Direction $\vec{\Omega}$ can then be written as follows:

$$\vec{\Omega} = \sqrt{1-\mu^2}\,\cos\varphi\;\vec{i} + \sqrt{1-\mu^2}\,\sin\varphi\;\vec{j} + \mu\,\vec{k}$$

where μ is the cosine of the polar angle, and φ is the azimuthal angle.

The assumption is made that, in this system, the solution is weakly dependent in the azimuthal direction (plane symmetry assumption), and so it is in x and y. By introducing an ε factor quantifying this low variation, and going to the $(\varepsilon \to 0)$, limit, a 1-D transport equation is obtained in the local system. Yet, in this local system, direction $\vec{\Omega}$ depends on space (since this system undergoes variation in space), which was not the case in the transport equation. Hence the need for an additional assumption, that the local system $(\vec{i}, \vec{j}, \vec{k})$ slowly varies in space (a variation quantified by the ε). With this assumption, the leakage term is written as follows:

$$\vec{\nabla}.(\vec{\Omega}\psi) = \vec{\Omega}.\vec{\nabla}\psi + (\vec{\nabla}.\vec{\Omega})\psi = \mu\frac{\partial\psi}{\partial z} + O(\varepsilon)$$

This results in a plane geometry local problem which can be solved accurately through the P_N method. If the $\psi^{1D}(z,\mu)$ solution of the plane geometry local problem is expanded on the Legendre polynomials basis, the following equation can be written:

$$\psi^{1D}(z,\mu) = \sum_{n=0}^{\infty} \psi_n^{1D}(z) P_n(\mu)$$

This expanding can be truncated at an N order chosen as odd. The expansion coefficients (harmonics) satisfy the following coupled system:

$$\begin{cases} \dfrac{d\psi_1^{1D}}{dz} + \Sigma_{r0}\psi_0^{1D} = S \\ \dfrac{n+1}{2n+1}\dfrac{d\psi_{n+1}^{1D}}{dz} + \Sigma_{rn}\psi_n^{1D} + \dfrac{n}{2n+1}\dfrac{d\psi_{n-1}^{1D}}{dz} = 0 \\ \Sigma_{rN}\psi_N^{1D} + \dfrac{N}{2N+1}\dfrac{d\psi_{N-1}^{1D}}{dz} = 0 \end{cases}$$

for $1 \le n \le N$.

It is worth to mention that:

$$\begin{cases} \Sigma_{rn} = \Sigma - \Sigma_{sn} \\ \Sigma_s(\vec{r}, \vec{\Omega}'.\vec{\Omega}) = \Sigma_s(\vec{r}, \mu) = \sum_{n=0}^{\infty} (2n+1)\,\Sigma_{sn}(\vec{r}) P_n(\mu) \end{cases}$$

The issue is to obtain the ψ approximation from ψ_1^{1D}. The following process can be used (by analogy with the scalar flux and the current in the diffusion equation):

- for even n, the equation can be written taking account of ψ weak dependence as a function of x and y :

$$\begin{cases} \psi_n = \psi_n^{1D} + O(\varepsilon) \\ \vec{\nabla}\psi_n = \dfrac{\partial \psi_n}{\partial x}\vec{\imath} + \dfrac{\partial \psi_n}{\partial y}\vec{\jmath} + \dfrac{\partial \psi_n}{\partial z}\vec{k} = \dfrac{d\psi_n^{1D}}{dz}\vec{k} + O(\varepsilon) \end{cases}$$

- for odd n, a $\vec{\psi}_n$ vector can be defined from the 1-D harmonic which satisfies:

$$\begin{cases} \vec{\psi}_n = \psi_n^{1D}\vec{k} \\ \vec{\nabla}.\vec{\psi}_n = \dfrac{d\psi_n^{1D}}{dz} \end{cases}$$

Thus the following equations can be written in the global system with an error in $0(\varepsilon)$. Making ε tend to zero brings back to a 1-D equation in the global system.

$$\begin{cases} \vec{\nabla}.\vec{\psi}_1 + \Sigma_{r0}\psi_0 = S & \\ \dfrac{n+1}{2n+1}\vec{\nabla}\psi_{n+1} + \Sigma_{rn}\vec{\psi}_n + \dfrac{n}{2n+1}\vec{\nabla}\psi_{n-1} = \vec{0} & 1 \le n \le N-1,\ n \text{ odd} \\ \dfrac{n+1}{2n+1}\vec{\nabla}.\vec{\psi}_{n+1} + \Sigma_{rn}\psi_n + \dfrac{n}{2n+1}\vec{\nabla}.\vec{\psi}_{n-1} = 0 & 1 \le n \le N-1,\ n \text{ even} \\ \Sigma_{rN}\vec{\psi}_N + \dfrac{N}{2N+1}\vec{\nabla}\psi_{N-1} = \vec{0} & \end{cases}$$

Hence a system of partial differential equations. Even equations are scalar, while odd equations are vector equations. This system can be closed only if adjoining a boundary condition set (*e.g.* even fluxes equal to zero on boundaries, or normal traces of odd fluxes equal to zero on boundaries in the case of symmetry). On order 1, diffusion equations can be found. Harmonic 0 stands for scalar flux, and harmonic 1 for current.

In the case of plane geometry or for an infinite homogeneous medium the method converges to the accurate transport solution (when n tends to the infinite). In contrast, in the general case, it converges to a different (though close) solution. Until then, no *a priori* error estimate has been obtained to measure the discrepancy between the SP_N solution and the accurate solution.

This approximation is available for the MINOS solver for static and kinetic calculations with anisotropic scattering [7]. The resolution process relies on even harmonics elimination, and on dual mixed finite element solving. It is also available for the MINARET solver. In this case a diagonalized form of the previous equations [8] is used, and the solving is performed through even harmonics elimination and discontinuous Galerkin finite-element discretization.

Diffusion approximation

The diffusion approximation enables the transport operator of the Boltzmann equation to be simplified under some assumptions, thereby leading to a simple equation fulfilled by the scalar flux.

The conventional way to derive the diffusion equation from the Boltzmann equation requires an expansion of the angular dependence of the flux within an energy group g, $\psi^g(\vec{r}, \vec{\Omega})$ based on spherical harmonics.

The approximation consists in truncating the development so as to reduce it to the first two terms by making the assumption that the sources are isotropic in the laboratory system:

$$\psi^g(\vec{r}, \vec{\Omega}) \cong \phi^g(\vec{r}) + \vec{J^g}(\vec{r}).\vec{\Omega} \qquad (14)$$

where $\phi^g(\vec{r})$ and $\vec{J^g}(\vec{r})$ represent the first two moments of the angular flux.

Equation (14) has a physical interpretation which corresponds to the assumption of a weak (linear at most) dependence of the flux according to direction $\vec{\Omega}$. If this approximation is introduced into the Boltzmann equation, various treatments can lead to the following equation, fulfilled by the scalar flux $\phi^g(\vec{r})$:

$$-\vec{\nabla}.D^g(\vec{r})\vec{\nabla}\phi^g(\vec{r}) + \Sigma_r^g(\vec{r})\phi^g(\vec{r}) = q^g(\vec{r}) \quad (15)$$

The terms are defined as follows:

- $-D^g(\vec{r})\vec{\nabla}\phi^g(\vec{r})$: neutron current which is proportional to the flux gradient; this is the **Fick's law**:

$$\vec{J^g}(\vec{r}) = -D^g(\vec{r})\vec{\nabla}\phi^g(\vec{r}) \quad (16)$$

  $D^g(\vec{r})$: **diffusion coefficient** given by the expression:

$$D^g(\vec{r}) = \frac{1}{3\Sigma_{tr}^g(\vec{r})} \quad (17)$$

  $\Sigma_{tr}^g(\vec{r})$: **transport cross section** in group g defined by:

$$\Sigma_{tr}^g(\vec{r}) = \Sigma^g(\vec{r}) - \bar{\mu}^g(\vec{r})\Sigma_s^g(\vec{r})$$

  $\bar{\mu}^g(\vec{r})$: cosine of the mean scattering angle in group g. If shocks are isotropic in the laboratory system, $\bar{\mu}^g(\vec{r})$ is equal to 0, and the transport cross section merely is the total cross section;

  $\Sigma_s^g(\vec{r})$: macroscopic scattering cross section in group g.

- $\Sigma_r^g(\vec{r})$: disappearance cross section from group g defined by:

$$\Sigma_r^g(\vec{r}) = \Sigma^g(\vec{r}) - \Sigma_s\left(\vec{r}, \vec{g} \to \vec{g}\right)$$

- $q^g(\vec{r})$: source term.

A second manner to get the diffusion equation, starting from an **integral form of the Boltzmann equation**, consists in assuming that sources and shocks are isotropic in the laboratory system, and that the scalar flux $\phi^g(\vec{r})$ and the total macroscopic cross section do not depend much on space. The scalar flux $\phi^g(\vec{r})$ is then developed into a **space Taylor series**, stopping it to the first order as follows:

$$\phi^g(\vec{r}) \cong \phi^g(\vec{r}_0) + \vec{\nabla}\phi^g(\vec{r})\big|_{\vec{r}=\vec{r}_0}.(\vec{r} - \vec{r}_0) \quad (18)$$

After a few transformations, we retrieve the diffusion equation (15), but with a diffusion coefficient equal to:

$$D^g(\vec{r}) = \frac{1}{3\Sigma^g(\vec{r})}$$

A third manner to get the diffusion equation relies on the assumption that the system's absorptions are very low, and so are the flux gradients. The Boltzmann equation is rewritten by inserting a ε ($\varepsilon \ll 1$) parameter, which measures the "smallness" of absorptions. An asymptotic analysis of this equation shows that on the first order, the scalar flux has to fulfill the diffusion equation (15). The peculiarity of this derivation is that assumptions are no longer made on the *a priori* unknown flux shape (weak space- or angle-dependence), but (partly at least) on the coefficients of the equation itself (the macroscopic absorption cross section is weak versus the total macroscopic cross section).

What are the benefits of the diffusion equation versus the transport equation?

First of all, a transition took place from a 6-dimensional phase space ($\vec{r}$, E, $\vec{\Omega}$) to a 4-dimensional phase space ($\vec{r}$, E). According to the previous assessment, this can reduce the number of degrees of freedom by a factor 100 to 1,000 in a numerical resolution.

On the other hand, the diffusion equation, to be met in several fields of physics (heat conduction, migration of chemical species through a medium, etc.) is a partial differential equation among the simplest and the most investigated by mathematicians and computer scientists. Consequently, it benefits from highly performing numerical resolution methods, which are continuously improved by the best specialists.

At last, it is worth to emphasize that, even when used far from its validity range, diffusion is a "robust" approximation, in that results, if not accurate, are qualitatively acceptable.

Practically, diffusion is applicable to almost homogeneous large systems (the dimension of a system being measured in numbers of mean free paths), similarly to power reactors with homogenized fuel assemblies. Industrial reactors are often computed, with satisfactory results, with few energy group diffusion theory, using as coefficients the quantities obtained with the help of accurate transport calculations. This point is dealt with below, pp. 193-213.

Space discretization for a given energy group

In this chapter, we present three types of space discretization methods: *Finite Difference Methods*, *Nodal Methods*, and *Finite Element Methods*.

We can also mention *the first-collision probability method*, based on the integral form of the transport equation that has been the privileged method of assembly codes for a number of years, in order to determine self-shielded multigroup cross sections for reactor core calculations. This method that suffers from the isotropic shock approximation in the laboratory system, is often replaced today by the more flexible and more precise *Method Of Characteristics* (MOC). However, it is still used in self-shielding calculations, in which energy treatment is of prime importance.

A comparison between these two methods is given in the insert, p. 84.

The Finite Difference Method is very easy to implement in Cartesian, cylindrical or spherical, geometry. Higher-order nodal (or finite volume) methods can also be used successfully for improved efficiency. Finite Difference Methods and nodal methods are often used in nuclear reactor physicists' community to solve the diffusion equation.

Finite Element Methods have been initially developed by mechanics scientists, and are based on the minimum energy calculation principle. They can be applied to solving either the diffusion equation, or the transport equation.

The space discretization methods, for a given energy group, are presented here in relation to the source diffusion equation. We assume that the energy (multigroup) discretization is already achieved, and we consider a given group g. In order to simplify notations, we deliberately omit the index on the group in the following.

The source diffusion equation in a given energy group is written as follows:

$$-\vec{\nabla}.\left(D\vec{\nabla}\phi(\vec{r})\right)+\Sigma_r(\vec{r})\phi(\vec{r})=q(\vec{r}) \qquad (19)$$

where $\phi(\vec{r})$ represents the scalar flux (not dependent on the angular variable), $\Sigma_r(\vec{r})$ the disappearance cross section from the group, and $q(\vec{r})$, the source term.

In what follows, for a purpose of simplification, we shall not use boundary conditions. Introducing these boundary conditions partially modifies discrete equations, but does not question their basis.

Finite Difference Methods

A simple way to solve the neutron diffusion equation on a space meshing is to assess this equation at the nodes of the meshing substituting differences for partial derivatives.

For a purpose of simplification, let us consider a 1-D geometry, $\mathcal{R}=[x_0,\ x_{N+1}]$, in which a space meshing is built: $x_0<x_1<\cdots<x_{i-1}<x_i<x_{i+1}<\cdots<x_{N+1}$

Assuming that the neutron flux is sufficiently regular, and using the *Taylor formula*:

$$\phi(x)=\phi(x_0)+(x-x_0)\phi'(x_0)+\frac{1}{2}(x-x_0)^2\phi''(x_0)+O(x^3)$$

it is possible to replace the differential operator of the diffusion equation by a Finite Difference operator:

$$\vec{\nabla}.\left(D\vec{\nabla}\phi\right)(x_i)\cong\frac{D_i^+}{(x_{i+1}-x_i)}[\phi(x_{i+1})-\phi(x_i)]-\frac{D_i^-}{(x_i-x_{i-1})}[\phi(x_i)-\phi(x_{i-1})]$$

where D_i^+ (resp. D_i^-) is the diffusion coefficient value within the interval $[x_{i-1},\ x_i]$ (resp. $[x_i,\ x_{i+1}]$).

By writing the diffusion equation at the meshing points, and after having substituted the previous Finite Difference operator for the differential operator, the resolution is finally focused on a matrix system in which the unknowns are the flux values at the meshing nodes:

$$A\phi=Q\ with\ \phi=\begin{pmatrix}\phi(x_0)\\ \dots\\ \phi(x_{N+1})\end{pmatrix}$$

As previously mentioned, the boundary condition treatment will not be specified here.

It is to be noted that the A matrix is symmetrical, positive definite, and with a dominant diagonal. Moreover, it is tri-diagonal (the flux in one point being connected only with its close neighbors). A number of direct or iterative methods exist to solve linear systems, which are well adapted to this system.

It can be observed that, if using the Taylor formula and evidencing the medium points $x_{i+\frac{1}{2}}$ of the intervals $[x_i,\ x_{i+1}]$, a matrix system is obtained which is of the same nature as that previously obtained, but with unknowns which are, in this case, the middle points of the meshing. In the first case, it will be referred to as **Finite Differences** at the mesh "**edges**", and, in the second case, as Finite Differences at the mesh "**centers**".

The Finite Difference method can be easily generalized to 3-D Cartesian geometries, and the properties of the global matrix are kept. This is why this method was first used as soon as square-pitch reactor cores (*e.g.* of the PWR type) started to be designed. As a matter of fact, iterative methods for solving the system are efficient, and do not require much memory space, which was compatible with the very first computer generations.

In contrast, the Finite Difference method cannot be generalized so easily to hexagonal-pitch geometries (*e.g.* fast neutron reactors).

This method converges in $O(h^2)$ where h is the maximum pitch of the space meshing. So the number of discretization points has to be strongly increased for approaching the accurate solution. This is especially true in the case of reactor core calculations, homogenized at assembly level.

The difficulty to generalize the Finite Difference method to hexagonal geometries as well as slow convergence with respect to space have led engineers to develop new space approximation methods, especially nodal methods.

Nodal Methods

Nodal methods are based on a semi-analytical resolution of the diffusion equation.

In order to illustrate the method, let us assume a 2-D Cartesian geometry $\mathcal{R}$, and a mesh $[x_i, x_{i+1}] \times [y_i, y_{i+1}]$ where the cross sections are constant.

Let us integrate the diffusion equation (19) in direction x over the interval $[x_i, x_{i+1}]$, and then in direction y over the interval $[y_i, y_{i+1}]$, and let us note as follows:

$$\begin{cases} \phi^i(y) = \int_{x_i}^{x_{i+1}} \phi(x,y)dx\,, \qquad q^i(y) = \int_{x_i}^{x_{i+1}} q(x,y)dx \\ \Lambda^i(y) = -\left(D\frac{\partial\phi}{\partial x}(x_{i+1},y) - D\frac{\partial\phi}{\partial x}(x_i,y)\right) \end{cases}$$

$$\begin{cases} \phi^j(x) = \int_{y_j}^{y_{j+1}} \phi(x,y)dy\,, \quad q^j(x) = \int_{y_j}^{y_{j+1}} q(x,y)dy \\ \Lambda^j(x) = -\left(D\frac{\partial\phi}{\partial y}\left(x,y_{j+1}\right) - D\frac{\partial\phi}{\partial y}\left(x,y_j\right)\right) \end{cases}$$

Differential equations are obtained in directions x and y:

$$\begin{cases} -D\frac{d^2\phi^j}{dx^2}(x) + \Sigma_r\phi^j(x) = q^j(x) - \Lambda^j(x) \\ -D\frac{d^2\phi^i}{dy^2}(y) + \Sigma_r\phi^i(y) = q^i(y) - \Lambda^i(y) \end{cases} \tag{20a}$$

$\Lambda^j(x)$ and $\Lambda^i(y)$ are called the "**transverse leakage**" in directions x and y.

At last, the integration of the diffusion equation on $[x_i, x_{i+1}] \times [y_j, y_{j+1}]$ leads to the **balance equation**:

$$\int_{y_j}^{y_{j+1}} \Lambda^i(y)dy + \int_{x_i}^{x_{i+1}} \Lambda^j(x)dx + \Sigma_r\overline{\phi} = \overline{q} \tag{20b}$$

with $\overline{\phi} = \int_{x_i}^{x_{i+1}}\int_{y_j}^{y_{j+1}} \phi(x,y)dxdy$

and $\overline{q} = \int_{x_i}^{x_{i+1}}\int_{y_j}^{y_{j+1}} q(x,y)dxdy$

Prior to establishing this equation, it can be observed that:

$$\begin{aligned} \int_{y_j}^{y_{j+1}} \Lambda^i(y)dy &= \int_{y_j}^{y_{j+1}} -\left(D\frac{\partial\phi}{\partial x}(x_{i+1},y) - D\frac{\partial\phi}{\partial x}(x_i,y)\right)dy \\ &= -(D\frac{d\phi^j}{dx}(x_{i+1}) - D\frac{d\phi^j}{dx}(x_i)) \end{aligned}$$

Nodal methods consist in solving differential equations in directions x and y taking into account the balance equation. This solution can be found analytically, or assuming a polynomial approximation of the unknowns.

In the case of the polynomial approximation, an either flat or quadratic approximation of transverse leakage is introduced. The system of equations (20a) and (20b) can then be solved step-by-step as follows:

- Integrating the differential equation according to y, assuming $\Lambda^i(y)$ as known, results in an analytical expression of $\varphi^i(y)$, which, once derived according to y, will give a value of $\int_{x_i}^{x_{i+1}} \Lambda^j(x)dx$
- Similarly, integrating the differential equation according to x, assuming $\Lambda^j(x)$ as known, results in an analytical expression of $\varphi^j(x)$ which, once derived according to x, will result in a value of $\int_{y_j}^{y_{j+1}} \Lambda^i(y)dy$
- Finally, the balance equation allows the integrated flux values $\overline{\phi}$ in the meshes to be calculated.

The unknowns introduced in this formulation are the transverse leakage at the mesh interface, and the flux in meshes. This formulation is akin to the mixed formulation with finite element approximation described hereafter (pp. 79 *et sq.*), and analogies, or even equivalences, can be demonstrated in some cases.

These methods have been generalized to hexagonal geometries.

Yet they suffer from their lack of mathematical foundations, which makes it difficult to introduce the notion of adjoint operator (contrary to the Finite Element Methods described in the following paragraph). This notion is used during perturbation calculations, which are the basis of studies of sensitivity to variations of parameters, such as geometrical parameters or nuclear data.

Finite Element Methods (FEM)

The neutron diffusion equation presented in the previous paragraph:

$$-\vec{\nabla}.\left(D\vec{\nabla}\phi(\vec{r})\right)+\Sigma_r\phi(\vec{r})=q(\vec{r}) \qquad (21)$$

can be rewritten thanks to the Rayleigh-Ritz method in an equivalent variational form. Here cross sections are assumed to be constant with respect to space.

The primal formulation and its space approximation

The **primal variational formulation** of the problem, the most immediate to be written, is the following:

Find $\phi \in V(\mathcal{R})$ such as:

$$\int_{\mathcal{R}} D\vec{\nabla}\phi.\vec{\nabla}w dr+\int_{\mathcal{R}}\Sigma_r\phi w dr=\int_{\mathcal{R}} qw dr \quad \forall\, w\in V(\mathcal{R})$$

where V is the Sobolev space of the functions which are L^2 integrable over the domain $\mathcal{R}$, as well as their derivatives.

There again, we do not take into account the boundary conditions.

For simplificity, we again limit ourselves to the 1-D geometry and its space meshing $\{x_i,\ i = 0 \text{ à } N+1\}$, in which the points are assumed equidistant in the interval $[x_0,\ x_{N+1}]$; h will then be the distance between two contiguous points.

As regards the **k-order Finite Element Method**, the discrete subspace V_h of V is introduced, being defined by:

$$V_h=\left\{\phi_h\in C^0([x_0,x_{N+1}])\ such\ as\ \ \phi_h|[x_i,x_{i+1}]\in\mathbb{P}_k, 0\le i\le N\right\}$$

where $\mathbb{P}_k$ is the k-degree polynomial space. Let us denote (w_ℓ) a basis of V_h.

The **discrete formulation** of the problem is as follows:
Find $\phi_h \in V_h$ such that:

$$\sum_{i=1,N}\int_{\mathrm{i}}^{i+1} D\vec{\nabla}\phi_h.\vec{\nabla}w_\ell dx+\sum_{i=1,N}\int_{\mathrm{i}}^{i+1}\Sigma_r\phi_h w_\ell dx = \sum_{i=1,N}\int_{\mathrm{i}}^{i+1} qw_\ell dx \quad \forall\, w_\ell$$

It is then rather easy to turn this problem into a matrix system $A\phi = Q$ where the unknowns are the coordinates of the flux ϕ_h in the basis (w_ℓ).

Of course, the 3-dimensional discrete formulation is generalized, with a discretization of the domain $\mathcal{R}$ into regular straight- or curved-edged polygons (quadrilateral/rectangular parallelepipeds, prisms, pyramids…). For example, in a 2-D configuration on a Cartesian meshing the polynomial bases are illustrated in Figure 29.

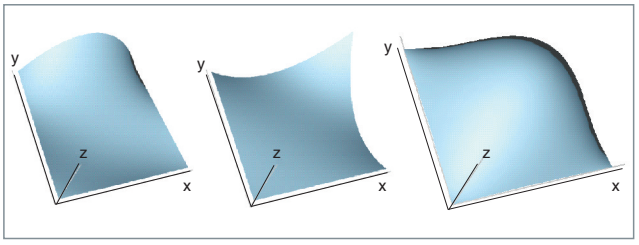

Fig. 29. 2-D 2nd-degree polynomial basis.

It can be shown that, in the case of a sufficiently regular domain $\mathcal{R}$, and under some conditions regarding cross sections, the solution to the discrete problem is, indeed, an approximation of the initial continuous problem, and that the order of the error is $0(h^{k+1})$.

Remarks

- It is possible to demonstrate the equivalence of Finite-Difference type approximations at mesh vertexes, and of 1-order Finite Element approximations, under the condition of numerically integrating (Gauss-Lobatto integration) the integrals involved in the discrete formulation.

- It has been also demonstrated that an error in $0(h^{k+2})$ can be obtained using a Gaussian integration; this is what is called the "**superconvergence**" phenomenon.

Flux approximation, as proposed here, provides a continuous solution over the domain $\mathcal{R}$. In contrast, the current (*i.e.* the flux derivative) is not continuous. This flux continuity can sometimes generate constraints concerning the domain discretization, especially at the core-reflector interface where the thermal flux undergoes a sharp rise of its level before getting null out of the core. This phenomenon is also visible at the interface of two assemblies of different natures (*e.g.* UOX and MOX). A good approximation of reality therefore requires a fine core discretization at the interface level, so as to allow to "follow at best" sharp variations in flux.

An alternative is to "release" the flux continuity constraint; this is possible using a mixed formulation of the problem.

The mixed formulation of the problem

Let us go back to the continuous formulation of the problem related to Equation (21), and let us introduce the auxiliary unknown $\vec{p}$, which represents the current:

$$\begin{cases}\vec{p}=-D\vec{\nabla}\phi(\vec{r})\\ \vec{\nabla}.\vec{p}+\Sigma_r\phi(\vec{r})=q(\vec{r})\end{cases}$$

The mixed variational formulation of the problem so written is as follows:

Find $(\phi,\vec{p})\in V(\mathcal{R})\times W(\mathcal{R})$ *such as:*

$$\begin{cases}\int_{\mathcal{R}}\frac{1}{D}\vec{p}.\vec{q}d\vec{r}+\int_{\mathcal{R}}\phi\vec{\nabla}.\vec{q}d\vec{r}=0 & \forall\,\vec{q}\in W(\mathcal{R})\\ \int_{\mathcal{R}} w\vec{\nabla}.\vec{p}d\vec{r}+\int_{\mathcal{R}}\Sigma_r\phi w d\vec{r}=\int_{\mathcal{R}} qwd\vec{r} & \forall\, w\in V(\mathcal{R})\end{cases}$$

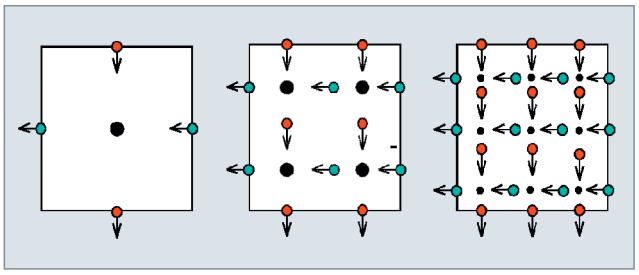

Fig. 30. 1-, 2- and 3-order mixed Raviart-Thomas finite elements in a Cartesian geometry (•:"flux" unknown, ⊷ : "current" unknown).

where V is the Sobolev space of the L^2 integrable functions (together with their derivatives), and W is the Sobolev space of L^2 integrable vector functions, with a L^2 integrable divergence.

The discrete formulation of this problem is obtained through discrete spaces of V and W. We shall not mention here the conditions to be fulfilled by these spaces, but we shall merely illustrate this discretization in the case of 2-D Cartesian meshing. In this special case, the finite elements used are represented in Figure 30:

Remarks

- The flux continuity constraint has been released, while keeping the current's continuity in the direction normal to the interface.

- It is possible to demonstrate the equivalence of Finite Difference type approximations at mesh centers, and of 1-order mixed Finite Element approximations, under the condition of numerically integrating (Gauss-Lobatto integration) the integrals involved in the discrete formulation.

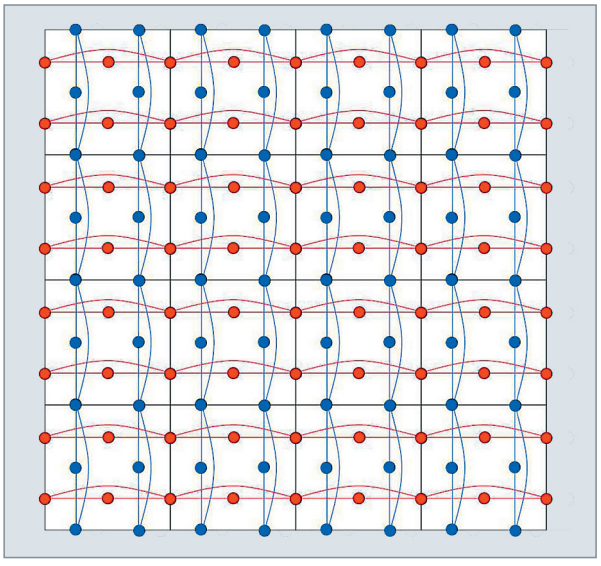

Fig. 31. Coupling of the "current" unknowns in a 2-D Cartesian geometry.

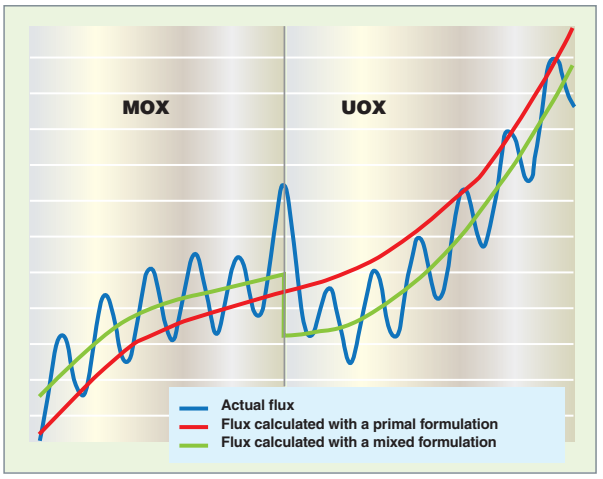

Fig. 32. Schematic representation of the fluxes calculated at an UOX/MOX interface.

The discrete problem resolution is performed on the unknown "current", after eliminating the unknown "flux" which is internal to the mesh. In the case or regular, Cartesian, or even hexagonal meshing, this resolution can be iterative, as shown in Figure 31. In addition, an efficient vector treatment of calculations can easily be achieved with this method.

Given the release of the flux continuity constraint, it is possible to add physical constraints of flux "jump" to the interfaces. The use of **ADF*** (discontinuity coefficients), especially at the UOX and MOX assembly interfaces, enables then flux discontinuity to be modeled.

Figure 32 **schematizes** an actual flux (arising from a fine transport calculation performed by a lattice code), a flux computed by an order-2 finite-element method with a primal formulation, which is continuous at the interface, but does not comply with the average value of the actual flux, and a flux calculated by an order-2 finite-element method with a mixed-formulation, that is discontinuous at the interface, but better fulfills the average value of the actual flux.

Angle and space discretization for a given energy group

Concerning the angular flux calculation in a given group, angle and space discretizations are simultaneously involved. Within this framework, we shall present the finite element method and the Method of Characteristics. For simplicity, cross sections are assumed to be constant with respect to space.

The Finite Element Method is particularly adapted to unstructured geometries.

The Method Of Characteristics (MOC), which benefits from the hyperbolic behavior of the transport equation, is often employed for assembly calculations, in which the aim is to treat unstructured geometries (fuel pins in a lattice, guide tubes, etc.) without using a meshing, which would require a high number of meshes to respect fissile volumes. (As it is known, at the first order, a 1% error in the pin volume may induce an error of about 1,000 pcm on the k_{eff}).

Finite Element Method

Let us now consider the source transport equation in a given group:

$$\vec{\Omega}.\vec{\nabla}\psi(\vec{r},\vec{\Omega}) + \Sigma\psi(\vec{r},\vec{\Omega}) = q(\vec{r},\vec{\Omega}) \qquad \vec{r} \in \mathcal{R} \qquad (22)$$

where $q\ (\vec{r},\vec{\Omega})$ gathers all the equation source terms.

Two variational formulations of the source transport problem can be written; one of the second order, which is close to the variational formulation obtained for the diffusion equation, the other of the first order, arising from Equation (22).

The even formulation of the transport equation

In this paragraph, the transport equation is assumed to have already undergone an angular discretization through the S_N *method*. The equations are thus written for a discrete set of values of $\vec{\Omega}$.

We have previously described the Finite Element Methods for solving a second-order equation, the diffusion equation.

A simple manner to treat this type of equation is to define the following unknowns:

$$\begin{cases} \psi^{+}(\vec{r},\vec{\Omega}) = \dfrac{1}{2}\left(\psi(\vec{r},\vec{\Omega}) + \psi(\vec{r},-\vec{\Omega})\right) \\ \psi^{-}(\vec{r},\vec{\Omega}) = \dfrac{1}{2}\left(\psi(\vec{r},\vec{\Omega}) - \psi(\vec{r},-\vec{\Omega})\right) \end{cases}$$

respectively called "**even flux**" and "**odd flux**".

Writing the transport equation for directions $\vec{\Omega}$ and $-\vec{\Omega}$, and summing (or subtracting) these two equations, the equation system, called "**even-odd formulation**", can be written as follows:

$$\begin{cases} \vec{\Omega}.\vec{\nabla}\psi^{-}(\vec{r},\vec{\Omega}) + \Sigma\psi^{+}(\vec{r},\vec{\Omega}) = q^{+}(\vec{r},\vec{\Omega}) \\ \vec{\Omega}.\vec{\nabla}\psi^{+}(\vec{r},\vec{\Omega}) + \Sigma\psi^{-}(\vec{r},\vec{\Omega}) = q^{-}(\vec{r},\vec{\Omega}) \end{cases}$$

The second equation of the system allows the odd flux to be eliminated, and to go back to the "**even formulation**" of the system:

$$-\vec{\Omega}.\vec{\nabla}\left(\frac{1}{\Sigma}\vec{\Omega}.\vec{\nabla}\left(\psi^{+}(\vec{r},\vec{\Omega})\right)\right) + \psi^{+}(\vec{r},\vec{\Omega}) = q^{+}(\vec{r},\vec{\Omega}) - \vec{\Omega}.\vec{\nabla}\left(\frac{1}{\Sigma}q^{-}(\vec{r},\vec{\Omega})\right)$$

This equation is of the second order, and an even flux approximation can be calculated through Finite Element primal methods.

The iterative solution on directions is generally accelerated through the so-called method of "**synthetic acceleration**", which allows calculation of an estimated error between two iterations by solving a diffusion equation. This even formulation of the transport equation leads naturally to the associated synthetic diffusion equation.

Remark

It is also possible to define a mixed formulation of the transport equation by keeping the odd flux as an unknown, in this case a scalar unknown, as opposed to the vector unknown (current) in the case of diffusion. This last formulation does not bring any improvement as for solving.

The discontinuous Finite-Element Method

Finite Element Methods have also been developed for first-order partial differential equations, such as the transport equation. One of these methods is based on discontinuous finite elements at mesh interfaces. Coupled with the S_N approximation, this method displays the advantage to benefit from a mesh-by-mesh solving which does not require the building, and so the solving, of the whole system for all the unknowns.

The **variational formulation** of problem (2) can be written as follows:

Find $\psi \in V(\mathcal{R})$ such that:

$$\int_{\mathcal{R}} \vec{\Omega}.\vec{\nabla}\psi\, w d\vec{r} + \int_{\mathcal{R}} \Sigma\psi w \mathrm{d}\vec{r} = \int_{\mathcal{R}} q w d\vec{r} \quad \forall\, w \in V(\mathcal{R})$$

where V is the Sobolev space of L^2 integrable functions as well as their gradients.

The absence of flux continuity determines the choice of discretization. The discontinuous finite element method consists in writing the flux on each mesh K like a polynomial, without imposing flux continuity at the interfaces between two adjacent meshes.

The **discrete formulation** can be written on mesh K as follows:

$$\int_{K} \vec{\Omega}.\vec{\nabla}\psi\, w d\vec{r} + \int_{\Gamma_e} \vec{\Omega}.\vec{n}_e\left(\psi_e^{+} - \psi_e^{-}\right) w \mathrm{d}\vec{r} + \int_{K} \Sigma\psi\, w d\vec{r} = \int_{K} q w d\vec{r}$$

Γ_e represents any incoming face of the mesh (see Fig. 33), $\vec{n}_e$ is the normal to Γ_e, w is a basis function that is a polynomial the degree of which depends on the required approximation order. As the flux on the mesh faces is not defined, the surface integral involves a flux discontinuity jump onto the enlightened faces: ψ_e^{+} is the "upwind" flux, assumed to be known, and ψ_e^{-} is the unknown flux of mesh K, restricted to face Γ_e.

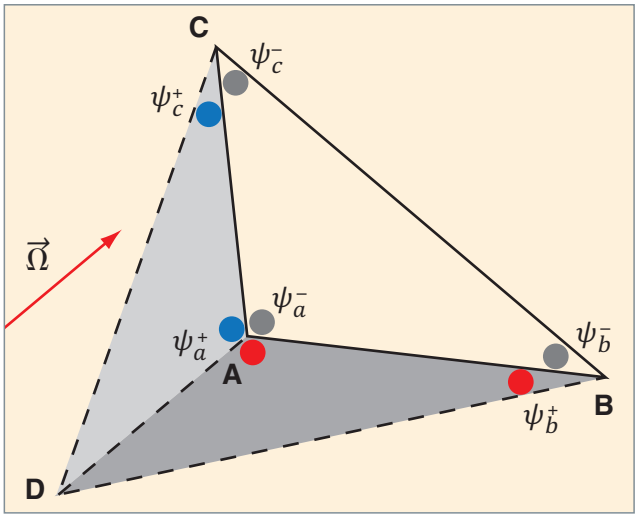

Fig. 33. View of solving principle on the ABC triangle for a given direction $\vec{\Omega}$. The incoming faces are faces ACD and ABD.

These equations are successively solved on each mesh according to a propagation front specific to each direction $\vec{\Omega}$.

As an illustration, let us assume the domain $\mathcal{R}$ meshed with triangles. Direction $\vec{\Omega}$ is a direction fixed by the S_N method. Let us also assume a linear approximation of the flux (w is a polynomial of a degree not exceeding 1). On ABC (Fig. 33), the flux ψ is written as follows:

$$\psi(x,y) = \psi_a^- w_A(x,y) + \psi_b^- w_B(x,y) + \psi_c^- w_C(x,y)$$

The aim is to compute the three fluxes $\psi_a^-, \psi_b^-, \psi_c^-$. The resolution has already been achieved on the two triangles with dotted sides. The upwind fluxes are the fluxes evaluated at blue and red dots. In order to calculate the fluxes at the points of the ABC triangle, a system of three equations with three unknowns has thus to be solved.

Remarks

- A variational formulation of the transport equation can be written in a space where the flux is continuous. Yet, it has been demonstrated that the solution is affected by oscillation problems.

- The solving method can be parallelized, for calculations are mesh-localized, and directions can be treated independently from one another upon an iterative method.

- The k - order method converges in $O(h^{k+1/2})$ towards the exact solution; it is worth to mention that the finite element methods previously described converge in $O(h^{k+1})$.

As for the solving of the equation's even formulation, iteration on angular directions is accelerated by solving a diffusion problem. In order to ensure consistency in the approximation of the two problems, *i.e.* transport and diffusion, a discontinuous Finite Element Method is used for solving the diffusion problem.

The variational form of the related diffusion problem can be written:

$$\int_K D\vec{\nabla}\phi.\vec{\nabla}w d\vec{r} + \int_{\Gamma_e} \alpha[\phi]\,[w]\,d\vec{r} + \int_{\Gamma_e} \overrightarrow{n_e}.\{D\vec{\nabla}\phi\}\,[w]\,d\vec{r} + \int_{\Gamma_e} \overrightarrow{n_e}.\{D\vec{\nabla}w\}\,[\phi]d\vec{r} + \int_K \Sigma\phi w d\vec{r} = \int_K q w d\vec{r}$$

As the fluxes are not defined on faces, surface integrals involve the operators [] and {}, which are the jump and the average respectively:

$$[\phi] = \phi^{ext} - \phi^{int} \quad and \quad \{\phi\} = \frac{\phi^{ext}+\phi^{int}}{2}$$

The first surface integral is a stabilization term with a penalizing parameter α. The third integral is a matrix symetrization term.

The α parameter is calculated as a function of the physical properties of the meshes on both sides of the interface.

Method Of Characteristics (MOC)

In mathematics, the characteristics method is a technique to solve first-order partial differential equations which, as it reformulates the problem in a curvilinear coordinate system, identifies curves referred to as "characteristic curves", or, more simply, "characteristics", along which the partial differential equation degenerates into an ordinary differential equation.

Due to its discretization, this is a computational method particularly well adapted to solving transport-type partial differential equations ([3], [4], [5], [6]). For today this is one of the most used methods for industrial calculations because it allows a good compromise between accuracy and computational time, still making it easier to describe complex arbitrary geometries precisely (thanks to an unstructured meshing), and ensuring a rigorous solution (taking into account very general boundary conditions and any anisotropy order for a shock). This method is available in the CEA's codes APOLLO2 and APOLLO3® [7]. A number of recent CEA's works ([8, 9, 10]) – on which this description is based – have focused on it. The method of characteristics is currently used as part of the multilevel scheme APOLLO2-A, implemented by AREVA in a partnership with the CEA for industrial calculation of pressurized water reactors and boiling water reactors [11].

The method of characteristics is presented in two dimensions, within an energy group g whose index is omitted in order to simplify notations. In this group, the Boltzmann multigroup integro-differential equation is written as follows:

$$\vec{\Omega}.\vec{\nabla}\psi(\vec{r},\vec{\Omega}) + \Sigma(\vec{r})\,\psi(\vec{r},\vec{\Omega}) = q(\vec{r},\vec{\Omega}) \tag{23}$$

where $q\,(\vec{r},\,\vec{\Omega})$ gathers the source terms of the equation.

Space and angle discretization

The method of characteristics relies on a space discretization into homogeneous regions, and an angle discretization called discrete ordinates (*cf.* Fig. 34).

Space variable: the geometrical domain D in which Equation (23) is solved, is partitioned into a set of I homogeneous regions D_i constituting an unstructured meshing:

$$D = \bigcup_{i=1,I} D_i$$

Cross sections and source terms are assumed to be constant per region with respect to space:

$$\begin{cases} \Sigma(\vec{r}) = \Sigma_i \\ q(\vec{r},\vec{\Omega}) = q_i(\vec{\Omega}) \end{cases}, \qquad \forall \vec{r} \in D_i, i = 1, I \tag{24}$$

Angle variable: it is worth to mention that the discrete ordinate formulation *(S_N)* consists in selecting a finite set of discrete directions and related weights:

$$\{\vec{\Omega}_n, \omega_n\} n = 1, N$$

The unknowns of the problem become the values that the angular flux takes for these discrete directions. In addition, the angular integration of an arbitrary function $f(\vec{\Omega})$ is achieved using a quadrature formula:

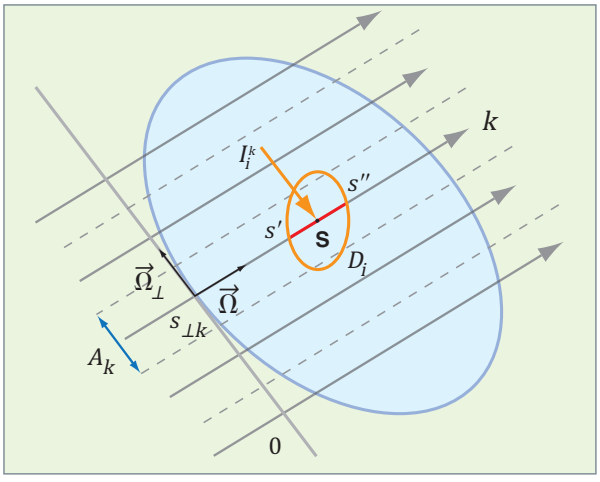

Fig. 34. The Method Of Characteristics (MOC): space and angle discretization.

$$\int_{4\pi} f(\vec{\Omega})\,d\vec{\Omega} = \sum_{n=1}^{N} \omega_n\, f(\vec{\Omega}_n) \tag{25}$$

For each angular direction $\vec{\Omega}$, a set of characteristic lines intercepting the boundaries of the domain's discretized regions provides a discrete set of points between which the homogeneous region approximation (24) can be achieved.

Let $\vec{\Omega}$ be the direction of the characteristic straight line k, and $\vec{\Omega}_\perp$ its perpendicular direction. All the points of the characteristic straight line k can be written as follows: $\vec{r} = s_{\perp k}\vec{\Omega}_\perp + s\vec{\Omega}$ where $s_{\perp k}$ characterizes the track k, and where s, which represents the curvilinear axis along a characteristic curve, varies. For a simplification purpose, we denote $\vec{r}_{0k} = s_{\perp k}\vec{\Omega}_\perp$.

On the characteristic straight line k, the transport equation can be written:

$$\frac{d\psi(\vec{r}_{0k} + s\vec{\Omega},\vec{\Omega})}{ds} + \Sigma(\vec{r}_{0k} + s\vec{\Omega})\psi(\vec{r}_{0k} + s\vec{\Omega},\vec{\Omega}) = q(\vec{r}_{0k} + s\vec{\Omega},\vec{\Omega}) \tag{26}$$

In the case of neutrons, the characteristic curves are straight lines colinear to $\vec{\Omega}$.

Integration along a characteristic

Transmission Equation

By integrating on a computational region D_i along the characteristic straight line k, the analytical solution to the characteristic equation (26) in any point $\vec{r}_{0k} + s\vec{\Omega}$ can be obtained as a function of the analytical solution at the entrance point $\vec{r}_{0k} + s'\vec{\Omega}$ through the following equation:

$$\psi(\vec{r}_{0k} + s\vec{\Omega},\vec{\Omega}) = \psi(\vec{r}_{0k} + s'\vec{\Omega},\vec{\Omega})\, e^{-\tau(s)} + \int_{s'}^{s} ds_1\, q(\vec{r}_{0k} + s_1\vec{\Omega},\vec{\Omega})\, e^{-\tau(s_1)} \tag{27}$$

where the optical path $\tau\,(s_1)$ is defined as follows:

$$\tau(s_1) = \int_{s'}^{s_1} \Sigma(\vec{r}_{0k} + s_2\vec{\Omega})ds_2 \tag{28}$$

Referring to Assumption (24) specifying that the cross sections and source term q are constant with respect to space in the calculation region D_i, Equation (27) becomes:

$$\psi(\vec{r}_{0k} + s\vec{\Omega},\vec{\Omega}) = \psi(\vec{r}_{0k} + s'\vec{\Omega},\vec{\Omega})\, e^{-\Sigma_i(s-s')} + \frac{q_i(\vec{\Omega})}{\Sigma_i}(1 - e^{-\Sigma_i(s-s')}) \tag{29}$$

So, by selecting the exit point $(\vec{r}_{0k} + s''\vec{\Omega})$ from region D_i, as the current point, it can be written as follows: (30)

$$\psi(\vec{r}_{0k} + s''\vec{\Omega},\vec{\Omega}) = \psi(\vec{r}_{0k} + s'\vec{\Omega},\vec{\Omega})\, e^{-\Sigma_i l_i^k} + \frac{1 - e^{-\Sigma_i l_i^k}}{\Sigma_i} q_i(\vec{\Omega})$$

where $l_i^k = s'' - s'$

Equation (30) is called the "**transmission equation**".

Balance equation

If we want obtain an average information about the whole of the characteristic line, it is sufficient to average Equation (29) along the optical path making s vary between s' and s'' so as to obtain:

$$\bar{\psi}_i^k = \frac{\psi(\vec{r}_{0k} + s'\vec{\Omega}, \vec{\Omega}) - \psi(\vec{r}_{0k} + s''\vec{\Omega}, \vec{\Omega})}{\Sigma_i \mathrm{I}_i^k} + \frac{q_i(\vec{\Omega})}{\Sigma_i} \qquad (31)$$

This equation, named the "**balance equation**", makes it possible to obtain flux values averaged along a path, while ensuring that the exact number of neutrons is kept in the system.

Transverse integration

In order to treat the transverse coordinate $s_\perp$, we have to define, for each direction $\vec{\Omega}$ a meshing in the transverse direction. Once this meshing is defined (meshes A_k on Figure 34), we can draw all of the tracks k of direction $\vec{\Omega}$ going through the center of the transverse meshes. All the resulting tracks are called "tracking".

It is important to note that the tracking only contains geometrical data: propagation angle, list of regions gone through, and corresponding intersecting lengths. This step is achieved only once, and contains all the geometric data required for the solver.

The previous equations (30) and (31) give access to variations of the angular flux along a characteristic line of direction $\vec{\Omega}$. In order to obtain the average angular flux over all of these regions, the transverse variable $s_\perp$ along direction $\vec{\Omega}_\perp$, perpendicular to $\vec{\Omega}$ has to be taken into account.

On the discretized region D_i of volume V_i, the average angular flux $\bar{\psi}_i$ is expressed as follows:

$$\bar{\psi}_i(\vec{\Omega}) = \frac{1}{V_i}\int dV\ \psi(s_\perp\vec{\Omega}_\perp + s\vec{\Omega}, \vec{\Omega}) = \frac{1}{V_i}\int ds_\perp \int ds\ \psi(s_\perp\vec{\Omega}_\perp + s\vec{\Omega}, \vec{\Omega})$$

The approximation of this integral is performed using a quadrature formula obtained through considering a set of parallel tracks that cover the region of interest. The volume D_i (Fig. 34) is scanned by a set of lines k which define a tube of transverse area A_k, of length l_i^k, of average flux on line $\bar{\psi}_i^k$. The mean value $\bar{\psi}_i$ on region D_i can so be approached through the following formula:

$$\bar{\psi}_i = \frac{\sum_k A_k l_i^k\ \bar{\psi}_i^k}{\sum_k A_k l_i^k} \qquad (32)$$

The summing is achieved on the characteristic lines k which are parallel to $\vec{\Omega}$ and which intercept region D_i.

Boundary conditions

There exist two types of boundary conditions frequently applied during the calculation of a reactor assembly, according to whether the domain boundary is seen as open or closed. A boundary is considered as open when neutrons can escape from the domain through, at least, one of the areas delimiting the boundary. Consistently, the term (simple or compound) "open paths" will be used when the boundary is open, and the term "cyclic paths", when the boundary is closed (Fig. 35). A further study of these boundary conditions is available in Reference [7].

Collision Probability Method and Method of Characteristics

The Collision Probability Method solves in each energy group the integral space-variable equation for the scalar flux. This method uses the flat source region approximation. It provides a matrix which connects the sources to the scalar fluxes per region, and whose elements can be interpreted as collision probabilities. As for the Method of Characteristics, the calculation of this matrix uses a drawing of parallel tracks for a finite set of angular directions, and it is shown that, for the same subdivision into regions and the same tracks, the collision probability and characteristics methods give the same results for 3-D geometries. It is so concluded that:

- The Method of Characteristics can be seen as an iterative solution of the collision probability method;
- the common idea that the collision probability method does not build any assumption relating to angular fluxes is false.

Reversely, the equivalence between the collision probability method and the method of characteristics is not exact in a 2-D *xy* geometry. Here the collision probability method uses special functions, the Bickley-Naylor functions, which accurately integrate the dependence on the polar angle, whereas, with the method of characteristics, this dependence is solved by numerical integration on this angle. However, the collision probability method can only be applied to problems with an isotropic shock. It therefore requires a transport correction which introduces an approximation difficult to control.

In addition, it leads to an algebraic system which has to be solved through a costly direct inversion, and whose matrices have to be stored by energy group. Owing to all these drawbacks, the collision probability method is only used for problems with relatively few regions, and, often, with degraded approximations (multicell approximation). So the method of characteristics remains the appropriate candidate for enhanced calculations, or for calculations where the collision anisotropy is high.

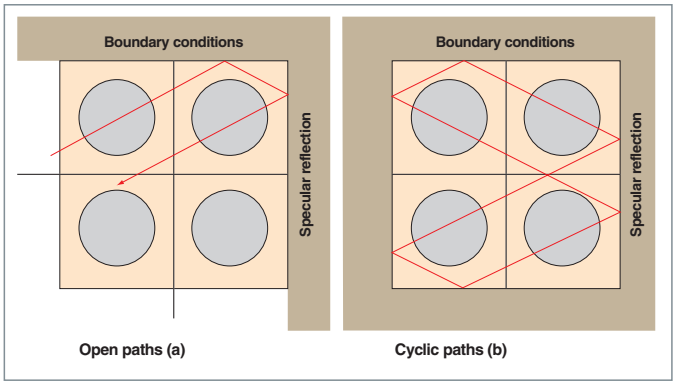

Fig. 35. Method of characteristics: open and cyclic paths.

References

[1] B. Davison, J. B. Skypes, *Neutron Transport Theory*, Oxford, Clarendon Press, 1957.

[2] J. J. Duderstadt, W. R. Martin, *Transport Theory*, New York, John Wiley & Sons, USA, 1979.

[3] E.M. Gelbard, *Simplified Spherical Harmonics Equations and their Use in Shielding Problems*, WAPD-T-1182 (Rev.1), Bettis Atomic Power Laboratory, February 1961.

[4] G. C. Pomraning, "Asymptotic and variational derivations of the simplified PN Equations", *Ann. Nucl. Energy*, 20(9), pp. 623-637, 1993.

[5] E.W. Larsen, J.M. McGhee, J.E. Morel, "Asymptotic Derivation of the Simplified PN Equations", *Proceedings of Topical. Meeting, Mathematical Methods and Supercomputers in Nuclear Applications*, M&C+ SNA 93, Karlsruhe, Germany, April 19-23, 1993.

[6] P.S. Brantley, E.W. Larsen, "A variational derivation of the simplified P3 approximation", *Proceedings of ANS Meeting on Mathematical Models and Supercomputing for Nuclear Applications*, Saratoga Springs, New York, 1997.

[7] A.M. Baudron and J.J. Lautard, "MINOS: A Simplified PN Solver for Core Calculation", *Nuclear Science and Engineering*, 155(2), pp. 250-263, February, 2007.

[8] A.M. Baudron and J.J. Lautard, "Simplified PN Transport Core Calculations in the APOLLO3 System", *International Conference on Mathematics and Computational Methods Applied to Nuclear Science and Engineering*, M&C 2011, Rio de Janeiro, RJ, Brazil, May 8-12, 2011.

[9] M. J. Halsall, "CACTUS : a Characteristics solutions to the neutron transport equations in complicated geometries", AEEWR-1291, Atomic Energy Establishment, UK, 1980.

[10] S. G. Hong, N. Z. Cho, "CRX : a code for rectangular and hexagonal lattices based on the method of characteristics", *Annals of Nuclear Energy*, vol. 25, pp. 547-565, 1998.

[11] K.S Smith, J.D. Rhodes, "CASMO-4 Characteristics methods for two dimensional PWR and BWR core simulations", *Trans Am. Nucl. Soc.*, vol. 83, pp. 294-296, 2000.

[12] R. Sanchez, L. Li Mao, S. Santandrea: "Treatment of boundary conditions in trajectory-based deterministic transport methods", *Nuclear Science and Engineering*, vol. 140, pp. 23-50, 2002.

[13] R. Sanchez, I. Zmijarevic, M. Coste-Delclaux, E. Masiello, S. Santandrea, E. Martinolli, L. Villatte, N. Schwartz, N. Guler, "APOLLO2 year 2010", *Nuclear Engineering and Technology*, vol. 42, n°5, pp. 474-499, October 2010.

[14] F. Févotte, *Techniques de traçage pour la méthode des caractéristiques appliquées à la résolution de l'équation de transport des neutrons en domaines multidimensionnels*, rapport CEA-R-6212, février 2009.

[15] G. Grassi, *Conception de nouveaux schémas multigrilles appliquées à la méthode des caractéristiques pour la résolution de l'équation de transport des neutrons*, rapport CEA-R-6211, février 2009.

[16] S. Santandrea, J.-C. Jaboulay, P. Bellier, F. Févotte, H. Golfier, "Improvements and validation of the linear surface characteristics scheme", *Annals of Nuclear Energy*, vol. 36, pp. 46-59, 2010.

[17] E. Martinolli *et al.*, "APOLLO2-A – AREVA's new generation lattice physics code: methodology and validation", Proc Int Conf on Advances in Reactor Physics to Power the Nuclear Renaissance (PHYSOR 2010), Pittsburgh, PA, USA, May, 9-14, 2010.

Bibliography

Self-shielding formalism

Livolant (M.), Jeanpierre (F.), *Autoprotection des résonances dans les réacteurs nucléaires*, Rapport CEA-R-4533-1974.

Grandotto-Biettoli (M.), *AUTOSECOL, Un calcul automatique de l'autoprotection des résonances des isotopes lourds*, Note CEA-N-1961, 1977.

Williams (M. L.), "Correction of Multigroup Cross-Sections for Resolved Resonance Interference in Mixed Absorbers", *Nuclear Science and Engineering*, 83, pp. 37-49, 1983.

Rimpault (G.), Grimstone (M.J.), "Validation of New Subgroup Algorithms for Resonance Self-Shielding in Heterogeneous Structures", *Proc. Int. Top. Meet. on Advances in Nuclear Engineering Computation and Radiation Shielding*, Santa Fe, New Mexico, USA, April 9-13, 1989.

Reuss (P.), *Théorie de l'absorption résonnante des neutrons*, Note CEA-N-2679-1991.

Sanchez (R.), *Module d'autoprotection du code APOLLO2*, Note CEA N- 2765-1994.

Bouland (O.), *Amélioration du calcul de l'autoprotection des résonances résolues par un traitement quasi-exact du ralentissement des neutrons*, Thèse de doctorat, Université Paris XI, Orsay, 1994.

Hébert (A.), "The Ribon Extended Self-Shielding Model", *Nuclear Science and Engineering*, vol. 151, pp. 1-24, 2005.

Coste-Delclaux (M.), *Modélisation du phénomène d'autoprotection dans le code de transport multigroupe APOLLO2*, Rapport CEA R- 6114, 2006.

Hfaiedh (N.), *Nouvelle Méthodologie de Calcul de l'Absorption Résonnante*. Thèse de doctorat, Université Louis Pasteur Strasbourg I, 2006.

Finite Element Method

Lesaint (P.) and Raviart (P. A.), "On a Finite Element Method for Solving the Neutron Transport Equation", in *Mathematical Aspects of Finite Elements in Partial Differential Equations*, p. 89, C. A. De Boor, Ed., Academic Press, New York, 1974.

Lautard (J.J.), "New Finite Element Representation for 3D Reactor Calculations", *ANS/ENS Meeting*, Munich,Germany, April 1981.

Kavenoky (A.) and Lautard (J. J.), "State of the Art in using Finite Element Methods for Neutron Diffusion Calculations", *ANS Topical Meeting on Advances in Reactor Computations*, Salt-Lake-City, USA,1983.

Lautard (J.J.) and Moreau (F.), "A Fast 3D Parallel Diffusion Solver Based on a Mixed Dual Finite Element Approximation", *Int. Conf. on Mathematical Methods and Supercomputing in Nuclear Applications*, Karlsruhe, Germany, 1993.

Ern (A.), Guermond (J.-L.), *Theory and Practice of Finite Elements*, Springer, New York, 2004.

Bernadi (C.), Maday (Y.), Rapetti (F.), *Discrétisation variationnelle de problèmes aux limites elliptiques*, Springer, New York, 2004.

Baudron (A.M.), Lautard (J.J.), "MINOS: A Simplified Pn Solver for Core Calculation", *Nuclear Science and Engineering*, vol. 155, number 2, pp. 250-263, February 2007.

To the origins of the Method Of Characteristics (MOC)

The **Method Of Characteristics** was presented for the first time by **Georg Friedrich Bernhard Riemann** in 1859, in an article titled *"Ueber die Fortpflanzung ebener Luftwellen von endlicher Schwingungsweite" ("On propagation of plane waves with finite amplitude in the air")* [1]. It is presented in Reference [2] by two authors, **H. M. Paynter** and **I. J. Busch-Vishniac**. This computational method displays a generic feature to treat linear or nonlinear problems of propagation in solid as well as liquid or gaseous media.

In the research field relating to the solving of the neutron transport equation, this method was first introduced in 1972 by the British scientist **J. R. Askew** in his article *"A characteristics formulation of the neutron transport equation in complicated geometries"* [3]. One of the interests of the **Method of characteristics** is, indeed, to allow a higher flexibility in the space discretization ("geometric flexibility") to be achieved for the physical system investigated. It is especially adapted for the so-called "nonstructured" geometric meshing. It is also interesting to treat neutron transport in physical configurations in which the *"streaming"* phenomenon is significant, *e.g.* in geometries displaying voids or a strong attenuation of the neutron flux.

The implementation of the method of characteristics in neutronics' computational codes gradually extended, as shown in 1980, in Reference [4] relating to **M. J. Halsall** and, then in 1981, in Reference [5] by **R. E. Alcouffe** and **E. W. Larsen** (Los Alamos National Laboratory, USA).

R. Sanchez is the one who introduced this method in the CEA's neutronics codes [6-7]. Today it is broadly applied to the solving of two-dimension problems. It is one of the lattice calculation methods that the **APOLLO** code developed at the CEA provides to nuclear reactor physicists.

The next step will be its three-dimensional space generalization.

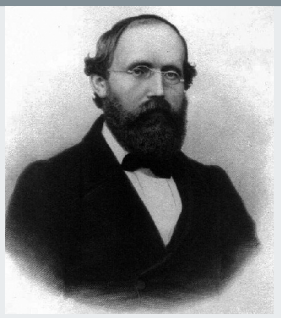

Georg Friedrich Bernhard Riemann (1826-1866) is a German mathematician who brought a major contribution to analysis and differential geometry.

References

[1] *Abhandlungen der Gesellshaft der Wissenshaften zu Göttingen*, Mathematisch- physikalishe Klasse 8, pp. 43 -65 (1858-59).

[2] J. Acoust, *"Remarks on Riemann's method of characteristics"*, Soc. Am. 84 (3), September 1988, pp. 813-821.

[3] Rapport technique AEEW-M 1108, *Atomic Energy Establishment*, Winfrith United Kingdom, 1972.

[4] M. J. Halsall, "CACTUS, a Characteristics Solution to the Neutron Transport Equations in Complicated Geometries", AEEW-R 1291, *Atomic Energy Establishment*, Winfrith, Dorchester, Dorset, United Kingdom, April 1980.

[5] *A review of characteristic methods used to solve the linear transport equation*, LAUR-136, ANS/ENS Joint Topical Meeting, Mathematical Methods in Nuclear Engineering, April 26-29, 1981, Munich, FRG.

[6] R. Sanchez, A. Chetaine, "A Synthetic Acceleration for a Two-Dimensional Characteristic Method in Unstructured Meshes", *Nuclear Science and Engineering*, 136, pp. 122-139, 2000.

[7] R. Sanchez, L. Mao, S. Santandrea, "Treatment of Boundary Conditions in Trajectory-Based Deterministic Transport Methods", *Nuclear Science and Engineering*, 140, pp. 23-50, 2002.

Guérin (P.), Baudron (A.M.), Lautard (J.J.), "Domain Decomposition Methods for Core Calculations Using the MINOS Solver", *Joint International Topical Meeting on Mathematics & Computations and Supercomputing in Nuclear Applications*, M&C +SNA 2007, Monterey April 15-19, 2007.

Wang (Y.), *Adaptive Mesh Refinement Solution Techniques for the Multi-group SN Transport Equation Using a Higher-Order Discontinuous Finite Element Method*, PhD Thesis, Texas A&M University, 2009.

Hébert (A.), *Applied Reactor Physics*, Montréal, Presses Internationales Polytechnique, 2009.

Moller (J.Y.), *Résolution de l'équation du transport des neutrons dans les cœurs de réacteurs nucléaires par la méthode (Galerkin) des éléments finis discontinus courbes*, thèse de l'université Henri Poincaré, Nancy, 2011.

Moller (J.Y.) and Lautard (J.J.), "MINARET, A Deterministic Neutron Transport Solver for Nuclear Core Calculations", *International Conference on Mathematics and Computational Methods Applied to Nuclear Science and Engineering* (M&C 2011), Rio de Janeiro, RJ, Brazil, May 8-12, 2011.

Mireille Coste-Delclaux, Cheikh M. Diop, Franck Gabriel, Jean-Jacques Lautard, Christine Magnaud, Fausto Malvagi, Sylvie Naury and Anne Nicolas
Department for Systems and Structures Modeling

Monte-Carlo Method for Solving the Boltzmann Equation

The Monte-Carlo probabilistic approach allows microscopic-scale "reality" to be simulated so as to reach macroscopic physical quantities: neutrons are individually followed, and events of interest are the interactions which they induce with the various nuclei of the atoms constituting the environment gone through: scatterings, capture, fission, reactions (n,2n), etc. This series of events is called a "**history**". Simulating a sufficient number of neutron histories is what makes it possible to quantify the macroscopic physical quantities of interest. The population of neutrons generated per second in a given instant in a PWR core in normal operation is an approximate 10^{19}. Now, current technology does not yet allow as many particles to be followed. With a representative sample of one billion (10^9) histories, the effective multiplication factor of a PWR core can now be determined with a statistical accuracy of a few *pcm*, and power per assembly with a 1% relative standard deviation.

The Monte-Carlo method applied to solving the neutron transport equation is assumed to be "**exact**", for it is able to reproduce particle-matter interaction phenomena "**with no approximations**" (as opposed to modeling through deterministic methods: *e.g.* no multigroup approximation) in physical systems displaying **any three dimensional geometry**. The counterpart however is its "time cost", due to the slowness of the statistical convergence of simulation. This induces a strong constraint on the size of the regions to be investigated, even if it is possible, in some situations, to obtain a flux estimation in one point of space. For the same reason, within the framework of neutronics studies, the resolution of the Boltzmann equation by the Monte-Carlo method is generally achieved in steady-state conditions.

The neutron transport codes based on the Monte-Carlo method simulate neutron propagation starting from pointwise nuclear data (cross sections, energetic and angular transfers, particle emission spectra…) provided in international evaluation files (*cf. supra*, pp. 21-38). This is the reason why they are often qualified as **continuous energy Monte-Carlo transport codes**, and they have got the status of **reference transport codes** with respect to deterministic transport codes.

General principles

Applying the Monte-Carlo method ([1], [2], [3]) to solve the Boltzmann equation is based on the latter's integral formulation presented *supra*, pp. 55-57.

The interest of this integral formulation lies in that it highlights the operators used to perform the simulation of neutron histories.

Prior to setting forth the general principles for applying the Monte-Carlo method to the resolution of the transport equation, it is useful to remind the definition of two physical quantities: detector response, and collision density.

A detector response, here denoted $R(Z)$, is the term currently used to specify a physical quantity of interest (*e.g.* flux or reaction rate) integrated in an area, Z circumscribed in the phase space. $R(Z)$ can be written by definition as follows:

$$R(Z) = \int_Z s_R(P)\psi(P)dP \qquad (1)$$

where $\psi(P)$ is the angular flux of neutrons at point P of phase space, defined by the triplet $(\vec{r}, E, \vec{\Omega})$, and $s_R(P)$ is the response or sensitivity function characterizing the quantity $R(Z)$. For instance, we can use: $s_R(P) = 1$ for flux calculation and $s_R(P) = \Sigma(\vec{r}, E)$ for the calculation of a reaction rate.

The collision density of neutrons corresponding to neutrons entering in collision at point P is formulated as follows:

$$\zeta(P) = \zeta(\vec{r}, E, \vec{\Omega}) = \Sigma(\vec{r}, E)\psi(\vec{r}, E, \vec{\Omega}) = \Sigma(P)\psi(P) \qquad (2)$$

where $\Sigma(\vec{r}, E) = \Sigma(P)$ represents the total macroscopic neutron cross section at point $\vec{r}$ and at the incident energy E.

It is convenient here to reformulate the expression giving $R(Z)$ by introducing the neutron collision density:

$$R(Z) = \int_Z \frac{s_R(P)}{\Sigma(P)}\zeta(P)dP \qquad (3)$$

The integral formulation of the Boltzmann equation (see inset p. 57) can be re-written with collision density $\zeta(P)$ in a compact formulation as follows:

$$\zeta(P) = \int_D K(P' \to P)\,\zeta(P') + Q(P) \qquad (4)$$

where $K(P' \to P)$ is the **kernel of the integral transport operator** which moves the particle from point P' to point P of the phase space D covered by the physical system investigated.

This integral operator is the product of the two operators displacement and collision whose kernels are respectively denoted $T(\vec{r}\,' \to \vec{r}, E, \vec{\Omega})$ and $C(\vec{r}, E' \to E, \vec{\Omega}' \to \vec{\Omega})$:

• The kernel of the displacement operator $T(\vec{r}\,' \to \vec{r}, E, \vec{\Omega})$ is given by:

$$T(\vec{r}' \to \vec{r}, E, \vec{\Omega}) d\vec{r} = \left[\exp\left(-\int_0^s \Sigma(\vec{r} - s'\vec{\Omega}, E)\, ds'\right) \right] \Sigma(\vec{r}, E)\, ds \tag{5}$$

with: $\vec{r} = \vec{r}\,' + s'\vec{\Omega}$.

By interpreting the macroscopic cross section $\Sigma(\vec{r}, E)$ as a probability density (the probability of interaction per unit length [cm^{-1}]), the expression (5) is interpreted as the product of probability $\exp\left(-\int_0^s \Sigma(\vec{r} - s'\vec{\Omega}, E)\, ds'\right)$ for the neutron not to have a collision along the path of length s, by the probability $\Sigma(\vec{r}, E)\, ds$ to collide on the elementary path between s and $s + ds$. In other words, it is interpreted as the probability density for the neutron to travel the distance $s = |\vec{r} - \vec{r}\,'|$ without undergoing any collision, and to collide in $\vec{r}$.

• The kernel of the collision operator $C(\vec{r}, E' \to E, \vec{\Omega}' \to \vec{\Omega})$ is given by:

$$C(\vec{r}, E' \to E, \vec{\Omega}' \to \vec{\Omega}) = \frac{\Sigma_s(\vec{r}, E' \to E, \vec{\Omega}' \to \vec{\Omega})}{\Sigma(\vec{r}, E')} \tag{6}$$

where $\Sigma_s(\vec{r}, E' \to E, \vec{\Omega}' \to \vec{\Omega})$ is the differential macroscopic scattering cross section of neutron, in energy and direction;

• $Q(P)$ represents the source particles which directly arrive at P without undergoing any collision:

$$Q(P) = \int_{DS} S(P_0) T(P_0 \to P) dP_0 \tag{7}$$

where DS refers to the $S(P_0)$ source area in the phase space.

Decomposition into a Neumann series

It can be shown that the $\zeta(P)$ solution to the integral equation (4) can be expressed by a series expansion named "**decomposition into a Neumann series**":

$$\zeta(P) = \sum_n^{\infty} \zeta_n(P) \tag{8}$$

in which each of the terms $\zeta_n(P)$ has a physical interpretation (see Fig. 36):

$\zeta_0(P) = Q(P)$ is the contribution to $\zeta(P)$ of neutrons directly arising from the source;
$\zeta_1(P)$ is the contribution to $\zeta(P)$ of neutrons which have undergone one, and only one, collision;
$\zeta_2(P)$ is the contribution to $\zeta(P)$ of neutrons which have undergone two collisions;
$\zeta_n(P)$ is the contribution to $\zeta(P)$ of neutrons which have undergone n collisions;

with:

$$\zeta_n(P) = \int_{DS} \dots \int_D S(P_0) T(P_0 \to P_1) \left[\prod_{k=1}^{n-1} K(P_k \to P_{k+1}) \right] K(P_n \to P) dP_0 \dots dP_n \quad n \geq 1 \tag{9}$$

the integrations being then performed on the phase space.

It can be observed that the random process of neutron propagation is a discrete *Markovian-type process*: the state of the particle at step n is determined from the knowledge of its state at the immediately previous step $(n-1)$, the history of a particle constituting a *Markov chain*.

This decomposition of $\zeta(P)$ into a *Neumann series* therefore shows that histories of any length arriving at the result area contribute to the quantity of interest $R(Z)$.

It naturally leads to the solution of the transport equation by the **Monte-Carlo method**, that is by simulating (on computer) the chain of events constituting the history of each source neutron: scatterings, absorptions, multiplications, leakages out of the physical system being investigated.

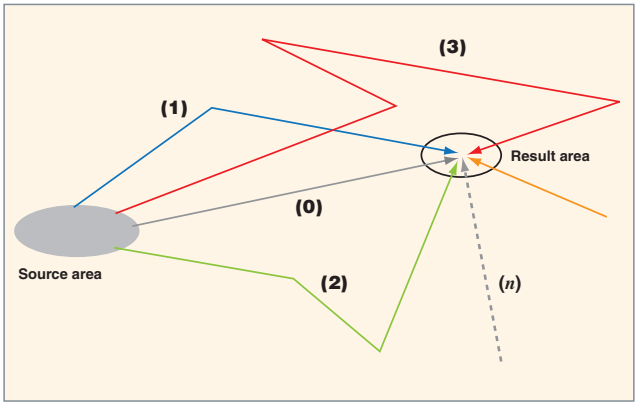

Fig. 36. Illustration of decomposition into a Neumann series. (n): order number of the collision, or number of collisions undergone by a neutron arising from the source area, before arriving at the result area.

Resolution of the transport equation with the Monte-Carlo method

Thus, the resolution of the transport equation through the Monte-Carlo method consists in the following steps:

a. To build a statistical process called "**game**", which, starting from a source, reproduces the particle history, represented by a set of paths and of collisions delimiting each path (scatterings, absorptions…). That results in a chain of event sites (source particle emission, collisions, disappearance): P_0, P_1, P_2, …, P_n…

b. To define a random variable $X(Z)$ that is coupled with the quantity of interest $R(Z)$: $X(Z)$ is referred to as "**estimator**" of $R(Z)$. When a neutron enters the result area Z during its history, this fact is recorded by assigning a value ϖ to $X(Z)$. For example, considering expression (3), if an interaction takes place in a point P of Z, then a value equal to: $(1 \times \frac{s_R(P)}{\Sigma(P)})$ is assigned to ϖ. The quantity ϖ is called "**score***" or "**tally***" or "**payoff***". At the opposite, if a neutron has not entered the result area during its history, the corresponding score is $\varpi = 0$.

c. To determine the "game rules", that is defining the probability densities with which events are selected. Regarding particles, that means choosing their paths, the nature of the interaction undergone, and, in the case of a scattering, their energy and direction after the shock. This is achieved in a random way, and in accordance with the physical characteristics of the particle source, and with the physical laws prevailing in their interactions with matter. The probability densities used to simulate the particle history have to be such that $E[X(Z)]$, the mathematical expectation of $X(Z)$, fulfills the following equation:

$$\mathrm{E}[X(Z)] = R(Z) \tag{10}$$

d. To perform the game M times independently, simulating M ($m = 1, M$) particle histories. In practice, N batches (or samples, or cycles, or generations) of M particles are simulated, hence a corresponding estimate $\tilde{X}_\nu(Z)$ of $R(Z)$, $\nu = 1, N$. The quantity is obtained through the empirical average:

$$\bar{X}_\nu(Z) = \frac{1}{M}\sum_{m=1}^{M} \varpi_{m,\nu}(Z) \tag{11}$$

where $\varpi_{m,\nu}(Z)$ is the score associated with the history m of the batch ν.

e. To assess the quantity of interest $R(Z)$ by applying the *law of large numbers* (N must be sufficiently large). $R(Z)$ is approached through the empirical average $\bar{X}_N(Z)$ of quantities $\tilde{X}_\nu(Z)$.

$$\bar{X}_N(Z) = \frac{1}{N}\sum_{\nu=1}^{N} \tilde{X}_\nu(Z)\ , \qquad \lim_{N\to\infty} \bar{X}_N(Z) = R(Z) \tag{12}$$

The central limit theorem states that quantities $\tilde{X}_\nu(Z)$ are distributed according to a Gaussian law, and the variance $\left[\varepsilon_{\bar{X}_N(Z)}\right]^2$ associated with their average, $\bar{X}_N(Z)$, is assessed without bias by:

$$\left[\varepsilon_{\bar{X}_N(Z)}\right]^2 = \frac{1}{N(N-1)}\sum_{\nu=1}^{N} (X_\nu(Z) - \bar{X}_N(Z))^2 \tag{13}$$

The confidence interval is defined as follows:

$$c(e) = \textit{probability}\ \{\bar{X}_N(Z) - e \le X(Z) \le \bar{X}_N(Z) + e\} \tag{14}$$

where e is a positive real, being calculated for a Gaussian probability density referring to the *central limit theorem*.

The usual values of e and of the corresponding values of the confidence interval are the following:
- $e = \varepsilon_{\bar{X}_N(Z)}$, $c(e) = 0.689$ (68.9 % of confidence)
- $e = 2\varepsilon_{\bar{X}_N(Z)}$, $c(e) = 0.954$ (95.4 % of confidence)
- $e = 3\varepsilon_{\bar{X}_N(Z)}$, $c(e) = 0.997$ (99.7 % of confidence).

Particularly, in the nuclear criticality-safety area, the computed value of the effective multiplication factor k_{eff} is given with a confidence interval corresponding to $3\varepsilon_{\bar{X}_N(Z)}$.

Figure 37 below schematizes the algorithm for simulating the history of particles which propagate in matter (the so-called "game").

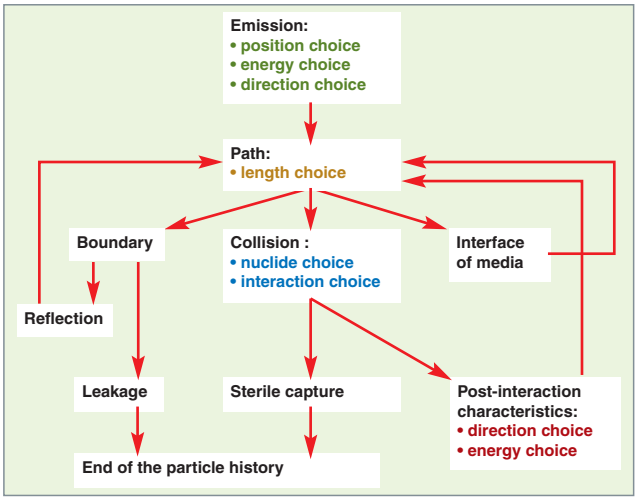

Fig. 37. General algorithm of particle history simulation using the Monte-Carlo method in a non-multiplying medium.

It is worth to mention here that two types of simulation can be carried out:

- a **natural** or analog **simulation** which uses the natural laws of occurrence of the physical phenomena initiated by the neutron;

- a **non-analog simulation**, often referred to as **biased simulation**, which uses artificial laws of occurrence of the physical phenomena initiated by the neutron, allowing to get a result in a shorter time than with analog simulation, for an equal variance (see inset, p. 102).

Event sampling laws – Building of the statistical process

As mentioned above, a neutron's history is built through the sampling (see inset, p. 93) of the successive events which take place from this neutron's birth to its disappearance. This event selection is carried out according to the probability laws that govern those events. Formally, these probability densities are defined as follows.

The first event of a history is a neutron's birth, which means determining the point P_0 of the phase space which belongs to the source area from which the neutron is made to emerge. This point is chosen using a probability density $f_0(P_0)$ which is built from the normalized distribution of the source $S_0(P_0)$ over its definition area DS within the phase space:

$$f_0(P_0) = \frac{S_0(P_0)}{\int_{DS} S_0(P_0) dP_0} \tag{15}$$

In practice the source often stands as a product of functions respectively depending on space, energy, and direction, and even time. So these variables are successively sampled through probability densities built according to the principle mentioned above. This is how the neutron's initial physical characteristics required to initiate its propagation are determined.

Once the point P_0 is known, the next point P_1 of the event chain is chosen using the probability density $f_1(P_1)$ deduced from the kernel of the integral transport operator:

$$f_1(P_1) = \frac{K(P_0 \to P_1)}{\int_D K(P_0 \to P_1) dP_1} \tag{16}$$

And so on: the point of the event chain P_i is chosen with the help of the probability density $f_i(P_i)$:

$$f_i(P_i) = \frac{K(P_{i-1} \to P_i)}{\int_D K(P_{i-1} \to P_i) dP_i} \tag{17}$$

In practice, densities exibit a factorized form complying with expressions (5) and (6): the neutron's path is chosen, and then the interaction, and so are, in the case of a scattering or a fission, the characteristics of the re-emitted neutron (direction and energy).

The neutron's path length between two successive collisions is sampled from expression (5). In the case of a propagation in a homogeneous medium, the path law (probability density) deduced from (5) can be simply expressed as follows:

$$f(s) = \Sigma(E)\, e^{-\Sigma(E)s} \tag{18}$$

where s is the path length. This length is sampled reversing the repartition function of $f(s)$ (18).

$$s = -\frac{1}{\Sigma(E)} \ln(1 - \xi) \tag{19}$$

where ξ is a random number uniformly selected between 0 and 1 (see insets, pp. 93 and 94).

Expression (6) relating to the collision operator kernel can be made explicit so as to display the probabilities of the different events associated with a collision (*cf.* Fig. 37): choice of the nuclide, choice of the interaction type, choice of the neutron's direction, and, possibly, energy after scattering, if the chosen interaction is a scattering. Considering a medium consisting of a homogeneous mixture of nuclides j, the collision operator kernel can be written as follows:

$$C(\vec{r}, E' \to E, \vec{\Omega}' \to \vec{\Omega}) = \sum_j \frac{\Sigma_j(\vec{r}, E')}{\Sigma(\vec{r}, E')} \sum_i \left[\frac{\sigma_{sj}(E')}{\sigma_j(E')}\right] \frac{\sigma_{ij}(E')}{\sigma_{sj}(E')} \nu_{ij} f_{ij}(E' \to E, \vec{\Omega}' \to \vec{\Omega}) \tag{20}$$

with:

- $\sigma_{sj}(E')$: the microscopic total scattering cross section at energy E' for nuclide j;
- $\sigma_j(E')$: the microscopic total cross section at energy E' for nuclide j;
- $\sigma_{ij}(E')$: the microscopic total scattering cross section at energy E' for the nuclear reaction of type i (elastic scattering, inelastic scatterings, [n, 2n] reaction, ...) on nuclide j;
- $\Sigma_j(\vec{r}, E')$: total macroscopic cross section at point $\vec{r}$, at energy E' for nuclide j;
- $\Sigma(\vec{r}, E') = \sum_j \Sigma_j(\vec{r}, E')$: total macroscopic cross section of the neutron propagation medium, *i.e.* a homogeneous mixture of nuclides j, at point $\vec{r}$, and at energy E';
- ν_{ij} : multiplicity of the neutrons produced during the interaction i on nuclide j : (n, 2n) reaction, fission, …;
- $f_{ij}(E' \to E, \vec{\Omega}' \to \vec{\Omega})$: energy and angle transfer probability density for the scattered particle related to the interaction of type i on nuclide j.

The interest of (20) is to highlight the following probabilities and probability density, directly used to achieve the Monte-Carlo simulation:

- $\frac{\Sigma_j(\vec{r},E')}{\Sigma(\vec{r},E')}$: probability for the choice of nuclide j;
- $\frac{\sigma_{sj}(E')}{\sigma_j(E')}$: probability for the neutron's non-absorption (or survival);
- $\frac{\sigma_{ij}(E')}{\sigma_{sj}(E')}$: probability for the choice of the scattering type;
- $f_{ij}\,(E'\to E, \vec{\Omega}'\to\vec{\Omega})$: energy and angle transfer probability density for the scattered particle related to the interaction of type i on nuclide j.

In the first three cases, the probabilities involved are of the discrete type.

The insets below present respectively the principle of event sampling and the random number generators currently used.

Sampling of a random variable according to a probability law

In practice, how can a value of the random variable be chosen in accordance with its probability density $f(x)$?

That means the two following main steps:

- Random number generators uniformly distributed over the interval $(0, 1)$ of the real straight line have been developed and made available on computers. Actually, the numbers are pseudo-random numbers, the random quality of which depends on the performance of the generator producing them. So, a random number ξ is chosen using an appropriate random number generator;

- The probability density $f(x)$ being defined on a segment (a, b) of the real straight line, we can establish the relationship existing between the number sampled on the interval $(0, 1)$, according to a constant probability density equal to one, and the variable x distributed over the interval (a, b) according to the density $f(x)$. This relationship is obtained through the expression of the equality of the distribution functions:

$$\int_0^{\xi} 1d\xi' = \xi = \int_a^x f(x')dx'$$

There exists a value of the variable x distributed according to density $f(x)$ which fulfills this equality and can be obtained as a function of ξ, by solving this equation in x.

Let us consider, for example, the choice of a path relating to a neutron moving in a medium characterized by a total macroscopic cross section Σ (cm^{-1}). The probability density associated with this path s is:

$$f(s) = \Sigma\, e^{-\Sigma s}$$

Hence the following expression:

$$\int_0^{\xi} 1d\xi' = \xi = \int_0^s f(s')ds' = \int_0^s \Sigma(E)e^{-\Sigma s'}ds'$$

which results in:

$$s = -\frac{1}{\Sigma}\ln(1-\xi)$$

For example, if $\Sigma = 0.791$ cm^{-1} and $\xi = 0.8$, then $s = 2.0347$ cm.

In the case of discrete probabilities p_i associated with a set of possible events i (*e.g.* the type of interaction of a neutron with a given nuclide), the selection of one among them is done through identifying the interval of the distribution function in which the random number ξ uniformly sampled in interval $(0, 1)$ is located. So, if $0 < \xi \le p_1$, event 1 is chosen.

If $\sum_{j=1}^{i-1} p_j < \xi \le \sum_{j=1}^{i} p_j$

event i is chosen.

Let us consider, for example, the three types of events induced by a neutron, *i.e.* scattering, sterile capture, and fission, for which respective macroscopic cross sections in the medium of interest, and at a given energy, are the following:

- Scattering: $\Sigma_s = 0.203$ cm^{-1},
- sterile capture: $\Sigma_c = 0.381$ cm^{-1},
- fission : $\Sigma_f = 0.207$ cm^{-1}.

The probabilities coupled with each of these three types of reaction are as follows:

- Scattering: $p_s = \frac{\Sigma_s}{\Sigma} = 0.2566$,
- sterile capture: $p_c = \frac{\Sigma_c}{\Sigma} = 0.4817$,
- fission: $p_f = \frac{\Sigma_f}{\Sigma} = 0.2617$.

Taking the scattering, sterile capture, and fission interactions in the arbitrary following order:

- If the sampled value of ξ has a value ranging from 0 to $p_s = 0.2566$, for instance, then scattering is selected;

- if ξ has a value ranging from $p_s = 0.2566$ to $p_s + p_c = 0.7383$, for instance $\xi = 0.71$, then sterile capture is selected;

- at last, if ξ takes a value ranging from $p_s + p_c = 0.7383$ to $p_s + p_c + p_f = 1$, for instance $\xi = 0.863$, then fission is simulated.

A generator of random numbers, ξ, provides a means to sample a random variable of a given probability density. A random number generator is designed to – almost – randomly choose a real number in the interval (0,1). Thus, numbers delivered by random number generators are qualified pseudo-random, for these generators are not (yet) able to reproduce hazard perfectly. The quality of a random number generator is so defined by its ability to reproduce hazard. This quality is reflected by a series of properties, among them the stochasticity and uniformity in the distribution of the random numbers generated, subjected to appropriate tests (*Marsaglia tests* [1, 2, 3], *Knuth tests* [4], and *L'Écuyer tests* [5, 6, 7] ...)

There exist several kinds of random number generators available on computers:

- *Linear Congruential Generators* (LCGs) [8]), such as DRAND48 [9];
- Feedback Shift Register generators, such as the *Generalised Feedback Shift Register* (GFSR [10, 11], arising from the *Multiplicative Lagged-Fibonacci Generator*) or the *Mersenne Twister* (TGSFR) [12, 13],
- shift register generators: SHR3 [14] (3-shift random number generator);
- the *"Blum Blum Shub"* generator [15]…

The transport code MCNP-5 uses a congruential random number generator [16]. The Monte-Carlo transport code TRIPOLI also uses DRAND48 generators operating in a *single-processor* mode, as well as GFSR and Mersenne Twister operating in a *multi-processor* or *parallel* mode.

Example of the linear congruential generator

The *linear congruential generator* generates a series of random numbers defined by the following recurrence:

$$X_{i+1} = (aX_i + c)\ (mod\, m),\ i = 1, \ldots, n,$$

where:
- a: is a positive integer chosen, referred to as the *multiplier*;
- c: is a positive or null integer chosen, referred to as the *increment*;
- m: is a positive integer referred to as the module.

The random number ξ_i which has a real value in the interval $(0, 1)$, is obtained through the division:

$$\xi_i = \frac{X_i}{m}$$

This iterative process is initiated by the datum of the first term of the series, X_0, called the *seed*.

The (deterministic) series so defined of (pseudo- or quasi-) random numbers is characterized by a period, after which the series is generated again identically. The quality of a random number generator can also be assessed with the length of its period (a sufficient length is required), its *reproducibility*, its *portability*, and its *velocity*.

As an illustration, the IBM System/360 computer of the seventies, a 32-bit machine, provided a congruential random number generator such as:

$$a = 7^5 \qquad c = 0 \qquad m = 2^{31} - 1 \qquad X_{i+1} = 7^5 X_i = 16{,}807\ X_i$$

It is shown that the maximum period of this generator is equal to $2^{31} - 2$ [17, 18].

The table below indicates the periods of random number generators used in Monte-Carlo computer codes:

Random number generator	Period	Use
DRAND48	2^{48}	Single processor
GFSR	$2^{607} - 1$	Multiprocessors (parallel simulations) Parallelization technique: Leap Frog
MERSENNE TWISTER	$2^{19,937} - 1$	Multiprocessors (parallel simulations) Parallelization technique: use of another generator

The *Mersenne Twister generator* was named after Marin Mersenne, a French mathematician (1588-1648): a Mersenne prime number is a prime number that can be put in the form $2^p - 1$ where p, too, is a prime number.

Research is underway to build a *Quantum Random Number Generator* (QRNG) [19].

References

[1] G. Marsaglia, and A. Zaman, "A new Class of Random Number Generators", *The Annals of Applied Mathematics*, vol. 1, nº 3, 1991.

[2] G. Marsaglia, "Random numbers for C: The END?" electronic billboard sci.crypt. random-numbers, January 20, 1999.

[3] G. Marsaglia, and W. W. Tsang, "The 64-bit universal RNG", Statistics & Probability Letters, vol. 66, nº 2, 2004.

[4] D. E. Knuth, *The Art of Computer Programming*, Massachusetts, Addison-Wesley Reading, 1969.

[5] P. L'Ecuyer, "Random number generation", in W. Haerdle, J.E. Gentle and Y. Mori, *Handbook of Computational Statistics*, Springer Verlag, chapter 2, pp. 35-70, 2004.

[6] L'Ecuyer, R. Simard, "Test01: A C Library for Empirical Testing of Random Number Generators", ACM Transactions on Mathematical Software, vol. 33, nº 4, art. 22, August 2007.

[7] X. Hugot, Y.K. Lee, "Verification Tool For Tripoli-4 Criticality Code Validation", *Proceedings of ICNC'2007*, St. Petersburg, p. 453, 2007.

[8] D. H. Lehmer, "Mathematical methods in large scale computing units", in *Proceedings of the Second Symposium on Large Scale Digital Computing Machinery*, Cambridge Harvard University Press, pp. 141-146, 1951.

[9] *DRAND48 Man*, Page: http://manpagesfr.free.fr/man/man3/drand48.3.html.

[10] T.G. Lewis, W.H. Payne, "Generalized Feedback Shift Register Pseudorandom Number", Algorithm, *Journal of the Association for Computing Machinery*, vol. 20, Nº 3, July 1973.

[11] S. Aluru, G.M. Prabhu, J. Gustafson, "A random number generator for parallel computers", *Parallel Computing* 18, 1992.

[12] M. Matsumoto, T. Nishimura, "Mersenne Twister: A 623-dimensionally equidistributed uniform pseudorandom number generator", *ACM: Transactions on Modeling and Computer Simulations, Special Issue on Uniform Random Number Generation*, 1998.

[13] F. Panneton, P. L'Ecuyer, M. Matsumoto, "Improved Long-Period Generators Based on Linear Recurrences Modulo 2", *ACM Transactions on Mathematical Software*, 32, pp. 1-16, 2006.

[14] G. Marsaglia, "Xorshift RNGs", *Journal of Statistical Software*, vol. 8, Issue 14, July 2003.

[15] L. Blum, M. Blum, and M. Shub. "A Simple Unpredictable Pseudo-Random Number Generator", *SIAM Journal on Computing*, vol. 15, pp. 364-383, May 1986.

[16] F. Brown, Y. Nagaya, *The MCNP5 Random Number Generator*, LA-UR-02-3782, Los Alamos National Laboratory, American Nuclear Society Winter Meeting, Washington DC, November 17-21, 2002.

[17] R. Y. Rubinstein, *Simulation and the Monte-Carlo Method*, New York, John Wiley & Sons, Coll. Wiley Series in Probability and Mathematical Statistics, 1981, pp. 25-26.

[18] S.K. Park, K. W. Miller, "Random number generators: Good ones are hard to find", *Communications of ACM, Computing Practices*, vol. 31, n° 10, October 1988.

[19] P. J. Bustard, D. Moffatt, R. Lausten, G. Wu, I. A. Walmsley, B. J. Sussman, "Quantum random bit generation using stimulated Raman scattering", *Optics Express*, vol. 19, nº. 25, pp. 25173-25180, 5 December 2011.

The "weight" of a neutron

In a strictly natural (or analog) simulation, the weight of the neutron is equal to one: one neutron represents one neutron, and it is recorded as one when it reaches the result area.

For reasons of optimized computational time, instead of simulating explicitly the particle capture, the trend is to multiply its unit-worth weight at the start of the simulation, by its survival probability equal to the ratio between the scattering cross section and the total cross section $\frac{\sigma_{sj}(E')}{\sigma_j(E')}$, and so on for each collision. This process justifies that the ratio is often referred to the "*implicit capture factor*".

As $\sigma_{sj}(E') < \sigma_j(E')$, the neutron weight w decreases with the collisions it undergoes, and tends to zero when the collision number tends to infinity. In this case, the neutron weight after n collisions is written $w_n = \left[\frac{\sigma_{sj}(E')}{\sigma_j(E')}\right]^n$. If the number of collisions is made to tend to infinity, the following result is obtained:

$$w_\infty = \lim_{n\to\infty}\left[\frac{\sigma_{sj}(E')}{\sigma_j(E')}\right]^n = 0.$$

In other terms, the "vital potential" and/or "information potential" of the neutron decreases from collision to collision. So, for a sufficiently high collision number, the neutron does not bring a higher significant contribution to the result of interest, and from the viewpoint of optimizing the computing time, the neutron is made to disappear through a relevant statistical process called "Russian roulette", when its weight falls under a fixed threshold.

So, the estimator of a response of interest also depends on the neutron weight.

The application of this simulation technique provides a first example of a simulation which is no longer strictly natural, since the capture is not explicitly simulated, hence leading to perform *non-analog simulation*.

Table 12 (see next page) gives orders of magnitude for a few characteristics of simulations relating to the calculation of the *effective neutron multiplication factor* (eigenvalue problem resolution), in a configuration met in fuel cycle's criticality studies.

Table 12.

Orders of magnitude related to a criticality benchmark

These simulations were performed on a 1.8-GHz Opteron processor.

Number of particle histories	Total number of sampling operations	Number of sampling per history	Number of collisions per history	Number of sampling per collision	Statistical accuracy	Computing time
$4\ 10^6$	10^9	256	32	8	20 pcm	900 s

As shown in the inset below, different mathematical forms can be associated with a given response, their choice being dictated by their convergence "rate" towards the value of interest. For example, in a little dense medium, the "track length estimator" converges more quickly that the "collision estimator". In some situations, thanks to a "point kernel estimator", a physical quantity can be computed at a point of the phase space: so it is for media with vacuum or of very low atom density.

Physical quantity estimators in a Monte-Carlo simulation

The table below presents various flux estimators, as well as the estimator of the particle current crossing a given surface:

Volume estimators of flux	Track length	$w\ell$
	Collision	$\dfrac{w}{\Sigma(\vec{r}, E)}$
Surface estimator of flux		$\dfrac{w}{\vec{\Omega}.\vec{n}}$
(Surface) estimator of current		w
Pointwise estimator of flux		$\propto w \dfrac{\Sigma_s(\vec{r}, E' \to E, \vec{\Omega}' \to \vec{\Omega})}{\Sigma(\vec{r}, E')} \dfrac{e^{-\tilde{\Sigma}}}{s^2}$

where:

w : neutron weight before collision;

ℓ : neutron path length between two collisions;

Σ : total macroscopic cross section of the medium in which the neutron propagates at a given energy E;

Σ_s : macroscopic scattering cross section of the medium in which the neutron propagates at a given energy E;

Σ_f : macroscopic fission cross section of the medium in which the neutron propagates at a given energy E;

$\vec{\Omega}$: neutron's propagation direction;

$\vec{n}$: normal to the surface considered;

$\tilde{\Sigma}$: optical path between collision point and flux calculation point:

$$\tilde{\Sigma} = \int_0^s \Sigma\left(\vec{r} - s'\vec{\Omega}, E\right) ds'$$

where s is the distance between collision point $\vec{r}\,' = \vec{r} - s\vec{\Omega}$ and calculation point $\vec{r}$.

The volume estimate of the flux is achieved in a given volume V of the space by "scoring" the values taken by the corresponding estimators during each event occurring in volume V. The reaction rates are obtained by multiplying the score by the microscopic or macroscopic cross sections relating to the reactions considered.

The expression of the collision estimator shows that it is not defined for a vacuum medium, for in this case $\Sigma = 0$. In such a medium, the track length estimator will be used: it will compute the lengths of neutron paths in volume V.

The so-called "point kernel estimator" is built considering any collision as a secondary neutron source. The term $\dfrac{e^{-\tilde{\Sigma}}}{s^2}$ occurring in the expression of this estimator corresponds with the flux without shock at the calculation point generated by a unit neutron source located at a s distance. The "point kernel" estimator is adapted to assess response in vacuum or in media of very low density. *A contrario*, in matter, it raises a singularity problem due to its behaviour in $\dfrac{1}{s^2}$, for a collision site may be very close to a calculation point, or even coincide with the latter [4], [5], [6].

The effective multiplication factor can also be assessed with various estimators:

- $w\nu$: at each fission, the number of fission neutrons generated ν is "scored";
- $w\nu\dfrac{\Sigma_f}{\Sigma}$: at each interaction on a fissile nucleus, the number of fission neutrons is computed;
- $w\ell\nu\Sigma_f$: at each path in the fissile medium (of length ℓ), the value taken by this expression is "scored".

Statistical convergence of a transport calculation using the Monte-Carlo method

At one or another step, engineering studies (industrial core calculations, reactor design/optimization, design basis for radiation shielding, shipping cask design…) are faced with the requirement to compute the physical quantities of interest with the best possible accuracy and in the shortest possible time. Monte-Carlo transport codes, which, as pointed out above, naturally display a time-consuming character compared to deterministic methods, tend to take up this challenge by implementing various strategies designed to speed up computational convergence.

Monte-Carlo simulation strategies

The following two examples are given as a first approach to the problematic of Monte-Carlo simulation strategies in nuclear reactor Physics.

Calculating fine power distribution in a PWR core

In order to determine power distribution in a PWR core, the user of a Monte-Carlo transport code defines space and energy scoring volumes, so that neutron flux and fission rates can be calculated within each of these volumes.

In a PWR, this number of space scoring volumes is equal to: *number of rods x number of fuel rings x number of axial steps*. Ideally, a fine mapping of power in a PWR core requires about: 40,000 x 4 x 30 = 4.8 10^6 (scoring) volumes. If a multigroup flux is to be computed in a 300 energy-group structure, that means a number of 40,000 x 4 x 30 x 300 = 1.44 10^9 (scoring) volumes. In a Monte-Carlo simulation, each of these volumes has to be visited by a sufficient number of neutrons to fulfill the statistical accuracy required for each of the computed physical quantities.

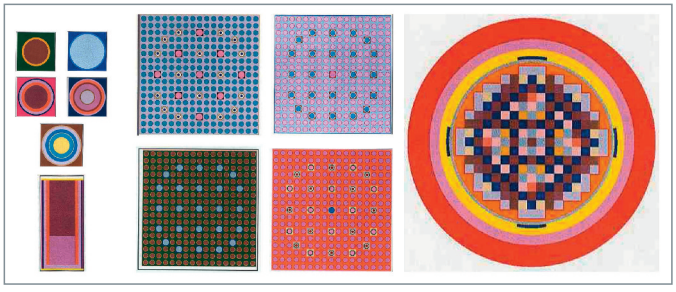

Fig. 38. Example of modeling of a fresh PWR core for the Monte-Carlo transport code TRIPOLI-4®, from the cell to the whole core consisting of its different 17x17 fuel-rod assemblies.

These figures are to be multiplied by the number of types of physical quantities to be computed, fluxes, and reaction rates. If a depletion (or burnup) calculation is considered, taking account of 200 nuclides in order to assess the material balance in a core, this number of scoring volumes has to be multiplied again, e.g. by a factor 50 if considering 50 burnup steps ranging from 0 to 60,000 MWd/t.

So this example shows that a high number of neutron histories will have to be simulated to get the value of each required tally with an acceptable statistical error, and that computing such a high number of tallies will significantly impact, of course, the computational time.

Calculating neutron flux attenuation in the structures of a nuclear reactor

Let us consider the example of the attenuation of a neutron flux by shields, of about several decades (up to 14 decades), as shown on Figure 39.

In such situations, reaching statistical convergence in "reasonable" simulation times is often illusory, hence the use of simulation acceleration methods.

Convergence and quality factor of a Monte-Carlo simulation

It can be shown that the variance σ^2 associated with a computed response varies as the inverse of the number of simulated particles:

$$\sigma^2 = \frac{1}{n} \qquad (21)$$

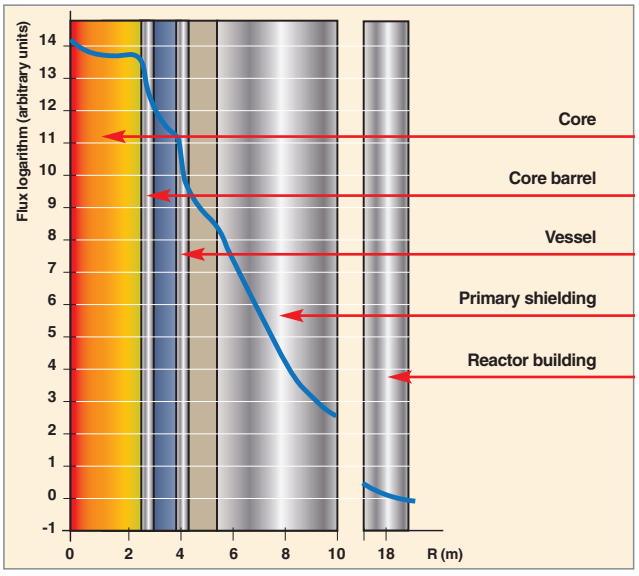

Fig. 39. Flux attenuation over 14 decades from the core to the outside of the reactor building.
(From A. Baur, *Protection contre les rayonnements, aspects physiques et méthodes de calcul*, CEA, 1985).

As a consequence, in order to decrease variance by a factor 10, a number 100 times higher of neutrons has to be simulated, and the computational time will be increased in the same proportions. This confirms that the Monte-Carlo method applied in natural simulation (or analog game) exhibits the drawback, already pinpointed, of converging "slowly".

Several strategies are available to the user to get the results of interest in the shortest possible time:

- Performing parallel calculations on a computer network, or on a massively parallel computer (see *infra*, pp. 149-161);
- Performing calculations in two steps: reference calculation during which relevant information about simulated particle histories are stored, and then use of this information by an appropriate functionality of the Monte-Carlo code, the latter allowing parametric studies to be carried out under some conditions;
- Using the most powerful processors available.
- Implementing *convergence acceleration techniques*, also called *variance reduction techniques*.

These strategies are summarized in Table 13, which gives orders of magnitude of their respective efficiencies. They are not exclusive of one another. Figure 40 shows the approximate progress in the number of neutron histories that can be simulated to carry out a study, as a function of computer development, going from about 5,000 in the sixties to one billion in the early 2000s, and hundreds of billions in 2013.

The first three strategies improve the "*extrinsic*" *quality* of simulation, which makes it possible to get results displaying sufficient statistical convergence in a shorter time.

Referring to the previous PWR example, the computational time required to get a fission rate in discretized volumes of a fuel rod with a statistical accuracy of 1 %, through a Monte-Carlo simulation, could be evaluated to approximately 100 years if using a 2 GHz mono-processor computer. So, theoretically, this time is expected to fall to about one year with a hundred of parallel processors, and to a few days with 10,000 processors.

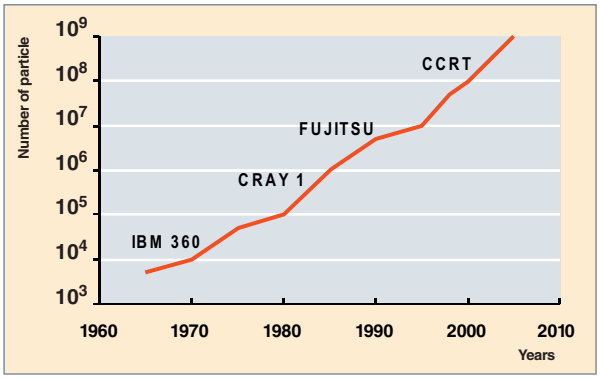

Fig. 40. Time evolution of the number of simulated particle histories as a function of increasing in computer power.

The fourth strategy aims at improving the *"intrinsic" quality* of a Monte-Carlo simulation. Generally, the simulation quality can be measured using a quantity called **figure of merit (FOM)**, defined by the following relationship:

$$FOM = \frac{1}{\sigma^2 t} \qquad (22)$$

where t is the simulation time, and σ^2 the variance. So the quality of simulation is all the better and consequently the figure of merit all the higher as a small value of σ^2 is reached in a short time t.

It can be observed that the *figure of merit* remains unchanged if the strategy only lies in increasing the number of particles simulated, since the computational time and the variance are respectively proportional and inversely proportional to the number of simulated particles.

Table 13.

Strategies for reducing computing times, and improving the quality of a Monte-Carlo simulation

Strategy	Possible gain	Comment
Parallel calculation	2 to 10,000	Proportional to the number of processors.
Information storage	100	Use of information relating to previously simulated particle histories in order to conduct parametric studies, or restart calculations. Counterpart: storage volume.
Processor advances	2	Application of the Moore law: processor power increases by a factor 2 every two years.
Convergence acceleration techniques	1 to 10^{15}	Efficiency in high neutron-attenuation problems over several decades. Developing this type of techniques for criticality calculations is more delicate, but is still a current topic.

A few specificities in the convergence of a critical calculation

A **critical*** calculation, as defined in *supra*, p. 56 (Equation 3), is aimed at determining the effective **multiplication factor***, an overall physical quantity relating to the whole of the fissile system investigated. As in the deterministic approach, the **power iteration method** is implemented, the principle of which is illustrated on Figure 41 for both a deterministic calculation (left), and a Monte-Carlo probabilistic calculation (right).

The Monte-Carlo simulation is performed by successive batches, the batch $(n+1)$ using as neutron source the fission neutrons arising from the previous batch (n). Since the initial source is arbitrary, the system tends to an equilibrium state as the number of simulated neutron cycles increases.

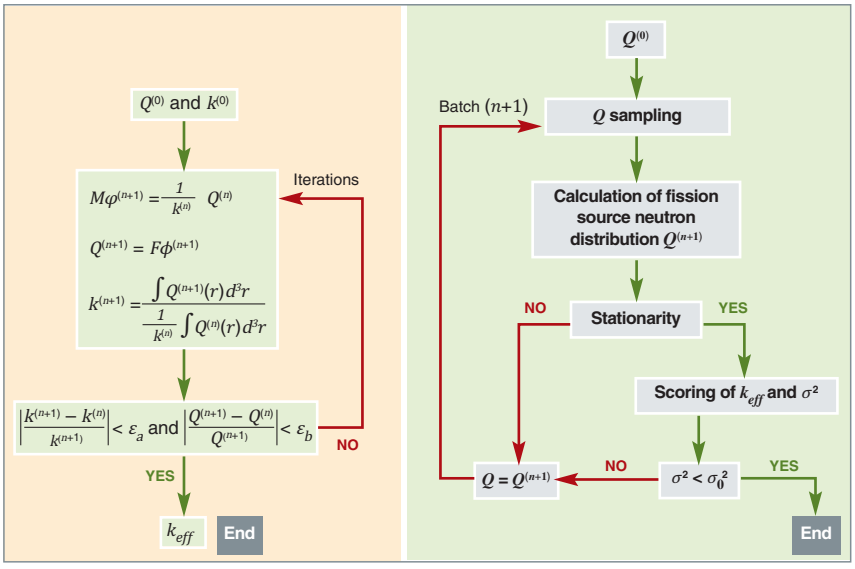

Fig. 41. Calculation of the effective multiplication factor, through the **power iterative method**. Deterministic one-energy group algorithm (left, source : J.J. Duderstadt, L. J. Hamilton, *Nuclear reactor Analysis*, John Wiley & Sons, 1976, p. 219), and probabilistic Monte-Carlo algorithm (right). In its integro-differential form (left), the resolved eigenvalue equation is in the form $M\phi = \frac{1}{k_{eff}} F\phi$ with $M = -\Omega.\overrightarrow{grad}\phi + \Sigma_a\phi$ and $F = \nu\Sigma_f\phi$. $Q^{(0)}$ stands for the (arbitrary) distribution of the initial neutron source, which allows to initiate the iterative resolution scheme.

The effective multiplication of neutrons is not the only eigenvalue satisfying the critical equation. The convergence of the iterative procedure for solving this equation uses the other eigenvalues and eigenvectors which are solutions to the critical equation. As shown in relationships (23) and (24), these eigenmodes (or higher order harmonics) "contaminate" the fundamental mode, though in such a manner that it decreases with the number of iterations. As a matter of fact, at the iteration step $(n+1)$, only considering the impact of the second harmonic, we get the following result:

$$k_{eff}^{(n+1)} \approx k_1 \left[1 + constant \times \left(\frac{k_2}{k_1}\right)^n \left(\frac{k_2}{k_1} - 1\right)\right] \qquad (23)$$

$$\phi^{(n+1)} \propto [u_1 + constant \times \left(\frac{k_2}{k_1}\right)^{n+1}] \qquad (24)$$

where:

k_1 is the first eigenvalue corresponding to the exact value of the effective multiplication factor k_{eff},

k_2 is the second eigenvalue;

u_1 is the first eigenvector corresponding to the fundamental mode.

Expressions (23) and (24) state that convergence first depends on the ratio $\frac{k_2}{k_1}$ between the first two eigenvalues of the critical state, the so-called "**dominance ratio**": the closer is k_2 to k_1, the slower is convergence, and, consequently, the higher is the number of iterations required to reach convergence, which is, for instance, the case of large physical systems such as nuclear power reactors.

It can also be observed on these expressions that the effective multiplication factor converges faster than neutron flux (or the neutron source distribution which is proportional to it).

Figure 42 represents a computational configuration known as "Computing the k_{eff} of the World", consisting of spherical fissile units, the central one being the most reactive.

Figure 43 shows the evolution of its k_{eff} as a function of the number of batches, for different initial distributions of the neutron source. It can be noted that convergence can be reached more or less "quickly" according to the case. k_{eff} is estimated by averaging the k_{eff} values obtained for each of the batches simulated **after reaching the equilibrium** in the neutron population. Reaching the equilibrium or **reaching stationarity** is the evolution stage of the neutron population characterized by the fact that neutrons have "lost the memory" of the initial computational conditions.

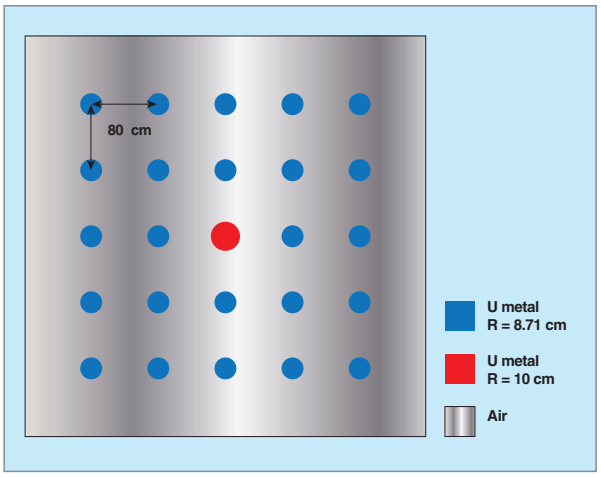

Fig. 42. OECD/NEA source convergence benchmark: problem n°4 (Whiteside's problem, "k_{eff} of the world") [7].

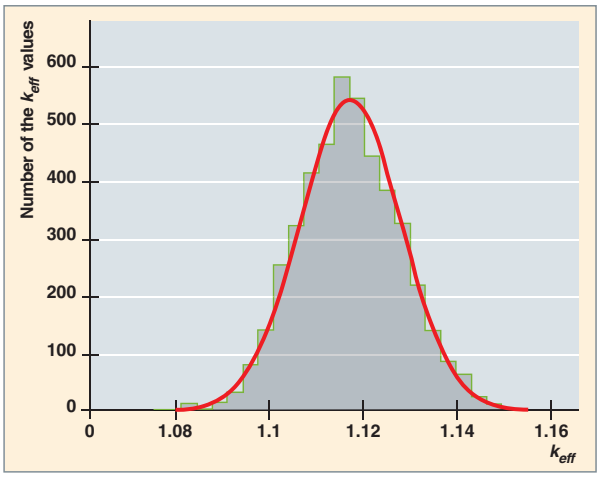

Fig. 44. Example of histogram of the k_{eff} obtained by Monte-Carlo simulation of the critical system schematized on Figure 42. The histogram obtained after a sufficient number of simulated batches displays the Gaussian shape as expected. The batches preceding the reaching of equilibrium are discarded.

Figure 44 shows an example of histogram of the values of the k_{eff} obtained by Monte-Carlo simulation.

In order to check that the distribution of the k_{eff} values generated at each batch does comply with a normal law, today several statistical tests, such as those of Kolmogorov and Cramer von Mises [8], are proposed in Monte-Carlo transport codes.

Tending to improve simulation quality, as defined above, requires to consider the issue of critical calculation convergence through the Monte-Carlo method in three aspects:

- diagnosis of the neutron population's stationarity condition in the fissile system under study;
- unbiased calculation of the neutron multiplication factor, the neutron source distribution and their associated variances;
- convergence acceleration.

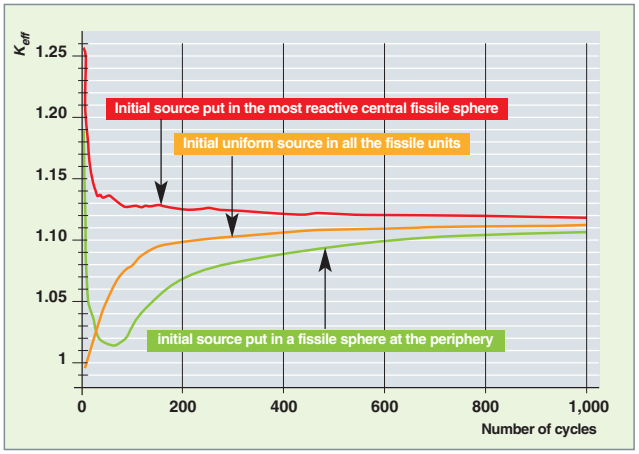

Fig. 43. Convergence of k_{eff} as a function of the number of cycles, and for various configurations of the initial (arbitrary) neutron source: initial source put in the most reactive central sphere, initial source put in a fissile sphere located at the periphery, initial uniform source in all the fissile units.

Searching for relevant criteria to determine whether a stationarity is reached

In the power iteration method, fission neutrons generated during the batch (n) are the source neutrons of the batch $(n + 1)$, which induces a statistical correlation between all of the simulated batches. What is at stake in reaching stationarity for the neutron population is unbiased assessment of the neutron multiplication factor (k_{eff}) and of the neutron flux. This unbiased assessment will be ensured if conditions for applying the central limit theorem are fulfilled, *i.e.* if neutron batches are statistically independent. How to detect this stationarity?

Some authors [9], [10], [11] have proposed an entropic criterion for diagnosing the neutron population equilibrium, this criterion being derived from Boltzmann's microscopic formulation of entropy. For this purpose, a spatial meshing has been defined on the system's geometry, and the entropy, S, of the fissile system of interest is determined as follows:

$$S = -\sum_{i=1}^{B} p_i \ln p_i \qquad (25)$$

where p_i represents the number of source particles in a mesh i, divided by the total number of particles, and B the total number of meshes. This entropy is computed at each cycle. When it is stabilized, stationary conditions are reached as shown on Figure 45 (see next page).

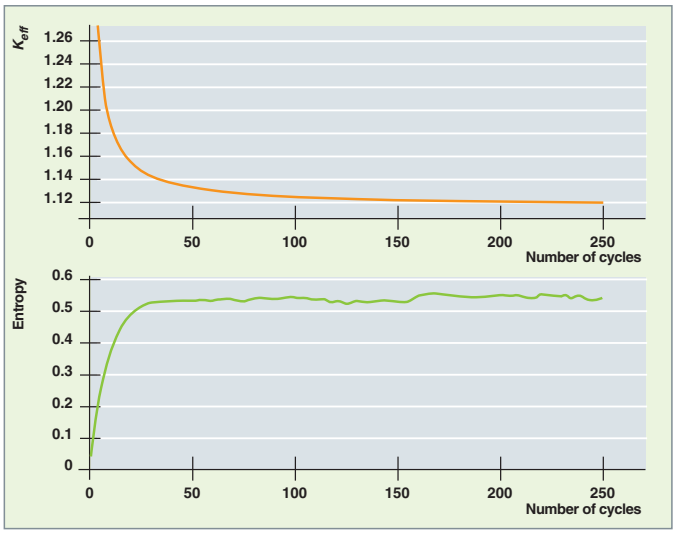

Fig. 45. Detection of the neutron source stationarity through a Boltzmann entropy calculation. A relative stabilization of entropy can be observed for a number of cycles (or batches) of about 50 (bottom curve). The k_{eff} is then assessed by averaging the evaluations achieved for all batches starting from the 50th [11].

The interest of this entropy-based criterion is that it has a physical meaning, and allows the whole phase space to be explored. Yet, this criterion proves insufficient when tackling with systems displaying low neutronic couplings, as for a PWR in which the dominance ratio is close to the unit due to its dimensions: the core center and its periphery display low coupling. The nature of the difficulty to make a Monte-Carlo critical calculation converge can be identified through variance analysis.

Calculating the variances of k_{eff} and neutron flux

In practice, the perfect stationarity can never be reached. This is due to the correlation between batches imposed by the power iteration method, that induces a propagation of statistical fluctuations from one batch to the following. Formulae (11), (12) and (13) applied to computing the average values of the k_{eff} and of the neutron flux, as well as the related variances, are no longer appropriate. It is shown that they have to be replaced by expressions including additional terms that take into account the various eigen modes of the fissile system of interest; otherwise, significant biases may be introduced in the estimated values [13], [14]. In particular, the inter-batch correlation being positive, not taking it into account leads to the underestimation of the variance. Now, these statistical effects are of prime importance, indeed, for large-sized neutronic systems such as PWRs, in which the **dominance ratio** is close to one. In practice, in order to reduce the impact of these biases on results, we make sure that:

$$\frac{1}{N \text{ (number of simulated neutrons per batch)}} < \frac{1}{\sqrt{M \text{ (number of batches)}}} \quad (26)$$

and that the N number is sufficiently high ($N > 1{,}000$).

A "reasonable" decrease in these statistical fluctuations therefore requires to simulate a sufficiently large number of batches and of particles per batch.

It is a long time since these problems were first identified and analyzed [13], [14]. As the power of current and future computers paves the way to full power reactor core calculations, these problems have been highlighted, and several authors have reviewed them, proposing various computational approaches of these statistical effects [8, 9, 12, 15, 16, 17, 18, 19, and 20]…, some of them being implemented in Monte-Carlo transport codes. One of them consists in making independent criticality calculation "packets" [21], the results of which can then be averaged in accordance with relationships (11), (12) and (13).

Acceleration of a Monte-Carlo simulation

The issue raised here is how to overcome the natural slowness of a Monte-Carlo simulation. Indeed, the answer lies in the use of *convergence acceleration techniques*, also called *variance reduction techniques*, with which a physical quantity (flux, reaction rate, etc.) can be assessed with a satisfactory statistical error while significantly reducing the simulation time.

The case of critical calculations

In criticality, the technique most used today consists in initiating the Monte-Carlo transport calculation with a neutron source distribution pre-computed with a deterministic code. It allows transient step time to be strongly reduced. Recent and pending works aim at a more ambitious objective, that is speeding up simulation convergence once the stationarity has been reached [18], [19]. The *Wielandt* (or deflation) *method*, among other explored approaches, is applied to the neutron transport Monte-Carlo simulation: it consists in bringing down the problem to be solved to a problem in which the dominance ratio is smaller, which, as previously seen, helps accelerate the convergence of the power iteration method implemented.

Biasing techniques in propagation

A special type of acceleration techniques are those referred to as **biasing techniques**. They consist in *artificially modifying* the physical laws prevailing in particle-matter interaction (probability to undergo a collision on a given nucleus, probability to induce a given reaction, probability of re-emission at a given energy and in a given direction during a scattering, etc.), in order to foster events which significantly contribute in the result of interest while minimizing the statistical distribution of their contributions. In counterpart, the estimator associated with the physical quantity of interest is also modified as shown in the short mathematical development presented in the next

inset. Referring to the same basic principle, different biasing techniques are implemented in a Monte-Carlo transport code, among which:

- The so-called "Russian roulette and splitting" technique, which artificially increases or reduces neutron population as a function of the areas where they are located,

- the so-called "exponential transform" technique, the principle of which is presented hereafter.

The principle of the "exponential transform" relies on a change of variable, from the natural flux $\psi(P)$ to the biased flux $\psi^*(P)$, through an arbitrary function $I(P)$ as follows:

$$\psi^*(P) = I(P)\psi(P) \qquad (27)$$

where P is a point $(\vec{r}, E, \vec{\Omega})$ in the phase space.

The role of the function $I(P)$ is to define the regions of the phase space which are significant with respect to the result of interest. This is why $I(P)$ is called **importance function**.

As we introduce this change of variable in the integro-differential form of the transport equation, we get a new equation that governs the biased flux $\psi^*(P)$, and the form of which is similar to the transport equation governing the neutron flux $\psi(P)$. The new equation differs from the latter, however, by the modified particle-matter interaction laws, in accordance with the Table 14 (next page).

The quantity $\varepsilon(P) = \frac{|\vec{\nabla} I(P)|}{I(P)}$ is sometimes called a "biasing parameter", and the vector $\vec{\Omega}_0(P) = \frac{\vec{\nabla} I(P)}{|\vec{\nabla} I(P)|}$ is referred to as the "direction of interest", that is the direction in which it is convenient to move neutrons so as to maximize the figure of merit.

Figure 46 below illustrates the operating mechanism of the exponential transform.

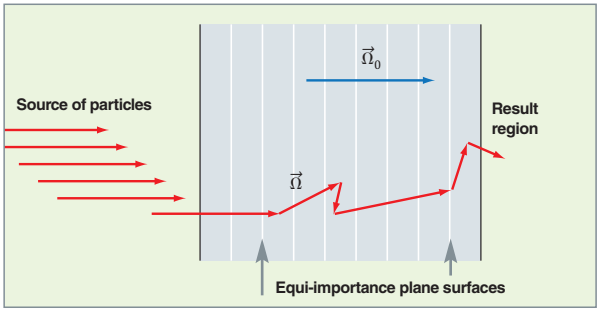

Fig. 46. Speed-up of a particle propagation calculation by the Monte-Carlo method illustrated in the case of neutron (or *gamma*) propagation in a shielding wall. In this example, the importance function $I(P)$ has been selected in such a way that equi-important surfaces be plane, the direction of interest being perpendicular to them.

Principle of biasing techniques

The problem to be solved can be formally summarized to calculating the mathematical expectation of a physical quantity defined by:

$$E[Y] = \int_D X g(X) dX$$

where X is a random variable, a "natural" estimator of Y, and $g(X)$ the probability density relating to the random variable X defined over a domain D.

Let us call $g^*(X)$ an arbitrary probability density associated with the random variable X. The mathematical expectation Y can be written as follows:

$$E[Y] = \int_D X g(X) dX = \int_D X \frac{g(X)}{g^*(X)} g^*(X) dX$$

That shows it is possible to assess **without bias** the quantity Y by building an event chain with a probability density $g^*(X)$, different from the natural probability density $g(X)$, providing $X \frac{g(X)}{g^*(X)}$, and no longer X, is taken as the new unbiased estimator of the quantity Y. In the background of neutron transport simulation with the Monte-Carlo method and, in practice, this means multiplying (or "correcting") the **neutron weight** (see *supra*, p. 95) for each event of interest, by the value taken by the ratio $X \frac{g(X)}{g^*(X)}$. The density $g^*(X)$ is often named, here, the *biased probability density*.

The terms "biasing" and "biased" are sometimes confusing, for the assessment performed here with the "biased density" $g^*(X)$ is strictly unbiased.

The **implicit capture** is a special illustration of this change of probability density coupled with an occurring event.

So the problem lies in finding the density $g^*(X)$ that results in the best possible intrinsic quality of simulation, in the meaning of the second expression of the expectation of Y, thereby significantly improving the figure of merit of Monte-Carlo simulation.

It is shown that, if a form built with the solution to the adjoint problem is taken for $g^*(X)$ (which requires to solve the adjoint transport equation, see *supra*, p. 58), then the ideal simulation can be reached, displaying a null variance on the result; this ideal simulation is referred to as **null variance game**.

However, the adjoint problem is at least as complex to solve as the direct problem. In other words, in practice, this theoretical result cannot be transposed as it is. Yet, solving this problem in relation to simplifying assumptions (infinite medium, monokinetic particles…) inspires efficient forms of biased density $g^*(X)$.

Table 14.

Biasing characteristics in the case of the exponential transform

	Analog simulation	Non analog simulation
Total cross section	$\Sigma(P)$	$\Sigma^*(P) = \Sigma(P) - \varepsilon(P)\vec{\Omega}_0(P).\vec{\Omega}(P)$ $\varepsilon(P) = \frac{\lvert\vec{\nabla}I(P)\rvert}{I(P)}$ $\vec{\Omega}_0(P) = \frac{\vec{\nabla}I(P)}{\lvert\vec{\nabla}I(P)\rvert}$
Track length probability density function	$f(s)ds = \left[\exp(-\int_0^s \Sigma(\vec{r} - s'\vec{\Omega}, E)\, ds')\right]\Sigma(\vec{r}, E)ds$	$f^*(s)ds = \left[\exp(-\int_0^s \Sigma^*(\vec{r} - s'\vec{\Omega}, E)\, ds')\right]\Sigma^*(\vec{r}, E)ds$
Collision operator kernel	$C(\vec{r}, E' \to E, \vec{\Omega}' \to \vec{\Omega})$	$C^*(\vec{r}, E' \to E, \vec{\Omega}' \to \vec{\Omega}) = \frac{I(\vec{r}, E, \vec{\Omega})}{I(\vec{r}, E', \vec{\Omega}')} C(\vec{r}, E' \to E, \vec{\Omega}' \to \vec{\Omega})$

As a matter of fact, the natural density $f(s)$ of the path choice s is replaced by biased density $f^*(s)$. Referring to the expression of $\Sigma^*(P)$, it can be observed that:

• $f^*(s)$ lengthens on average the paths of particles going in the direction of interest $\vec{\Omega}_0(P)$:

$\vec{\Omega}_0(P).\vec{\Omega}(P) > 0$ and $\Sigma^*(P) < \Sigma(P)$

• $f^*(s)$ shortens on average the paths of particles going opposite to the direction of interest $\vec{\Omega}_0(P)$:

$\vec{\Omega}_0(P).\vec{\Omega}(P) < 0$ and $\Sigma^*(P) > \Sigma(P)$

As mentioned above, the particle weight will have to take into account this change in the path sampling law, being multiplied by the ratio between the natural density $f(s)$ and the modified density $f^*(s)$ as follows:

$$\frac{f(s)}{f^*(s)} = \frac{\left[\exp(-\int_0^s \Sigma(\vec{r} - s'\vec{\Omega}, E)\, ds')\right]\Sigma(\vec{r}, E)}{\left[\exp(-\int_0^s \Sigma^*(\vec{r} - s'\vec{\Omega}, E)\, ds')\right]\Sigma^*(\vec{r}, E)}$$

Figures 47 and 48 help display the efficiency of applying this acceleration technique in the case of a stationary fixed-source transport. Recent works propose to implement it in critical calculations.

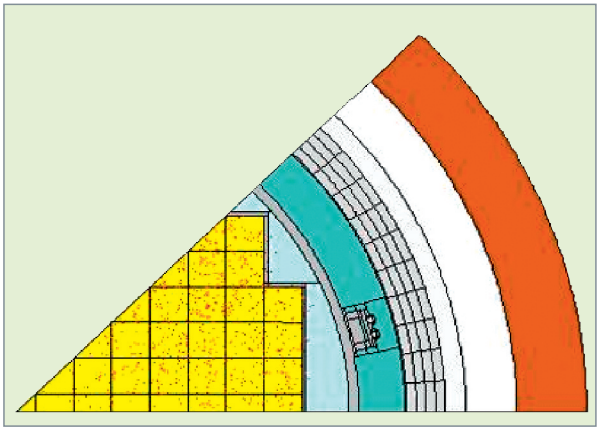

Fig. 47. Natural or analog simulation of neutrons generated in the reactor core: the points represent the location of collisions. Too few neutrons can reach the outer structures of the core (especially the vessel) to allow the neutron fluence to be evaluated with an acceptable statistical accuracy.
This simulation was performed with the Monte-Carlo transport code TRIPOLI.

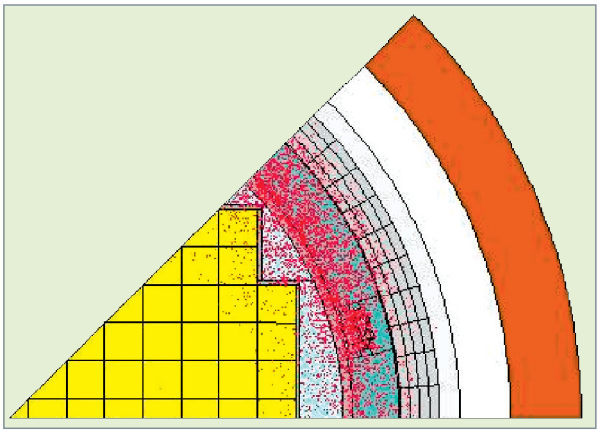

Fig. 48. Non-analog or "biased" simulation of neutrons generated in the reactor core: the distribution of the points representing the location of collisions shows the efficiency of the exponential transform technique that "pushes" neutrons to the areas of interest, here the barrel and internal wall of the nuclear reactor vessel for which neutron fluence received is being estimated. This simulation was performed with the Monte-Carlo transport code TRIPOLI.

In the TRIPOLI Monte-Carlo transport code, the importance function is automatically built according to an adjoint approach, using a shortest-path algorithm drawn from the graph theory, the **Dijkstra algorithm** [22], [23]. Several other techniques for reducing variance, such as "Russian roulette" and "splitting" (neutron breaking into several other neutrons) are jointly used in a same simulation. Ongoing works try to improve the performance of $I(P)$ importance functions, using **neural-network*** based techniques [24].

Perspectives

As part of nuclear reactor physics, the Monte-Carlo method applied to neutron transport allows the treatment of either core physics problems (k_{eff}, calculations, in-core power distribution…) or radiation protection problems (stationary-source calculation: determination of fluxes, heatings and dose rates…) generated by neutron propagation over variable distances that can reach up to several hundreds of meters (*e.g.* the "skyshine effect"). According to the same principles, it simulates the propagation of the *gamma* radiation generated in a nuclear facility. In addition, it allows an increasingly finer simulation of physical reality (resonant up-scattering [25]), calculations of physical parameter perturbation and/or uncertainty propagation [26, 27, 28, 29], as well as transport treatment in a stochastic medium [30], making them benefit from its specific features (continuous-energy, three-dimensional calculation). The ever increasing power of computers [31] paves the way for Monte-Carlo treatment of kinetics [32], and of couplings between physical phenomena, such as Monte-Carlo transport and nuclide generation/depletion (see inset *infra*, pp. 136 and 137), or Monte-Carlo transport and core thermal-hydraulics [33].

References

[1] N. Metropolis, S. Ulam, "The Monte-Carlo Method", *Journal of the American Statistical Association*, 247, 44, pp. 335-34, 1949.

[2] I. Lux, L. Koblinger, *Monte-Carlo Particle Transport Methods : Neutron and Photon Calculations*, CRC Press, 1991.

[3] J.C. Nimal, J. Rastoin, *Méthodes de Monte-Carlo*, Note CEA-N 533, avril 1965.

[4] H. Rief, A. Dubi, T. Elprin, "Track Length Estimation Applied to Point Detectors", *Nuclear Science and Engineering*, 87, pp. 59-71, 1984.

[5] F.H. Clark, "Variance of Certain Flux Estimators Used in Monte-Carlo Calculations", Nuclear Science and Engineering, 27, pp. 235-239, 1967.

[6] N. Authier, J.P. Both, J.C. Nimal, "New Photon Biasing Schemes for the 'One-More-Collided-Flux-Estimator's Method", *Nuclear Science and Engineering*, 137, pp. 146-155, 2001.

[7] G. E. Whitesides, "A Difficulty in Computing the k-effective of the World," *Trans. Am. Nucl. Soc.*, 14, p. 680, 1971.

[8] Y. Richet, "Suppression du régime transitoire initial des simulations Monte-Carlo de criticité", *Thèse de Doctorat*, École des Mines de Saint-Étienne, décembre 2006.

[9] T. Ueki, F. B. Brown, D. K. Parsons, D.E. Kornreich, "Autocorrelation and Dominance Ratio in Monte-Carlo Criticality Calculations", *Nuclear Science and Engineering*, 145, pp. 279-290, 2003.

[10] T. Ueki and F. B. Brown, "Stationarity Modeling and Informatics-Based Diagnostics in Monte-Carlo Criticality Calculations", *Nuclear Science and Engineering*, 149, pp. 38-50, 2005.

[11] E. Dumonteil, A. Le Peillet, Y.-K. Lee, O. Petit, C. Jouanne, et A. Mazzolo, "Source Convergence Diagnostics using Boltzmann Entropy Criterion. Application to different OECD/NEA criticality benchmarks with the 3-D Monte-Carlo code Tripoli-4", Physor, 2006.

[12] E. Dumonteil, T. Courau, "Dominance Ratio Assessment and Monte-Carlo Criticality Simulations : Dealing with High Dominance Ratio Systems", *Nuclear Technology*, 112, pp. 120-131, November 2010.

[13] R. C. Gast and N. R. Candalore "Monte-Carlo Eigenfunction Strategies and Uncertainties", *Proceedings of the NEACRP Meeting of a Monte-Carlo Study Group*, ANL-72-2 (NEA-CRP-L-118), pp. 162, 1974 ; E.M. Gelbard, R.E. Prael, "Monte-Carlo work at Argonne National Laboratory", *Proceedings of the NEACRP Meeting of a Monte-Carlo Study Group*, ANL-72-2 (NEA-CRP-L-118), p. 202, 1974.

[14] J. Brissenden and A. R. Garlick, "Biases in the estimation of k-eff and its Errors by Monte-Carlo Methods", *Annals of Nuclear Energy*, 13, 2, pp. 63-83, 1986.

[15] T. Ueki, T. Mori, and M. Nakagawa, "Error Estimations and their Biases in Monte-Carlo Calculations", *Nuclear Sciences and Engineering*, 125, p. 1, 1997.

[16] L. Demaret, A. Nouri, L. Carraro, and O. Jacquet, "Accurate Determination of Confidence Intervals in Monte-Carlo Eigenvalue Calculations", *Proceedings of ICNC'99*, p. 66, 1999.

[17] Y. Dufek, *Development of New Monte-Carlo Methods in Reactor Physics – Criticality, Non-Linear Steady State and Burnup Problems*, PhD, Stockholm, Sweden, June 2009.

[18] P. David Griesheimer and R. Brian Nease, "Spectral Analysis of Stochastic Noise in Fission Source Distributions from Monte-Carlo Eigenvalue Calculations", *Progress in Nuclear Science and Technology*, 2, pp. 706-715, 2011.

[19] S. Christoforou, J.E. Hoogenboom, "A Zero-Variance-Based Scheme for Monte-Carlo Criticality Calculations", *Nuclear Science and Engineering*, 167, pp. 1, 91-104 (2011) ; S. Christoforou, A Zero-Variance-Based Scheme for Monte-Carlo Criticality Simulations, *PhD, Technische Universtiteit Delft*, October 2010.

[20] F. X. Hugot, Y. K. Lee, F. Malvagi, "Recent R&D around the Monte-Carlo code TRIPOLI-4 for criticality calculation", *Proceedings of International PHYSOR-2008*, CD ROM, Interlaken, Switzerland, September 14-19, 2008.

[21] N. Petrov, N. P. Kolev, G. Todorova, F.X. Hugot, T. Visonneau, "TRIPOLI-4 Solutions of VVER-1000 Assembly and Core Benchmarks", *Proceedings of International Conference M&C 2009*, Saratoga Springs, New York, May 3-7, 2009.

Dice
Egyptian Antiquity
Louvre Museum © D.R.

The notion of hazard is old, as is shown by the dice above, which go back to the Higher Antiquity. The invention of the **Monte-Carlo method** is assigned to the naturalist **Georges-Louis Leclerc, Comte de Buffon**, who proposed an original probabilistic method - well-known as the *"Buffon's needle"* experiment - to obtain an estimation of the π number value [1].

In his dissertation, Buffon presents the issue dealt with in his mathematical work: « *L'Analyse est le seul instrument dont on se soit servi jusqu'à ce jour dans la science des probabilités, pour déterminer et fixer les rapports du hasard ; la Géométrie paroissoit peu propre à un ouvrage aussi délié ; cependant si l'on y regarde de près, il sera facile de reconnoître que cet avantage de l'Analyse sur la Géométrie, est tout-à-fait accidentel, et que le hasard, selon qu'il est modifié et conditionné, se trouve du ressort de la géométrie aussi-bien que de celui de l'analyse ; … »*. Once the problem so stated, Buffon dealt with it referring to the example of the "franc-carreau" game. *"Buffon's needle"* is dealt with in the second part of this dissertation as follows: *« Je suppose que dans une chambre, dont le parquet est simplement divisé par des joints parallèles, on jette en l'air une baguette, et que l'un des joueurs parie que la baguette ne croisera aucune des parallèles du parquet, et que l'autre au contraire parie que la baguette croisera quelques-unes de ces parallèles ; on demande le sort de ces deux joueurs. On peut jouer ce jeu sur un damier avec une aiguille à coudre ou une épingle sans tête…»*

Later on, the junction established between mathematicians' works, on the one hand, *i.e.* works of **G. F. Cantor** (1845-1918) on the *set theory*, of **E. Borel** (1871-1956), **H. Poincaré** (1854-1912), **A. A. Markov**, **H. Lebesgue**, **A. N. Kolmogorov**, … on *probabilities*, *random processes*, and the *measure theory*, and, on the other hand, works of the physicists **J. C. Maxwell** and **L. Boltzmann** on the gas theory (see *supra*, p. 48) were crucial indeed in spreading the stochastic approach in research on physical phenomena.

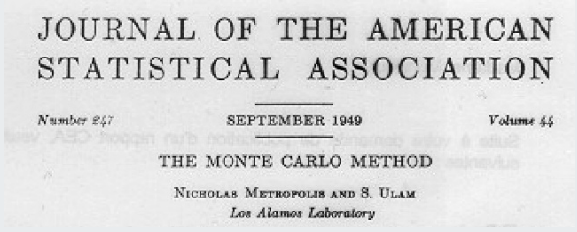

JOURNAL OF THE AMERICAN STATISTICAL ASSOCIATION

Number 247 SEPTEMBER 1949 Volume 44

THE MONTE CARLO METHOD

NICHOLAS METROPOLIS AND S. ULAM
Los Alamos Laboratory

Before bearing this very name, the Monte-Carlo method was initially used by **E. Fermi** in Rome to investigate neutron slowing-down [2].

It was especially in the background of World War II -, with the atomic bomb development at Los Alamos (USA) - and of the advent of early electronic machines and computers, that this method took its boost. The name of this method – ***Monte-Carlo*** – is assumed to have been the code name assigned to a secrete work achieved at Los Alamos atomic research center (New Mexico, USA). It was to be developed by **J. von Neumann**, **S. Ulam**, and **N.C. Metropolis** [3, 4]. The **Monte-Carlo method** was increasingly used together with the ongoing rise in computer power, emphasized by books and articles presenting it [5, 6, 7, 8, 9, 10, 11]. The development of the American Monte-Carlo particle (neutron, *gamma*, electrons…) transport code MCNP is in the straight line of the Monte-Carlo method pioneers' legacy [12]. In France, at the CEA, neutron transport softwares based on the Monte-Carlo method – ZEUS, POKER – were written in the sixties [7], [8], [9]. The first version of their successor, **TRIPOLI**, was issued in the 1970s [11].

A few historical references

[1] Comte de BUFFON, *Essai d'arithmétique morale,* dans *Histoire Naturelle générale et particulière*, Supplément, Tome Quatrième, pp. 95-105, 1777 (http://www.buffon.cnrs.fr/). In fact, this mathematical work had been submitted earlier to the French *Académie des sciences*. On Saturday, April 25th, 1733, the mathematicians A. Clairaut and P. L. Moreau de Maupertuis "issued the following statement about a memoir presented by M. Le Clerc: «On request of the *Académie* we have examined a memoir by M. Le Clerc dealing with the game of *Franc-Carreau*...»" (http://gallica.bnf.fr/ark:/12148/bpt6k55728h.f166).

Georges-Louis Leclerc, Comte de Buffon (1707-1788).

Andrey Andreyevich Markov (1856-1922).

Henri Lebesgue (1875-1941).

Andrey Nikolaevich Kolmogorov (1903-1987).

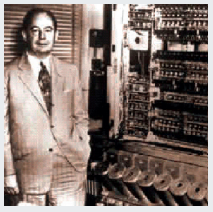

John von Neumann (1903-1957).

Stanislaw Ulam (1909 -1984).

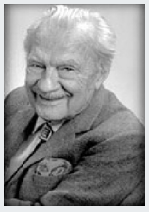

Nicholas Constantine Metropolis (1915-1999).

[2] E. Segrè, Les Physiciens modernes et leurs découvertes – *Des rayons X aux Quarks*, Paris, Fayard, coll. "Le temps des Sciences", p. 304, 1984.

[3] N. Metropolis, S. Ulam, "The Monte-Carlo Method", *Journal of the American Statistical Association*, 247, 44, 335-34, 1949.

[4] N. Metropolis, "The Begining of the Monte-Carlo Method", in *Los Alamos Science Special Issue*, pp. 125-130, 1987.

[5] J. Spanier, *Monte-Carlo Methods and their Application to Neutron Transport Problems*, WAPD-195, AEC Research and Development Report, Bettis Atomic Power Laboratory, Pittsburgh, Pennsylvanie, USA, July 1959.

[6] J. Spanier et E. M. Gelbard, *Monte-Carlo Principles and Neutron Transport Problems*, USA, Addison-Wesley Publishing Company, 1969.

[7] J.-C. Nimal, J. Rastoin, *Méthodes de Monte-Carlo*, Note CEA-N-533, 1965.

[8] C. Devillers, S. Katz, J.C. Nimal, *Quelques remarques sur la pondération dans les méthodes de Monte-Carlo*, Note CEA-N-644, 1967.

[9] J. M. Lanore, *Utilisation d'une méthode de Monte-Carlo pour la propagation des neutrons à grande distance*, Note CEA-N-934, 1968.

[10] J. M. Hammersley, D.C. Handscomb, *Les Méthodes de Monte-Carlo*, Paris, Dunod, coll. « Monographies Dunod », 1967.

[11] J. H. Halton, "A Retroscpective and Prospective Survey of the Monte-Carlo Method", *SIAM Review*, 12, 1, 1-63, January 1970.

[12] G. W. McKinney, J. W. Durkee, J. S. Hendricks, M. R. James, D. B. Pelowitz, L. S. Waters, F. X. Gallmeier, *MCNPX Overview*, LA-UR-06-6206, 2006.

[13] S. Katz, J. C. Nimal, *Programme de Monte-Carlo polycinétique à trois dimensions : TRIPOLI-01*, Note CEA-N-1919, 1976.

[22] P. J. Dossantos-Uzarralde, *Automatisation de la recherche des fonctions d'importance dans un code Monte-Carlo*, Thèse de doctorat, Université Paris 6, 1990 ; J.-P. Both, G. Dejonghe, J.-C. Nimal, P. J. Dossantos-Uzarralde and T. Vergnaud, "Automated importance generation and biaising techniques for Monte-Carlo shielding techniques by the TRIPOLI-3 code", Proceedings of Physor 90 International Conference, (XII)-59–68, Marseille, France, April 1990 ; J.P. Both, J.C. Nimal, T. Vergnaud, "Automated Importance Generation and Biasing Techniques for Monte-Carlo Shielding Techniques by the TRIPOLI-3 code", *Progress in Nuclear Energy*, 24, pp. 273-281, 1990.

[23] B. Morillon, *Méthode de Monte-Carlo non analogue – Application à la simulation des neutrons*, Thèse de doctorat, Université Paris XI-Orsay, Note CEA-N-2805, janvier 1996.

[24] E. Dumonteil, "On a New Variance Reduction Technique : Neural Network Biasing – A Study of Two Test Cases with the Monte-Carlo Code TRIPOLI-4", *Nuclear Technology*, 112, pp. 793-798, December 2009.

[25] A. Zoia, E. Brun, C. Jouanne, F. Malvagi, "Doppler broadening of neutron elastic scattering kernel in TRIPOLI-4®", *Annals of Nuclear Energy 54*, 218-226, 2013.

[26] H. Rief, "Generalized Monte-Carlo Perturbation Algorithms for Correlated Sampling and Second-Order Taylor Series Approach", *Annals of Nuclear Energy*, 11, 9, pp. 455-476, 1984.

[27] G. Dejonghe, J. Gonnord, J.C. Nimal, "Perturbation Calculations by the Correlated Samples Method", *Proceedings of the International Meeting on Advances Nuclear Engineering Computational Methods*, Knoxville, Tennessee, vol. 2, April 9-11, 1985).

[28] B. Morillon, *Perturbation dans le transport des neutrons par la méthode de Monte-Carlo*, Note CEA-N 2838, octobre 1998.

[29] Y. Nagaya, T. Mori, "Estimation of reactivityworth with differential operator sampling method", *Joint International Conference on Supercomputing in Nuclear Applications and Monte-Carlo 2010 (SNA + MC2010)*, Tokyo, Japan, October 17-21, 2010.

[30] A. Mazzolo, "Probability density distribution of random line segments inside a convex body: Application to random media", *Journal of Mathematical Physics*, V. 44, pp. 853-863, 2003.

[31] K. Smith, "Nuclear Mathematical and Computational Sciences: A Century in Review, A Century A new." *Invited Keynote Speaker*. Gatlinburg, Tennessee, USA, May 2003.

[32] B. L. Sjenitzer and J. E. Hoogenboom, "A Monte-Carlo method for calculation of the dynamic behaviour of nuclear reactors", *Progress in Nuclear Science and Technology*, 2, pp. 716-721, 2011.

[33] J. E. Hoogenboom, A. Ivanov, V. H. Sanchez, C. M. Diop, "A flexible coupling scheme for Monte-Carlo and thermal-hydraulics codes", *International Conference on Mathematics and Computational Methods Applied to Nuclear Science and Engineering* (M&C 2011), Rio de Janeiro, RJ, Brazil, on CD-ROM, Latin American Section (LAS) / American Nuclear Society (ANS) ISBN 978-85-63688-00-2, May 8-12, 2011.

Cheikh M. Diop, Éric Dumonteil,
François-Xavier Hugot and Fausto Malvagi
Department for Systems and Structures Modeling

Methods for Solving the Generalized Bateman Equations

General principles

In a medium irradiated by a neutron flux, nuclide composition evolves over time by **transmutation***, due to nuclear reactions and to the radioactive **decay*** of the generated radionuclides.

Table 15 gathers the main nuclear phenomena responsible for change in the composition of the irradiated medium. Following a nuclear reaction or a radioactive process (highlighted in red), the nucleus ${}^{A}_{Z}X$, of atomic number Z and mass number A, is transmuted into another nucleus.

Table 15.

Nuclear reactions and radioactive processes contributing to isotopic composition change in a nuclear reactor

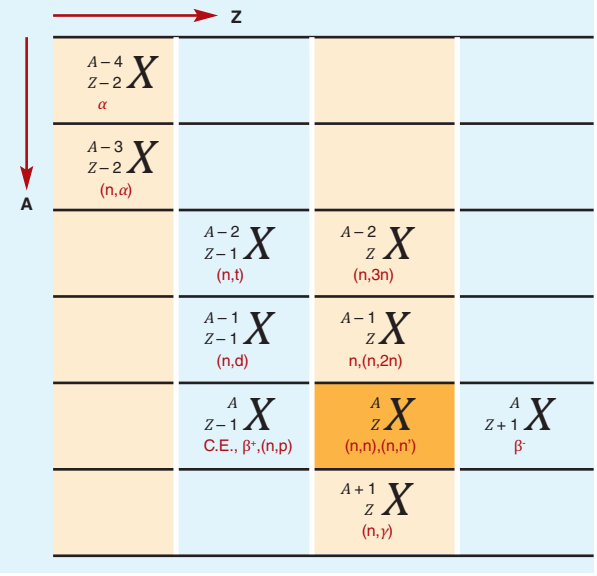

These nuclear phenomena are responsible for the space and time isotopic **generation/depletion** of a fuel irradiated by neutrons with respect to **heavy nuclei** and **fission products*** (FPs) in a fuel irradiated by neutrons. So it is of the depletion of **activation products** (AP) formed in reactor structures, and of the generation/depletion of spallation products (SP) formed, *e.g.* in a **hybrid system*** such as an accelerator driven subcritical reactor.

Thus, the JEFF-3.1.1 evaluation includes all of these nuclides, classified into heavy nuclei and fission products in the following Table 16:

Table 16.

Nuclide distribution in nuclear data evaluation JEFF-3.1.1 [1], [2] **among the following classes: heavy nuclei, fission products, and fissile systems**	
Total number of nuclides	3,852 (226 stable)
Heavy nuclei	863 (Z > 80: Hg)
Fission products (FPs)	1,314
Fissile nuclei (or "fissile systems")	39

All of these father and daughter nuclides are described as part of **decay chains** of variable length according to the case. Thus, the decay chains of heavy nuclei and fission products are used for nuclear reactor calculation, possibly with a certain number of simplifications, relating, *e.g.* to the half-lives of radioactive nuclei, or to their capture power.

Several physical quantities are derived from concentrations $N_i(\vec{r}, t)$ of nuclides i: **reaction rates***, *gamma*, *beta* and *alpha* **decay heats*** and corresponding radiation sources.

The space dimension appearing in the generalized Bateman equations is imposed by both the space distribution of nuclide concentrations present before irradiation (initial concentrations), and the neutron flux through the various reaction rates. So these equations have to be solved consistently with the space computational scheme (space meshing) adopted in the transport equation resolution.

In the case of nuclear fuel, where there is a strong interdependence between neutron flux and concentrations, the discretized time steps are defined so that neutron flux can be assumed to be constant in them. In practice, the variables that are often used instead of time are two quantities representative of element irradiation (see Table 5, *supra*, p. 13):

- **Neutron fluence***, expressed in neutrons per kilobarn (n/kb);
- **burnup***, expressed in megawatt day per ton (MW·d/t).

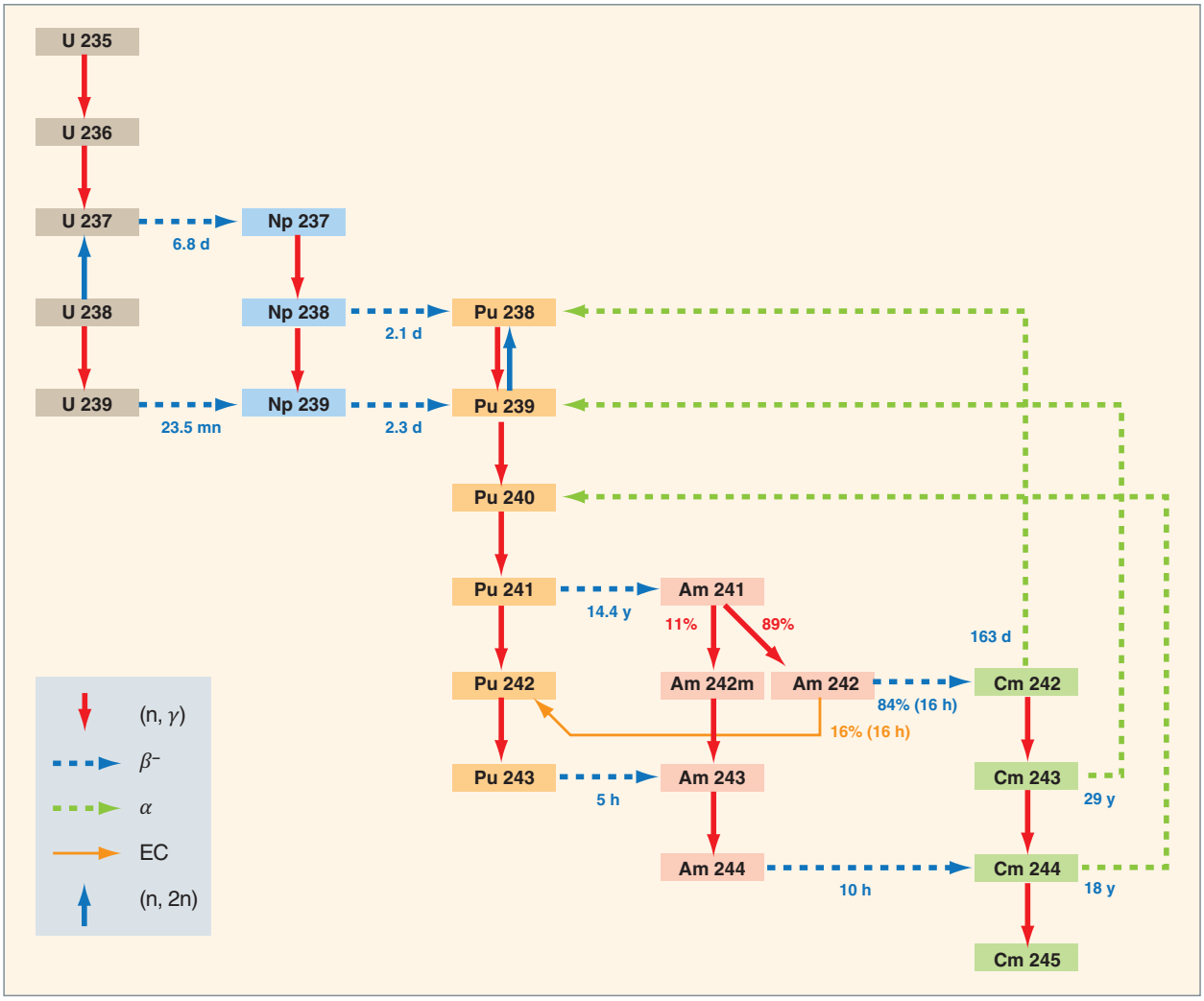

Fig. 49. Extract from the simplified decay chain of heavy nuclei present in a light-water reactor core. This schematic view shows how actinides, especially plutonium, are formed, through nuclear reactions and radioactive decays.

For instance, the 45,000 MW·d/t burnup of a 4.5% enriched UOX fuel will be subdivided into a fifty or so burnup steps, accounting for a 3- or 4-year residence time in reactor.

The solving of the generalized Bateman equations presented *supra*, p. 49, is achieved through various methods, chosen as a function of the nature of the problem considered:

- Searching for an analytical solution as a linear combination of exponentials;
- Matrix exponential method using a limited development of the exponential function;
- Computational methods using discretization of time (or of the related variable).

The principles of resolution through analytical or Runge-Kutta computational method are set out hereafter. In the following, we show the results of a burnup calculation that illustrates, on the one hand, the significant changes in fuel's heavy nuclei composition during its residence in the reactor core, and, on the other hand, core poisoning by two fission products: xenon 135 and samarium 149.

Analytical solution of the Bateman equations

When the decay chain is described without any closed path, it is always possible to arrange nuclides so that the i^{th} nuclide calculation only uses nuclides already calculated.

Let us state c_{ik} the coefficient leading to nuclide i from nuclide k by decay and/or nuclear reaction, and b_i a source term (neutron induced fission here) feeding nucleus i. Coefficients c_{ik} and b_i are assumed to be constant on the burnup step considered.

Omitting the space variable for simplification, the equation to be solved that gives the concentration of nuclide i as a function of time t, computed from the start of the burnup step, is written as follows:

$$\frac{dN_i(t)}{dt} = b_i + \sum_{k=1}^{i-1} c_{ik} N_k(t) - c_{ii} N_i(t) \tag{1}$$

The solution is written in the following form:

$$N_i(t) = N_i^S + \sum_{k=1}^{i} F_{ik} e^{-c_{kk} t} \tag{2}$$

where coefficients N_i^S and F_{ik} are defined by:

$$N_i^S = \frac{1}{c_{ii}} \left[b_i + \sum_{k=1}^{i-1} c_{ik} N_k^S \right] \tag{3}$$

assuming that $c_{ii} \neq 0$

$$F_{ik} = \frac{1}{c_{ii} - c_{kk}} \left[\sum_{j=k}^{i-1} c_{ij} F_{jk} \right] \quad 1 \leq k \leq i-1 \tag{4}$$

assuming that $c_{ii} \neq c_{kk}$

$$F_{ii} = N_i(0) - N_i^S - \sum_{j=1}^{i-1} F_{ij} \tag{5}$$

where $N_i(0) = N_i(t = 0)$

It shall be noted that in the absence of flux, this solution is always less costly than a solution by numerical discretization.

Numerical resolution of the Bateman equations

When closed paths are considered, a numerical resolution scheme has to be used. The scheme presented here is of the **Runge-Kutta** type, **of order 4**, this order being chosen as a good compromise between accuracy and computational cost.

The generation/depletion equations to be solved can be written in a general matrix form as follows:

$$\frac{dN(t)}{dt} = S(t) + A(t)N(t) \tag{6}$$

with:

- $N(t)$: vector of the concentrations of the nuclides considered;
- $S(t)$: vector of the source term;
- $A(t)$: generation/depletion matrix, the non-diagonal elements of which contain the feeding terms, and the diagonal elements, the terms of nuclide disappearance by radioactive decay and/or nuclear reaction.

The matrix coefficients are defined as follows:

$$A_{ii}(t) = -\lambda_i - \varsigma_i(t) \tag{7}$$

$$A_{ij}(t) = \lambda_{i \leftarrow j} + \varsigma_{i \leftarrow j}(t) \tag{8}$$

where the terms λ_i, $\lambda_{i \leftarrow j}$, respectively relating to the decay of nuclides i and j, and $\varsigma_i(t)$ and $\varsigma_{i \leftarrow j}(t)$, corresponding to the microscopic reaction rates associated with nuclides i and j, have been previously defined (see *supra*, p. 49).

It can be seen that, according to expressions (7) and (8), the depletion matrix mainly depends on time through the flux, which is a datum provided by transport codes. Its values can be known at any moment, either because they are tabulated, or because they can be interpolated from the tabulated values. If performing a calculation over a "not too broad" irradiation range, the generation/depletion matrix may be assumed to be constant and equal to its expression at the middle point of the irradiation step.

In practice, when the middle point of the irradiation step is not a point corresponding with a tabulated result, the elements of the generation/depletion matrix are computed from the interpolated values between two tabulation points surrounding the burnup middle point.

This assumption, coupled with the possibility to know the generation/depletion matrix at various burnup values, can justify the use of a Runge-Kutta type numerical scheme, without a new calculation of the generation/depletion matrix between two elementary time steps. That type of numerical techniques is named after the two German mathematicians who developed them, **Carl David Tolmé Runge** (1856-1927), and **Martin Wilhelm Kutta** (1867-1944).

This numerical scheme is based on the joint use of the Euler method, for solving first-order differential equations, and of the Taylor development at a fixed order of $N(t)$ and of its derivate. It is stated as follows:

$$G(N) = S(t) + A(t)N(t) \tag{9}$$

The 4-order **Runge-Kutta scheme** is then written as follows:

$$\begin{aligned}
N^{(0)} &= N^{(n)} \\
N^{(1)} &= N^{(0)} + \frac{\Delta t}{2} G(N^{(0)}) \\
N^{(2)} &= N^{(0)} + \frac{\Delta t}{2} G(N^{(1)}) \\
N^{(3)} &= N^{(0)} + \Delta t\, G(N^{(2)}) \\
N^{(4)} &= \frac{\Delta t}{2} G(N^{(3)}) \\
N^{(n+1)} &= \frac{1}{3}(N^{(1)} - N^{(0)}) + \frac{2}{3} N^{(2)} + \frac{1}{3} N^{(3)} + \frac{1}{3} N^{(4)})
\end{aligned} \tag{10}$$

where Δt is the time mesh width.

The error associated with this numerical scheme is proportional to Δt^4.

The history of neutron flux has been implicitly assumed to be known. In fact, in core calculations, neutron flux is not known in advance: the transport equation and the depletion equations have to be solved simultaneously. In practice, they are solved sequentially by time steps (or by neutron fluence, or burnup steps), joining to the numerical process previously described a **"prediction-correction" procedure**, which anticipates the variation in neutron flux over the discretization interval considered; this technique allows a refined calculation of concentrations at the upper bound of this interval.

Examples of typical irradiation calculations in reactor physics: generation/depletion of heavy nuclei and fission products

Generation/depletion of heavy nuclei

Fuel used in current French reactors is either uranium-based fuel called UOX, or mixed uranium and plutonium oxides, called MOX. Two types of nuclei can be distinguished in these fuels: on the one hand, "fissile" nuclei, such as uranium 235, plutonium 239, and plutonium 241, and, on the other hand, "fertile" nuclei, which generate a fissile nucleus by neutron capture. Uranium 238, which yields a fissile nucleus, plutonium 239, by capture of a neutron followed by radioactive decays, is an example of "fertile" nuclide.

During irradiation, as will be seen later on, fission products are formed in fuel, as well as new heavy nuclei mainly arising from neutron capture reactions. The nuclides generated, and their amount, depend on the initial composition of fuel, as well as of the neutron spectrum. Figures 50 and 51 respectively illustrate, versus irradiation, the production or disappearance of uranium and plutonium isotopes in a 4.5% – enriched PWR – UOX fuel, and in a MOX fuel with a 5.6% plutonium average initial content.

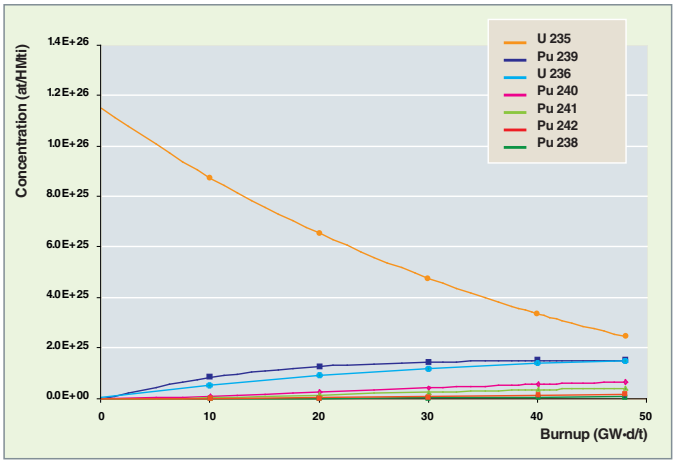

Fig. 50. Depletion of the main U, Pu nuclei in an UOX fuel.

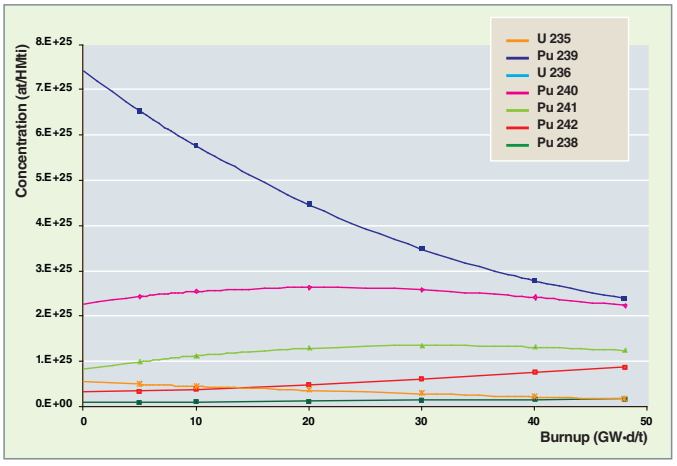

Fig. 51. Depletion of the main U, Pu nuclei in a MOX fuel.

Poisoning by fission products

The main effect relating to the formation of fission products in fuel is the possible loss of reactivity due to their neutron capture. This is what is referred to as **poisoning***. The most significant poisons in thermal neutron reactors, the effects of which will be examined below, are xenon-135 and samarium-149.

At the end of irradiation, the poisoning due to all of fission products reaches a dozen thousand pcm in water reactors. The fifteen most absorbing fission products alone account for over 80% of the total capture of fission products. Among them are the following nuclides: Rh 103, Gd 155, Cs 133, Nd 143, Nd 145, Sm 151, and Eu 153.

This penalizing negative reactivity in reactors can however become an asset in fuel cycle related studies, especially in the field of nuclear criticality-safety. In the latest years, a number of studies have been conducted about what is called the

"**burnup credit***", which consists in taking fuel burnup into account in nuclear criticality-safety studies.

Poisoning by xenon-135

Xenon-135 is a rare gas arising from fission according to the chain presented on Figure 52.

This is one of the main poisons in thermal neutron reactors, taking into account, on the one hand, its high fission yield for uranium 235 and plutonium 239 (6.5% and 7.2%, respectively), and, on the other hand, its exceptional capture cross section in the thermal energy range ($\sigma_c = 3.10^6$ *barns*). In normal operation, xenon poisoning is about 3,000 pcm in a PWR; this asymptotic negative reactivity (xenon generation and disappearance are balanced) is reached after one or two days of constant-flux operation.

When the reactor shuts down, iodine 135 is no longer generated by fission, and xenon 135 no longer disappears by neutron capture. The iodine 135 stock piled up during operation decreases, generating xenon 135, and the latter's quantity increases up to reaching a maximum after an approximate 10 hours, before decreasing again. In a PWR, the maximum negative reactivity due to this "xenon peak" is of about 3,700 pcm, which can prevent the reactor to restart instantaneously. So it is indispensable to take account of the existence of this phenomenon in core design.

Moreover, this **xenon effect** may be the origin of perturbations in power distribution in the reactor core owing to its particularly high capture cross section.

Poisoning by samarium 149

The depletion chain leading to samarium-149 is presented on Figure 53. This isotope is stable, and exhibits an absorption cross section of 60,000 barns in the thermal energy range. After a few weeks of operation, at equilibrium, that is when there is as much samarium formed as samarium destroyed, negative reactivity brought by samarium-149 is about 600 pcm.

If the reactor has been operating at constant flux for several weeks, and is finally shut down very quickly, the amount of stable samarium stays in the reactor, and increases due to the decay of prometheum-149 that displays a half-life of 53 hours (see Figure 52). Hence an increase in poisoning that reaches an asymptotic value proportional to the flux prevailing in the reactor before shutdown. Contrary to the xenon effect, there is no transition through a negative reactivity maximum. The amount of samarium decreases only when the reactor starts up again, by neutron absorption.

References

[1] A. Santamarina *et al.*, *The JEFF-3.1.1 Nuclear Data Library – Validation Results from JEF-2.2 to JEFF-3.1.1*, JEFF Report 22, OECD 2009 NEA n° 6807, 2009.

[2] M.A. Kellett, O. Bersillon, R.W. Mills, *The JEFF-3.1/-3.1.1 radioactive decay data and fission yields sub-libraries*, JEFF Report 20, OECD 2009 NEA No. 6287, 2009.

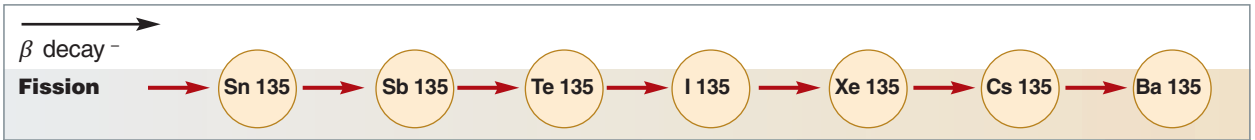

Radioactive half-life	0.85 s	1.70 s	19.0 s	6.61 h	9.09 h	$2.3\ 10^6$ years	Stable
Cumulated yield (for a thermal neutron inducing a fission)							
U 235	$9.3\ 10^{-4}$	$1.8\ 10^{-1}$	3.68	6.32	6.58	6.58	6.58
Pu 239	$5.9\ 10^{-5}$	$3.9\ 10^{-2}$	1.92	6.19	7.23	7.24	7.24

Fig. 52. Xenon-135 depletion chain.

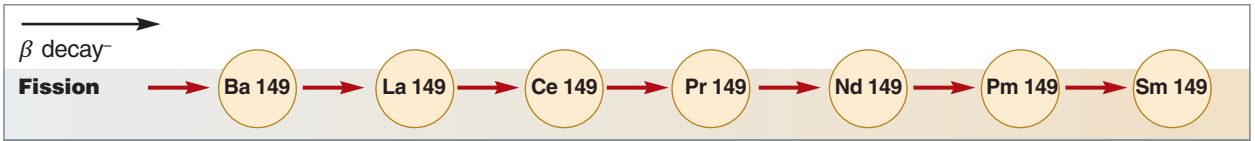

Radioactive half-life	0.35 s	1.20 s	5.20 s	2.27 mn	1.73 h	53 00 h	Stable
Cumulated yield (for a thermal neutron inducing a fission)							
U 235	$1.5\ 10^{-3}$	$1.0\ 10^{-1}$	$8.3\ 10^{-1}$	1.04	1.05	1.05	1.05
Pu 239	$1.8\ 10^{-4}$	$3.9\ 10^{-2}$	$7.1\ 10^{-1}$	1.21	1.25	1.25	1.25

Fig. 53. Samarium-149 depletion chain.

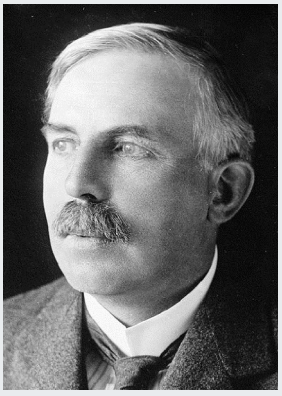

Ernest Rutherford (1871-1937)
Nobel Prize in Chemistry
in 1908

Frederick Soddy (1877-1956)
Nobel Prize in Chemistry in 1921

LX. *Radioactive Change.* *By* E. RUTHERFORD, *M.A., D.Sc., Macdonald Professor of Physics, McGill University, and* F. SODDY, *M.A. (Oxon.).*

CONTENTS.

I. The Products of Radioactive Change, and their Specific Material Nature.
II. The Synchronism between the Change and the Radiation.
III. The Material Nature of the Radiations.
IV. The Law of Radioactive Change.
V. The Conservation of Radioactivity.
VI. The Relation of Radioactive Change to Chemical Change.
VII. The Energy of Radioactive Change and the Internal Energy of the Chemical Atom.

§ 1. *The Products of Radioactive Change and their Specific Material Nature.*

IN previous papers it has been shown that the radioactivity of the elements radium, thorium, and uranium is maintained by the continuous production of new kinds of matter which possess temporary activity. In some cases the new product exhibits well-defined chemical differences from the element producing it, and can be separated by chemical processes. Examples of this are to be found in the removal of thorium X from thorium and uranium X from uranium. In other cases the new products are gaseous in character, and

§ 4. *The Law of Radioactive Change.*

The view that the radiation from an active substance accompanies the change gives a very definite physical meaning to the law of decay of radioactivity. In all cases where one of the radioactive products has been separated, and its activity examined independently of the active substance which gives rise to it, or which it in turn produces, it has been found that the activity under all conditions investigated falls off in a geometrical progression with the time. This is expressed by the equation

$$\frac{I_t}{I_0} = e^{-\lambda t}$$

where I_0 is the initial ionization current due to the radiations, I_t that after the time t, and λ is a constant. Each ray or

Ernest Rutherford was a physicist and a chemist, who was born in New-Zealand, and who spent his life in England. Being an exceptional experimentalist, he gave a clear insight of the atomic structure, *i.e.* a positively charged atomic nucleus surrounded with negatively charged electrons. He discovered *alpha* and *beta* radiation arising from uranium as he investigated air ionization induced by this radiation. Working with the chemist **Frederick Soddy**, he determined the relationship between **radioactivity** and **change in chemical species** in 1902 [1].

A little later on **F. Soddy** identified radioactive nuclides of different masses but with the same chemical properties, which led to the notion of **isotope**.

E. Rutherford and **F. Soddy** especially investigated the radioactive family of thorium, and established the **exponential decay law which governs decay chains** [1], [5].

The discovery of this law had a significant impact, indeed, on the understanding of the Earth's history. Through clever experiments, **Buffon** (1707-1788) had already upset the age of a few thousand years commonly attributed to the Earth in Europe, bringing it to 80,000 years, and even reviewing it once to a few million years. In the mid-19th century, geology in full expansion announced several hundred million years. In the early 20th century, radioactivity brought the Earth's age beyond one billion years, to the deep dissatisfaction of the almighty and "anti-Darwinian" physicist **Lord Kelvin** (1824-1907), who long focused on the age of one hundred million years he had deduced from the application of heat diffusion laws [3].

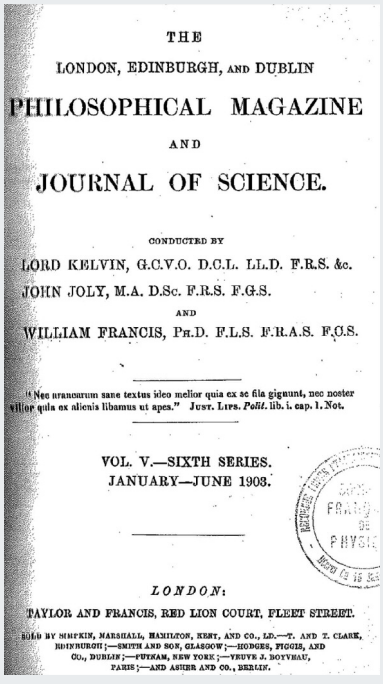

THE
LONDON, EDINBURGH, AND DUBLIN
PHILOSOPHICAL MAGAZINE
AND
JOURNAL OF SCIENCE.

CONDUCTED BY
LORD KELVIN, G.C.V.O. D.C.L. LL.D. F.R.S. &c.
JOHN JOLY, M.A. D.Sc. F.R.S. F.G.S.
AND
WILLIAM FRANCIS, PH.D. F.L.S. F.R.A.S. F.C.S.

"Nec aranearum sane textus ideo melior quia ex se fila gignunt, nec noster vilior quia ex alienis libamus ut apes." JUST. LIPS. *Polit.* lib. i. cap. 1. Not.

VOL. V.—SIXTH SERIES.
JANUARY—JUNE 1903.

LONDON:
TAYLOR AND FRANCIS, RED LION COURT, FLEET STREET.
SOLD BY SIMPKIN, MARSHALL, HAMILTON, KENT, AND CO., LD.—T. AND T. CLARK, EDINBURGH;—SMITH AND SON, GLASGOW;—HODGES, FIGGIS, AND CO., DUBLIN;—PUTNAM, NEW YORK;—VEUVE J. BOYVEAU, PARIS;—AND ASHER AND CO., BERLIN.

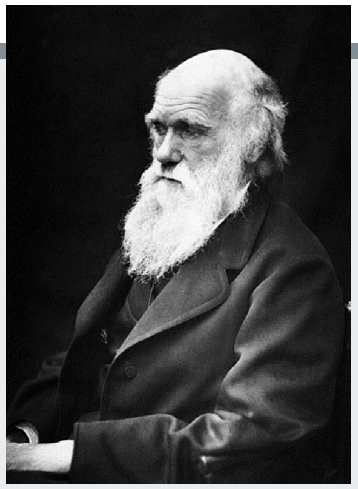

Charles Robert Darwin (1809-1882)

Harry Bateman (1882-1946)

Following the evolution theory of **Charles Robert Darwin** (1809-1882) [and also **Alfred Russel Wallace** (1823-1913)], emerging **nuclear physics** thus contributed in durably setting up a new paradigm of the natural history of the Earth, of the Solar System, and of the Universe: diachronic, evolutionary and genealogical.

The general solution to the differential equations governing over time the concentrations of nuclides involved in decay chains [4], [5] was set up by **Harry Bateman**, an English-born mathematician who migrated to the United States and was deeply interested in physics-mathematics. These equations are currently referred to as the **Bateman equations**. ***Generalized*** **Bateman** equations – or **depletion** (or **evolution**, or **burnup**) **equations** - that also take into account irradiation by a neutron flux, similarly to what occurs in an operating nuclear reactor core, were solved for the first time in 1949 by **William Rubinson**, a scientist working at the *Chemistry Department of the Brookhaven National Laboratory* (USA) [6].

Cheikh M. Diop, Tan Dat Huynh,
Anne Nicolas, Aimé Tsilanizara
Department for Systems and Structures Modeling
and Bénédicte Roque
Department of Reactor Studies

References

[1] E. Rutherford, F. Soddy, "Radioactive Change", *Philosophical Magazine and Journal of Science*, Jan-Jun, pp. 576-591, 1903.

[2] http://www.larecherche.fr/idees/histoire-science/quel-age-a-terre-01-10-2009-86743

[3] C. Darwin, *On the Origin of Species by Means of Natural Selection, or the Preservation of Favoured Races in the Struggle for Life*, London, John Murray, 1859.

[4] H. Bateman, "The solution of a system of differential equations occurring in the theory of radioactive transformations", *Proceedings Cambridge Philosophical Society*, vol. 15, pp. 423-427, 1910.

[5] R. D. Evans, *The Atomic Nucleus*, New York, Mac Graw-Hill Book Company, 1955.

[6] W. Rubinson, "The Equations of Radioactive Transformation in a Neutron Flux", *Journal of Chemical Phvsics*, vol. 17, number 6, pp. 542-547, June 1949.

Methods for Time Resolution of Coupled Space-Dependent Kinetics Equations

Circumscribed to neutronics, the general Boltzmann equation governing neutron flux in any point of the reactor core and at any instant t, has been previously presented *supra*, p.60. This equation has two neutron source terms respectively corresponding with **prompt neutrons*** and **delayed neutrons***. The crucial role played by delayed neutrons in the control of a nuclear reactor has already been mentioned in this Monograph.

In normal operation, the aim is to maintain the reactor in an equilibrium state characterized by a null balance between neutrons generated in it (mainly by neutron-induced fission), and neutrons disappearing by absorption and leakage out of the reactor core. Even in normal operation, the physical properties of the reactor (isotopic composition, temperature, dimensions…) are constantly being modified due to the physical processes taking place in it, so that in practice this critical state is maintained by acting on the devices able, at any moment, to reduce the discrepancy to criticality to 0 ($\delta k = 0$). This control of the reactor is performed particularly through control rods, whose more or less deep insertion into the reactor core allows the value of the parameter δk to be controlled.

This chapter is devoted to the kinetics of nuclear reactors at "short" times over which delayed neutrons play a role of prime importance.

As already explained in "The nuclear reactor physicist's approach" (see *supra*, p. 51) the complexity of the actual physical configurations (heterogeneities, large size…) to be investigated leads to introduce reasonably simplified assumptions in order to solve transport and depletion equations. The so-called model of "**point kinetics of nuclear reactors**" hereafter described is based on this approach. It is characterized by two first-order coupled linear differential equations which respectively govern the time evolution of the total neutron population in the reactor, and that of delayed neutron precursors; they are assumed to be valid in any point of the reactor core, the variables space and energy being neglected. The presentation of this model is preceded by the listing of the general principles that prevail in the transition from space-dependent kinetics equations described *supra*, pp. 59 and 60, to point kinetics equations. In this transition, the quantities referred to as "**effective**" are introduced: they play a key role, indeed, for they make it possible to "preserve the physics" of the real configuration.

The role of delayed neutrons in reactor control

Let us take the example of a thermal neutron reactor, and let us only consider, as a first step, the prompt neutron population, that accounts for over 99% of the total neutron population (*i.e.* prompt neutrons + delayed neutrons). The average lifetime ℓ of a neutron in the thermal energy range is about $\ell \approx 10^{-5}$ s.

It can then be shown that the neutron flux in any point of the reactor core undergoes an exponential evolution as a function of time as does $e^{\frac{\delta k}{\ell}t}$ where δk is the excess of the neutron multiplication factor with respect to the unit: $\delta k = k_{eff} - 1$. **Reactivity***, denoted ρ, is defined as $\rho = \frac{\delta k}{k_{eff}} = \frac{k_{eff}-1}{k_{eff}}$. The stable or **critical*** state of the reactor corresponds with $\delta k = 0$ or $\rho = 0$.

The quantity $T = \frac{\ell}{\delta k}$ is the time constant that characterizes the evolution of the neutron population in the reactor of interest; it is named "**reactor period**".

If $\delta k = 10^{-4}$, then $T = 0.1\ s$, and within one second the initial neutron flux is multiplied by the factor $e^{10} \approx 2.2\ 10^4$, which definitely makes it impossible to perform any control of the reactor.

Although few in proportion (less than 1%), the delayed neutrons have the effect of lengthening very significantly the reactor period. For instance, delayed neutrons due to induced fission on uranium 235 make the reactor period move from $T = 0.1\ s$ to $T = 866\ s$.

Within one second, the initial neutron flux is then multiplied by the factor $e^{\frac{1}{866}} \approx 1.00116$, which makes possible to perform the reactor control.

At last, it is necessary to distinguish **static reactivity*** that measures the discrepancy to criticality of a "fixed" reference fissile system, and **dynamic reactivity*** that includes an additional term resulting from a perturbation of the reference system.

General principles

In this Section we come back to the guidelines of the paper presented on this topic by J. Lewins in Reference [1]. In accordance with what has been written above, the aim here is to describe the behavior of the nuclear reactor strictly as a function of time. For this purpose, we start again from the space-dependent kinetics equations (*supra*, pp. 59 and 60), replacing the neutron flux by the total neutron density in these equations, as follows:

$$\frac{\partial n(\vec{r},E,\vec{\Omega},t)}{\partial t} = -v\vec{\Omega}.\vec{\nabla}n(\vec{r},E,\vec{\Omega},t) - v\sum_k N_k(\vec{r})\,\sigma_k(E)n(\vec{r},E,\vec{\Omega},t) + \sum_k N_k(\vec{r})\int_0^\infty dE'\int_{4\pi} d\vec{\Omega}'\,\sigma_{s,k}(E'\to E,\vec{\Omega}'\to\vec{\Omega})v'n(\vec{r},E',\vec{\Omega}',t) + \frac{1}{4\pi}\sum_k N_k(\vec{r})\int_0^\infty dE'\,\nu_{p,k}(E')\sigma_{f,k}(E')\chi_{p,k}(E'\to E)v'n(\vec{r},E',t) + \frac{1}{4\pi}\sum_{k\in F}\sum_i \lambda_i^{(k)}C_i^{(k)}(\vec{r},t)\chi_{d,i}^{(k)}(E) + S_{ext}(\vec{r},E,\vec{\Omega},t) \quad (1)$$

$$\frac{dC_i^{(k)}(\vec{r},t)}{dt} = -\lambda_i^{(k)}C_i^{(k)}(\vec{r},t) + N_k(\vec{r})\beta_i^{(k)}\int_0^\infty dE'\,\nu_{t,k}(E')\sigma_{f,k}(E')v'n(\vec{r},E',t) \quad (2)$$

For the purpose of clarifying the presentation, we shall not consider any outer source, and we shall assume that there is only one fissile nucleus, denoted k_0.

Moreover, we shall neglect the dependence of the number of neutrons emitted by fission, and of the fission spectrum, on the incident neutron's energy. According to these assumptions, Equation (1) can be rewritten as follows:

$$\frac{\partial n(\vec{r},E,\vec{\Omega},t)}{\partial t} = -v\vec{\Omega}.\vec{\nabla}n(\vec{r},E,\vec{\Omega},t) - v\sum_k N_k(\vec{r})\,\sigma_k(E)n(\vec{r},E,\vec{\Omega},t) + \sum_k N_k(\vec{r})\int_0^\infty dE'\int_{4\pi} d\vec{\Omega}'\,\sigma_{s,k}(E'\to E,\vec{\Omega}'\to\vec{\Omega})v'n(\vec{r},E',\vec{\Omega}',t) + \frac{1}{4\pi}N_{k_0}(\vec{r})\nu_{p,k_0}\chi_{p,k_0}(E)\int_0^\infty dE'\,\sigma_{f,k_0}(E')v'n(\vec{r},E',t) + \frac{1}{4\pi}\sum_i \lambda_i^{(k_0)}C_i^{(k_0)}(\vec{r},t)\chi_{d,i}^{(k_0)}(E) \quad (3)$$

The following simplified notations are used:

- $n \equiv n(\vec{r},\ E,\ \vec{\Omega},\ t)$
- $\chi_p \equiv \chi_{p,k_0}(E)$: energy spectrum for fission prompt neutron emission.
- $\chi_{d,i} \equiv \chi_{d,i}^{(k_0)}(E)$: energy spectrum for delayed neutron of family i.
- $\beta_i \equiv \beta_i^{(k_0)}$: fraction of delayed neutron of family i.
- $\lambda_i \equiv \lambda_i^{(k_0)}$: decay constant of family i.
- $\beta = \Sigma_i\ \beta_i$: delayed neutron total fraction.
- $C_i \equiv C_i^{(k_0)}(\vec{r},t)$: concentration of precursors of family i.
- $1-\beta$: prompt neutron fraction.

The following quantities are defined:

- neutron disappearance and transfer rate, denoted in a simplified manner Rn:

$$Rn \equiv v\vec{\Omega}.\vec{\nabla}n(\vec{r},E,\vec{\Omega},t) + v\sum_k N_k(\vec{r})\,\sigma_k(E)n(\vec{r},E,\vec{\Omega},t) - \sum_k N_k(\vec{r})\int_0^\infty dE'\int_{4\pi} d\vec{\Omega}'\,\sigma_{s,k}(E'\to E,\vec{\Omega}'\to\vec{\Omega})v'n(\vec{r},E',\vec{\Omega}',t)$$

- rate of fission-induced neutron production, denoted in a simplified manner Fn :

$$Fn \equiv \frac{1}{4\pi}N_{k_0}(\vec{r})(\nu_{p,k_0}+\nu_{d,k_0})\int_0^\infty dE'\,\sigma_{f,k_0}(E')v'\int_{4\pi} d\vec{\Omega}\,n(\vec{r},E',\vec{\Omega},t)$$

If we note that the prompt neutron generation rate is written as follows:

$$\frac{1}{4\pi}N_{k_0}(\vec{r})\nu_{p,k_0}\chi_{p,k_0}(E)\int_0^\infty dE'\,\sigma_{f,k_0}(E')v'n(\vec{r},E',t) = (1-\beta)\chi_p Fn$$

we can then rewrite Equations (3) and (2) as follows:

$$\frac{\partial n}{\partial t} = -Rn + (1-\beta)\chi_p Fn + \frac{1}{4\pi}\sum_i \chi_{d,i}\,\lambda_i C_i \quad (5)$$

$$\frac{dC_i}{dt} = -\lambda_i C_i + 4\pi\beta_i Fn \quad (6)$$

The total neutron production operator is introduced:

$$Pn \equiv [1-\beta]\chi_p Fn + \sum_i \beta_i\chi_{d,i}Fn \quad (7)$$

Finally, the following system of equations can be derived:

$$\frac{\partial n}{\partial t} = Pn - Rn - \sum_i \beta_i\chi_{d,i}Fn + \frac{1}{4\pi}\sum_i \chi_{d,i}\,\lambda_i C_i \quad (8)$$

$$\frac{dC_i}{dt} = 4\pi\beta_i Fn - \lambda_i C_i \quad (9)$$

In order to describe the nuclear reactor behavior only as a function of time, Equations (8) and (9) are angle, energy and space integrated over the whole reactor core. The second equation is previously multiplied by the energy spectrum of delayed neutrons $\chi_{d,i}$, and then both equations are multiplied by a weight function w to be defined.

$$\frac{\partial}{\partial t}\int\int\int w\, n\, d\vec{\Omega}dEd\vec{r} = \int\int\int w\, Pn\, d\vec{\Omega}dEd\vec{r} - \int\int\int w\, Rn\, d\vec{\Omega}dEd\vec{r} - \int\int\int w\, \beta_i \chi_{d,i} Fn\, d\vec{\Omega}dEd\vec{r} + \int\int\int w\, \frac{1}{4\pi}\sum_i \chi_{d,i}\, \lambda_i C_i\, d\vec{\Omega}dEd\vec{r} \quad (11)$$

$$\frac{\partial}{\partial t}\int\int\int w\, \chi_{d,i}\, C_i\, d\vec{\Omega}dEd\vec{r} = \int\int\int w\, 4\pi\beta_i \chi_{d,i}\, Fn\, d\vec{\Omega}dEd\vec{r} - \int\int\int w\, \lambda_i\, \chi_{d,i}\, C_i\, d\vec{\Omega}dEd\vec{r} \quad (12)$$

Now, the following "effective" kinetic quantities are defined:

• weighted number of neutrons in the reactor:

$$[n]_{eff} = \int\int\int w\, n\, d\vec{\Omega}dEdr$$

• weighted number of precursors in the reactor:

$$[C_i]_{eff} = \frac{1}{4\pi}\int\int\int w\ \chi_{d,i}\, C_i\, d\vec{\Omega}dEdr$$

• average number of neutrons generated in the reactor:

$$[P]_{eff} = \frac{\int\int\int w\, Pn\, d\vec{\Omega}dEdr}{\int\int\int w\, n\, d\vec{\Omega}dEdr}$$

• effective delayed neutron fraction for the family i :

$$[\beta_i]_{eff} = \beta_i \frac{\int\int\int w\ \chi_{d,i}\, Fn\, d\vec{\Omega}dEdr}{\int\int\int w\, Pn\, d\vec{\Omega}dEdr}$$

• effective delayed neutron fraction:

$$[\beta]_{eff} = \sum_i [\beta_i]_{eff}$$

• average number of neutrons transferred from one point of the phase space to another in the reactor:

$$[R]_{eff} = \frac{\int\int\int w\, Rn\, d\vec{\Omega}dEdr}{\int\int\int w\, n\, d\vec{\Omega}dEdr}$$

• reactivity:

$$[\rho]_{eff} = \frac{[P]_{eff} - [R]_{eff}}{[P]_{eff}}$$

Reactivity appears as the difference between the neutron generation term and the neutron transfer and disappearance term normalized by the generation term;

• average time of neutron multiplication in the reactor:

$$[\Lambda]_{eff} = \frac{1}{[P]_{eff}}$$

$[\Lambda]_{eff}$ is about 25 microseconds in a thermal neutron power reactor.

The two equations (11) and (12) then assume the simple following forms:

$$\frac{\partial [n]_{eff}}{\partial t} = \frac{[\rho]_{eff} - [\beta]_{eff}}{[\Lambda]_{eff}}[n]_{eff} + \sum_i \lambda_i [C_i]_{eff} \quad (13)$$

$$\frac{\partial [C_i]_{eff}}{\partial t} = \frac{[\beta_i]_{eff}}{[\Lambda]_{eff}}[n]_{eff} - \lambda_i [C_i]_{eff} \quad (14)$$

Besides, it can be shown that the weight function w deduced from the solution of the adjoint critical state equation:

$$0 = [P^+ - R^+]n_0^+ \quad (15)$$

is an optimum choice [1].

From the physical viewpoint, this angle, energy and space weighting by the adjoint quantity n_0^+ of the critical density n_0 means that all the neutrons do not bring the same contribution to reactivity. This contribution varies depending on their position in the phase space; the neutrons created in the regions where neutron density is the highest, "weigh" more than those created at the periphery of the core, the latter having a higher leakage probability than the first.

The direct solution of space-dependent kinetics equations (1) and (2) is still seldom used owing to its high cost in computing time. However, thanks to current and future computational powers, it can be considered through either the deterministic or the stochastic route, as shown in References [2] and [3].

With the help of Equations (13) and (14), time evolution can be determined depending on reactivity, and on the weighted number of neutrons and precursors in the reactor. Quantities $[\rho]_{eff}$, $[\beta_i]_{eff}$ and $[\Lambda]_{eff}$, present in these equations, are generally determined by respectively replacing in their definition w and n by n_0^+ and n_0, which requires the solving of the critical equation and of its adjoint equation.

These equations can be directly established as part of the **point kinetics theory**, often used in nuclear reactor Physics.

Point kinetics equations

Within the framework of point kinetics, the neutron population is modelled considering time alone, with the reactor properties averaged in angle, space, and energy. So the point kinetics model means to assume that the whole reactor is concentrated in one and the same spatial point, and that all the neutrons have the same velocity vector.

The evolution of the total number of neutrons depends on three parameters:

- The effective multiplication factor;
- the mean lifetime of neutrons in the reactor;
- the parameters of delayed neutrons.

In the paragraph establishing the equations of spatial kinetics (*supra*, pp. 59 and 60), it was shown that delayed neutron precursors are not treated individually: their contributions to delayed neutron generation are distributed among a few groups or **families of precursor nuclei**. The number of families is denoted I. Today conventional reactor calculations involve six or eight of these families, each of them highlighted by the index i, $1 \leq i \leq I$ exhibiting the following characteristics:

- The total quantity of delayed neutrons issued from the nuclei belonging to this family, denoted β_i ;
- a decay constant, denoted λ_i (or the associated mean lifetime, denoted τ_i) which accounts for the rate of production of the delayed neutrons arising from this family.

These characteristics, issued from the smoothing of the measurements conducted after activation of fissile materials, are, in the case of uranium 235, gathered in Table 17 (see below). In this table, the line “Mean value” also mentions the characteristics to be used if ever a coarser treatment of delayed neutron generation were to be achieved, by gathering all of the precursor nuclei in a single family.

Point kinetics equations can be directly established by performing a balance of the total number of neutrons $n(t)$ and of the number of precursors in each family $C_i(t)$.

Over a time interval dt, $n(t)\frac{dt}{\ell}$ neutrons disappear, generating an average number of $n(t)\frac{dt}{\ell}k_{eff}(1-\beta)$ prompt neutrons by fission. Over the same time interval, $\sum_i \lambda_i C_i(t)$ delayed neutrons appear following the decay of precursors.

Furthermore, over a given time interval dt, $\lambda_i C_i(t)$ precursors of the family i disappear while $n(t)\frac{dt}{\ell}k_{eff}\beta_i$ appear.

This is how **point kinetics equations** are obtained:

$$\begin{cases} \dfrac{dn(t)}{dt} = \dfrac{k_{eff}(1-\beta)-1}{\ell}n(t) + \displaystyle\sum_i \lambda_i\, C_i(t) \\ \dfrac{dC_i(t)}{dt} = \dfrac{k_{eff}\beta_i}{\ell}n(t) - \lambda_i C_i(t) \end{cases} \tag{16}$$

By expressing the effective multiplication factor as a function of reactivity ρ, $k_{eff} = \frac{1}{1-\rho}$, the system of equations (16) can be rewritten as follows:

$$\begin{cases} \dfrac{dn(t)}{dt} = \dfrac{\rho-\beta}{\dfrac{\ell}{k_{eff}}}n(t) + \displaystyle\sum_i \lambda_i\, C_i(t) \\ \dfrac{dC_i(t)}{dt} = \dfrac{\beta_i}{\dfrac{\ell}{k_{eff}}}n(t) - \lambda_i C_i(t) \end{cases} \tag{17}$$

Table 17.

Decay constants, delayed neutron proportions, and mean lifetime in the case of U 235 fission
(data issued from JEFF3.1)

Precursor Groups	λ_i (s^{-1})	$\tau_i = \frac{1}{\lambda_i}$ (s)	β_i (pcm)
1	$1.247\ 10^{-2}$	$8.021\ 10^{1}$	22
2	$2.829\ 10^{-2}$	$3.535\ 10^{1}$	102
3	$4.252\ 10^{-2}$	$2.352\ 10^{1}$	61
4	$1.330\ 10^{-1}$	7.516	131
5	$2.925\ 10^{-1}$	3.419	220
6	$6.665\ 10^{-1}$	1.500	60
7	1.635	$6.117\ 10^{-1}$	54
8	3.555	$2.813\ 10^{-1}$	15
Mean value	$7.681\ 10^{-2}$	$1.302\ 10^{1}$	665

It can be noticed that this system displays the same form as the system built by general equations (13) and (14), the effective quantities $[\rho]_{eff}$, $[\beta_i]_{eff}$ and $[\Lambda]_{eff}$, used as parameters in these equations being here replaced by quantities ρ, β, and $\frac{\ell}{k_{eff}}$. This latter value, generally denoted ℓ^*, stands for *neutron lifetime in a critical reactor*.

As a first approach, it may be considered that the normal operation of reactors takes place as a succession of ranges where reactivity is maintained constant (through control rods inserted more or less deeply, at values maintained during a certain time).

So the differential equation system (17) is a linear homogeneous system with constant coefficients whose solution is a linear combination of $(I+1)$ specific solutions. These specific solutions are sought for the neutron population, and for the precursor population, in the following form:

$$\begin{cases} n_j(t) = A_j \exp(\omega_j t) \\ C_{ij}(t) = B_{ij} \exp(\omega_j t) \end{cases} \qquad 1 \le j \le I+1$$

where ω_j is a parameter to be determined.

So the general solution can be written as follows:

$$\begin{cases} n(t) = \sum_{j=1}^{I+1} A_j \exp(\omega_j t) \\ C_i(t) = \sum_{j=1}^{I+1} B_{ij} \exp(\omega_j t) \end{cases}$$

It is shown that the ω_j are the solution of an equation in ω , referred to as the "**Nordheim equation**":

$$\rho = \ell^* \omega + \sum_i \frac{\beta_i \omega}{\omega + \lambda_i} \qquad (18)$$

Once the possible values of ω_j have been found, the solving of the whole problem is finalized through determining constants A_j and B_{ij}, starting from the initial conditions $n(t=0)$ and $C_i(t=0)$.

A practical way to proceed is to solve the Nordheim equation graphically. Its roots are evidenced tracing the horizontal line ρ in a diagram that represents the function $f(\omega)$ mentioned in the second member of Equation (18) (Fig. 54).

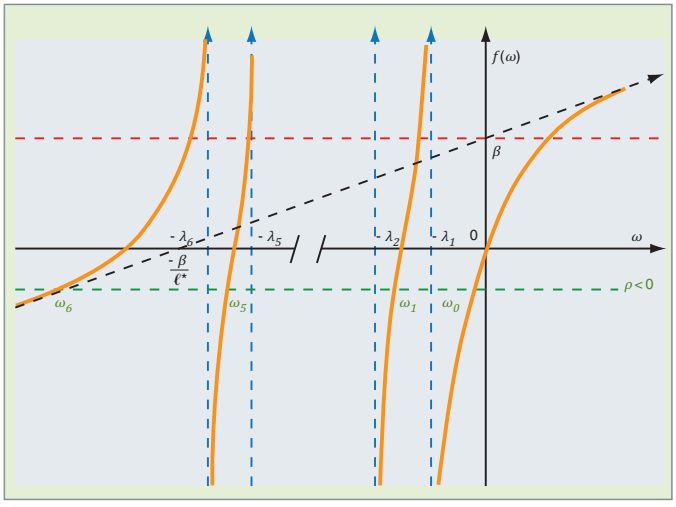

Fig. 54. Graphical resolution of the Nordheim equation. Case of negative reactivity.

As shown on this graph, $(I+1)$ roots can always be found, I being the number of delayed neutron families. Among these $(I+1)$ roots, I are always negative and correspond with transients, while the last one, of the same sign as reactivity, corresponds with the asymptotically dominant mode.

In the case of very high reactivity (that corresponds with accidental conditions), the expression of the biggest root of the Nordheim equation, denoted ω_0, can be made explicit with simple considerations of orders of magnitude, *i.e.* approximately:

$$\omega_0 \simeq \frac{\rho - \beta}{\ell^*}$$

This expression can also be written as follows:

$$\omega_0 \simeq \frac{k_{eff}(1-\beta) - 1}{\ell}$$

where $k_{eff}(1-\beta)$ represents the contribution of prompt neutrons alone to the multiplication factor.

This formula shows that, if $k_{eff}(1-\beta) > 1$ (or $\rho > \beta$), the reactor diverges with only prompt neutrons, the neutron population multiplying with the period:

$$T_0 \simeq \frac{\ell^*}{\rho - \beta} = \frac{\ell}{k_{eff}(1-\beta) - 1}$$

that is extremely fast, according to the law:

$$n(t) = n_0 \exp\left(\frac{\rho - \beta}{\ell^*} t\right)$$

The reactor is in such a case referred to as "prompt critical", and the value $\rho = \beta$ (β about 665 pcm for uranium 235 according to Table 17) appears as the upper limit beyond which the reactor behavior is controlled by prompt neutrons.

In contrast, when reactivity is very small and lower than β, the reactor behavior is described by:

$$\omega_0 \simeq \frac{\rho}{\tau}$$

where

$$\tau = \ell^* + \sum_i \frac{\beta_i}{\lambda_i} \simeq \sum_i \frac{\beta_i}{\lambda_i}$$

Time τ is characteristic of the fissile nucleus, and is equal to about 0.0866 s in the case of uranium 235.

The neutron population then multiplies with the period:

$$T_0 \simeq \frac{\tau}{\rho} \simeq \frac{\tau}{k_{eff} - 1}$$

according to the law:

$$n(t) = n_0 \exp\left(\frac{\rho}{\tau} t\right)$$

So the control of the reactor is quite possible as small reactivity is introduced.

It can also be observed that a complete stop of nuclear chain reaction only becomes effective by the end of delayed neutron emission that is after a few minutes.

Three-Dimensional Kinetics

Modeling the incidental or accidental situations of a reactor core requires taking account of the fast variation in the neutron population within the reactor core. The envelope accident considered for design basis, with respect to the uncontrolled evolution of nuclear fission, is the ejection of a control rod. This ejection is induced by a failure of the control rod drive mechanism, and is due to a difference in pressure between the reactor vessel and the containment. It results in a very intense, local runaway of nuclear fission (a few milliseconds), yet limited by the neutron feedbacks, which enable the reactor to be immediately shut down. It is understandable that an accurate investigation of this type accident requires an associated 3-D neutronics and thermal-hydraulics model. The spatial neutronic kinetics equations have been set out above, *supra*, pp. 59 and 60.

Usually, they are solved in the following simplified form:

$$\frac{1}{v}\frac{\partial \psi(\vec{r}, E, \vec{\Omega}, t)}{\partial t} + \vec{\Omega}.\vec{\nabla}\psi\left(\vec{r}, E, \vec{\Omega}, t\right) + \Sigma(\vec{r}, E, t)\psi(\vec{r}, E, \vec{\Omega}, t) = Q\left(\vec{r}, E, \vec{\Omega}, t\right) \quad t \in [t_0 \ t_1] \tag{19}$$

with:

$$Q\left(\vec{r}, E, \vec{\Omega}, t\right) = Q_s\left(\vec{r}, E, \vec{\Omega}, t\right) + Q_p(\vec{r}, E, t) + Q_d(\vec{r}, E, t)$$

$$Q_s\left(\vec{r}, E, \vec{\Omega}, t\right) = \int_{4\pi} d\vec{\Omega}' \int_0^{\infty} \Sigma_s(\vec{r}, E' \to E, \vec{\Omega}.\vec{\Omega}', t)\psi\left(\vec{r}, \mathrm{E}', \vec{\Omega}', t\right) dE'$$

$$Q_p(\vec{r}, E, t) = \frac{1}{4\pi}\chi_p(E) \int_0^{\infty} \nu_p(\mathrm{E}')\Sigma_f\left(\vec{r}, E', t\right)\phi(\vec{r}, E', t) d\mathrm{E}'$$

$$Q_d(\vec{r}, E, t) = \frac{1}{4\pi}\sum_i \lambda_i \ \chi_{d,i}(E)\, C_i(\vec{r}, t)$$

Here we work with a mean prompt fission spectrum independent of the incident neutron's energy, an average number of emitted prompt neutrons, and precursor families independent of the fissile system.

After having integrated Equation (2), the concentration $C_i(\vec{r}, t)$ of the precursor i is expressed as a function of the scalar flux as follows:

$$C_i(\vec{r}, t) = \mathrm{e}^{-\lambda_i(t-t_0)} C_{0i}(\vec{r}, t) + \int_{t_0}^{t} \mathrm{e}^{-\lambda_i(t-s)} \int_0^{\infty} \beta_i \ \nu\Sigma_f(\vec{r}, E', s)\phi(\vec{r}, E', s)\, dE' ds \tag{20}$$

Solving such an equation is very costly as it is expressed in a seven-dimensional space. The times for a typical calculation can be estimated assuming that the space is discretized into 10^3x10^3x10^2 points, that the angle requires about 50 directions, that the energy is discretized into twenty or so groups, and that time discretization needs about 10^3 steps of 10^{-2} s. In addition, iterations are necessary to take into account thermal-hydraulics feedbacks. This results in about 10^{11} unknowns. Each unknown is coupled by a matrix system. By estimating the filling ratio of the matrix system to 100, an estimate of about 10^{16} floating operations can be obtained for a three-dimensional kinetics simulation.

In order to reduce this high cost in computing time, various approximations have been proposed over the years, depending on power available on computers.

Simplification models

The first simplifying model relies on the angular discretization. A diffusion operator ($-\vec{\nabla}.\mathrm{D}\vec{\nabla}$) is most often used, for which the unknown becomes the scalar flux: $\phi(\vec{r}, E, t)$. More recently, was introduced the SP_N operator (see *supra*, p. 74), for which the unknown is then a set of harmonics, among which the scalar flux and the current. At the present time, thanks to the power of new parallel machines, full-transport kinetics problems can be solved, the unknowns then being the angular fluxes.

The second model is related to the time model. It leads to a number of variants (adiabatic, quasi-static, improved quasi-static, local quasi-static, generalized quasi-static, multiscale, "single-step" or "multistep" three-dimensional… methods). Approximations deal with the system's initial state or behavior over time, which of course may result in a loss in the model's accuracy. Therefore, a good compromise has to be found for the time/accuracy ratio by the user.

The point kinetics model has already been described. This model can only lead to the average behavior of the core. That is, it does not include local spatial information, which makes it applicable to the sole problematic of core operation, and does not allow its use to tackle the severe accident problematic.

The early 3-D time models have been developed since the 1960s [5]. They rely on a principle of space and time factorization, with a shape function that is space-dependent and possibly time-dependent, and an amplitude function that is time-dependent and possibly space- dependent.

$$\phi(\vec{r},\ E,\ t) = a\,(\vec{r},\ E,\ t)\ f\,(\vec{r},\ E,\ t) \qquad (21)$$

The method can be seen as a separation of the fast and slow variations in flux (versus time). Thus, $a\,(\vec{r},\ E,\ t)$ is a function which represents the fast behavior over time, and $f\,(\vec{r},\ E,\ t)$ is a shape flux (in n/cm²/s) that slowly varies versus time.

Quasi-static method (QS)

The principle of the quasi-static method has been proposed by Henry in 1958. In this model, only amplitude $a\,(t)$ is computed as a function of time, and shape f is maintained at its initial value $f\,(\vec{r},\ E,\ t_0)$:

$$\phi(\vec{r},\ E,\ t) = a\,(t)\ f\,(\vec{r},\ E,\ t_0)$$

Amplitude only depending on time is the solution of a point kinetics equation, the coefficients of which can be obtained by the shape projection on a weighting function that, optimally, is the adjoint flux. Shape calculation can be performed again during the transient, for a given static state, providing the point kinetics coefficients are computed again.

Improved Quasi-Static method (IQS)

The variable separation achieved in the quasi-static method is a strong assumption. This is why it was quickly converted into the Improved Quasi-Static (IQS) form. The idea is to introduce a slow time dependence denoted T for the shape, while keeping a fast-variation point amplitude:

$$a\,(\vec{r},\ E,\ t) = a\,(t) \text{ and } f\,(\vec{r},\ E,\ t) = f\,(\vec{r},\ E,\ T)$$

However, due to the time dependence of f, it is necessary to add a normalization condition so as to ensure the unicity of the factorization. Usually, in the IQS method, it is imposed what follows:

$$\iint \frac{1}{v}\frac{\partial f(\vec{r},E,t)}{\partial t}\phi^*(\vec{r},E,t_0)d\vec{r}\,dE\ = 0$$

This condition *a posteriori* validates the assumption of slow variation over time of the shape function. Other weighting functions, apart from the adjoint flux $\phi^*(\vec{r},\ E,\ t_0)$, are possible. Yet, a variational reasoning shows that using the initial adjoint flux minimizes the error in calculation.

So two scales of time discretization are introduced, first a coarse scale $T \in [T_i\ T_{i+1}]$, on which the shape is evaluated, and secondly a fine scale (a subdivision of the previous one) $\Delta t_k\ \in [t_k\ t_{k+1}]$, on which the amplitude alone is evaluated.

A solution is given, alternately, to the following problems:

- A point kinetics problem that gives a, knowing f;
- a 3-D kinetics problem on the coarse time step that gives f, knowing a.

Solving is performed as follows. Let us consider the 3-D equations where ϕ is replaced by the product af. In order to obtain the first equation on amplitude a, these equations are condensed in space and energy, after multiplication by the initial adjoint flux. The time derivative of the shape flux disappears thanks to the normalization condition. In order to obtain the equations on shape, the equation treatment is identical to that of a full 3-D system. An additional term appears so as to take into account the variation in amplitude, which leads to a system coupled with amplitude that may be solved by a fixed-point iterative method (in practice, a single iteration is performed). For time discretization, as the variation is slow, low-level schemes can be used. All the major (diffusion and transport) core computer codes at least apply one of the quasi-static methods (generally, the improved quasi-static method).

The improved quasi-static method is available, for instance, for the MINOS finite-element solver of the CRONOS2 code [6]. Integrating the IQS method in the MINOS context has made it possible to benefit from the advantages of the solver fastness. However, in practice, to get an accuracy equivalent to that of a 3-D resolution, requires a very fine time discretization [7].

Local quasi-static method

The flaw of the previous method lies in the strong assumption of an amplitude constant in space and energy. Thus, in fine time steps, variations in space and energy, *e.g.* related to a strong heterogeneity of the medium, are not sufficiently taken into account. In order to overcome this flaw, attention is focused on other approaches partly integrating the quasi-static principle, given its gain in computing time but with a more local condensation of the shape.

The idea is to achieve a decomposition of the spatial domain into subdomains, and locally transpose the global assumptions of the quasi-static method. So the subdomains will display a quasi-static amplitude/shape decomposition (with an amplitude only depending on time, and a shape weakly depending on time). A more realistic model could, hopefully, be obtained, for instance by adapting these subdomains to the medium's properties.

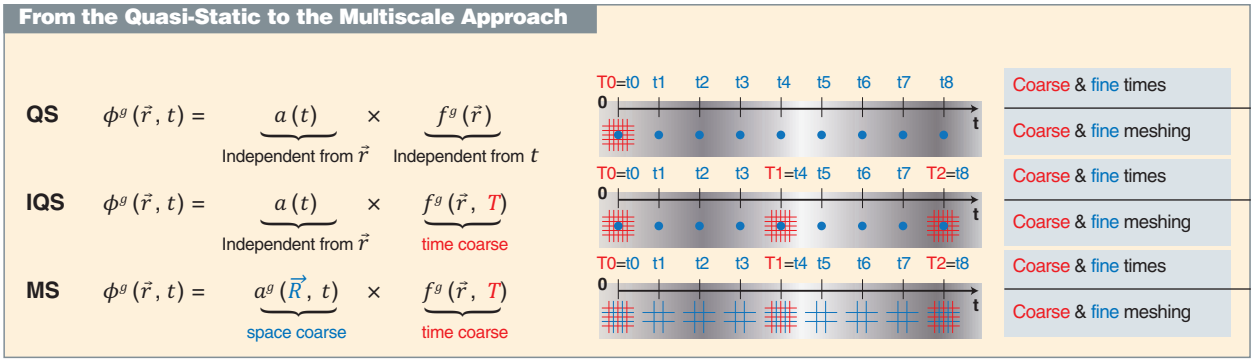

Fig. 54. Principle schematics of quasi-static, improved quasi-static, and multiscale modeling.

Multiscale (MS) approach

Here the purpose is to extend the principle of the local quasi-static method so as to improve the model's accuracy while keeping the advantages of a local approximation. The idea is to keep the factorization with two time scales, while introducing, for the amplitude function, a coarse variation in space (on a coarse spatial meshing, built on the resolution fine one) [8].

This approach entails that two simultaneous kinetics problems have to be solved on different scales and using the same solver. In the MINOS context, studied by S. Chauvet [8], the discontinuous representation of the flux makes the implementation easier (though the continuity of the normal current has to be imposed). Moreover, more benefit can be drawn from existing tools, which are optimized in the environment of the available code (*e.g.* MINOS). The problematic mainly lies in how to optimize the time / accuracy ratio.

Starting from existing methods, and locally optimizing the resolution methods suitable for the context (coarse time step or broad spatial meshing), this method saves computational time in contrast with a full 3-D method.

Modal synthesis method

The modal synthesis method is an extension of the original quasi-static method in which a solution is looked for in the form of a superposition of known and pre-calculated shape functions (modes), denoted f_m. Regarding the energy condensation method, the following expansion is used:

$$\phi(\vec{r},E,t) = \sum_m a_m(t) f_m(\vec{r},E)$$

The equations giving the coefficients $a_m(t)$ are obtained through condensation, using weighting functions, and integrating over the space and energy domain. A preliminary step is eliminating the differential equations of precursors using equations (20).

The result is a system of coupled integro-differential equations on the functions $a_m(t)$ that can be solved through a time discretization and a "single-step", or "multistep" scheme.

The system's solution can exist only if the various modes are linearly independent. A possible choice is using the space and energy harmonics of the static operator ; the best choice, in the variational meaning, for the weighting functions is then to use adjoint harmonics.

Three-Dimensional Kinetics Methods

The first applications of the Three-Dimensional Kinetics Methods go back to the years 1970. They were first applied to a Finite Difference discretization for the space variable (use of the diffusion operator), a multigroup discretization for the energy variable, and a "single-step" scheme for the time variable. Concerning three-dimensional calculations, the Finite Difference Method proved too costly in memory, and was replaced by Finite Element Methods that lead to more condensed matrices, and allow an easy reconstruction in the meshes. We describe this approach first used in the CRONOS code [6], and then in the APOLLO3® code in SPN (MINOS solver [9]), and, more recently, in transport (MINARET solver [10]) with discontinuous finite elements (see *supra*, p. 81).

Let us consider the kinetics equation in which the precursor equations have been previously integrated, as shown above. A multigroup energy discretization is used.

The diffusion operator is selected as spatial operator. Let us consider a time step $[t_p\, t_{p+1}]$, over which a time integration is achieved. Assuming v^g constant over a time step, the kinetics equation then results in what follows:

$$\frac{1}{v^g}\left(\phi^g_{p+1}(\vec{r}) - \phi^g_p(\vec{r})\right) + \int_{t_p}^{t_{p+1}} \left(\vec{\nabla}.D^g(\vec{r},t)\vec{\nabla}\phi^g(\vec{r},t) + \Sigma^g(\vec{r},t)\phi^g(\vec{r},t)\right)dt = \int_{t_p}^{t_{p+1}} Q^g\left(\vec{r},\vec{\Omega},t\right)dt$$

where it has been set: $\phi_p^g(\vec{r}) = \phi^g(\vec{r}, t_p)$ and $\phi_{p+1}^g(\vec{r}) = \phi^g(\vec{r}, t_{p+1})$.

Then assumptions on the time variations of cross sections, of the diffusion coefficient, and of the flux are made. They are written as follows:

$$\Sigma^g(\vec{r}, t) = l_p(t)\ \Sigma_p^g(\vec{r}) + l_{p+1}(t)\ \Sigma_{p+1}^g(\vec{r})$$

$$D^g(\vec{r}, t) = l_p(t) D_p^g(\vec{r}) + l_{p+1}(t) D_{p+1}^g(\vec{r})$$

$$\phi^g(\vec{r}, t) = \omega_p(t) \phi_p^g(\vec{r}) + \omega_{p+1}(t) \phi_{p+1}^g(\vec{r})$$

with:

$$\Sigma_q^g(\vec{r}) = \Sigma^g(\vec{r}, t_q), \mathrm{D}_q^g(\vec{r}) = \mathrm{D}^g(\vec{r}, t_q)$$

$$\forall\ g \in G\ ,\ q = p, p+1$$

Various choices on the functions $\omega_p(t)$ and $l_p(t)$ are possible. The cross sections and the diffusion coefficient are assumed to be of linear variations over the time step. As regards the flux, the choice of a linear variation in t leads to the conventional Crank-Nikolson scheme, and the choice of a parabolic representation in t allows the implicit scheme to be obtained, among other benefits. In the simulations of accident transients, both schemes can be used successively: the Crank-Nikolson scheme, more precise, is used during power excursion, and the implicit scheme, more stable, is used in the power drop phase due to control rod drop.

Let us then consider a spatial representation on a finite element basis. The flux is then expanded into the following form:

$$\phi_q^g(\vec{r}) = \sum_i \phi_q^{ig} P_i(\vec{r}) \quad \forall\ g \in G\ , \qquad q = p, p+1$$

The $\phi_q^g(\vec{r})$ are replaced by their representation in the kinetics equation, integrated over the time step. After multiplication by weighting functions $P_j(\vec{r})$ (Galerkin method), integration is performed over the full spatial domain. This results in a matrix system of order $N \times G$ (N being the number of nodes in the finite element basis, and G the number of energy groups). At each step, a linear system has to be solved:

$$A_{p+1} \phi_{p+1}^{ig} = A_p \phi_p^{ig} + Q_p^{ig}$$

The previous system is solved by iterations, using various acceleration methods. The "rebalancing" method by condensation on energy groups is quite efficient; it is equivalent to a preconditioning by a quasi-static method.

The extension of the method to the SP_N MINOS solver (Cartesian and hexagonal geometry) complies with the same principle. Yet, due to the mixed approximation used, two different representations are introduced on the time step for even (scalar) fluxes and odd (vector) fluxes. The matrix system to be solved over the time step is written in terms of odd fluxes. Using this solver and according to the user's choice, the differential term

$$\frac{1}{v}\frac{\partial}{\partial t}$$

of Equation (19) can be taken into account on the scalar flux alone, or on the flux and the current, or on all the harmonics.

The S_N transport kinetics can help improve modeling in strongly heterogeneous configurations. The TORT-TD code [11] can perform such calculations for Cartesian and cylindrical geometries. The time scheme is an implicit scheme, and space discretization is of the finite-difference type. More recently, the S_N transport kinetics has been implemented for the MINARET solver of the APOLLO3® code. The time algorithm is also "single-step" implicit, the space discretization uses discontinuous finite elements of any order, and the meshing is radial-unstructured, and axial-cylindrical. The user may, at his convenience, take into account the time differential term

$$\frac{1}{v}\frac{\partial}{\partial t}$$

for the scalar flux alone or for all the components of the angular flux. The angular sweep is parallelized.

A 3D-Kinetics application example is given in this Monograph in the case of a steam line break accident (see *infra*, p. 225).

References

[1] J. Lewins, *Nuclear Reactor Kinetics and Control*, Oxford, Pergamon Press, 1978.

[2] B. L. Sjenitzer and J. E. Hoogenboom, "A Monte-Carlo method for calculation of the dynamic behaviour of nuclear reactors", *Progress in Nuclear Science and Technology*, vol. 2, pp. 716-721, 2011.

[3] B. L. Sjenitzer and J. E. Hoogenboom, "General purpose dynamic Monte-Carlo with continuous energy for transient analysis", in *Proceedings PHYSOR* (Knoxville), 2012.

[4] G. R. Keepin, *Physics of Nuclear Kinetics*, Addison-Wesley, Massachussetts, 1965.

[5] A. Henry, "The application of reactor kinetics to the analysis of experiments", *Nuclear Science and Engineering*, 3, pp. 52-70, 1958.

[6] J.J. Lautard, S. Loubière and C. Fedon-Magnaud, "CRONOS a Modular Computational System for Neutronic Core Calculations", *Specialist IAEA meeting, Advanced Calculational Methods for Power Reactors*, Cadarache, France, 1990.

[7] M. Dahmani, A.M. Baudron, J.J. Lautard and L. Erradi, "Application of the nodal mixed dual technique of spatial reactor kinetics using the improved quasi static method", *Proc. ANS Topical Mtg., Mathematics*

and Computation, Reactor Physics and Environmental Analysis in Nuclear Applications, vol. 1, Madrid, Spain, 1999.

[8] S. Chauvet, A. Nachaouia, A.M. Baudron and J.J Lautard, "A Multi-Scale Quasi-static Method for the Neutronic Kinetics", *International Conference on the Physics of Reactors*, Casino-Kursaal Conference Center, Interlaken, Switzerland, September 14-19, 2008.

[9] D. Schneider, J.C. Le Pallec, A.M. Baudron "Mixed dual finite element method for the solution of the 3D kinetic simplified PN transport equations", *Nuclear Mathematical and Computational Sciences*, Gatlinburg, Tennessee, April 6-11, 2003.

[10] A.M. Baudron, J.J. Lautard, Y. Maday, and O. Mula, "Towards a time-dependent neutron transport parallel solver" submitted to Proc SNA/MC conf. Paris, 2013.

[11] A. Seubert, A. Sureda, J. Bader, J. Lapins, M. Buck, E. Laurien, "The 3-D time-dependent transport code TORT-TD and its coupling with the 3D thermal-hydraulic code ATTICA3D for HTGR applications", *Nuclear Engineering and Design*, 251, pp. 173-180, 2012.

Anne-Marie Baudron, Patrick Blanc-Tranchant, Mireille Coste-Delclaux, Cheikh M. Diop, Jean-Jacques Lautard and Anne Nicolas
Department for Systems and Structures Modeling

Neutronics Computer Codes and High-Performance Computing

Studies performed by reactor physicists require an access to the physical quantities of interest such as reactor power, particle fluxes, isotopic concentrations… For this purpose it is necessary to solve the equations that govern neutron propagation in space and time *(Boltzmann equation)*, and those that govern time evolution in concentrations of nuclides present and formed in the various materials of fuel and of all the reactor's structures *(generalized Bateman equations)* [see *supra*, pp. 45-49].

Numerical simulation implements computational tools that solve the above mentioned equations. These tools are based on:

- *Physical-mathematical formalisms* that describe the physical phenomena investigated;
- *modelings*, *i.e.* descriptions of the physical system and the phenomena that take place in it basing upon relevant assumptions that make calculations and their optimization practical;
- *numerical methods* that treat physical-mathematical formalisms within the frame of the defined modelings;
- *computer science* and algorithmics coupled to the selected numerical methods to be implemented on computers.

Two main classes of algorithmic approaches are available to solve the Boltzmann equation: *deterministic* approaches and the so-called stochastic or probabilistic approaches. Two corresponding families of codes have therefore been developed:

- *Deterministic codes*, in which the result is obtained by solving the Boltzmann equation and/or its simplified version that is the *diffusion equation*. These tools are those which are usually utilized to perform calculations of operating reactors, coupling them if need be to thermal-hydraulic or mechanical computer codes. The Boltzmann equation is solved taking into account either its integral form or its integro-differential form. The main resolution methods and models used are detailed *supra*, pp. 61-86;
- codes based on the *Monte-Carlo method*, which solves the Boltzmann equation starting from its integral form (see *supra*, pp. 89-106). This method is considered as the reference computational route.

A given modeling to calculate a nuclear reactor (particle flux, isotopic concentrations, effective multiplication factor, various reaction rates…), with a pre-established computational time/accuracy compromise, requires to choose among the different options available in relation to:

- Nuclear data;
- fine-scale discretization in space and energy;

- physical phenomena decoupling;
- the equation adopted (deterministic or Monte-Carlo calculation, transport or scattering);
- the resolution method (characteristics, collision probabilities, nodal methods…);
- the anisotropy description;
- the succession of computational sequences;
- …

This set of alternatives dedicated to calculating a reactor type, with one or several precise objectives (design, tool validation, accident analysis…) is referred to as a "**computational** (or **calculation**) **scheme**". Some of them are described in chapter titled "Reactor Neutronics Calculation", pp.193-213. In practice, a computational scheme is executed through specific instructions written in a high-level computer language called a "**command language**". These particular instructions which specify the selected calculation options and the computational sequences to be applied are "encapsulated" in sets likely to be easily handled by users, the so-called "**computational procedures**".

As a general rule, **computational tools** assigned to a given study refer to a consistent set, often called a "**computational code package**", which consists of the following items:

- The ***computational software(s)*** [or ***code(s)***];
- the ***basic physical data*** (cross section libraries…) needed to implement the software;
- the ***computational schemes*** and corresponding **computational procedures**;
- the ***verification, validation and qualification file*** (experiments, benchmarks…), a tool for demonstrating the ability of the software used to perform accurate calculations;
- the ***documentation*** coupled to the software, procedures and libraries used (user manual, calculation scheme computational procedures report, identification report, document for library contents description…).

The code package limits for use, biases and uncertainties are assessed and transferred to the user. For example, the NARVAL and HORUS-3D forms, further described (pp. 143-147), are respectively dedicated to the calculation of nuclear propulsion reactors and of the Jules Horowitz Reactor (JHR). They consist of computer codes such as APOLLO2, for calculation of multi-parameter cross section libraries, CRONOS2 for 3-D core calculation, TRIPOLI-4® for reference calculation, and DARWIN-2 for burnup calculation, as well as of referenced nuclear data libraries, and of validated, documented calculation options, the whole of it being usable in a given qualification area (see *infra*, pp. 165-182).

Main Computer Codes

In the chapter dedicated to the neutron physicist's approach, we have seen that for reasons of memory size and computational time, adapted discretizations and physical phenomena uncoupling are implemented for reactor modeling. As already mentioned, the deterministic calculation of a reactor is divided into two parts. The first one deals with the precise solving of the Boltzmann equation, in both space and energy, on a small area of the core (*e.g.* one assembly, a pattern of a few assemblies…). This step provides space-homogenized and energy-condensed constants, which are used as coefficients of the Boltzmann equation or the diffusion equation for the second computational step. The latter consists in solving these equations on the full, usually three-dimensional, reactor core, keeping spatial and energetic meshes less detailed than in the first step.

Initially, computer codes were dedicated to either of these steps. This subdivision is still preserved in currently employed codes. The first computational step is usually called a "**spectral calculation***", or "**lattice calculation***", while the second is referred to as "core calculation*" (see *supra*, pp. 51-54, and *infra*, pp. 193-213). In both cases, the Boltzmann (and diffusion) equations as well as the Bateman equations are solved through different techniques adapted to the problems to be solved (see the previous chapters).

The computer codes briefly described herein are the following:

- The **APOLLO2*** lattice code and the **CRONOS2*** core code (mainly used for thermal neutron reactors);
- the **DARWIN-2*** time evolution (burnup) code;
- the **ERANOS*** computational code package (dedicated to fast spectrum reactors);
- the new multi-purpose platform **APOLLO3®*** and **MENDEL***;
- the Monte-Carlo transport code **TRIPOLI-4®***.

A few computational codes, referred to as "simplified", are also mentioned in the final part of this review.

These computer codes are developed within a partnership with French nuclear actors. They benefit from ongoing improvements through R&D programs and the various PhD dissertations achieved within this framework.

APOLLO2

APOLLO2 [1] [2] is a spectral multigroup two-dimensional computer code that solves the neutron transport equation using different methods:

- The *collision probabilities* (exact, and in a numerically approximated formulation referred to as "multicell") [see *supra*, p. 84];
- the space nodal methods and the angle S_N-type methods, for Cartesian geometries (see *supra*, pp. 72-74);
- the *Method Of Characteristics* (MOC), the latter (see *supra*, pp. 82-85) being available for any type of geometries, described through a man-machine interface (MMI) named "SILENE" [3].

It is possible to combine the different flux calculation methods with one another in order to reach a quality solution within a reasonable computational time.

The development of the Characteristics Method, coupled with algorithmic and numerical advances, has yielded significant advances in **core physics*** with APOLLO2, through achieving two-dimensional (2-D) full-core calculations with an accurate geometrical description and without intermediate homogenization stages.

APOLLO2 can be used with any energy multigroup structure of cross sections: there exists a library of 12,000 energy groups or so that enables reference calculations to be performed, while usual calculations are achieved for about 300 energy groups. The nuclear self-shielding computational method which is implemented in it (see *supra*, pp. 65-72), is both precise and original; this is one of the code's major assets. For it is based on a *twofold space and energy equivalence*, and on the use of cross sections represented as **probability tables***. Particularly, it is worth to mention the accurate treatment of nuclear mixtures.

APOLLO2 also performs fuel generation/depletion calculations.

The code is mainly used to calculate thermal or epithermal spectrum reactors; it was validated on a high number of critical experiments, among which those achieved in the ÉOLE reactor. Its validation area covers the use of MOX and UOX fuels, of various absorbers and neutron poisons (**B_4C***, **gadolinium***, **AIC***…). After being widely used with a cross section library* issued from JEF-2.2 nuclear data evaluation, it is now coupled with the new library issued from JEFF-3 nuclear data evaluation (see *supra*, pp. 21-37). Using the SILENE interface enables the user to generate consistent data for APOLLO2 and for Monte-Carlo code TRIPOLI-4®, which makes it possible to safely perform calculation validation.

Most of APOLLO2 applications aim at achieving multi-parameterized libraries of space-homogenized, energy-condensed cross sections which are used as input data for core calculations. APOLLO2 is the spectral code of all French nuclear actors (EDF, AREVA-NP, CEA). It is also the lattice code of the NURISP European project (www.nurisp.eu/www/nurisp/index.php). At last, it is included in the CRISTAL *criticality code package* (see *infra*, p. 242) and in the DARWIN *cycle computational*

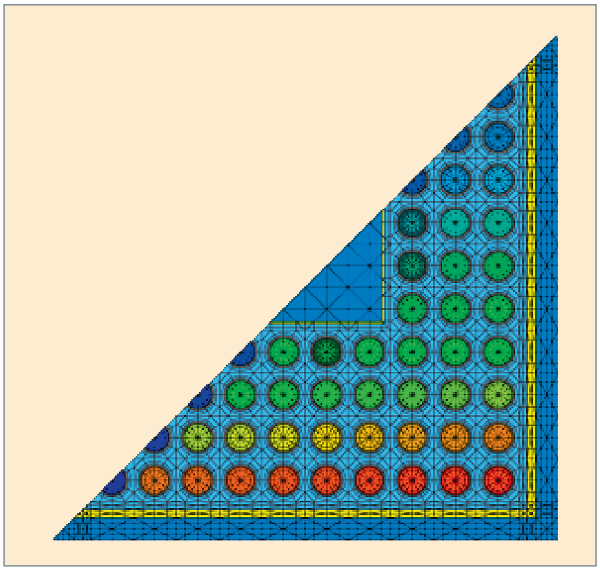

Fig. 55. APOLLO2, calculation of a benchmark for an ATRIUM-type BWR assembly. Half-assembly [4].

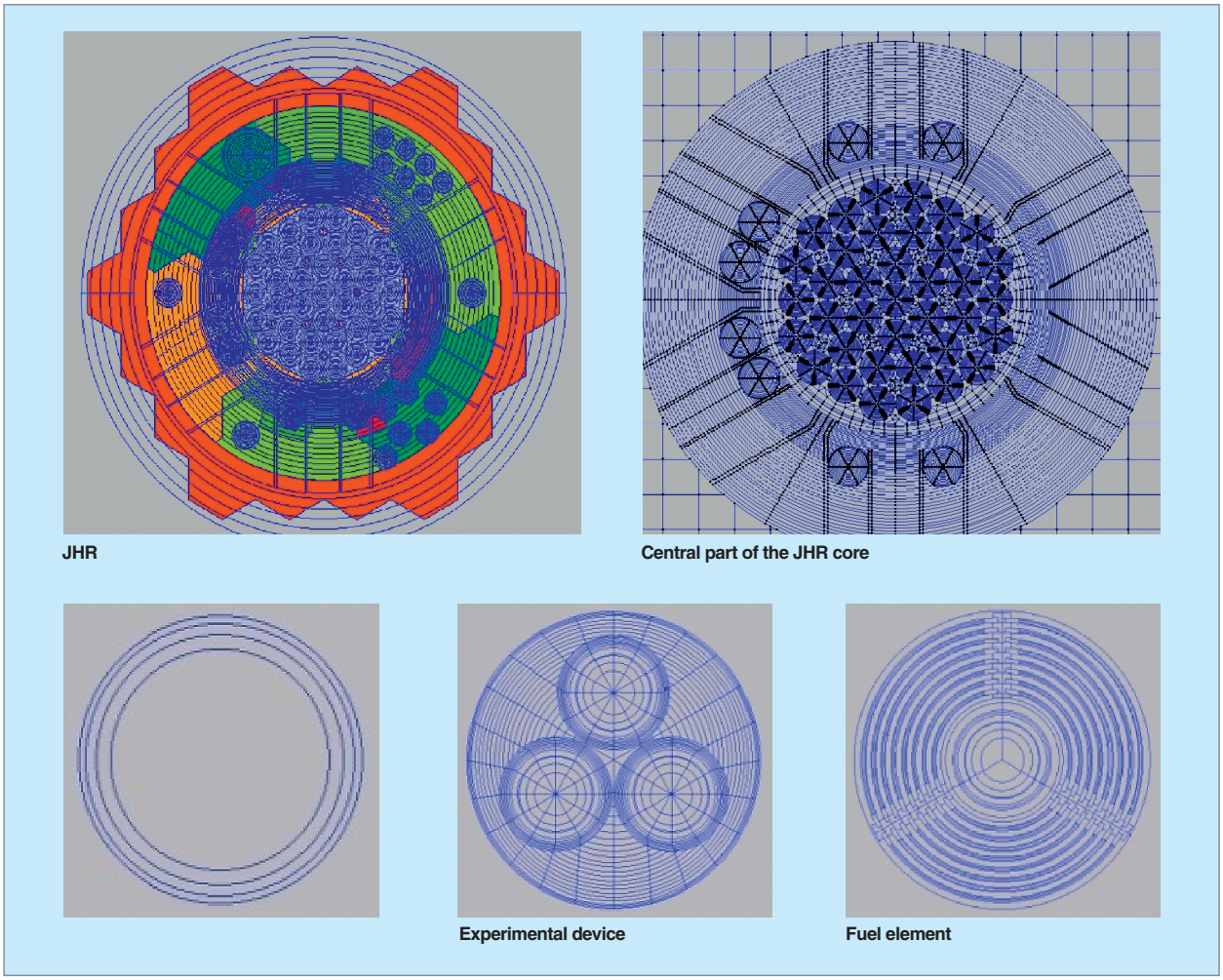

Fig. 56. APOLLO2: meshing for the Jules Horowitz Reactor (JHR).

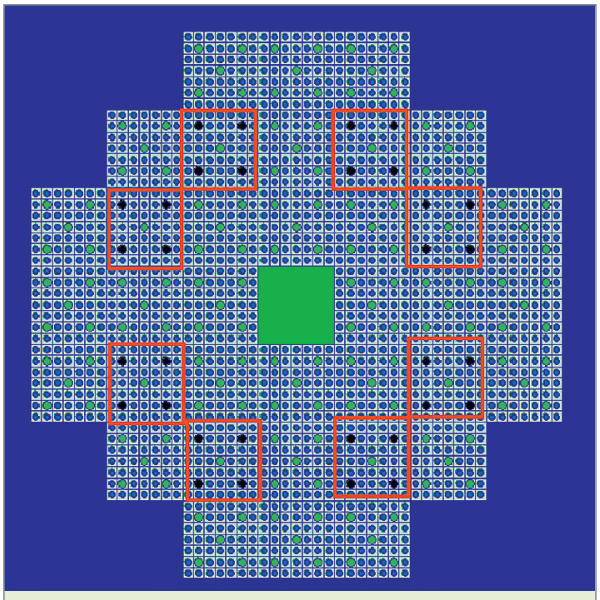

Core and reflector geometry

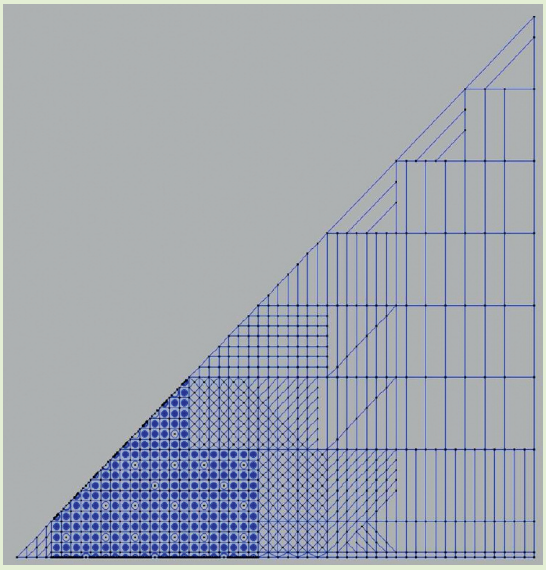

Core and reflector meshing

Fig. 57. APOLLO2: meshing for a design of a research reactor.

code package (see the next page). A high number of modules for edition, condensation, homogenization, as well as of functionalities for calculation branch and result archiving are available in APOLLO2.

The following illustrations (Fig. 55, 56 and 57) are drawn from APOLLO2 calculations performed within different research frameworks. Referring to the specific case of research reactors, they show the geometrical modeling abilities and the possible mesh refinements provided by the APOLLO2 code.

CRONOS2

The purpose of the CRONOS2 code [5] [6] is **3-D*** reactor core calculation, in order to determine reactivity, power distribution maps, absorber efficiencies, core behavior under time evolution, in normal or accidental conditions…

CRONOS2 is a multi-purpose code: the type of reactor to be calculated is not predetermined by any feature in its organization or structure. Consequently, computational models based on CRONOS2 have been made for a very high number of reactor cores: plate-fuel reactor cores, cores of High Temperature Reactors (HTRs), Pressurized Water Reactors (PWRs), Boiling Water Reactors (BWRs), of the Jules Horowitz experimental Reactor (JHR), as well as of various research reactors.

Fed with *neutron data* issued, for example, from the spectral code APOLLO2, it solves either the neutron transport equation, or a version of this equation referred to as the simplified transport equation (SPN), or the diffusion equation. These *neutron data* are space homogenized and energy condensed cross sections, according to meshes selected by the user. CRONOS2 is used to treat the depletion of fuel, and, if need be, of absorbers. The depletion chains described are of any kind, and only depend on the libraries, initially built in APOLLO2, which contain the cross sections of the nuclides to be treated explicitly under depletion (heavy nuclei, fission products, or absorbers…).

Methods for flux calculation available in CRONOS2 are nodal methods, Lagrangian **finite elements***, **mixed finite elements***, and **isoparametric finite elements***, and finite differences, described *supra*, pp. 61-66.

CRONOS2 is endowed with a simplified thermal-hydraulics model which can be used to calculate normal or incidental operating conditions.

The types of geometries that can be used in the CRONOS2 code are Cartesian and/or hexagonal geometries that correspond to nearly all existing reactors. The usual description of such homogeneous areas is not always sufficient for a reactor to be computed accurately. Recent developments enabling the code to treat isoparametric finite elements offer capabilities of meshing refinement for complex core modeling, as illustrated below for one sixth of **HTR*** core, and for the JHR core.

CRONOS2 is used to carry out a high number of studies (both for analysis and design) and expertise. In incident or accident situations, it can be coupled with thermal-hydraulics codes and system codes (see *infra*, pp. 215-226). Just like APOLLO2, it belongs to the class of computational code packages for

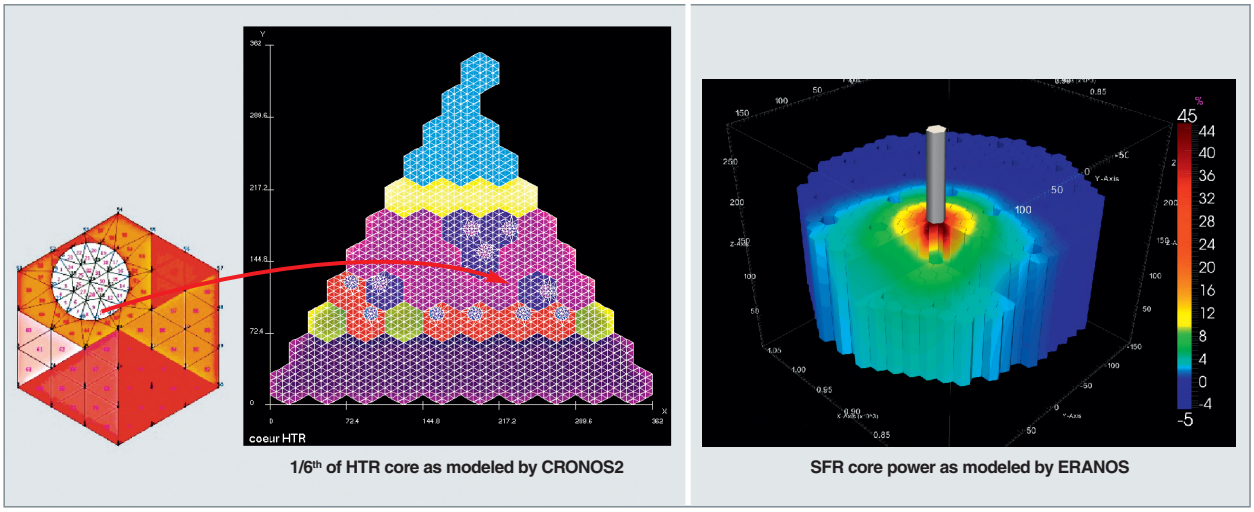

Fig. 58. Two types of reactor core modeling. Left: meshing of 1/6th of a HTR core. Right: withdrawal of an off-centered control rod from a low void effect core (CFV) inducing a local 45% power increase.

nuclear reactors, among which the following can be mentioned:

- NARVAL, for naval propulsion;
- HORUS3D, for the Jules Horowitz Reactor (JHR);
- ANUBIS, dedicated to calculations for OSIRIS reactor operation;
- NEPHTIS, for calculation of High Temperature Reactors (HTRs).

ERANOS

The scope of the ERANOS system [7] is that of fast spectrum reactors, ranging from "conventional" fast neutron reactors to innovating Generation IV reactors.

The nuclear data libraries of ERANOS are currently based on JEF-2.2 evaluated data, as well as on those drawn from JEFF-3.1.1. A fine energy meshing library (1,968 energy groups) contains the main nuclei; two other libraries include all of the nuclides available in coarser meshing. This whole depends on the application considered (calculation of the neutron spectrum's fast component, and of the thermal component, shielding calculations). To the JEF-2 library is also assigned an "adjusted" version, the so-called ERALIB1, which takes into account the experimental feedback through a statistical adjustment process. This experimental feedback is based on 400 measurements performed in critical mockups.

Cell or lattice calculations are achieved with the ECCO code [8], included in ERANOS, in which the neutron transport equation is solved with the collision probability method. Resonance self-shielding is based on the so-called "subgroup method", that enables neutron slowing-down to be treated with a fine energy mesh (1,968 groups), and so makes it possible to perform reference calculations.

The core is computed by solving the diffusion or transport equation with various methods (only S_N for transport), and with various geometrical descriptions: 2-D, 3-D, and RZ, rectangular or hexagonal geometries.

ERANOS also achieves depletion calculations.

Calculation of sensitivities, uncertainties, and kinetic parameters is made easier by many functionalities based on the perturbation theory. There also exist computational models dedicated to describing reactor operation (loading, unloading, management…), as well as a number of capabilities for editing the quantities handled in the code.

DARWIN

DARWIN* [9] [10] is the computational code package dedicated to studies focused on fuel cycle as a whole, either in core or out of core (fabrication, in-core stay, storage in pool, transport, recycling, storage, geological disposal…), as well as to safety studies, whatever the reactor type. It provides a solution to the main problems raised by fuel cycle, as, *e.g.* monitoring of radioactive materials amounts, residual power removal, radiation protection, determining of the contamination level, etc., by calculating a set of physical quantities related to radioactivity phenomena.

The basic quantity is the concentration of each nuclide obtained by solving the generalized Bateman differential equations. The latter govern the evolution over time of the isotopic population generated/depleted by two types of essential physical phenomena, that is nuclear reactions (fission, radiative capture…) and radioactive disintegrations.

The other physical quantities are masses, activities, residual power (α, β, γ, neutrons), spectra of emitted radiations, neutron sources, radiotoxicities; they are deduced from computed concentrations.

DARWIN identifies and quantifies all types of pathways for a given nuclide.

The nuclear daughter chains treated mainly correspond to the broad nuclide families of interest for nuclear reactor physics, that is fission products, heavy nuclei, activation products, and, secondarily, spallation products. They can be full or simplified, depending on applications.

Neutronic input data are drawn from transport calculations carried out as an initial step, especially with APOLLO2, ERANOS, or TRIPOLI-4®, according to the studies performed.

The new platform: APOLLO3® and MENDEL

The lifetime cycle of computational codes for nuclear reactors is of about fourty years, including a full use period of twenty years or so: APOLLO2 and CRONOS2 have been developed since 1985, starting from the previous generation (APOLLO1 and CRONOS1). Now, if new and innovating developments have been continuously integrated in these tools, one can but recognize that their inner organization (the so-called "software architecture") has become insufficiently robust along time to enable them to experience new advances in a simple and efficient way. Moreover, computer architecture and processor power are significantly progressing, hence allowing performing calculations which could be deemed a mere utopia at the time when these codes were initiated.

Other reasons also induce teams in charge of developing codes to initiate a new generation: challenges related with the modeling of new nuclear reactor types, displaying very heterogeneous cores, innovating fuels, and a wide variety of geometries. Thus, the requirements formulated by the 4th Generation reactor designers are highly stimulating and structuring, as they assign new objectives to R&D. Of course, nuclear reactor designers and physicists are not the only to prove creative: computer scientists and physicists generate innovating models and algorithms. Some of the latter have been implemented in the current generation of computational codes: for example, the numerous methods to accelerate flux calculations, or the self-shielding model for the rigorous treatment of mixed resonant nuclei. Others, like the spectrum codes transition to 3-D, or the simple, natural exchange with Monte-Carlo codes, need a new definition of code architecture to be easily achieved. Tools dedicated to activities for evaluation and treatment of

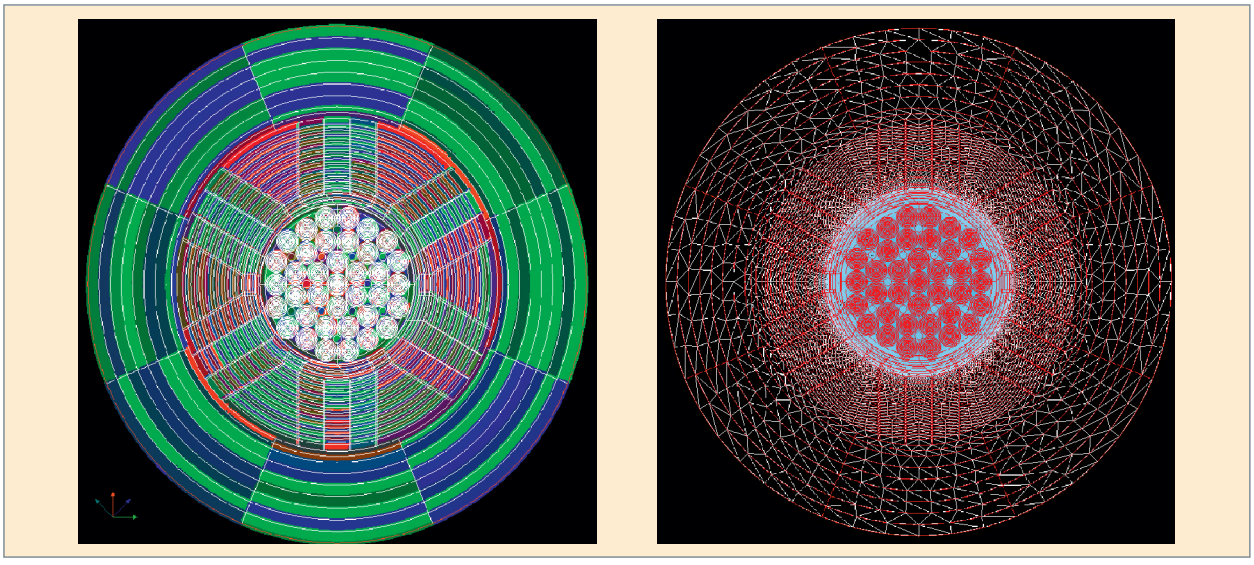

Fig. 59. APOLLO3®. Jules Horowitz Reactor: calculations with the MINOS solver (Cartesian-mesh SP_N solver, left figure) and the MINARET solver ("unstructured"- mesh scattering solver, right figure) [11]

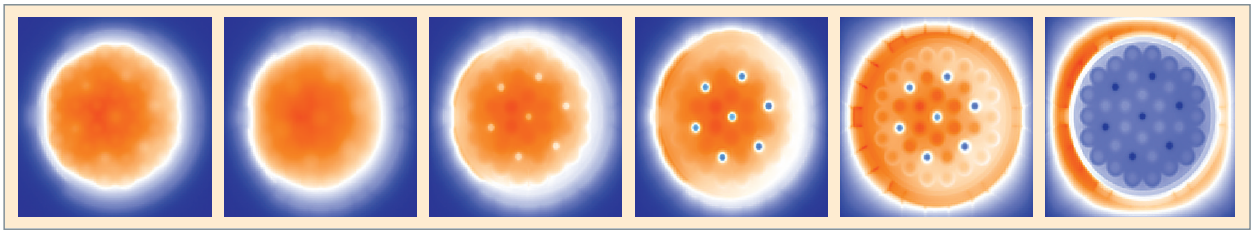

Fig. 60. APOLLO3®, flux distribution as a function of neutron energy in the Jules Horowitz Reactor (JHR) (by decreasing order of neutron energy) [11].

nuclear data that are the key input data of neutronics codes, are also subjected to similar upgrading and innovation requirements.

As part of a rationalization approach, the will to unify tools dedicated to calculating the different reactor types also provides a guideline for making new neutronics codes. Thus, APOLLO3® is the new multi-purpose code under development, which displays a unique organization for the parts "core" and "spectral code". It includes new functions, such as unstructured spatial mesh computing. A first version of APOLLO3® was delivered to users in December 2012.

Another challenge to be faced by APOLLO3® is how to perform 3-D generalized calculations with an accurate geometry description. That implies an optimum operation of new computer architectures (parallel computers, multi-core processors…) likely to significantly reduce computational times and use the required memory sizes. Hence the achievement of calculations in a single step, which is one of the "key" goals of neutronics code development.

The APOLLO3® code was used on the CEA's **TERA100** computer in parallel mode, on 33,000 computational cores, in order to perform calculations of a sodium-cooled reactor core. It was thus demonstrated that studies requiring several months on conventional architectures could be carried out within a few hours.

Whatever the target considered - core calculations or other purposes such as residual power and activation calculations -, fuel depletion is treated by the **MENDEL*** code. The latter may be used independently, or be shared by APOLLO3® and TRIPOLI-4®. In contrast with its predecessor, DARWIN, MENDEL has been restructured, especially as regards input (nuclear data) organization. Another of MENDEL's advances lies in its ability to determine uncertainties, possibly in relation to statistical analysis models, in particular through the URANIE platform [13].

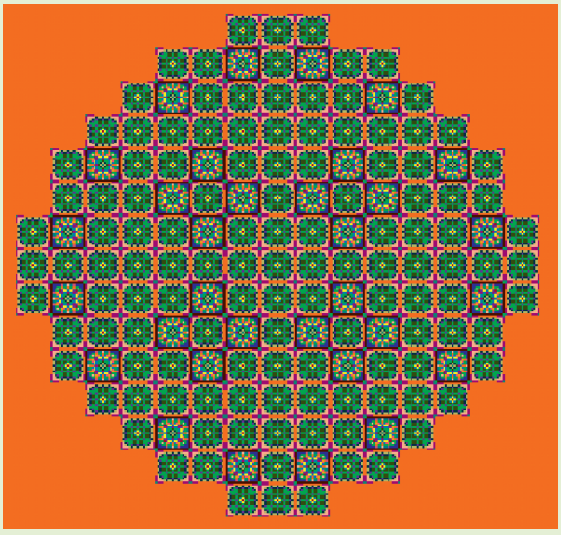

Core geometry

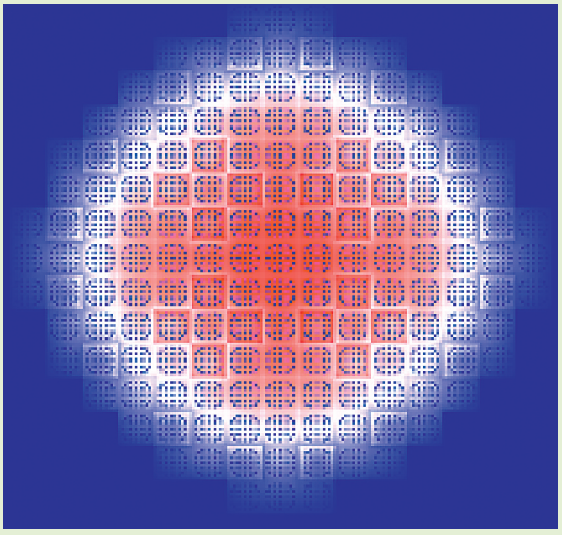

Integrated power map

Fig. 61. APOLLO3®, pressurized water reactor (PWR): heterogeneous 3-D SPN-transport calculation. Left: core geometry. Right: integrated power map [12].

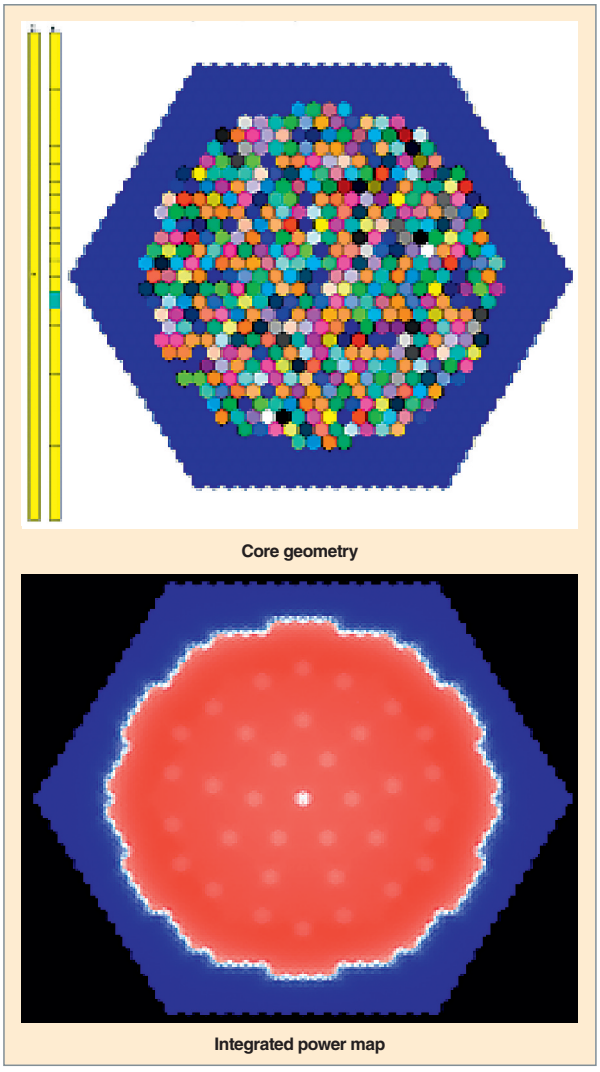

Fig. 62. APOLLO3®, sodium-cooled fast reactor (SFR): 3-D heterogeneous computing in S_N transport. Left: core geometry. Right: integrated power map.

The TRIPOLI-4® Monte-Carlo code

The TRIPOLI *(TRIdimensionnel POLYcinétique)* code family has been developed by the CEA since the sixties. TRIPOLI-4® represents the fourth generation, whose innovating development in the C++ language, initiated by J.P. Both, goes back to the early nineties [14] [15].

TRIPOLI-4® solves the neutron and photon transport equation by the Monte-Carlo method (see *infra*, pp. 89-106) in 3-D geometries, with the pointwise (or "continuous") energy representation of nuclear reaction cross sections, hence the name "continous-energy code". Its privileged scopes are **core physics*** (critical problem resolution, determination of power distribution), **criticality*** (resolution of the source critical, subcritical problem), **radiation protection*** (resolution of a fixed source problem). TRIPOLI-4® treats the coupled transport of neutrons and *gammas*, which result from neutron-induced nuclear reactions.

Specific functionalities, such as the treatment of the electromagnetic cascade (coupled electron-positron-photon transport), have been implemented in order to extend its scope to nuclear instrumentation and medical applications,

It covers all of the functionalities that a state-of-the-art general-purpose use code is liable to offer to its users [16]. Since 2004 it has been available at the **OECD/NEA*** data bank [17], and is used by many nuclear companies.

The types of particles usually simulated are photons and neutrons displaying energy lower than 20 MeV. The cross sections used are drawn from international evaluations at ENDF/B format: JEF-2.2, JEFF-3, ENDF/B-VI, and B-VII, JENDL-3.3, etc. Pointwise energy cross sections are used at the "PENDF" format directly drawn from the treatment of the evaluation considered (see *supra*, pp. 31-37).

In the code, geometrical descriptions are performed through both surface definition and volume combinatorial mode. Other modes of description exist, especially through the ROOT "library" [18]. For the ROOT tool developed and used to analyze CERN experiments can be coupled with TRIPOLI-4®, thereby providing the user with new geometrical shapes and powerful pre- and post-processing functionalities.

Neutron and photon sources can be described in any way, *i.e.* in space, energy, angle, or even in time. Possible scores are particle fluxes, and reaction rates derived from them, currents, energy deposits, **DPA***, **pka***, generated gases, dose equivalent rates, as well as the neutron multiplication factor in a critical calculation. Statistical tests are performed in order to ensure a suitable convergence for the user.

Several variance reduction methods are available to optimize Monte-Carlo codes. As revealed by their name, for an identical fixed computational time and an identical final result (average **score***), they allow lower score variances to be reached, which ensures better accuracy. In radiation protection simulations, these methods are often indispensable to drive particles to the areas of interest.

In order to solve these radiation protection problems, TRIPOLI-4® uses performing and automatic techniques to reduce variance (*e.g.* particle attractors to the areas of interests in the phase space). It is also endowed with a perturbation calculation functionality that implements the correlated sampling method, as well as the method based on a Taylor expansion of the physical quantity of interest.

TRIPOLI-4® operates in both a monoprocessor and a parallel mode within a multiprocessor architecture. TRIPOLI-4® calculations in a parallel mode have enabled simulations of over 150 billion neutrons to be performed [20].

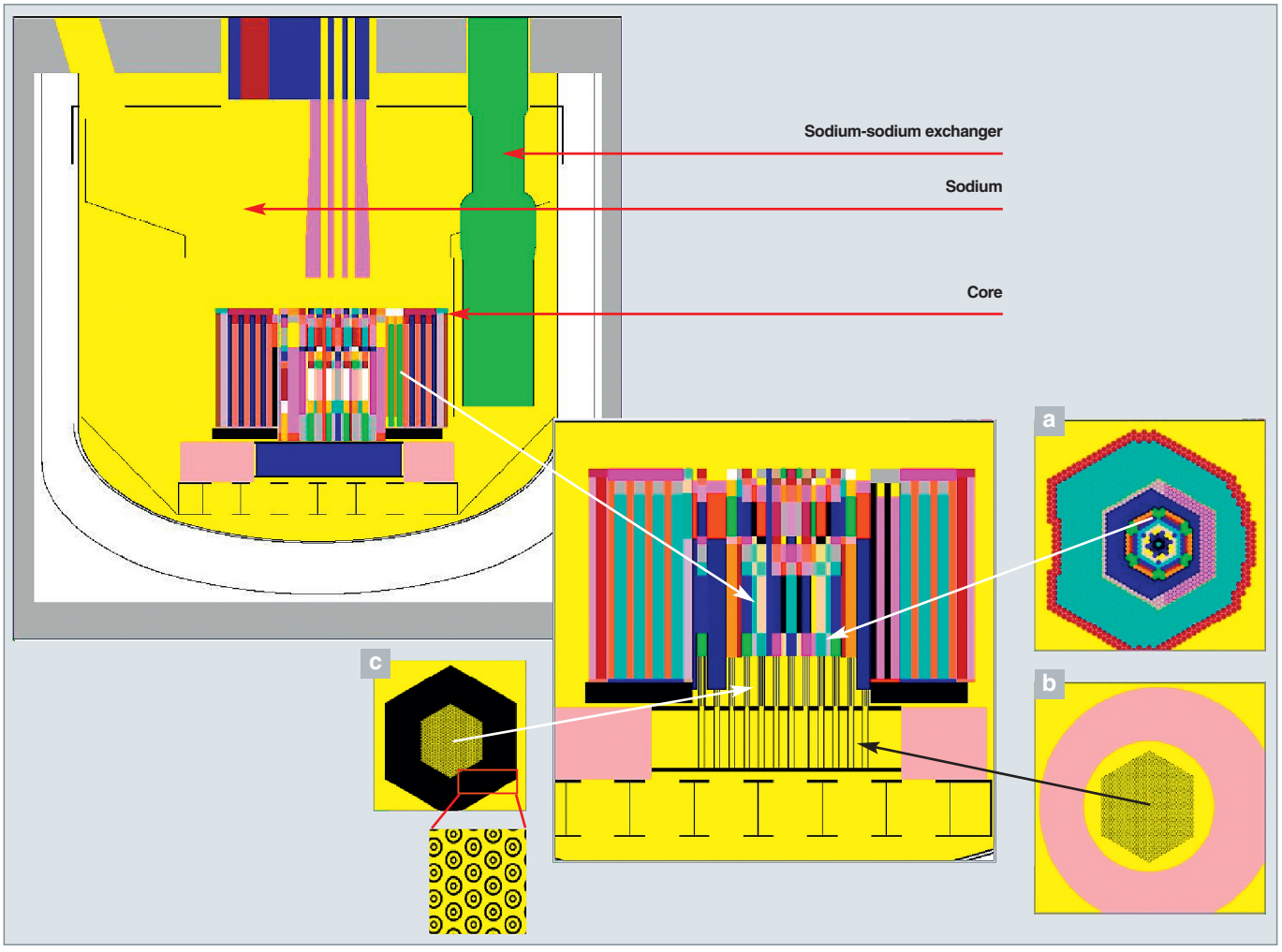

Fig. 63. TRIPOLI-4®: detailed modeling of the PHÉNIX reactor for dismantling calculations. (a), (b) and (c): horizontal sections of the core at different heights.

Coupling of Monte-Carlo neutron transport with other physical phenomena, such as radionuclide depletion in a reactor core or thermal-hydraulics phenomena stands as a prime stake, and raises problems relating to the stochastic feature of this coupling. These problems induce a R&D which aims at successfully achieving this type of coupling in accident situations in a more or less long term. The inset below briefly describes the operational coupling achieved between TRIPOLI-4® and MENDEL.

Coupling of Monte-Carlo neutron transport with calculation of isotopic fuel depletion opens promising routes to reactor physics and fuel cycle. Thus, TRIPOLI-4® has already been used in parallel with APOLLO2 to examine the impact of an UMo fuel on the cycle duration and performance of the ILL (Institut Laue Langevin) high flux experimental reactor.

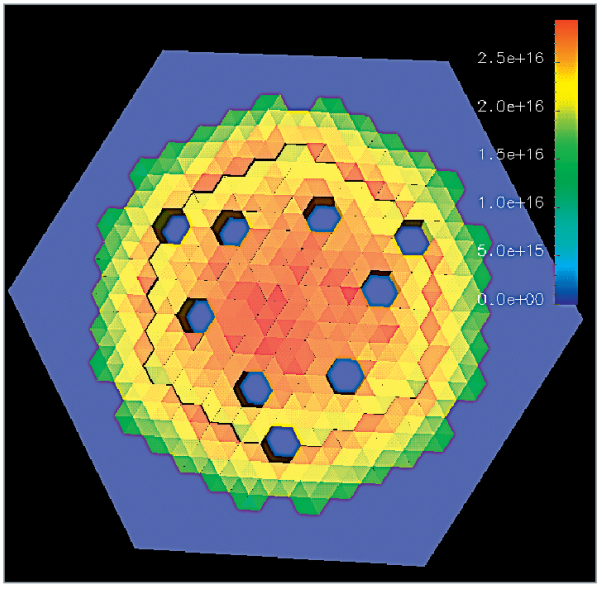

Fig. 64. TRIPOLI-4®, calculation of the PHÉNIX reactor: power distribution per assembly [19].

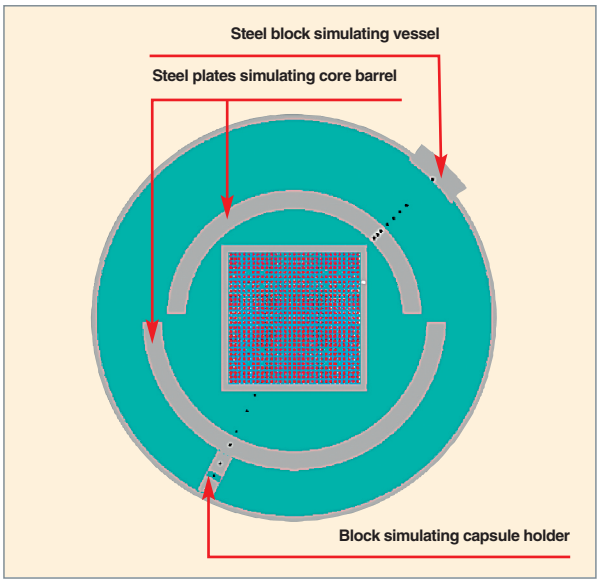

Fig. 65. TRIPOLI-4®, modeling of the FLUOLE experiment in the research nuclear reactor ÉOLE (an experiment that aims at validating the determination of the neutron fluence received by a PWR vessel).

The agreement between the results of probabilistic (TRIPOLI-4® and MENDEL) and deterministic (APOLLO2) calculations has corroborated the CEA's answers to the operator (see Fig. 67 and 68).

Besides, Monte-Carlo transport-thermal-hydraulics couplings are also achieved as shown by various thesis works [22], [23], and by developments within the framework of, *e.g.* the European project NURISP [24], [25]. This paves the way to being able to perform not only 3-D core calculations, especially for PWRs exhibiting significant tridimensional effects, but also transient calculations in accident situations.

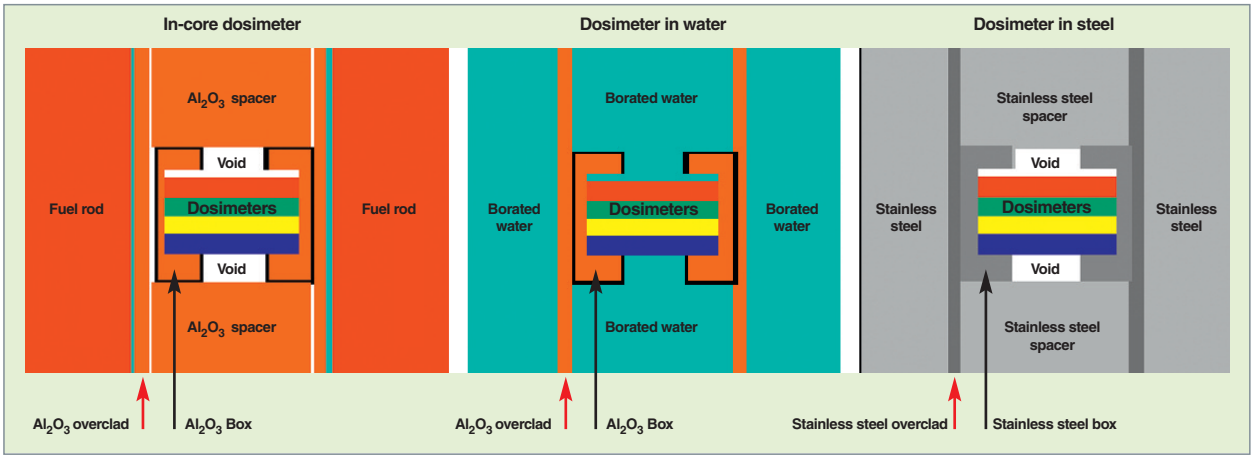

Fig. 66. Description of the dosimeters selected [20].

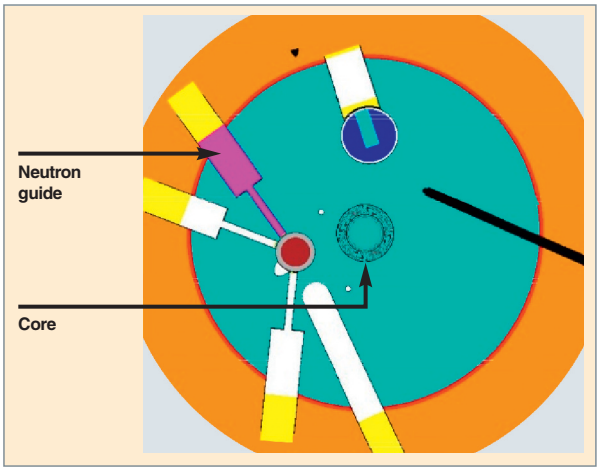

Fig. 67. Horizontal section of the High Flux Reactor (HFR) at the Laüe Langevin Institute [21].

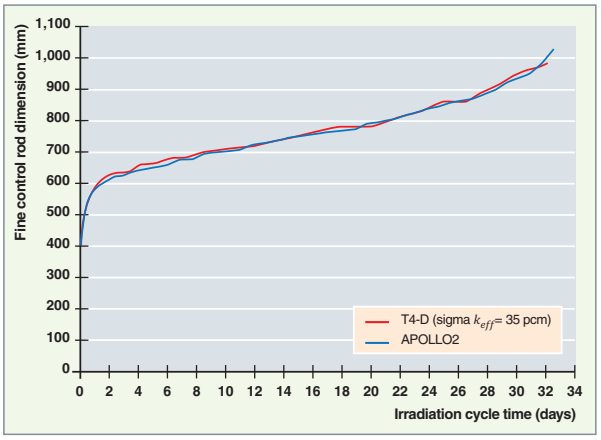

Fig. 68. Comparison between TRIPOLI-4® / MENDEL calculation and the APOLLO2 deterministic code calculation to determine the fine control rod dimension of the High Flux Reactor (HFR) during an irradiation cycle [21].

TRIPOLI-4®: the Monte-Carlo burnup code

Up to the years 2000, core calculations with the help of Monte-Carlo transport codes were performed for a limited number of steady state configurations, for the purpose of validating deterministic calculations. Increased power of computers now makes it possible to contemplate such "time evolution" (or generation/depletion or burnup) calculations – as is done in a deterministic core calculation – by coupling the neutron transport solver with the solver of time evolution equations (Bateman equations) for nuclide concentrations in nuclear fuel. Computer codes performing this type of coupling are called "**Monte-Carlo burnup codes**" (or "Monte-Carlo evolution or depletion codes"), an English phrase often used in French, too, with the French corresponding term "***Monte-Carlo évoluant***". The name assigned to some of these codes used is given at the end ot fhis inset. Coupling between the Monte-Carlo code **TRIPOLI-4®** and the **MENDEL** generation/depletion solver is briefly described hereafter.

These two softwares are coupled through computer interfaces so as to build schemes of coupling between transport calculation and generation/depletion calculation. Coupling consists, first, in computing fluxes and reaction rates with the Monte-Carlo transport code (assuming the concentrations of media as fixed), and then in using these results to evaluate the concentrations after irradiation during a given time, with the help of the generation/depletion code (this time, assuming the fluxes as fixed). With an iteration on this computation sequence, it is then possible to build first or second-order time evolution schemes, *e.g.* of the "predictor-corrector" type. With **TRIPOLI-4®**, it is also possible to change the geometry or composition of the objects being calculated, and to define irradiation conditions according to various possible modes (through the flux or reaction rate data, or even by mixing the two approaches). The execution can be controlled interactively or not, according to the user's choice. The latter can also select a keyword control mode, or can directly program its computing sequences in the data set.

A strong R&D activity is focused on developing Monte-Carlo burnup code type calculation schemes due to specific issues raised by the probabilistic approach, as, *e.g.* statistical convergence, and uncertainty propagation. With this respect, special attention has to be given to studying the accurateness of the result obtained, for the latter may be flawed by various systematic errors (the so-called "biases"), which are to be quantified. These errors can be related with:

- spatial discretization (an assumption of uniformity of concentrations in unit volumes) and time discretization (an assumption of stationary flux in each of the time intervals of the time (or fluence or burnup) discretization, as for deterministic calculations);
- the random feature of the evaluated reaction rates, inherent to the Monte-Carlo transport, which induces a bias on the concentrations calculated with deterministic generation/depletion equations [1]. This bias is due to the nonlinear feature of the generation/depletion equations with respect to reaction rates (or the neutron flux), and propagates along the various steps of the iterative procedure. Figure 70, drawn from [3], highlights the occurrence of such a bias on the calculation of a fuel rod. The behavior of this bias was investigated with the TRIPOLI-4® code, performing several types of simulations: 1x1, 5x5, 10x10, 20x20, 100x100, and 1,000x1,000, in which the first number stands for the number of batches, and the second, for the number of neutrons per batch. This study points out the importance of the number of sampled neutrons, which allows this source of error to be reduced arbitrarily.

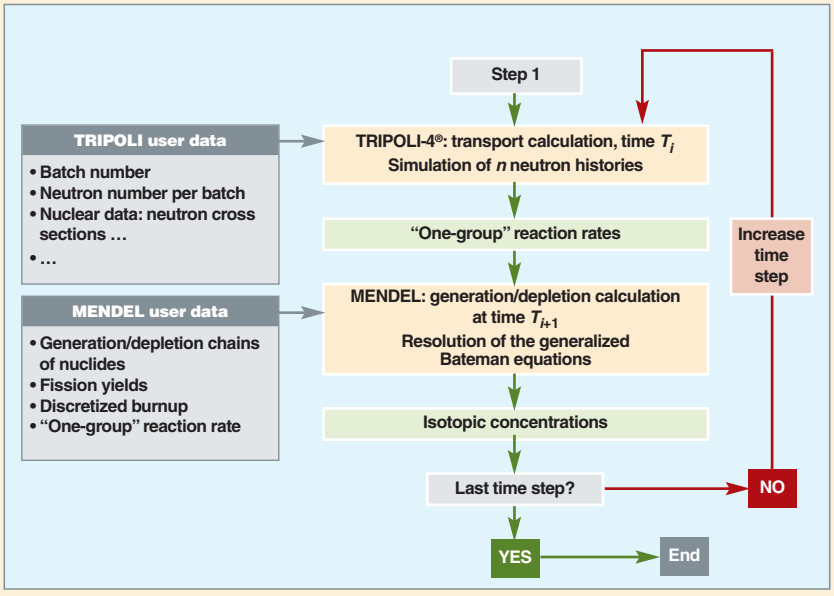

Fig. 69. Principle of the Boltzmann / Bateman coupling with the TRIPOLI-4® Monte-Carlo code and the MENDEL generation/depletion solver.

References

[1] http://root.cern.ch/drupal/

[2] E. Dumonteil, C.M. Diop, « Biases and statistical error bars in Monte-Carlo burnup calculations : an unbiased stochastic scheme to solve Boltzmann/Bateman coupled equations », *Nuclear Science and Engineering*, vol. 167, N2, pp. 165-170, 2011.

[3] E. Brun, E. Dumonteil and F. Malvagi, « Systematic Uncertainty Due to Statistics in Monte-Carlo Burnup Codes: Application to a Simple Benchmark with TRIPOLI-4-D », *Progress in Nuclear Science and Technology*, vol. 2, pp. 879-885, 2011.

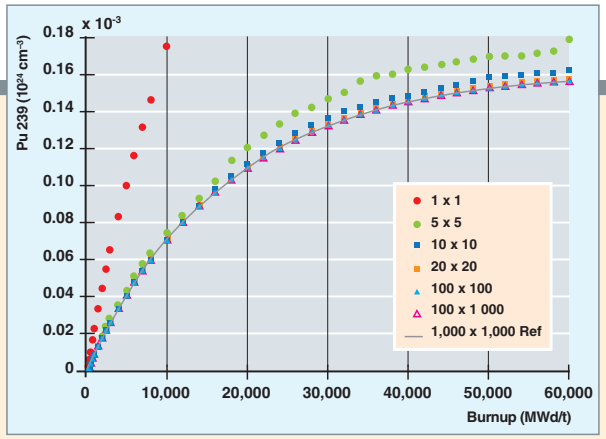

Fig. 70. Computational bias evidenced on Pu-239 concentration in a burnup Monte-Carlo code.

The following table gives other examples of software systems which couple a Monte-Carlo transport code and a burnup (evolution) code.

Examples of software systems coupling a Monte-Carlo transport code and a burnup (generation/depletion) code

Name of the coupled software system	Coupled codes	
	Monte-Carlo transport code	Burnup code
MOCUP *(Idaho National Engineering Laboratory, USA)*, 1995.	MCNP	ORIGEN2
MCB (*Royal Institute of Technology, Sweden*), 1999.	MCNP	CINDER
MCWO, *(Idaho National Engineering & Environmental Laboratory, USA)*, 1999.	MCNP	ORIGEN2
MONTEBURNS *(Los Alamos National Laboratory, USA)*, 1999.	MCNP	ORIGEN2
MURE *(Laboratoire de Physique Subatomique et de Cosmologie de Grenoble, Institut de Physique Nucléaire d'Orsay, France)*, 2000.	MCNP(X)	Specific generation/ depletion module
MCODE *(MIT, USA)*, 2002.	MCNP	ORIGEN2
ALEPH *(SCK -CEN, Belgium)*, 2005.	MCNP(X)	ORIGEN2
MCNP-ACAB *(Universidad Politecnica de Madrid, UPM, Spain)*, 2005.	MCNP	ACAB
MCNPX *(Los Alamos National Laboratory, USA)*, 2006.	MCNPX	CINDER90
MCOR *(Pennsylvania State University, USA, AREVA, Erlangen, Germany)*, 2006.	MCNP	ORIGEN-S, and then KORIGEN
VESTA *(IRSN, France)* generical interface, 2008.	MCNP, MORET…	ORIGEN2, PHOENIX…

"Simplified" codes

In some cases, simple and fast calculation requirements, the accurate knowledge of the situations to be modeled, and their systematics have entailed the development of the so-called "simplified" computational codes.

Let us mention a few of them:

- The **NARMER*** code (succeeding the MERCURE and NARCISSE codes), dedicated to *gamma* radiation protection, which enables dose rate and heating calculations to be performed by the so-called "straight-line approximation". To use it properly, it is indispensable to get specific input libraries (cross sections, buildup factors). It is mainly validated through comparisons with reference calculations performed with the TRIPOLI-4® code;

- The **CÉSAR*** code [26], which allows fast calculations for material balances. It uses libraries gathering input chiefly drawn from APOLLO2, and is validated by comparison with DARWIN;

- The **FAKIR** code, which determines the residual power of irradiated fuels [27], [28];

- The **STRAPONTIN** code developed by EDF and dedicated to fast isotopic and mass balance calculations particularly used for strategic planning of the nuclear fuel cycle [29].

Main reactor physics codes

The neutronics codes developed and used in the world's nuclear reactor physics community are presented below in Tables 19 and 20, successively relating to deterministic transport and probabilistic transport through the Monte-Carlo method, and isotope time evolution. Yet this record is not exhaustive. A few of the main features of these codes are reported in it. It can be seen that generally industries have developed their specific core code.

Deterministic transport codes

Table 18.

Deterministic neutronics codes

Those highlighted with a star (*) include an isotopic depletion solver.

Name	Organization	Applications Equation	Cross section library	Geometry	Self-shielding	Flux solver
AEGIS*	Nuclear Engineering, Limited - Nuclear Fuel Industries - Nagoya University (Japan)	Lattice/core Transport	172 groups	Any 3-D	Equivalence (URR) and ultrafine mesh (RRR)	2-D: MOC
AGENT	Purdue University (USA)	Core Transport	Self-shielding macroscopic cross sections	Any 3-D (by R-functions)	–	3-D: 2D coupling (MOC)/1-D(FDM)
ANC	Westinghouse (USA)	Core Diffusion	PARAGON (2 groups)	3-D XYZ	–	3-D: Nodal diffusion
APOLLO2*	CEA (France)	Lattice/core Transport	172/281 groups and over	Any 2-D (MOC), cell lattices (Pij and SN)	Equivalence (RRR) subgroups (URR)	2-D: Pij, MOC, S_N
APOLLO3®* (TH)	CEA (France)	Lattice/core Transport	172/281 groups and over / Self-shielding microscopic cross sections (APOLLO2, ECCO, APOLLO3®)	Any 2-D (MOC), any 3-D cell lattice (Pij and S_N)	Equivalence, (RRR) subgroups (URR)	2-D: Pij, MOC, S_N 3-D: diffusion, SP_N transport , S_N transport , MOC
ATTILA*	LANL, and then Transpire Inc. (USA)	Core Transport	Self-shielding macroscopic cross sections	Any 3-D (tetraedric mesh)	–	3-D: S_N
CASMO*	Studsvik Scandpower (USA)	Lattice/core Transport	586 groups	2-D LWR lattice	Equivalence	2-D: MOC
CHAPLET 3D	TEPCO - Osaka University (Japan)	Core Transport	Self-shielding macroscopic cross sections	Any 3-D	–	3-D: 2-D (MOC)/1-D (FDM or MOC or NEM coupling)
COCCINELLE	EDF (France)	Diffusion Simplified transport	APOLLO2 (2 groups)	3-D XYZ	–	3-D: Diffusion
CRONOS2* (TH)	CEA (France)	Core, Diffusion Transport, Simplified transport	APOLLO2, ECCO (multigroup)	3D XYZ, and HEX-Z	–	3-D: Diffusion, SP_N transport , S_N transport
DeCART (TH)	KAERI (Corea) - ANL (USA)	Core Transport	Microscopic cross sections	3D XYZ	Subgroups	3-D: CMFD, 2-D homogenization *via* MOC; 1-D axial solution *via* NEM
SCALE DENOVO	ORNL (USA)	Core Transport	Self-shielding macroscopic cross sections	3-D XYZ structured	–	3-D: S_N
TRIVAC	École Polytechnique Montréal (Canada)	Core Diffusion, Simplified transport	DRAGON	3D XYZ and HEX-Z	–	3-D: diffusion, SP_N transport

CMFD: Coarse Mesh Finite Difference
FDM: Finite Difference Method
NEM: Nodal Expansion Method
(TH): taking thermal-hydraulics feedback into account
XYZ: 3-D Cartesian geometry
HEX-Z: 3-D hexagonal Z-axis geometry
RZ: 2-D cylindrical geometry
RO: 2-D cylindrical geometry
ROZ: 3-D cylindrical geometry

Name	Organization	Applications Equation	Cross section library	Geometry	Self-shielding	Flux solver
DRAGON*	École Polytechnique Montréal (Canada)	Lattice Transport	172 groups	Cartesian or hexagonal lattice	Equivalence (Stammler), subgroups	2-D and 3-D: Pij, MOC
ERANOS*	CEA (France)	Core Diffusion, Transport	ECCO	RZ, XYZ, HEX-Z	–	2-D: S_N(R-Z), 3-D: P_N (XYZ or HEX-Z)
ERANOS/ ECCO	CEA (France)	Lattice Transport	1968, 172, 33 groups	Cartesian or hexagonal lattice	Subgroups	2-D: Pij
HELIOS2*	Studsvik Scandpower (USA)	Lattice Transport	177 (n)/48 (γ) or 49 (n)/18 (γ) groups	Any 2-D lattice	Subgroups (Dancoff factor, MOC calculation)	2-D: Pij, MOC ("long" and "short")
Lancer 02*	Global Nuclear Fuel - GE Energy, Nuclear (USA)	Lattice Transport	118/190 groups	BWR lattice	Approximated models (Wigner, Bell, Dancoff, Williams)	2-D: MOC (after condensation of 19-group sections)
PARAGON*	Westinghouse (USA)	Lattice Transport	70 (n)/48 (γ0) (n)/48 groups	Cartesian cell lattice	Equivalence (Stammler)	2-D: Pij (cells coupled by interface currents)
PARCS	Purdue University (USA)	Core Diffusion	TRITON (multigroup)	3-D XYZ, HEX-Z, ROZ	–	3-D: Nodal diffusion
SCALE/ TRITON*	ORNL (USA)	Lattice Transport	238/44 groups et 27 (n)/18 (γ) groups	Any 2-D	Pointwise (50,000 to 70,000 points) S_N ou P_{ij} transport)	2-D: MOC ("short" characteristics)
SCOPE2*	Nuclear Engineering, Limited - Nuclear Fuel Industries - Nagoya University (Japan)	Core Transport	AEGIS (9 groups)	3-D XYZ rod by rod	–	SP_3 transport
SHARP/UNIC	ANL (USA)	Lattice/core Transport	>10,000 groups	Any 3-D	Not required	3-D: P_N + finite elements, MOC
SIMULATE*	Studsvik Scandpower (USA)	Core Diffusion	CASMO	3-D LWR	–	3-D: nodal scattering by 2-D/10 synthesis
SMART	AREVA (France)	Core Diffusion	APOLLO2 (2 groups)	3-D XYZ	–	3-D: Nodal diffusion
PARTISN	LANL (USA)	Core Transport	Self-shielded macroscopic cross sections	1-D, 2-D (XY, RZ, or RT), 3-D (XYZ or RTZ)	–	3-D: S_N
WIMS*	Serco (UK)	Lattice Transport	172 groups	LWR, HWR, GFR Lattices	Equivalence (RRR), Subgroups (URR)	2-D: P_{ij}, S_N, MOC 3-D: MOC, Diffusion, Hybrid Monte-Carlo

Monte-Carlo transport codes

Other Monte-Carlo transport codes exist, used in the medical, particle physics and, sometimes, nuclear reactor physics areas: EGS4 (USA), FLUKA (Italy, CERN), GEANT4 (CERN), MCNPX (USA), PENELOPE (Spain)… They concern energy ranges much broader than those covered by Table 19, up to several GeV and beyond, as well as many types of particles other than neutrons and *gammas*, especially charged particles (protons, deuterons, α, ions). They are able to treat spallation reactions (see *supra*, p. 39 and Ref. [30]), of high interest in relation to the issue of nuclear waste transmutation.

Table 19.

Main particle transport codes using the Monte-Carlo method: 0-20 MeV energy range

A few of their specificities are mentioned. Those highlighted with a star (*) include, or can use, an isotopic depletion solver.

Name	Organization	Particles	Types of problems	Cross section representation	3-D geometry	Variance reduction techniques	Parallelization
KENO-6#	Oak Ridge National Laboratory (USA)	Neutrons	Eigenvalue (k_{eff})	Pointwise, Multigroup	Surface	–	Yes
MCBEND	AMEC, ANSWERS Software Service (UK)	Coupled neutrons and photons (n,γ)	Fixed source	Pointwise	Combinatorial, Holes	Splitting/Russian *roulette* "Woodcock tracking"	–
MAVRIC	Oak Ridge National Laboratory (USA)	Coupled Neutrons and photons (n,γ)	Fixed source	Multigroup	Surface	Importance (adjoint calculation with S_N code)	Yes
MCNP-5#	Los Alamos National Laboratory (USA)	Coupled neutrons and photons (n,γ) Electrons positrons	Eigenvalue (k_{eff}) Fixed source; time-dependent	Pointwise, probability Tables	Surface, Hierarchical	Splitting/Russian *roulette* (weight window)	Yes
MCU#	Kurchatov Institute (Russia)	Neutrons photons Electrons positrons	Eigenvalue (k_{eff}) ; Fixed source; time dependent	Pointwise	Combinatorial, Hierarchical	"Woodcock tracking"	Yes
MC21#	Knolls Atomic Power Laboratory and the Bettis Atomic Power Laboratory (USA)	Neutrons Photons	Eigenvalue (k_{eff}) ; Fixed source	Pointwise, probability Tables	Combinatorial, Hierarchical	–	Yes
MONK#	AMEC, ANSWERS Software Service (UK)	Neutrons	Eigenvalue (k_{eff})	Pointwise, multigroup	Combinatorial, holes, CAD import	"Woodcock tracking"	Yes
MORET-4, 5	IRSN (France)	Neutrons	Eigenvalue (k_{eff})	Multigroup self-shielded (APOLLO2, DRAGON), Pointwise and probability tables (URR)	Combinatorial	"Woodcock tracking"	–
MVP#	JAEA (Japan)	Coupled neutrons and photons (n,γ)	Eigenvalue (k_{eff}) ; Fixed source time-dependent	Pointwise, probability tables (URR)	Combinatorial	Splitting/Russian *roulette*	Yes
PRIZMA#	RFNC – Zababakhin Institute of Technical Physics (Russia)	Neutrons photons charged particles	Eigenvalue (k_{eff}) ; Fixed source time-dependent	Pointwise, probability tables	–	Importance	
SERPENT#	VTT Technical Research Centre of Finland	Neutrons	Eigenvalue (k_{eff}) ; Fixed source	Pointwise	Surface	"Woodcock tracking"	Yes
TRIPOLI-4®#	CEA (France)	Coupled neutrons, photons (n,γ) electrons positrons	Eigenvalue (k_{eff}) ; Fixed source time-dependent	Pointwise, probability tables (URR, possible RR), multigroup self-shielded cross section (APOLLO2)	Combinatorial and surface (possible mixture)	Exponential transformation Splitting/Russian *roulette*	Yes

Generation/depletion (burnup) codes

Table 20.

Codes for time evolution of radionuclide concentrations			
Name	**Organization**	**Resolution method**	**Nuclides**
CINDER	Bettis Atomic Power Laboratory, Los Alamos National Laboratory (USA)	Analytical (linear generation/depletion chains)	Heavy nuclei, fission products, activation products, spallation products
DARWIN	CEA (France)	Analytical Runge-Kutta numerical method (belongs to the family of "time step methods")	Heavy nuclei, fission products, activation products, spallation products
FISPACT	UKAEA, Culham Science Centre (UK)	Matrix formulation, numerical resolution	Activation products (oriented to radiation protection, such as those relating to neutron activation of structures in a fusion device). Complementary of the FISPIN code.
FISPIN	AMEC, ANSWERS Software Service (UK)	Numerical, approximation of the term derivate (belongs to the family of "time step methods")	Heavy nuclei, fission products, a few activation products (structural materials)
ORIGEN	Oak Ridge National Laboratory (USA)	Matrix exponential	Heavy nuclei, fission products, activation products, spallation products

References

[1] R. Sanchez, J. Mondot, Z. Stankovski, A, Cossic, I. Zmijarevic, « APOLLO2: a user oriented, portable, modular code for multigroup transport assembly calculations », *Nuclear Science and Engineering*, 100, pp. 352-362, 1988.

[2] R. Sanchez, I. Zmijarevic, M. Coste-Delclaux, E. Masiello, S. Santandrea, E. Martinolli, L. Villatte, N. Schwartz, N. Guler, « APOLLO2 Year 2010 », *Nuclear Engineering and Technology*, vol. 42, n° 5, pp. 474-499, October 2010.

[3] Z. Stankovski, « Implementation of the component concept in SILENE 2D/3D Pre & Post Processing GUI », M&C+SNA 2007, April 15-19, Monterey, USA, 2007.

[4] I. Zmijarevic *et al.*, « Industrial application of APOLLO2 to Boiling Water Reactors », PHYSOR 2006, Vancouver, BC, Canada, September 10-14, 2006.

[5] J.J. Lautard, S. Loubière and C. Fedon-Magnaud, « CRONOS a Modular Computational System for Neutronic Core Calculations », *Specialist IAEA meeting, Advanced Calculational Methods for Power Reactors*, Cadarache, France, 1990.

[6] J.J. Lautard, C. Magnaud, F. Moreau, A.M. Baudron, *CRONOS2 : un logiciel de simulation neutronique des cœurs de réacteur*, Rapport scientifique DRN, SERMA/LENR/PU/00/2746/A, 2000.

[7] G. Rimpault *et al.*, « The ERANOS Code and Data System for Fast Reactor Neutronic Analyses », PHYSOR 2002, Seoul, Korea, 2002.

[8] G. Rimpault *et al.*, « Algorithmic Features of the ECCO Cell Code for Treating Heterogeneous Fast Reactor Subassemblies », *International Topical Meeting on Reactor Physics and Computations*, Portland, Oregon, May 1-5, 1995.

[9] A. Tsilanizara, C.M. Diop, B. Nimal, M. Detoc, L. Lunéville, M. Chiron, T.D. Huynh, I. Brésard, M. Eid, J.C. Klein, B. Roque, P. Marimbeau, C. Garzenne, J.M. Parize, C. Vergne, « DARWIN : An Evolution Code System for a Large Range Application », *Journal of nuclear Science and Technology*, Supplement 1, pp. 845-849, March 2000.

[10] L. San-Felice, R. Eschbach, P. Bourdot, A. Tsilanizara, T.D. Huynh, « Experimental Validation of The Darwin2.3 Package for Fuel Cycle Applications », PHYSOR 2012 – *Advances in Reactor Physics – Linking Research, Industry, and Education*, Knoxville, Tennessee, USA, April 15-20, 2012.

[11] P. Guérin, A. M. Baudron, J. J. Lautard, « Domain Decomposition Methods for Core Calculations Using The MINOS Solver », M&C+SNA 2007, Monterey, USA, April 15-19, 2007.

[12] P. Guérin, A.M Baudron, J.J. Lautard, « A component mode synthesis method for 3D cell by cell SPn core calculation using the mixed dual finite element solver MINOS », M&C 2005, Avignon, France, September 12-15, 2005.

[13] A. Boulore, Ch. Struzik, F. Gaudier, « Modeling of the Uncertainty of Nuclear Fuel Thermal behaviour using the URANIE framework », *The First International Conference on Advances in System Simulation*, SIMUL 2009, Porto, Portugal, September 20-25, 2009.

[14] J.P. Both, H. Derriennic, B. Morillon, J.C. Nimal, « A Survey of TRIPOLI-4 », *Proceedings of the 8th International Conference on Radiation Shielding*, Arlington, Texas, USA, pp. 373-380, April 24-28, 1994.

[15] J.P. Both, A. Mazzolo, Y. Péneliau, O. Petit, B. Roesslinger, *Notice d'utilisation du code TRIPOLI-4.3 : code de transport de particules par la méthode de Monte-Carlo*, rapport CEA-R-6043, 2003 ; TRIPOLI-4® Project Team, *TRIPOLI-4 User Guide*, CEA-R-6316, 2013.

[16] E. Brun, E. Dumonteil, F. X. Hugot, N. Huot, C. Jouanne, Y. K. Lee, F. Malvagi, A. Mazzolo, O. Petit, J. C. Trama, A. Zoia, « Overview of TRIPOLI-4® version 7 Continuous-Energy Monte-Carlo Transport Code », ICAPP 2011, Nice, France, May 2-5, 2011.

[17] http://www.nea.fr/abs/html/nea-1716.html

[18] http://root.cern.ch/root/html

[19] F. X. Hugot, Y. K. Lee, F. Malvagi, « Recent R&D around the Monte-Carlo code TRIPOLI-4® for criticality calculation », *Proceedings of International Conference*, PHYSOR 2008, CD-ROM, Interlaken Switzerland, 2008.

[20] D. Beretz, S. Bourganel, P. Blaise, C. Destouches, N. Huot, J.M. Girard, C. Doumergue, H. Philibert, R. Brissot, M. Dumont, « FLUOLE : A new relevant experiment for PWR pressure vessel surveillance », *Reactor Dosimetry State of Art 2008, Proceedings of the 13th International Symposium*, Akersloot, May 25-30, 2008.

[21] G. Campioni, B. Desbrière, « HFR Advanced Computation's Models », *Proceedings of International Conference*, PHYSOR 2008, CD-ROM Interlaken, Switzerland, 2008.

[22] N. Capellan, *Couplage 3D neutronique thermohydraulique. Développement d'outils pour les études de sûreté des réacteurs innovants*, Université Paris Sud XI, Orsay, France, 2009.

[23] F. Vaïana, *Couplage Neutronique- Thermohydraulique. Application au Réacteur à Neutrons Rapides refroidi à l'Hélium*, Thèse de doctorat, Université de Grenoble, France, 2009.

[24] J. E. Hoogenboom, A. Ivanov, V. Sanchez and C. Diop, « A Flexible Coupling Scheme for Monte-Carlo and Thermal-hydraulics Codes », *The 2011 International Conference on Mathematics and Computational Methods Applied to Nuclear Science and Engineering*, M&C 2011, Rio de Janeiro, RJ, Brazil, May 8-12, 2011.

[25] D. P. Griesheimer, « Common Monte-Carlo Design Tool (CMCDT) for Reactor Design and Analysis », http://www.ornl.gov/sci/nsed/outreach/presentation/2008/Griesheimer_seminar.pdf, *Knolls Atomic Power Laboratory and the Bettis Atomic Power Laboratory seminar*, April 9, 2008.

[26] J.M. Vidal, J.P. Groullier, A. Launay, Y. Berthion, A. Marc, SGN, H. Toubon, « CÉSAR: A Code for Nuclear Fuel and Waste Characterisation », *Proceedings of International Symposium Waste Management 2006*, February 26 – March 2, Tucson, Arizona, USA, 2006.

[27] T.D. Huynh, J.C. Nimal, M. Zachar, « FAKIR 5.0 A PC Code for Residual Decay Heat Power and Activity Calculation (Fuel After Heat Keyboard Instant Result) », *Proceedings of the 8th International Conference on Radiation Shielding*, April 24-28, 1998, pp. 113-120, Arlington, USA, 1994.

[28] T.D. Huynh, *Développement et mise au point de la bibliothèque physique du système PEPABAC (progiciel FAKIR) à l'aide des codes PEPIN et APOLLO 1*, Thèse, Université Paris 11, Orsay, 1995, Note CEA-N-2815, 1996.

[29] F. Laugier, C. Garzenne, E. Cabrol, "Very fast isotopic inventory and decay heat calculations in PWR spent nuclear fuel for industrial application, M&C 2005, International topical meeting on mathematics and computation, Avignon (France); 12-15 Sep 2005, IAEA-INIS 4005483, vol. 40, Issue 22 ; S. Marguet, Paris, *La physique des réacteurs nucléaires*, Lavoisier, Éditions TEC & DOC, 2011, note, p. 915.

[30] J.-C. David, *Spallation : comprendre pour prédire !?*, Thèse HDR, Université de Strasbourg, France 2012.

Cheikh M. Diop, Éric Dumonteil, Anne Nicolas, Odile Petit, Michel Soldevila, Jean-Christophe Trama, Aimé Tsilanizara,
Department for Systems and Structures Modeling.
Cyrille de Saint-Jean and Yannick Pénéliau
Reactor Study Department.

Computational Code Packages: Two Examples

NARVAL: a neutronics code package applied to naval propulsion reactors

Despite a high similarity of physical behavior with pressurized water reactors (PWRs), nuclear propulsion reactors (NP) display the following specificities: a small size, which generates significant [neutron] leakage, a particular geometry, the use of specific burnable poisons, and, finally, control by heterogeneous mobile absorbing rods. As a result, these reactors are objects which are far from "standard" land power systems, hence the need to model them somewhat differently.

NARVAL *(formulaire Neutronique Appliqué aux Réacteurs de propulsion naVALe)* is a neutronics code package of naval propulsion cores whose early preliminary version goes back to the early nineties, and whose first version was delivered to AREVA TA as soon as 1999. It is now fully mature with its fourth version delivered in December 2009, and steadily upgraded since then.

Initially based on using JEF-2.2 nuclear data libraries and APOLLO2 and CRONOS2 chained codes applied in the **LWR*** reactor types for civilian applications, NARVAL integrates a high number of additional procedures specific to naval propulsion. The first step of this code package consists in solving the energy problem on a basic pattern (2D small portion of the core, corresponding to an assembly), and then to perform a flux calculation with a precise method (S_N method), using a fine meshing for the energy variable (172 energy groups), together with a generation/depletion (or burnup) code calculation of isotope concentrations. This step ensures the availability of accurate data that constitute an input library for core calculations. As a second step, a three-dimensional core-scale calculation taking into account core burnup during its irradiation is performed using the diffusion method after cross section condensation on four energy macrogroups, spatial homogenization of neutron constants, and equivalence step in relation to the equation change (transition from the - exact transport equation to the simplified - diffusion equation – see *supra*, pp. 51-54).

The NARVAL *development, validation and qualification approach* is summarized below. First of all, the computational numerical validation step achieved at time zero with the help of the continuous-energy Monte-Carlo reference code TRIPOLI-4® makes it possible to quantify modeling biases at three scale levels: basic cell, assembly and core, apart from the choice of optimum deterministic calculation options.

As regards the *qualification* (or *experimental validation*) *phase*, it lies on experience feedback from cores of onboard nuclear reactors, from land prototypes RNG and RES *(Réacteur d'ESsais pour la propulsion navale)*, and from the AZUR critical mockup. NARVAL then simulates the irradiation of these cores, and the most significant experiments, and computes the time evolution of the isotopic fuel inventory at a very fine space scale. Its results can then be compared with the isotopic analyses carried out after dissolution of either fuel or irradiated neutron poisons.

The three-dimensional calculation of a naval propulsion core under depletion, in a heterogeneous geometry, means a few dozen millions of computational meshes: today, it takes about one hundred hours on a 2.3-GHz - 16-Go RAM LINUX computer. This code package is used by AREVA-TA for design and safety studies.

The NARVAL package treats these cores in their whole current complexity with key safety parameter uncertainties deemed satisfactory. Yet, given the increased performances related to these core lifetime expected by the CEA/DAM/DPN project owner, the code package must be developed to further improve the integral quantities, such as the overall reactivity of the core or the integral efficiency of absorbing rods, and local quantities, such as power and burnup factors, or isotopic concentrations, for configurations increasingly heterogeneous. More recent nuclear data drawn from the JEFF-3 evaluation, physical models, and higher-performance solvers, such as the Method Of Characteristics (MOC) implemented in the APOLLO2 code or even hybrid calculation schemes associating NARVAL with the Monte-Carlo code TRIPOLI-4®, are scheduled to be used in the second major version of the code package (NARVAL-2).

In addition, in response to the technical specifications of needs expressed by AREVA-TA, NARVAL adapts itself to evolutions and innovations contemplated on nuclear propulsion cores through addition of computational methods and procedures

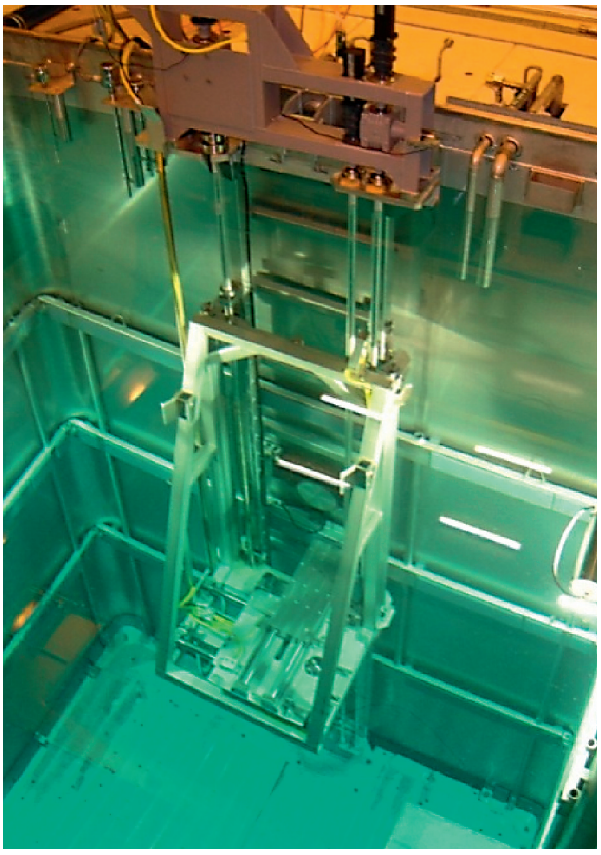

Fig. 71. Gammametry bench immersed in order to measure fine burnup distribution on the reactor fuel plates of the **RES*** *(Réacteur d'ESsais pour la propulsion navale).*

used to treat transient-related problems with the help of couplings between disciplines such as thermal hydraulics and spatial kinetics). Special attention is also paid to improving the ease of use and portability of the computational code package, in response to the various AREVA-TA constraints of use all along the steps of feasibility, design and safety studies.

In addition to the NARVAL qualification approach, a significant effort is being devoted to the design of new experimental programs, focused on two axes:

- Irradiated fuel and poison expertise;
- core instrumentation and target uncertainties, consistently with higher target accuracy in computational code packages.

As a final step, NARVAL is to rely on the new APOLLO3® neutronics code.

HORUS3D: a new neutronics simulation tool for the Jules Horowitz Reactor

In order to meet design needs relating to the future **Jules Horowitz research Reactor (JHR)**, it proved necessary to develop a computational model enabling the prime contractor AREVA-TA, under the responsibility of the project owner CEA/DEN, to conduct studies in support of design and safety report establishment.

The full chain of simulation tools dedicated to design studies is called HORUS3D *(Horowitz Reactor simulation Unified System)*. It was developed in various CEA units, and is related to neutronics, photonics, cycle calculation, as well as core and system thermal-hydraulics. As regards the neutronics components gathered in HORUS3D/N, this chain is mainly based on codes APOLLO2, CRONOS2 and TRIPOLI-4®, and on the European nuclear data library JEFF-3.

The JHR core has undergone numerous modifications during the feasibility and definition studies. With the aim of optimizing core performance in terms of flux, engineers have selected an irregular arrangement of the so-called *"Pâquerette"* (daisy-like) assemblies. In addition, in order to make it possible to vary the position of out-of-core experiments during irradiation, the reflector has been fitted with mobile elements placed in "waterways", which was done disregarding the modeling symmetry and simplicity. The result of these technological options is the new reactor geometry shown on Figure 72 below.

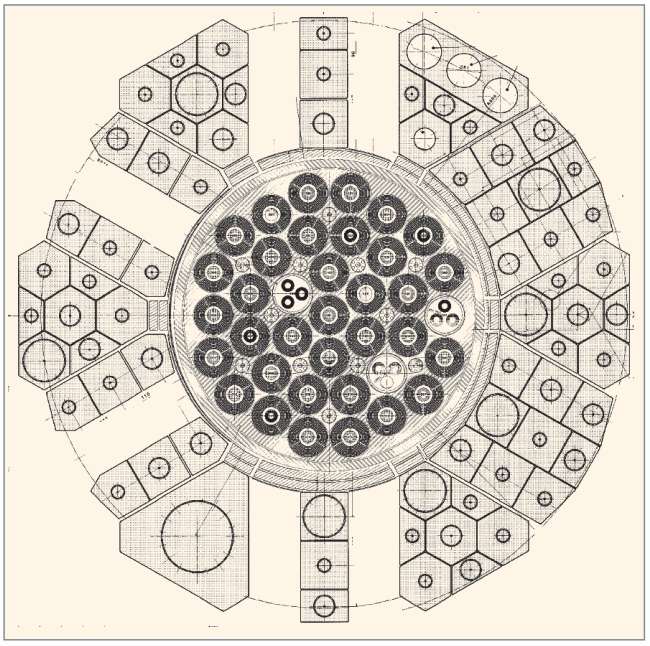

Fig. 72. "Pâquerette" (daisy-like) geometry of the Jules Horowitz Reactor (JHR) core and reflector.

Concerning neutronics calculations, the most accurate solution would have been to use the Method Of Characteristics (MOC), which today is the reference route for deterministic depletion calculations, as it allows a heterogeneous description of the geometry. Modeling biases can be limited thanks to it, among other reasons because of a very accurate geometrical description, including in the case of unstructured geometries (see *supra*, p. 82) However, the APOLLO2 code currently treats two-dimensional geometries alone, which does not allow treatment of all of the needs involved in the design of a reactor and of experimental devices in the case of the JHR. As a consequence, the joint use of APOLLO2, CRONOS2 and TRIPOLI-4® has allowed designer requirements to be fulfilled, before APOLLO3® can fulfill them in the future by treating 3D heterogeneous geometries.

Since 2007, HORUS3D/N has allowed the 3D irregular *"Pâquerette"* (daisy-like) geometry of the JHR core to be taken into account with CRONOS2, by implementing the "isoparametric finite element" method in this code, especially suited to memory size needs due to the JHR mesh complexity.

The conforming isoparametric finite elements with an irregular triangular mesh can reproduce the "Pâquerette" core as homogeneous meshes. Then the key element is fuel element modeling with dodecagons, thereby keeping the rotational symmetry by taking account of fuel plate stiffeners. Figure 73 below shows how the *"Pâquerette"* core is discretized into hexagonal "superfinite elements" (SFE), meshed with the SILENE tool (meshing tool of the APOLLO2, CRONOS2 and TRIPOLI-4® codes). The triangular meshing specific to each hexagon can take account of lattice irregularity as well as of the geometrical complexity of the lattice-vessel-reflector interface.

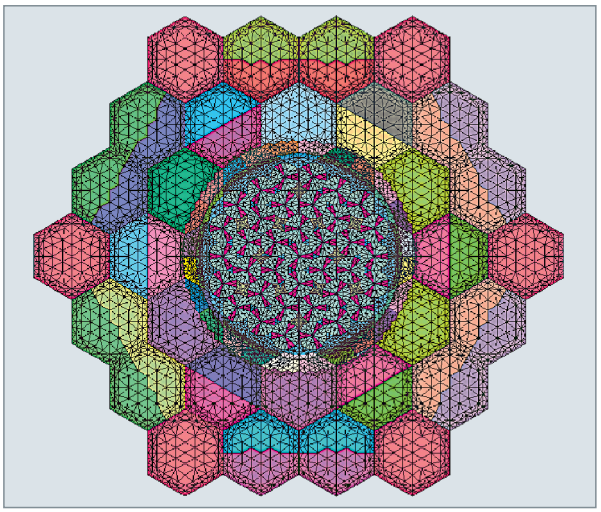

Fig. 74. CRONOS2 mesh with isoparametric finite elements, generated with the GAIA generator.

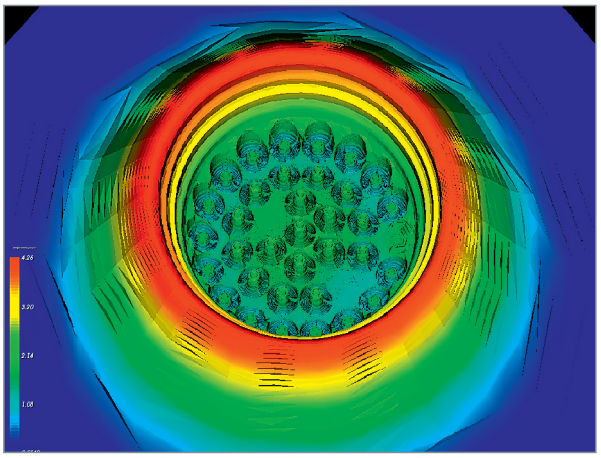

Fig. 75. 3-D distribution of thermal flux in the JHR, calculated with the HORUS3D/N neutronic simulation package.

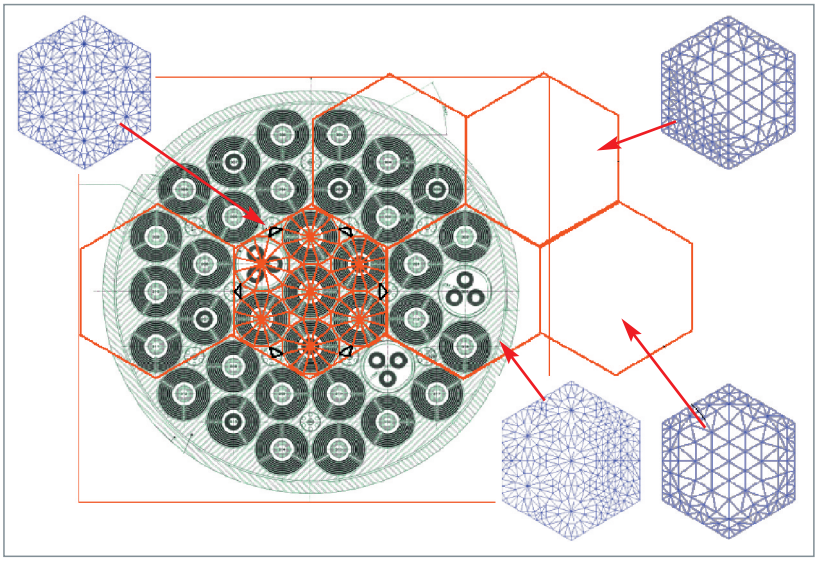

Fig. 73. Meshing of the JHR *"Pâquerette"* core into hexagonal finite macro-elements.

Automation and reliability of the JHR modeling is ensured by a dedicated graphical interface, named "GAÏA". The first version of the code package was used by the AREVA-TA prime contractor to finalize development studies.

In HORUS3D/N, the 3-D homogeneous optimized modeling selected requires to differentiate 70,000 meshes in space to calculate flux, as well as fuel depletion (*i.e.* change over time in its composition as a function of irradiation). Energy meshing for flux calculation results in six energy groups (*e.g.* PWR core calculation is usually performed with two energy groups, and naval propulsion cores, with four groups). In order to reach a sufficiently precise 3-D homo-

geneous modeling of the core, it is necessary to build libraries of space-homogenized and energy-condensed nuclear data for each core component (fuel, reflector and structures). These libraries are obtained through fine heterogeneous modelings with 172 energy groups, with special attention paid to the cross section data processing in relation to the self-shielding phenomenon (see *supra*, pp. 65-72).

The current performance of the calculation scheme stands as the best compromise between accurateness and computational time, and complies with the accurateness requirements expressed by the prime contractor. On a 3 GHz Pentium-type Linux machine, a depletion calculation requires about seven CPU hours depending on the configuration.

As compared to TRIPOLI-4® standard calculations, reactivity is predicted to be better than 200 pcm in a low-perturbation configuration, and 400 pcm in a perturbed configuration consisting of experimental devices and control absorbers. The power per assembly discrepancy is lower than 2%. An illustration of the JHR 3D heterogeneous-geometry modeling with the TRIPOLI-4® code is given below (Fig. 76).

Under depletion, HORUS3D/N is validated versus a 20-energy group, 2-D transport calculation using the TDT-MOC (Method Of Characteristics) solver of the APOLLO2 code (see Fig. 77). Between the TDT-MOC APOLLO2 calculations and the TRIPOLI-4® standard calculations, the reactivity deviation observed is 120 pcm. Typical deviations compared to the TRIPOLI-4® values are 1.6% and 1.9%, respectively in per-assembly and per-plate power distributions.

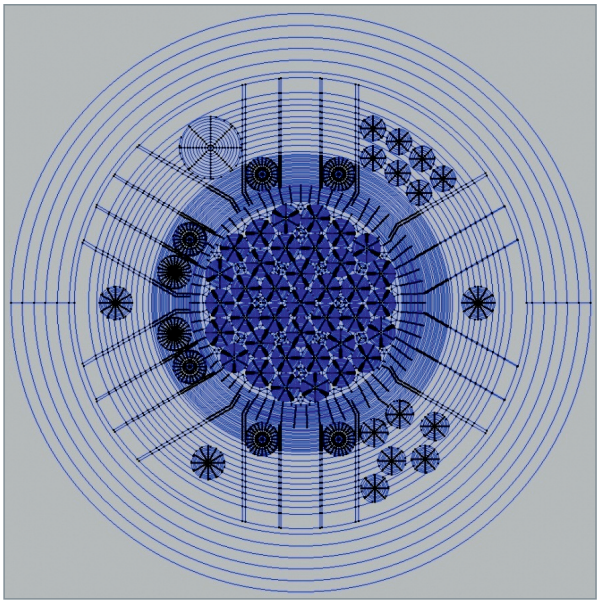

Fig. 77. 2-D APOLLO2 calculation geometry of the bare JHR core.

Following the code package qualification, performances in terms of biases and uncertainties applicable to the studies conducted with HORUS3D/N are defined basing on experiments designed and achieved by CEA/DEN.

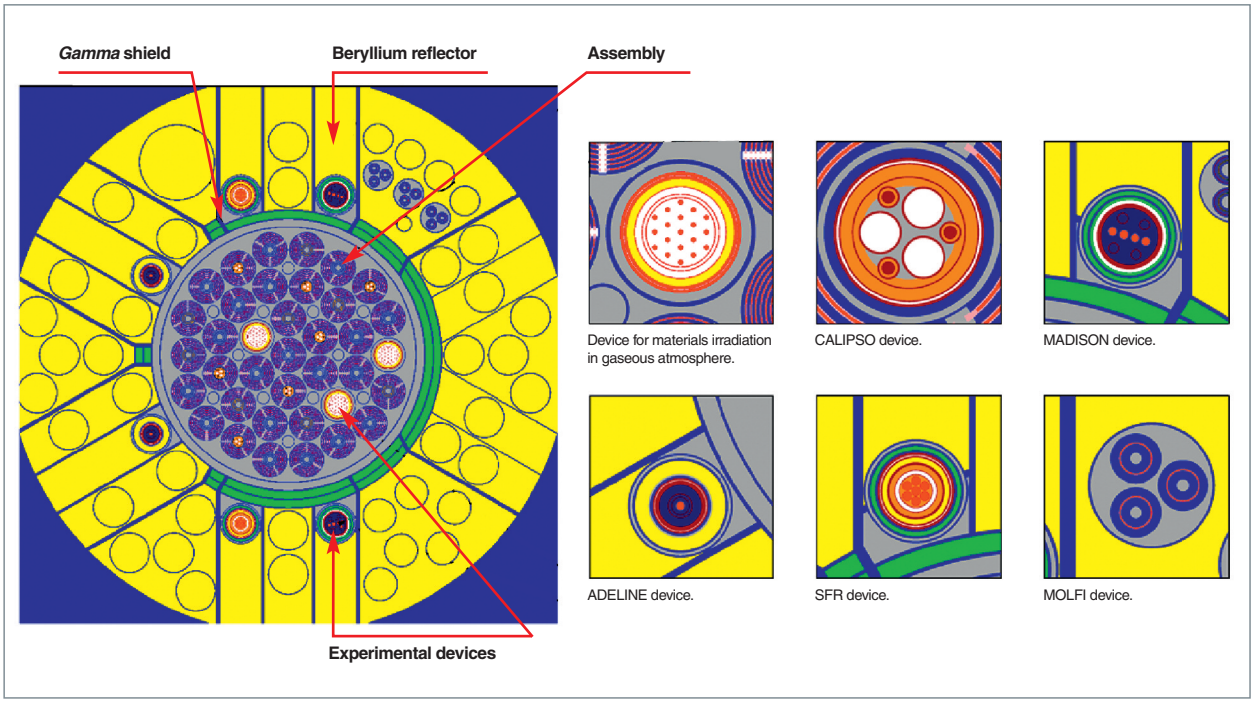

Fig. 76. Heterogeneous TRIPOLI-4® modeling of the JHR, with a maximum experimental loading (gas devices, Calipso, Molfi, Madison, SFR, and Adeline).

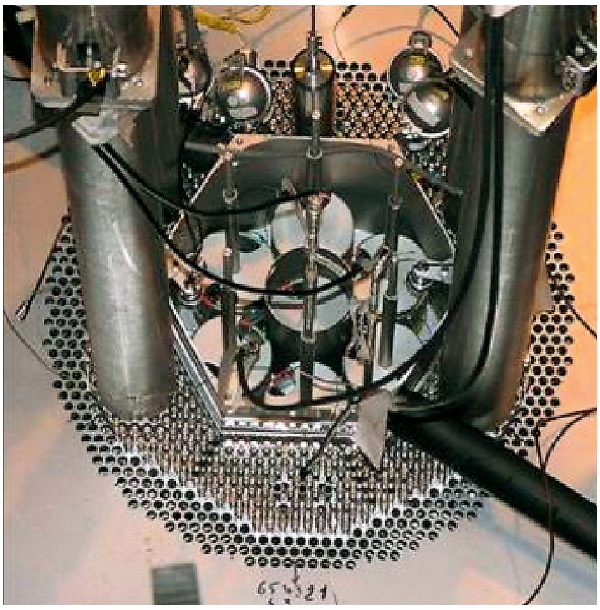

Fig. 78. AMMON core in a reference configuration, loaded in ÉOLE.

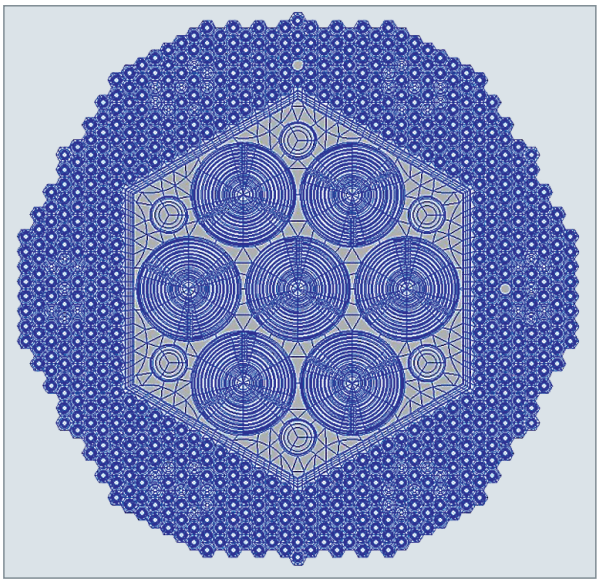

Fig. 79. APOLLO2 modeling of the AMMON core in a reference configuration.

In particular, basic experimental programs named VALMONT and ADAPh were achieved as a first step, respectively in the MINERVE and, then, ÉOLE and MINERVE reactors:

- The VALMONT program achieved in 2004 has qualified the neutronics calculation of an UMoAl-HEU-fuel core allowing related uncertainties to be reduced and controlled;

- the ADAPh program achieved in 2005 has resulted in a first qualification of the calculation of prompt and delayed photon heating in materials.

The specific experimental program **AMMON*** (see Fig. 78 and Fig. 79) – containing 7 JHR assemblies – in the ÉOLE reactor from 2010 to 2013. It will result *in fine* in the qualification of HORUS3D/N (for neutronic calculations) and P (P for photonic calculations) with respect to most of the JHR integral neutron and photon quantities and of reactivity effects.

Current software tools can treat a broad spectrum of applications which goes beyond reactor physics itself. If the intrinsic quality of these computational softwares meets the final user's needs in many cases, this user often expresses strong expectations, especially as regards their flexibility, their reliability, their ability to be automated, to be coupled and to provide uncertainties in relation to computed quantities.

Advances in calculation methods, increasing computational power, improved geometrical modeling softwares, and development of powerful softwares for processing big volumes of data, promise a significant change in the engineer's practice.

APOLLO3®, the new-generation computational system under development, aims at addressing these stakes with increased efficiency.

Anne Nicolas,
Department for Systems and Structures Modeling
Jean-Pascal Hudelot and Jean-Marc Palau
Reactor Study Department

High-Performance Computing

Introduction

In the field of nuclear reactor Physics, **High-Performance Computing** (**HPC***) paves the way for evolutions and changes in the way to perform a numerical simulation and to use it. **HPC** refers to all the methods for treating complex applications with powerful machines able to manage huge volumes of numerical data.

As a matter of fact, evolutions in computational codes (algorithms, numerical methods…), and efficient use of increasing computing powers continuously improve accuracy and fineness in modeling [1].

The data so obtained through numerical simulation are also more complete as a result of generalizing **three-dimensional (3-D) calculations**, and taking account of **multiphysics phenomena***, and even a higher number of power plant components simulated simultaneously (coupled thermal-hydraulics / neutronics, three-dimensional treatment of reactor core and nuclear steam supply system). That helps reach far better accuracies within times of the same order of magnitude as those corresponding to simplified models conventionally used.

These ongoing advances in the field of modeling and numerical simulation are indispensable for:

- Reducing uncertainties;
- optimizing facility design and, so, related costs;
- improving safety;
- optimizing facility operation;
- improving physics knowledge.

As a function of the objectives to be reached with the help of HPC, various techniques can be used. The objectives to be attained by HPC fall into four broad classes as follows:

- **Multiparameter calculations:** this is the basic technique for optimization. HPC is an excellent tool to take account of more parameters, and reduce the optimized-solution *"time to market"*. This also allows the use of learning techniques, such as **neural networks***, so as to automatically find an optimized set of parameters;
- **a very high-resolution physics:** that is, the one which adheres most closely to the real physical world, tending to best simulate all of physical phenomena at the various temporal and spatial scales, which inescapably requires higher memory space and increased computational power;
- **a more realistic physics:** by systematically using the most possibly realistic physical model instead of a simplified model or of pre-established values. That means not only higher computational power, but also robust and easy-to-use coupled systems;
- **real-time simulation:** it is already existing, but improved modeling could help get more realistic simulators, and reduce the number of assumptions.

From now on, HPC is seen as mixed with the use of **supercomputers***. Even if that may seem a little reducing, it is clear that, from the engineer's workstation to the supercomputer, intensive calculation has to rely on the ability to use a high number of calculation resources (**computer cores***), and this simultaneously (or in parallel). Without pretending to be comprehensive, the following paragraphs set forth the guidelines of HPC use in Monte-Carlo and deterministic neutron transport codes, as well as its development outlooks, including the evolution of hardware architectures.

HPC for Monte-Carlo simulations

The Monte-Carlo method for solving the neutron transport equation is an excellent, natural candidate to make use of parallelism. As the simulation process is based on a statistical processing of independent particle paths, each particle can be simulated by a different processor. So Monte-Carlo methods are qualified as *"embarrassingly parallel"*.

Principles for a parallel implementation

In order to control the simulation process, a monitor is required to control the whole simulation, an so is another process in charge of collecting simulation results. These two processes can be executed on a same processor or on different processors.

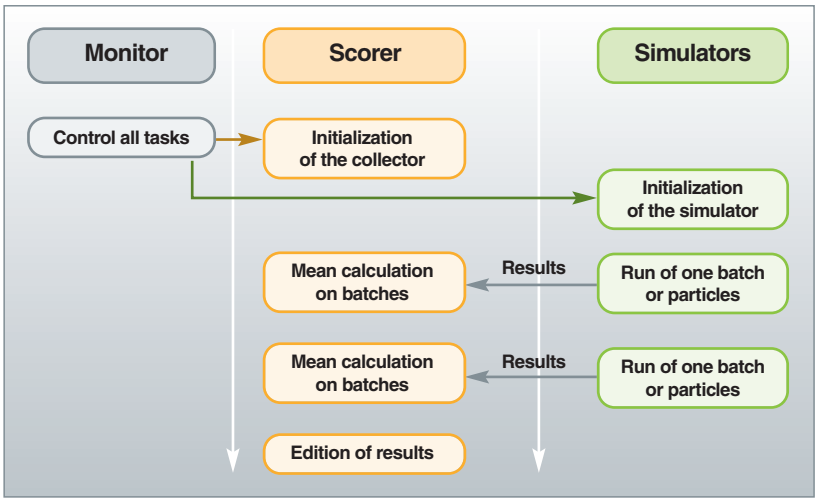

Fig. 80. Principle for parallelism implementation in an MC simulation – Case of the TRIPOLI-4® code.

For this implementation part, the model used is a **MPMD** approach, "MPMD" standing for "Multiple Program Multiple Data": *i.e.* different programs are executed in parallel using different data. It is based on a "master / slave" model, a master being identified as being in charge of simulation control, and the processes of simulation and collecting being separated ([2, 3, 4, 5]).

This principle is applied in the TRIPOLI-4® code ([5, 6, 7, 8]) and is schematically described on Figure 80.

The main benefits of this model lie in its easy implementation and portability; it is also well adapted to independent particle simulation. Another advantage is that this implementation is fault-tolerant. For if one of the simulators happens to fail, whether this is due to a hardware or software failure or to a computational numerical problem (non convergence), the monitor can send the corresponding particle batches to another simulator. Thanks to these features, even if over half the simulators is lost, simulation can still go on.

Other features have also been installed during TRIPOLI-4® execution, such as backup / restart procedures: the current state of the TRIPOLI-4® simulation is stored in different files which enable simulation to start again at any time.

From the viewpoint of mathematics and algorithmics, the main issue lies in the parallel version of the **random number generator*** [10] (see *supra*, pp. 94 and 95), the latter having to display the following properties:

- Independence with respect to the number of processors;
- no correlation between sets for different processors;
- on each processor, the generator can be initialized independently (no communication between processes).

An example of this parallel random generator is that based on the GFSR algorithm (GFSR: Generalized Feedback Shift Register) [10]. The chief benefits of this random number generator are its high execution rate and its very long period (2^{607}) (see *supra*, pp. 94 and 95).

Performances

The way to assess parallel performances of Monte-Carlo simulations is fully different from the conventional efficiency measurement: it is based on a factor which measures simulation quality, referred to as the "Figure of Merit" (FOM), and defined as follows:

$$FOM = \frac{1}{\sigma^2 \times \tau}$$

where σ^2 is the variance coupled with the computed quantity, and τ the simulation time (see *supra*, pp. 89-106).

The speedup or the FOM is expected to increase linearly with the number of processors, which is generally verified as shown on Figure 81.

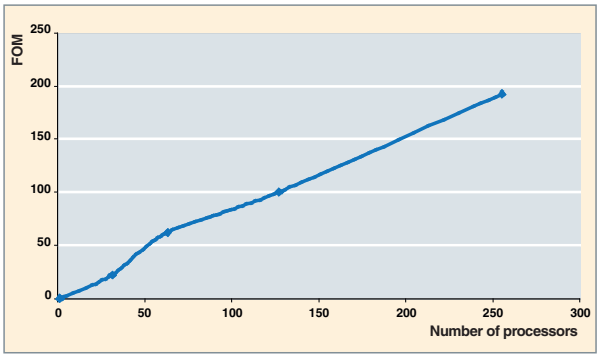

Fig. 81. Typical behavior of the "Figure of Merit" on a Monte-Carlo simulation using the TRIPOLI-4® code.

This type of behavior is regularly verified for simulations going up to 1,000 processors, in which efficiency is still of an approximate 90%.

One of the advantages of the parallel implementation of the TRIPOLI-4® code is that the monitor can help dynamically control the load balance of each simulator. Thus, the number and size of batches can be adjusted so that there is a minimum queuing file on simulators, thereby maximizing the overall efficiency of simulation.

Yet, there may be jams, indeed, that make it hard to get an ideal efficiency. Even if performance can be adjusted, the collector may prevent from getting an optimum computing speedup for a very high number of simulators (> 1,000). Some alternatives are being investigated, such as the implementation of a collector tree, so as to share the load of result collecting. Another alternative might be to avoid on-line collecting, and pile-up results after simulation. Nevertheless, special attention has to be paid to the amount of data to be stored.

Expected challenges

However, even if some Monte-Carlo simulations are naturally parallel, as seen above, reaching the **petaflop*** and beyond scale (over 10,000 cores) is still a challenge, as for many other applications. Therefore, a huge amount of data will have to be coped with, either on the network, or on the file system, in order to store simulation results.

If geometry complexity is further increased, and so is the number of computational variables (*e.g.* the reaction rates on a full reactor core on the rod or pellet scale), storing all these data in memory raises a problem. For, in the parallelism model used, all the input data (geometry, compositions, nuclear data…), as well as the output data are duplicated on each processor (see Fig. 82).

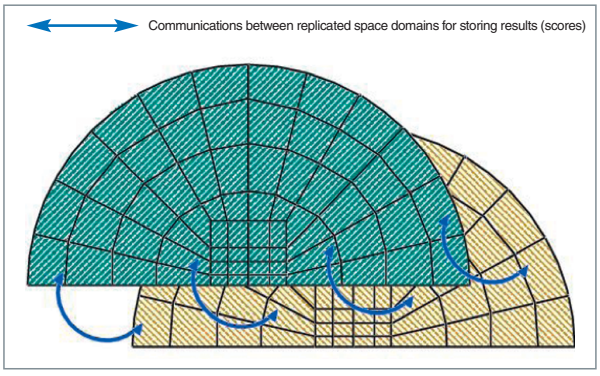

Fig. 82. Domain replication (history based parallelism).

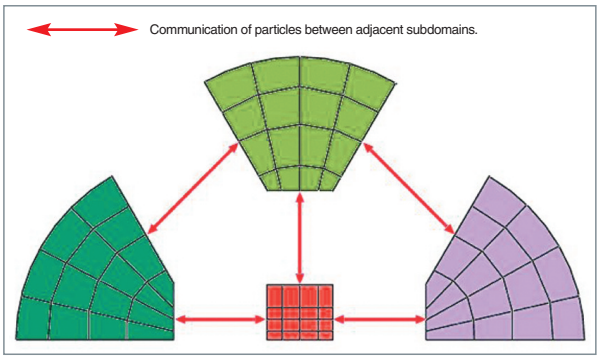

Fig. 83. Domain decomposition (space parallelism).

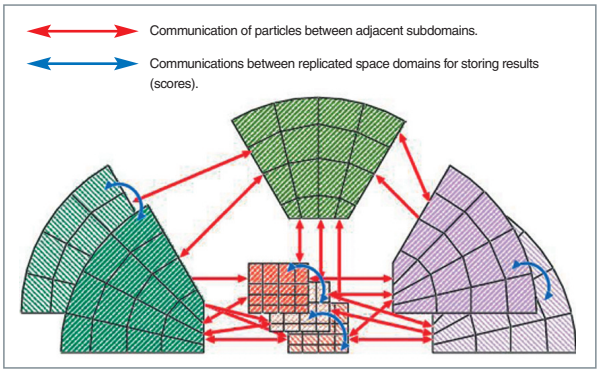

Fig. 84. Domain decomposition and domain replication (space parallelism and history based parallelism).

So, the limit is not only relating to computational time as it is today, but also to memory size. An alternative would be to mix task parallelism with data parallelism, and to divide the computational range so as to distribute it among the different processors (see Fig. 83).

But this parallelism is "against nature" for Monte-Carlo simulations, and induces delicate problems, such as the load unbalance, as well as efficiency losses due to communication traffic between processors.

In the MERCURY code, both models are implemented [11] so as to make use of the benefits of both, spatial and particle, parallelism models (see Fig. 84).

This type of approach is also considered for the MNCP code, in which innovating data transfer paradigms are being investigated in order to tackle the problem of task parallelism mixing with data parallelism for a Monte-Carlo simulation [12].

Such approaches do not include any particular assumption about machine architecture. Another alternative likely to help solve the problem of data duplication in memory, is taking account of the evolution of architectures, in which the number of computational units sharing a common memory is continuously increasing. Thus, the idea here is to have only one copy

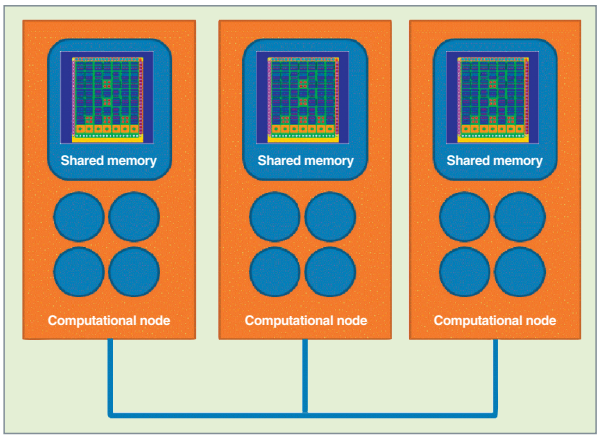

Fig. 85. Principle for data sharing within a same computational node, and for duplication among calculation nodes.

of data within a computational node, which has several computational units sharing these data, and duplicate them among the various computational nodes. This principle is displayed on Figure 85.

There exist many other areas in which High-performance Computing and Monte-Carlo transport can be explored. Among these areas, it is worth to mention the use of computing accelerators or many core architectures, such as GPU or Intel Xeon Phi.

HPC in the deterministic approach

The various levels of parallelism

In deterministic approaches, three main levels of parallelism can be considered:

- The first level concerns multi-parametrized calculations. The goal is to achieve a set of calculations independent from each other, on a set of computational resources. So, in this case, calculation and data flows (input data and results) have to be managed on the whole of computational resources. A well-known example is the calculation of a multi-parametrized library for *core calculation*. Calculations of the various assemblies and loading conditions are all independent from each other, and so can be computed simultaneously.

- The second level corresponds to multidomain calculations. Here the aim is parallel managing of a set of calculations on data which are not necessarily independent. Among the treatments of interest, let us quote, for example, **isotope depletion calculations*** and thermal-hydraulics feedbacks… For this level, it can be generally considered that the spatial dependence of data is very low, and that a massively parallel approach is well adapted. In cases when the spatial dependence of data is strong, domain decomposition techniques are generally used. This is typically the case in transport equation resolutions.

- The third level mainly deals with fine-grained parallelism of solvers, making use of the parallelization inherent to the numerical methods considered.

These different levels are illustrated in the following pages, which describe a few representative examples [13].

First level: multi-parameterized calculations

The main interest of this level is to use the "brute force" of HPC for solving problems with huge amounts of independent calculations at "human-time" scale solving.

An example can be found in HPC use to reduce simulation uncertainties (*e.g.* thanks to finer space and energy discretizations…), or to gain margins with the help of optimization techniques.

One obvious way to reduce uncertainties is to make use of deterministic approaches. Another way consists in using a less intrusive method based on a stochastic approach (sampling). As it can be questioned due to required computational resources, this sampling method however proves quite interesting when the deterministic approach is too complex to be implemented. It is worth mentioning the coupled (thermalhydraulics-neutronics) problems, or isotopic depletion calculations.

As regards optimization problems, a very good example lies in the optimization of core loading schemes using genetic algorithms [14]. A tool based on URANIE/VIZIR and the APOLLO3® code [15] was designed and successfully applied to optimize model fuel loading in the case of heterogeneous PWR cores. This tool makes it possible to assess over ten million different configurations in less than ten hours using more than 4,000 processors. An illustration of different types of solutions is given on Figure 86, on the following page.

The main benefit of this type of method is to enable engineers to test various configurations, and reduce some design constraints, which would not have been possible without the joint use of genetic algorithms and HPC. Examples of different solutions are given on Figure 87.

This type of approach is getting generalized at CEA, and is now applied in support of the **ASTRID*** studies with the TRIAD tool. It is interesting to note that a prototyping exercise, following the access to a major computational resource, has allowed to demonstrate to physicists in charge of nuclear reactor design the potentialities of a tool and of an approach thanks to HPC, and how, two of three years later, thanks to the increase

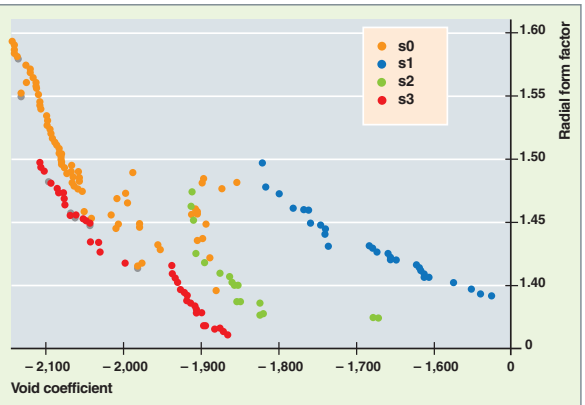

Fig. 86. Pareto fronts: solution sets found by genetic algorithms according to various optimization strategies relating to the void coefficient and the radial form factor, s0,s1,s2, and s3 standing for various layouts of the fertile assemblies in the core.

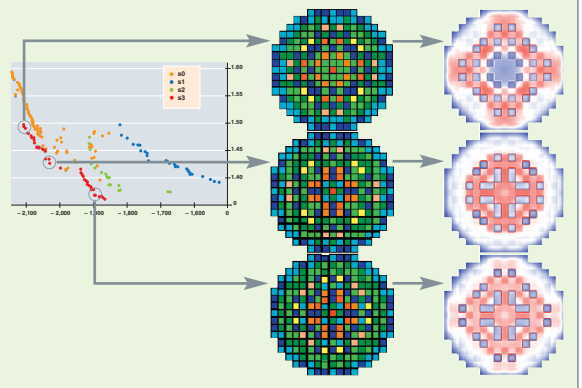

Fig. 87. Illustration of various loading pattern-related solutions: Pareto fronts (left), loading patterns (center), corresponding power distribution maps (right).

in accessible computational power, what was a mere exercise may become a design tool for computer-assisted reactor design.

Second level: multi-domain calculations

This level corresponds to the most general use. In most of parallel scientific applications, this level is used through the **domain decomposition*** technique. As part of neutronics, all calculations which are spatially independent are concerned. For example, in a typical two-step core calculation (see *infra*, pp. 193-213), all sequences relating to cross-section management, feedbacks, isotopic depletion…, are locally coupled with the geometrical domain cell, and can so be performed in parallel. To put it in a nutshell, in a 3-D standard nuclear reactor core calculation, all the steps are spatially independent, and can so be conducted in parallel, except for one of them: neutron flux calculation. Even if all the previous steps are conducted in parallel, the main problem remains data flow management and data distribution among processes. So it is necessary to prepare a well-thought code architecture design in order to get optimum data structures liable to ease and optimize in-parallel data flow management.

Concerning the calculation of the fluxes themselves, conventional techniques of domain decomposition can be used [16]. Concerning the transport equation solver [17], additional degrees of parallelism can be found, for example for the other dimensions of the equation can be used, *e.g.* angle or energy dimensions. Many solvers have been implemented in parallel, making use of parallelism either in angle and energy [18, 19, 20], or in space [21, 22, 23], or in the three of them [24].

Figure 88 below shows the performance obtained with the transport solver MINARET of the APOLLO3® code, through parallelism based on angular directions calculation. The exercise, which took place on CCRT's TITANE and CEA's TERA-100, allowed the architecture and computational behavior of the solver to be validated for a massive parallelism use of up to 33,000 computational cores, on a realistic configuration: ESFR-type 3D core calculation (even if such an increase in order is not physically useful).

Another degree of parallelism can be used during the use of multi-level techniques. For instance, the coupling of a fine solution of the transport equation at the assembly level with a coarse 3D core solution. Typical examples of the implementation of these techniques can be found in the 3-D COBAYA code [25] (see Fig. 89), or in the MINOS diffusion solver as part of an original approach based on a modal synthesis method. [26].

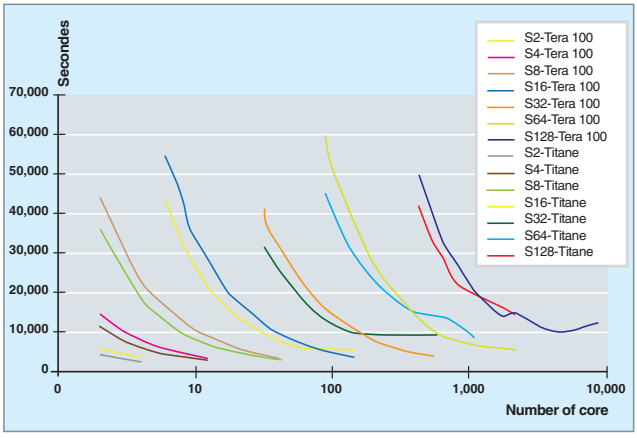

Fig. 88. Computational time of a 3-D simulation conducted with the MINARET transport solver of the APOLLO3® code on the TITANE and TERA-100 CEA's supercomputers.

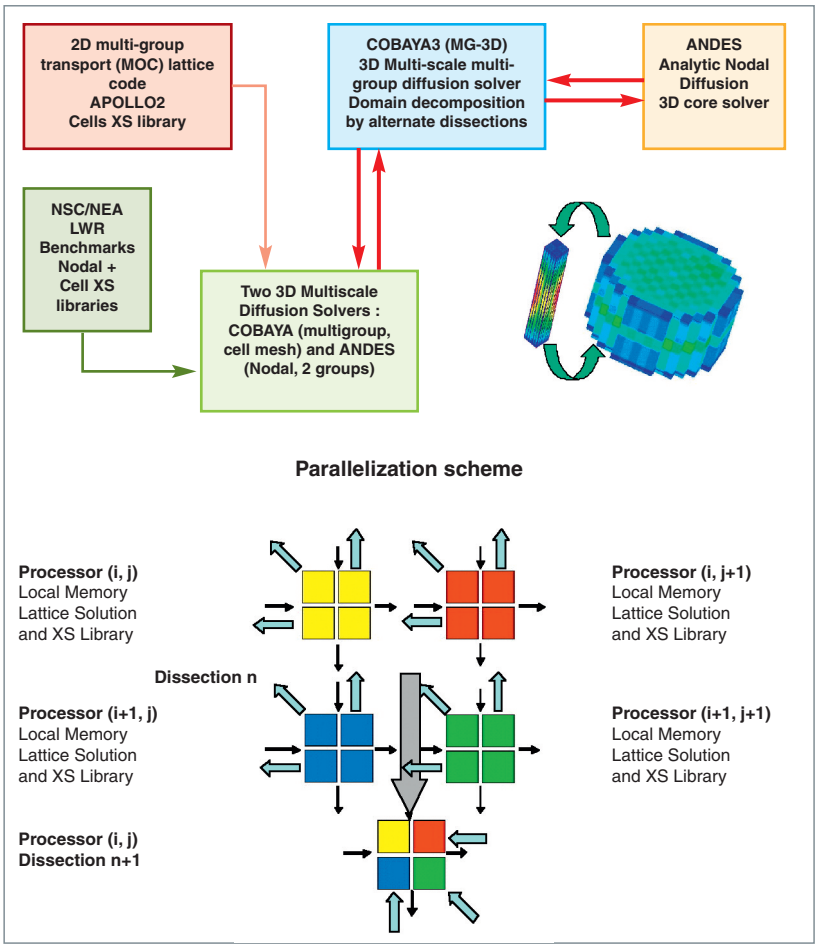

Fig. 89. Parallelism principle used in the COBAYA code (Source: NURESIM Project).

This multi-level approach of parallelism is also well suited to 3-D calculations, especially when the method presents intrinsically low parallelism, or very difficult to parallelize. One typical example is the Method Of Characteristics (MOC) [see *supra*, pp. 82-85] used to find the solution to the neutron transport equation. Indeed this method can be parallelized, but it requires quite advanced parallelism techniques in order to get an interesting efficiency [27, 28, 29]. One alternative is to couple a 2D approach with a coupling in the third direction, and to compute 2D planes in parallel (Fig. 90). This approach is used, for instance, in the DeCART code [30] and in the UNIC code [31].

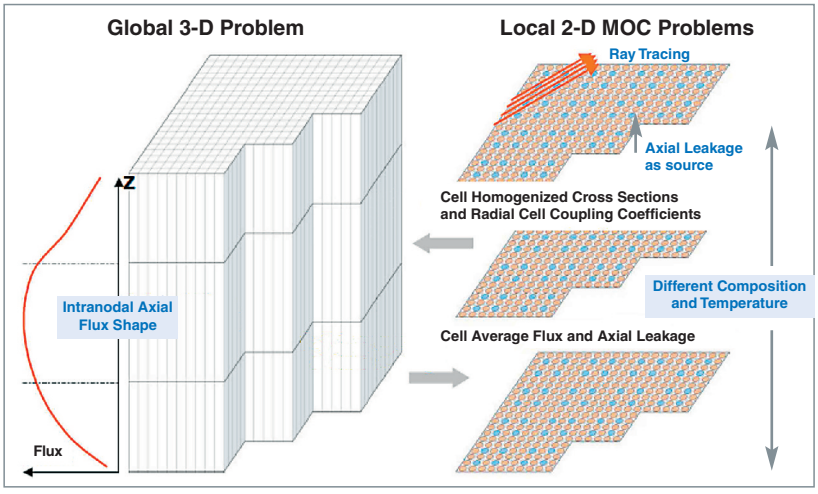

Fig. 90. 3-D MOC method based on the synthesis of plane 2-D MOC calculations.

Third level: fine-grained parallelism

This level is generally used on shared-memory architectures, and makes use of the intrinsic parallelism of algorithms. These techniques experienced much success in the early years 2000 with the HPF, and then OpenMP languages [21, 22, 32]. On current multi-core architectures, it is increasingly interesting to combine this *fine grain* level with the previous level so as to improve the overall performance of algorithms.

Hybrid parallelism

As a result of race for power, supercomputers are now fitted with the most powerful accelerators, such as graphical cards (GPUs). These new-generation architectures display the advantage of providing a quite interesting computational performance / electric power ratio. Yet they mean an additional heterogeneity in codes prior to their being used.

First experimentations have been achieved around the simplified transport solver MINOS, as part of the APOLLO-3® project. So it is possible to mix a domain decomposition approach and GPU acceleration [18].

Figure 91 above shows the results obtained for a 3-D PWR-core calculation, in a two-group, cell-per-cell scattering. As can be observed, speedups to 30 computational units prove very interesting as compared with conventional CPUs.

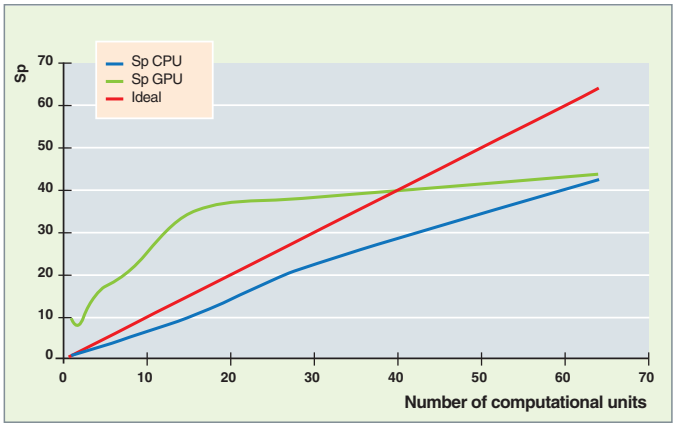

Fig. 91. Compared speedup (Sp) between CPU (blue curve), GPU (green curve), and ideal speedup (red curve). On the y axis, the number of computational units.

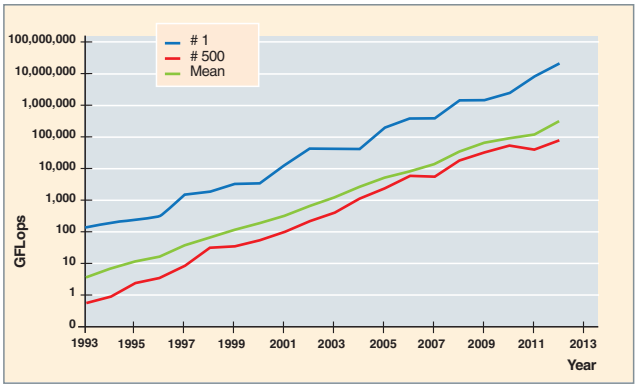

Fig. 92. Evolution of computational power in TOP 500.

Hardware architecture evolution for scientific high-performance computing

This paragraph aims at providing information about machine architecture evolution and trends predicted over the next dozen of years.

Part 1 presents the evolutions of computational machines over the last twenty years, as well as the main trends likely to be deduced from them, thereby allowing next evolutions to be better anticipated.

Part II gives an overview of current architectures, and focuses on French machines.

Finally, the last part introduces the issue of machine architectures over the next ten years, especially in relation to the **exascale*** target.

Evolutions over the last twenty years

A simple, representative way to trace back the evolution of computational machines is to base on the TOP 500 classification (http://www.top500.org) which twice a year, since 1993, has recorded the 500 machines proving most powerful in the world on the basis of a linear algebra benchmark.

Machine power evolution

Figure 92 presents the evolution in the *peak power* of the first-rank machine, as well as of the last-rank machine. The average peak power of the ranked machines as a whole is also mentioned.

As can be observed, power is constantly increasing. Another interesting item is the first rank-last rank transition time, which is between 7 and 8 years or so.

Figure 93 below shows the evolution over years in the number of processors or computational cores for the first-rank and the last-rank machine, as well as the evolution in the average number of processors for the whole of classified machines.

The curves are less smooth than on the previous figure, but the conclusions are the same. This means that an increase in computational power requires an increase in the number of computational units. As on Figure 93, the number of cores in TOP 500 last-rank machine is the number of cores in the first-rank machine eight years earlier.

To sum up it all, the trend to a massive increase in parallelism does not only concern the most powerful machine in the world, but also all of the machines.

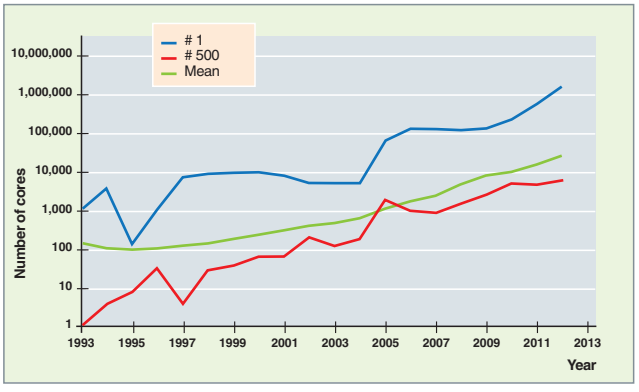

Fig. 93. Evolution of the number of cores in TOP 500.

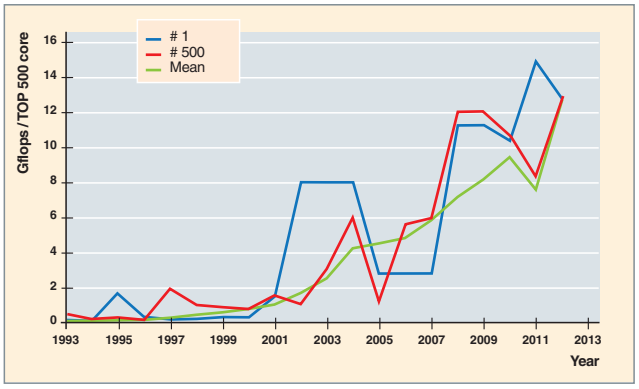

Fig. 94. Power evolution in a computational core.

This is corroborated by the following graph (Fig. 94) which represents power evolution in a computational core.

On this curve deviances between Number 1 and the last machine are not systematically constant over years. The processor of machine n°1 is not necessarily more powerful than that of the last-rank machine. In particular, it can be observed that in 2012 computing power was identical for both extremes. This is mainly due to the standardization of the components used. As a matter of fact, there is actually no more specialized processor for HPC.

Another important remark is that the unit power of a processor has increased by a factor 100 between 1993 and 2012. Now, according to the Moore law, this factor should be about 8,000… In contrast, the total machine power has progressed by a factor exceeding 150,000.

So it is obvious that an increase in machine power is mainly based on an increase in parallelism level.

Memory evolution

Figure 95 presents the evolution in total machine memory size, only for the machine ranking first in TOP 500.

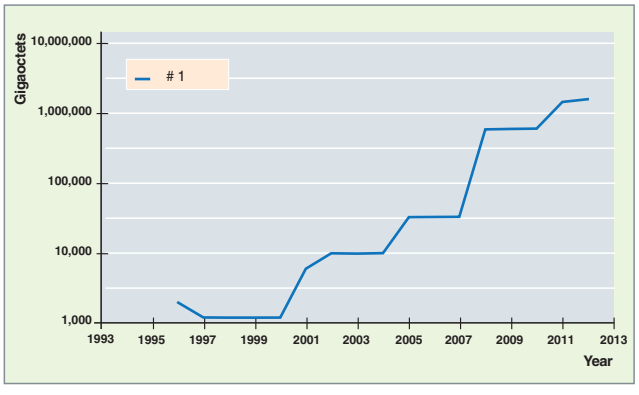

Fig. 95. Evolution of memory capacity in TOP 500.

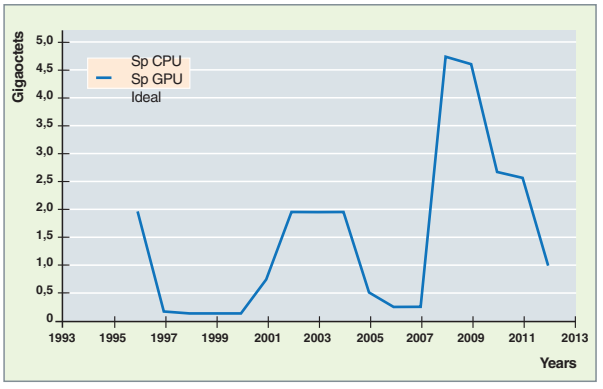

Fig. 96. Memory evolution per computational core.

It can be observed that there is a regular and significant increase in the total memory capacity of computational machines.

But what about the memory per computational core? Its evolution is represented above on Figure 96.

Obviously, if clear-cut variations could be observed during past years, the memory size per core has not increased since 1996, or even has somewhat decreased.

As a conclusion, the total overall memory of machines is rising, proportionally to power (though the slope is less sharp), but the memory per computational core either remains constant, or decreases. That means this overall memory space is increasingly shared by computational units (cores, multicore processors) within a computational node, and increasingly distributed among computational nodes.

Current architectures and computational powers

All computational machines are parallel, ranging from the workstation to the supercomputer ranking first in TOP 500.

As mentioned above, processors themselves are parallel in that they have become multicore. They are also *"multithreaded"*. These multicore processors are themselves aggregated within a shared-memory computational node, these nodes being linked with one another by a connection network. As regards their architecture in the past years, they have fluctuated, on the average, between *homogeneous* (*i.e.* with processors being all identical, or at least of the same type) massively parallel architectures, and *heterogeneous*, accelerator-based architectures. Tables 1 and 2 below present the first ten machines of TOP 500 in June 2012 and November 2011.

Table 21.

The first ten machines of TOP 500 in June 2012

On the blue background, the machines fitted with an accelerator.

Machine	Processor technology	Processor rate MHz	Accelerator/ Co-Processor	Core per *socket**
BlueGene/Q	PowerPC	1600	None	16
K computer	Sparc	2000	None	8
BlueGene/Q	PowerPC	1600	None	16
iDataPlex	Intel SandyBridge	2700	None	8
NUDT YH MPP	Intel Nehalem	2930	NVIDIA 2050	6
Cray XK6	AMD x86_64	2200	NVIDIA 2090	16
BlueGene/Q	PowerPC	1600	None	16
BlueGene/Q	PowerPC	1600	None	16
Bullx B510	Intel SandyBridge	2700	None	8
Dawning TC3600	Intel Nehalem	2660	NVIDIA 2050	6

Table 22.

The first ten machines of TOP 500 in November 2011

On the blue background, the machines fitted with an accelerator.

Machine	Processor technology	Processor rate MHz	Accelerator/ Co-Processor	Core per *socket*
K computer	Sparc	2000	None	8
NUDT YH MPP	Intel Nehalem	2930	NVIDIA 2050	6
Cray XT5-HE	AMD x86_64	2600	None	6
Dawning TC3600	Intel Nehalem	2660	NVIDIA 2050	6
HP ProLiant SL390s	Intel Nehalem	2930	NVIDIA 2050	6
Cray XE6	AMD x86_64	2400	None	8
SGI Altix ICE	Intel Core	3000	None	4
Cray XE6	AMD x86_64	2100	None	12
Bull bullx super-node S6010/S6030	Intel Nehalem	2260	None	8
BladeCenter QS22/LS21	Power	3200	IBM PowerXCell 8i	9

Table 23.

List of various machines accessible in France, with their world rank, number of cores, and power in Teraflops
(*i.e.* 10^{12} floating point operations per second).

Rank	Site	System	Number of core	Power in TeraFlops
9	CEA/TGCC/GENCI	CURIE TN – BULL Bullx	77,184	1,667.2
17	CEA	TERA-100 – BULL Bullx	138,368	1,254.5
29	EDF	Zumbrota – IBM BlueGene/Q	65,536	838.9
30	CNRS/IDRIS/GENCI	IBM BlueGene/Q	65,536	838.9
75	CINES/GENCI	JADE – SGI Altix	23,040	267.9
97	CEA/CCRT	AIRAIN – BULL Bullx	9,440	203.9
104	EDF	Ivanohe – IBM iDataPlex	16,320	191.3
115	CEA	TERA-100 Hybrid – BULL Bullx	7,020	274.6
149	CNRS/IDRIS/GENCI	IBM BlueGene/P	40,960	139.3
162	CEA/TGCC/GENCI	CURIE Hybrid – BULL Bullx	5,040	198.2
168	CEA/CCRT/GENCI	TITANE – BULL Novascale	11,520	130
201	EDF	Frontier2 – IBM BlueGene/P	32,768	111.4
245	CEA/TGCC/GENCI	CURIE TN – BULL Bullx	11,520	104.4

It can be observed that in November 2011 60% of TOP 10 machines were accelerator-based, falling to 40% only in June 2012… As a matter of fact, a new proportion inversion can be predicted…

Thus, to go on increasing computational power, while remaining in a reasonable thermal envelope, one of the routes is to use accelerators (graphic cards - GPUs - being currently used). Yet, **IBM BlueGene** machines or the **Fujitsu K machine** (which is commercially distributed) provide alternatives based on homogeneous processors.

The interested reader is invited to read the article http://www.hpcwire.com/hpcwire/2012-07-05/green500_turns_blue.html?page=2 dealing with Green 500 analysis. Green 500 classification (http://www.green500.org/ is symmetrical to that of TOP 500, but here the classification criterion is the computational power/electrical power ratio. This article shows that in the last classification, BlueGene/Q machines rank first in contrast with the latest years, when the first-rank machines in this list were accelerator-based.

Table 23 (left) summarizes the various machines accessible in France (without mentioning access procedures, the potential users of the listed machines being the DEN or its customers).

Considering the civilian CEA's machines alone, that accounts for over 110,000 computational cores, and practically 2 petaFLOPS.

Future architectures and computational powers

Two distinct periods of time, and so two different architecture generations, can be distinguished: multipetascale machines, which, to sum up it all, will lie on present technologies, and exascale machines, which will require huge technological breakthroughs to reach the exaflop power needed for an acceptable electrical consumption.

Multipetascale machines

These machines already exist. So, in the next years, evolutions of present architectures will be available with the homogeneous MPP line (BlueGene/Q, R…), and hybrid architectures based on the GPU and the new Intel MIC-technology processor, Xeon Phi (http://www.pcinpact.com/news/71737-intel-xeon-phi-mic-knight-corner-coprocesseur.htm).

The TACC's (Texas Advanced Computing Center) next machine, Stampede, will provide about 20 petaFLOPS in early 2013, *i.e.* 5 petaFLOPS with conventional processors, and 15 petaFLOPS with Xeon Phi.

A no negligible advantage of this new accelerator is that available programming models and languages are the same as those for conventional CPUs. Such is not the case for GPUs. Programing languages, models and environments for the HPC represent a broad topic which is not considered in this short review.

Exascale machines

According to some specialists, exascale machines are expected to be available by 2018-2020. What mainly guides their design, apart from the fact that they have to reach the exaFLOPS (10^{18} floating point operations per second), is electrical consumption. As a matter of fact, if they kept the same type of technology as that adopted for current petaFLOPS machines, feeding these machines would require the equivalent of a nuclear power plant's electrical output. It is hard to predict what the exascale machine architectures will be. So it is preferable to turn to area specialists, referring to an extract of the ***International Exascale Software Project*** (IESP)'s Report ***Roadmap 1.1***, http://www.exascale.org/iesp/Main_Page)

To sum up it all: an even higher parallelism (beyond 100 million cores), a reduced memory size per core, and necessarily tailored programing models.

A very high number of uncertainties still exist in relation to these machines. For, even if they are bound to be built, they will be so "unique" that they will have probably to be considered as major research instruments, and there will be only a few of them worldwide according to **Marc Snir**, Director of the *Mathematics and Computer Science Division at the Argonne National Laboratory* (USA).

Report Roadmap 1.1

«As a result of these and other observations, exascale system architecture characteristics are beginning to emerge, though the details will become clear only as the systems themselves actually develop. Among the critical aspects of future systems, available by the end of the next decade, which we can predict with some confidence are the following:

- Feature size of 22 to 11 nanometers, CMOS in 2018;
- Total average of 25 picojoules per floating point operation;
- Approximately 10 billion-way concurrency for simultaneous operation and latency hiding;
- 100 million to 1 billion cores;
- Clock rates of 1 to 2 GHz;
- Multithreaded, fine-grained concurrency of 10- to 100-way concurrency per core;
- Hundreds of cores per die (varies dramatically depending on core type and other factors);
- Global address space without cache coherence; extensions to PGAS (*e.g.* AGAS);
- 128-petabyte capacity mix of DRAM and nonvolatile memory (most expensive subsystem) Explicitly managed high-speed buffer caches; part of deep memory hierarchy;
- Optical communications for distances > 10 centimeters, possibly intersocket;
- Optical bandwidth of 1 terabit per second;
- System wide latencies on the order of tens of thousands of cycles;
- Active power management to eliminate wasted energy by momentarily unused cores;
- Fault tolerance by means of graceful degradation and dynamically reconfigurable structures Hardware-supported rapid thread context switching;
- Hardware-supported efficient message-to-thread conversion for message-driven computation;
- Hardware-supported, lightweight synchronization mechanisms;
- 3-D packaging of dies for stacks of 4 to 10 dies each including DRAM, cores, and networking.

Because of the nature of the development of the underlying technology most of the predictions above have an error margin of +/-50% or a factor 2 independent of specific roadblocks that may prevent reaching the predicted value».

It is difficult to know the impact of these architecture evolutions on lower-class machines,given the constant observed in the past years: what guides the computer engineering market is not scientific calculation.

As a result, even if a few exceptional machines are built on the basis of leading-edge technologies, it is uncertain whether these technologies will be used in machines dedicated to output. For the volume of this output will not be sufficient to ensure the cost efficiency of their basic components.

Such a strategy, shared by all the continents, is summarized on the following figure, which provides the Japanese government's strategic view of HPC.

Synthesis

The various trends of machine architecture evolutions can be summarized as follows:

- For over ten years, and at least for the coming ten years, the unique route to increase machine performance requires a *constant increase in the parallelization degree, and this at all levels*: in a computational core with *multithreading*, within a processor with several computational cores, and within a computational node with several processors per node. In 2012, this parallelization degree is about one million cores for the first TOP 500 machines, or 100,000 for European machines;
- computational core power will experience only a very slight increase, or even will decrease in order to reduce electrical consumption;
- memory size per core will remain constant, or even will tend to be reduced;

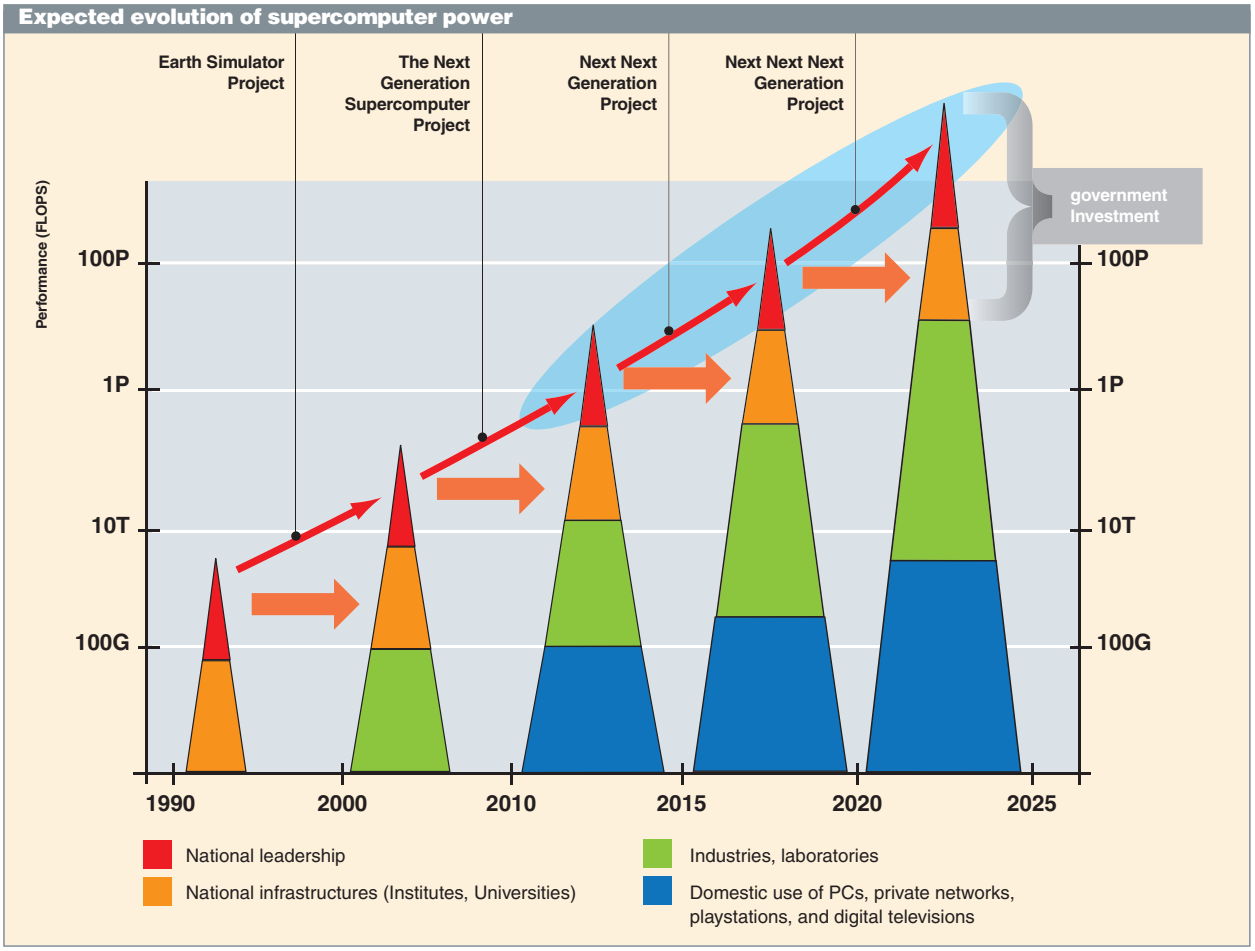

Fig. 97. The Japanese government's strategic view of High-Performance Computing (HPC).

- the type of processor to be used is not clear, and there are still many options: standard Intel processors, or GPUs, or Intel Phi accelerators;

- exascale machines are expected to be available by the end of the next decade, and will be probably reserved to some scientific challenges. Therefore, some exaFLOP systems will presumably coexist with multi-petaFLOP machines. Yet it is hard to say whether architecture homogeneity will be ensured. Will exaflop-related technological choices impose those regarding multipetascale machines?

- whatever the future architectures, taking into account the strong increase in parallelism degree clearly emerges as a *must*.

References

[1] C. Calvin and D. Nowak, "High Performance Computing in Nuclear Engineering", Chapter *in Handbook of Nuclear Engineering*, Springer, 2010.

[2] F. Brown, J. Goorley and J. Sweezy, "Mcnp5 Parallel Processing Workshop", *Workshop M&C 2003*, Gatlinburg, Tennessee, USA, April 6-11, 2003. http://mcnp-green.lanl.gov/publication/mcnp_publications.html

[3] L. Deng and Z-S Xie, "Parallelization of MCNP Monte-Carlo Neutron and Photon Transport Code in Parallel Virtual Machine and Message Passing Interface", *Journal of Nuclear Science and Technology*, vol. 36, nº 7, pp. 626-629, 1999.

[4] T. Goorley, F. Brown, and L. J. Cox, "MCNP5TM Improvements For Windows PCS", *Nuclear Mathematical and Computational Sciences*, Gatlinburg, Tennessee, April 6-11, 2003, on CD-ROM, American Nuclear Society, LaGrange Park, IL, USA, 2003.

[5] J.C. Trama and FX Hugot, "TRIPOLI-4: Parallelism Capability", *ANS Winter meeting*, Washington, DC, USA, November, 11-15, 2007.

[6] J.P. Both, A. Mazzolo, Y. Péneliau, O. Petit, B. Roesslinger, *Notice d'utilisation du code TRIPOLI-4.3 : code de transport de particules par la méthode de Monte-Carlo*, rapport CEA-R-6043, 2003.

[7] J.C. Trama, "Overview of TRIPOLI-4.5", *Proceedings of 11th International Conference on Radiation Shielding*, April 13-18, 2008, Callaway Gardens, Pine Mountain, Georgia, USA, 2008.

[8] F.X. Hugot, Y.K. Lee and F. Malvagi, "Recent R&D around the Monte-Carlo code Tripoli-4 for criticality calculations", *Proceedings of PHYSOR 2008 Conference*, Interlaken, Switzerland, September 14-19, 2008.

[9] P. Hellekalek, "Don't trust parallel Monte-Carlo!", *ACM SIGSIM Simulation Digest archive*, vol. 28, Issue 1 (July 1998), 1998.

[10] T.G. Lewis and W. H. Payne, "Generalized Feedback Shift Register Pseudorandom Number Algorithm", *Journal of the ACM*, vol. 20 (July 1973), Issue 3, pp. 456-468, 1973.

[11] R. Procassini, M. O'Brien and J. Taylor, "Load Balancing Of Parallel Monte-Carlo Transport Calculations", *M&C 2005*, Avignon, France, Septembre 12-15, 2005.

[12] P. Romano, B. Forget, F. Brown, "Towards Scalable Parallelism in Monte-Carlo Particle Transport Codes Using Remote Memory Access," *Proc. SNA + MC2010*, Tokyo, Japan, October 17-20, 2010.

[13] C. Calvin, "HPC Challenges for Deterministic Neutronics Simulations Using APOLLO3® Code", *Progress in Nuclear Science and Technology Journal*, 2, pp. 7007-705, 2011.

[14] J.M. Do *et al.*, "Fuel loading pattern for heterogeneous EPR core configuration using a distributed evolutionary algorithm", *Proceedings of M&C 2009*, Saratoga Springs, New York, USA, May, 3-7, 2009.

[15] H. Golfier *et al.*, "APOLLO3: a common project of CEA, AREVA and EDF for the development of a new deterministic multi-purpose code for core physics analysis", *Proceedings of M&C 2009*, Saratoga Springs, New York, USA, May, 3-7, 2009.

[16] B. F. Smith, P. Bjorstad and W. Gropp, *Domain Decomposition – Parallel Multilevel Methods for Elliptic Partial Differential Equations*, Cambridge University Press, 1996.

[17] R. Roy and Z. Stankovski, "Parallelization of neutron transport solvers", *Recent Advances in Parallel Virtual Machine and Message Passing Interface*, LCNS, vol. 1332, pp. 494-501, 1997.

[18] E. Jamelot, J. Dubois, J-J. Lautard, C. Calvin, A-M. Baudron, "High Performance 3d Neutron Transport On Petascale And Hybrid Architectures Within APOLLO3® Code", *M&C 2011*, Rio de Janeiro, Brésil, May 2011.

[19] M. Zeyao and F. Lianxiang, "Parallel Flux Sweep Algorithm for Neutron Transport on Unstructured Grid", *The Journal of Supercomputing*, vol. 30, issue 1, 2004.

[20] Z. Stankovski, A. Puill, L. Dullier, "Advanced plutonium assembly parallel calculations using the APOLLO2 code", *M&C 97*, Saratoga Springs, NY, USA, 1997.

[21] J. Ragusa, "Application of Multithread Computing and Domain Decomposition to the 3-D Neutronics FEM Code CRONOS", *International Conference on Supercomputing in Nuclear Applications*, Paris, France, Sept. 2003.

[22] J. Ragusa, "Implementation of Multithreaded Computing in the Neutronics FEM Solver Minos", *Proceedings of the ANS Mathematics and Computations International Conference*, Gatlinburg, Tennesse, April 2003.

[23] P. Guérin, A-M Baudron and J-J. Lautard, "Domain decomposition methods for core calculations using the MINOS solver", *M&C + SNA 2007*, Monterey, California, April 15-19, 2007, on CD-ROM, American Nuclear Society, LaGrange Park, IL, 2007.

[24] G. E. Sjoden, *PENTRAN: A parallel 3-D S_N transport code with complete phase space decomposition, adaptive differencing, and iterative solution methods*, Thesis (PhD). The Pennsylvania State University, Source DAI-B 58/05, p. 2652, Nov. 1997.

[25] J.J. Herrero, C. Ahnert, J.M Aragonés, "Spatial Domain Decomposition for LWR Cores at the Pin Scale", *ANS Winter meeting*, Washington, DC, USA, November, 11-15, 2007.

[26] P. Guérin, A-M Baudron and J-J. Lautard, "Component mode synthesis methods applied to 3D heterogeneous core calculations, using the mixed dual finite element solver MINOS", *PHYSOR 2006*, Vancouver, Canada, September 10-14, 2006.

[27] M. Dahmani and R. Roy, “Scalability Modeling For Deterministic Particle Transport Solvers”, *International Journal of High Performance Computing Applications*, vol. 20, nº 4, pp. 541-556, 2006.

[28 G. Wu and R. Roy, “Parallelization of Characteristics Solvers for 3D Neutron Transport”, *Recent Advances in Parallel Virtual Machine and Message Passing Interface*, LCNS, pp. 344-351, 2001.

[29] M. Dahmani and R. Roy, “Parallel solver based on the three-dimensional characteristics method: Design and performance analysis”, *Nuclear Science and Engineering*, 150 (2), pp. 155-169, 2005.

[30] J. Han Gyu *et al.*, “Methods and performance of a three-dimensional whole-core transport code DeCART”, *PHYSOR 2004*, Chicago, Illinois, April 25-29, 2004, on CD-ROM, American Nuclear Society, Lagrange Park, IL, 2004.

[31] G. Palmiotti *et al.*, “UNIC: Ultimate Neutronic Investigation Code”, *M&C + SNA 2007*, Monterey, California, April 15-19, 2007, on CD-ROM, American Nuclear Society, LaGrange Park, IL, 2007.

[32] F. Coulomb, “Parallelization of the DSN Multigroup Neutron Transport Equation on the CRAY-T3D using CRAFT”, *Proceedings of the Eighth SIAM Conference on Parallel Processing for Scientific Computing*, PPSC, 1997.

Christophe Calvin
Department for Systems and Structures Modeling

Qualification and Experimental Neutronics

Ensuring Neutronics Computational Tools Quality

The Verification, Validation and Qualification Approach

The Verification, Validation and Qualification (VVQ) approach of a scientific computational tool is a process which consists in evaluating its ability to predict real phenomena for a defined scope. In particular, it aims at reaching uncertainty quantification, and controlling computational biases associated with quantities used and/or obtained in the studies carried out with this tool.

Two conventional steps: code verification and validation

- **The first step is that of verification***: the goal of this approach is to ensure that the equations of the physical model used in the computational code are correctly solved from the mathematical, numerical and computer viewpoint. The approach may concern one, several, or the whole physical phenomena treated. Verification may include a comparison with calculation cases which can be solved analytically, or have been solved by a reference code. The latter is trusted because it has already followed the different steps of the VVQ approach successfully. In the specific case of neutronics, the availability of two major types of independent computational tools (deterministic codes and Monte-Carlo codes, as explained *supra*, pp. 125-142) makes verification easier, through cross-comparisons between calculations. As part of this verification step, the accuracy of the code's input data does not have a crucial importance: it is sufficient that these data be identical in the compared calculations.

- **The second step is that of validation***, an approach to ensure that, after due verification of the code at a previous step, experiment is reproduced by the results of a numerical simulation arising from this code. The two characteristics tested in this step are the quality of input data and the extent of the validity domain V of the model within the space of its parameters (Fig. 98). This validity domain is the intersection of the relevance domain P of the model (that in which the model's approximations are assumed to be valid), and of the E domain, in which it has been successfully compared with experiment. The higher the validity domain V, the more validation is trusted. As opposed to the verification step, the quality of input data is here of prime importance. In the specific case of neutronics codes, comparison with experimental results highlights the importance of nuclear data.

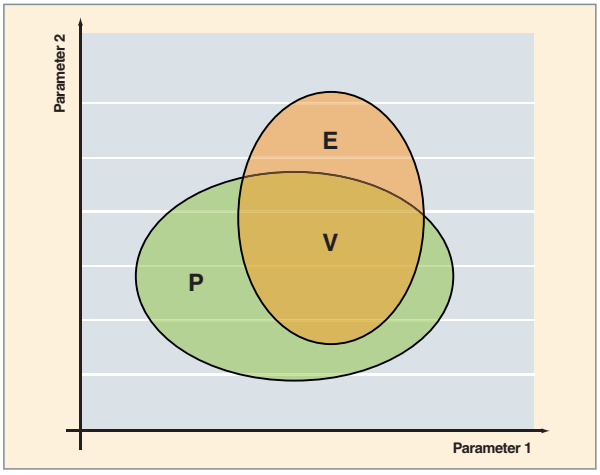

Fig. 98. A computational code is characterized by its relevance domain P within the space of its input parameters. It is confronted to experiment in a domain E, and validated in the domain V, the intersection of the P and E domains.

One peculiarity of neutronics lies in that Monte-Carlo codes can be used as a reference code. This is why the comparison with these Monte-Carlo codes is sometimes named "numerical validation", especially as relatively complex calculations are being implemented (chaining of solvers and deterministic physical models).

A third step: computational code package* qualification

- **The qualification* of a computational code package (computer code, calculation schemes, and associated input data)** is the whole of the processes allowing a computational code and its basic data to be deemed as "good for service", within the limits of a defined validity domain V and with controlled uncertainties (Fig. 99). Such processes include proofs of the quality of basic data, as well as the code's verification and validation established during the two previous steps.

What is mentioned above is general, and could be applied to any computational code. In the special case of neutronics codes, input data are displayed under a particularly complex code package, mainly because neutron cross sections

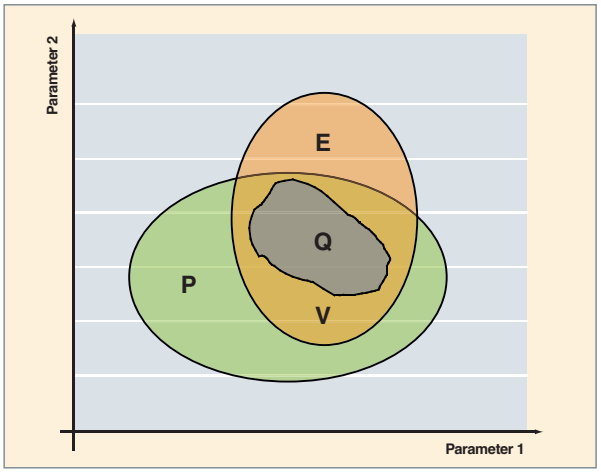

Fig. 99. A computational code package is qualified in the space of its input parameters, within its qualification domain Q. This domain, more limited than the validity domain V of the code used, is that in which computational uncertainties are deemed to be acceptable given the use considered for the computational code package.

strongly depend on the neutron energy (see *supra*, pp. 65-72). The quality proofs of these data are of prime importance, for in most current neutronics calculations; uncertainties about basic nuclear data represent the main source of uncertainty.

A major point of the VVQ approach: quality proofs of nuclear data

The proofs of nuclear data quality are obtained by interpreting experimental results from two types of so-called "integral" experiments of quite a different nature:

- The so-called "**separate-effect** integral experiments", also called "separate-effect analytical experiments" (*e.g.* oscillation experiments in the MINERVE reactor, or spectrum index measurements in MINERVE/EOLE/MASURCA). These experiments are devoted to improving knowledge of nuclear data about a particular nucleus. For example, such measurements can bring information about averaged cross sections on an energy spectrum of the incident neutron. They play a crucial role, for they are complementary of differential microscopic measurements (see the chapter dealing with nuclear data in this Monograph);

- Integral measurements focused on **global effects** (*e.g.* in research nuclear reactors such as ÉOLE and MASURCA, or in a power reactor). The aim is to measure critical sizes of experimental lattices, including absorber rod weight, critical concentrations of soluble absorbers, temperature coefficients (fuel or moderator), power distributions, or even kinetic parameters. These experiments display a higher number of degrees of freedom (*i.e.* a higher number of parameters and/or isotopes) than the analytical experiments previously presented. They provide information about the quality of a full library of nuclear data.

In most of these cases, which refer to "simple" experimental situations, result interpretation is achieved through Monte-Carlo calculations, for which calculation biases are assumed to be known. The calculation-measurement discrepancy can then be directly assigned to the involved nuclear data.

Quantifying neutronics calculation uncertainties

Computational code packages* used in neutronics are dedicated to a specific use for a given **reactor type***. They consist of the neutronics code, the useful input data, and the calculation schemes considered for using the code. The goal of computational code package quantification is to provide, for a given design (PWR, BWR, fast neutron reactor, naval propulsion reactor…), a "nuclear data library, computational code, model choice in the code, definition of calculation succession (chaining)" set, as well as an evaluation of uncertainties in computational results.

Within this framework, a modeling step is undertaken, including various choices: space (geometry) meshing, energy (cross section) meshing, solver choice, nuclear data (libraries), chaining of the various computational steps, in relationship with the aimed target (predesign, reference calculation, design calculation…). These calculation schemes are then verified through comparisons with reference calculations, hence the evaluation of the computational biases linked with the used methods.

Finally, validation is performed by using a high number of integral experiments so as to cover at best the scope associated with the reactor project. So it is crucial to correctly define the qualification experimental base, referring to critical mockups (*e.g.* ÉOLE, MASURCA, and MINERVE) and research nuclear reactors (*e.g.* MÉLUSINE, **OSIRIS***, JHR, and RES), and power reactors (typically, the EdF fleet reactors, Phénix, SPX…), selecting the representative experiments likely to validate the modeling of each parameter. If this base does not cover the scope of interest, then new experimental programs are designed so as to ensure a better coverage of this scope through their good representativeness.

Then comes the indispensable step of quantifying uncertainties that originate in the following items:

- The choice of the physical model, which by definition consists in a simplified representation of simulated physical phenomena; in order to evaluate the systematic uncertainty brought by these approximations or simplifications, a comparison can be done with a Monte-Carlo type reference calculation;

- numerical calculation, which bears systematic uncertainties related to solving the physical model's equations; in order to evaluate the latter, meshes are refined, and convergence is enhanced;

- technological data relating to the reactor investigated (*e.g.* reactor geometry as well as fuel composition are known only within some accuracy);

- nuclear data, arising from experiments or theoretical models which are by themselves uncertain.

These last two sources of uncertainties with regard to the calculation input data may be of systematic or stochastic nature. Generally, in order to evaluate their importance, a sensitivity analysis is carried out. It is often the uncertainty about nuclear data which predominantly contributes to the overall uncertainty about the neutronics calculation. With a view to contributing in the evaluation of computational uncertainties for an industrial nuclear reactor core, benefiting from rich experimental bases and from comparisons with reference calculations, it is indispensable to use all or part of the uncertainty analysis resulting from these calculations of "simple" situations. This step, referred to as "transposition", is more or less complex to achieve; it is of prime importance to evaluate the impact of nuclear data uncertainties on neutronics calculation results.

So it is understandable that there is a feedback between nuclear data, codes, and experiments dedicated to validation. This feedback is illustrated in the following schemes (Fig. 100) that summarize the steps of the VVQ approach: establishing data, verifying and validating computational codes, and qualifying computational code packages for a dedicated, specific purpose.

The results computed using this computational code package are confronted with the experimental results collected on a set of experiments, selected so as to best represent the diversity of the configurations met, so that:

- The computational code may be questioned, which entails a corrective action;

- basic physical data can be considered again, with a re-evaluation of the cross sections from the international benchmarks used;

- the experiment may be questioned.

Uncertainty propagation, sensitivity calculations

Several methods of uncertainty propagation are available. An often used computational formalism is the one based on a Taylor development of the first order of the physical quantity of interest G in the neighborhood of the average value of the X parameters it depends on [1]. This formalism may be formally represented by the following mathematical expression:

$$\mathrm{Cov}\,G = {}^{t}S_{G/X}.\mathrm{Cov}X.S_{G/X}$$

where:

- $S_{G/X}$: is the sensitivity vector of the physical quantity G with respect to X parameters. G sensitivity to the variation of X parameters is expressed by the partial derivative vector $\partial G/\partial X$, also called **sensitivity profile***;

- ${}^{t}S_{G/X}$: transposed from $S_{G/X}$;

- Cov$X$: is the variance-covariance matrix of X parameters; it contains the uncertainty data about the X parameters as well as their correlations, to be propagated on G;

- Cov$G$: is the resulting variance-covariance matrix related to the G quantity: the Cov$G$ diagonal contains the uncertainty values of interest.

When G is analytically expressed as a function of X, it is possible to directly obtain the *sensitivity profiles* by derivation. In the general case, the *sensitivity profiles* are deduced from solving the **adjoint equation*** of that fulfilled by the quantity of interest G.

In neutronics, this typical formalism (sometimes brought to a higher order) has been introduced in deterministic transport codes and burnup codes (*cf.* References [2] to [5]).

The probabilistic Monte-Carlo method allows three-dimensional error propagation calculations to be performed, using the *correlated sampling method* [6], [7]. It is shown that the impact on the quantity of interest G of the variation in one or several parameters X appears as a multiplicative factor of the G estimator, so that in a same simulation it is possible to assess G and the perturbation impact on this same quantity. In addition to its three-dimensional feature, the advantage of the correlated sampling method lies in that it allows low and relatively high variations on the X parameters, going up to several dozen percents.

Within the framework of this probabilistic approach, it is still possible to introduce the *Taylor series expansion* of the physical quantity of interest in order to calculate sensitivity coefficients using the Monte-Carlo method [7], [8], and reuse them according to the first- or second-order deterministic formalism.

A third approach consists in directly sampling the X parameters with a Monte-Carlo method according to the probability density of the uncertainty related to them (*e.g.* a Gaussian den-

...

sity), and computing the value of the corresponding G quantity. Repeating this operation a sufficient number of times results in getting a probability distribution of quantity G, from which the average value and the related variance can be deduced. This approach exhibits a higher cost in computational time, and yet brings much more information, since it gives access to the statistical distribution of G. In nuclear reactor physics, this stochastic approach is implemented on the URANIE platform [9] developed at the CEA.

It must be pointed out that taking into account correlations between the various X parameters adds a further degree of difficulty in uncertainty propagation calculation relating to a both comprehensive and overall approach [10].

Treating uncertainties is a crucial R&D area due to its safety stakes and economic impacts. It has been the topic of numerous works, seminars, and summer schools, with the joint contribution of research scientists of various backgrounds, inducing tests of new approaches such as "chaos polynomial models" [11].

References

[1] D. L. Smith, *Probability, Statistics, and Nuclear Uncertainties in Nuclear Science and Technology*, OECD Nuclear Energy Agency, Nuclear Data Commitee Series, Neutron Physics and Nuclear Data in Science and Technology, vol. 4, 1991.

[2] A. Kodeli, *Études des incertitudes sur la fluence dans les cuves des REP – Ajustement des données de base*, Note CEA-N-2749, janvier 1994.

[3] J. M. Kalfez, G.B. Bruna, G. Palmiotti, M. Salvatores, "Burnup Calculations with Time-Dependent Generalized Perturbation Theory", *Nuclear Science and Engineering*, 62, 1977, p. 304.

[4] J. Rebah, Y.K. Lee, J.C. Nimal, B. Nimal, B. Duchemin, L. Lunéville, "Sensitivity and Uncertainty Analysis for Fission Product Decay Heat Calculations", *Proceedings of the 8th International Conference on Radiation Shielding*, April 24-28, 1998, Arlington, USA, pp. 84-91, 1994.

[5] A. Gandini, "A Generalized Perturbation Method for Bi-linear Functionals of the Real and Adjoint Neutron Fluxes", *J. Nuclear Energy*, 21, 755-765, 1967.

[6] G. Dejonghe, J. Gonnord, J.C. Nimal, "Perturbation Calculations by the Correlated Samples Method", *Proceedings of the International Meeting on Advances Nuclear Engineering Computational Methods*, Knoxville, Tennessee, April 9-11, 1985, vol. 2, 1985.

[7] H. Rief, "Generalized Monte-Carlo Perturbation Algorithms for Correlated Sampling and Second Order Taylor Series Approach", *Annals of Nuclear Energy*, vol. 11, n°9, 1984, pp. 455-476.

[8] B. Morillon, *Perturbation dans le transport des neutrons par la méthode de Monte-Carlo*, Note CEA-N 2838, octobre 1998.

[9] J.P. Both, "Treatment of Cross Section Uncertainties in the transport Monte-Carlo Code TRIPOLI-4", ICRS'9, Tsukuba, Ibaraki, Japan, October 17-22, 1999, *Journal of Nuclear Science and Technology*, Supplement1, pp. 420-426, March 2000.

[10] A. Boulouré, C. Struzik, F. Gaudier. "Uncertainty and sensivity analysis of the nuclear fuel thermal behavior". *Nuclear Engineering and Design*, 253, pp. 200-210, 2012.

[11] O. Leray, *Détermination, maîtrise et réduction des biais et incertitudes de la réactivité du Réacteur Jules Horowitz*, Thèse de Doctorat en Sciences, Université de Grenoble, 25 septembre 2012.

[12] J. M. Martinez, "Analyse d'incertitudes, Modèles simplifiés par polynômes de chaos", Séminaire incertitude de Bruyères le Châtel, 23 avril 2006.

Bibliography

Cacuci (D.), *Uncertainty and sensitivity analysis*, USA, Chapman and Hall/CRC, 2003.
http://www.oecd-nea.org/science/wpec/sg33/methods/SU_References.pdf

Usachev (L.N.), *Proc. Int. Conf. On Peaceful Uses of Nucl. Energy*, Geneva, vol. 5, 503, 1955.

Weinberg (A.) et Wigner (E.) *The Physical theory of neutron chain reactor*, The University of Chicago Press, 1958.

Williams (M.L.), "Development of depletion perturbation theory for coupled neutron/nuclide fields", *Nuclear Science and Engineering*, 70, 20-36,1979.

Takeda (T.) and Umano (T.), "Burnup sensitivity analysis in a fast breeder reactor – Part I : sensitivity calculation method with generalized perturbation theory", *Nuclear Science and Engineering*, 91, 1-10, 1985.

Rimpault (G.) *et al.*, " Methodology for a Large Gas-Cooled Fast Reactor Core Design and Associated Neutronic Uncertainties " *Proc. Int. Conf. PHYSOR'2004*, Chicago, USA, 04/2004.

Archier (P.) *et al.*, "Nuclear data uncertainty propagation for neutronic key parameters of CEA's SFR v2b and CFV sodium fast reactor designs", *Proc. Int. Conf. PHYSOR 2012*, Knoxville, USA, 2012.

Fig. 100. The steps of the VVQ approach: establishing data; verifying and, then, validating computational codes; and qualifying computational code packages for a dedicated, specific use.

As mentioned above, the Monte-Carlo method availability to neutron physicists to verify deterministic calculations is an asset frequently used for the past few years. Using the latest computational resources (HPC, see *supra*, the chapter devoted to High-Performance Computing) as well as the Monte-Carlo method has induced qualitative jumps with respect to accuracy and analysis.

Thanks to the joint use of Monte-Carlo / HPC / accurate measurements, the impact of nuclear data can be assessed, and so it is of the impact of modeling biases by comparing Monte-Carlo / deterministic methods, providing the nuclear data used in both computing systems is fully consistent. Furthermore, the Monte-Carlo code used as a reference must have undergone the whole VVQ process above mentioned.

In order to complete the verification, validation and qualification approach, benchmarks can be carried out to get an estimate of neutronics calculation uncertainties (see the recent international benchmarks mentioned hereafter). These benchmarks are an integral part of the approach for qualifying a computational code package, for they contribute to enhance trust in the computational codes and code packages used.

Bibliography

Oberkampf (W. L.), Trucano (T. G.), Hirsch (C.), "Verification, validation, and predictive capability, in computational engineering and physics", *Computational Engineering and Physics, Appl. Mech. Rev.*, vol. 57, n° 5, September 2004.

Orlov (V. V.), Van'kov (A. A.), Voropaev (A. I.), Kazanskij (Y. A.), Matveev (V. I.), Mugorov (V. M.) et Khodarev (E. A.), "Problem of fast reactor physics related to breeding", *Atomic Energy Review*, vol. 4, n° 118, pp. 989-1077, 1980.

Rider (W. J.), Kamm (J. R.) and Weirs (V. G.), *Verification, Validation and Uncertainty Quantification Workflow in CASL*, SAND2010-234P, December 2010.

Bernard Bonin,
Nuclear Energy Division
Cheikh M. Diop, Anne Nicolas
Department for Systems and Structures Modeling
and Cyrille de Saint-Jean
Reactor Study Department

Experimental Neutronics. Experiments in Critical Facilities

Background and needs in experimental neutronics

Since the early age of nuclear reactor history, experiment has constantly accompanied computational modeling. Although neutronics relies on equations perfectly representative of the phenomena involved, the amplitude of energy ranges, the multiplicity of materials and of their characteristics, and the geometrical complexity of cores make it indispensable to carry out experimentation on reactors in order to qualify the whole of physical data and computational models. So will it be in the future, especially in the case of computational models designed to be applied to new, or little used, neutronic configurations.

The CEA ensures the qualification of basic data and of neutronics computational code packages thanks to the design and achievement of experiments on three Zero Power Reactors, also called "**critical facilities**", or "**mockups***" (or *Zero power reactors* [ZPR]), set up at Cadarache: ÉOLE, MINERVE and MASURCA, described in detail in the DEN Monograph "Research Nuclear Reactors".

These critical facilities are reactors in which very low powers are involved. They display a neutronic behavior likely to be extrapolated to basic physical phenomena encountered in power reactors, thanks to the linearity of the Boltzmann equation prevailing in neutron transport.

However, this is true only under certain conditions: coupling neutronics with thermal-hydraulics (especially through temperature) destroys the linearity of phenomena. Of course this effect limits the extrapolative feature of critical facilities results, but, for all that, does not cancel their interest for separate-effect experiments, particularly for nuclear data qualification.

These facilities are flexible, adaptable, of easy access, and easy to instrument. A detailed description of these experimental devices can be found in the DEN Monograph "Research Nuclear Reactors".

The ÉOLE critical facility, of very low power (<100 W), is dedicated to neutronics studies of moderated light water **lattices***, especially those of Pressurized Water Reactors (PWRs), as well as of Boiling Water Reactors (BWRs) [Fig. 101].

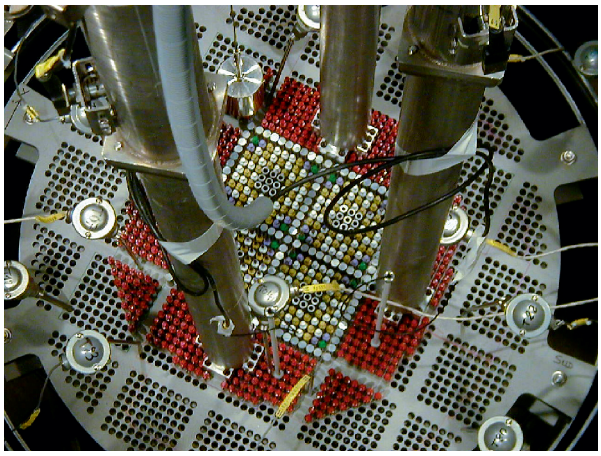

Fig. 101. View of the FUBILA 100% MOX ABWR core configuration in the ÉOLE critical facility.

Its central component is a vessel of 2.3 m in diameter and 3 m in height. At the center, another smaller vessel (~1 m in diameter and 1 m heigth) can house any type of water reactor lattice thanks to a set of interchangeable grids. **Reactivity*** can be controlled at any moment through four safety rods.

Criticality* is reached by adjustment of soluble boron concentration in the moderator (light water), or by adjustment of the number of fuel rods. Divergence is achieved, and power can be stabilized between 0 and 100 W (maximum authorized power) with the help of a fine control rod.

A large number of fuel types (UO_2, PWR and BWR type MOX), and absorbing materials, poisons, or structural materials (natural and enriched B_4C, AIC, Hf, UO_2-Gd_2O_3, pyrex, Zy-2, steel…) can be used. Due to the experimental techniques used and its almost unique flexibility, ÉOLE stands as a rare, efficient tool dedicated to light water reactor physics.

The MINERVE reactor is a pool reactor, in which the very low power (< 100 W) core, immersed under 3 m of water, consists of high-enriched metal uranium plates (Fig. 102). At the center of this "driver" core, a cylindrical cavity houses experimental lattices to be studied. Several types of lattices can so be investigated, thereby allowing generation of neutron spectra representative of **fast neutron***, **epithermal neutron***, **thermal neutron***, and very thermal neutron reactors. At the center of the cavity, a special apparatus, called an "oscillator", is used to measure reactivity on specific specimens with the help

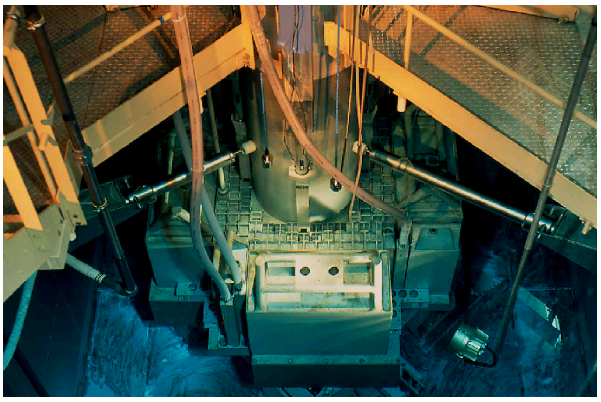

Fig. 102. Overview of MÉLODIE core in MINERVE pool.

of a rotative control system used to compensate for changes in reactivity (the rotation angle of this system's absorbing parts is proportional to the reactivity introduced in the core). Reactivity effects varying from 0.1 to 10 **pcm*** can be measured with this tool, with a precision of about 0,01 pcm.

The MASURCA reactor, of low power (< 5 kW), is dedicated to neutronics studies of **fast neutrons***, or epithermal neutrons reactors (Fig. 103).

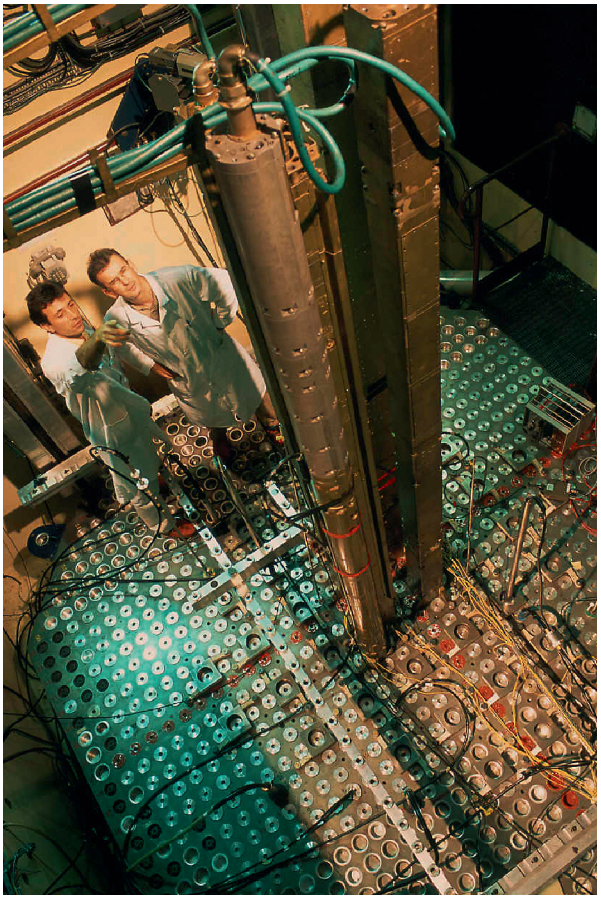

Fig. 103. Two experimentalists on the MASURCA reactor roof.

This reactor is of a "Meccano®" type. It can contain cores with a volume up to 6 m^3, and consists of square-section tubes individually loaded with fuel or coolant rodlets or platelets representative of fast or epithermal neutron lattices to be investigated.

This facility can help study a quasi-infinite number of combinations and solutions representative of the problems to be treated (MOX, metal Pu, depleted, natural and enriched UOx, thorium, graphite, gas, sodium, lead, steel, ferrite, CaH_2, ZrH_2…). This facility, which displays high flexibility in loading and operation, allows the validation of innovating core alternatives for fast or epithermal neutron reactors, such as **GFRs***, **HTRs***, and **hybrid systems***.

Critical facilities and integral experiments

The design of an **integral experiment*** aims at making this experiment as representative as possible with respect to the expressed qualification needs (computational tools and nuclear data libraries for a given type of reactor). It also uses chained *sensitivity calculations* and *uncertainty calculations*.

Two types of integral experiments can be distinguished. "Fundamental"-type experiments aim at qualifying nuclear data libraries by measuring fundamental parameters, such as **multiplication factors*** k_{eff}, **spectrum indices***, **cross sections***, U 238 **conversion factor***, **temperature coefficient***, or **effective delayed neutron fraction*** β_{eff}. "Mockup"-type experiments aim at qualifying calculation methods as a whole (code and nuclear data library), through project parameters such as reaction rate distributions, soluble boron efficiency, control rod cluster worth, or **void coefficients of reactivity*** (sodium or void).

Conducting experimental programs in neutron physics implies using a number of experimental techniques to get the various physical parameters to be used for **computational code package*** qualification, together with its uncertainty. These techniques can be classified into three main families:

- Measuring techniques to determine absolute **reactivity*** (reactivity scale) or relative reactivity (difference between two levels of reactivity);
- *"in-core"* or "post-irradiation" measuring techniques to determine absolute or relative (level of perturbation) **reaction rate*** and **flux*** distributions;
- measuring techniques to determine absolute or relative *gamma* or neutron **doses***.

For each parameter or phenomenon measured, several experimental techniques have generally to be used simultaneously in order to get and manage the related **target uncertainty***.

Determining experimental parameters requires control of systematic and statistical experimental uncertainties. The simultaneous use of several measuring techniques allows a decrease in the systematic term of the uncertainty. The achievement of several series of measurements with the same experimental technique, as well as the intrinsic improvement of this technique make it possible to decrease the statistical term of the uncertainty.

Fission chambers to measure neutron flux in research nuclear reactors

The so-called *"in-core"* measuring techniques are based on the use of neutron detectors referred to as **fission chambers*** (Fig. 104). The interest of these small-sized detectors lies in getting local measures of neutron flux with an accurate positioning.

A fission chamber consists of a leaktight enclosure filled with inert gas (generally argon), inside which two electrodes are placed, one of which, the anode, bears a fissile material lining characterizing the chamber (U 235, Pu 239, Pu 241…). The general features of a fission chamber are as follows:

- Bias voltage: 50 - 500V
- Gas pressure: 5 - 20 bars;
- Lining thickness < 1mg/cm^2.

During fission, a high number of orbital electrons are ejected so that fission fragments are strongly ionized. One of fission products (the heaviest) is absorbed by the supporting electrode, while the other ionizes the rare gas of the chamber. Charges are collected on the anode, and are transferred along a coaxial cable inside the instrumentation tube so as to generate the measuring signal. So, it is considered as an on-line, *"in core"* measurement, which nevertheless requires an ad hoc

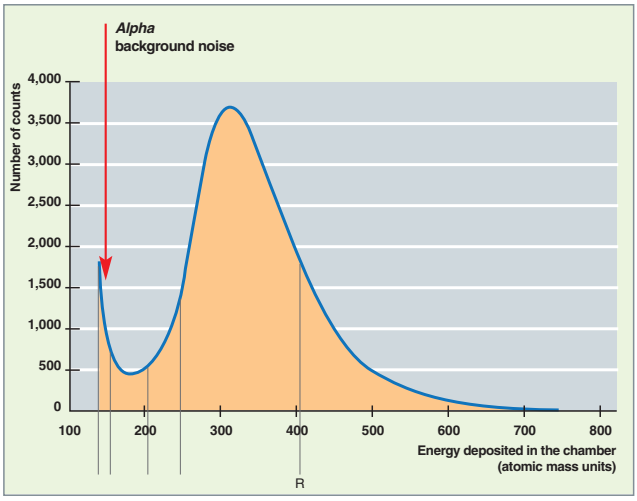

Fig. 105. Example of a PHA (Pulse Height Amplifier) spectrum obtained with a fission chamber. Fission spectrum of a Pu-241-lined chamber in the MISTRAL experiment.

measuring channel (an instrumentation tube through which the measuring sensor can be inserted). This fission chamber is connected with an electronic measuring channel consisting of a pre-amplifier, an amplifier, and a multichannel analyzer so as to get a count spectrum, to be processed in the following step (Fig. 105).

So these on-line measuring methods are used:

- Either for measuring axial or radial reaction rate distributions for a specific nucleus (the doping nucleus of the chamber) (see Fig. 106 on the next page);

- or for measuring spectrum indexes, through the ratio between measures of two reaction rates using two different fission chambers. The various ratios measured allow the neutron spectrum to be characterized; each nucleus used having a specific response to different neutron energies. This type of measures requires a preliminary chamber calibration in a fully thermal neutron flux, obtained through a so-called "thermal column", or in a pure fission spectrum, using a so-called "Mark III" device.

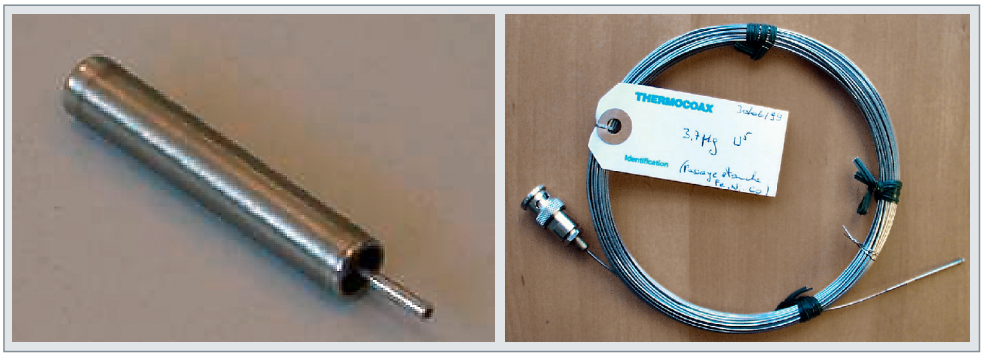

Fig. 104. Miniature fission chambers (4 mm and 1.5 mm).

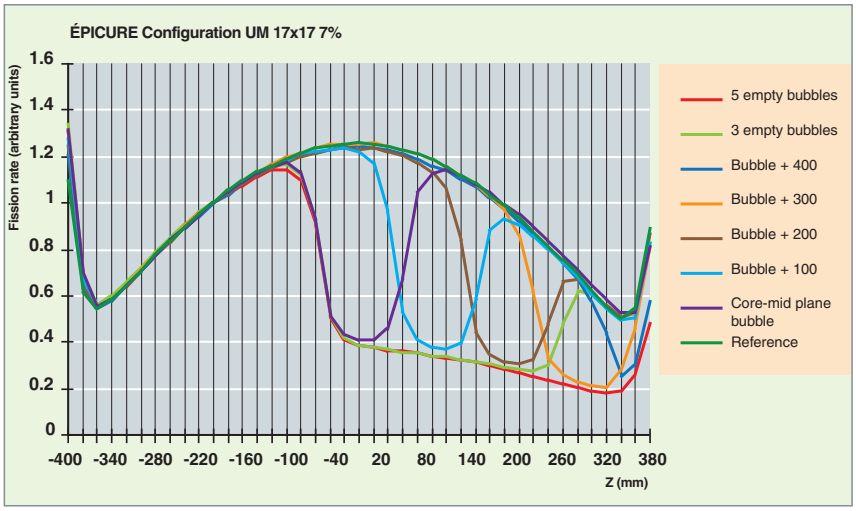

Fig. 106. Fission-chamber measurement of fission rate distribution versus the axial dimension in the ÉOLE core (fissile stack 800 mm high) with a "bubble" axially moving in the center of ÉOLE.

Examples of measuring methods to determine reactivity

Measuring techniques and signal acquisition and processing channels applied to determine **reactivity*** are used to assess the reactivity difference between two given states of one or several configurations, and so to infer reactivity coefficients, or reactivity worth. We shall give four examples below.

- The "critical" measuring technique is based on the knowledge of all of the critical parameters of a configuration (number and type of fuel and absorber rods, concentration in burnable poisons, core geometry, date, and plutonium aging if need be). The time evolution of the neutron population $N(t)$ is measured: as the reactor is slightly supercritical, the neutron population increases exponentially according to the following law:

$$N(t) = N(0)e^{\frac{k-1}{\ell}t}$$

where k is the multiplication factor, and ℓ the average neutron lifetime.

From this measurement, determining the doubling time t_d of the neutron population makes it possible to trace back to the residual reactivity, or excess reactivity, of the configuration under study, with the help of its Nordheim curve $\rho = f(t_d)$, extracted from the inverse kinetics equations.

- The "subcritical" measuring technique uses the Source Amplification Method (SAM). This technique is based on the fact that, for a subcritical state, the product of reactivity by the neutron population is a constant, that is $\rho N = C^{te}$. Reactivity effects related to the introduction of the neutron source are measured by subcritical counting operations on various fission chamber-type monitors, located at different positions in the core so as to limit spatial effects. This counting is then compared to the one obtained in the reference core, and calibrated referring to a well-known/ standard reactivity effect (the fine control rod of the core is generally used to determine the constant). Such a comparison directly provides the variation in reactivity.

- The **kinetic*** measuring technique is based on reactor power follow-up versus time during the motion of an absorber. Inverse kinetics equations then allow determination of the reactivity related to this perturbation, based on the known values of delayed neutron constants and neutron lifetime.

- The so-called "oscillation" measuring technique, which relies on the oscillation of small samples made of the material of interest. This technique is specifically used on the MINERVE reactor, and consists in inducing small periodic perturbations of the neutron population. Experimentally, the material to be investigated is periodically extracted from an oscillation channel placed in the center of the MINERVE experimental zone, and is replaced by a known material. That induces an overall flux perturbation on the whole reactor, resulting in a variation in the neutron population level. It is sensitive to the neutron flux importance in the perturbed area, to the variation in generation and absorption rates, and to the **transfer function*** in the reactor. So, the variation in the effective multiplication factor, induced by the perturbation, provides the variation in reactivity $\Delta\rho$ introduced by the considered sample.

Measurement of the effective delayed neutron fraction

The delayed neutron fraction measurement belongs to the so-called "neutron noise" measurement category. Its relies on measuring neutron fluctuations induced in low-power reactors by random phenomena, such as absorption, neutron leakage, or neutron generation. In the power spectral density (PSD, in French: DSP "*Densité Spectrale de Puissance*") [1], based on the spectrum analysis of neutron fluctuations, it is assumed that the causes of neutron noise are random phenomena likely to be described as Poisson processes, statistically considered as a source of white noise. The spectral density of this noise source is given by the following expression:

$$\left|\overline{\delta s(\omega)}\right|^2 = 2\frac{N}{\Lambda}\frac{\overline{\nu(\nu-1)}}{\bar{\nu}}$$

where N is the neutron "population", and Λ, the neutron generation time, while ν is the number of neutrons emitted by fission.

Point kinetics equations allow the fluctuations δN of the neutron population N in the reactor to be linked to the noise source $\delta s(\omega)$. The related mathematical development is out of the scope of this Monograph. Let us simply mention that the reactor behaves as a high-cut filter with respect to the noise source: the neutron population cannot undergo very fast (*i.e.* high-frequency) fluctuations due to the finite neutron generation time and to the occurrence of delayed neutrons.

Fluctuations in the neutron population fulfill the following equation:

$$\frac{|\delta N(\omega)|^2}{N^2} = 2N\Lambda\frac{\overline{\nu(\nu-1)}}{\bar{\nu}}\frac{1}{(\beta_{eff}-\rho)^2+\omega^2\Lambda^2}$$

So, measuring the neutron population's spectral density, named $DSP \equiv \frac{|\delta N(\omega)|^2}{N^2}$, brings information about the proportion of delayed neutrons, and the neutron generation time.

The measurement of this power spectral density as a function of frequency relies on a technique based on the study of correlations between two fission detections at instants t and $t+T$. The use of two correlated detectors allows the noise of the detector electronic devices to be neglected. This is why the technique is called "correlated power spectral density", or intercompared power spectral density (IPSD). It is implemented using two specific, strongly charged fission chambers, operating in a current mode and placed at the core peripherals, as close to the fuel as possible. Generally, they are placed in symmetrical positions, so as to reduce the detection of uncorrelated events as far as possible.

As the reactor behaves as a filter, the power spectral density displays a low-frequency plateau, its amplitude/level giving the value of β_{eff}. The final expression which ensures the connection between the value of the power spectral density at low frequency and the delayed neutron fraction is the following:

$$DSPI = 2\frac{DV_1V_2}{F}\frac{1}{(\beta_{eff}-\rho)^2}$$

where $\frac{DV_1V_2}{F}$ is a constant which can be determined independently from power spectral density, describing the response of the fission chambers employed for noise measuring, as a function of their operating voltage V_1 and V_2.

The cutoff frequency ω_c of the power spectral density equals to $\frac{\beta_{eff}-\rho}{\Lambda}$. So, this measuring technique not only gives access to the delayed neutron fraction, but also to the neutron generation time Λ.

The previous equations show the interest to achieve delayed neutron measurements as close as possible to criticality, for which the reactivity value is null. Such an approach allows a significant increase in measuring accuracy, while reducing the related uncertainty.

The total uncertainty on the β_{eff} value is about 1.6%, without taking into account the uncertainty coming from the Diven factor D, which contributes by 3% to 1σ on the β_{eff}^2.

As shown in the equations above, the measurement of the effective delayed neutron fraction is intimately connected with the measurement of reactivity ρ : the latter is a dimensionless number, most often expressed in **pcm***, *i.e.* pour cent mille. (10^{-5}) Yet, as delayed neutrons play an important role in reactor control, it is relevant to employ a more physical unit for reactivity: according to a convention issued from the United States, reactivity is expressed in "**dollars***": 1 dollar = 1 * effective *beta*. So, according to this convention, reactivity in "dollar" units equals to:

$$\rho_{\$} = \frac{\rho}{\beta_{eff}}$$

To sum up it all, a reactor will not be prompt critical as long as its reactivity will remain lower than 1 dollar.

It can be said that reactivity ρ expressed in pcm is an absolute value, and that reactivity $\rho_{\$}$ expressed in dollars is a relative value. However, a comparison with simulations can well and truly be performed using reactivity estimations in dollars in as much as the effective *beta* will have been computed in a previous step.

Reaction rate measurement methods

The measuring techniques, together with their signal acquisition and processing channels, can be classified into two types of techniques:

- The so-called *"in core"* (or in-reactor) measuring techniques for real-time determination of reaction rates: measurement is based on a direct characterization of the neutron population, mainly using miniature fission chambers;

- the so-called "post-irradiation" measuring techniques for determining reaction rates: , the measurement is based on the determination of the *gamma* population issued from fission products or activation products decay.

The post-irradiation methods are based on integral and special-peak *gamma-scanning* methods, in which the activity of *gammas* arising from fission or capture is determined through measuring channels, which include semiconductors (diode), a preamplifier, an amplifier and a counting scale.

Thus, a so-called "integral" *gamma-scanning* measurement consists in determining the total activity of fission products *gammas* above a 550 keV energy, thereby taking into account only events proportional to fission (capture, **pair creation***, and ***Bremsstrahlung*** events are not taken into account).

However, this technique requires considering *gamma* activity decay versus time.

The so-called "special-peak" *gamma-scanning* measurement consists in determining the absolute activity of a given *gamma* ray, in order to determine the neutron-induced fission or capture rate (Fig. 107 and 108).

Fig. 107. *Gamma*-spectrometry measurement on critical mockups ÉOLE / MINERVE. Insertion of UO_2 or MOX fuel rods under a germanium diode.

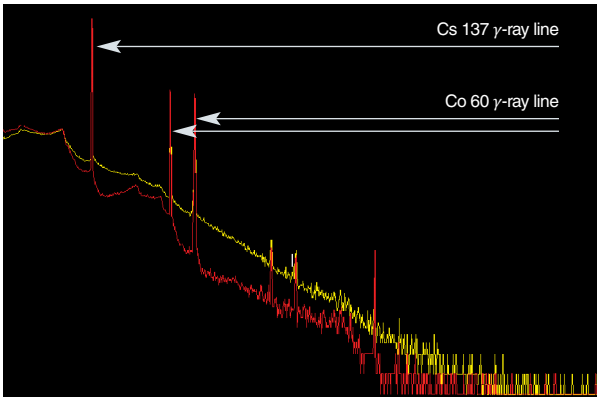

Fig. 108. *Gamma*-spectrometry measurement on a fuel rod. An example of how dead time is taken into account in fission products spectra: the red and yellow spectra have been respectively obtained with and without rejection of pile-up signals in electronic detectors.

These various measuring techniques are mainly used in determining parameters of interest for reactor physics, such as, *e.g.* reactivity effects:

- Absorber (Hf, AIC, natural B_4C, enriched B_4C, $UO_2Gd_2O_3$, …) efficiency;
- control rod cluster efficiency;
- soluble boron differential and integral coefficient of reactivity;
- temperature coefficient of reactivity;
- void coefficient of reactivity.

Apart from reactivity-related parameters, experiments on critical mockups can also help determine other types of parameters such as **spectrum indexes***, or relative (rod-per-rod) power distribution. They can also be used to investigate 2-D and 3-D rod bowing, rod substitution, or void effects.

Finally, experiments on critical mockups bring invaluable information about the quality of neutron cross sections characterizing involved nuclei.

Neutronics calculations compared with experiment in the difficult case of high temperature reactors: the HTTR benchmark

Among the IAEA joint research programs, the CRP-5 (Common Research Program) proposed in 1998 a core physics benchmark relating to the startup steps of the HTTR (High Temperature Test Reactor). This reactor diverged in Japan in November 1998. Built by JAERI (Japan Atomic Energy Research Institute), the HTTR is a reactor moderated with graphite (prismatic blocks) and helium-cooled. The coolant outlet temperature is 950 °C for a thermal power of

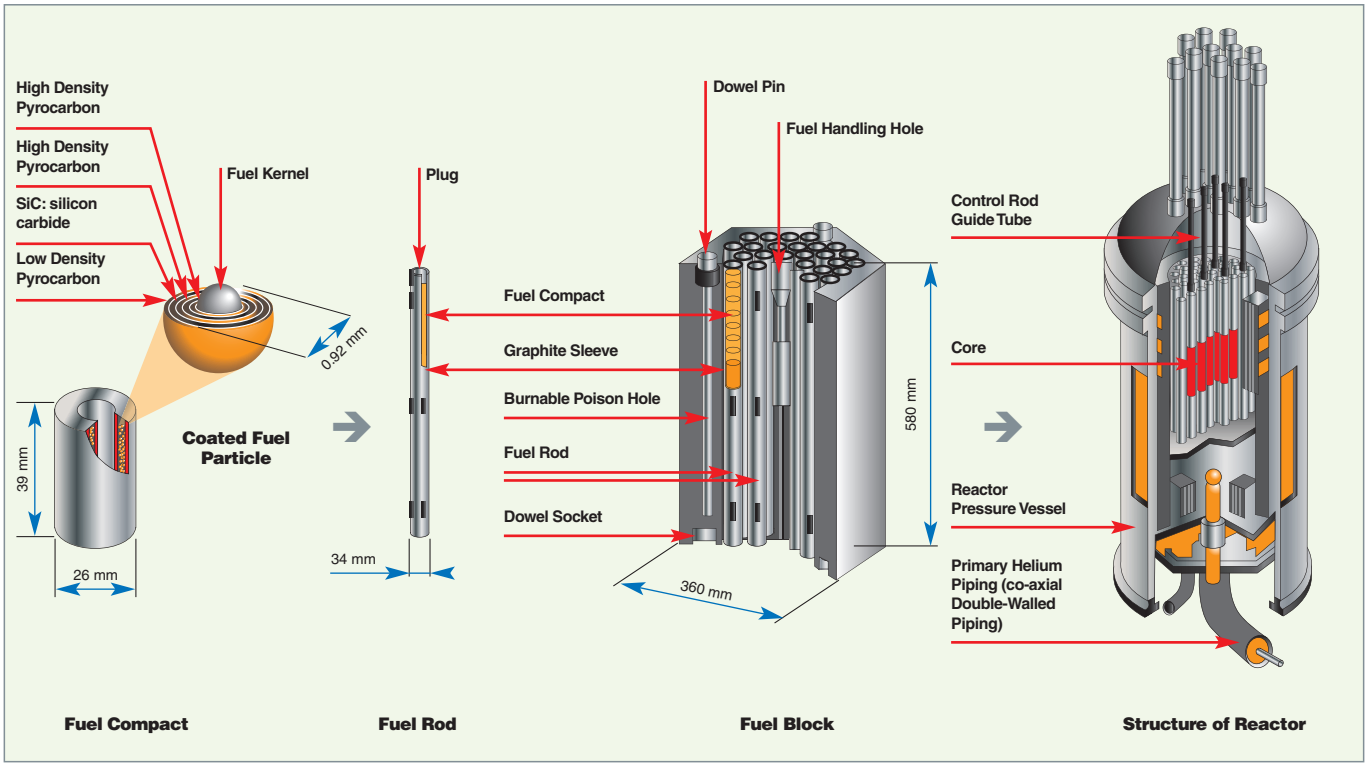

Fig. 109. Cutaway view of the HTTR prismatic fuel block and core.

30 MW. The reactor core dimensions (about 230 cm effective diam. and 290 cm high) approximately correspond to half the size of the VHTR-type gas reactor cores proposed in Generation IV. Figure 109 displays the geometrical features of this type of concept: fuel, contained in embedded, spherical micro-particles, is agglomerated with graphite so as to constitute annular fuel compacts. These fuel compacts are then axially piled up, thereby forming fuel bars, which are inserted in a graphite block 60 cm high. The reactor core consists of these piled-up prismatic fuel blocks.

The computational benchmark proposed by JAERI in 1998 was aimed at evaluating the number of fuel stacks loaded in the core at the first divergence, as well as the excess reactivity of the core in different configurations during fuel loading. Regarding the benchmark-related calculations at the CEA [2], they were carried out with the APOLLO2, CRONOS2 and TRIPOLI-4® codes (see *supra*, pp. 125-142, the chapter dealing with computational tools in this Monograph).

Concerning the calculation of the effective multiplication factor during the different core loading steps, two schemes have been selected. The first computational scheme (APOLLO2 - CRONOS2) is based on the approach used for pressurized water reactor cores, in which the scattering calculation constants are issued from the energy and space homogenization of the fuel assembly calculated in an infinite medium as part of the transport theory. The second scheme (APOLLO2 – TRIPOLI-4®) has been set up for the calculation of the HTTR startup neutronics benchmark.

As far as modeling difficulties are concerned, it is worth to mention that coupling graphite and highly fragmented fuel in this type of reactor maximizes neutron absorption in the **resonances*** of heavy nuclei. As a result, it is rather delicate to choose among the various assumptions issued in treating resonant cross sections (**self-shielding*** calculations). The approximations done in self-shielding models, which result in uncertainties well controlled today in water reactor calculations, may be enhanced in the case of HTRs.

Besides, the choice of helium as coolant results in broad gas flow sections across the core. Now, these gas channels constitute preferential leakage paths (**streaming***) for neutrons having a direction close to that of gas flow, as neutrons can move easily in helium. Treating this leakage in core calculations stands as one of the key problems of modeling in this reactor type, especially for channels in which control rods are inserted.

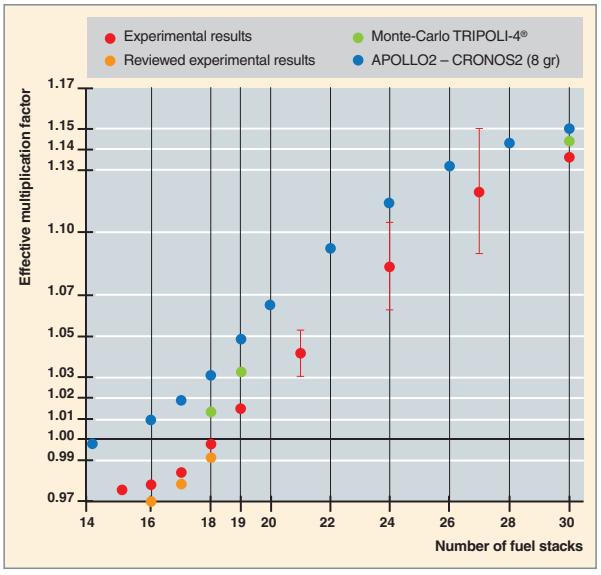

Fig. 110. Evolution of the effective multiplication factor of the HTTR core calculated with various models as a function of the number of fuel elements loaded in the core [2].

As evidenced in the general conclusions of this benchmark, issued from the intercomparison of many calculation results for a full-core configuration (30 fuel stacks), there is a good agreement between the results of deterministic and probabilistic calculations, and experiment (Fig. 110) [3].

In contrast, deviations can be evidenced in intermediate configuration (*e.g.* 20 fuel stacks).

In the annular configuration (18 fuel stacks) close to the first critical state, calculations still overestimate reactivity in contrast with experiment, though to a lesser extent. Monte-Carlo codes at best predict a critical core with 18 stacks, that is with about 600 to 800 **pcm*** of excess reactivity.

Apart from experimental uncertainties (impurities, reactivity measures…), the assumptions generally set forth to explain these deviations are random geometry treatment (particles in compacts) and cross section accuracy. The 3-D neutron scattering calculations performed on an annular-configuration core exhibit a deviation of about 900 pcm with Monte-Carlo calculations, and evidence the limits of applying a two-step deterministic calculation scheme based on a fuel-scale transport calculation and a core-scale scattering calculation.

It will be possible to escape these limitations in the new computer code APOLLO-3®, through a systematic use of the 3D transport.

An illustration of the difficulties inherent to existing multi-scale modeling in a prismatic-block annular reactor, and of the resulting spectral heterogeneity is given through the heat flux distribution map calculation in the full-core configuration (Fig. 111).

The high heat flux gradients observed on the right figure result from the occurrence in the core of many control elements (the latter being prismatic graphite blocks pierced with three cavities for control rod insertion), which play an important role in the slowing-down and thermalization of neutrons generated by fission in fuel elements.

However, the difficulties met in this HTTR annular configuration are not directly transposable to other reactors of the HTR type (GT-MHR, PBMR…). In particular, the startup annular core, very heterogeneous, of low thickness, and fitted with a central reflector, in which the high number of elements with "holes" enhances the streaming effect, is not representative of a power reactor. So, in this respect, the HTTR will remain indeed a reference in terms of modeling difficulties.

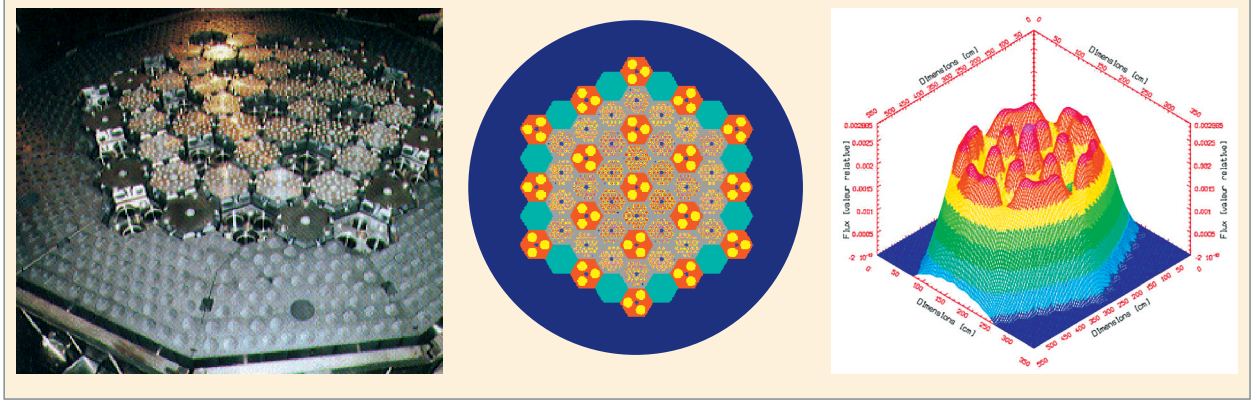

Fig. 111. Thermal flux variation in the HTTR reactor core – Full-core configuration, with all the rods withdrawn.

International benchmark databases

The **validation*** of the code and nuclear data set requires quality experiments. This is why an international effort has been undertaken for the world property of neutronics experiments to benefit to everybody, seeing that each experiment be described as accurately as possible, and be internationally reviewed by peers before being integrated in the international base. A standardized experiment, the results of which are interpreted by the international community before being recorded in an international database, is what specialists call a "**benchmark***".

The benchmark description is standardized with guides specific to each experimental field. The benchmark starts with a detailed experiment and facility description, including photographs, schematics, tables of numerical values, and texts explaining experimental data in detail. For instance, in the criticality field, the benchmark first includes the description of the geometry and materials likely to lead to a critical state. Experiment results are then considered as a second step. An evaluation of experimental data is carried out, in which the various, especially technological, uncertainties are discussed. Later on, the evaluator recommends, and justifies, simplifications, hence the generation of one or several models: this is the benchmark specifications step. Finally, as all this evaluation work can but use transport codes, the corresponding computational results are provided. Each database is distributed in electronic form, in a pdf format.

Benchmark experiments benefit from a fine evaluation of experimental uncertainties, especially those relating to geometry and materials compositions. Knowing the uncertainty about integral quantities is crucial for transport code validation and the improvement of nuclear data (see *supra*, p. 165). A guide applicable to the different data bases *(ICSBEP Guide to the Expression of Uncertainties)* defines the framework of experimental uncertainty evaluation.

Three broad categories of experiments result in computerized databases: criticality, reactor physics, and shielding.

As regards criticality, the database *"International Criticality Safety Benchmark Evaluation Project"* (ICSBEP [4]) gathers about 516 evaluations, *i.e.* 4,405 critical, near critical, or subcritical configurations. So people involved in validation can select the relevant experiments in this base, and easily transpose their descriptions into the language of the code to be validated. This database is divided into various categories of critical experiments according to fuel enrichment and nature, and neutron spectrum. For instance, the database subset LEU-COMP-THERM-15 includes the evaluation of a 335 VVER-dedicated critical experiment series, carried out in the research nuclear reactor ZR-6 (Fig. 112). The title LEU-COMP-THERM means "Low-Enriched Uranium fuel in a solid compound form, in a thermal neutron spectrum". This particular category currently includes 94 evaluations, each of them containing many critical configurations.

This database dedicated to criticality, *i.e.* prediction of the effective multiplication factor, is attractive to reactor physicists, but many other neutron quantities have to be measured to validate transport codes.

The goal of the IRPhE Project [5] is to meet neutron physicists' specific needs. The compilation named "International Handbook of Evaluated Reactor Physics Benchmark Experiments" includes 53 series of experiments, close to reactor physics issues: that is, in particular, in-reactor fuel irradiation experiments including isotopic composition analysis, and

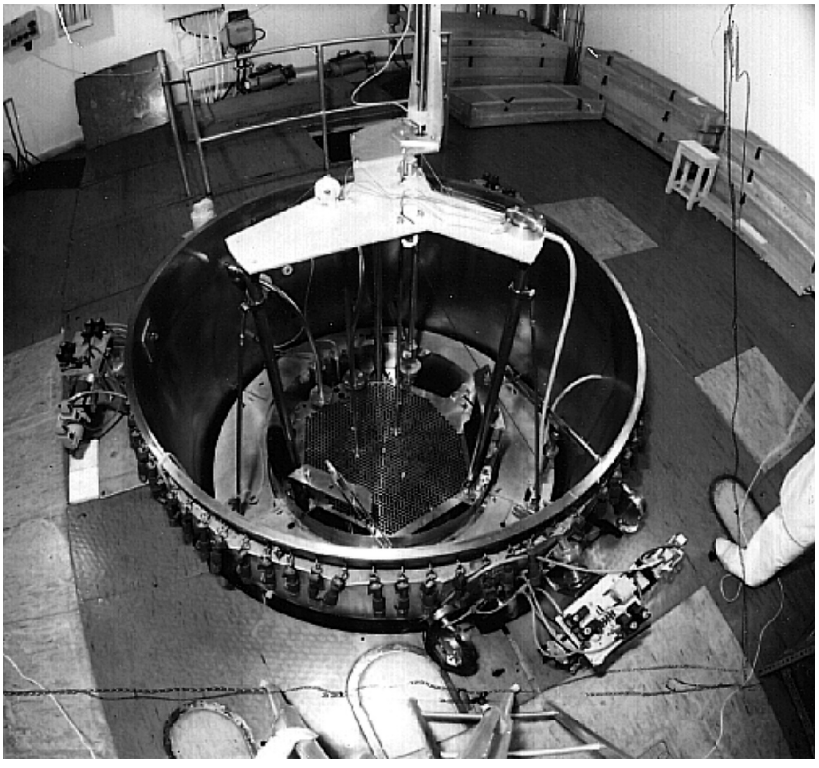

Fig. 112. Top view of the Hungarian reactor ZR-6 used for critical experiments dedicated to VVER reactors.

reactivity coefficient measurements including the study of reactivity sensitivity to materials temperatures, material composition, or material insertion in the reactor, as well as kinetics, power distribution and spectrum measuring.

The **SINBAD Project** [6,7] (Shielding Integral Benchmark Archive Database) gathers a broad set of integral experiments dedicated to codes and nuclear data involved in the design basis of shielding for fission or fusion reactors, and also of shielding for accelerators. Integral quantities are generally derived from the response of energy-threshold detectors. The database includes 45 nuclear reactor shielding experiments, 23 experiments dedicated to neutron shielding in the fusion field, and, finally, 23 for shielding in accelerators. Among the 45 reactor shielding experiments, it is worth mentioning two of them. First, the VÉNUS-3 experiment [8], [9], conducted in Belgium in 1988, gives access to a significant quantity, *i.e.* **vessel fluence***, by measuring threshold detector activation, according to the Ni 58 (n,p), In 115 (n,n'), and Al 27 (n,α) reactions. The achievement of this experiment in conditions close to those of a nuclear reactor makes it attractive to validate transport codes in addition to nuclear data.

Even very old experiments still prove useful in these benchmarks, since their results can be re-interpreted with modern tools. The Naïade experiment [10] conducted between 1960 and 1964, in the periphery of the heavy water reactor ZOÉ located at Fontenay-aux-Roses, was re-evaluated in 2005, and integrated in the SINBAD base [7]. The experiment schematic on Figure 113 indicates the principle of this experiment conducted on a thermal column: thermal neutrons coming from the reactor core are turned into fission neutrons in an uranium plate. These fission neutrons are then propagated through support blocks of various materials, successively selected among graphite, light water and steel. The latter are instrumented with different detectors located at various depths in the block thickness, along the central axis of the thermal column (Fig. 113). The response of these detectors gives access to fluence, for example, in neutronics conditions relatively simple and, so, useful for nuclear data validation.

The OECD's Nuclear Energy Agency (OECD/NEA) plays a federating role on an international scale in order to preserve the historical feedback drawn from integral experiments, especially those conducted in shut-down facilities, and by specialists who have retired or given up this field.

Other benchmarks

In this last part, we have gathered two particular applications dedicated to the TRIPOLI-4® code validation: the GONDOLE experiment in the OSIRIS reactor, dedicated to the study of steel aging under irradiation, and the FLUOLE experiment, which aims at validating propagation calculation in PWR-representative water-steel laminates.

Study of steels behavior under neutron flux, using an experimental device put in the OSIRIS reactor*

A neutronics calculation was performed to interprete a steel specimen irradiation experiment conducted in the OSIRIS reactor (Fig. 114) [11], [12]. This experiment was aimed at investigating radiation damage in steels, and establishing the toughness curve of PWR vessel steels. As part of this experiment, dosimetric measurements were achieved on the following detectors located in a device in the core peripherals: Fe 54 (n,p) Mn 54, Ni 58 (n,p) Co 58, In 115 (n,n') In 115m, Cu 63 (n,α) Co 60. Calculations/measurements comparisons relating to each of these reactors show a good agreement, better than 10%.

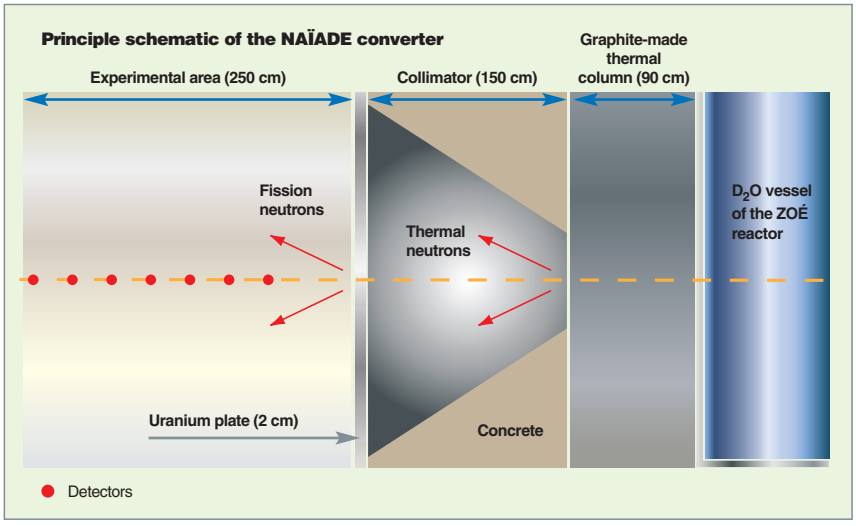

Fig. 113 : Principle of an integral experiment on a thermal column. (Sectional view of the NAÏADE converter) [9].

Interpretation of the FLUOLE experiment conducted in the critical mockup ÉOLE

The aim of the FLUOLE experiment [13] is to validate the computational schematic of neutron fluence on a PWR vessel. Neutron propagation is achieved with the Monte-Carlo transport code **TRIPOLI-4®*** coupled with the nuclear data **evaluation*** JEFF-3.1. The experiment is representative of a 1300-MWe PWR, and was achieved in the ÉOLE reactor of the CEA Cadarache Center (Fig. 115).

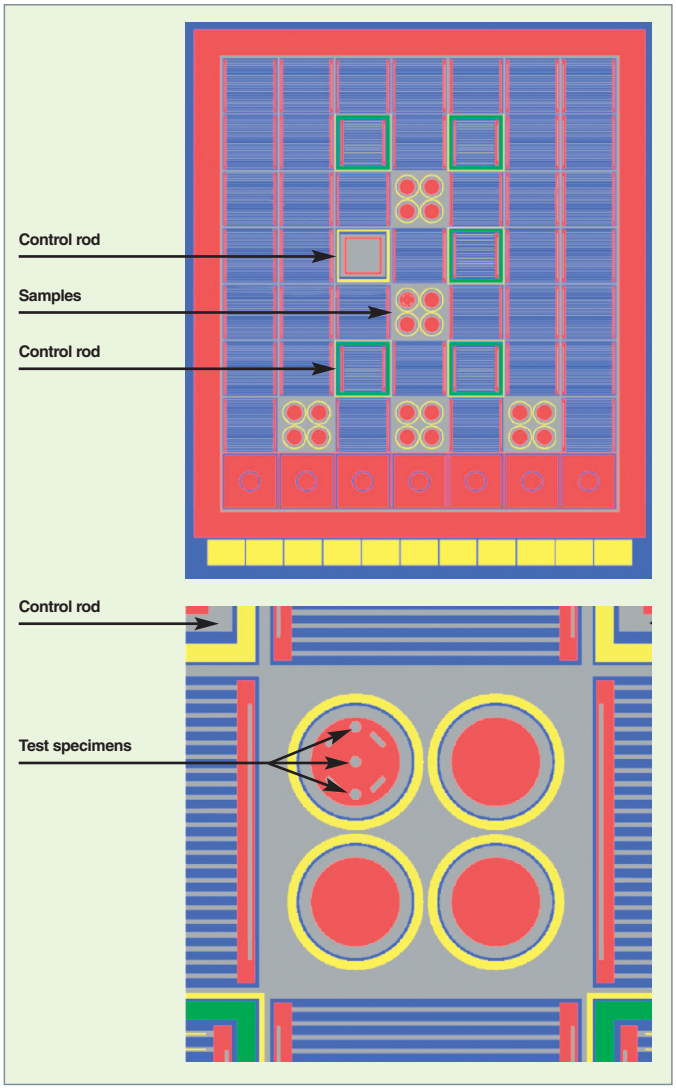

Fig. 114. TRIPOLI-4® modeling to simulate the OSIRIS reactor and the experimental device containing steel specimens.

Calculation/measurement comparisons were particularly focused on the following dosimetric reactions: Ni 58 (n, p) Co 58, Co 59 (n, γ) Co 60, Fe 54 (n, p) Mn 54, Au 197 (n, γ) Au 198. Especially owing to the very reduced size of the result acquisition areas (a few mm^3), about 100 billion neutron histories were simulated, which required to employ 100 processors during a fortnight.

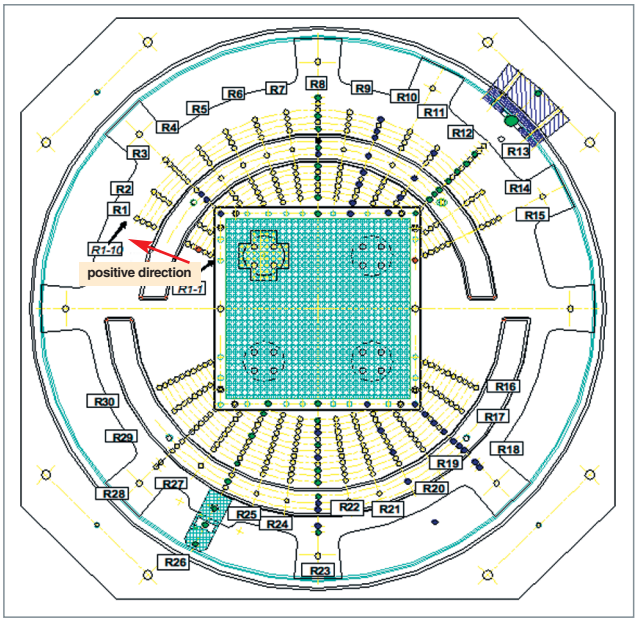

Fig. 115. The ÉOLE reactor, in the configuration of the FLUOLE experiment [13].

References

[1] A. Santamarina, P. Blaise, L. Erradi and P. Fougeras "Calculation of LWR eff kinetics parameters: validation on the MISTRAL experimental program", *Annals of Nuclear Energy*, http://dx.doi.org/10.1016/j_anucene.2012.05.001.

[2] F. Damian, X. Raepsaet, F. Moreau, "Code and Methods Improvement in HTGR Modeling at CEA", *Conférence Internationale PHYSOR 2002,* Seoul, October 2002.

[3] X. Raepsaet, F. Damian, U. A. Ohlig, H.J. Brockmann, J. B. M. De Hass, E. M. Wallerbos, "Analysis of the European results on the HTTR's core physics benchmarks", *Nuclear Engineering & Design*, 222, pp. 173-187, 2003.

[4] *International Handbook of Evaluated Criticality Safety Benchmark Experiments*, http://www.oecd-nea.org/science/wpncs/icsbep/handbook.html

[5] *International Handbook of Evaluated Reactor Physics Benchmark Experiments*, http://www.oecd-nea.org/science/wprs/irphe/irphe-handbook/handbook.html

[6] *Integral Benchmark Archive Database, SINBAD*, http://www.oecd-nea.org/science/shielding/sinbad/sinbadis.htm

[7] I. Kodeli, H. Hunter and E. Sartori, "Radiation Shielding And Dosimetry Experiments Updates In The SINBAD Database", *Radiation Protection Dosimetry*, vol. 116, nº 1-4, pp. 558–561, 2005.

[8] *VENUS-3 LWR-PVS Benchmark Experiment*, NEA-1517/69, 1988.

[9] Y.K. Lee, "Analysis of the VENUS-3 PWR pressure vessel surveillance benchmark using TRIPOLI-4.3 Monte-Carlo Code", *12th International Symposium on Reactor Dosimetry*, Gatlinburg, USA, May 8-13, 2005.

[10] J.C. Nimal, *New Interpretation Of The Naïade 1 Experiments*, NEA/NSC/DOC15, 2005.

[11] H. Carcreff, A. Alberman, L. Barbot, F. Rozenblum, D. Beretz, Y. K. Lee, "Dosimetry Requirements fo Pressure Vessel Steels Toughness Curve in the Ductile to Brittle Range", *Journal of ASTM International*, vol. 3, n° 3, 2006.

[12] Y. K. Lee, F. Malouch, "Analysis of OSIRIS in-core surveillance dosimetry for GONDOLE steel irradiation program by using TRIPOLI-4 Monte-Carlo code," *ISRD-13, International Symposium on Reactor Dosimetry*, Alkmaar, Netherlands, May 25-30, 2008 (2008).

[13] D. Beretz, S. Bourganel, P. Blaise, C. Destouches, N. Huot, J.M. Girard, C. Doumergue, H. Philibert, R. Brissot, M. Dumont, "FLUOLE: A new relevant experiment for PWR pressure vessel surveillance", *Reactor Dosimetry State of Art 2008, Proceedings of the 13th International Symposium*, Akersloot, May 25-30, 2008.

Philippe Fougeras, Patrick Blaise,
Reactor Study Department
Stéphane Bourganel, Yi-Kang Lee, Maurice Chiron,
Frédéric Damian and Claude Mounier
Department for Systems and Structures Modeling

Neutronics Applications

Classification of Neutronics Application Fields

As an introduction to this Section, we propose a synthetic classification of the major application fields of neutronics, in its extended meaning, mentioning their specificities as well as related study needs.

The major application fields

The engineering studies or applications mentioned here are related to facilities of various research organizations and industrial companies: CEA, CNRS, EDF, AREVA, GDF-SUEZ, ANDRA… Table 24 below records existing types of physical configurations, connecting them with the physical quantities of interest to be computed and the corresponding goals.

This table shows four major research areas relating to nuclear reactors: core physics, radiation protection (radiation shielding), nuclear criticality-safety, and nuclear instrumentation, although this Monograph is mainly focused on core physics.

The Introduction to this Monograph details the main physical quantities of interest relating to these application fields.

Table 24.

Recorded types of actual physical configurations to be met in neutronics applications, in relation to the physical quantities of interest to be computed and the corresponding concrete objectives

Facilities	Types of problems / Goals	Physical quantities of interest (out of flux)
Power reactors, Research nuclear reactors	Reactor power determination. Getting quantities relating to core design basis, fine power distribution, burnups, and critical parameters (**control rod*** dimension and efficiency, concentration…), **burnable poison*** burnup. Core conditions monitoring, criticality control under loading. Response of *in-core* and *ex-core* detectors (fission chambers…).	**Effective multiplication factor k_{eff}** **Reaction rates*** Power distribution (rods, assemblies) **Reactivity*** Isotopic concentrations ***Gamma* heating***
	Study of incidental and accidental situations (kinetics, transients).	**Effective multiplication factor k_{eff}*** Power peak
	Reactor vessel and internals lifetime.	**Neutron fluence*** Structure damages
	Accessibility to the various facility areas, studies of incidental and accidental situations.	**Dose rates*** (*gammas*, neutrons, charged particles)
	Facility safety, design basis of devices used for residual heat removal (cooling circuits, pool…).	**Residual power*** (*gammas*, *betas*, *alphas*, delayed neutrons)
	Nuclear instrumentation: design of experimental devices and experiments. Experiment interpretation.	Reaction rates **Activities***
Dismantling	Structural activation. Contribution in drawing out dismantling scenarios for a nuclear facility. Classification of irradiated structures in terms of waste.	Activities Isotopic concentrations **Radiotoxicities*** *Gamma* dose rate

Facilities	Types of problems / Goals	Physical quantities of interest (out of flux)
Fuel cycle facilities: enrichment, fabrication, spent fuel treatment	Nuclear criticality safety analysis. Facility design basis with respect to criticality risk control, studies of accidental situations for crisis management, definition of standards, and qualification. Facility design basis so as to ensure protection of men and equipment.	Effective multiplication factor Activities Isotopic concentrations Dose rates (*gammas*, neutrons, charged particles)
Fuel casks	**Shipping cask***, containers design. Nuclear criticality safety in incidental or accidental situations.	Effective multiplication factor Dose rates (*gammas*, neutrons)
Waste packages	Design of waste packages. Determination of their content (*gamma* spectrometry, neutron interrogation…). Study of **radiolysis*** in the container or in the host rock of the disposal site. Nuclear criticality safety of a waste storage or waste disposal facility.	Effective multiplication factor Activities Dose rates (*gammas*, neutrons) *Gamma* heating
Fusion devices: tokamak, inertial confinement (laser)	Shielding design basis. Accessibility to the various facility areas. Maintenance operations. Materials behavior under irradiation (first wall, superconducting magnets). Neutronics of tritium breeding blankets (calculation of tritium generation in the **fertile*** blanket: tritium breeding).	Reaction rates Deposited energy, damage Dose rates (*gammas*, neutrons, charged particles)
Particle accelerator, spallation devices, hybrid systems	Facility design. Accessibility to the various facility areas. Maintenance operations. Resistance and lifetime of the **spallation*** target. Neutronics and shielding of **hybrid systems***.	Neutron source Effective multiplication factor Reaction rate Isotopic concentrations Activities Radiotoxicities ***Bremsstrahlung**** *gamma* source Photo-neutron source Dose rates (*gammas*, neutrons, charged particles)
Irradiator	Food preservation, sterilization of medical equipment.	*Gamma* dose rates
Medicine: irradiation devices, sources	Cancer treatment (boron neutron therapy…). Optimization of radiation collimation and energy spectra. Medical diagnoses (radioactive tracers).	Dose rates (*gammas*, neutrons, charged particles). Activities.
Space	Propulsion core design. Astronaut protection, equipment integrity.	Neutronic quantities Dose rates (neutrons, *gammas*, charged particles). Damage.

Study needs for the various applications of neutronics

Study needs can be classified into the three following levels, by increasing order of integration:

- **Description of the physical configuration** to be investigated;
- **methods, computational schemes and algorithms** used for modeling;
- **industrial use of neutronics computational softwares**.

Study needs on the "physical configuration" level

This level corresponds to defining the type of *situations and physical objects* to be calculated. Here five studyareas can be distinguished as follows:

- Power reactors, research nuclear reactors, and onboard nuclear steam supply systems (NSSS);
- experimental devices, excluding fission reactors;
- non-energy generating industrial facilities;

- medical and/or medicine-oriented facilities;
- nuclear instrumentation.

Nuclear power reactors, research nuclear reactors, and onboard nuclear steam supplied systems (NSSS)

The code application "objects" can be subdivided as follows:

- GEN. II and GEN. III **PWR*** or **BWR*** type reactors and fuels: facilitating the approval steps by safety authorities (reference alternatives, and qualification);
- **GEN. III*** reactors: reactor and fuel cycle facility evolution induced by expected changes in operation and supply constraints: optimized fuel use, safety ensured in out-of-design-basis conditions, increased **conversion factor***, extended lifetime;
- **GEN. IV*** reactors: orientation and evaluation studies relating to reactor types and related fuel cycle, including fast neutron reactors. The **ASTRID*** project is involved in this outlook, and so are the concepts of **hybrid systems***;
- permanently shut-down reactors: **GEN. I*** reactors, research reactors (TRITON, SILOÉ, RAPSODIE…), and onboard nuclear steam supply systems (NSSS): dismantling strategy and operations with man and/or remote-controlled (robotics) intervention;
- research nuclear reactors: **OSIRIS***, **ORPHÉE**, **ILL**, **RES***, **JHR***…;
- onboard nuclear steam supply systems: naval propulsion, space propulsion;
- front-end (fabrication…) and back-end (spent fuel treatment…) fuel cycle plants, whose needs are mainly related to criticality and radiation protection;
- waste disposal and storage sites: site design, design of packages which are to undergo physico-chemical phenomena initiated by their radioactive content (*e.g.* **radiolysis***), and likely to impact on their integrity. In deep disposal, what is to be investigated is the host rock behavior;
- on-site or training-center simulators;
- design simulators.

Ten examples of topics are identified hereafter. For each of them, the main objectives to be reached are mentioned, together with the related modeling issues.

Core Physics

Study topic	Modeling issue
Studies of "current" concepts	• 3-D rod-by-rod transport, detailed isotope generation/depletion;
• **UNGG / MAGNOX / AGR*, PWR*, BWR*, RBMK*, VVER***, **fast neutron reactors*, CANDU***, research nuclear reactors, onboard nuclear steam supply systems (NSSS).	• Directly taking instrumentation into account in calculations; • Optimization methods using **HPC***; (genetic algorithms, probabilistic methods…);
Studies of "new" concepts	• Neutronics / thermal-hydraulics coupling;
GFR*, SFR*, GT-MHR*, VHTR*, hybrid systems*, research nuclear reactors, and onboard nuclear steam supply systems (NSSS).	• Thermal-mechanics / Chemistry coupling; • Design simulator; • Online calculator: extrapolation calculations (predictive evaluations);
Fleet optimization (scenario studies)	• Simulator: representation of real-time neutronics and thermal-hydraulics core behavior; • Experiment substitution in some cases; • Neutron noise.

Safety: accidental situations

Study topic	Modeling issue
Reactivity accident	
• Steam Line Break (SLB) accident; • Rod ejection (RIA); • Spurious boron dilution; • Valve opening accident in the secondary coolant circuit; …	• Transients; • Neutronics - thermalhydraulics coupling; • Thermal-mechanics coupling (pellet-clad interaction); • Coupling evolution (nuclide generation/depletion) with release formalism and transport codes;
Degraded core studies, ***corium****	
• Radioactive products release in an accidental situation;	• Transport of electrons arising from the *beta* decay of radioactive products.

Criticality

Study topic	Modeling issue
Fissile materials behavior in fuel cycle, in incidental and accidental situations	• Varied geometrical configurations;
• Nuclear criticality safety analyses; • Nuclear criticality safety calculations;	• Broad (fast to thermal) neutron spectrum; • Isotopic variety of materials;
New fuels, new facilities…	• **Burnup credit***.

Safety/Radiation protection in relation to fissile materials

Study topic	Modeling issue
Design basis, approval	
• Dose equivalent rate and residual power of the **cask*** and of containers; • Dose equivalent rate during a criticality accident.	• Measure interpretation (determining functions for radiation transfer between source point and measuring point).

***In-core* and *ex-core* instrumentation response**

Study topic	Modeling issue
Achieving neutronic control of PWR nuclear plant units, calculating neutron flux measuring chamber response	
• Establishing neutron flux maps; • Providing information about core conditions: - Case of partial or total voiding, *e.g.* water level; - **Axial offset***… • Calculating the average or local irradiation of assemblies (**burnup***) • Studying the impact of removing neutron sources used for reactor startup; • Determining *gamma* radiation influence on the signal delivered by neutron flux measuring chambers.	• Out-of-core propagation for parametric studies and calculations/measurements comparisons; • Uncertainty propagation in calculations; • Nuclear heating (measurement, nuclear data, detector response function); • **Collectron*** response; • Coupling between deterministic and probabilistic modeling (uncertainty propagation).

Vessel surveillance dosimetry

Study topic	Modeling issue
Ageing, irradiation resistance of materials, reactor lifetime depending on management schemes under consideration (extended operation…)	
• Determination of **neutron fluence*** and *gamma* fluence on reactor vessel and internals.	• Taking into account overall uncertainties (basic nuclear data, technological data…); • Relevance of damage indicators in matter: neutron flux > 1 MeV, neutron flux > 0.1 MeV, displacements per atom (**dpa***), reaction rate for the physical interpretation of measures; • Coupling between deterministic and probabilistic modeling; • Measurement interpretation.

Spent fuel treatment, fuel fabrication

Study topic	Modeling issue
Shielding design basis, conditions of accessibility and stay at plant workstations	
• Shield nature and thicknesses: optimization, calculation of neutron and *gamma* dose equivalent rates.	• (Monte-Carlo and S_N) reference methods and "simplified" methods (attenuation along a straight-line path) to treat strongly heterogeneous geometries and lacunar media (pipe, gaps of various kinds, cable passageways…).

Dismantling

Study topic	Modeling issue
Calculations relating to nuclear reactor and facility dismantling: UNGG, EL4 (Brennilis), research nuclear reactors, PWRs, accelerators…	
• Neutron mapping, structural activation, isotopic inventory, radiation sources, spectra, equivalent dose rate, heating.	• Optimizing computational schemes; searching for calculation cost/accuracy compromise (numerous geometrical configurations, decay chains and related study of pathways). • Controlling approximations and uncertainties.

Radiation-induced ambient dose rate

Study topic	Modeling issue
Dose equivalent rate in and out of the reactor building (skyshine…)	
Dose equivalent rate in reactor pit and reactor building, measuring point detection [examination]	• Monte-Carlo: developing importance maps for simulation in order to perform a one-step calculation (in relation to the complex geometry of the whole reactor building structures) for neutrons and *gammas*.

Waste management

Study topic	Modeling issue
Radioactive waste storage and disposal studies. Deep disposal studies in underground laboratories	
• Inventory/isotopic analysis of any irradiated object: fuel, clad, structures… Industrial and research reactor waste. Radiotoxicity; • 3-D mapping of radiation in the host rock of a waste disposal site; limitations of delivered doses during handling of irradiated waste packages; • *Gamma* heating for **radiolysis*** study: gas formation and explosion risk in packages and host rock; • Dose equivalent rate in handling and storage galleries.	• Neutron emission in vitrified waste packages; • Full radioactive inventory; • Investigating nuclide pathways; • Coupling with the "process" steps… • Interpretation of measured actinide doses in waste drums.

Experimental devices other than nuclear fission reactors

Even if fission reactors constitute the main field of application of neutronics, other devices rely on this discipline. Some are mentioned in the table below:

Study topic	Modeling issue
*Thermonuclear **fusion*** machines: *• **Tokamak*** (magnetic confinement): **ITER*** *• Inertial confinement machine: **LMJ**** *Particle accelerators:* *• **GANIL***: (e.g. SPIRAL-2)* *• **SOLEIL***: (e.g. MARS line)* *• **ESS****	
• Shielding design basis (dose equivalent rate, activation, heating, damage); • Ambient dose rate; • Radioactive inventory, radiation sources; • Definition and interpretation of experiments; • Contribution in defining the operating procedures of the machine.	• 3-D propagation of neutral and charged particles at intermediate energies; • Electromagnetic shower; • Coupling between intermediate-energy codes and low-energy codes.

Non-energy producing industrial facilities

Study topic	Modeling issue
Irradiators (food, medical instrument sterilization…);	
• Shielding design basis; • Ambient dose rate (dose equivalent rate…).	• "Simplified" methods to treat strongly heterogeneous geometries and media exhibiting gaps (pipes, gaps of various types, cable passageways…).

Medical facilities for in-reactor radionuclide production

Study topic	Modeling issue
• *Proton accelerator for proton-therapy* • *Gamma irradiator of cancer tumor* • *Innovating reactors and systems for* ***Boron Neutron Capture Therapy (BNCT)****	
• Shielding design basis; • Collimator optimization; • Neutron source generation; • Neutron spectrum optimization; • Irradiation simulation (aided treatment).	• 3-D propagation of neutral and charged particles at intermediate energies; • Electromagnetic shower; • Intermediate-energy / low-energy code coupling.

Nuclear instrumentation

Study topic	Modeling issue
Detector design: *for core monitoring (prevention of unflooding accident and core compaction accidents…)*	• Calibration of detection instruments; • On-line flux measuring; • Irradiation resistance;
Experiment design *Optimization of irradiation conditions and measurement sorting*	• Reduction of experimental uncertainties; • Neutrino source (fundamental physics).

Study needs on the modeling level

This level refers to physical-mathematical methods/models and to the algorithms developed and implemented in computational softwares in order to solve particle transport and kinetics equations (Boltzmann), time isotopic generation/depletion (Bateman) equations, (Navier-Stokes) flow equations. The fineness of geometrical representation, the degree of accuracy, and computational time performance are related to this level. So the latter controls the predictive character and the possible use of calculation tools which are expected by users to do ever more and better in an ever decreasing time.

Schematically, the predictive ability of a computational tool can be assessed through comparisons with measurements on given representative configurations and related uncertainties. At this very level are defined **computational schemes***, *i.e.* the specific modes of use of one or several computational softwares to treat a given situation, possibly including the coupling with other disciplines (thermal-mechanics, thermal-hydraulics, physical-chemistry…).

Two types of calculation are required:

- ***The reference calculation***, which is as close as possible to physical reality: *e.g.* the fine rod-per-rod power distribution of a nuclear reactor core. A reference calculation tool can be used for various purposes as follows:
  - the computational validation of physical-numerical models;
  - the generation of physical data/ quantities for other computational tools;
  - the analysis of physical phenomena;
  - the validation of basic physical data (cross sections…);
  - numerical experiments: complementary/alternative to experiment;
- ***the design*** or ***preliminary design calculation*** which gives an order of magnitude. A design calculation tool has to be performing with respect to computing time, and easy to implement. Parametric and pre-optimizing calculations can be carried out with this tool.

Study needs on the industrial level

This level specifies the requirements and selection criteria to perform ***"production" calculations***: selection of nuclear data libraries, computational codes and schemes, automation / reliability of computational chaining (procedure setting-up), conviviality, performance criteria, portability, quality (procedure setting-up, maintenance, assistance, expertise, verification and validation, internal and external acknowledgement, especially with respect to safety authorities, etc.).

Code user groups or ***forums*** enhance the "continuous" transfer of users' needs and feedback to developers, and makes problem solving and solution sharing easier.

The following chapters deal with nuclear reactor calculations, with a description of the state-of-the-art for the different reactor types (see *infra*, pp. 193-213). Strictly speaking, a coupled treatment of neutronics, thermal-hydraulics, thermal-mechanics and mechanics is required. If the neutronics - thermal-hydraulics coupling is indispensable to calculate power reactors, combining thermal-mechanics and, sometimes, mechanics becomes indispensable to describe accidental sequences in reactors (see *infra*, pp. 215-225). Other applications of neutronics deal with fuel cycle physics calculations (see *infra*, pp. 227-234), and nuclear criticality-safety calculations (see *infra*, pp. 235-246). At last, other applications of neutronics which have resulted in recent developments at the CEA, have been gathered in the last Chapter of this Section (see *infra*, pp. 235-246) in order to illustrate their diversity.

Cheikh M. Diop and Anne Nicolas
Department for Systems and Structures Modeling

Reactor Neutronics Calculation

This chapter, focused on reactor calculation, naturally starts with the listing of the quantities to be computed, detailing in what they help demonstrate the reactor ability to fulfill its mission (power production, experiments) in a safe and optimal way from a technical and economical viewpoint. The available tools and methods, presented in the previous Chapters, will be briefly recalled later on.

Neutron life in a reactor

Due to their lack of electrical charge, the only possible form of interaction for neutrons as they go across a reactor core lies in collisions with the medium's atoms (nuclei). Between two shocks, neutrons follow rectilinear, uniform paths (considering the framework of classical mechanics, and seeing gravity as negligible). Given the materials (combination of fuel's heavy nuclei with the light nuclei of structures, coolant, and moderator) and the probabilities involved (cross sections), their path from birth to disappearance (on the average) consists of the following components:

- A high number of scatterings resulting in a gradual slowing-down of neutrons;
- leakage towards the system's outer part, in limited number;
- a final absorption that may be:
  - either sterile, hence the neutron disappearance,
  - or fertile, hence the formation of a fissile nucleus, leading to the birth of new neutrons by fission;
- a fission.

Fission neutrons are generated at high energy (2 MeV, *i.e.* a velocity of 14,000 km/s). Then they undergo a series of collisions with the moderator's atomic nuclei that slow them down. Once they have been sufficiently slowed down (to a so-called "thermal" velocity, of the order of 1 km/s, below which they can no longer slow down, because the medium's thermal motion gives them as much energy as is lost through collision), neutrons can finally be absorbed by a fuel nucleus, thereby inducing the latter's fission… and the generation of new neutrons that undergo the same cycle. It is worth to mention that this is true for the so-called "thermal reactors". Regarding fast reactors, neutrons are absorbed by fuel nuclei, in order to induce fissions, without having to undergo slowing-down.

	H	D	C	O	U
A	1	2	12	16	238
σ_a (barns)	0.33	$0.5.10^{-3}$	3.10^{-3}	$0.3.10^{-3}$	2.7
N_c (2 MeV – 1 eV)	15	20	92	121	1,731

Very efficient slowing-down — Required enrichment to a few %

Characteristics of the main moderators (and comparison with uranium): mass number, thermal capture cross section, and number of shocks required to slow-down one neutron. Light-water hydrogen slows down neutrons quite efficiently, but also captures them. Heavy-water deuterium does not exhibit this drawback.

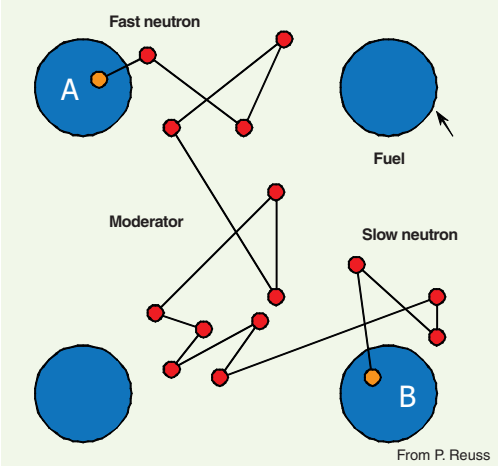

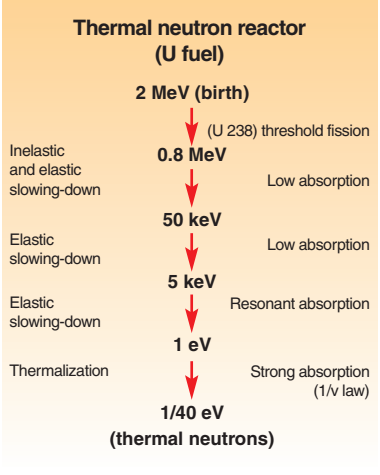

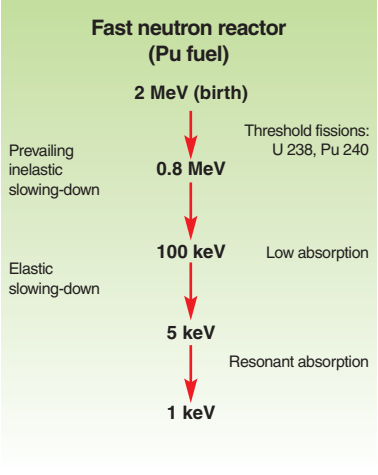

The slowing-down of a neutron in a thermal neutron reactor and in a fast neutron reactor.

Neutronics applications to reactors are described starting from two typical examples: the calculation of pressurized water reactors (**PWR***), and that of sodium-cooled fast reactors (**SFRs***). Special emphasis is put on why and how the calculation schemes set up for these two types of reactors have been adapted, or even transformed, to calculate other types of reactors: boiling water reactors (**BWRs***), research nuclear reactors, **heavy water reactors***, high-temperature reactors (**HTRs***), gas-cooled fast reactors (**GFRs***), etc.

The quantities to be computed

Neutron flux

Knowing the energy distribution (spectrum) as well as the space distribution of neutrons is of prime importance, since these quantities determine local reaction rates in the core. In this respect, the spectrum and the neutron flux play a prominent role in core design basis and its performance.

Reactivity and its evolution

In normal operation, core **reactivity*** is null at every instant, as the reactor is just **critical*** (k_{eff} = 1). This reactivity results from the equilibrium between fuel's potential reactivity that decreases as fuel burns (through burning of fissile nuclei), and the **negative reactivity*** brought by the various neutron absorbers present in the core (fission products generated by fissions, soluble boron in the primary coolant circuit of pressurized water reactors, **control rods***, **burnable poisons***, etc.). So it is crucial to know the time evolution of every component in order to permanently maintain the equilibrium, and determine the cycle length, *i.e.* the operating time between two fuel loading operations.

In a shutdown situation, safety rules impose a subcriticality (k_{eff} < 1) level that depends on the situation considered (hot shutdown at **nominal power***, hot shutdown at zero power, cold shutdown, etc.). At last, in an accidental situation, the variation speed of the power released by the core is determined by the supercriticality (k_{eff} > 1) level.

Knowing reactivity and its evolution over time are therefore fundamental, whatever the core situation may be.

Change in reactor power by inserting a reactivity step

A control rod is extracted during a given T time, and then is brought back to its initial position, which temporarily increases reactivity ρ. The solving of kinetics equations allows the evolution of the neutron population to be determined (Fig. 116):

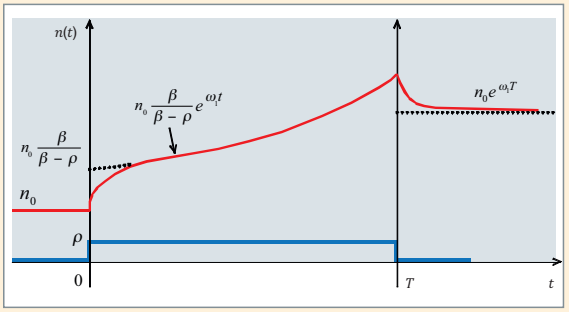

Fig. 116. Neutron population evolution after inserting a reactivity step.

It can be shown that the neutron population $n(t)$ will reach a final value different from the initial value.

$$n_\infty = n_0 e^{\omega_1 T} \text{ where } \omega_1 = \frac{\rho\lambda}{\beta - \rho}$$

λ and β being the delayed neutron parameters for a single family.

In this case, a power increase adjustable through the reactivity step height and duration has been achieved. The case mentioned here is that of a low power reactor, for which thermal effects are negligible. In practice, temperature effects have to be taken into account, for they are prevailing in the control of power reactors.

Feedback coefficients

These coefficients express reactivity response to variations in core characteristics, whether deliberate (*e.g.* change in operating point), or not (*e.g.* accidental situations, such as the Steam Generator Tube Rupture (SGTR) or the Loss of Coolant Accident (LOCA) in pressurized water reactors).

The core features which may undergo variations may be related to fuel temperature, moderator or coolant temperature. In that case, the resulting variations in reactivity are referred to as *temperature effects*. They modify the critical equilibrium described in the previous paragraph, and have to be exactly compensated by a variation in reactivity of opposite charge.

Another core feature likely to undergo changes is the amount of coolant: boiling/evaporation, partial or total voiding… When coolant's neutron weight is not negligible, as is the case for fast neutron reactors, as well as for PWRs and BWRs, in which it plays the role of a neutron moderator, induced variations in reactivity may be significant. Generally, one prevailing principle, at the design step, will be to keep stabilizing **temperature coefficients*** or void **coefficients of reactivity*** with respect to the core's critical conditions: increases in temperature, or reactor voiding, have to result in a decrease in reactivity.

A key feedback for reactor stability: the Doppler Effect

The nuclei constituting the material through which neutrons move, are not motionless, and it is important to take their motion into account in cross section formulation, especially in relation to resonances. When the medium's temperature increases, the cross section "flattens", the resonance peak widens, and the cross section integral is preserved (see *supra*, Fig.14, p. 34). According to the target nucleus of interest, the Doppler Effect yields different effects. As regards U 238, a mostly absorbing nucleus, generally prevailing in nuclear fuel, the Doppler Effect increases neutron capture probability, and so has a negative effect on core reactivity. When reactor power increases, temperature increases, U 238 capture resonances widen, and the capture rate increases, which induces a decrease in reactivity of about -3 pcm/°C. This feedback contributes in the intrinsic stability of water reactors. It is fundamental for their safety.

Power distribution

Power distribution among the various core areas, also called "power distribution", is a fundamental quantity with respect to both safety and the technico-economical optimization of the core.

As a matter of fact, concerning safety, an upper limit is imposed on the ratio between maximum power and average power, not to be exceeded in normal operation for reactor safety to be ensured in the case of an accident. As regards optimization, given a fixed maximum power, the goal is to ensure that the power released in all the core areas be as close as possible to this maximum; as released power determines the rate of fuel burnup. A uniform power distribution leads to a uniform fuel burnup, which is therefore optimum with respect to fuel use; *a contrario*, a non-uniform burnup often entails a shortened time of irradiation cycle and removal of incompletely burned fuel.

Efficiency of the various reactivity control devices

Obviously, calculating the efficiency of the various reactivity control devices is a prime component of reactor safety demonstration. These control devices (boron dissolved in the primary coolant system and absorbent control rod clusters for PWR, BWR control rod cross, burnable poisons, etc.) are used either to maintain the core in a critical condition (zero reactivity) in normal operation, or to bring back the core to a subcritical condition in the case of a shutdown or an accidental situation.

Isotopic composition of the various core materials

As regards reactors, isotopic composition calculation mainly concerns fuel, that is heavy nuclei and fission products, as well as absorbers, in particular burnable poisons. However, the only elements to be taken into account are those having a significant neutronic "weight" – *i.e.* an effect on core reactivity –. Fuel cycle physics studies require a much more detailed knowledge of the **material balance*** in order to determine the **residual power*** of fuel, activity, radiotoxicity, etc. Tools used for these studies are presented *supra*, pp. 127-142.

Power level for accident transients

The quantity to be calculated to assess the consequences of an accident on the core, and, more generally, on the whole system is the time evolution of the absolute power level and of its distribution in the core. This is a notable difference with respect to normal operation. As a matter of fact, in this case, core power is an input datum that is necessary to normalize **neutron flux** level since, in accordance with theory, flux in a critical core is calculated up to a constant multiplication factor.

Burnup distribution

The **burnup*** of a fuel element determines its isotopic composition. In addition, it has to be known, and so computed, to allow fuel management in reactors which fuel is reloaded by core fraction (this is the case of all nuclear power reactors and of many research nuclear reactors). As a matter of fact, this is the burnup distribution that determines the end of cycle when one or several fuel elements have reached their technological burnup (depletion) limit. Besides, the fuel loading pattern for the next cycle, *i.e.* the location of each (fresh or spent) fuel element in the core, is established on the basis of the burnup distribution in the end-of-cycle core.

Other quantities

Residual power

Residual power is the thermal power delivered by a shut-down nuclear reactor, mainly arising from the **activity** of **fission products**. A few seconds after reactor shutdown, this residual power accounts for about 7% of reactor power before its shutdown. As shown by the **Fukushima*** accident, the removal of this power is a fundamental safety issue.

Nuclear heating

The nuclear heating induced by neutrons, and by ***gamma**** photons, too, is an important quantity, especially for research nuclear reactors. In these reactors, nuclear heating on experimental irradiation devices has to be taken into account for the design basis of their coolant circuit and/or the shields to be interposed between the core and these devices to limit the *gamma* flux received by them.

Materials damage

The resistance over time of the constituent materials of a nuclear reactor core depends on the dose received by these materials that may be damaged, deformed, or embrittled by irradiation. For this reason, it is important to be able to assess this dose, particularly for some crucial or non-replaceable components, such as the reactor vessel. The main quantities of interest are **fluence*** (time integrated dose or flux) and the number of **displacements per atom** (**dpa***) on reactor vessels and internals.

Available tools

What are the tools available to the nuclear reactor physicist to compute these quantities?

Nuclear data

First of all, for all the nuclides of interest, he has at his disposal qualified nuclear data in a form suitable for computer codes: generally energy **multigroup*** (or groupwise) for deterministic codes, and pointwise (continuous-energy) for codes implementing the Monte-Carlo method. After being put in the convenient form, these data are gathered in "libraries" that, for each nuclide, contain the interaction **cross sections*** for the various neutron-and photon-induced reactions, as well as other nuclear parameters of interest: **radioactive half-life***, **neutron multiplicity**, fission energy, etc.

The "libraries" that contain these data essentially differ by the evaluation they arise from, and, in the case of multigroup libraries, by the energy meshing adopted.

These nuclear data have been qualified by calculation, through a comparison, on very simple experiments, between very accurate calculation results and measures. As a matter of fact, using very accurate calculations - the so-called "reference calculations" - ensures that most of the observed discrepancy arises from nuclear data, and not from the calculation method.

Chapters concerning "Nuclear Data" (see *supra*, pp. 19-38) give detailed information about nuclear data, their evaluation and their treatment.

Codes and methods

Methods for solving equations governing the evolution of the neutron population, as well as the **nuclear reactor physicist's approach** are presented *supra*, p. 51-54. The main computational [computer] codes used for nuclear reactor calculations are presented *supra*, pp. 127-142.

To sum up it all, there exist two types of computational methods, which are complementary: the Monte-Carlo method, and deterministic methods. The first one is selected to perform reference calculations, and validate usual calculations. The other methods are used to develop the computational models dedicated to the usual calculation of nuclear reactors.

Experimental neutronics

Measurements of reactivity, reaction rates, and isotopic compositions of irradiated fuels, achieved in research nuclear reactors or in power reactors according to the case, are confronted with calculation results in order to establish the whole qualification of computational schemes. This **qualification*** is completed by comparisons with calculations known to be more accurate (*e.g.* calculations based on the Monte-Carlo method).

Neutronics application to pressurized water reactors (PWRs)

The implementation of the usual two-step computational scheme for the calculation of a PWR in normal operation takes place as follows: for each type of assembly present in the core (Fig. 117), a lattice code, such as the **APOLLO2*** code, is used to carry out a set of calculations, so as to constitute a multiparameter library of neutron characteristics, that can be used in the core calculation performed by a core computer code such as the **CRONOS2*** code (see also *supra*, the nuclear reactor physicist's approach, pp. 51-54). The neutron features of the reflector surrounding the core are determined as mentioned hereafter, p. 198. The assembly types available in the core may differ depending on the supplier, the fuel (MOX, UOX), the burnable poisons (gadolinium) and the absorber control rod clusters.

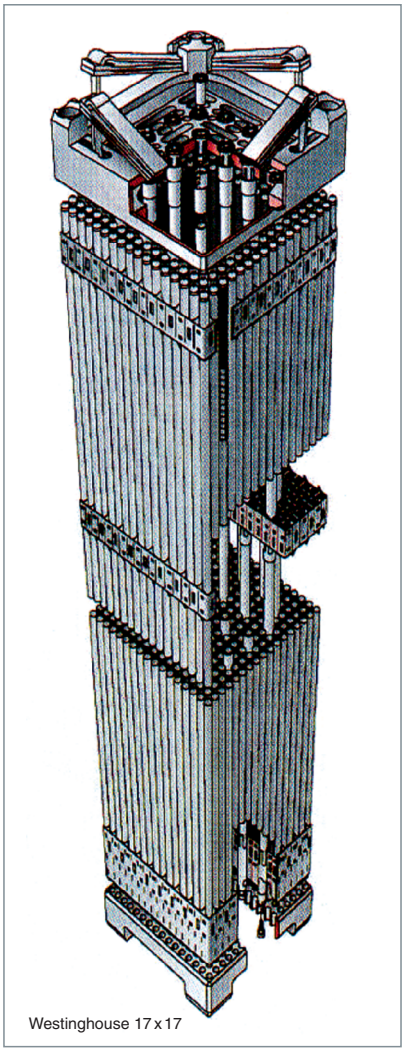

Fig. 117. A pressurized water reactor fuel assembly.

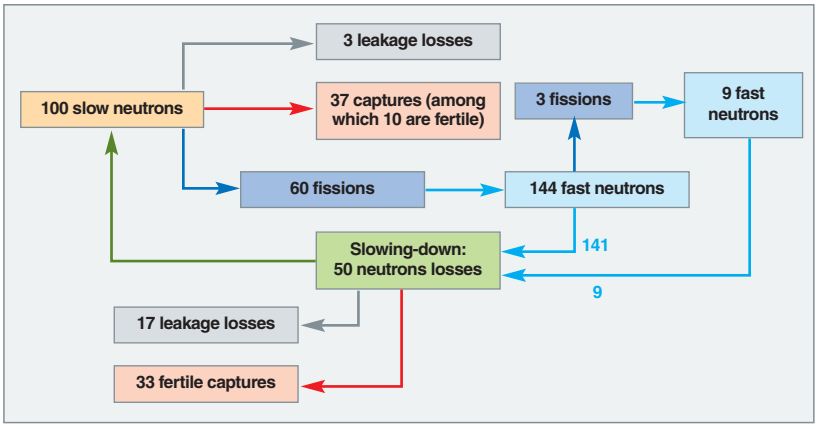

Fig. 118-a. Neutron balance of a water reactor.

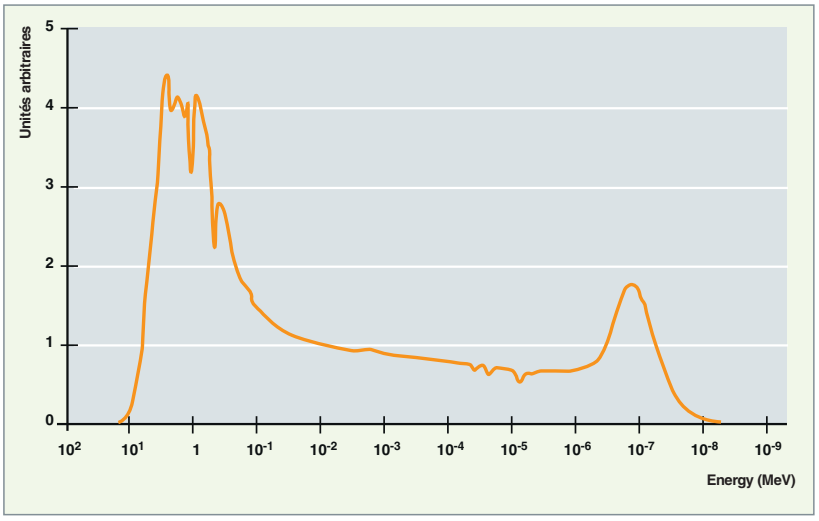

Fig. 118-b. Neutron spectrum of a pressurized water reactor.

Figures 118-a and 118-b above show the neutron balance of a pressurized water power reactor, as well as the spectrum of the neutrons present in the core.

Assembly depletion (or burnup) calculation in nominal conditions

For this calculation, the operating parameters T_m, ρ_m (moderator temperature and density), and T_c Tc (fuel temperature) are fixed at their nominal value. Boron concentration (Cb) takes an arbitrary mean value, generally 600 **ppm***.

A horizontal section of the **assembly*** is described in detail: each **rod*** is represented with its fuel (split into concentric rings in order to take into account the spatial variation in neutron resonant absorption), its **clad***, and the associated **moderator*** part; spacer grids are diluted in the moderator to take into account their absorption.

According to the degree of accuracy desired, the flux is calculated on this geometric model using, in most cases, the **Method Of Characteristics*** or the **Collision Probability Method*** (P_{ij} method, most often employed in the "multicell" approximation to couple cells with one another). The calculation is most often performed with 281 energy groups, according to the threefold compromise computational time/library volume/desired accuracy.

The resonance **self-shielding*** is computed distinguishing four or six concentric rings in non-gadolinium-bearing fuel rods, and eleven in gadolinium-bearing rods.

The depletion (or burnup) calculation is carried out by solving the **Bateman*** equations at a constant specific power, on as many media as there are rings in the fuel rods. Thus, in a simple scheme, the different rods are not distinguished with respect to the depletion. So all outer rings evolve similarly, and so it is for other rings. For higher accurateness, rods can be distinguished so as get a differentiated depletion of each ring in each assembly rod. Sixty computational steps or so are required to reach an average discharge burnup of 60 GWd·/t.

Self-shielding is recomputed a dozen times during the depletion in order to take variations in isotopic concentrations into account.

The so-called "branch" assembly calculations

For a subset of depletion steps, a fixed-burnup assembly calculation is achieved from the concentrations stored at the end of the previous calculation for a certain number of value triplets of parameters moderator density (ρ_m), fuel temperature (T_c), and soluble boron concentration (Cb). These calculations aim at taking into account, on the one hand, the possible insertion of control rod clusters in the assembly, and, on the other hand, thermal-hydraulics feedbacks. If the study is focused on an accidental situation including in-core steam appearance, the moderator temperature T_m, uncoupled from the density parameter ρ_m in the area in steam, is added as a parameter.

As for calculations in nominal conditions, resonance self-shielding is calculated on an average cell including four or six rings in non-gadolinium-bearing fuel rods, and eleven in gadolinium-bearing rods.

These branch calculations are performed (n+1) times, with n equal to the number of control rod clusters likely to be inserted in the assembly. For example, for a 900MWe PWR, n equals 2, because an assembly can receive a black rod cluster (*i.e.* 24 absorber rods) or a grey rod cluster (*i.e.* eight absorber rods and sixteen steel-made rods). For the first calculation series, the assembly is deprived of control rod cluster, as is the case for the depletion (or burnup) calculation in nominal conditions.

The flux is calculated on the same model as in the depletion (or burnup) calculation, and through the same method; it is then used to homogenize the assembly, either in its totality, or "by pieces", that is, cell per cell in practice. Total homogenization consists in replacing the assembly by a neutronically equivalent homogeneous "mix". Cell per cell homogenization consists in replacing the assembly by a series of homogeneous "mixes", each of them equivalent to a cell or to an assembly cell group. The assembly homogenization degree is determined by the core calculation refinement level of interest (assembly per assembly calculation, referred to as "**homogeneous calculation**", or rod per rod calculation, referred to as "**heterogeneous calculation**").

The homogeneous "mix(es)" is (are) characterized by few (usually two)-energy-group cross sections that are determined using this same flux, through "condensation" of 281-group cross sections. According to this type of method and the geometric model used in core calculation, an equivalence can be possibly performed in order to correct these sections, and take account of the change in the transport equation modeling between Step 1 (assembly-scale fine transport) and Step 2 (core-scale diffusion or simplified transport).

The two-energy-group macroscopic sections of the homogeneous, assembly-equivalent "mix" are then stored in a multiparameter library, in which parameters are: burnup, fuel temperature T_c, moderator density ρ_m, possibly moderator temperature T_m, boron concentration Cb, and the type of inserted control rod cluster.

A few nuclides can be particularized (an operation which consists in isolating their concentration and their microscopic cross sections in the library all along the depletion) so as to explicitly treat their depletion during the cycle in core calculation. As regards the PWR, these are xenon-135 and samarium-149, *a minima*, *i.e.* fission products, the time evolution of which is particularly followed up on the core scale. As a matter of fact, they are the chief contributors in core neutron poisoning on account of their very high thermal neutron capture cross section. In the case of PWR cores, it is possible, in some cases, to perform the so-called "macroscopic" depletion (or burnup) calculations, in which only the Xe 135 and Sm 149 concentrations are followed up.

If all the nuclides of the multiparameter library are particularized, this is what is called a "microscopic" depletion on the core scale.

Calculation of reflector neutron characteristics

The reflector is generally represented by a layer of homogeneous material 20 cm thick surrounding the active part of the core on all its faces. The neutron characteristics of this dummy material are determined so as to reproduce the reflecting properties of the actual materials surrounding the core: baffle assembly, water, core barrel, assembly top and bottom nozzles, etc.

Core calculation

For the calculation of a cycle, core depletion is computed through chaining of flux calculations, assuming power constant between two calculation steps. Thanks to increases in burnup computed for every core mesh, the cross sections to be used at the following step can be determined through interpolation in the multiparametrized library. At each step, the code determines boron concentration Cb that makes the core critical, and calculation chaining can go on up to a previously fixed minimum boron concentration, that corresponds to the end of the cycle.

The homogeneous calculation of a cycle takes place as follows:

- The core is modeled in 3-D, with 20 or 30 axial meshes on the active part, four radial meshes per assembly (to take into account the power gradients experienced by fuel assembly during its residence in the core). The flux is generally calculated by solving the two-group diffusion equation through a **mixed finite element*** method or a nodal method;

- thermal-hydraulics feedbacks are taken into account thanks to a thermal-hydraulics model. So each space mesh of the core is differentiated from the others by its own parameter (T_c, ρ_m, T_m, Cb); the cross sections used are deduced by interpolation as a function of the parameters of the cross sections available in the multiparameterized library;

- the code provides the critical concentration of boron, power distribution per space mesh, and burnup distribution, and this at each depletion step of the computed cycle;

- if need be, the power peak (*i.e.* power released in the "hotter" mesh of the core normalized to the average power) is calculated by factorization: first, the "hottest" computational mesh (*i.e.* a quarter-fraction of assembly) is pinpointed in the core calculation results, so as to note its power $P^{\max}_{x,y,z}$; then, the cell-per-cell power distribution (referred to as "fine structure") $P_{x,y,z}$, is recovered in the multiparameterized library of the corresponding assembly; and finally, the "pin power peak" value is calculated as the product $P_{x,y,z}.P^{\max}_{x,y,z}$.

In the case of very heterogeneous cores or very dissymmetrical situations or when a more precise knowledge of power distribution is required, a core heterogeneous calculation can be achieved; in this case, each cell is represented by a homogeneous mix. In this type of heterogeneous calculation, the core model for the thermal-hydraulics calculation is coarser than the neutronics model (*i.e.* per assembly or per assembly quarter, instead of cell per cell). Thus, the neutronics quantities computed cell per cell are averaged on an assembly quarter or on an assembly before being transferred to the thermal-hydraulics calculation.

Neutronics application to sodium-cooled fast reactors (SFRs)

The initial motivation for investigating this reactor type is the possibility to make these reactors able to produce as much fissile material as is burnt by them, or even more, that is to reach a conversion factor higher than the unit in an U-Pu cycle. This is only possible with fast neutrons, because in this energy range alone is the ratio between fertile captures and fissions sufficiently high. So, neutron slowing-down is to be avoided as much as possible after their emission by fission, which excludes the presence of light materials in the reactor core.

In comparison with that of thermal reactors, the neutronics of **fast neutron reactors*** exhibits a number of specificities, briefly presented below.

Neutronic specificities of fast neutron reactors

In these reactors, the amount of very light nuclei is much lower than in a water reactor, so neutron slowing-down is less efficient, and energy loss by collision is lower on the average. This makes it necessary to perform multigroup calculations with an energy meshing finer than in a thermal neutron reactor, whether on the scale of assembly calculation or of core calculation. In addition, reaction thresholds (inelastic scattering…) can be better taken into account thanks to this meshing.

Apart from specific devices (*e.g.* moderated assemblies for long-lived waste transmutation), there are practically no thermal neutrons in the neutron spectrum. As a result, many "poisons" (neutron absorbers) in the thermal spectrum no longer are so in the fast spectrum: for instance, there is not any xenon poisoning, and the reactivity loss due to accumulated fission products is significantly lower. The self-shielding effects, too, are lower, while remaining significant.

The mean free path of neutrons is much higher, typically of the order of a few centimeters. This means that a fast neutron reactor core is more "coupled" than a thermal core of the same size, that zonal instabilities are less strong, that flux depression in fuel pins is generally negligible, and that heterogeneity effects are lower on the whole. At last, there is a huge neutron leakage out of the core: for example, about 30% of the neutrons generated in the Phénix core leak out of the latter (and, in this very case, are almost fully recovered by the **fertile blankets***).

Design constraints of fast neutron reactors

Several schemes of the so-called Generation IV fast cores have recently emerged, displaying an evolutionary or more innovating character versus existing concepts. As any design result, they originate in compromises and optimizations, between more or less antagonist design constraints, some of which are detailed below.

The reaction **cross sections*** being much lower in the fast spectrum than in the thermal spectrum, it is necessary to have a very high neutron flux (typically a few 10^{15} n/cm^2/s, *i.e.* 10 to 15 times more than in a PWR). The first consequence of these low cross section values is the high amount of fissile* material required to make the reactor **critical***. In order to minimize this fissile material that accounts for a heavy U 235 or Pu 239 initial inventory, a dense core, highly enriched in fissile material (U 235 or Pu 239), and endowed with a high power density, has to be designed. This high power density in fuel is expressed by high nominal temperatures, likely to exceed 2,000 °C in the centerline fuel pellets, and 600 °C in the clads, hence low temperature margins in the case of an accident. Now, this constraint of high power density can be eased if large amount of Pu are readily available.

On the other hand, the high neutron fluxes of fast neutrons lead to a strong damage in the core's constituent materials: marked structural swellings and creeps, in competition with **pellet-clad interactions***, make it necessary to conduct research on **structural materials optimization** likely to push back the neutron limit of irradiation. Today, the latter is about 150 GW·d/t_{ox} for fuel, and 180 dpa **NRT*** for clads; this optimization will have to be pursued for classes of materials considered in Gen. IV reactors.

Fast neutron reactors are characterized by a high **flexibility in the conversion factor**: they may be designed as **burners***, **converters***, or **breeders***; the two crucial parameters governing this feature are the fuel Pu/(U+Pu) content, and the more or less high abundance of fertile zones likely to recover neutrons leaking out of the core, especially numerous in the fast spectrum.

A high conversion factor in fuel also means a decrease in the reactivity loss under depletion, and so the efficiency required for absorbers, so that it attenuates the effects of an accidental ejection of the latter.

It is also worth to mention that part of the conversion factor can be sacrificed to transmute undesirable nuclei (long-lived waste transmutation). In the long term, introducing fast reactors in the nuclear reactor fleet would result in modulating the amounts of long-lived waste generated within certain limits. But minor-actinide transmutation in fast reactors has to cope with hostile constraints: generally, the cost to pay is an increase in the **void coefficient of reactivity***, accompanied with a decrease in the Doppler **feedback coefficient*** and the **delayed neutron*** fraction, which makes it necessary to limit the isotopic abundances, and so the amounts of minor actinides destroyed at each run.

There exist **positive reactivity effects** in a fast reactor, because the nominal core is not in its most critical configuration; in particular, reactivity is increased by core compaction. Moreover, a local hardening of the neutron spectrum due to **coolant voiding** in the fuel area also increases reactivity in the case of a U-Pu fuel. This effect can be compensated at various degrees by increased leakage due to coolant loss, by playing on the geometry and compositions of the core and of its close environment: “flat” core, absorbent heterogeneities present in the core, such as fertile plates or rings, strong increase in the sodium volume fraction just above the core (sodium plenum), etc. The spectrum component, too, can be reduced by decreasing the sodium amount in the fuel areas, at the expense of reducing heat transfer capacities and, so, power density. A judicious combination of these options can lead to a very significant decrease in reactivity effect due to coolant voiding, which, *e.g.* will result in reduced energy releases in the case of a core meltdown accident, and a more favorable behavior during loss of coolant flow accidents.

The amplitude of some feedbacks (**Doppler effects**, expansion effects) can be modulated within some limits. In particular, the major factors impacting on Doppler feedback are the Pu/(U+Pu) content of fuel and spectrum hardness. Here optimization is more delicate, because high amplitude of Doppler feedback, or reduced amplitude at the opposite, may be favorable according to the accidents or the accident process step.

In order to illustrate antagonisms between design objectives with a simple example, let us consider the trends resulting from increased fuel Pu/(U+Pu) abundance:

- The fuel conversion factor decreases, as neutron leakage out of fuel, likely to be recovered by fertile materials, increases; but, generally, there is an incomplete compensation, and the total conversion factor (core + blankets) decreases;

- the void coefficient of reactivity decreases (lower spectrum effect, and increased leakage), and so does the amplitude of the Doppler feedback.

So, an objective of increased conversion factor is most often opposed to an objective of decreased void coefficient of reactivity, as well as to an objective of decrease in the reactivity reserve required for reactor operation. But it is in agreement with an objective of increased temperature feedbacks. Thus, designing sodium-cooled fast reactors (SFRs) likely to be converters, while having a low void coefficient of reactivity, requires the search for a compromise.

The design of the Generation IV prototype ASTRID core rather well illustrates this search for a compromise: the ASTRID low void effect core (CFV: *Cœur à Faible coefficient de Vidange*) (Fig. 120) solves the void problem, since it displays a global void coefficient of reactivity equal to zero. This design stands as a very significant advance in safety in contrast with the previous SFR concepts.

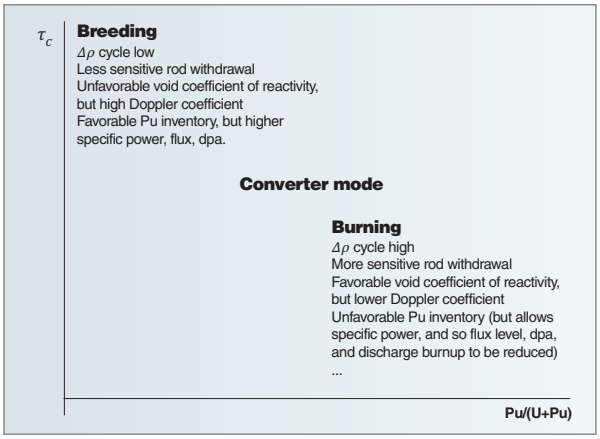

Fig. 119. Conversion factor (τ_c) as a function of the plutonium fuel content Pu/(U+Pu): representation of the terms of the design compromise of a fast neutron reactor.

Assembly calculations

Fast reactor core modeling (Fig. 121), too, is achieved in a conventional way, through a two-step approach: assembly calculations and core calculations. These two calculation steps are performed at the CEA with the ERANOS* computer code.

Assembly calculation is achieved with a fine energy meshing (1,968 energy groups), the group width being about the average logarithmic energy loss by collision on an actinide nucleus. Neutron slowing-down, a non-negligible component of which is due to heavy nuclei, can thus be taken into account correctly.

A horizontal cross section of the assembly is described in detail: for example, in the case of a hexagonal assembly with pins and spacer wires, each pin is represented as follows: fuel (without zoning, given the high mean free path of neutrons), clad integrating spacer wire and coolant; the fuel bundle is surrounded by a hexagonal structured tube, also represented. Simpler (homogeneous, or two-area cylindrical) modeling of fuel cell is possible for fast prospective calculations; the heterogeneity effects on the multiplication factor are then about a few per thousand.

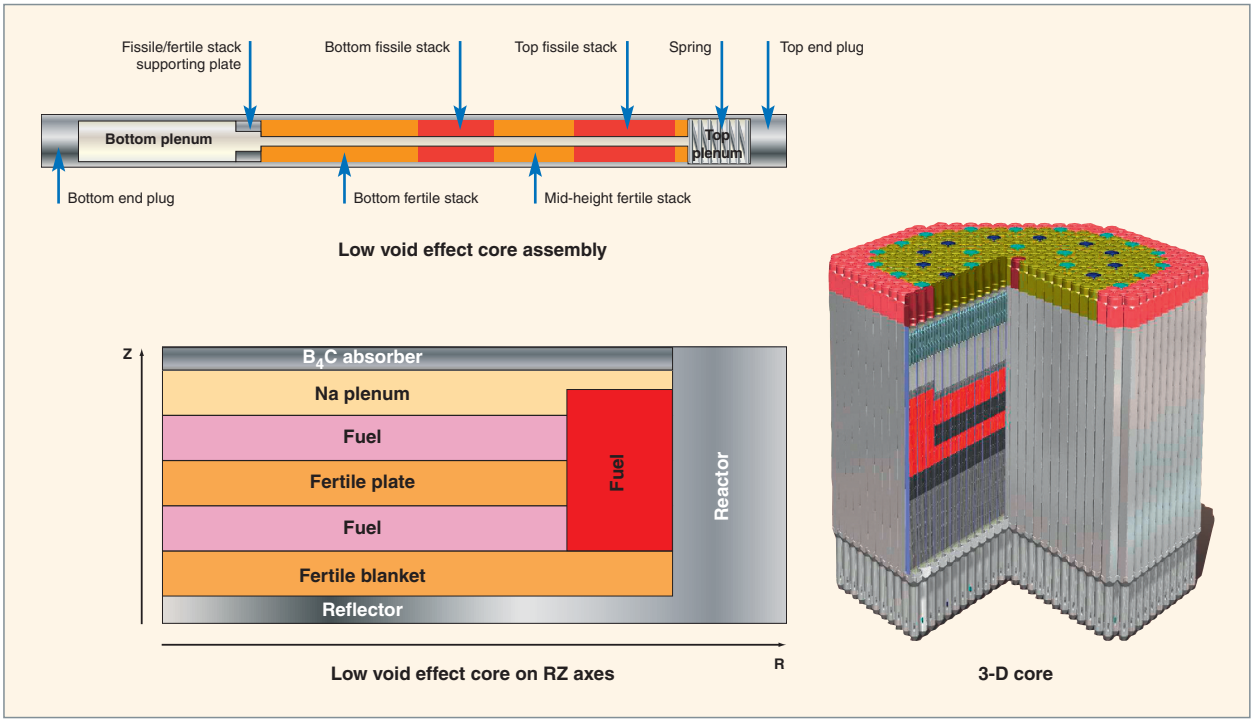

Fig. 120. A picture of the low void effect core (CFV) of the ASTRID fast neutron reactor prototype.

Flux in the fuel element is calculated as part of an infinite lattice on this geometric model, using a **collision probability method***, accurate on simple models, and approximate on full assemblies. Resonance self-shielding is achieved for all resonant isotopes with the help of a subgroup method, in a full geometric description. A broad-group energy condensation and a homogenization can be performed for core calculations to be fed with sets of broad-group homogeneous cross sections. These operations are conducted so as to preserve the neutron balance of the cell.

Given the low neutron weight of fission products, and as the self-shielding phenomenon undergoes little change over the cycle, it is not necessary to take fuel depletion into account at the assembly calculation level. Depletion (or burnup) calculation is generally achieved at the same time as core calculation.

Subcritical assemblies (blankets, reflectors) are treated similarly, but often in a simplified manner, imposing in their peripheral part a source simulating leakage out of fuel areas.

Core calculations

An often used energy meshing contains 33 energy groups, whose boundaries are selected among those of the fine 1,968 group meshing. This meshing is much finer than that generally used in core calculations of pressurized water reactors (*i.e.* two or four groups).

Diffusion theory gives accurate results when neutron flux is close to isotropy, which is the case, excepted in presence of strong absorptions not compensated, or in the neighborhood (approximately one mean free path) of interfaces such as core/blanket or core/reflector interfaces. Flux solvers in diffusion theory are available in one-, two-, or three-dimensional **finite differences***. In a hexagonal geometry, the radial meshing can be refined by discrete steps (7, 19, 37… points per assembly), if taking high flux gradients into account, especially in core peripherals and in blankets.

However, diffusion theory tends to overestimate leakage. In a fast neutron reactor, this is expressed by an under-estimate of the core's multiplication factor of a few per thousand. There is also a notable impact on some reactivity effects strongly dependent on leakage, such as the void coefficient of reactivity, or the neutron distribution in the neighborhood of core boundaries. This is why the transport theory tends to be used as much as possible. In the present state, this can be done in a (XY or RZ) two-dimensional geometry, using a S_N **method***, or in a (XYZ or HEX, Z) three-dimensional geometry, using a **nodal variational method***. A fine flux reconstruction inside the meshes is possible in the latter case.

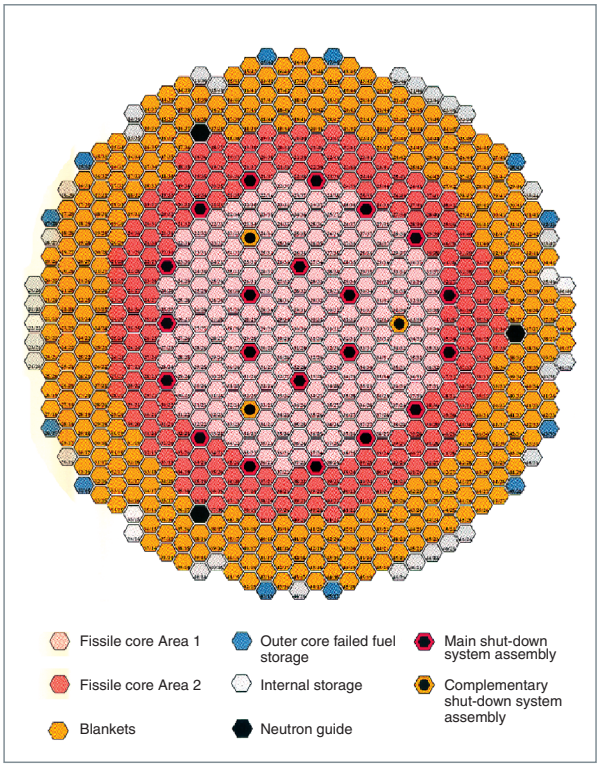

Fig. 121. General scheme of the SUPERPHÉNIX core.

Core evolution is processed by chaining flux calculations and depletion (or burnup) calculations at constant power.

Treatment tools give access to the quantities of interest for the project: neutron balance, material balance and conversion gain, and power distribution and peaks.

It is worth to especially mention the use of perturbation tools, based on the definition of an "**adjoint flux***", or "neutron importance". As the reactions of interest are generated over a very broad energy range, these tools strongly contribute to a detailed physical analysis, invaluable to the nuclear reactor physicist and the designer. In particular, they can help calculate in a simple way the sensitivities to nuclear data of a wide variety of parameters (multiplication factor, ratios between reaction rates, etc.).

Finally, as in the case of water reactors, computational chaining that can be easily parameterized makes it possible to determine cycles at equilibrium, or to perform a fine follow-up of a power core.

Feedback on nuclear data

For fast and intermediate-energy incident neutrons, reaction cross sections are known with a lesser accuracy than in the thermal range. From the project parameter viewpoint, the impact of this lesser knowledge often results in an uncertainty that goes far beyond the target uncertainty required by designers; this is another typical problem of fast reactor neutronics. Sensitivity studies referred to as above can then help define trends for specific nuclear data to be re-examined by evaluators, so that the resulting experimental value prediction can be better focused, and associated to rather reduced uncertainties.

From pressurized water reactor (PWR) to boiling water reactor (BWR)

Even if they are not available in the French fleet, boiling water reactors (**BWRs***) stand as an important component of the world nuclear power fleet. The absence of the secondary cooling circuit on the BWRs makes them less costly on purchase. Reversely, due to the two-phase coolant, their neutronics design is more complex than that of pressurized water reactors.

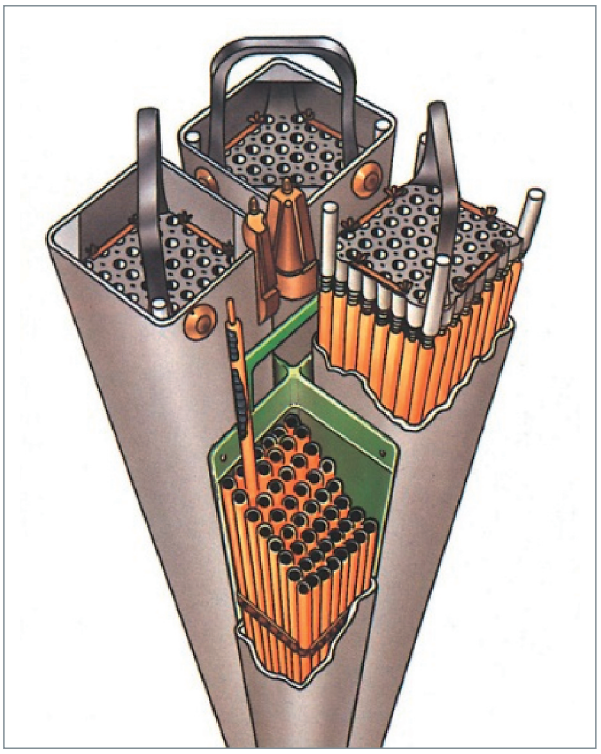

Fig. 122. A Boiling Water Reactor fuel assembly.

Assembly calculations

The BWR assembly design is quite different from that of a PWR design (Fig. 122):

- Fuel rods are enclosed in a box that includes in its center a big-sized “water hole”. This water hole, in which water remains liquid, brings an additional moderation, which avoids the appearance of power peaks in the assembly peripherals, in the upper part of the core (where the void fraction in the box is high);

- a liquid water flow from bottom to top in the core separates the assemblies, thereby bringing the peripheral rods of the assemblies an additional moderation in the upper part of the core;

- the control rod crosses are inserted between the assemblies, and not in the assemblies, as is the case for PWRs.

This heterogeneous design, which decouples the assemblies from one another, ensures high flexibility in the assembly composition (fuel enrichment, fuel poisoning with burnable poisons, etc.). However, it also entails spectrum variations (energy distribution of neutrons), very high from one rod to another, in addition to the axial variation in spectrum due to the gradual steam appearance.

An accurate treatment of these spectrum variations requires a much finer spatial meshing, on the assembly level, than for PWR assemblies. In addition, the steam present at the top of the core enhances the impact of rod coupling due to the increased neutron **migration area***. This entails the use of an accurate resolution method, such as the **method of characteristics***.

At the top of the core, the motion of the neutron spectrum towards the **epithermal*** region, due to under-moderation, requires to take account of the **resonance*** overlapping of some heavy nuclides during the resonance self-shielding calculation.

In order to maintain the computational time at an allowable level, though using accurate, and thus time-consuming, methods, **self-shielding*** treatment and flux calculation in the assembly, *i.e.* the two major items of the total computational time, have to be uncoupled to the utmost. They are set out here, in relation to what was achieved with the APOLLO2 code.

- Self-shielding is locally treated for a certain number of nuclides, with a simple geometric model (*e.g.* a single fuel rod); it is treated on the whole assembly only for a small number of nuclides, for which it is important to take inter-cell coupling into account;

• The flux is calculated with a multi-level scheme that implements several methods and several meshings in both space and energy; the model and the method can so be adapted to the physical problem to be treated;

The depletion (or burnup) calculation is repeated – which is another difference with respect to the PWR computational scheme –, for several void fraction values between 0% and 80%.

So, the calculations performed to build the multiparameterized cross section library include an additional parameter, the **void fraction***. The calculations are repeated for each void fraction value corresponding to a depletion calculation. However, the library does not contain the boron concentration parameter, since boron is not used in BWRs for reactivity control.

The multiparameterized library is built at the end of these calculations just as for PWRs, with a slight difference: all the nuclides, the concentration of which varies under depletion, are particularized so that a detailed depletion calculation can be performed as part of core calculation.

Core calculations

The core model used and the computational methods are not basically different from those used for PWRs. The core is described in the form of homogeneous assemblies, assuming that an inserted control cross is integrated in the four neighboring assemblies.

The thermal-hydraulics model has to be able to treat two-phase situations.

Finally, in contrast with a PWR, the generation/depletion (or evolution) in the concentrations of fuel's various nuclides is always followed up on the core scale. The depletion of nuclei is explicitly treated by solving the Bateman equations using the microscopic cross sections contained in the multiparameterized library. As a matter of fact, a "macroscopic" depletion, such as that to be performed in the case of PWRs, is not suitable here given the space variation of the neutron spectrum.

The case of innovating water reactors

Current light water reactors (PWRs or BWRs) are optimized to use low-enriched U 235-based uranium; hence a limited use of the energy potential of fuel's heavy nuclei, about a few percent. Studies relating to innovating water reactors are aimed at improving the use of matter in core by modifying core neutron design (Fig. 123). Increasing mean neutron energy (**spectrum*** hardening) enhances conversion of U 238 that, by neutron capture and radioactivity, is turned into plutonium, a **fissile*** resource. This objective is reached by reducing the **moderator-to-fuel ratio*** (*i.e.* the ratio between moderator volume and fuel volume), while increasing plutonium abundance in the fuel rods loaded in the core, and introducing **fertile*** targets bearing depleted uranium (heterogeneous core).

Such changes in core geometry and fuel loading entail an adjustment of neutronics calculation:

• Spectral hardening effect as well as increased plutonium content make it necessary to adjust multigroup cross section **self-shielding*** models in lattice transport codes: taking into consideration **resonance*** overlapping of the various heavy nuclei in fuel becomes indispensable;

• the fine assessment of coolant **void effect*** that is a key parameter in the reactor's safety, requires the control of nuclear data uncertainties in the field of higher energies. Given the heterogeneous in-core loadings considered (a mixture of fissile plutonium-bearing assemblies and fertile depleted uranium-bearing assemblies), the assumption of an assembly calculation in an infinite medium usually retained in

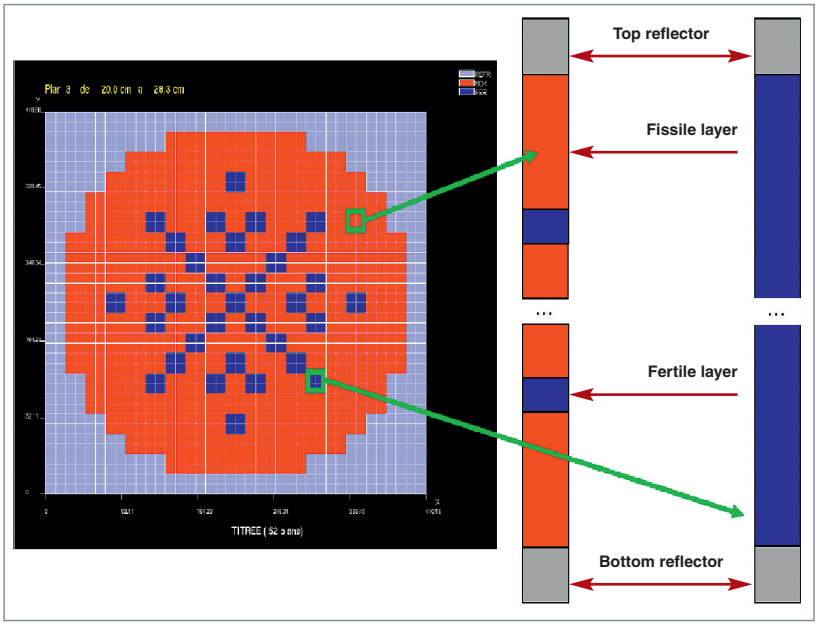

Fig. 123. Twofold heterogeneity of under-moderated light-water-reactor cores.

lattice codes is less allowable. Thus, better taking into consideration interfacing effects between the various fuel assemblies requires calculations on assembly patterns (*e.g.* a 3x3 pattern);

- an adjustment is also needed for reactor core-scale calculation: increase in / adaptation of the energy **group*** number, **depletion** calculation model enabling all or part of heavy nuclei to be taken into consideration ("fine" depletion model).

From PWR to research nuclear reactors: OSIRIS and the JHR

In addition to nuclear power reactors, research nuclear reactors are also required, especially to explore matter's structure, to investigate materials under irradiation, and to produce medical radioisotopes. These reactors, of low power when compared with nuclear power reactors, are designed to produce a high neutron flux.

In small-sized cores of research reactors such as **OSIRIS*** or the **Jules Horowitz reactor*** (**JHR***), the assumption of an infinite lattice to calculate assembly constants is more questionable than in big-sized cores, and leakage is much higher. Significant spectrum transients develop that lead to using space and energy meshings with a much higher degree of refinement in core calculations.

Research reactor cores also differ from big-sized nuclear power cores by the structure of their fuel assemblies. As a matter of fact, the latter most often consists of fuel plate clusters, these plates being flat in the case of OSIRIS, and bent in the case of the JHR: that entails the systematic use of two-dimensional flux computational methods. Similarly, reflectors generally display a more complex structure.

An additional difficulty, often observed in the case of heavy water reactors, too, is the very pronounced heterogeneity of the core: in OSIRIS, reactivity control elements are fully separated from fuel elements, and have comparable dimensions with respect to the latter. In addition, some fuel assemblies in the core are replaced by experimental devices; this configuration entails a specific calculation scheme for the modeling of these reactors.

Experimental devices in the core have an impact on core reactivity and power distribution, to be taken into account for reactor operation.

Yet, this very pronounced heterogeneity of the core is associated with low **feedbacks*** (the temperatures of the various media are space uniform). Hence a simplification, since the libraries dedicated to core calculation are no longer multiparameterized, and can be directly built as a result of the depletion calculation.

The OSIRIS reactor case

ANUBIS, the computational scheme developed by the CEA for the OSIRIS reactor operation, is a scheme derived from the two-step scheme implemented for PWRs.

Assembly calculations

For the various types of assemblies in the core, assembly calculations are performed according to a two-level scheme that achieves a good compromise between accuracy and computational time:

- The resonance self-shielding calculation is performed at 172 energy groups with a very simple geometric model representing a one-dimension traversing path of the assembly of interest; so, this is a succession of infinite plates representing the various media to be found along this path. As a result of this calculation, achieved through the collision probability method (P_{ij}), the cross sections of the different media (fuel, clad, structures) are condensed into twenty energy groups;

- the flux depletion calculation in the assembly is achieved through the ***S_N*method** on a detailed two-dimensional, 20-energy-group geometric model, with self-shielding calculations rerun. As regards the calculation of the control assembly and of the assembly bearing experimental devices that do not contain fuel, the geometric model consists of the assembly to be calculated, surrounded with eight fuel assemblies standing as a neutron source.

As a result of these calculations, a library parameterized for the burnup alone is built for a little number of media (from one to four according to the type of assembly) within a six-energy-group meshing.

Core calculation

The 3-D geometric model of the core is a "container" consisting of the vessel and the associated outer structures (radial and axial reflectors, beryllium "wall", etc.). This container is filled with 49 assemblies of different types, in accordance with the reactor loading scheme. The geometric models of these assemblies each include a few dozen homogeneous meshes in the x-y plane (homogenized fuel with its clad and the related moderator, lateral structures). Axially, the core is split into a little less than 100 meshes.

Flux calculation is performed by solving the diffusion equation or the simplified six-energy-group transport equation using a mixed finite element method.

Fuel depletion is treated as in the PWR case; the only nuclei individually treated are xenon, samarium and boron.

One of the difficulties in this calculation is related to the special structure of control elements. As a matter of fact, they are followed with a fuel element, the depletion of which under flux is stopped when inserting the control element in the core induces its withdrawal from the core. The depletion starts again when the rod is withdrawn, bringing the "follower" fuel element back to the core.

This calculation directly gives access to the quantities of interest, excepting the fine distribution of power (4 areas per fuel plate) that is "rebuilt" starting from two elements:

- The fine (plate per plate) distribution of power in an assembly within an infinite lattice, resulting from the assembly calculation;
- power distribution in the homogeneous assembly, resulting from core calculation that provides information about power gradient in the core assembly.

The case of the Jules Horowitz Reactor (JHR)

OSIRIS and the JHR mainly differ by fuel element shape, reactivity control element structure, and in-core fuel element layout.

The JHR fuel elements consist of twenty-four bent plates grouped so as to form eight concentric cylinders, with a channel in the center likely to house a control rod, an experimental device, or an inert aluminum rod (Fig. 124). With such a configuration, the JHR core displays a lesser heterogeneity than the OSIRIS core. Besides, the lattice consisting of the thirty-seven locations available in the core (among which thirty-four are filled with fuel assemblies) is not regular, and this feature has made it necessary to use a solver adapted to irregular three-dimensional geometries in the CRONOS2 code.

The HORUS-3D computational scheme developed for the JHR three-dimensional calculation is a conventional two-step scheme. It is worth to mention the use of a one-step two-dimensional computational scheme that consists in calculating a horizontal section of the whole reactor with APOLLO2, using the method of characteristics. This very scheme is also used to determine the neutronics constants of the radial reflector.

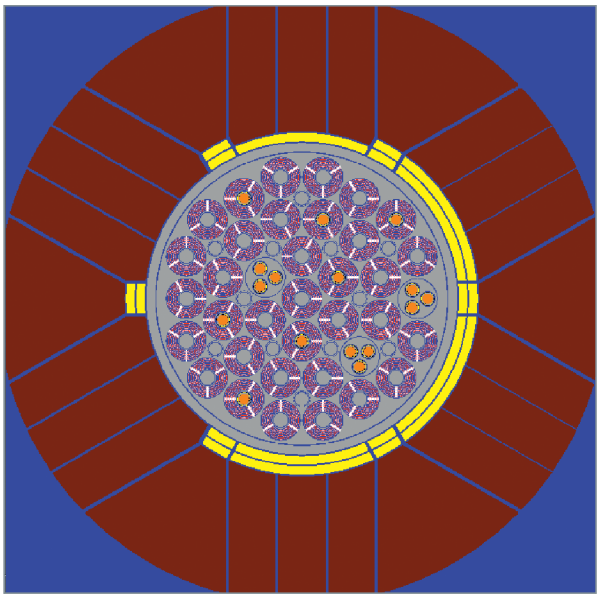

Fig. 124. Scheme of the Jules Horowitz Reactor core.

Assembly calculations

The calculation of the flux under depletion in the various types of assemblies (with control rod, aluminum mandrel, experimental device) is performed in the actual geometry, in an infinite lattice, using the 172-energy group collision probability method.

The elements without fuel, consisting of a group of three experimental devices, undergo a special treatment: they are modeled with a homogeneous environment representative of the fuel assemblies surrounding them.

Following these calculations, the assemblies are fully homogenized, and a six-energy group cross-section library parameterized as a function of burnup is built for each type of assembly. The library relating to the assembly with a control rod is fitted through a transport-diffusion equivalence procedure.

Calculation of the Jules Horowitz Reactor core

As is the case for OSIRIS, flux calculation is performed by solving the diffusion equation or the six-energy group simplified transport equation. The single peculiarity of this calculation lies in the use, with the CRONOS2 code, of special finite elements specifically created to allow this type of irregular core to be calculated. These finite elements have also been implemented to calculate high-temperature reactors (see the following Section). With these finite elements, the core, the vessel and the reflector are described with macro-hexagons containing a variable number of assemblies and experimental devices depending on their position; each fuel element is described by a dodecagon. The whole is meshed according to a triangular pattern (Fig 125). The complex management of these objects

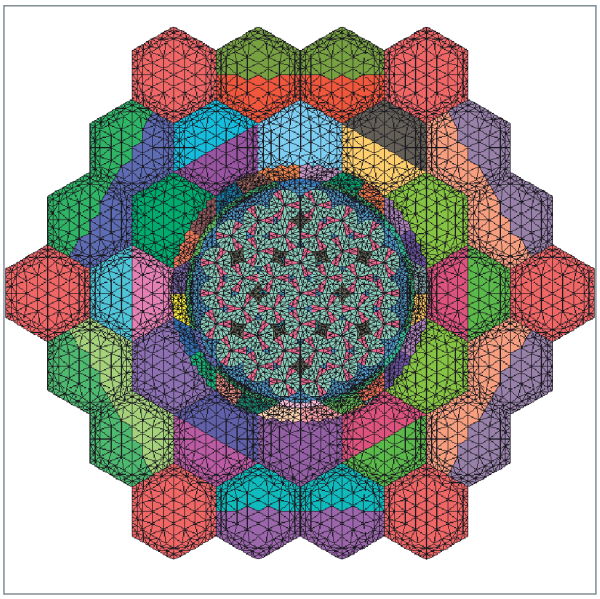

Fig. 125. Space meshing of the Jules Horowitz Reactor core, with its vessel surrounded by its reflector.

is made transparent to the end user through a specific interface. Axially, the core is cut out into a little less than forty meshes.

From PWR to high-temperature reactors (HTRs)

High-Temperature Reactors (HTRs) are gas-cooled reactors currently being investigated within the Generation IV Forum framework. Their interest chiefly lies in their high yield for electric power conversion and their intrinsic safety (see the Monograph "Gas-Cooled Reactors").

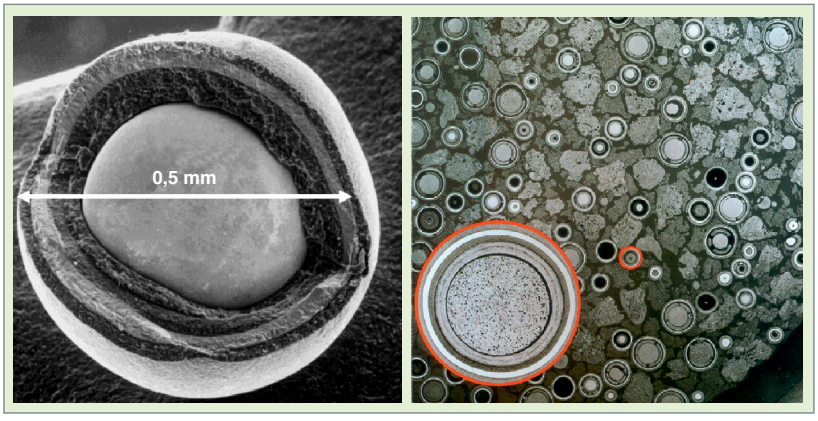

Fig. 126. A "TRISO" fuel particle for high temperature reactors. Sectional view of a HTR fuel element.

HTRs' most striking specificity is the twofold heterogeneity of their fuel element (Fig. 126). As a matter of fact, in a HTR (prismatic block concept), fuel element (*i.e.* the compact) contains uranium oxide as embedded micro-particles that are agglomerated into a graphite matrix. Volume proportions are variable from one concept to another, but a compact generally contains a particle volume much lower than 40%.

It is worth to mention the other following specificities:

- The use of graphite as a moderating material of lower efficiency than hydrogen to slow down neutrons, and low power density of cores result in big-sized cores;
- the availability in assemblies of big-sized channels for control rod insertion that constitute privileged leakage passages for neutrons.

In addition, the emergence of the passive safety concept applied to HTRs has led to an annular core design that is aimed at favoring residual power release in case of Loss Of Forced Convection (LOFC). These annular-geometry cores are characterized by a low-thickness (about 1 m) fuel area, the neutron behavior of which is strongly influenced by inner and outer graphite reflectors: very high variations in neutron spectrum can be observed between the core inner "face" and outer "face". Another HTR peculiar feature is to contain control elements in the reflectors.

Combining twofold heterogeneity, in-core significant spectrum gradients, and control element arrangement (in reflectors) makes it complex to treat cores with a conventional two-step scheme currently applied to other reactor types. However, that structure has been maintained through code development works and computational scheme adaptation.

Assembly calculation

Calculating flux under depletion in the various assembly types (standard assembly and control assembly) is carried out using the collision probability method (in a so-called multicell formalism), or the method of characteristics, with a 172 group energy meshing. The effect of twofold heterogeneity is explicitly taken into account by an ad hoc formalism. This calculation is performed in nominal operating conditions.

As in the case of PWRs or BWRs, multiparameterized libraries dedicated to core calculation are issued from several series of "branch" calculations corresponding to variations in different parameters: as regards the HTR, burnup, fuel temperature, moderating

graphite temperature, and control rod presence are taken into account.

These branch calculations are performed according to a twofold level: a first level allows compacts (graphite matrix and embedded particles) to be homogenized, and their 8-energy-group cross sections to be computed, in order to limit the second-level computational time; in this second level, except for the homogenized compact, the assembly is described in its actual geometry, if need be together with the control rod. The flux is calculated through the 8-energy-group method of characteristics; it is used to homogenize the assembly in one or several areas according to the core model adopted, and to create multiparameterized libraries. The libraries are adjusted through a transport-diffusion equivalence procedure, and the streaming (neutron leakage) effect in control rod insertion channels is taken into account by a correction of the diffusion coefficient.

Core calculation

As in the case of the JHR, in-core flux is calculated according to the 8-energy-group diffusion theory. A function of the CRONOS2 code (momentum method) has been used to add a spatial heterogeneity level within the assembly, and refine its geometrical description, especially to take account of control rod off-centering and **burnable poisons*** presence. Each assembly is split radially into 50 to 100 meshes, and axially into 70 to 100 meshes. CRONOS2 allows the "mixture" of triangular and quadrangular meshes, thereby reducing the number of meshes required for the geometric description of the core (Fig. 127).

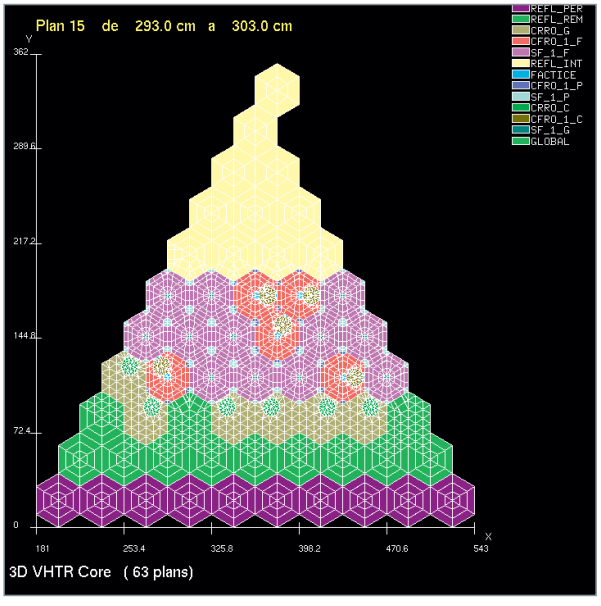

Fig. 127. Three-dimensional space meshing of a very high temperature reactor (VHTR) core.

Core depletion is treated explicitly by solving the **Bateman equations***, for the same reasons as in the case of BWRs. **Thermal feedbacks*** are treated through a coupling with the **CAST3M*** code, six areas being differentiated per assembly.

This calculation provides the critical control rod insertion value, and power distribution per mesh.

From Sodium Fast Reactor to Gas-cooled Fast Reactor

Gas-cooled Fast Reactors (GFRs), currently investigated as part of the Generation IV forum, display specificities which make them distinct from sodium-cooled analogous reactors.

First of all, they allow a higher temperature thermodynamic cycle thanks to the use of heat-resisting materials. These materials often are ceramics containing large amounts of "light" nuclei such as carbon (*e.g.* silicon carbide [SiC]), and are used as both fuel matrices, and structural materials constituents, in substitution of steel. The desired maximization of the inner conversion ratio leads to select a fuel of higher density than oxide (*e.g.* carbide), and to optimize reflectors around the core (with materials such as Zr_3Si_2 or ZrC). On the whole, that leads to a neutron spectrum more degraded than in sodium-cooled reactors, that is slightly shifted to lower energies (yet, there is never a sufficient amount of"light" elements to result in a significant thermal component). Moreover, the energy distribution of neutrons is affected by the presence of new elements (C, Si, Zr, He…), and the absence of others (O, Na, Fe, Cr, Ni…). Taking account of a fine multigroup energy meshing (1,968 groups) allows these spectrum effects to be properly integrated in assembly calculation.

Secondly, and this is what most impacts the computational chain on the assembly calculation scale, the fuel assembly pattern may differ significantly from that used for sodium-cooled reactors, with, *e.g.* plate assemblies as shown on Figure 128. This peculiar geometry has required to adapt the usual **collision probability method*** for the assembly's neutron calculation. On the other hand, as gas is a coolant of low efficiency, its volume fraction is higher than would be that of sodium (40 to 65% instead of an approximate 35%), which may induce heterogeneity effects and preferential leakage directions for neutrons ("streaming"). So these directional effects have to be taken into account on the assembly calculation scale. The core calculation and isotopic generation/depletion model remains unchanged.

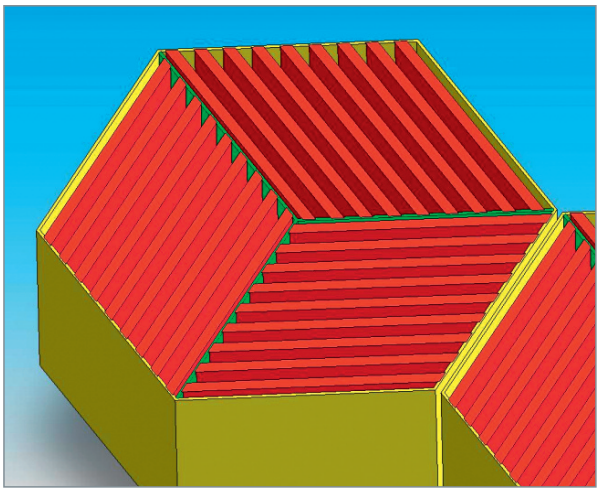

Fig. 128. Fuel element for a gas-cooled fast reactor.

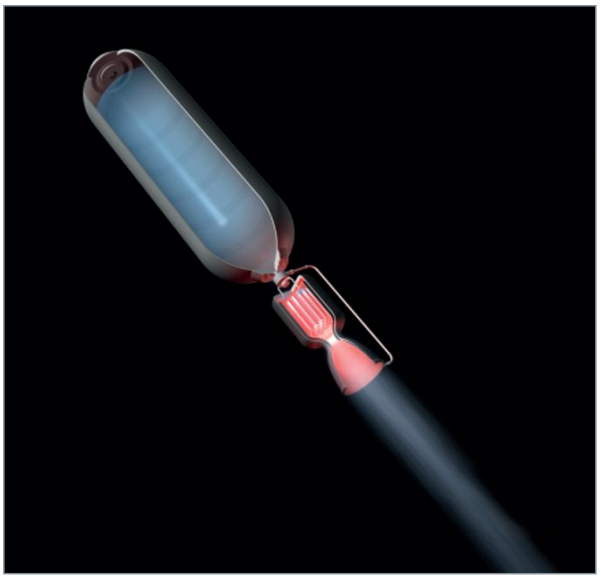

Fig. 129. Thermal space propulsion.

Nuclear space reactor

Given their multipurpose features (high power under low weights, potentially long operating time), nuclear reactors stand as an attractive energy source for space missions.

Potential uses of a nuclear space reactor

Two main types of use of nuclear reactors can be considered in space: power generation and propulsion. Both of them require compliance with specific constraints in terms of neutronics.

Electricity generation

The first application is power generation. The nuclear reactor is then conventionally used as a power generator, whether for supplying a planetary base with power, or meeting power needs of a probe or a space exploration vessel. It can also be coupled with ionic propellers that consume large amounts of power: this is then *nuclear power propulsion, likely to be used for long periods of time (years) with moderate thrusts (hundreds of millinewtons), so as to propel a probe already freed from the Earth's attraction*. This application does not require nuclear reactors operating at very high temperatures (typically 1,300 K).

Nuclear thermal propulsion

The second application is *nuclear thermal propulsion* that generates significant thrusts (tons) during short times (about 1 mn) to free from the Earth's attraction. It uses the conventional thermodynamical route of heating the material to be ejected. This principle is illustrated on Figure 129. Heat generated within the nuclear reactor is the primary energy source. Pure hydrogen current is heated in it at a high temperature (2,500 K to 3,000 K) before being pressure regulated through a suitable flow nozzle. Using this technique that by the way is simple and close to conventional chemical propulsion, allows twice higher ejection speeds.

Neutronics-related design basis

The rules and constraints for the design basis of these reactors, necessarily small as they are to be shipped, are very peculiar. As a matter of fact, optimizing a land-based nuclear reactor relies on the search of a **critical*** reactor with a sufficient **irradiation cycle*** while minimizing the investment in **fissile*** material. In the spatial background, these goals are changed. The investment in fissile material and the latter's proper use no longer are key criteria, since the total amount loaded is low, and these reactors are only related to a few spatial projects. The key points of the design basis of a nuclear reactor designed for spatial applications are the following, in increasing order of priority:

- **Mass** minimization;
- **a long operating time**, usually ranging between 7 and 10 years for power generation;
- tending to a **high core outlet operating temperature**, whether for *nuclear thermal propulsion* or for power generation. The goal is not only to obtain a reasonable conversion yield, but also – and above all – to reduce the surface of the radiating heat sink, the only possible cold source in space.

In the case of nuclear thermal propulsion, very high temperatures and high power density are necessary only for a relatively short operating time.

In addition, the use of a **uranium fuel** is imposed by the safety objectives relating to the use of nuclear sources in space.

Design

Mass minimization constraint

Using a space nuclear reactor leads to an argument quite different from that of a land-based reactor. The choice of the neutron spectrum deeply impacts on the mass of the onboard reactor. On the one hand, a **thermal neutron*** reactor core can be used, likely to enhance U 235 fission (higher probability of neutron-nucleus interaction at a low incident energy of the neutron), but it requires the addition of moderating materials (see **moderator***). On the other hand, a **fast neutron*** reactor core can be used, only containing fissile material and structural materials, but then the low fission **cross section*** in the fast spectrum will tend to increase the critical size of the core.

Using good moderators such as hydrogenated materials (Zr_xH_y, Li_xH_y…), the critical size of a high-enriched uranium, well-**thermalized*** core is smaller than that of a core operating in the fast neutron range, which leads to a lighter reactor.

This is illustrated on the following figures that take as an example the case of parametric studies conducted on an oxide fuel, ZrH-moderated, and using NaK as a **coolant***. As shown on Figure 130, each **moderator-fuel ratio*** corresponds to a different **neutron spectrum***. On Figure 131, critical masses of bare or beryllium-**reflected*** cores clearly evidence a minimum for moderator-fuel ratios neighboring 7.

The choice of a thermal neutron spectrum represents the best solution as regards reactor mass minimization. However, other constraints have to be taken into account.

Temperature constraint

For nuclear thermal propulsion reactors, whose core has to be operating at high temperature, the conclusions may prove different as regards the neutron spectrum to be selected. As a matter of fact, the temperature use range of performing moderators (efficient slowing-down materials, such as hydrogenated materials) is often narrow, and makes it more complex to design a high-temperature, high power density core. Design basis then leads to various technological choices that rely on using heat-resisting materials (based on graphite or other materials) that often have proven to be moderators of low efficiency. The previous trend is then reversed. In this case, the choice of a fast spectrum is privileged so as to minimize the reactor mass. As a matter of fact, using thermal neutrons with this type of moderator would result in prohibitive core sizes.

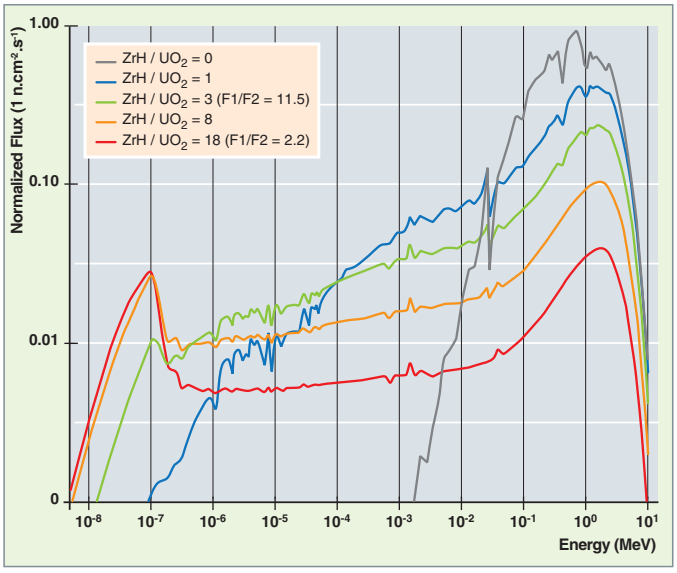

Fig. 130. Neutron flux for various core moderator-to-fuel ratios using zirconium hydride.

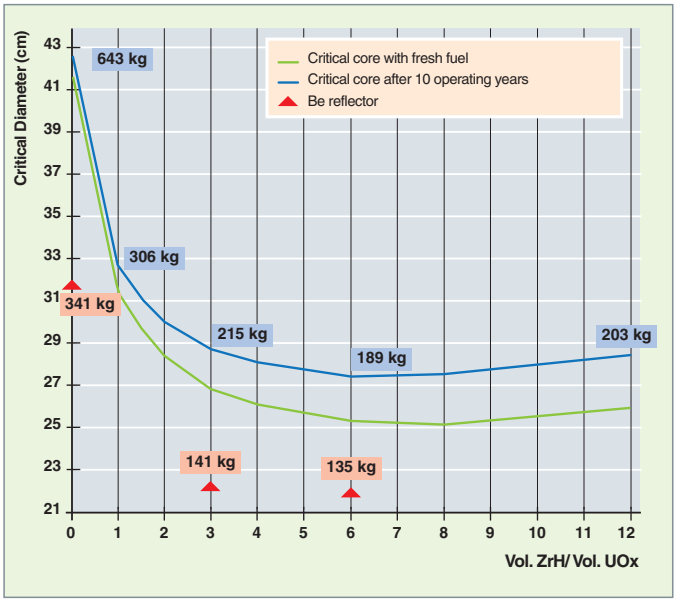

Fig. 131. Example of evolution in the mass of a nuclear space reactor depending on the selected moderator-to-fuel ratio and neutron spectrum. The green and blue curves stand for a bare core; the full triangles, for a beryllium-reflector core.

Time-of-use constraint

One of the specificities of the power generating space reactor is its time of use. The critical configuration of the reactor has to be maintained over a long operating time: generally, about 7 to 10 years, with a power demand likely to vary between 20 and 100 % according to the mission steps.

In such conditions, the fast core will ensure a better control of **reactivity*** evolution due to its high initial fissile material inventory, often much higher than one hundred kilograms of U 235 as against fifteen kilograms or so in a thermal neutron reactor. Reactivity loss due to fuel burnup is a less salient problem. The **burnup*** rates reached (specific energy in MWd/t or in fissioned atom %) are also low. In contrast, materials damage, proportional to the flux of high-energy neutrons (E_n > 1 MeV) integrated over time (***fluence****), is higher in the case of a fast neutron reactor.

Synthesis

The benefits and drawbacks of the two possible neutron spectra in small-sized space reactors are summarized in the following Table 25:

Table 25.

Issue of the (thermal or fast) neutron spectrum alternative in terms of technological constraints

+ stands for favorable – for unfavorable

Type of core	Fast	Thermal
Critical size and mass of the system	– –	+ +
Fuel burnup	+ +	– –
Reactivity control	+ +	– –
Power distribution	+ +	– –
Irradiation resistance of materials (dpa, swelling…)	– –	+ +
High temperature control	+ +	– –

Up to 100 kWe, competition between fast and thermal neutron spectra results from an optimization integrating the whole of the system's parameters. The small size of the thermal reactor will be limited by the maximum burnup allowable for fuel, by a more delicate in-core beginning of life reactivity control, and also by more important power peaks. In contrast, the higher mass of the fast core will be compensated by higher operating temperatures (reduced heat sink size) and a less thick shielding due to the lower flux level in this reactor exhibiting a larger critical size.

If the choice of neutron spectrum is not trivial for small power reactors, operating constraints in space lead to fast neutron reactors when the goal is reaching powers of the order of the MWe. So, for this power range, the designer has to carry out the design basis of a fast neutron reactor associated with a uranium fuel. This can be seen as a peculiarity of nuclear space applications, since, in land-based applications, the fast neutron reactor is rather contemplated with a plutonium fuel, thereby paving the way to breeding.

Neutronics simulation

Reactor control

Small-sized nuclear space reactors are very often controlled by **neutron leakage***. As a matter of fact, the neutron balance evidences a neutron leakage ratio higher than 50 % of neutrons generated in the core. Therefore the conventional approach lies in using shutters or cylinders with **absorbing*** sections, located in the reflector (see Fig. 132 on the following page) as reactivity control tools.

Yet, one of the difficulties of nuclear space reactor design also lies in that their core is not in its most reactive configuration. In the case of a launching failure, some precautions have to be taken in order to avoid any uncontrolled **divergence*** risk by water ingress in the reactor core. The analysis of the "flooding" situation often leads to consider the use of additional absorbers laid out either in the core as **burnable poison*** or

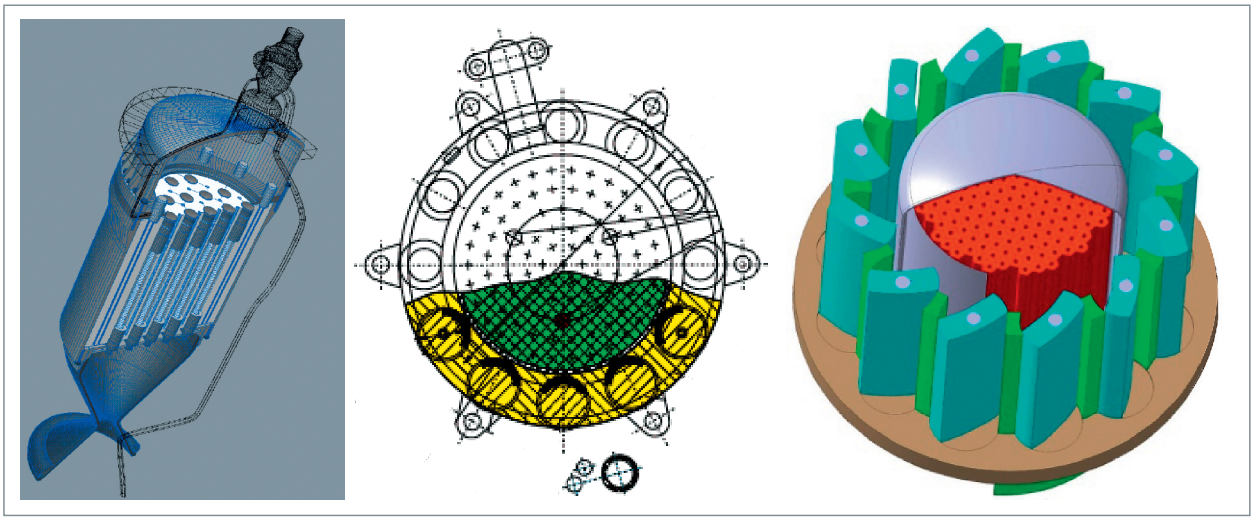

Fig. 132. Example of leakage control systems in nuclear space reactors: nuclear thermal propulsion studies MAPS (CEA/CNES), TOPAZ reactor (ex-USSR), and OPUS reactors (CEA).

small **control rods*** used only once, or, *e.g.* by covering the reactor vessel with a B_4C boron carbide coating.

Nuclear space reactor modeling

The small-sized, very heterogeneous nuclear space reactor is hardly liable to undergo a simplified simulation of the transport equation under the diffusion approximation. As a result, neutron design basis is to be at least issued from 2D fine transport calculations on a core radial description (Fig. 133, following page). As regards the assessment of axial neutron leakage, it is deduced from transport calculations on a RZ axisymmetrical representation of the core. This first approach gives access to reactivity assessment (core k_{eff}), as well as to other neutron parameters, such as **temperature coefficients***, power peaks, control system weight… It also allows prediction of reactivity evolution and, so, of the reactor's potential lifetime.

An alternative, but also complementary approach, consists in directly using 3-D simulations based on Monte-Carlo methods, since the small size of the geometries, as well as the **migration areas*** observed in these cores are liable to undergo this kind of modeling without reaching prohibitive computational times. It is important to note that these calculations, considered as references, may be used to validate deterministic approaches. As a matter of fact, the experimental qualification basis is rather narrow and little documented. It goes back to either U.S. Nerva experiments (1959-1972), or to experiments conducted in the ex-USSR, among which some are still accessible today through collaborations between, *e.g.* the CEA and the Kurchatov Institute. Figure 134 shows the *Narcisse* Russian experiment that will help validate the tools and methods employed to predict the neutronic behavior of nuclear space reactors.

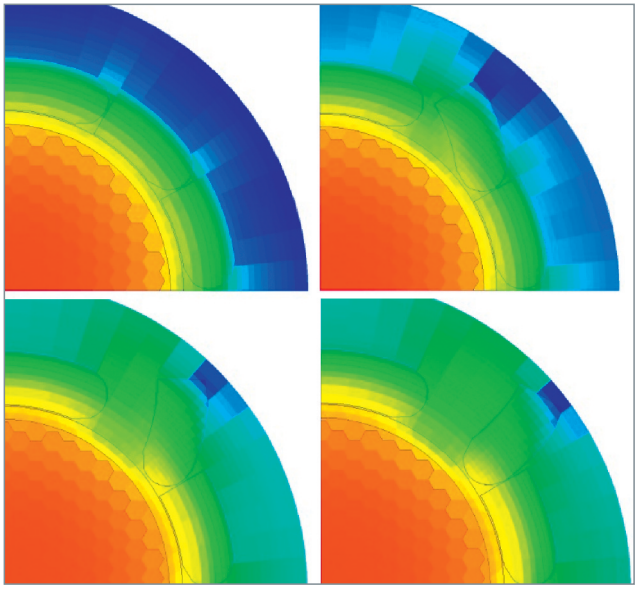

Fig. 133. Neutron flux distribution in the fast neutron reactor OPUS, calculated with the neutronics code APOLLO2 for gradual control opening (0, 30, 60, 90 °).

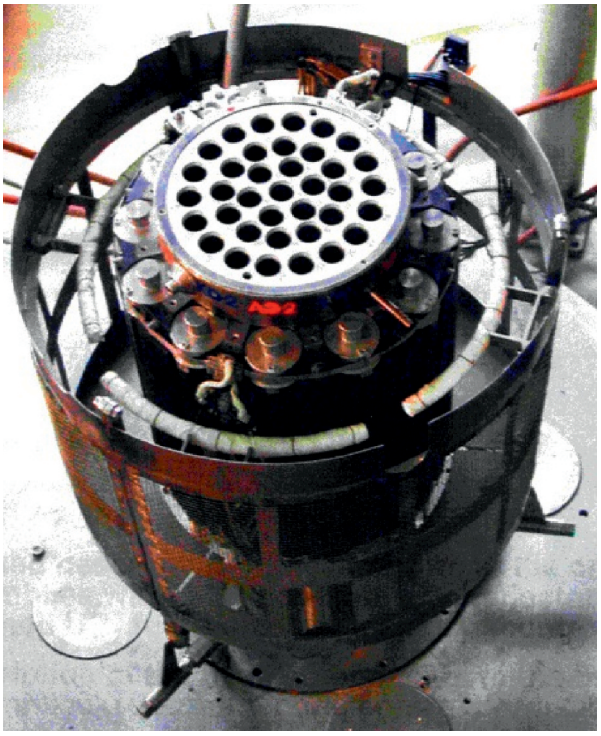

Fig. 134. View of the NARCISSE critical experiment achieved at the Kurchatov Institute.

Example of reactor characteristics of an electric-power generator in the 100-500 kWe range

The OPUS studies currently conducted at the CEA as part of competitive intelligence activities are complementary to the ERATO program achieved in the eighties in relation to power generators. While the ERATO reactor allowed the potentialities of a liquid metal-cooled (Na, and then Li for a more innovating solution) fast reactor to be explored, the OPUS reactor relies on the gas-cooled fast reactor type, and makes it possible to achieve synergies through the R&D endeavors of the Gen. IV land-based reactors.

The approach adopted for the design basis of the OPUS reactor takes into account a power range and a time of use that are variable. The concept is to keep a single reactor scheme for all of the cases to be considered. The reactor so defined is evolutionary, and can meet the needs of both small power and short time missions, and larger-scale missions that require powers of about 500 kWe over periods of time ranging from 7 to 10 years. That leads to the core parameters gathered in Table 26, where only the last values depend on the required power level and lifetime.

Table 26.

Core parameters of the OPUS nuclear space reactor designed at the CEA	
Core radius/height	24 cm / 48 cm
Core mass/volume	300 kg / 87 l
Reactor mass	690 kg
Core reactivity k_{eff} (BOL)	1.073
Flow area	10 % (180 cm^2)
Neutron migration area (M2)	130 cm^2
Doppler effect*	- 0.02 pcm/K
Expansion effect	- 0.6 pcm/K
Control shutter efficiency	11,300 pcm
Maximum efficiency of 3 shutters	4,500 pcm
Mean flux in fuel	$1.8.10^{13}$ $n.cm^{-2}.s^{-1}$
Maximum fast fluence on fuel particle	$7.7.10^{20}$ $n.cm^{-2}$ (E_n > 1MeV)
Mean specific power	4.6 W/cm^3
Mean burnup fraction	~ 0.5 % at.

It is worth pointing out that a reactivity excess indicates that a gain can be obtained on the core mass through reducing its critical radius, and optimizing the reactivity required for small power missions. However, the reactor mass only accounts for about one third of the overall mass of the power generation system, and an overview of the parameters shows that this gain is partly compensated by an increase in the biological shielding mass.

No spatial application has ever been found for nuclear fission reactors: until now only radioactive sources have been shipped. Nevertheless, given their polyvalence, these reactors are likely to be used in the future, particularly for long missions to the planet Mars.

Michel Soldevila, Xavier Raepsaet
Department for Systems and Structures Modeling
and Jean Tommasi
Reactor Study Department

Neutronics Coupled with Other Disciplines

Why this coupling is required

In nuclear reactors, neutron balance depends on fuel temperature and coolant density. All these data involve the coupled solution of the **Boltzmann*** and **Navier-Stokes*** equations, as well as those which govern fuel behavior.

Neutronics studies coupled with other disciplines are mainly used for design and safety of nuclear systems. Safety demonstration makes it necessary to determine margins with respect to the consequences induced by the severest accidental sequences. For this purpose, neutronics, thermics and thermal-hydraulics simulations have to be set up so as to take into account various normal and accidental operating transients. Theoretically, the analysis should be conducted simultaneously for the three disciplines, since:

- **Cross sections*** depend on fuel temperature and moderator density;
- fuel thermics depends on fuel irradiation, neutron power, and thermal exchange with **coolant*** fluid (which is also used as a **moderator*** in water reactors);
- the fluid thermal-hydraulics depends on the power source term released by convection (fuel wall) and by *gamma* radiation.

For the reactor's normal operation, the neutronics / thermal-hydraulics coupling is achieved through cross sections, which are re-evaluated for each spatial mesh, and as a function of the change in fuel and moderator properties; the latter are generally evaluated through an optimized model integrated in the core code.

Until a yet recent period, the three disciplines were relatively disconnected in the approach used to describe accidental situations in safety reports. In this approach, thermal-hydraulics calculations had to involve power distributions in rods computed at each time step. Neutronics feedbacks were determined in them by 3-D neutronics calculations in representative stationary situations. For the calculation of the transient, these core (fuel and moderator) reactivity **feedbacks*** were taken into account by **kinetics*** neutronics calculations, either by considering the core as a point (point kinetics model), or by considering a 1-D approach (1-D kinetics model) at best. The drawback of this approach lies in that, in order to be **conservative***, phenomenological corrective factors, penalizing for several quantities, such as power distribution, reactivity coefficients…, have to be applied in safety studies.

Today, thanks to the development of neutronics codes, reactivity transient simulations can be performed in order to obtain 3-D kinetic responses. These reactivity transients originate in uncontrolled motions of control rods, cooling of the primary coolant system, or change in the moderator's thermal-hydraulics conditions and in boron concentration. Related variations in power may be global, or local and restricted to a few assemblies, or even to a few fuel rods. In addition, the core power level prior to the accident and its burnup history may influence results in transient conditions. Conventionally, neutronics codes use cross sections tables likely to be used for the description of neutron properties in the various core media, for various states: these properties are computed, and then parameterized as a function of, *e.g.* burnup, soluble boron concentration (for PWRs), fuel temperature, moderator density, void fraction for BWRs…, as well as of history parameters (for BWRs, the time spent at different void fractions) In normal operating conditions, neutronics simulation generally relies on simplified models of fuel thermics and thermal-hydraulics.

Today, with the progress of computer performance, it can be considered to interconnect disciplines, and so to reduce the conservatism applied in uncoupled approaches, and get information about every point in the reactor. In the eighties, the CEA conducted the first 3-D rod ejection accident simulation with neutronics / thermal-hydraulics coupling. Today, such simulations are routinely used by the industry, and advances targeted by works underway are boosted by improved fuel modeling. For transients that involve a modeling of the whole reactor (core and circuit, as in a steam pipe break), the CEA has developed a modeling based on a system including the CRONOS, FLICA, and CATHARE codes.

Couplings

In nuclear reactors, neutronic (N), thermal (T), hydraulic (H), and mechanical (M) phenomena are intimately coupled.

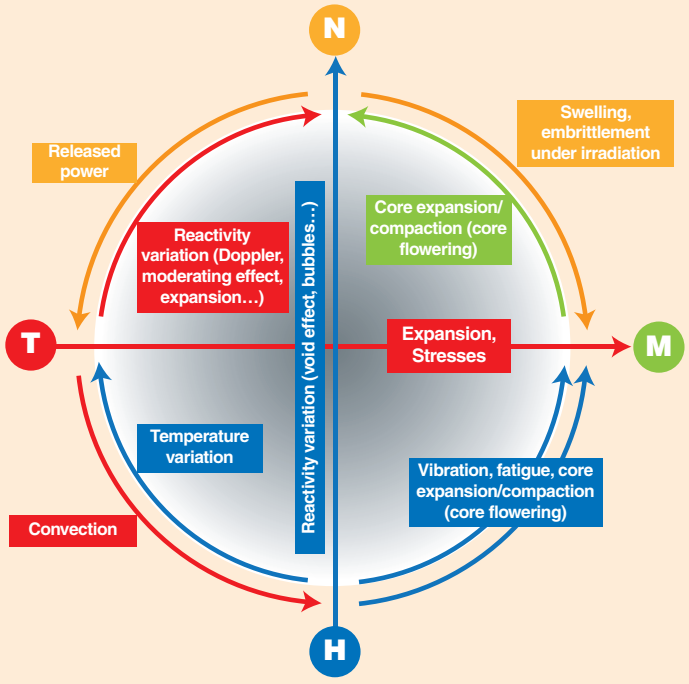

Fig. 135. Coupling between phenomena in a nuclear reactor core.

Of course, neutronics is coupled with thermics, since the energy released as heat in the reactor core arises from nuclear reactions. Conversely, any variation in core temperature changes its reactivity through the Doppler effect, which modifies neutron-nucleus interaction cross sections, and through expansion, which modifies nuclear density in the core.

Thermics and hydraulics are coupled so intricately that they cannot be dissociated (hence the term "thermal-hydraulics"). For any change in the coolant flow regime modifies the core temperature field, and, reciprocally, if temperature changes, this has an impact on coolant fluid flow through convection, and, possibly, by coolant vaporization phenomena on the wall.

Hydraulics and neutronics are coupled, too: the coolant fluid absorbs neutrons to a little extent, and slows them down (a little as in the case of a fast reactor, and more in the case of a water reactor). If the coolant is vaporized, or leaks out of the reactor (*e.g.* because of an accidental primary coolant system leak), this results in a change of neutron absorption and slowing down. Hence a variation in core reactivity.

The core's mechanical structure is designed to maintain in a stable way the distribution of fuel elements, absorbers and moderators in the core, for this distribution determines the core reactivity. However, this structure can undergo slight deformations: it experiences expansion (thermal-mechanics coupling), it swells under irradiation (neutronics-mechanics coupling), and it vibrates, for coolant flow is turbulent (hydro-mechanics coupling). All these effects may induce a variation in reactivity. For instance, a variation in the stresses maintaining fuel bundles together induces the fuel element flowering phenomenon, which much impacts the core's neutronic behavior.

Calculations of large cores of thermal neutron reactors systematically combine neutronics and thermal-hydraulics. A very current challenge of nuclear R&D consists in treating all disciplines jointly, and taking into account couplings within a same simulation platform.

Principles of neutronics / thermal-hydraulics coupling

There exist several alternatives when developing a coupled model. Let us mention two of them:

- implicit coupling, which means treating the full system of coupled equations;
- explicit coupling, which separately solves the neutronics and thermal-hydraulics equation systems, and manages the coupling through data exchange and a steady-state, fixed-point type iterative algorithm.

The advantage of the first solution is that it is direct, and so does not require data exchange between codes, or data treatment to achieve the correspondence between two equation systems separately resolved. However, the major drawback of this model lies in that a full computer code has to be developed in order to ensure that the whole equation system can be solved at one and the same time.

The second solution that has been adopted, is easier to implement, since it does not need any basic rebuilding of the existing computer codes. So it is necessary to work out a set of procedures and/or functions likely to allow the treatment of data and the management of computational meshings. This alternative requires external iterations between codes, and a tool to control codes and manage information exchange.

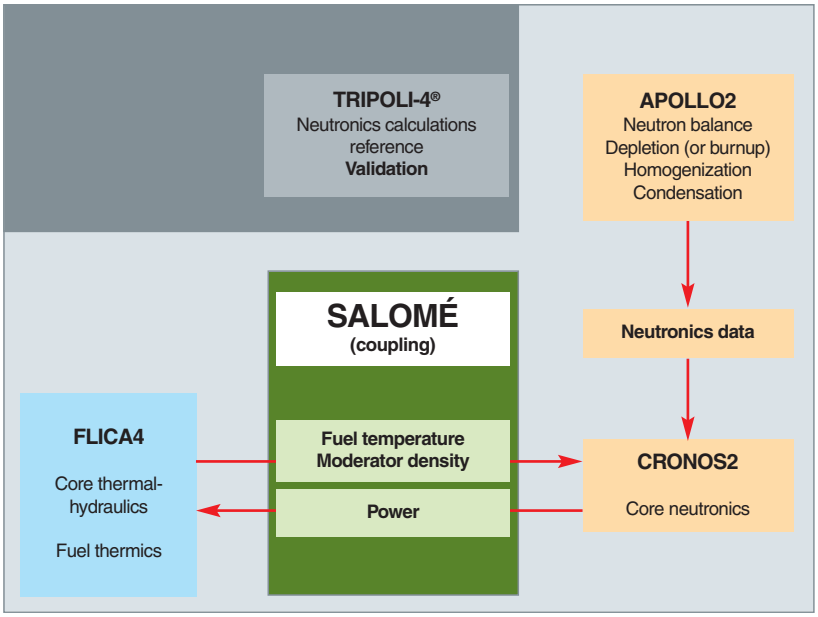

Fig. 136. Schematization of neutronics / thermal-hydraulics coupling.

Figure 136 shows the schematic view of a core calculation that implements, on the **SALOMÉ* platform**, all of the neutronics computer codes APOLLO2 and CRONOS2, and the thermal-hydraulics code FLICA4, mainly developed for **PWRs*** and **BWRs***. Details on neutronics codes are given *supra*, pp. 125-142.

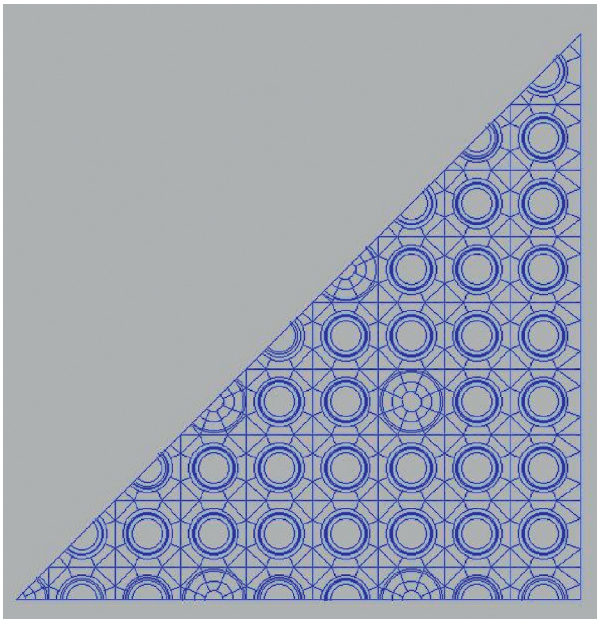

Fig. 137. Typical geometry for a fuel assembly calculation with APOLLO2.

Core calculation is performed within two main steps.

The **first step** consists in computing a two-dimensional assembly as accurately as possible (expliciting all its geometrical features and the materials it is made of), by solving the neutron transport equation and the fuel depletion (or burnup) equations with the **APOLLO2*** code. Figure 137 presents a typical geometry treated with the solver using the method of characteristics. This step does not involve coupling with thermal-hydraulics, and the boundary conditions imposed are reflection on all the assembly faces (this assembly being represented in an "infinite medium").

In a first step, **depletion calculations** are made to obtain the **material balances*** on the assembly. The assembly and rod cross sections are then computed as a function of the parameters of the core state (burnup, void history for BWRs, moderator density, fuel temperature, soluble boron concentration…). The latter are obtained with the help of a set of "branch" calculations, in which the core state parameters are made to vary one by one. A set of several dozen thousand calculations is performed in order to parameterize the assembly-related nuclear data.

This step is validated through reference calculations achieved using for example the Monte-Carlo code **TRIPOLI-4®***.

In a **second step**, core calculation is performed in three dimensions, for example with the **CRONOS2*** and **FLICA4*** codes coupled through the **SALOMÉ*** platform.

The CRONOS2 code solves the multigroup diffusion and transport equations on a simplified core geometry, using the cross sections determined during the previous step (*i.e.* one set of cross sections per assembly), with the actual core boundary conditions. The FLICA4 code solves the 1D fuel thermics and two-phase flow equation using a 3-D four-equation model (mass conservation, momentum and energy balance of the water-steam mixture, and mass balance for steam) for the calculation of inter-assembly transverse flow rates. It receives the power distribution computed by CRONOS2, and determines the thermal-hydraulics variables that will be taken into account in computing neutron data. After a maximum dozen of iterations, at a given moment and for steady operating conditions, this process gives access to power distribution, the thermal-hydraulics field, and core reactivity. The SALOMÉ platform is the coupling tool used to exchange data and control the CRONOS-2 and FLICA-4 codes.

Coupling Examples

Couplings in boiling water reactors

In a PWR, on a power demand from the supply network, the system meets this need by opening the steam-turbine inlet valve: steam is then brought, and pressure and saturation temperature decrease in the secondary coolant system of the steam generator; primary water, a little cooler, goes back to the core inlet, which increases the latter's reactivity, and the power level required can so be reached naturally.

On a similar demand to a BWR, pressure and saturation temperature decrease in the reactor; the bubble volume increases, reactivity decreases, and, instead of meeting the power increase demand, the reaction cannot be sustained. In order to avoid this phenomenon, additional power grid demand actuates flow pump speedup and/or control rod withdrawal. The moderating valve of the turbine is set to keep upstream pressure constant. When pressure rises in the reactor following rod withdrawal, the moderating valve opens so as to let in more steam, and thus tends to maintain upstream pressure.

In order to control reactor power, fine control can act on:

• Rod control position;

• the flow rate Q_e of water inlet to the core.

Preferential control is that of the water flow rate Q_e which does not induce any local perturbation of neutron power. The action on control rods is generally subordinated to the action on the recirculation flow rate, at least in modern reactors whose pumps integrated in the vessel bottom exhibit reduced inertia.

The BWR (Boiling Water Reactor) neutronics is close to that of a PWR, but, due to the high boiling ratio in the BWR, for a comparable **moderator-to-fuel ratio*** (*i.e.* the under-moderation required for the temperature and void coefficients to be always negative, thereby ensuring steadiness and safety), the BWR ratio of volumes V_{H_2O}/V_{UO_2} is higher (2.50 to 2.70 instead of 2.05).

Water enters the core at a temperature slightly lower than saturation temperature, and boiling then develops along fuel clads. The **nucleate boiling*** regime ensures good conditions of heat exchange. In normal operation, clad surface temperature is only a few dozens of Celsius degrees higher than coolant temperature. Boiling crisis, beyond which **film boiling*** would take place with a sharp drop in wall heat flux, can be avoided by limiting the Minimum Critical Heat Flux Ratio (MCHFR) to 1.9.

The **void fraction*** (channel fraction filled with steam) varies depending on service conditions. Corresponding variations in density in the moderator entails a strong coupling between neutronics and thermal-hydraulics.

The water column rising into the core channels remains liquid in the 40 to 70 first centimeters before starting to boil and form steam bubbles in the remaining active core height. Steam bubbles in the core constitute vacancies which strongly reduce reactivity: the reactivity loss goes from -160 pcm/ % void **(*pour cent mille* parts per percent of void)** at the first core beginning of cycle to -100 pcm / % void close the end of a cycle at equilibrium. Close to the end of a cycle, the void effect can be limited by pushing up the recirculation flow rate (which decreases the volume fraction of steam).

An increase of the water flow rate in the core moves the boiling area upwards, and entails an increase in reactivity and reactor power, hence a rise in steam production. The permanent co-occurrence of the two water phases (liquid and steam), and the evolution of global and local transients during a cycle make it absolutely necessary to model the core by **coupling neutronics and thermal-hydraulics, basing on a two-phase thermal-hydraulics model**. For instance, during a failure of the turbine inlet, pressure increases excessively in the core, which induces steam condensation, and so reactivity insertion and a significant variation in spectrum.

Core behavior simulation relies on the use of a coupled "computational scheme", the principle of which has been previously described in this chapter.

The strong heterogeneity of BWR assemblies requires a neutron flux calculation using elaborate methods to solve the Boltzmann equation (Method Of Characteristics), an approach validated by reference Monte-Carlo TRIPOLI-4® calculations. As for PWRs, the data so produced for core calculation depend on burnup, fuel temperature, and moderator density; another parameter called "void history" has been added so as to differentiate assemblies depending on their evolution in a low or high void fraction area. This parameter is directly correlated with the plutonium amount generated in the assembly: the higher the void fraction, and so the harder the spectrum, the higher is the plutonium amount generated.

Figure 138 shows the reactivity behavior in an assembly assumed to be in an infinite medium, depending on burnup, and for several void fraction values respectively representative of the void conditions at the core inlet, core mid-height, and core outlet. This result was obtained with the APOLLO2 code.

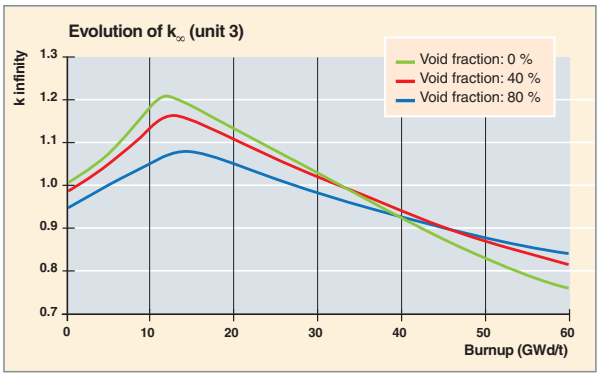

Fig. 138. Reactivity behavior versus burnup, for three void fraction values: 0%, 40%, and 80%.

At the CEA, the latest works on boiling water reactors have dealt with:

- Developing an industrial and reference computational scheme for the various types of BWRs available;
- defining a global CRONOS2/FLICA4 neutronics/thermal-hydraulics computational scheme;
- achieving the physical analysis of BWR abilities to recycle plutonium [4];
- analyzing the new Japanese concepts of tight-lattice BWRs that aim at increasing conversion factors (*e.g.* Japanese projects BARS and HCBWR).

Couplings in gas-cooled high-temperature reactors (HTRs)

Gas-cooled high temperature reactors exhibit a specific neutronic behavior, due to particle fuel and graphite moderator (see the DEN Monograph "*Gas-cooled reactors*"). In contrast with water reactors, in which both functions of **coolant*** and **moderator*** are ensured by water, helium coolant here practically plays no role of neutron moderation due to its low density. This uncoupling gives the designer much freedom in the choice of HTR neutronic features.

Graphite is a poor moderator due to the relatively high atomic mass of carbon: a very high number of elastic scatterings has to be undergone by fission neutrons for them to reach the range of thermal energies. This results in a significant number of neutrons in the epithermal range (*i.e.* from a few eV to a few dozen keV), in contrast with other reactor types, with a strong probability for absorption in the resonances of heavy nuclei during the slowing-down phase. Fuel particles deprived of their surrounding graphite matrix and directly bathed by the gas display a neutron spectrum shifted towards high energies.

Using a very fragmented fuel also enhances neutron absorption in the resonances of heavy nuclei. In a conventional fuel, whether a plate or a rod, one part of absorbing heavy nuclei, especially U 238, is hidden to the neutrons that are preferentially captured in the peripherals of fuel. In the HTR, fuel in the form of micro-particles increases this capture probability. Taking into account the fact that helium is transparent to neutrons, using a graphite matrix containing fuel micro-particles entails the following features:

- The HTR is designed with a **ratio of moderator to fuel*** varying from 500 to 1 000 carbon atoms for one heavy nucleus. This results in a high moderator volume, and so big-sized cores;
- HTRs rely on a high U 235 enrichment owing to the strong neutron absorption of U 238. This high enrichment is also necessary to draw benefit from good performance in fuel particle burnup fractions, so as to make up for fissile material disappearance by fission;
- At last, the HTR is characterized by a broad **migration area*** of neutrons (sum of the square of the lengths actually followed by the neutron before being absorbed), on the one hand during its slowing-down, and on the other hand during its motion by scattering in the thermal state. In the HTR, the slowing-down length in graphite is quite significant. The resulting broad migration area (*i.e.* 450 cm^2 against 50 cm^2 in a PWR) leads to high **neutron leakage*** levels. For instance, 10% of the neutrons leave the annular core of the **GT-MHR*** without being absorbed. Because of these leaks, **reflectors*** play a rather predominant role in the neutronic behavior of the core. Peculiarly, they exhibit a non-negligible positive **temperature coefficient***, which makes it necessary to take account of the thermal **feedback*** effects of reflectors, in addition to those of the core.

In order to draw benefit from the HTR flexibility, it may be useful to design complex and strongly heterogeneous core configurations. Furthermore, some HTR concepts have to ensure a passive removal of **residual power*** in the case of a depressurization accident, which entails annular-shaped cores, well suited for heat transport to the reflectors. The annular configuration induces strong spatial variations in the neutron spectrum, and so core-reflector interfaces hard to model. In addition to these strongly heterogeneous (3-D) annular core configurations, the use of **control rods*** in the reflector and a thermal feedback effect of the reflector have to be taken into account. Figure 139 shows the multi-scale feature in the HTR reactor core.

A computational scheme was developed at the CEA between 2005 and 2008, basing on the **APOLLO2*** and **CRONOS2*** codes, coupled with the **CAST3M*** code for thermal feedback calculation.

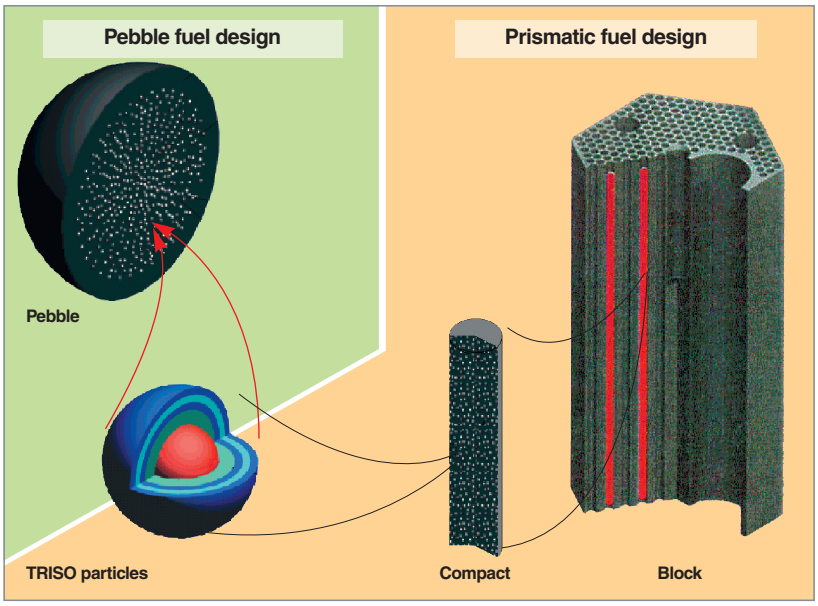

Fig. 139. Structure of the fuel used in gas-cooled high-temperature reactors.

An application result is shown on Fig. 141 that presents the impact of coupling on the core eigenvalue, on **Axial-Offset***, and on axial power profiles. The coupling impact is significant, especially on axial offset that goes from -2% to +5%, and on power distribution.

This coupled system can help conduct studies in static conditions (how to reach steady cycle with inserted control rods), as well as in kinetics in order to model **design basis* transients*** for this reactor type.

Coupling between neutronics codes and thermal-hydraulics codes is achieved by an explicit method, through an external connection. This method consists in solving the two physical problems independently, and exchanging the coupling data at the end of each resolution. This procedure is repeated as many times as necessary until reaching a steady state during which the physical parameters fluctuate under a certain defined limit.

The basic neutronics model selected for coupling is that of a computational scheme called **NEPHTIS***, developed by the CEA for AREVA-NP and EDF. The neutronic modeling of HTR cores treats core calculation as two distinct steps: the first one deals with assembly calculation to generate cross section libraries, using the APOLLO2 code. The second is devoted to the calculation of the whole core according to the scattering theory, using CRONOS2. The thermal-hydraulic model for these cores is based on standard conservation equations for both the coolant and the solid part of the core.. It takes into account the various heat transfer phenomena occurring in HTR cores: conduction, radiation, as well as convection due to coolant gas flow.

The principle of the coupling retained is presented on Fig. 140: the CRONOS2 neutronics code and the CAST3M thermal-hydraulics code exchange temperature and power data through PIPE-type files.

The application of the coupling system has been implemented on the GT-MHR core, basis of current studies on the VHTR.

Various approaches exist to classify accidental transients for HTRs. The most current uses initiating events as a classifying criterion.

The **ATWS*** (Anticipated Transient Without Scram) is a power transient coupled with a penalizing assumption that is the reactor's automatic shutdown system (RAS) cannot be triggered. It belongs to the class of "Transients related to reactivity control". This type of transient is relatively slow (several minutes), but can yet be considered as fast versus neutronics phenomena observed. As a consequence, a fine modeling of neutronics, graphite thermics and core thermal-hydraulics is required all along the transient and in every point of the reactor. The ATWS stands as a privileged application for the coupling system developed at the CEA.

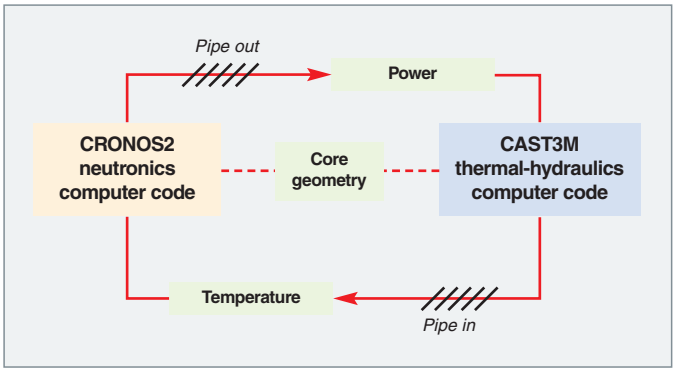

Fig. 140. Principle of the CAST3M-CRONOS thermal-hydraulics/ neutronics coupling for a HTR core.

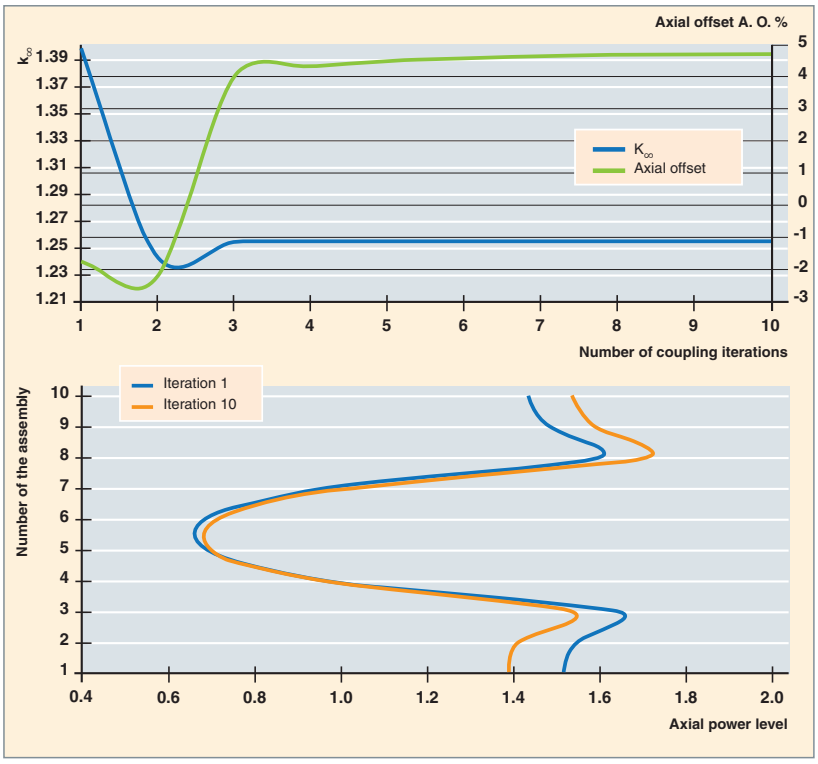

Fig. 141. Illustration of how the neutronics/thermal-hydraulics coupling taken into account impacts reactivity, axial offset, and axial power distribution of the core.

As a rule, there are two sets of automatic shutdown systems in a high-temperature reactor:

1. The main shutdown system consisting of the fine control rods and the safety rods (for the automatic shutdown of the reactor);

2. The backup shutdown system consisting of absorbing B_4C balls injected into the core: if the main shutdown system fails, the second system is operated by hand or automatically.

In an ATWS transient, it is assumed that the main shutdown system is not triggered, or does not detect the variation in reactivity in the core; it is also assumed that the absorbing ball injection system does not intervene.

The transient scenario (Fig. 142) is broken down into two parts that can be treated independently from each other:

1. Initially the core is in a state of equilibrium. Xenon is assumed to be in equilibrium everywhere in the core. One of the fine control rods already inserted in the core up to 170 cm deep is inserted 7 further cm deep within 20 seconds, and remains in this position during ten minutes. The rod insertion corresponds to a reactivity deviation of 50 pcm.

2. Ten minutes later on, the fine control rod is brought back to its initial position within 20 seconds.

At the start of the transient, reactor power is reduced to 79% of **nominal power***. Due to the dynamic effects the power then increases during about 2 minutes, and after 4 minutes, it is stabilized at 97 % of its initial level (Fig. 143).

The second ATWS phase takes place 10 minutes after the transient being initiated. The ATWS initiating rod is brought back to its initial equilibrium position (170 cm), at the same rate as during the first transient phase. Following this motion, reactor power increases up to an approximate 125% of the reactor's nominal power, without the automatic shutdown system being triggered. Beyond 4 minutes, the reactor recovers its initial power, and remains steady (Figure 143).

During the second ATWS phase, the core's power reaches 732 MWth. This power increase is accompanied with a temperature rise which locally reaches 1,410 °C. This temperature rise then brings down the core power level following the thermal feedback effects taken into account in coupling. Without coupling, the power reached in the second transient phase would be quite significant (*i.e.* several orders of magnitude versus the result with coupling), due to the strong **Doppler*** coefficient of this type of core, about 6 pcm/°C. Consequently, temperatures would exceed the allowable safety thresholds (about 1,600 °C for this type of fuel).

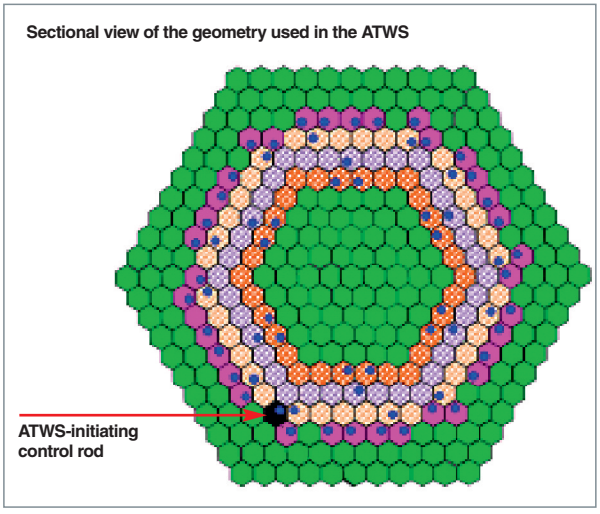

Fig. 142. Horizontal cut view of the geometry used in the ATWS, and localization of the ATWS-initiating control rod.

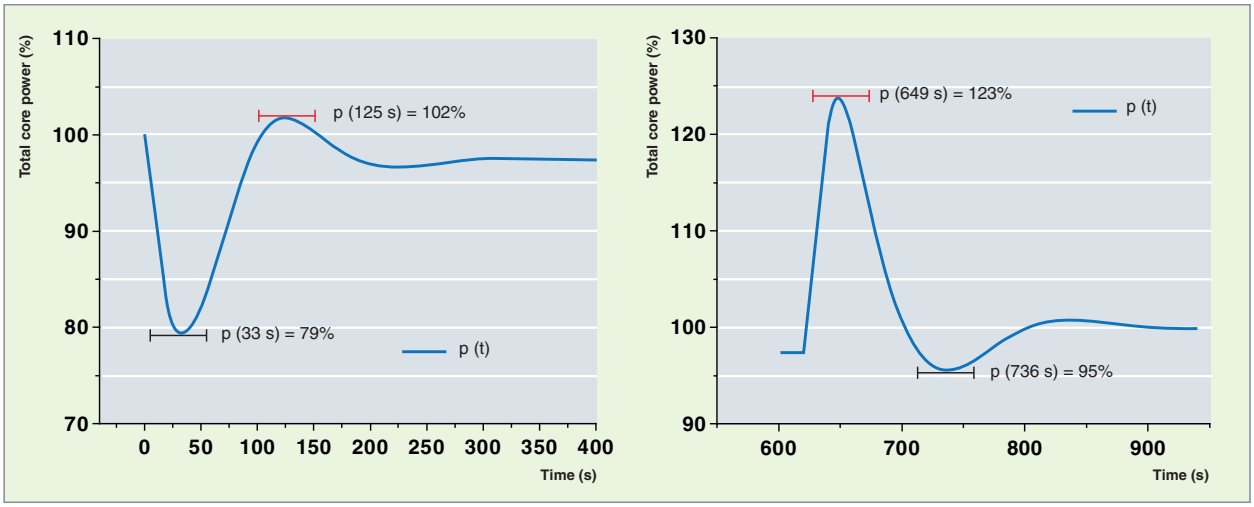

Fig. 143. Time evolution of total core power over the two ATWS steps: control rod insertion step (left figure), and return-to-equilibrium step (right figure).

The outlet temperature of helium during the ATWS also fluctuates. Figure 144 illustrates the variation in the helium outlet temperature at the lower core **plenum*** (in a HTR, helium flows from top to bottom in the core). This variation in temperature does not go beyond 140 °C.

The coupling system applied through the ATWS and other accidental or operating transients makes it possible to initiate design basis and safety studies for the future VHTR concept.

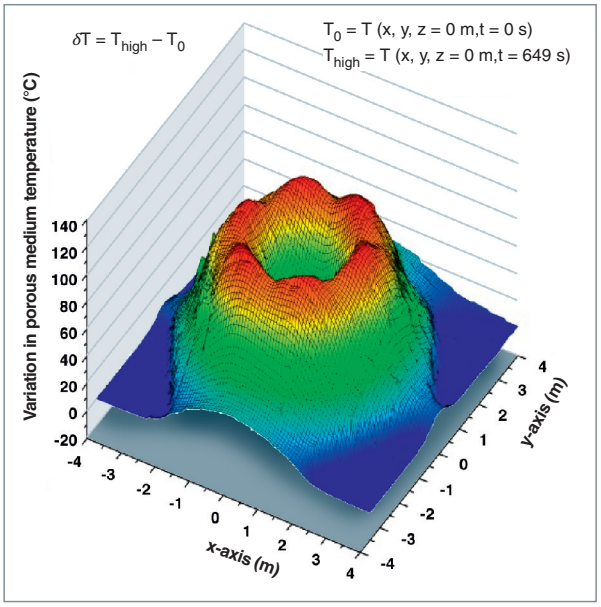

Fig. 144. Temperature variations during a power transient. Variation of outlet helium temperature between the initial critical state (p_0 = 600 MWth) and the maximum power state (p_{max} = 732 MWth).

It will also be used to optimize some features of the reactor, such as the helium outlet temperature rise, while preserving the safety criteria.

Reactivity Initiated Accident (RIA)

Phenomenology

In a nuclear power plant, safety is guaranteed by fuel confinement, which shall not be questioned in any case. This confinement is ensured by three successive barriers:

- The clad separating fuel from the remainder of the core;
- the reactor vessel containing the whole of the core;
- the reactor containment in which the whole of the primary coolant circuit is enclosed.

A reactivity initiated accident (RIA) is an accident induced by an accidental insertion of reactivity in the core; in this case, the resistance of the first barrier (clad) may be affected. In a PWR the conventional initiator of such an accident is the ejection of a control rod assembly. This accident may be qualified as significant due to the consequences it might have, but also as hypothetical due to the related probability occurrence (10^{-6} to 10^{-4} per nuclear plant unit and per year).

The RIA leads to a sudden, significant release of energy in a localized area of the core (*i.e.* the area surrounding the assembly where the control rod assembly ejection has taken place). Two types of transient may take place depending on the reactivity brought by the ejected control rod assembly $\rho_{\text{control rod assembly}}$ and the delayed neutron fraction β present in the core:

- Prompt overcritical type transients corresponding to $\rho_{\text{control rod assembly}} > \beta$ (kinetics controlled by prompt neutrons) This type of transient may be met when the initial core power is low, most of the control rod assembly being inserted in the core and, so, very strongly antireactive;

- Overcritical type transients corresponding to $\rho_{\text{control rod assembly}} < \beta$ (kinetics controlled by delayed neutrons). This situation is a core configuration with an initial power close to the nominal level; the accident-initiating control rod assembly is inserted less deeply than in the previous case, so that its withdrawal will bring a lesser reactivity.

These two transients correspond to two distinct types of neutron kinetics.

Calculating an RIA situation

The aim of RIA calculation is to check that the safety-related criteria associated with this accident are fulfilled. These criteria are empirical, and result from experimentations conducted in the SPERT-CDC and PBF reactors in the USA (in the seventies) on fresh/irradiated UOX fuel (33 GWd/tU), and then in the NSRR reactor in Japan (in the eighties) on UOX and MOX fuels with irradiated up to 70 GWd/tU, and, finally, more recently, in the CABRI reactor at CEA/Cadarache (France) on UOX and MOX fuels with a burnup range equivalent to that used for NSRR tests. Basically, the criteria are of the thermal type, and focus on fuel and clad temperature, as well as on energy deposited in fuel.

In the case of low-burnup fuels (thus subjected to the criteria based on the SPERT-CDC and PBF tests), the analysis of a RIA transient is focused on following up the thermal behavior of the core's hot spot (or hot pellet) after the ejection of the core's control rod assembly exhibiting the highest negative reactivity, the core being in a penalizing state with respect to the parameters controlling the transient. Thus in the case of a PWR loaded with UOX fuel, the analysis is performed in an end-of-cycle core for which k_∞ is minimal (penalizing configuration).

The thermal behavior at the hot spot is directly correlated with the local power evolution during the transient, that is factorized in $P_{\text{core}}(t) \times F_Q(t)$ where:

- $P_{\text{core}}(t)$ is the core power;

- $F_Q(t)$ is the internal peaking factor (or hot spot factor).

It is assumed that, in the initial situation, core power, *i.e.* $P_{\text{core}}(t \leq 0)$, is constant, and so the neutron population is stable. When the control rod assembly is ejected, the core equilibrium is broken. The example presented below corresponds to a situation when the core is critical at a very low power level (*i.e.* a power level equal to residual power $10^{-4} * P_{\text{nominal}}$); the scenario is a prompt overcritical type transient that corresponds to $\rho_{\text{control rod assembly}} > \beta$.

Core power evolution takes place in the five following steps represented by Areas 0 to 4 on Fig. 145.

Following the ejection of the control rod assembly (Area 0), $P_{\text{core}}(t)$ increases very suddenly (exponential evolution) without however inducing a significant temperature rise in the core, given the low initial power level (Area 1).

The Doppler feedback then takes place, and counterbalances the inserted initial reactivity. Power evolution slows down and finally decreases (peak shape in Area 2, Fig. 145).

Simultaneously with a decrease in the energy deposition dynamics, fuel/coolant heat transfer takes place. The moderator density feedback then occurs in addition to the Doppler effect. A new state of equilibrium is reached (Area 3, Fig. 145). Following the **power peak***, core reactivity reaches the delayed neutron fraction (β).

In practice, this state can never be reached (solid-line curve in Area 4, Fig. 145), because the RIA scenario includes the emergency shutdown (*i.e.* all the core's control rod assemblies being dropped, except for the second control rod assembly exhibiting the highest negative reactivity, which constitutes a penalizing factor of the scenario). This event definitively stifles the nuclear chain reaction (dotted curve in Area 4, Fig. 145).

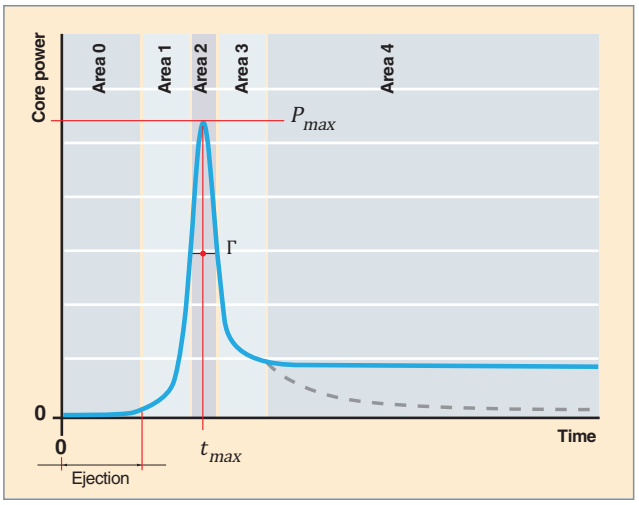

Fig. 145. Typical power time evolution during a reactivity accident.

The internal peaking factor is defined as follows:

$$F_Q(t) = max_{x,y,z}\,[F(x,y,z,t)]$$

where $F(x,y,z,t)$ stands for the normalized 3-D power distribution in the core.

During the five steps previously described, the evolution of the internal peaking factor is as follows.

As the control rod assembly is ejected from the core, the power distribution map is deformed around the ejection spot, thereby resulting in an increase of the internal peaking factor (Area 0, Fig. 146).

Once the assembly has been ejected, the deformation level gets stable around the so-called "ejected static" state ($F_Q^{Stat\ Eject}$). As long as the core power has not reached the threshold for fuel thermics activation, the deformation remains constant (plateau phase in the evolution of the internal peaking factor in Area 1, Fig. 146).

Feedbacks then take place (Doppler feedback in Area 2, and moderator density feedback in Area 3, Fig. 146), so that the power distribution map is flattened, thereby inducing a decrease in the internal peaking factor.

Apart from any emergency shutdown mechanism, the core reaches a new state of equilibrium characterized by a new deformation of the power distribution map, and the internal peaking factor reaches a stable state (F_Q^{Asympt}).

The results displayed here have been obtained through a neutronics/thermalhydraulics core kinetics 3D modeling, which gives access to powers in all of the core's rods.

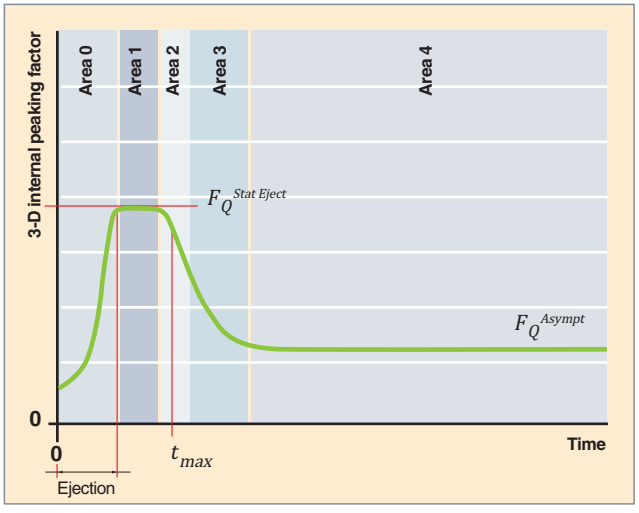

Fig. 146. Typical evolution of an internal peaking factor during a RIA.

Starting from point kinetics analysis, it can be shown that:

- Maximum power reached in the core P_{max} is proportional to $(\rho - \beta)^2$ and inversely proportional to the Doppler temperature coefficient;
- The power peak mid-height width Γ is inversely proportional to $(\rho - \beta)$;
- Deposited energy is proportional to $(\rho - \beta)$ and inversely proportional to the Doppler coefficient.

It can be shown that the Doppler effect, intrinsic to fuel, controls the prompt neutron transient. In the reactor design basis, or in the definition of the assembly loading pattern in the core, the aim is to make sure that the efficiency of the ejected control rod assembly is such that deposited energy is lower than the established limit value.

One example of accidental transient: Steam Line Break (SLB) accident

Phenomenology

The SLB is a design basis accident of pressurized water reactors (PWRs), which involves coupled physical phenomena: thermal-hydraulics of the secondary coolant circuit (location of the accident-initiating breach), primary-secondary heat exchange through steam generators (SGs), thermal-hydraulics of the primary coolant circuit, core neutronics and thermal-hydraulics.

The predictable scenario of a Steam Line Break (SLB) is as follows: the accident-initiating secondary breach induces a large steam leak, which withdraws an increased energy amount from SGs, hence a sudden cooling of the primary coolant circuit. This cooling induces, first, a power increase (increase in reactivity by moderator effect), and second, a pressure drop by a primary fluid shrinkage effect. These two coupled effects may lead to boiling crisis, and so to fuel clad damage. The nuclear power plant engineered safeguard systems are actuated during the transient: steam isolation valves can slow down, or stop, steam leakage (at the utmost, a single steam generator is emptied); the automatic shutdown of the reactor (RAS) [control rod drop] limits the neutron reaction

Table 27.

A few orders of magnitude characteristic of the reactivity insertion accident (RIA)	
Ejection time	0.1 s
Power peak width Γ	60 ms
Emergency shutdown	1 s
Transient time	2 s
Maximum power P_{max}	10 $P_{nominal}$
Maximum value of internal peaking factor $F_Q^{Ejected\ Static}$	20

runaway, and the safety injection can reduce pressure drop, as well as reactivity, by inserting concentrated boron later on (typically within a 70-80 seconds delay).

The Steam Line Break (SLB) is an accident characterized by dissymmetry, for the loop corresponding to the steam breach behaves differently from the other loops. Core cooling is not uniform, which is expressed by a power distribution distortion. During the RAS, this deformation may be enhanced by the non-insertion of a control rod assembly in the best cooled area (penalizing assumption with respect to the accident).

For the French PWR reactor type, the initial conditions of the design basis accident correspond to hot shutdown (maximum SG energy and minimum primary energy), with an end-of-cycle core (maximum moderator effect).

With respect to safety, the discriminating parameter is the minimum Critical Heat Flux Ratio (CHFR) which has to be computed during the transient in order to ensure that boiling crisis is not reached.

Simulation

The complexity of a SLB simulation originates in the need to describe phenomena of different natures and time scales: neutronics, 3-D core and Nuclear Steam Supply System (NSSS) thermal-hydraulics.

Two types of simulation can be carried out; in the so-called "uncoupled simulation", several steps are taken sucessively as follows:

- First, neutron coefficients (cross sections and feedback coefficients) are computed depending on fuel features and management;

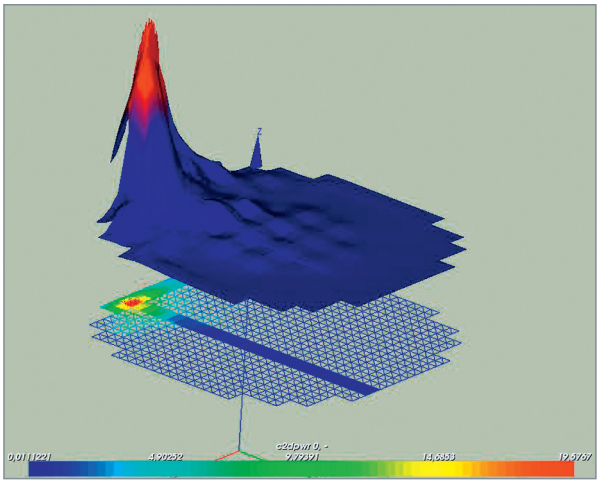

Fig. 147. Envelope of the normalized 2D power distribution, as obtained with all the control rods dropped (excepting the rod with the highest negative reactivity) during a Steam Line Break (SLB) accident.

- secondly, the NSSS thermal-hydraulics features (geometry, pressure drop, operating point, in-vessel mixing…) are used as input data for the thermal-hydraulics code that generates a detailed modeling of the core;

- finally, the overall transient calculation is achieved taking into account the full NSSS and its safety engineered systems, with a simplified core modeling (point kinetics + 1-D TH, the latter being based on multiple 3-D static calculations), or a fine core modeling (3-D kinetics + 3-D TH). Risks of boiling crisis can be quantified in relation to the evolution of the 3-D power map and of local thermal-hydraulics conditions during the transient (Fig. 147).

As regards 3-D coupled simulation, it gives access to the maximum values reached in the reactor for the following parameters: power peak, clad temperature, etc. Moreover, the flow and neutron flux evolution during the transient has an impact on the core behavior that obviously cannot be described by point kinetics. But primary temperature return to equilibrium between core inlet and outlet can be taken into account by 3-D core simulation, which allows a better assessment of feedback effects.

Bibliography

Lautard (J.J.) *et al.*, « CRONOS, un logiciel de simulation neutronique des cœurs de réacteurs », Rapport scientifique DRN, 1999.

Toumi (I.) *et al.*, « FLICA4 : a three dimensional two-phase flow computer code with advanced numerical methods for nuclear applications », *Nuclear Engineering and Design*, 200, pp. 139-155, 2000.

Toumi (I.) *et al.*, "Specifications of the General Software Architecture for code Integration in ISAS", *Euratom Fusion Technology*, ITER Task S81TT-01, 1995.

Lenain (R.) *et al.*, "Physical analysis of plutonium recycling in BWRs", GLOBAL'99, August 29-September 3, Jackson Hole, USA, 1999.

Damian (F.) *et al.*, "VHTR Neutronic Calculation Scheme: Validation Elements using MCNP and TRIPOLI-4® Monte-Carlo Codes", M&C 2005, September 12-15, Avignon, France, 2005.

Limaiem (I.), Damian (F.), Raepsaet (X.), "VHTR Core Modeling: Coupling between neutronic and thermal-hydraulics" M&C 2005, September 12-15, Avignon, France, 2005.

Royer (E.), Raimond (E.), Caruge (D.), "CEA-IRSN participation in the MSLB benchmark", *Nuclear Technology*, vol. 142, pp. 154-165, May 2003.

Mignot (G.), Royer (E.), Rameau (B.), Todorova (N.), "Computation of a BWR Turbine Trip with CATHARE-CRONOS2-FLICA4 Coupled Codes", *Nuclear Science and Engineering*, vol. 148, October 2004, pp. 235-246.

Bruna (G.B.), Le Pallec (J.C.), *and al.*, « HEMERA: a 3D computational chain for PWR safety analysis », PHYSOR 2008, September 14-19, Interlaken, Suisse, 2009.

LE PALLEC (J.C.), POINOT (C.), CROUZET (N.), ZIMMER (S.), "HEMERA V2: An evolutionary tool for PWR multiphysics analysis in SALOME platform", ICAPP 2011-2011 May, Nice, France.

Nuclear Fuel Behaviour Under Reactivity-initiated Accident (RIA) Conditions, State-of-the-art Report, OCDE 2012 NEA No. 6847, 2010.

S. SANTANDREA *et al.*, "Improvements and validation of the linear-surface characteristics scheme", *Annals of Nuclear Energy*, 36, pp. 46-59, 2009.

Éric ROYER, Christine POINOT-SALANON,
Frédéric DAMIAN, Jean-Charles LE PALLEC
Department for Systems and Structures Modeling
and Edwige RICHEBOIS
Department for Facility and Packaging Projects

Fuel Cycle Physics

Nuclear fuel cycle (Fig. 148) is the whole of operations aimed at providing nuclear reactors with fuel, and then managing irradiated fuel from ore mining to waste management.

Managing nuclear materials in fuel cycle requires several parameters relating to nuclear fuel properties at each step of the cycle: control of the materials quantities involved, criticality risk prevention, removal of the residual power generated by these materials, protection against ionizing radiation and control of waste package contamination level…

The knowledge of these parameters relates to the neutronics field: so nuclear fuel use is simulated at each point of the cycle so as to determine physical quantities such as isotope composition (the so-called "material balance"), residual power, activity, (*alpha*, *beta*, *gamma* and neutron) radiation sources and spectra, and radiotoxicity. These quantities that are computed through solving the neutronic depletion equations, allow characterizing fuels and structures irradiated in a reactor.

Neutronics equations provide the possibility to calculate the amounts of the various nuclei being formed at every instant in and out of the reactor through the combined processes of

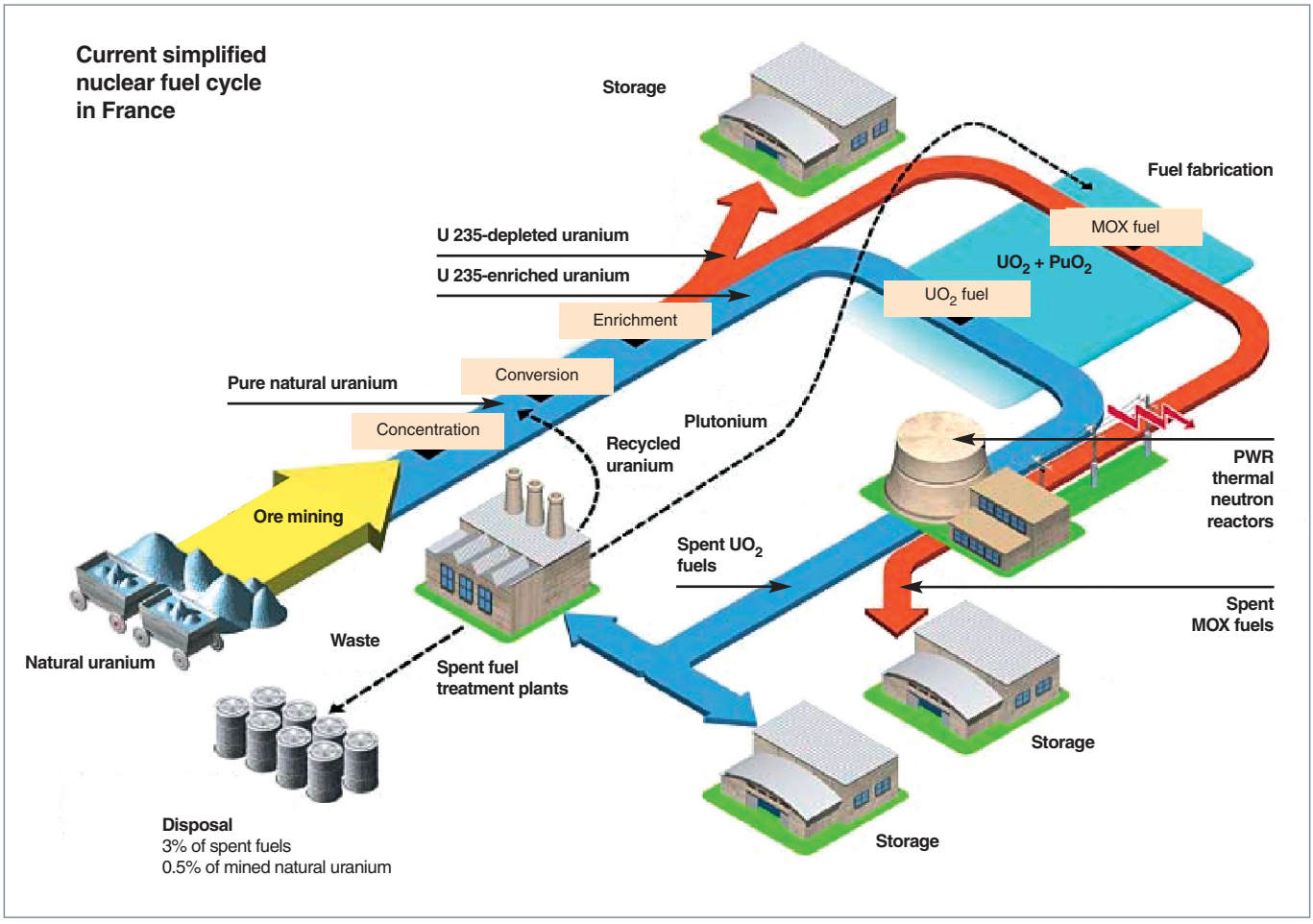

Fig. 148. Fuel cycle in France.

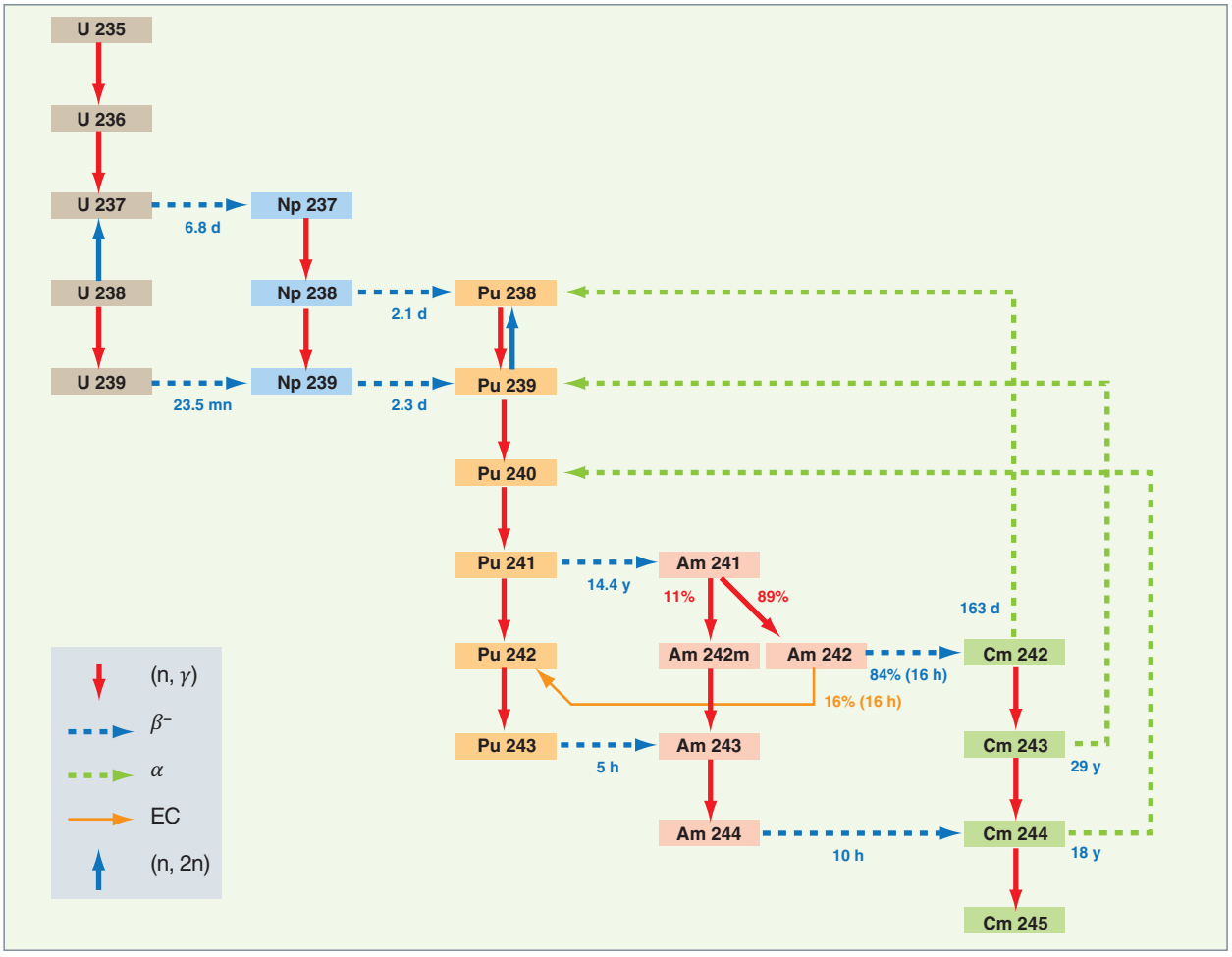

Fig. 149. Extract from a decay chain of the main heavy nuclei present in a reactor core. This scheme shows how actinides, especially plutonium, are formed.

nuclear reactions and radioactive decays (Fig. 149), thereby allowing a "material balance" to be determined.

In fuel cycle studies, it is worth to mention three tools developed by CEA/DEN as a support for these activities:

- The **DARWIN** (a French acronym for *Développement Appliqué au Recyclage Vérifié et Validé pour les Installations Nucléaires*: development applied to recycling, verified and validated for nuclear facilities) code package, developed at CEA/DEN in cooperation with EDF and AREVA, is designed to compute these quantities in every point of the cycle and at any instant, from the end of irradiation to the cooling times corresponding with geological disposal situations. It is dedicated to studies dealing with the whole cycle of present (UOX, MOX), or innovating (GEN. IV) fuels, for any reactor type of interest (PWRs, fast reactors, BWRs, advanced reactors). DARWIN is based on the chaining of neutronics computational tools (APOLLO2, ERANOS, PEPIN2), and uses nuclear data (cross sections, fission yields, decay constants…) mainly arising from JEFF-3 evaluations for actinides, fission products, and activation products.

- The simplified **CÉSAR** (a French acronym for *Code d'Évolution Simplifié Appliqué au Retraitement*: simplified depletion (or burnup) code applied to spent fuel treatment) code that has been jointly developed by the CEA and AREVA since the 1990s, allows a simplified fast depletion (burnup) of a fuel assembly all along its history (fabrication, irradiation, cooling, and storage). Its development was aimed at providing accuracy and fastness in calculations, flexibility and safety of use, so that it may become the code under operation at La Hague spent fuel treatment plant. This tool is validated with respect to DARWIN that is the reference tool for fuel depletion; CÉSAR therefore benefits from the whole of its qualification.

- Criticality risk prevention is treated by the **CRISTAL*** code package.

The presence of fissile nuclear materials in fuel cycle facilities (laboratories and plants) and in shipping casks induces a specific risk, referred to as “criticality risk”. This is the risk to gather the conditions for triggering and sustaining a fission nuclear chain reaction.

The critical state depends on a number of factors, especially:

- the fissile material mass loaded in each device, and the latter’s geometric shape;

- the concentration of uranium or plutonium solutions;

- the presence in the fissile medium of nuclei that slow down neutrons (*i.e.* moderating nuclei), or absorb them (neutron poisons…).

A criticality accident would have severe radiological consequences on staff in most cases, even though all mechanical consequences are seldom prejudicial, and it might entail radioactive materials releases outside the facility.

Criticality risk prevention first relies on assessing, through calculation, the criticality conditions of all the devices enclosing, or likely to enclose, fissile materials. It is also based on the operator's analysis of the operating conditions of these devices.

The new-generation criticality **code package*** named **CRISTAL*** that is dedicated to safety studies, has been developed for this purpose since 1995.

It is worth to mention another major industrial application of these tools, that is the “**Burnup Credit***”. The negative reactivity induced by fuels irradiation in a nuclear reactor core is named “**burnup credit***”. It is due to the decrease in the fissile isotope mass, and to the formation of actinides and fission products absorbing neutrons. As late as in the 1980s, criticality studies neglected the reactivity loss resulting from fuel assembly residence in the reactor core, as part of a safety approach. As a result, the features selected for fuel assemblies were those of assemblies prior to irradiation. The methodology for computing the “burnup credit” was drawn up by the CEA as soon as the early 1980s, to partially take into account the burnup of Light-Water Reactor uranium-oxide fuels in criticality studies.

In relation to neutronics applied to fuel cycle, four typical actions are detailed in this Chapter.

Qualification (or experimental validation) of the “material balance” calculation

Most of the quantities computed for the cycle’s needs are derived from computing isotopic concentrations. This is why a considerable qualification work relating to this quantity for the isotopes of interest in the physics of fuel cycle (see Table 28, next page) is carried out at CEA/DEN that is in charge of setting up the qualification reports of the DARWIN code package.

These reports have to cover the present needs of the French fleet (UOX and MOX PWRs, fast neutron reactors), as well as issues relating to foreign spent fuel treatment, especially those in relation to Boiling Water Reactors (BWRs). Besides, new needs related with the treatment of spent fuels from research nuclear reactors are emerging today.

This qualification is conducted comparing the results of the DARWIN calculation and experimental results. The latter are of two types: isotopic analyses of samples of fuels irradiated in EDF reactors (for UOX- and MOX-PWRs), or in PHÉNIX (for fast neutron reactors), and analyses arising from dissolutions of full assemblies in spent fuel treatment plants (La Hague, Marcoule Pilot Facility).

Present qualification reports deal with actinides U, Pu, Np, Am and Cm, as well as with fission products of interest in criticality studies, burnup credit studies, or residual power calculations (see Table 28, p. 230). The range covered is related with UOX-PWRs, with enrichments between 3.1% and 4.5% up to burnups of 85 GW·d/t, and MOX-PWRs with an average Pu abundance of 5.6% reaching burnups of 60 GW·d/t. Qualification studies are underway so as to extend the average Pu abundances in MOX fuels; they are part of the EDF *PARITE-MOx* program (9.77% Pu), and then *PARITE-MOx Nouvelle Teneur* program (10.78%).

A first qualification of the material balance calculation for BWR fuels in cooperation with AREVA was conducted in 2004, and then reviewed in 2009 with the latest nuclear data (issued from the European database JEFF-3). For this type of fuel, it is necessary in neutronics calculations to take account of an additional parameter, that is void fraction.

Regarding the long-term behavior of spent fuels packages, recent programs have provided first qualification results for long-lived radionuclides: Se 79, Sr 90, Zr 93, Pd 107, Sn 126, I 129, and C 14. Furthermore, this qualification has required R&D programs relating to chemical analysis processes that had never been implemented to measure the above mentioned isotopes.

In the future, qualification will have to be extended to more exotic, not well-known isotopes, such as the following activa-

Table 28.

The nuclides of interest in fuel cycle physics regarding the quantity calculated

(at T > 1 year for residual power)

Material Balance	Residual Power	Neutron Source	Activity	Radiotoxicity	Burnup Credit (FPs)
U 232	U 239	Pu 238	Ac 227	Np 237	Mo 95
U 234	Np 236	Pu 240	Ra 226	Pu 238	Tc 99
U 235	Np 239	Am 241	Ra 228	Pu 239	Ru 101
U 236	Pu 238	Cm 242	Th 232	Pu 240	Rh 103
U 238	Am 241	Cm 244	U 233	Pu 242	Ag 109
Np 236	Cm 242	Cm 246	H3	Am 241	Cs 133
Np 237	Cm 244	Cm 248	Be 10	Am 243	Nd 143
Pu 236	Sr 90+Y 90	Cf 252	C 14	Cm 243	Nd 145
Pu 238	Ru 106+Rh 106		Ca 41	Cm 244	Sm 147
Pu 239	Ag 110m		Cl 36	Cm 245	Sm 149
Pu 240	Cs 134		Nb 94	Se 79	Sm 150
Pu 241	Cs 137+Ba 137m		Mo 93	Kr 85	Sm 151
Pu 242	Ce 144+Pr 144		Fe 55	Zr 93 + Nb 93	Sm 152
Pu 243	Pm 147		Fe 60	Tc 99	Eu 153
Pu 244	Eu 154		Ni 59	Pd 107	Eu 155
Am 241	Zr 95+Nb 95		Ni 63	Sn 126	Gd 155
Am 242m	Sb 125+Te 125m		Ag 108m	I 129	
Am 243	Y 91		Ho 166m	Cs 135	
Cm 243	Ru 103			Sm 151	
Cm 244	Sr 89				
Cm 245	Eu 155				
Cm 246	Co 60				
Cs 133	Cr 51				
Cs 134	Mn 54				
Cs 137					
Nd 145					
Nd 146					
Nd 148					

tion products: Co 60, Be 10, Cl 36, and Ca 41. For this purpose, experimental programs are under definition jointly with industry.

Qualification feedback towards nuclear data

The qualification studies of the DARWIN code package can help determine trends relating to the degree of validity of some nuclear data. From the result of the comparison between calculation and experiment, and controlling uncertainties in computational models and reactor operating conditions, it is possible to assign most of the resulting discrepancy to some nuclear data.

This is illustrated by the example of the work conducted on Eu 154, an isotope that can be used as a burnup indicator in fuel cycle facilities, and that is also important for the calculation of residual power and of **burnup credit***. The comparison of the calculation / experiment results conducted within the framework of the DARWIN qualification showed a very high over-estimation, of about 100%, in the calculation of the material balance of this isotope. A study of related nuclear data evidenced that the theoretical model formerly used in the JEF2.2 evaluation to generate the Eu 154 capture cross section was not suitable. The comparison between, first, known experimental data relating to the measurement of this cross section, and, second, international evaluations, made it possible to propose a new capture cross section in JEFF3.1.1 (Fig.150). This new evaluation has led to an improvement of this fission product data that is now computed at less than 5% (UOX with a 45 GW·d/t burnup).

The release of the nuclear data evaluation JEFF-3.1.1 in 2008 has resulted in a significant improvement in the material balance calculated by DARWIN, particularly for the following isotopes: U 236, Pu 242, Am 242m, Am 243, Cm 244, Cm 245, Nd 143, Sm 147, Sm 150, Sm 152, Gd 155, Eu 153, Eu 154, Eu 155.

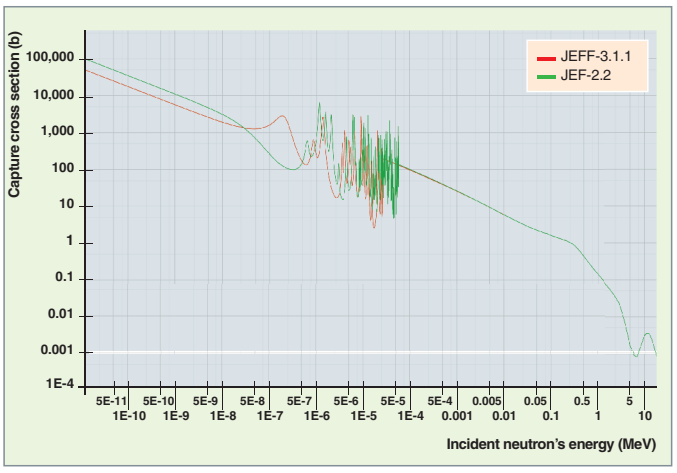

Fig. 150. Comparisons of europium-154 capture cross sections (in barns) in JEFF-3.1.1 (red) and JEF-2.2 (green) nuclear data libraries.

Residual power calculation

After the shutdown of a nuclear reactor, the radioactive decay of the elements formed during fuel irradiation generates the emission of radiations, sources of heat. This non-negligible amount of heat is called "**residual power***". The removal of this thermal power has to be ensured in the reactor, but also in all of the fuel cycle facilities in order to avoid the damaging of the protective structures set up between fuel and its environment.

These problems are especially important in the following fuel cycle units:

- At the reactor level, immediately after a sudden shutdown (as, *e.g.* after the earthquake at Fukushima);
- for all of the machines used for transfer, packaging, or transport of spent fuel assemblies;
- for the treatment plants in which the residual thermal power might induce an overheating of fuel solutions, thereby leading to evaporation and facility obstruction;
- for all the units dedicated to **storage*** of spent fuel assemblies or radioactive waste, in which the degradation of the stored object or of the container has to be avoided.

So it is important to know the degree of reliability to be assigned to a calculation of the "residual power" value.

Figures 151 and 152 below respectively illustrate how actinides and fission products contribute to the residual power expressed in Watt per ton of initial heavy metal of a (4.5% U 235 enriched) UOX fuel for a specific burnup of 60 GW.d/t, as a function of fuel cooling time (calculations performed with the DARWIN code package for cooling times over 1 year).

Qualification works for computing residual power with DARWIN were achieved for long cooling times, that is times for which the fuel cycle stages of interest, with respect to the residual heat problematic, are transport, treatment, storage, and disposal. They consist in interpreting calorimetric measurements of spent fuel assemblies performed by the SKB Company in the buildings of the centralized repository of Sweden. A calorimeter was specially designed to carry out residual power measurements from 50 W to 1,000 W on PWR and BWR type spent fuel assemblies, with an uncertainty lower than 2%.

Basing on thirty or so measurements, for PWR 17x17 and 15x15 assemblies, DARWIN was qualified for residual power calculation over long cooling times (between 10 and 30 years). Calculation/measurement discrepancies show a slight underestimation of residual power calculation (an average of -2.2%), yet covered by the related uncertainty (± 3.4 %).

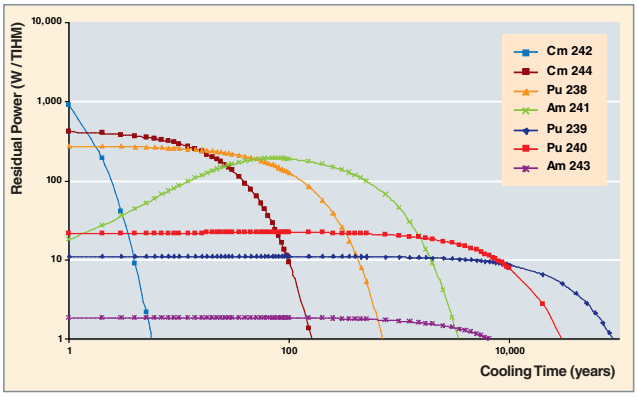

Fig. 151. Actinide contribution to residual power in a (4.5%-enriched) UOX fuel for a 60-GW.d/t burnup.

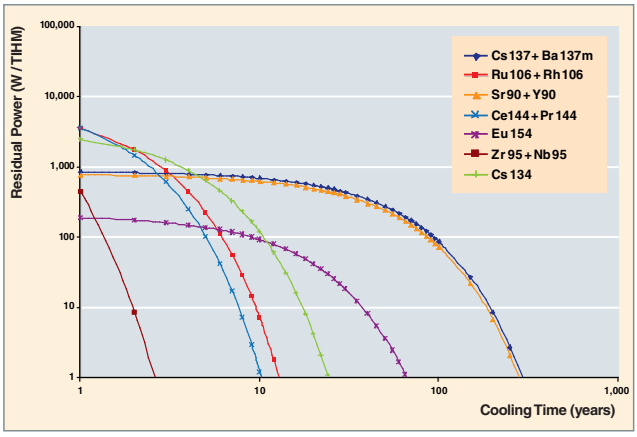

Fig. 152. Fission products contribution to residual power in a (4.5%-enriched) UOX fuel for a 60-GW.d/t burnup.

Recent studies have also evidenced that for cooling times over one year or so, uncertainties about decay energies and constants are generally low with respect to uncertainties about the material balance. In addition, beyond 100 years, residual power is mainly related to the α disintegrations of actinides. Consequently, determining the uncertainty about residual power beyond 100 years fully depends on qualifying the calculation of the material balance of the actinides involved, especially Pu 238, Pu 239, Pu 240, Am 241, Cm 242 (for MOX), and Cm 244.

Studies have been conducted for a few years at CEA/DEN in order to determine, or even reduce the uncertainties about residual power calculation, particularly at short times. They are more especially dedicated to the safety features relating to the removal of this power immediately after the reactor shutdown. According to the consequences for safety, engineers have to add 1, 2, or even 3 error estimations to computed residual power, this margin being all the higher as the severity of the accident is high. This uncertainty depends on basic uncertain-

ties about nuclear data (cross sections, fission yields, de-excitation heat, radioactive half-life of each nuclide), on uncertainties about computational models, and on uncertainties about the operating conditions of the reactor.

In view of this, two major actions are being conducted:

- The first one is relating to the development of propagation of uncertainties tools related to nuclear data, through probabilistic methods (CEA/DEN's **URANIE*** platform coupled to the depletion solver) or deterministic methods. In parallel, actions are underway to improve knowledge of decay data and fission yields values for all of the isotopes involved in residual power calculation, as part of developing the JEFF3 nuclear data evaluation.

- The second action relies on achieving a fine integral measurement of residual power. The MERCI experiment has consisted in irradiating a PWR type fuel rod in the OSIRIS research nuclear reactor (Fig. 153), and then in measuring the released power by calorimetry. The specificity of this experiment lies in that it takes account of all the nuclei, actinides and fission products contributing to residual power, in contrast with former (1970) experiments only based on elementary fissions. Furthermore, measurements have started at a rather short cooling time, of about twenty minutes. This experiment is detailed in the following paragraph.

Measuring residual power: the MERCI experiment

The purpose of the MERCI experiment is to measure the residual power released by a PWR UO_2 fuel sample in a short time after a reactor shutdown in order to validate, or even reduce, the uncertainties relating to this quantity.

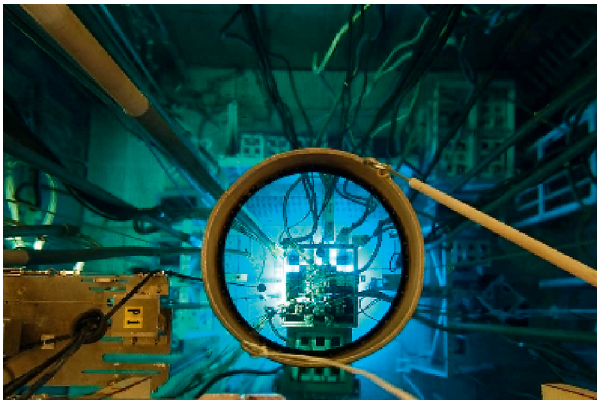

Fig. 153. OSIRIS core in which the MERCI experiment was carried out.

Experiment principle and difficulties

The MERCI (a French acronym for *Mesure de l'Énergie Résiduelle d'un Combustible Irradié*: measurement of the residual energy of an irradiated fuel) experiment consists in irradiating a fuel rod in the OSIRIS pool reactor (CEA/Saclay), and in measuring the released residual power by calorimetry. This principle presents an innovating character in that this is the first integral measurement performed with an industrial type fuel (UOX pellets used for PWR power reactors) in laboratory conditions. In this experiment, residual power can be known after a cooling time of only 26 minutes following the reactor shutdown, including all the evolutions undergone by the various isotopes present in fuel (captures and transmutations).

The first difficulty in performing the MERCI experiment lies in the step of transfer from the irradiation unit to the calorimeter that has to be achieved as fast as possible to give access to the measurement at short cooling times. The calorimeter design is another significant difficulty due to the accuracy required for the measured thermal power (1%). In order to take account of the residual power component transferred by the *gamma* radiation, it was necessary to include in the calorimeter a bulk tungsten containment in which the fuel rod was placed. In such conditions, getting the residual power value entails correcting the raw measurement of residual *gamma* leakage outside the calorimeter (of about 4%), and taking the thermal inertia phenomena into account. In order to ensure that these phenomena are of the second order, once the first instants of the measurement elapsed, an extremely accurate temperature control (+ 0.01 K) is required. These difficulties are increased by the location of the calorimeter, put in a shielded cell. A patent was registered for this calorimeter, named MOSAÏC.

Project schedule

EDF selected the MERCI experiment in 1998, in response to a recommendation of the French nuclear safety authority asking that the residual power values selected for its new fuel management projects be confirmed. The project took place from 1999 to 2009.

The years 1999 to 2004 were devoted to investigating the feasibility study and design basis of the experiment and of the calorimeter. The equipment development was carried out from 2005 to 2007, and the experimental step itself took place in 2008.

Given its both deeply innovating and technical profile, the MERCI experiment has called for the mobilization of the CEA Nuclear Energy Division's (CEA/DEN) major skills for several years, and in various fields (neutronics, thermics, thermal-hydraulics, mechanical engineering, instrumentation, chemistry…), relying on simulation tools (DARWIN-2/PEPIN-2,

FAKIR, TRIPOLI-4®, APOLLO2) and on the operation of the DEN's main facilities (OSIRIS, ATALANTE, LECI, analysis laboratories). The operational control of this set of skills and tools, ranging from the experimentation design to its achievement in reactors, and then up to its detailed interpretation, helped federate teams distributed among eight CEA's units and three CEA's centers.

Technical features

- The irradiation device of the MERCI rod was set up in the core peripherals, in the OSIRIS research reactor pool, 10 cm far from the reactor vessel. Thanks to this location, the specified burnup (3 to 4 GW·d/t) could be reached within an acceptable irradiation time (less than two months). As the aim of the experiment was to validate computer codes and nuclear data, special attention was paid to the acquisition of the physical parameters of interest and to the instrumentation (two poles of dose integrators for integrated-profile recovery, collectrons continuously indicating neutron flux axially and azimuthally, and a fission chamber for periodic flux measurements).

- The MOSAÏC calorimeter (Fig. 154) is dedicated to measuring the decay kinetics of the residual power from an irradiated fuel rod placed in a bulk tungsten shield absorbing γ radiation in a very broad power range going from 300 W to 4 W. This calorimeter (see Figure 154) consists of a low-pressure two-phase water-steam containment (0.026 absolute bar), likely to keep the tungsten shield temperature constant (20°C) by evaporation. This two-phase containment is isolated from the outside by a high-vacuum containment (10^{-3} absolute Pa), the latter being surrounded by a polyurethane thermal insulation. A condenser located in the vacuum containment removes power. The enthalpy balance at the terminals of this condenser reflects the instantaneous residual power. Terms of the second order are added to this balance for thermal losses and inertial storage to be taken into account. Thermal losses are extremely limited thanks to the thermal insulation of the calorimeter, and to the absence of thermal gradient between the device and the shielded cell atmosphere.

In order to minimize the corrective terms that are maximum just after inserting the rod into the calorimeter, the latter was equipped with an insertion device likely to optimize the temperature of the rod as the latter is being inserted. This calorimeter was patented in 2008.

Experiment progress

- **Step n°1:** December 2007-March 2008: rod irradiation achieved in the peripherals of OSIRIS within 55 equivalent full power days (EFPD), at an average linear power density per cycle fluctuating between 260 and 312 W/cm;

- **Step n°2:** March 17, 2008: rod transfer from its irradiation location to the calorimeter placed in a hot cell. That step mobilized a CEA team of 20 persons, and lasted 26 minutes while complying with all of the safety and security measures inherent to irradiated nuclear fuel handling (Fig. 155);

- **Step n°3:** March-May 2008: residual power measurement during 49 days with the MOSAÏC calorimeter installed in a shielded cell. Then, γ-spectrometry and neutron-radiography post-irradiation examinations and chemical analyses were performed on the rod in order to characterize its irradiation (burnup determination).

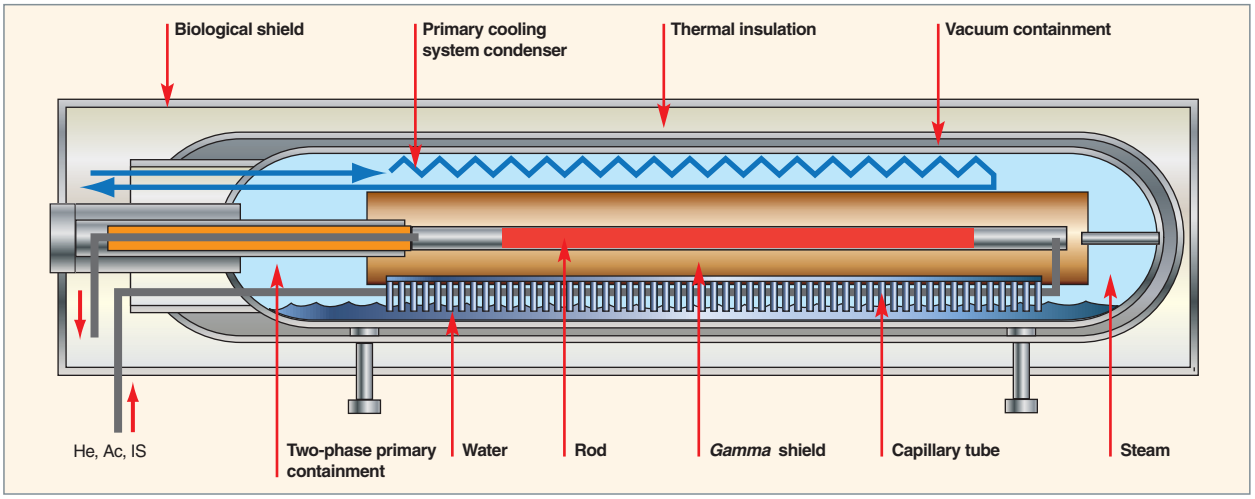

Fig. 154. The MOSAÏC calorimeter.

Fig. 155. The MERCI experiment: a true team work!

Results obtained

The project has come to an end experimentally. The analysis has highlighted the following results:

- The MERCI rod irradiation in the peripherals of OSIRIS was achieved complying with the required irradiation conditions (time and power range), and with a suitable operation of the instrumentation (integrators, collectrons, and fission chambers);

- the calorimetric measurement (see Figure 156) that displays an exponential decay kinetics qualitatively in accordance with prediction, was obtained with the required accuracy in the 45 mn - 60 day range following the rod drop: ± 1% (the measurements acquired before a 45 mn cooling time could not be used due to the pronounced inertial behavior of the calorimeter);

- the required qualitative and quantitative *gamma* spectrometry and isotopic analyses (U, Pu, and burnup indicators Nd, Cs) were achieved on the MERCI rod;

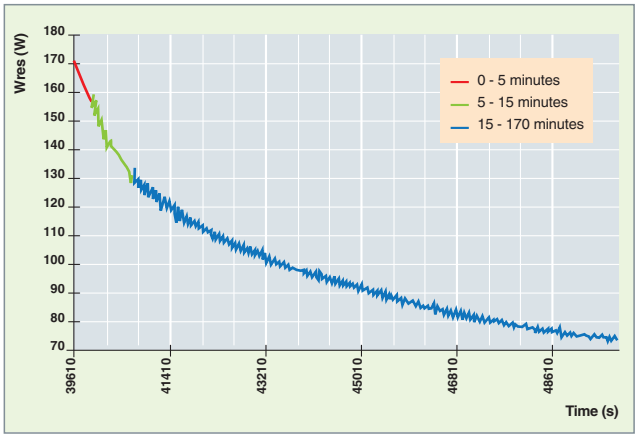

Fig. 156. Measurement of residual power versus time.

- all the experimental data collected during the experiment, with the help of the instrumentation and of the MERCI experiment, could be exploited.

The scientific balance of the program appears as particularly satisfactory, with a validation of the basic principles and of the original technical solutions retained, and, above all, with objectives attained in terms of transfer time and measurement accuracy concerning the two-phase calorimeter.

The interpretation of residual power with computer codes has shown calculation / measurement discrepancies ranging from +0.5% to +6%, included in the 2 standard-deviation interval, for cooling times between 45 minutes and 2 days, and discrepancies around + 1% for cooling times between 45 minutes and 42 days.

Operators have already expressed a pronounced interest for the project: first, EDF that has contributed to the joint financing of the program since its very start, and, secondly, more recently, GDF-SUEZ.

Finally, a second experiment focusing on a MOX rod is considered, justified by a more significant contribution of heavy nuclei to residual power. In addition, it is contemplated to pursue the MERCI program on rod sections irradiated in (UOX, MOX) PWRs.

Bénédicte Roque,
Reactor Study Department
Danièle Gallo and Stéphane Bourganel
Department for Systems and Structures Modeling

Bibliography

San-Felice (L.), Eschbach (R.), Bourdot (P.), Tsilanizara (A.), Huynh (T.D.), Ourly (H.), "Experimental Validation Of The Darwin2.3 Package For Fuel Cycle Applications", *PHYSOR 2012 – Advances in Reactor Physics – Linking Research, Industry, and Education*, Knoxville, Tennessee, USA, April 15-20, 2012, on CD-ROM, American Nuclear Society, LaGrange Park, IL, 2010.

Tsilanizara (A.), Diop (C.M.), Nimal (B.), Detoc (M.), Lunéville (L.), Chiron (M.), Huynh (T.D.), Brésard (I.), Eid (M.), Klein (J.C.), Roque (B.), Marimbeau (P.), Garzenne (C.), Parize (J.M.), Vergne (C.), "DARWIN : An Evolution Code System for a Large Range Application", *Journal of Nuclear Science and Technology*, Supplement 1, pp. 845-849, March 2000.

Jaboulay (J. C.) and Bourganel (S.), "Analysis Of Merci Decay Heat Measurement For PWR UO_2 Fuel Rod", *Nuclear Technology*, vol. 177, pp. 73-82, Janv. 2012.

Criticality

Handling fissile materials in facilities other than nuclear reactors (in the front- and back-end of the **fuel cycle***), in quantities higher than a certain value (**critical mass***), may lead, in the absence of any precursor, to the triggering of an uncontrolled **nuclear chain reaction***: the **criticality accident***. This involves an intense emission of neutron and *gamma* radiation, as well as a strong heating of **fissile*** material, and the release of gaseous radioactive **fission products*** and aerosols (hence, an irradiation and contamination risk).

The feedback on the criticality accidents that took place in laboratories and plants [1] shows that the fissile materials masses involved may be low (slightly more than 1 kg of plutonium for some of them). As for the duration of a criticality accident, it may be no more than a "flash" of about one millisecond, or last for dozens of hours when the conditions for a fast material dissemination during the first power peak are not available.

Generally, fuel cycle facilities are not much liable to sustaining supercritical conditions during long periods of time: as soon as criticality is reached, a power peak takes place, which either tends to disseminate material, thereby entailing a definitive return to subcritical conditions, or leads to periods when the divergent reaction successively stops and starts again, with time intervals more or less long, depending on the environment characteristics (thermal exchange, flows…). As a consequence, energies involved in a criticality accident are not sufficient to induce significant material damage (the energy generated during a criticality accident is between one hundred and one million times lower than that evaluated during the Tchernobyl accident), and the impact on the environment are lower. Despite that, the consequences of such accidents are generally disastrous for the facilities (which seldom start again after the accident), and exposure to irradiation of the operators working near the place of the accident, may be high, or even deadly.

Since 1945, twenty-two criticality accidents have been reported in fuel cycle facilities all over the world [1]. Nine persons died, and thirty-seven other persons were significantly irradiated. The last criticality accident took place in Japan in 1999 (the Tokaï Mura accident, described in the following pages of this chapter). It lasted 20 hours.

Preventing the criticality risk relies on basic principles, which are simple, but require rigorous studies conducted by specialists of this discipline, constant vigilance from all facility actors, and criticality experts' strong commitment in nuclear facilities.

Criticality: a question of neutron balance*

The effective multiplication factor

The criticality conditions of a fissile medium (*e.g.* U 235), in which fission reactions take place, result from the balance of neutrons yielded by fission reaction, and from their loss by absorption or leakage (Fig. 157).

Thus, the status of this medium is characterized by the **effective multiplication factor***, k_{eff}, that expresses the **neutron*** multiplication capability in the fissile medium. It is defined as follows:

$$k_{eff} = \frac{Production}{Absorption + Leakage}$$

If $k_{eff} < 1$, the chain reaction is inhibited. This is the **subcritical*** state, which characterizes the safe state of interest in the operation of nuclear facilities distinct from reactors.

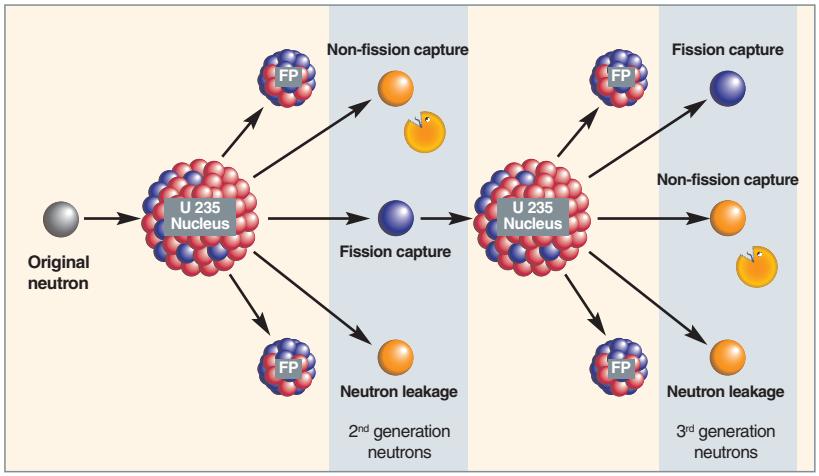

Fig. 157. Neutron balance following a fission reaction between a neutron and a U 235 nucleus.

If k_{eff} = 1, the chain reaction is controlled. This is the just critical state, for which neutron population remains constant, *i.e.* the target state in nuclear operating reactors, and, reversely, the state that shall never be reached in other nuclear facilities or in fissile materials transport.

If k_{eff} > 1, an uncontrolled nuclear chain reaction starts, thereby entailing a significant yield of neutrons which is not compensated by neutron absorption in the medium or by their leakage out of the latter. This is the **supercritical*** state that leads to the criticality accident.

As part of the preventive approach intended to avoid such a criticality accident, evaluations are carried out in such a way that at any instant, the multiplication factor k_{eff} of a unit or working post must be lower than 1, with a sufficient safety margin.

Apart from the various **cross sections*** (fission, non-fission capture, scattering…), several parameters (mass, geometric shapes, materials…) directly impact on the various terms of the neutron balance. In order to illustrate the various phenomena involved, a case of application based on the Tokaï Mura criticality accident is also proposed in the following pages. The criticality engineer's approach consists in "playing" with these parameters for the sum of neutrons absorbed and of neutron leakage be significantly higher than the number of yielded neutrons referred to as "useful" (*i.e.* those yielding fission reactions, thereby contributing to increase the system's multiplication factor k_{eff}), seeing that:

- fission reactions, which are sources of "useful" neutrons, are limited as much as possible;
- neutron disappearance by leakage out of the fissile medium, or their absorption by non-fission capture are boosted as much as possible.

It is to be noted, too, that the evaluation of a system, seldom isolated from its environment, has to take account of the following items:

- A neutron which has escaped from the system, may be scattered by the environment, and go back to the system with a probability not equal to zero (neutron reflection);
- The system may have in its environment other systems containing fissile material into which neutron leakage can penetrate, and thus contribute to add neutrons likely to induce fission reactions in it (neutron interaction).

These various phenomena are presented hereafter.

"Useful" neutron production

Fissile material mass

Neutron production increases with the number of fissile nuclei in the medium, and, so, the fissile material mass (increase in the total uranium quantity, or in uranium enrichment in the fissile isotope U 235). For that means a higher probability for neutrons to meet a fissile nucleus and induce a fission reaction (Fig. 158).

Limiting the mass of fissile material, or uranium enrichment, contributes to decrease the multiplication factor k_{eff} of the system; limiting uranium enrichment allows an increase in critical masses.

Dry uranium masses, of density 18.93 (bare sphere), resulting in a k_{eff} of 1:
- **4,045 kg** of **10%** U 235 enriched uranium;
- **53 kg** of **93.5%** U 235 enriched uranium.

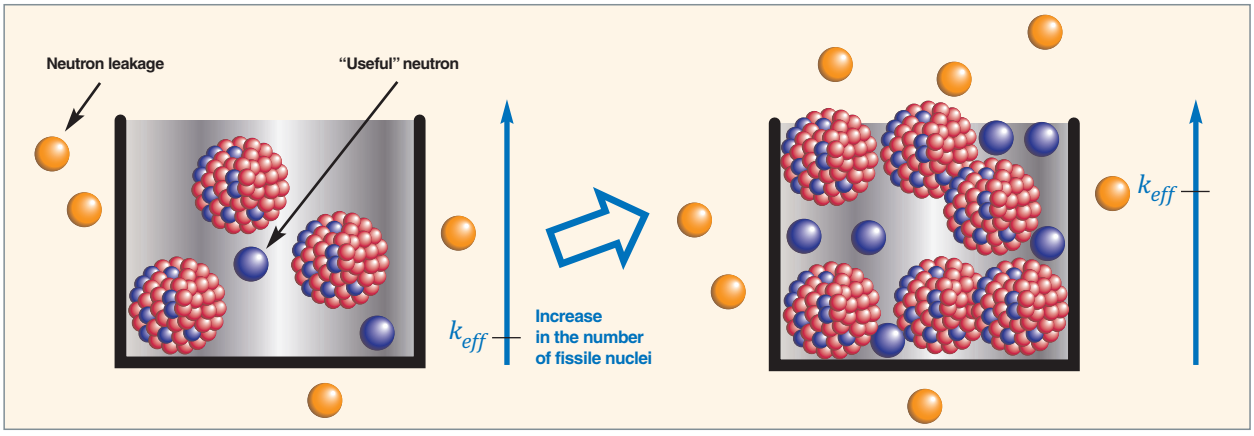

Fig. 158. Increase in the generation of "useful" neutrons due to increase in the number of U 235 nuclei.

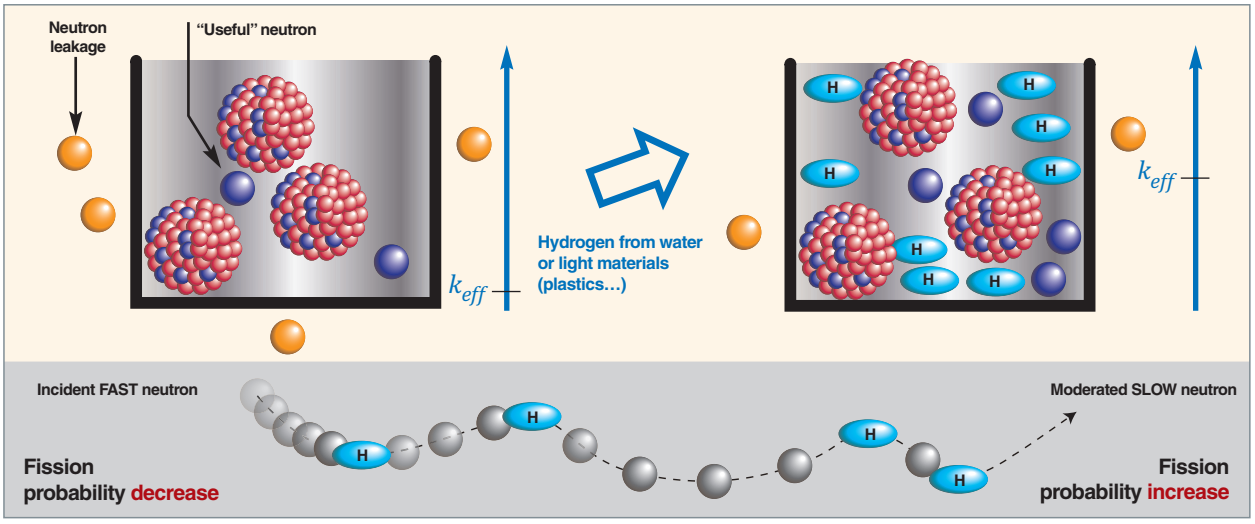

Fig. 159. Increase in useful neutron production by moderating neutrons with hydrogen from water or plastic materials.

Neutron moderation

The probability for a neutron to be absorbed by a fissile nucleus and to induce a fission reaction is all the stronger as the incident neutron energy is low, that is when **slow***, **moderated*** or **thermal neutrons*** are involved. **Moderation*** is a phenomenon of neutron slowing-down by successive collisions against **moderating*** nuclei. The lighter the nuclei (hydrogen from water or plastics, carbon…), the more efficient is neutron moderation (Fig. 159). Slowing down a neutron requires 18 shocks in water, 110 shocks in graphite, 2,000 shocks in lead; this is why, practically, all criticality accidents in fuel cycle facilities take place when using fissile materials solutions.

So fission reactions are often favored by any process likely to slow down neutrons.

Limiting the amount of moderating materials in fissile material may contribute to decrease the system's multiplication factor. In studies, water is generally taken into consideration as a moderating element.

Masses of **93.5%** U 235 enriched uranium, of density 18.93 (bare sphere), resulting in a k_{eff} of 1:
- **53 kg** of U without **moderation** (dry);
- **1,5 kg** of total U with **optimum moderation**.

Optimum moderation being defined as the water amount leading to the minimum critical mass.

Neutron losses by non-fission capture

Nuclei have a more or less strong probability to absorb neutrons by non-fission capture. So absorbed neutrons are definitely lost for neutron production by fission reaction (see Fig. 160 on the following page).This is referred to as poisoning, **neutron poisons*** or neutron absorbers. Poisons usually encountered are the following:

- Hydrogen which, though favoring fission reactions at low dilution due to its moderating effect, becomes a poison when occurring in high amounts in fissile material as a result of non-fission capture;
- uranium 238 and plutonium 240, which exhibit high non-fission neutron capture probabilities for some neutron energy values;
- boron, cadmium, gadolinium and hafnium, which also have high non-fission neutron capture probabilities, and are used as poisons in fissile materials solutions and in the structures of some equipment;
- some stable fission products occurring in fuels irradiated in reactors…

Adding, or taking into account, neutron poisons in fissile material or its environment contributes to decrease the system's multiplication factor.

Masses of **93.5%** U 235 enriched uranium, of density 18.93 (bare sphere), resulting in a k_{eff} of 1:
- **1,5 kg** of U with optimum moderation;
- **4 kg** of U with optimum moderation in presence of 1 g/l of boron.

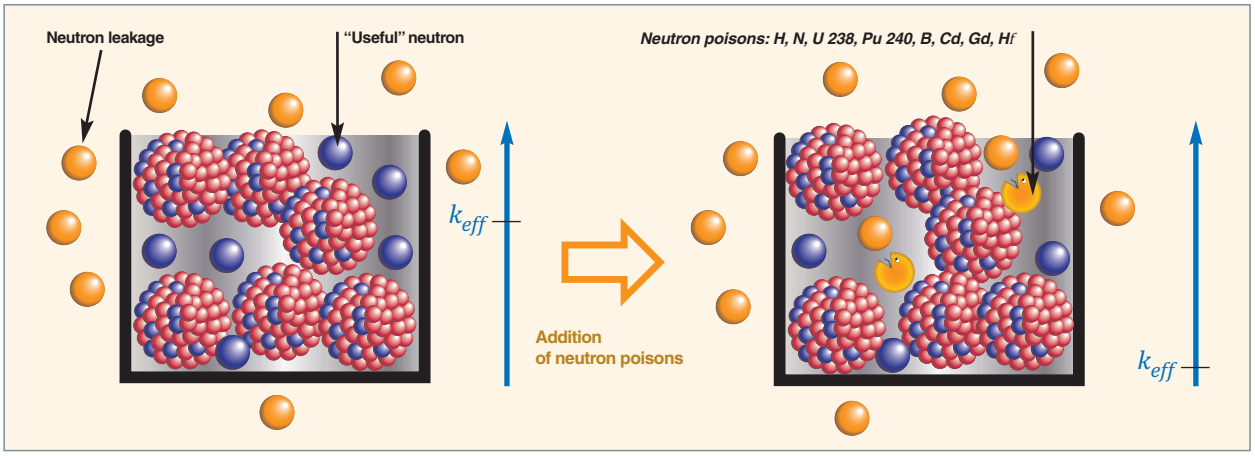

Fig. 160. Increase in neutron absorption by non-fission capture, following the addition of a neutron poison to the U 235 solution.

Neutron losses by leakage out of fissile medium

Decrease in fissile material density

In a dry medium, or a medium of low moderation, the higher the fissile medium density, the stronger the probability for a neutron to interact with a fissile nucleus, and so to induce a fission reaction (Fig. 161).

Limiting fissile material density makes it possible to increase critical masses.

Masses of **93.5 %** U 235 enriched uranium in dry conditions (bare sphere), resulting in a k_{eff} of 1:

53 kg d'U (metal)	**105 kg** d'U (sintered pellet)	**3,093 kg** d'U (powder)
density 18.93	**density 10.96**	**density 2**

Geometry

The larger the outer surface of the fissile medium, the higher the proportion of neutrons going across this surface (leaking out of it). So, geometrical shapes and dimensions more or less favor neutron leaking out of the fissile medium.

Generally speaking, for a constant mass, lesser geometrical dimensions entail an increase in the probability for a neutron to leak out of the fissile medium without the latter inducing fission reactions.

In some cases, these leaks can be sufficiently high to ensure an equipment criticality risk equal to zero (characterized by a k_{eff} value lower than 1), whatever the moderation, and the amount of fissile material may be. Equipment is then said to be of "safe geometry" (Fig. 162).

Playing on the system's geometry (shapes and dimensions) may contribute to decrease the system's multiplication factor (Fig. 163). As the sphere displays the smallest surface, it is the least prone to neutron leakage, thereby favoring neutron production by fission reaction.

Masses of **93.5 %** U 235 enriched uranium of density 18.93, in dry conditions, resulting in a k_{eff} of 1:

61 kg of U **cubic** shape	**58 kg** of U **orthocylindrical** shape	**53 kg** of U **spherical** shape

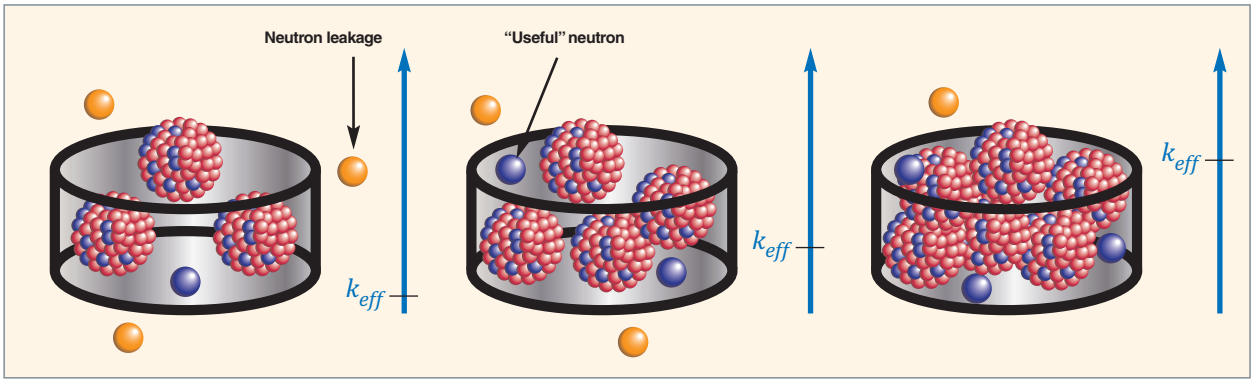

Fig. 161. Limiting fissile material density makes it possible to increase critical masses.

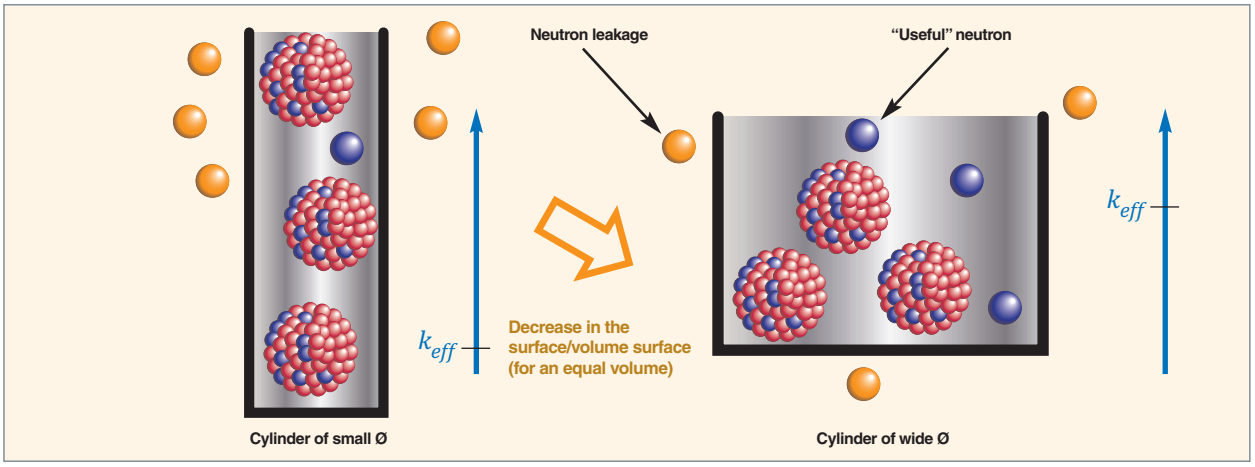

Fig. 162. Decrease in neutron leakage by decreasing the surface/volume ratio of equipment containing U 235.

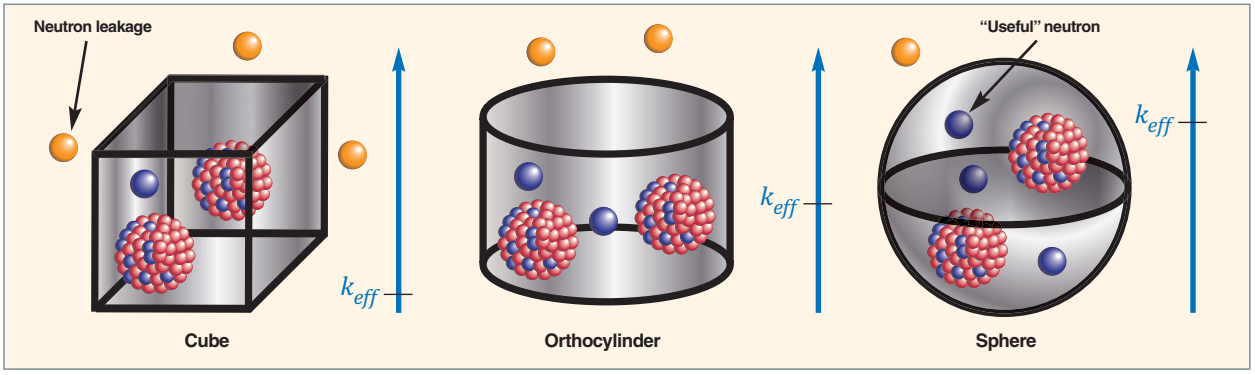

Fig. 163. Increase in the k_{eff} of a piece of equipment as a function of its geometry for a constant mass and volume.

Neutron contribution by reflection or interaction

Reflection

Neutron escape from the system is seldom total: part of the neutrons escaping from the fissile medium may come back to the latter (and so take part in useful neutron production), after being scattered in the neighboring materials: structural materials, cooling system, partitions, walls, ceiling, machines, staffs… This is referred to as neutron leakage reflection towards fissile medium (Fig. 164). Some materials display more or less reflecting properties, which vary depending on their chemical composition, their amount, and their proximity to fissile material.

In studies, water is generally taken into account as a reflecting element. Yet, some materials are more reflecting than water, such as, *e.g.* concrete or lead.

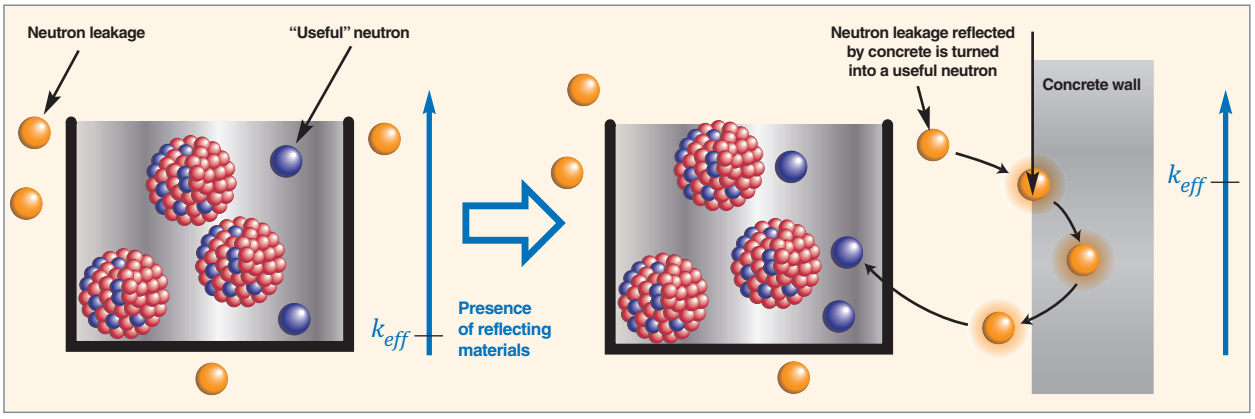

Fig. 164. Neutron leakage reflection in the materials neighboring the equipment containing U 235.

Masses of **93.5 %** U 235 enriched uranium of density 18.93, in dry conditions, resulting in a k_{eff} of 1:

53 kg of U bare sphere	**24 kg** of U surrounded by 20 cm of **water**	**21 kg** of U surrounded by 60 cm of **concrete**	**22 kg** of U surrounded 25 cm of **lead** and 20 cm of **water**

Putting ineffective reflector materials near fissile material, or making reflector materials more distant from fissile material may contribute in decreasing the system's multiplication factor k_{eff}.

Neutron interaction

When several devices containing fissile material face each other in a facility, one part of neutrons leaving a device can penetrate in the other neighboring device's fissile material and interact with it (Fig. 165). This is referred to as neutron interactions between devices. They increase the multiplication factor k_{eff} of both devices as a whole, as they increase useful neutron generation in each of the devices.

The interaction between both devices can be attenuated by interposing a neutron-absorbing shield (Fig. 166), or increasing the distance between them (if this distance is sufficiently high, both devices can be considered as neutronically isolated, that is the k_{eff} of the devices as a whole corresponds to the highest k_{eff} of the devices.

IInfluence of the various physical phenomena on critical mass value

Table 29 shows the influence of the various physical phenomena on the critical mass of uranium (k_{eff} = 1).

In studies relating to nuclear criticality safety, when allowed by operating conditions, the critical mass values considered are those obtained with a spherical shape, optimum moderation, and reflection by water (possibly by concrete or lead if need be).

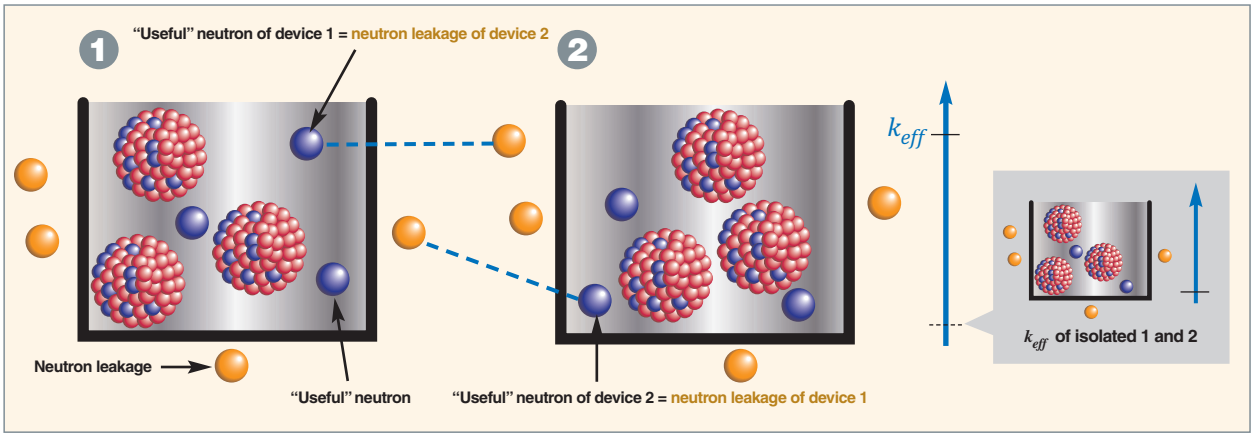

Fig. 165. Neutron interactions favoring useful neutron generation in devices 1 and 2 containing U 235.

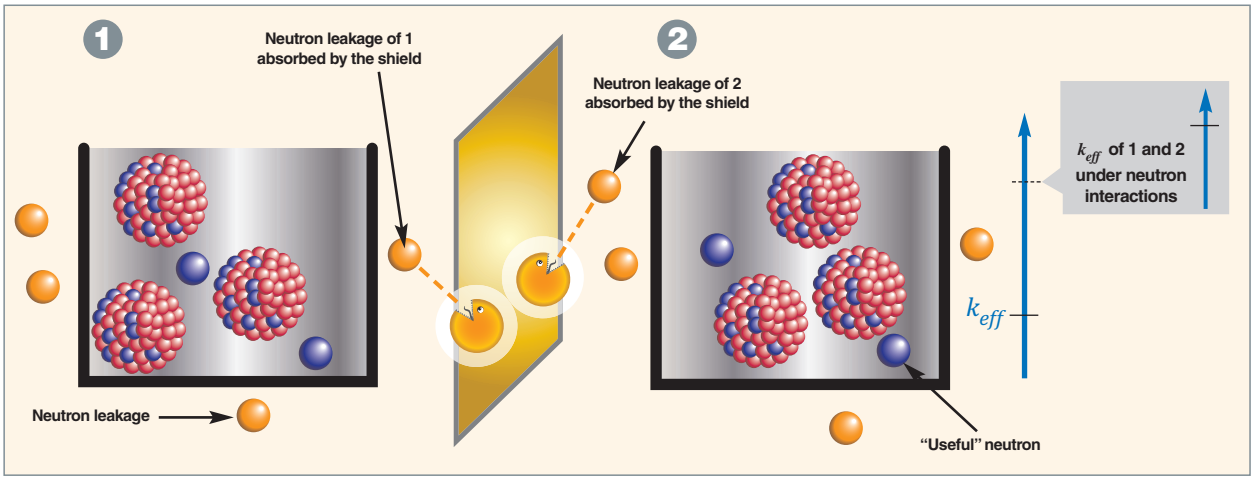

Fig. 166. Decrease in neutron interactions by interposition of a neutron-absorbing shield between devices 1 and 2 containing U 235.

Table 29.

Sphere-shaped masses of 93.5%* U 235 enriched uranium resulting in a k_{eff} of 1				
		Metal	**Sintered**	**Powder**
Bare	**Dry**	53 kg / 4 045 kg* Orthocylindrical: 58 kg Cubic: 61 kg	105 kg	3,093 kg
	Optimum moderation**	1.5 kg Poisoned by 1 g/l of boron: 4 kg		
Surrounded by 20 cm of water	**Dry**	24 kg	45 kg	619 kg
	Optimum moderation**		843 g	
Surrounded by 60 cm of concrete	**Dry**	21 kg	36 kg	235 kg
	Optimum moderation**		749 g	
Surrounded by 25 cm of lead and 20 cm of water	**Dry**	22 kg	40 kg	296 kg
	Optimum moderation**		614 g	

* Excepting contrary mention for which uranium is 10% U 235 enriched.
** The optimum moderation does not depend on fissile material's density.

When these values are too much penalizing, critical mass calculations are performed for 3D configurations (modeling of a particular piece of equipment and its layout, studies of the impact of neutron interactions between the various pieces of equipment of a cell…).

Safety criticality studies

Criticality control modes

As shown in the paragraph titled "Criticality: a question of neutron balance", there exists a broad variety of parameters which impact on the criticality state of a system containing fissile materials, and so, practically, a broad variety of methods to maintain this system in a subcritical state. In criticality engineers' language, this is referred to as "criticality control modes". The aim is to impose a limit to a criticality parameter (or to several of them): fissile material mass, fissile material geometry, fissile material concentration in solutions, moderation, or poisoning.

Neutronics codes (see *supra*, pp. 125-142) allow the k_{eff} value of a system to be calculated as a function of these parameters. The results of these calculations are often transcribed into "standards", which give the mass and volume in a spherical shape, the diameter of an infinite-height cylinder, or the thickness of an infinite-section plate thickness for a critical or subcritical system, with a determined safety margin.

Basic Safety Rule N°I.3.c

In France, generally speaking, the **nuclear safety*** approach relies on the **defense in depth*** principles: *i.e.* implementing any measures to avoid incidents (prevention), getting means allowing any anomaly likely to result in an incident to be detected (monitoring), predicting the implementation of means likely to limit the consequences of a possible accident, and circumscribe and stop the accident (consequence limitation). All nuclear risks or likely to have "nuclear" consequences are considered in this manner. However, in the case of a criticality accident, as the latter displays no precursor sign, it is practically impossible to detect it, and so to anticipate it…, as long as the system's k_{eff} is strictly lower than 1. For, as long as the k_{eff} is lower than 1, the neutron population is negligible, and it is practically impossible to detect the criticality accident before the transition to a critical situation. This is why nuclear criticality-safety mainly relies on prevention.

The Basic Safety Rule (RFS (French acronym for *Règle fondamentale de sûreté*) N° I.3.c [2]) issued by the French **regulatory authority for radiation protection and safety*** stands as a methodological reference for preventing criticality risk for nuclear designers as well as for nuclear operators and criticality experts. It defines the scope of the various criticality control modes, and also explains the related design, operating or administrative constraints. It also shows how to determine the limit of the criticality control mode, given the determination of the reference fissile medium. The latter is the medium which, among all those to be met in a Unit, in normal and abnormal operating conditions, leads to the lowest limits owing to its fissile material abundance, its composition, and its dilution law (physico-chemical nature of fissile material, isotopic composition, density, moderation).

Studies for criticality risk prevention are so conducted basing on this methodology, in compliance with both the defense-in-depth concept and the double contingency principle [2] that specifies that the facility shall be designed and operated with the following purposes:

- "in no case shall a criticality accident result from a single anomaly: component or function failure, human error (*e.g.* non-compliance with an instruction), accidental situation (*e.g.* fire);

- if a criticality accident may result from the simultaneous occurrence of two anomalies, it shall then be demonstrated that:
  - both anomalies are strictly independent;
  - the occurrence probability of each of both anomalies is sufficiently low;
  - each anomaly is evidenced through suitable and reliable monitoring tools, within an acceptable period of time allowing intervention."

Neutronics computer codes used for criticality studies

Evaluating criticality conditions in nuclear fuel cycle facilities and fissile materials transport casks first entails investigating the neutron population behavior and treating neutronics equations, especially the equation of neutron **transport*** in matter, aiming at:

- Assessing the k_{eff} value for configurations determined by 3-D calculation;

- defining the criticality parameter values determined by 1-D calculation.

For this purpose, analyses for preventing the criticality risk are based on the conclusions of the criticality calculation notes which display the values calculated using neutronics codes.

In France, calculations are usually achieved with the **CRISTAL*** package [3]. The latter consists in an integrated set of nuclear criticality-safety calculation softwares developed and qualified within the framework of an IRSN, AREVA and CEA collaboration, taking into account the needs relating to all of the applications to be considered. The last evolutions were aimed at modeling fuel burnup (disappearance of uranium and plutonium nuclei, and appearance of new actinides and fission products which impact favorably on subcriticality thanks to their neutron-absorbing properties) in order to take account of the "**burnup credit***", *i.e.* the reactivity margin due to fissile material disappearance and to the formation of these nuclides. This modeling is achieved through coupling with the **DARWIN*** or **CESAR*** codes.

The CRISTAL package (Fig. 167) includes:

- Nuclear data libraries (mainly based on the European evaluation **JEFF***), which contain basic information common to all calculations (**cross sections***, **resonance*** parameters, **fission yield***, **radioactive half-life***…);

- validated and qualified procedures (for the standard route);

- specific calculation codes;

- interfacing tools (for the standard route).

The overall architecture of the CRISTAL package is structured into two calculation routes which use common nuclear data:

- The "standard route", which implements a formulation using several energy groups of cross sections (multigroup cross sections), allowing:
  - multigroup probabilistic calculations with the computer code **MORET5***, using cross sections libraries issued from the **APOLLO2*** deterministic code to determine k_{eff} for 3-D configurations;
  - deterministic calculations with the **APOLLO2*** computer code (calculations with the so-called integro-differential method or S_N) to determine k_{eff} or geometrical dimensions for a given k_{eff} (1-D configurations);

- the "reference or pointwise route", based on the **TRIPOLI-4®*** pointwise Monte-Carlo code.

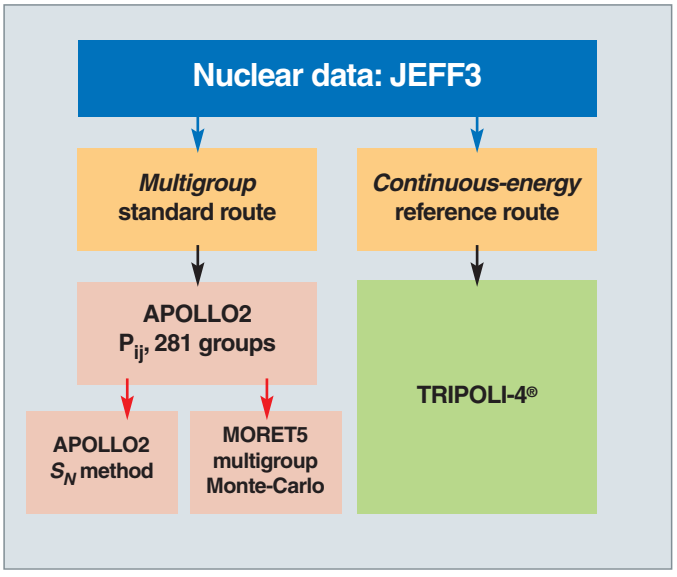

Fig. 167. Simplified block diagram of the CRISTAL formula in its version 2.

Criticality in glove boxes

The purpose is to determine the following items for this type of operations:

- The reference fissile medium;
- the criticality control mode(s);
- the related limit(s);
- the measures implemented in the facility to guarantee these limits.

Let us consider, for instance, a nuclear facility for which an operator has to handle, in a glove box, fuel rod sections (sintered pellets) of mixed uranium and plutonium oxides of various isotopic abundances (that is, the U 235 enrichment is variable versus U 238, the Pu 239 abundance is variable versus the other plutonium isotopes (Pu 240, Pu 241 and Pu 242), and the U/U+Pu is variable).

Determining reference fissile medium and criticality control mode

The Basic Safety Rule (RFS) I.3.c [2] specifies that, for the units implementing small amounts of fissile materials, which is often the case for glove boxes, the most appropriate criticality control mode is the limitation of fissile material mass to the whole of the glove box (Fig. 168).

The reference fissile medium is plutonium in metallic form, displaying isotope-239 purity (*i.e.* 100% in Pu 239), and of a maximum theoretical density of 19.86. For this medium is an "envelope" for all of the fissile media implemented in the facility (uranium oxide fuels and mixed uranium and plutonium fuel), since it leads to the lowest values of critical masses.

Fig. 168. Operator handling uranium and plutonium fuel rod sections in a glove box.

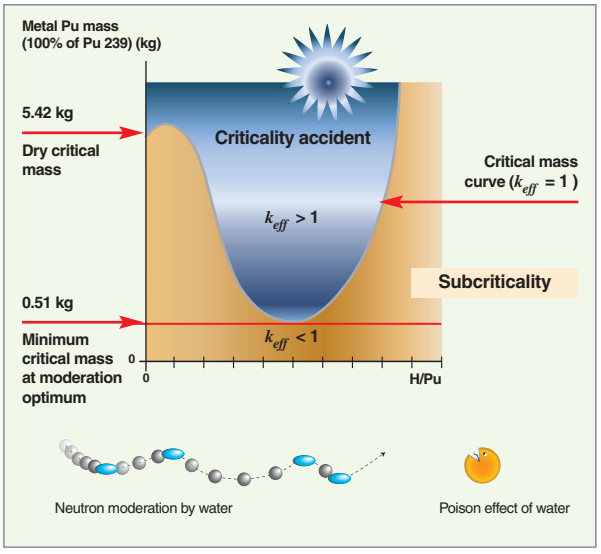

Fig. 169. Critical mass (k_{eff} = 1) of plutonium (metal form, 100% of isotope Pu 239, and density 19.86), versus the moderator-to-fuel ratio H/Pu (reflection by 20 cm of water).

The reflection conditions retained are water occurrence, taking account of the distance from the concrete walls and of the absence of lead in the unit. Water is also retained for moderation conditions, given the absence of materials more moderating than water.

Determining limits related to reference fissile medium and criticality control mode

The criticality standards set out by neutronics codes are aimed at determining the variation in a critical mass of plutonium, in metallic form, pure in isotope-239, versus moderation (defined as the moderator-to-fuel ratio H/Pu, *i.e.* the ratio between the number of hydrogen atoms and the number of plutonium atoms). This curve is displayed on Figure 169. Basing on the latter, values corresponding with a k_{eff} equal to 1 can be obtained as follows:

- 510 g of plutonium corresponding to the minimum value of the curve on Figure 169 (it accounts for the lowest amount of plutonium resulting in criticality, whatever the moderation and geometry conditions may be); this is referred to as "**minimum critical mass**";

- and also, if the masses to be handled are higher due to operating needs, 5.42 kg of plutonium, providing the absence of moderation is guaranteed (in dry conditions) in normal and incidental operating conditions.

Safety margins are applied to these critical limits in order to guarantee the absence of criticality risk in all normal and incidental situations considered as presumable. For this purpose, a safety coefficient of 0.7 is applied. This coefficient of 0.7 is used for control mode by mass limitation, providing that the

analysis demonstrates that the risk to introduce an amount of fissile material equal to twice the mass limit (double batching) is excluded. Otherwise, the coefficient to be applied is 0.43. Thus, the obtained mass limits respectively are 350 g of plutonium with no moderation limit, and 3.7 kg of plutonium in dry conditions. The latter case makes it possible to significantly increase the mass limit in the glove box.

How to ensure compliance with the limits

In order to ensure compliance with the limits of 350 g and 3.7 kg of plutonium, in both cases rules will have to be worked out at the facility to ensure fissile materials management and the absence of fissile materials build-up in the glove box, given the absence of any material more moderating than water. Furthermore, in the second case, the absence of moderation will have to be ensured by forbidding the insertion into the glove box of any moderating material, as well as water use in case of fire. On the other hand, further safety studies will have to demonstrate the absence of risk of water being brought in by internal flooding (spraying from pipe, oil leak from a jack or an engine…), and by external flooding (flood, rain…).

As a result, the more criticality control modes are used, the more constraints are imposed for design, administration or operation (Fig. 170). This is why the dialogue between criticality experts and the operator is crucial to find the most suitable solution likely to ensure an efficient operation of the facility in fully safe conditions with respect to the criticality risk.

In addition, criticality risk training sessions are provided to operators.

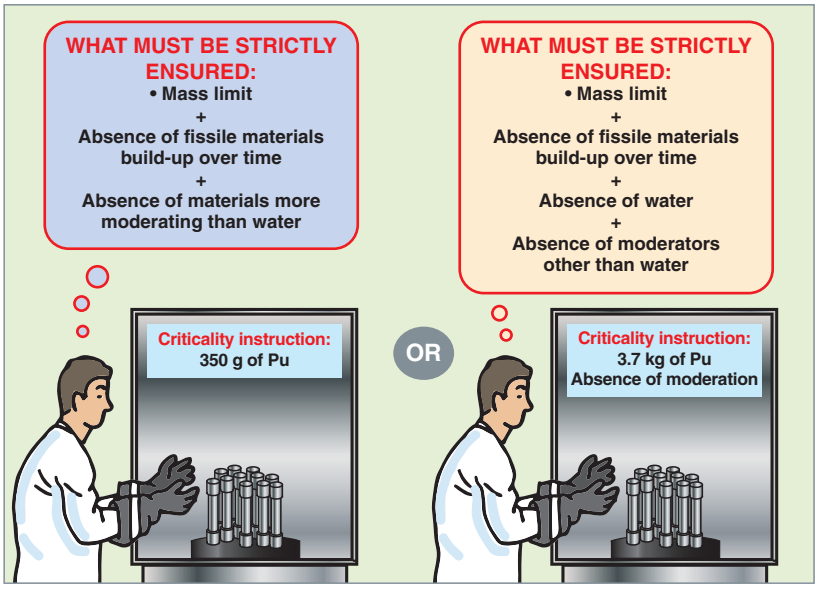

Fig. 170. Limit constraint in the glove box as a function of the presence or absence of moderation.

Tokai-Mura criticality accident (Japan)

The last criticality accident took place on September 30, 1999 in Japan, in a workshop at the nuclear fuel fabrication plant of Japan Nuclear Fuels Conversion Company (JCO) located 15 km far from the Tokai-Mura site (150 km North-East of Tokyo). It was classified at Level 4 of the International Nuclear and Radiological Event Scale (**INES***), which consists of eight levels. This accident lasted for 20 hours, and resulted in about 2.5 10^{18} fissions [1].

Reading the previous paragraphs of this Chapter dealing with criticality is required for a good understanding of what follows.

Accident circumstances

The accident took place during operations of dissolution in nitric acide of 18.8% U 235 uranium powder in order to obtain uranyl nitrate. The process authorized by the Japanese safety authorities consisted in dissolving uranium powder in a safe geometry device. Now, the volume of this device, too low, did not allow a sufficiently high uranyl nitrate amount to be obtained. Several consecutive dissolutions proved to be necessary, thereby entailing batches of heterogeneous uranium concentration. So, without taking advice from a criticality expert, the managers decided to replace the safe geometry dissolver, first selected, by a precipitation tank of a broader diameter, fitted with a mechanical stirrer likely to make easier the operation of concentration homogenization in the various dissolution batches. As that latter tank was not of safe geometry, the absence of criticality risk was guaranteed in the whole equipment by an uranium mass limit of 2.4 kg.

The two operators filled the tank with 7 buckets, each of them containing 2.4 kg of powder of uranium dissolved in nitric acid (Fig. 171). During the voiding of the last bucket, an operator observed a blue flash characteristic of a criticality accident **(Čerenkov effect*)**: 16.6 kg of uranium were present in the tank.

The criticality accident resulted from several anomalies and from non-compliance with rules.

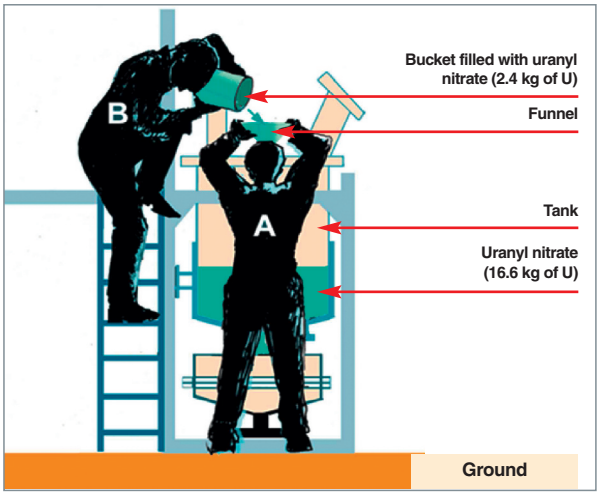

Fig. 171. Position of the two operators during the criticality accident that took place at Tokai-Mura (Japan) on September 30, 1999.

Factors that led to the accident

The first factor was the replacing of the safe geometry equipment by equipment of bigger size, entailing a significant decrease in the number of neutrons in the solution likely to escape from it, and, so, an increase in the k_{eff} value.

Secondly, the mass limit of 2.4 kg guaranteeing an operation without criticality risk and with high safety margins was not complied with in the bigger size equipment. As neutron production grew with the number of fissile nuclei in the medium, the occurring 16.6 kg of uranium significantly increased the k_{eff} value.

Finally, the water cooling system (reflector) brought back to the fissile medium neutrons which would have escaped in the absence of water. So occurring water around the tank increased the k_{eff} value to over 1. Here, again, complying with the mass limit of 2.4 kg would have resulted in an operation with no criticality risk. In addition, if there had been no water around the tank, the accident would not have taken place for the 16.6 kg of uranium, but for a higher amount.

Interventions to stop the accident

In order to stop the accident, the operator had to void the cooling system by breaking the pipe. Then, a neutron poison, boron, was introduced into the tank so as to reduce k_{eff} significantly and definitively.

Consequences

During this accident, 136 persons on the site were irradiated at very variable doses, among whom three of them seriously. The two employees involved in the accident (see Figure 171), who had received **doses*** much higher than the lethal dose, died after respectively three and seven months of intensive care. The foreman, located in a neighboring room at an approximate 5 m distance from the vessel, received a dose which could initiate a cancer in the long term. About a hundred other persons (133 firemen and operators who intervened to stop the accident) were irradiated much less severely, and, presumably, for most of them, without any directly observable effect on their health.

Several hundreds of other people on the site are assumed to have potentially received very low doses. In the neighboring of the site, the 160 inhabitants present within a 350 m radius from the building containing the vessel were evacuated, while the 320,000 others, within a 10 km radius, were ordered to stay confined at home till the end of the accident out of precaution. Measurements performed in air, water or plants have evidenced occurring iodine (a volatile fission product) only in very few points and as traces.

Lessons learned

The organization set up by JCO and approved by the Safety Authority was not suitable. Especially, in case of change in the process, requesting the Safety and Quality Assurance managers was only optional. There was no criticality expert on the Center site, nor regular inspections by safety authorities. Furthermore, the instructions to be complied with in order to avoid any criticality accident were not displayed (mass limits as a function of U 235 enrichment).

The operators had not been informed about the criticality risk. The foreman and the operators had quite a number of years of experience in operations implementing 5% U 235 enriched uranium. The operators transposed their experience in U 235 5% enriched uranium to U 235 18.8% enriched uranium without knowing the risks involved.

The severity of this accident has induced all of safety authorities and operators in each country implementing nuclear facilities to undertake a review of current procedures and practices in relation to criticality risk prevention.

Liability and compensation issue

Two years later on, the then plant head and five other persons (among them the foreman) were inculpated for non-compliance with nuclear safety rules and for professional negligence.

JCO paid a compensation amount of about 100 million Euros to the workers exposed to a dose of over 0.25 Sievert, to the population located 350 m far from the place of the accident, and to the industrial and agricultural activities with respect to the accident-related losses in the fields of agriculture, fishing and industry and to the costs assumed by the village in its management of the accident consequences.

Finally, the accident induced a broad debate over nuclear industry, which then met about one third of Japan's needs in electric power.

Conclusions

If no criticality accident has been blamed for in France till now, no doubt this is mostly due to the relevance of the defense-in-depth and multiple-barrier concepts implemented in safety demonstrations, to the rigorous operation of facilities, and to the specific organization in relation to the criticality risk at the CEA (this organization being based on engineers' skills in CEA facilities, at CEA centers, and at the national level), as well as to the performing, operational software tools developed.

Yet, despite all the measures taken to avoid the criticality accident, and the organization set up, such a possibility cannot be totally excluded indeed. This is why, from the sixties until now, the CEA has strengthened its nuclear criticality-safety approach as part of the defense-in-depth third level (limitation of accidental consequences), especially as follows:

- Conducting significant, comprehensive experiments and studies in order to know the phenomenology and potential consequences of a criticality accident;
- developing CEA's ability to detect such an accident; implementing a fast, efficient intervention structure;
- acquiring the knowledge required to control accidents (design-step study of the engineered safety systems likely to be set up), and restricting its consequences on workers, the public, and the environment.

References

[1] *Les Accidents de criticité dans les usines et les laboratoires*, DSNQ/MSN/FT/2001/007.

[2] Règle Fondamentale de Sûreté n°I.3.c du 18 octobre 1984 : Règles applicables à la prévention des risques dus aux rayonnements ionisants – Risque de criticité.

[3] J.M. Gomit, J. Miss, A. Aggery, C. Magnaud, J.C. Trama, C. Riffard, "CRISTAL Criticality Package Twelve Years Later and New Features", International Conference on Nuclear Criticality 2011, 19-22 September 2011, Edinburgh.

Bibliography

Clefs CEA n°45, *Physique nucléaire et sûreté*, octobre 2001.

Dominique Mijuin and Emmanuel Gagnier
Department for Systems and Structures Modeling

Other Examples of Neutronics Applications

This overview of neutronics applications is completed with a few additional examples of studies conducted with the transport codes developed at the CEA.

Lifetime of a nuclear reactor: reactor vessel neutron fluence

Neutron **fluence*** is one of the physical parameters involved in assessing the reactor's lifetime. For the fluence of neutrons with an energy over 1 MeV, is one of the parameters of the relationship giving the ductile-brittle transition temperature shift of vessel steel. An order of magnitude of that neutron fluence over 40 operating years is 6 10^{19} n.cm^{-2}.

About one hundred million neutron histories are simulated to obtain the neutron flux impinging on the vessel, after 3 to 4 attenuation decades, with a suitable statistics (*i.e.*, a typical deviation of less than 1%) [Fig. 172]. The implementation of a simulation acceleration technique is therefore required to reach statistical convergence in such physical configurations (see *supra*, pp. 89-106).

The calculation of the ex-core chamber response relies on a similar approach [3] [4].

Ambient dose rate in a nuclear reactor building

Neutrons escaping from a nuclear reactor core follow "passages" ("**streaming***" phenomena), and propagate through the facility, thereby inducing the activation of the various structures encountered. They so induce neutron and *gamma* dose rate levels in the different areas of the reactor building. For a radiation protection purpose, the level of these dose rates is predicted by computing. The facility size (Fig. 173) and its technical complexity lead to implement 3-D Monte-Carlo transport calculations.

Nuclear reactor dismantling: neutron activation of structures

Studies conducted for the **dismantling*** of a nuclear reactor more especially deal with the radioactivity induced by neutrons in the whole of its structures all along its operation. The neutron activation of these structures is investigated by simulating neutron propagation in the facility using a (Monte-Carlo or S_N) transport code. The neutron flux so computed is then transferred to a nuclide generation/depletion code which determines activity according to the reactor's operating history and

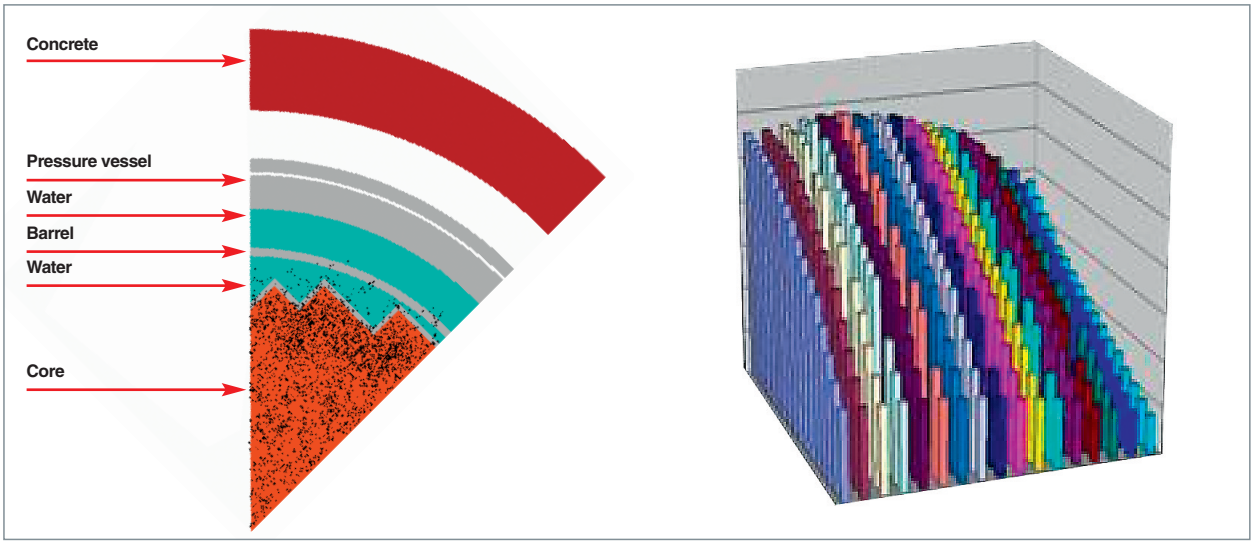

Fig. 172. On the left-hand side, simulation of neutron propagation with the TRIPOLI-4® Monte-Carlo transport code in order to determine neutron fluence on a pressurized water reactor (PWR) vessel (representation of the reactor 1/8th). On the right-hand side, as an example, rod-per-rod description of a neutron source in a peripheral assembly, modelled in TRIPOLI-4® [1] [2].

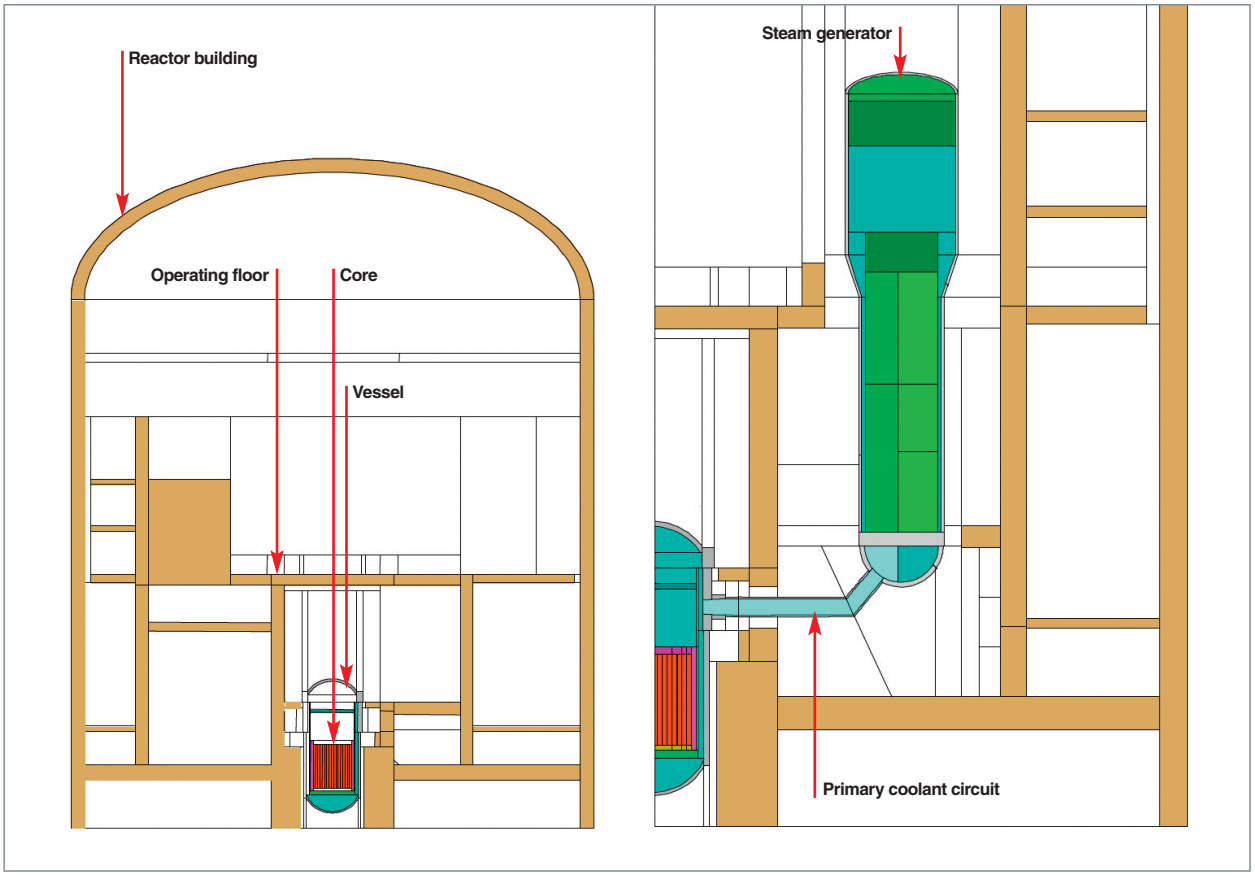

Fig. 173. Schematic view of the reactor building containment of the European Pressurized Reactor (EPR) (operating floor, steam generator area, etc.), used to determine neutron and *gamma* equivalent dose rates around the operating reactor, using the Monte-Carlo transport code TRIPOLI.

the period of time considered after its final shutdown (Fig. 174). So these calculations can lead to a thorough inventory of the radionuclides occurring in the various reactor's structures at any moment. A three-dimensional activity and radiotoxicity map can be deduced from it, to be used to manage all of the waste arising from the reactor's dismantling (Fig. 174).

In addition, these calculations provide the radioactive-decay *gamma* source terms which allow determination of the related dose equivalent levels, an information indispensable for decommissioning operations.

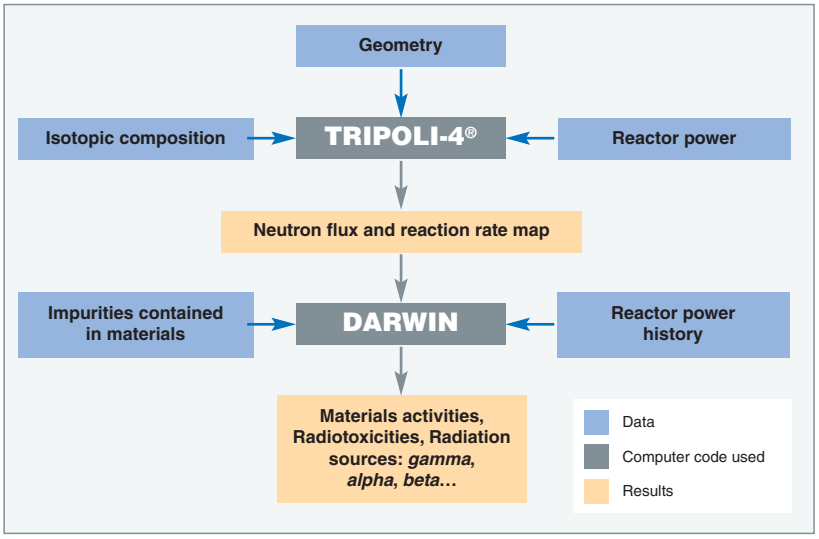

Fig. 174. An example of computational scheme dedicated to nuclear reactor dismantling studies [5] that uses the TRIPOLI-4® 3D Monte-Carlo transport code and the DARWIN time nuclide generation/depletion code. This computational scheme was applied to the configurations shown on Figures 175 and 176.

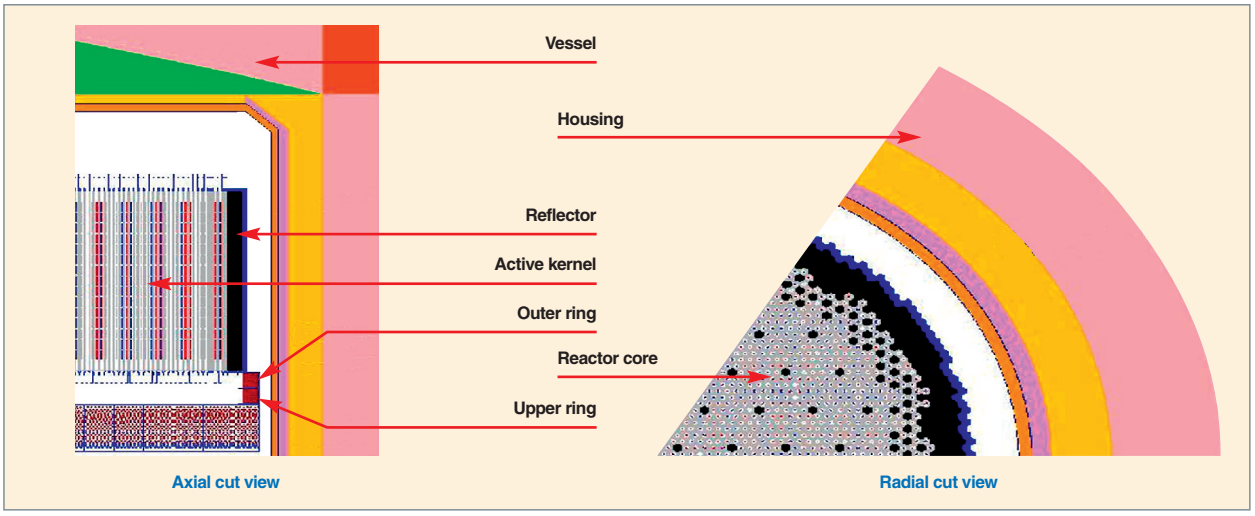

Fig. 175. Modeling of a natural uranium-graphite-gas (**UNGG***) type reactor, for the purpose of dismantling studies, achieved with the **TRIPOLI-4®*** Monte-Carlo transport code for neutron propagation, and with the **DARWIN*** code for radioactivity calculations: especially radiological inventory, activity, radiotoxicity, and *gamma* and *beta* source terms.

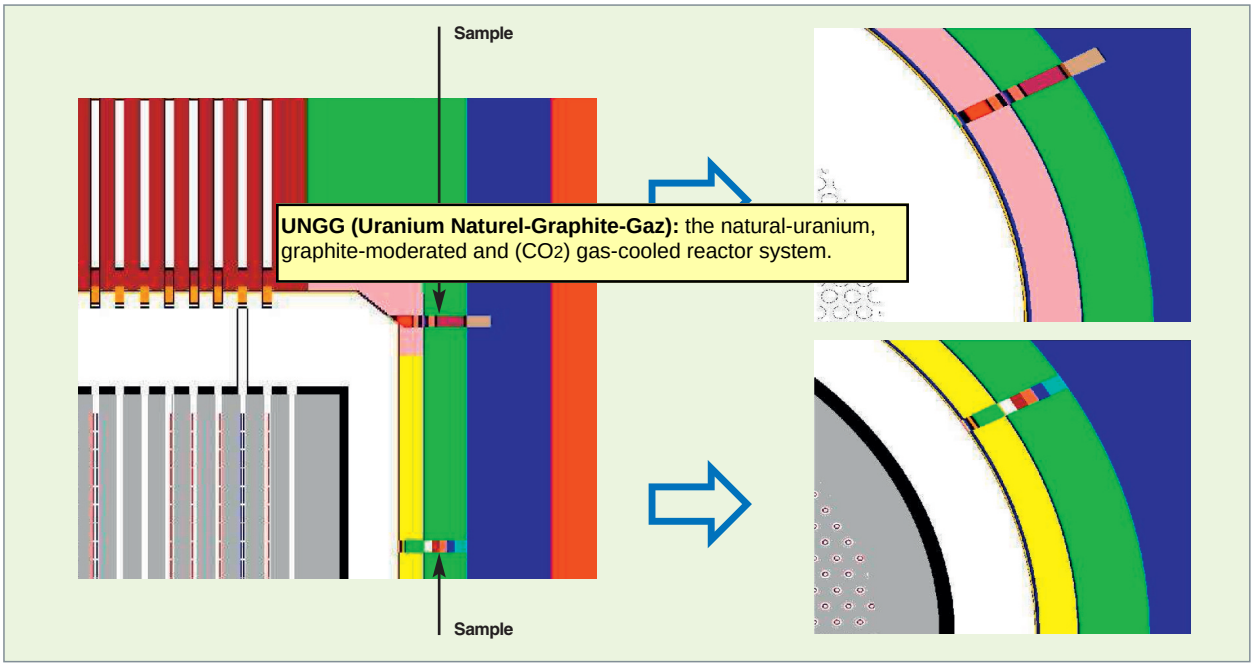

Fig. 176. Fine modeling of a natural uranium-graphite-gas (**UNGG***) type reactor in order to compare calculation results with activity measurements achieved on samples collected in various places of the reactor housing [6].

Thermonuclear fusion: heating and neutron activation of structures

The studies of heating and neutron activation of fusion device (magnetic or inertial confinement) structures are carried out with the same computational codes as those used for the nuclear reactor dismantling studies. The example below illustrates the TRIPOLI-4® modeling of a module of the **ITER* tokamak***.

The calculation results shown on Figure 178 are related with first wall heating in the plasma chamber. They were respectively obtained by the American **MCNP*** and TRIPOLI-4® Monte-Carlo transport codes [7]. Another example of study is provided by reference [8] dealing with the design of the test module of the ITER lithium-lead blanket ("Fast Neutron Generator Helium Cooled Lithium-Lead (FNG HCLL) Test Blanket Module [TBM]").

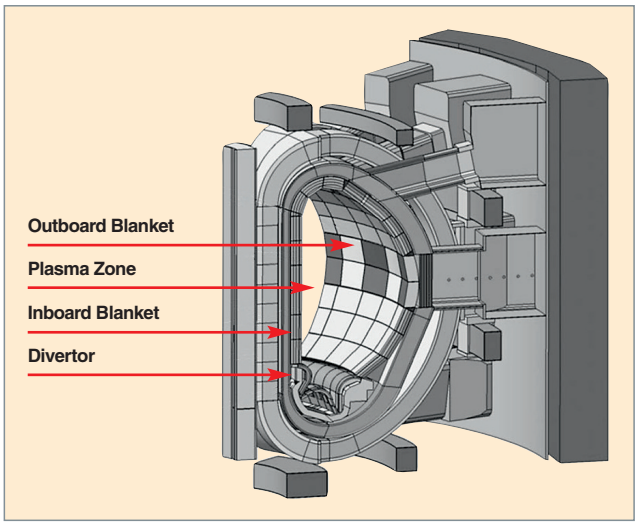

Fig. 177. Benchmark model of the ITER tokamak [7].

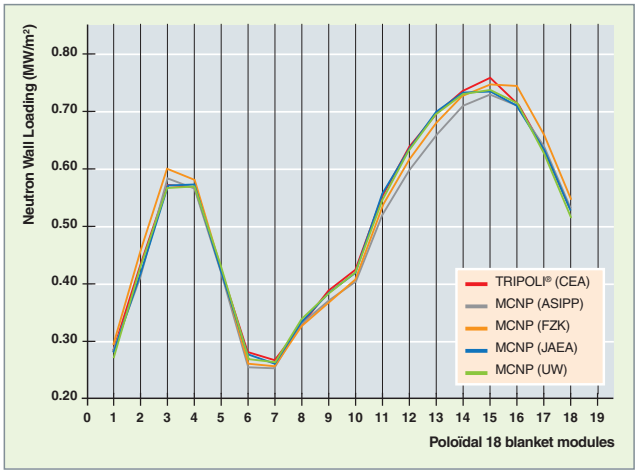

Fig. 178. Calculation of heating in ITER first wall, using **TRIPOLI-4®*** and MCNP Monte-Carlo neutronics codes. The results are reported for each of the 18 modules of the device.

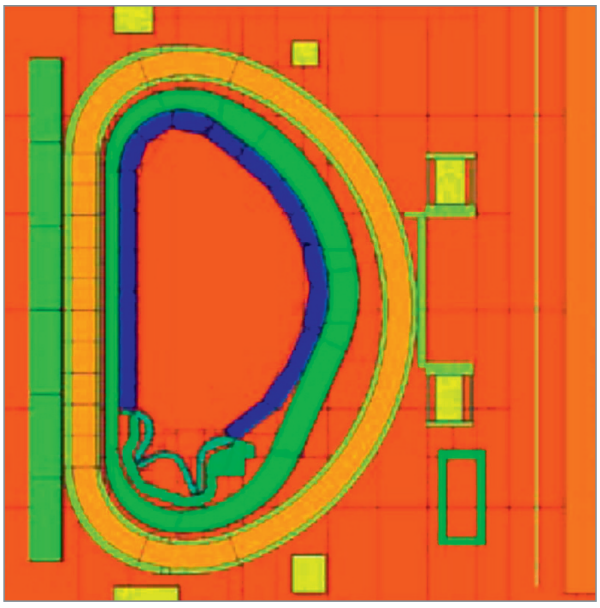

Fig 179. Cut view of the ITER tokamak displayed using the T4G tool of the TRIPOLI-4® code [9].

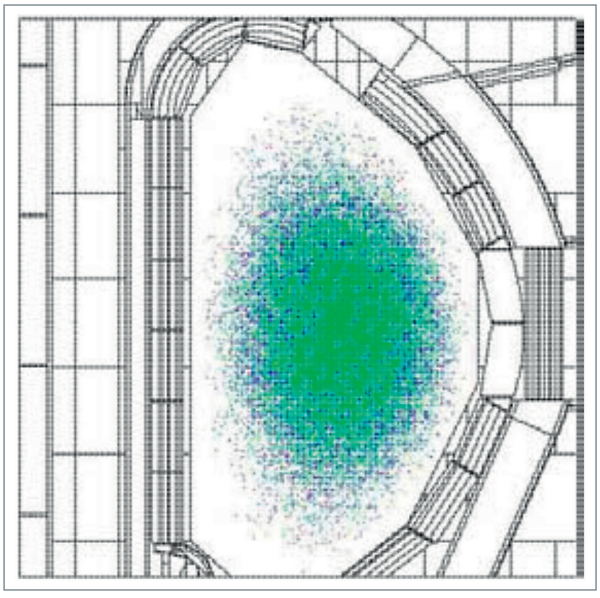

Fig. 180. Cut view of the ITER tokamak showing the sampling of the source neutrons arising from deuterium-tritium fusion reactions [9], [10].

References

[1] S. Bourganel, O. Petit, M. Chiron, C. Diop, "Pseudo-Adjoint Monte-Carlo Method 3D Particle Transport for Nuclear Application Parametric Studies", 14th Biennial Topical Meeting of the Radiation Protection and Shielding Division, Carlsbad New Mexico, USA, April 3-6, 2006.

[2] S. Rollet, C. Diop, M. Chiron, S. Bourganel, "Core contribution calculations with TRIPOLI-4 Green's functions and MCNP4C adjoint in PWR neutron transport studies", ICRS-11 – RPSD-2008, Callaway Gardens, Pine Mountain, Georgia, USA, April 13-18, 2008.

[3] C. Trakas, O. Petit, "TRIPOLI-4 Green's Functions & MCNP5 Importance to Estimate ex-core Detector Response on a N4 PWR", Proceedings of the *Joint International Conference on Supercomputing in Nuclear Applications and Monte-Carlo 2010* (SNA + MC2010), Hitotsubashi Memorial Hall, Tokyo, Japan, October 17-20, 2010.

[4] S. Bourganel, O. Petit, C. M. Diop, "3D Particle Transport using Green's functions in TRIPOLI-4® Monte-Carlo Code. Application to PWR neutron fluence and ex-core response studies", *Nuclear Technology*, October 2013.

[5] I. Brésard, F. Marcel, M. Messaoudi, G. Imbard, G. Betsch, J .M. Parize, J .C. Nimal, "Radiological Characterization of Nuclear Reactors Structures, Calculations and Measurements Comparisons", Proceedings of the *1998 ANS Radiation Protection and Shielding Division Topical Conference, Technologies for the New Century*, April 19-23, 1998 Knoxville, Tennessee, USA, 1998.

[6] F. Laye , M.-C. Perrin, “Comparison of Activation Calculations with Measurements For The Biological Shield of The Bugey 1 Graphite-Gas Reactor”, *5th EPRI International Decommissioning and Radioactive Waste Workshop*, October 31 – November 2, 2006.

[7] L. Lu, Y. K. Lee *et al*., “Development of Monte-Carlo auto-matic modeling functions of MCAM for TRIPOLI-ITER application,” *Nucl. Instr. Meth. Phys. Res.*, A605, 384, 2009.

[8] C. Fausser, Y. K. Lee, R. Villari, Q. Zeng, J. Zhang, A. Serikov, J.-C. Trama, F. Gabriel, “Numerical benchmarks TRIPOLI - MCNP with use of MCAM on FNG ITER Bulk Shield and FNG HCLL TBM mock-up experiments”, *Fusion Engineering and Design*, 86, pp. 2135–2138, 2011.

[9] F.-X. Hugot and Y. K. Lee , “A New Prototype Display Tool for the Monte-Carlo Particle Transport Code TRIPOLI-4”, *Progress in Nuclear Science and Technology*, vol. 2, pp.851-854, 2011.

[10] Y. K. Lee, O. Petit, “Display of Collision Sites with TRIPOLI-4 Monte-Carlo Code,” *ANS - RPSD topical meeting*, Las Vegas, NV. USA, Apr. 18-23, 2010.

Stéphane Bourganel, Maurice Chiron, Cheikh M. Diop, François-Xavier Hugot, Frédéric Laye, Yi-Kang Lee, Jean-Christophe Trama
Department for Systems and Structures Modeling
and Clément Fausser
Reactor Study Department

Neutronics: its Successes and Future Challenges

As a conclusion of this monograph, it seems relevant to take an overview of the neutronics discipline in order to analyze its status, look backwards at its successes, and consider the challenges it will have to face.

Initially a mere branch of Nuclear Physics, neutronics has very soon become an autonomous branch of Physics. As seen above, its applications are numerous and varied, and deal with the various aspects of reactor physics and fuel cycle, nuclear instrumentation, nuclear criticality safety, and radiation protection. Neutronics is now indispensable to nuclear industry, for the design, operation and safety demonstration of its facilities. It has reached a sufficient level of maturity to participate in a genuine simulation of these facilities. This maturity, put into effect under the form of neutronic calculation codes developed at CEA and used by industry, does not mean the end of the work: many challenges are still awaiting nuclear reactor physicists, and expectations for progress are still high.

Neutronics simulation: a necessarily multiscale approach

The basic phenomenon of neutronics is the nuclear reaction. The mean free path of neutrons in matter is extremely dependent on their energy, the latter being able to vary in a nuclear reactor's core over more than ten orders of magnitude. This makes it necessary to describe neutronics phenomena within a very broad range of spatial scales. One of the major challenges of neutronics lies in the management of these various space and energy scales. The methods developed are significantly clever and efficient. Neutronics describes phenomena using coupled, nested scales, through an energy and space “multiscale” approach, in which the microscopic description of the system provides data for a more macroscopic description: neutronics has thus paved the way to a “multiscale” approach applied to other disciplines.

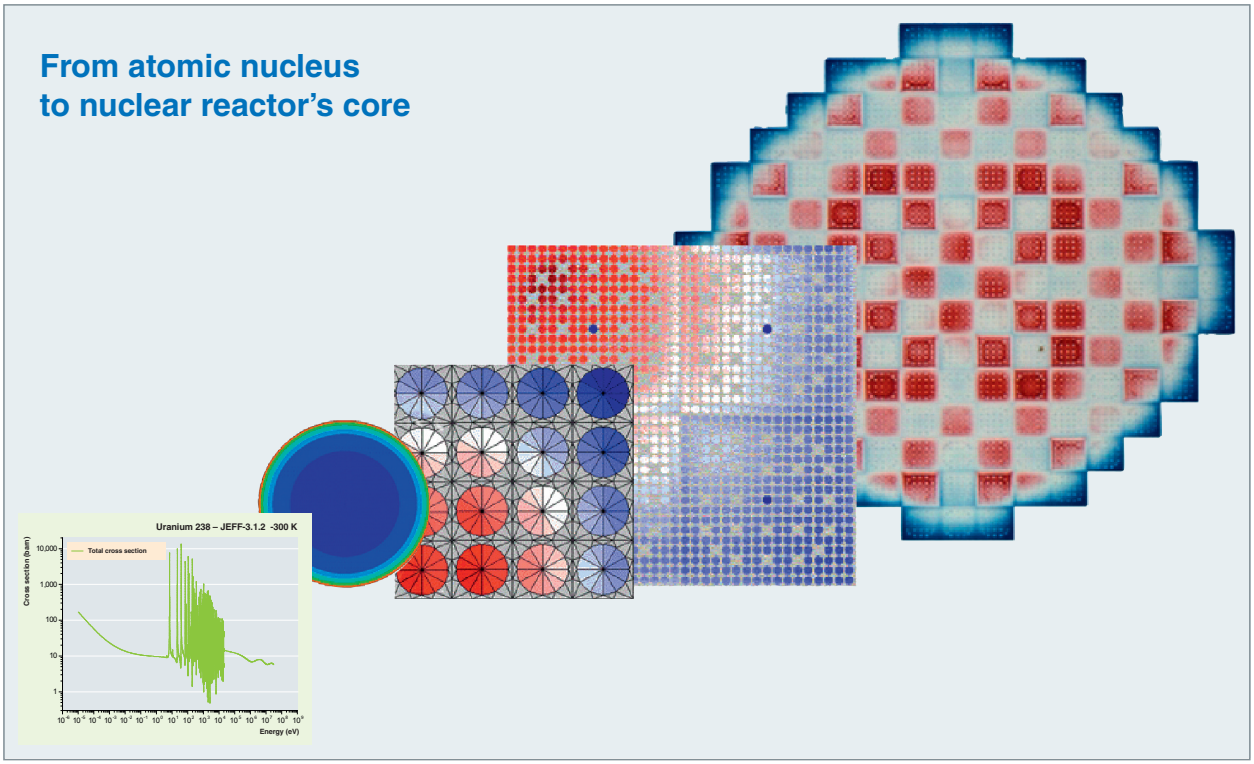

Fig. 179. Multiscale description of a nuclear reactor's neutronic behavior.

Coupling neutronics with other disciplines

Nuclear systems are complex systems, involving numerous coupled physical phenomena, which makes it necessary to describe them as a whole, through a "multiphysics" approach, with the contribution of a number of physics disciplines. One of the challenges for future neutronics is systemizing its coupling with other disciplines, especially thermal-hydraulics and thermal-mechanics.

Towards 3+1 dimensional direct simulation

Today, deterministic neutronics calculations relating to reactor cores are still performed as two steps which combine two- or three-dimensional calculations, for reasons of computational time. The increase in calculation capacities now makes it possible to perform three-dimensional direct calculations (*i.e.* without any homogenization step) on meshings of over ten million meshes. The CEA accompanies this evolution developing the APOLLO3® code. A number of reactor concepts involving large or very heterogeneous cores will fully benefit from these advances. Moreover, simultaneously taking into account the time and space aspects of a reactor's core neutronic evolution in a 3+1 D approach constitutes an important challenge, paving the way for the detailed description of transient phenomena.

What about the status of Monte-Carlo simulation?

One of the neutronics specificities is the development and success of Monte-Carlo codes. Thanks to the fine simulation likely to be performed through them (if assuming, of course, the required cost in calculation time!), these codes are used as reference codes, and their results have the hybrid status between a calculation result and an experimental result. It will be interesting to see how stochastic and deterministic codes will evolve. The exponential increase in calculation power makes the use of Monte-Carlo codes ever more accessible. This is why the CEA is developing the TRIPOLI-4® code. It might take a long time, however, for these codes to dislodge deterministic codes, which are much more flexible and much easier to use for parametric studies.

Instead of looking them as competing tools, it is probably more fruitful to emphasize the possible synergies between both families of codes. For example, a deterministic calculation can contribute to accelerate a Monte-Carlo simulation significantly. Conversely, a Monte-Carlo calculation can be used to elaborate homogenized and/or condensed nuclear data for a later use in deterministic codes.

Synergy between simulation and experiment

With simulation development, the status of experiment is changing: it becomes experiment for validating or determining basic data, and it may take the form of experiments designed to isolate a particular effect. That may help reduce much heavier and much more costly integral experiments on whole systems, but obviously the latter cannot be fully dropped. So the ÉOLE, MINERVE, and MASURCA critical mockups still available at the CEA remain tools of invaluable interest.

Coping with uncertainties

One of the major challenges to be taken up in simulating complex system behavior is how to assess uncertainties, as the latter may arise from uncertainties on initial data, on the model itself, or on the resolution of its constitutive equations. Neutronics cannot escape the rule: improving accuracy means improving margins in reactor design and operation. It also means making progress in safety and radiation protection. The coupling of neutronics with other disciplines (thermal-hydraulics, thermal-mechanics) adds another degree of difficulty to the mastery of the uncertainty propagation in neutronic numerical simulation.

Improving nuclear data

Higher accuracy in future "reference" neutronics calculations will mostly result from improvement of nuclear data. For, even if Monte-Carlo codes are good candidates to get the status of reference code in neutronics, their results will be good only if the basic nuclear data provided are accurate.

Nuclear data integration does mean a special challenge indeed, due to the high diversity of experiments giving access to those data. For the aim is to integrate as validated data experiment-based information as different as measurements of differential cross sections on spectrometers, and reactor noise measurements or oscillation experiment results on critical mockups. The first display a status of "raw" data, and can be integrated practically as they are; the second require a model for their integration. In addition, the microscopic theory of nuclear reactions provides an increasingly precise tool for nuclear data evaluation. How can all these data be used with a minimum loss of information? Here lies a true methodological difficulty which has not yet been fully overcome.

Nevertheless, the nuclear reactor physicists' community has been able to get appropriate structures to build a few standardized, federative databases, whose quality is ensured by a robust process of evaluation through expertise. In particular, the CEA is a major actor in the building of the JEFF3 European base, which may be used as an example for the setting-up of similar databases in other scientific and technical fields.

Simulation-dedicated platforms

Using numerical simulations has always been an inescapable component in the design and safety demonstration of nuclear facilities. This requirement is based on the observation that some experiments, especially those dealing with reactor safety, cannot be achieved on full scale. The CEA has got specialized in these numerical simulations, first of all in the neutronics field. For computer codes and related databases capitalize knowledge stored over time in relation to systems modeling. The design of major computer codes is long and complex. It is based on a very broad number of skills: physicists, experimentators, computer scientists, computer engineers, mathematicians… Simulation has long consisted in developing overall computer codes dedicated to describing a physical phenomenon or a particular process. Now, as observed in the last ten years, it could be fruitful to subdivide calculation into generic modules, and gather these modules, and the databases feeding them, on platforms likely to make them exchange data, the outputs from some of them being likely to be used as inputs by the others. This new paradigm of simulation through software platforms has paved the way to multiphysics and multiscale simulation, and has broadened its scope. Neutronics, which has been a pioneering discipline in building simulation platforms, perfectly fits within this framework, that at CEA takes the form of the SALOMÉ platform construction.

Simulation codes have a lifetime much longer than the computers on which they run: given the time needed to develop codes, and the time of use, which may cover 20 to 30 years, it is a *must* to fully anticipate the needs they will have to meet, and the diversity of the computer machines on which they will be used. This is why the major neutronics codes developed at the CEA/DEN have to be considered as long-term investments, similarly to those for experimental facilities.

Numerical simulation and high-performance computing

As could be seen all along this Monograph, High-Performance Computing (HPC) has induced a boost of the neutronics discipline, a progress made possible by adapting the computational codes and models to the architecture of these new machines, which is a "must" for a full use of supercomputer power. In order to develop and implement simulation platforms, the CEA/DEN teams can use supercomputers or computer networks among the most powerful in Europe. Their most consuming simulations requiring the highest computing powers can be performed on the whole of computer tools available at the very large-scale computing center TGCC *(Très Grand Centre de Calcul)* operated by CEA, that is: the CEA's CCRT, and CURIE, the petaflop machine financially supported by the French national major equipment for enhanced computing GENCI *(Grand Équipement National de Calcul Intensif)*.

The use of these tools is structured within the framework of networks or centers of excellence, such as the *Maison de la Simulation* (House of simulation), which is a joint laboratory gathering CEA, CNRS, INRIA, Paris-Saclay University, and Versailles-Saint-Quentin University, and a multidisciplinary center of excellence likely to take up challenges relating to enhanced calculation.

These computer machines and related structures will soon allow tools such as "numerical (or digital) reactors" or "numerical factories" to be developed, so that the impact on a facility of a modified design choice, or input item, may be evaluated very quickly. Nuclear reactor physicists do play a crucial role in this program that, though demanding long-lasting efforts, stands as an extremely attractive challenge, indeed, for the CEA's research scientists.

Bernard Bonin
Scientific Division

Glossary – Index

Note to the readers.– This set of terms and definitions is strictly intended to be a translation of the French DEN Monograph Glossary and is provided only for convenience purposes. Accordingly, the definitions herein may differ from standard or legally-binding definitions prevailing in English-language countries.

Absorber (neutron)**:** see **Neutron absorber*.**

Accelerator-driven system (ADS): see **Hybrid system***.

Actinides: rare-earth elements with atomic numbers ranging from 89 to 103. This group corresponds to the filling up of electron subshells 5f and 6d. Actinides exhibit very close chemical properties. **9, 22, 28, 29, 108, 190, 200, 228, 229, 231, 242.**

Activation (or **radioactivation**)**:** the process whereby a stable **nuclide*** is turned into a **radioactive*** nuclide. It tends to make certain nuclides radioactive, particularly within structural materials in reactors, through bombardment by **neutrons*** or other particles. **9, 29, 32, 107, 131, 141, 180, 185, 189, 190, 228, 230, 247-249.**

Activation products: nuclides* generated by neutron capture. Generally, this term specifically refers to nuclides generated in fuel, in **core*** structures, and in the remainder of reactor structures, excluding transformations of heavy nuclei. The most important activation products are tritium, carbon 14, chlorine 36, manganese 54, iron 55, cobalt 60, molybdenum 93, and niobium 94. **131, 141, 230.**

Activity: for a radioactive substance, the number of spontaneous nuclear transitions per unit time within a **radionuclide*** population or a mixture of radionuclides. It is expressed in **becquerels*** (Bq). 1 becquerel is equivalent to one disintegration per second. **10, 12, 13, 41, 57, 131, 176, 185, 186, 195, 196, 230, 248, 249.**

ADF: see **Assembly Discontinuity Factor***.

Adjoint flux: the solution of the adjoint transport equation. **58, 121, 202.**

ADS: Accelerator-Driven System. See **Hybrid system***. **39- 41.**

Advanced Sodium Technological Reactor for Industrial Demonstration: see **ASTRID***.

AGR (Advanced Gas cooled Reactor)**:** the second generation of British reactors using low-enriched uranium, graphite as moderator, and carbon dioxide as coolant. **187.**

Alpha*:** see **Radioactivity. **10, 22, 32, 40, 47, 107, 112, 173, 227, 248.**

ANDRA: *Agence Nationale pour la gestion des Déchets RAdioactifs*. The French national radioactive waste management Agency. **185.**

APOLLO, **APOLLO2**, **APOLLO3®:** deterministic transport neutronics computer codes. **16, 18, 54, 62, 65, 67, 69, 71, 73, 82, 85, 87, 122, 123, 126-135, 138, 140, 141, 143-147, 152-154, 160, 177, 178, 196, 203, 206, 212, 217, 219, 220, 228, 233, 242, 254.**

Assembly calculation: see **Spectrum calculation***. **52, 70, 198, 199, 201-203, 205-209, 217, 220.**

Assembly Discontinuity Factor (**ADF**)**:** a factor introduced in the deterministic transport equation resolution methods to treat interfaces between assemblies. **54, 80.**

Assembly (**fuel**)**:** see **Fuel assembly***.

ASTRID (Advanced Sodium Technological Reactor for Industrial Demonstration)**:** an integrated technology demonstrator designed for industrial-scale demonstration of 4th-generation sodium-cooled fast reactor (SFR) safety and operation, which is being investigated at the French Alternative Energies and Atomic Energy Commission (CEA: *Commissariat à l'énergie atomique et aux énergies alternatives*). **21, 29, 152, 187, 201.**

ATWS (Anticipated Transient Without Scram [Safety Control Rod Axe Man])**:** a power transient associated with a penalizing assumption, that is the reactor's automatic shutdown cannot be triggered. It belongs to the class of "transients related to reactivity control". **221, 222.**

Axial offset: in a nuclear reactor, the axial deformation of power distribution compared to a symmetrical distribution. **188, 220, 221.**

Barn: the unit used to measure **cross sections*** (1 barn = 10^{-24} cm^2). **11.**

Barrier (**confinement**)**:** see **Confinement barrier***.

Bateman equations (**generalized**)**:** a set of coupled equations governing the time evolution of nuclei concentrations within an irradiated medium (*e.g.* a nuclear reactor core), taking into account both neutron-nucleus interactions and radioactive decay phenomena. **11, 12, 13, 14, 49, 51, 52, 54, 59, 107, 108, 109, 113, 125, 136, 198, 204, 208.**

Becquerel (**Bq**)**:** a unit of radioactive decay equal to one disintegration per second. 37 billion becquerels are equal to 1 curie (Ci). 30,000 disintegrations per second occur in a household smoke detector. As the becquerel is a very small unit, large multiples are often used: mega-, giga-, or terabecquerel (MBq, GBq, and TBq corresponding respectively to 10^6, 10^9, and 10^{12} Bq). **13.**

Benchmark: a model intercomparison exercise based on a set of experimental data. In its first meaning, this term refers to a reference value (or experiment), the results of which are interpreted by the international community before being integrated in an international database. **41, 70, 96, 100, 104, 126, 128, 136, 154, 155, 170, 176, 177, 178, 179, 180, 181, 182, 226, 250, 251.**

Beta*:** the **delayed neutron fraction, generally expressed in **pcm*** *(pour cent mille)*. Some fission products generated in the reactor's **core*** emit neutrons, sometimes with a delay up to a few dozen seconds after fission. Though bringing little contribution to **neutron balance***, these very neutrons enable **nuclear chain reaction*** to be controlled and regulated. The "effective *beta*" is the product of *beta* by a coefficient larger than 1, which expresses the higher neutron efficiency of delayed neutrons in the core due to their energy being lower than that of **prompt neutrons***. **175.**

Beta* radiation:** see **Radioactivity.

Black rod: a **control rod*** consisting of neutron-absorbing materials, and contributing to **criticality*** control in a nuclear reactor. **198.**

Blanket: an area located in the peripheral part of a reactor **core*** and containing **fertile*** material. **9, 186, 200-202, 249, 250.**

BNCT: Boron Neutron Capture Therapy. See **Boron therapy***.

Boiling crisis: for a **coolant*** in contact with a heated surface, the passage from **nucleate boiling*** to **film boiling***, that results in a sharp degradation of the heat transfer coefficient. This complex

local thermal-hydraulics phenomenon includes **film boiling*** and dryout. In a nuclear reactor, a specific follow-up is given to boiling crisis, for this phenomenon may cause a severe damage in **fuel clad***, and so affect the integrity of the first **confinement barrier***. 195, 218, 225.

Boiling water reactor (**BWR**)**:** a nuclear reactor moderated and cooled with ordinary water, brought to boiling in the core in normal operating conditions. 129, 135, 166, 171, 187, 194, 195, 203, 204, 208, 217-219, 228, 229.

Boltzmann equation: a kinetic equation in which internal forces only act as the result of binary collisions between particles. It is applicable in the case of short-range inter-particle forces (ordinary gases). In reactor physics this equation describes neutron transport in matter. 11-14, 16, 43-45, 47, 49, 51, 52, 55, 58, 61-65, 75, 76, 89, 125, 127, 171, 218.

Boron Neutron Capture Therapy: see **Boron neutron therapy***.

Boron neutron therapy (or **Boron Neutron Capture Therapy**, **BNCT**)**:** a boron neutron capture therapy especially used to treat brain tumors. Capture induces the emission of *alpha* particles likely to destroy tumor cells in a very finely localized area. 186, 191.

Bq: see **Becquerel***. 13.

Breeder reactor (or **breeder**)**:** a nuclear reactor able to generate more **fissile*** material than is burnt in it. The new fissile nuclei are generated through capture of **fission* neutrons*** by **fertile*** nuclei (non-fissile under the action of **thermal neutrons***) after a certain number of r**adioactive decays***. 200.

Breeding: an operating mode of a nuclear reactor in which the **conversion factor*** is higher than 1. 186, 201, 211.

Bremsstrahlung: the electromagnetic radiation appearing when a charged particle is slowed down (or accelerated) by an electromagnetic field. For example, it is emitted by a highly energetic electron as it goes through the Coulomb field of a nucleus. 21, 32, 176, 186.

Burnable poison: a **neutron poison*** deliberately introduced into a reactor so as to help control long-term variations in **reactivity*** through its gradual disappearance. 211.

Burnup (or **burn-up**) (also called **burnup fraction** or **burnup rate**)**:** strictly speaking, the percentage of heavy atoms (uranium and plutonium) that have undergone **fission*** over a given time interval (referred to as "burnup fraction"). It is commonly used to determine the amount of thermal energy generated in a reactor per unit mass of **fissile*** material, from fuel loading to unloading operations, and is then expressed in megawatt.days per ton (MW.d/t) (this is referred to as "**specific burnup***": see this term). **Discharge burnup*** is the value for which a fuel assembly must be effectively unloaded, *i.e.* after several irradiation cycles. 13, 97, 107, 109, 110, 136, 143, 144, 188, 195, 198, 199, 201, 205, 206, 208, 211, 213, 215, 219, 223, 229-231, 233, 234.

Burnup code: see **Depletion code***.

Burnup credit (or **burn-up credit**)**:** the difference between the **reactivity*** of non-irradiated fuel in a given medium and lower reactivity of the same fuel after irradiation (negative reactivity brought by fission products). The burnup credit can be taken into account in **criticality*** studies. 111, 188, 227, 230, 242.

Burnup fraction: see **Burnup***.

Burnup rate: see **Burnup*** and **Specific burnup***.

BWR: see **Boiling Water Reactor***.

Calculation scheme: see **Computational scheme***.

CANDU (CANada Deuterium Uranium)**:** a Canadian type of natural-uranium, heavy water-cooled and -moderated nuclear power reactors. One of the specific features characterizing the CANDU reactor, of a unique design, lies in its ability to be refuelled at full power. 187.

Cask: a shielded container used for transport and, possibly, storage of radioactive materials. 97, 186, 188.

CAST3M: a simulation computer code dedicated to mechanics and thermics (materials, structures, fluids). 208, 220.

CCRT *(Centre de Calcul Recherche et Technologie)***:** a CEA research and technology computational center in which computers are chiefly used by the industrial branches of the CEA and of industrial partners. 98, 153, 157, 255.

Cell: see **Lattice***. 18, 52, 54, 63, 66, 70, 84, 97, 127, 130, 138, 139, 143, 154, 155, 174, 197, 198, 199, 202, 207, 232-234, 241.

Čerenkov effect: the emission of visible light appearing when a charged particle moves through a given medium at a speed greater than the speed of light in this medium. Radiation is emitted as a shock wave coupled with the particle. Thus decay of **radioactive*** nuclei releases electrons at speeds greater than the speed of light in water, and these electrons interact with the latter giving off their energy through emission of a blue light cone. The same phenomenon may take place in matter during a **criticality*** accident. 244.

CÉSAR: a "simplified" fuel cycle computer code. 137, 142, 228, 242.

Chain reaction: see **Nuclear chain reaction***.

Cherenkov effect: see **Čerenkov effect***.

Clad: see **Fuel clad***.

Code package (or **computational code package**)**:** a tool consisting of nuclear data libraries, **computer codes***, as well as validated and qualified calculation procedures, designed for calculation of physical quantities of interest in neutronics. 21, 126, 127, 129, 130, 143-145, 147, 165-172, 228, 229-231, 242.

Code package (**qualification**)**:** see **Qualification of a code package***.

Collectron: see **Self-powered neutron detector***.

Collision probability method ($\mathbf{P_{ij}}$)**:** see p. 84 in particular. See also pp. 69, 84, 127, 130, 205-208.

Computational code: see **Computer code***.

Computational code package: see **Code package***.

Computational scheme (or **calculation scheme**)**:** see pp. 125 and 126. See also **Code package*** and **Core calculation***. 51, 126, 146, 177, 178, 181, 196, 204-207, 218-220, 248.

Computer code (or **Computational code**)**:** a computational numerical program that consists of coded mathematical formulae related to the simplified representation (modeling) of a system or process for simulation purposes. 16, 18, 21, 23, 27, 28, 35, 37, 52, 54, 62, 65, 67, 69, 71, 73, 80, 85, 87, 89, 94, 97, 103, 104, 121-123, 127-146,150-154, 160, 165, 166, 168, 169, 178, 180, 181, 196, 199, 203, 206, 208, 212, 215, 217, 220, 225, 226,228, 234, 242, 247, 249, 250, 254.

Condensation: for a given **multigroup*** meshing, an operation that consists in defining a coarser multigroup meshing on which the physical quantities of interest are computed using an equivalence method. 52, 53, 122, 123, 129, 139, 143, 198, 202, 217.

Confinement barrier (or **containment barrier**)**:** a device able to prevent or limit dissemination of radioactive materials. In a nuclear reactor, all the physical components that isolate fuel **radionuclides*** from the environment. In a **pressurized water reactor***, these successive components are fuel clad, primary coolant circuit envelope (including vessel), and reactor containment. 222, 223, 246.

CONRAD (COde for Nuclear Reaction Analysis and Data assimilation)**:** a code system dedicated to nuclear data evaluation. 21, 23-26, 28, 35, 36.

Conservative approach: the quality of a calculation approach or method that takes into account assumptions enhancing the effects of phenomena likely to alter the performance of a material, piece of equipement, or facility, and to affect **nuclear safety*** or **radiation protection***. 215.

Control rod: a movable rod, or group of rods moving as an integral unit, containing a neutron-absorbent material (boron, cadmium…), and acting on the **reactivity*** of a nuclear reactor core depending on its position in the core. 28, 120, 185, 218.

Control rod cluster: see **Control rod***.

Conversion factor: the ratio, for a given time interval, between the number of **fissile* nuclides*** generated, and the number of fissile nuclides destroyed. A reactor is said to be a **converter reactor*** when its conversion factor is equal to 1, and a **breeder reactor*** when its conversion factor is greater than 1. 172, 187, 199, 200, 201, 208, 219.

Converter mode: the operating mode of a nuclear reactor in which the reactor produces as much **fissile*** material as it consumes (see also **Conversion factor*** and **Breeder reactor***). 200.

Converter reactor (or **converter**)**:** a nuclear reactor operating in the **converter mode***. 200.

Coolant: a liquid or gas used to remove heat generated by **fissions*** from the **core*** of a **nuclear reactor***. In a **pressurized water reactor*** (PWR), water plays the role both of coolant and **moderator***. 52, 172, 177, 193, 194, 195, 200, 201, 203, 204, 207, 208-210, 215, 216, 219, 220, 224, 239.

Core: the central area of a **nuclear reactor*** that contains **fuel assemblies***, **coolant*** and **moderator***, and in which **nuclear chain reaction*** takes place. 9, 17, 45, 51-54,59, 62, 63, 89, 97, 101, 104, 108, 115, 117, 120, 121, 126-148, 152-155, 171-229, 232, 247, 253.

Core calculation: the second step in the two-step computational scheme of a nuclear reactor, the first one being referred to as **spectrum calculation***. This step is achieved using for example the **CRONOS2*** code. 52-54, 63, 121, 126, 127, 130, 136, 153, 154, 196, 198, 199, 202, 204-205, 206, 208, 209, 217, 218, 220.

Core melting: a nuclear accident during which **nuclear fuel*** is brought to a sufficiently high temperature for nuclear fuel to be melt into a corrosive magma (**corium***) at the bottom of the reactor **vessel***. 200.

Core physics: the study of nuclear reactor cores, a major area of neutronics. 127.

Corium: a mixture of molten materials resulting from the accidental melting of a **nuclear reactor* core***. 188.

CRISTAL: a criticality code package based on the **APOLLO2***, **MORET4***, **MORET5***, and **TRIPOLI-4®*** codes, and on the **JEF-2*** and **JEFF-3*** nuclear data evaluations. 129, 228, 229, 242, 246.

Critical: qualifies a medium in which a **nuclear chain reaction*** is self-sustained, *i.e.* in which the number of **neutrons*** generated equals the number of lost neutrons. The **multiplication factor*** is then strictly equal to 1, and the reaction is strictly sustained; the number of fissions observed during successive time intervals remains constant. **Criticality*** expresses a strict equilibrium between neutrons yielded by fission, (n, 2n) reactions…, and neutrons lost by absorption and leakage. When neutron yields by fission are higher than losses by absorption or leakage, the system is referred to as **supercritical***; otherwise, it is known as a **subcritical*** system. 7, 13, 15, 16, 38, 51, 54-56, 58, 61, 97, 99-101, 103, 115, 117-119, 128, 130, 133, 143, 166, 171, 172, 174-176, 178-182, 185, 194-196, 199, 200, 202, 209-213, 218, 222, 223, 225, 229, 235-241, 243, 254.

Critical mass: the minimum mass of **fissile*** material nuclei required for the number of **neutrons*** produced during a **chain reaction*** to be equal to the number of neutrons absorbed. See also **critical***. 15, 235, 237, 240, 243.

Critical mockup: a reactor dedicated to experimental neutronics studies, in which very low powers are involved. Its neutronic behavior can be directly extrapolated to physical phenomena encountered in power reactors, thanks to the linearity of neutronics equations. 16, 130, 143, 166, 171, 172, 176, 181, 254.

Criticality: the characteristic configuration of a mass of material containing **fissile*** elements, and possibly other elements, with a composition, proportions, and a geometry such that a **nuclear chain reaction*** can be self-sustained within it. 9, 39, 47, 51, 73, 91, 96, 98, 101, 104, 110, 111, 115, 129, 133, 171, 175, 178-188, 192, 194, 227, 228, 229, 235-246, 253.

Criticality accident: the initiation of an uncontrolled **nuclear chain reaction*** corresponding to an effective **multiplication factor*** k_{eff} higher or equal to 1. 9, 188, 229, 235, 236, 241-246.

Criticality excursion: in a medium where nuclear reactions take place, a controlled or accidental increase in neutron flux up to exceeding **criticality***. 51.

CRONOS, **CRONOS2:** deterministic neutronics computer codes used for calculation of reactor **cores***. 121, 122, 124, 126, 127, 129, 130, 131, 138, 141, 143-145, 160, 177, 178, 196, 206, 208, 215, 217, 218, 220, 226.

Cross section (**macroscopic**)**:** see **Macroscopic cross section***.

Cross section (**microscopic**)**:** see **Microscopic cross section***.

Cumulative fission yield (or **cumulative yield** or **cumulated fission yield**) [of a fission product]**:** the **primary fission yield*** to which are added all the contributions from the radioactive **decay*** of parent nuclei that yield this fission product (definition adopted in nuclear data libraries). 27, 111.

DARWIN, **DARWIN2:** neutronics computer codes used to model how **fuel*** evolves under irradiation (radionuclide concentrations, residual power, radiation sources…). 126, 127, 129-132, 137, 141, 228, 230, 231, 233, 234, 242, 248, 249.

Daughter products: see **Radioactive filiation***.

Decay (**radioactive**)**:** the transformation of a **radionuclide*** into a different nuclide by spontaneous emission of *alpha*, *beta*, or *gamma* radiation, or by electron capture. The final product is a nucleus of lower energy and higher stability. Each decay process has a well-defined **radioactive half-life***. 8, 12, 19, 28, 31, 32, 35, 36, 45-47, 49, 59, 107, 112, 231, 242.

Decay chain: a series of **nuclides*** that arises from successive **radioactive disintegrations*** or **nuclear reactions***, starting from a parent nuclide. See also **Radioactive filiation***. 107, 108, 131, 189, 228.

Defense in depth: a concept in which several successive lines of defense are set in place in a nuclear facility so as to prevent the occurrence of accidental situations due to technical, human, or organizational failures or, if ever they occur, to limit their effects. 241, 246.

Degree of moderation: see **Moderator-to-fuel ratio***.

Delayed neutrons: neutrons* emitted by **fission*** fragments a long time after fission (a few seconds on the average). Although they account for less than 1% of emitted neutrons, they are those

which allow reactor control *in fine* using this delay. 8-10, 27, 46, 47, 52, 55, 59, 60, 115-119, 172, 174, 175, 194, 200, 223.

Depletion: see **Fuel depletion*** and **Depletion code***.

Depletion code (also called **generation/depletion code**, **isotopic depletion code** or **burnup code**)**:** a computer code for modeling **fuel depletion***. It is also referred to as "**burnup code**" or "**isotopic depletion code**". It may also be called an "**evolution code**". 134, 136, 137, 141, 228, 247.

Design basis: the working out of a nuclear facility's characteristics as part of its design step in order to meet pre-established criteria and comply with regulatory practice. 33, 97, 120, 144, 180, 185-191, 194, 209-211, 222, 224, 225, 233.

Design basis accident (or **DBA**)**:** a reference accident, the study of which is used for the **design basis*** of a reactor with respect to **safety***. 225.

Deterministic method (or **deterministic calculation**)**:** a method for calculating the behavior of complex systems that is based on the analytical or computational numerical resolution of equations fully or partially describing these systems. In **neutronics***, deterministic methods are used for the computational numerical resolution of the transport equation, in order to determine the **neutron flux***. They generally require the discretization of space, energy, and time variables. They are much used for **nuclear reactor*** design. 51-53, 126, 127, 136, 143, 152, 178.

Diffusion equation: an equation derived from the **Boltzmann equation***, in the so-called diffusion approximation (Fick's law). 44, 52, 62, 75-78, 81, 129, 130, 143, 199, 206, 217.

Direct disposal: the action of directly disposing of spent fuel without going through the fuel treatment and recycling steps. 130, 186, 187, 190, 202, 227, 228, 231, 233.

Discharge burnup: see **Burnup***.

Disintegration (**radioactive**)**:** the transformation of an unstable nucleus into a stable, or unstable, nucleus, during which the number and nature of nucleons within the nucleus are changed. 8, 49, 248.

Dismantling: the whole set of technical operations required for dismounting, and possibly disposing of, a piece of equipment or a part of a nuclear facility. 9, 29, 134, 185, 187, 189, 247-249.

Disposal (**of radioactive waste**) (or **radioactive waste disposal**, or **radwaste disposal**)**:** the placing of radioactive waste in a facility designed to ensure its permanent confinement. For the facility in which waste is placed without scheduling further retrieval, see the term **Repository***. Retrieval would however be possible in the case of a reversible disposal (see also **Radioactive waste storage***). Deep geological disposal of radioactive waste is the disposal of these materials in an underground facility specially managed for this purpose. 130, 186, 187, 190, 196, 227, 228, 231.

Divergence: the state of a reactor at the very moment when **core criticality*** is reached; by extension, the startup sequence of a nuclear reactor that takes place prior to reaching core criticality. 15, 171, 177, 211.

Dollar: a **reactivity*** unit. The dollar is defined by the reactivity / **delayed neutron*** proportion ratio = 1, with the cent as a submultiple. 175.

Domain decomposition: a numerical, algorithmic technique implemented to parallelize computer codes. For example, the MINARET solver of the **APOLLO3®*** code uses domain decomposition techniques to run on processors operating in parallel. 151-154.

Doppler effect: in **neutronics***, the broadening of neutron cross section resonances resulting from the thermal motion of the target nuclei. This effect contributes to ensure the stability of a nuclear reactor, bringing down the **reactivity*** of its **core*** as core temperature rises. 201, 222, 224.

Dose: the amount of energy imparted to a medium by ionizing radiation. In radiation protection, the general term "**dose**" conveys a special meaning when used in association with one or several qualifier adjectives, such as "absorbed", "collective", "effective", "equivalent", or "individual". Absorbed energy may be weighted or not according to radiation type or quality. 28, 104, 133, 137, 172, 185, 186, 188-190, 196, 233, 245-248, 257.

Dose rate: the quotient of the increment in **dose*** in a time interval by that time interval (energy absorbed in matter per unit mass and unit time).The SI standard unit is the **gray*** per second (Gy/s). 28, 137, 188-190.

Dosimetry: dose* measurement. It is aimed at assessing, through a measurement or an appropriate calculation, the amount of energy absorbed in a given mass of material. 32.

dpa: Displacements Per Atom. A unit of radiation damage in materials. The dpa number is the number of times that each atom of a given sample of solid material has been ejected from its site under irradiation. This is an appropriate unit to quantify irradiations in metals. 28, 133, 189, 196, 200, 201, 211.

ECCO: deterministic transport neutronics computer code. It is part of the **ERANOS* code package** dedicated to **fast neutron reactors***. 37, 67, 130, 138, 139.

ECIS *(Équations Couplées en Itérations Séquentielles)***:** coupled-equations in sequential iterations. A computer code dedicated to nuclear reaction models. 23, 24.

Effective delayed neutron fraction: see ***Beta****.

Effective multiplication factor+ (***k_{eff}***) [also called **effective multiplication constant**]: see **Multiplication factor***.

Elastic scattering: a scattering process in which the energy of the scattered particle does not change in the center-of-mass system. 10, 11, 25, 31, 45, 46, 52, 53, 55, 56, 57, 66, 68, 70, 76, 89, 90-93, 95, 101, 120, 122, 193, 199, 219, 236, 239.

Electron: a negatively charged elementary particle that is a constituent of the atom. In an atom having a Z atomic number, Z electrons orbit around the atomic nucleus. 10, 21, 22, 32, 47, 105, 112, 133, 140, 173, 188.

Enrichment: a process that, in the case of uranium, allows, by various means (gaseous diffusion, ultracentrifugation, selective laser excitation), an increase in the concentration of (**fissile***) **isotope*** 235 relative to isotope 238, which is predominant in natural uranium. See also **Fuel cycle***. 71, 179, 186, 203, 219, 227, 229, 236, 243, 245.

Epithermal neutrons: neutrons having an energy in the (approximate) 1 eV-20 keV range, thus exhibiting a kinetic energy greater than that of **thermal neutrons***. In this energy domain, neutron-nucleus interactions exhibit resonances, so that their **cross sections*** may vary by several orders of magnitude. 22, 128, 171, 172, 203, 219.

EPR: European Pressurized Reactor. 21, 29, 52, 60, 251.

ERANOS: a European neutronics code mainly dedicated to calculations of fast neutron reactor cores. 54, 127, 130, 131, 139, 141, 201, 228.

ESFR: European Sodium cooled Fast Reactor. A collaborative European project. 153.

Evaluation (**of nuclear data**)**:** a work that consists in producing a nuclear data library from experimental measurements and theoretical models of nuclear physics. 11, 21-29, 31-35, 37, 58, 89, 107, 128, 131, 133, 143, 168, 181, 228, 230, 232, 242, 254.

Evolution code: see **Depletion code***.

Fast neutron reactor (or **fast reactor**, **FR**)**:** a **nuclear reactor*** in which the amount of materials likely to slow down **neutrons*** is kept low, so that most **fissions*** may be caused by **fast neutrons***. 23, 29, 37, 77, 130, 133, 142, 166, 172, 187, 193, 194, 195, 199, 201, 202, 208, 210, 211, 228, 229.

Fast neutrons: neutrons* of a **nuclear reactor*** that exhibit a kinetic energy much greater than **thermal neutrons***. These neutrons, released during fission*, move very quickly (20,000 km/s). Their energy is about one million **electronvolts***. 15-17, 23, 37, 66, 67, 127, 130, 133, 142, 171, 172, 187, 193, 194, 197, 199-201, 208, 211.

Feedback (**reactivity**)**:** see **Reactivity feedback***.

Fertile: refers to a **nuclide*** likely to be directly or indirectly turned into a **fissile*** nuclide through **neutron capture***. This is the case for uranium 238, which yields plutonium 239. Otherwise, the material containing the nuclides is said to be "sterile". 25, 110, 153, 186, 193, 197, 199-201, 204.

Film boiling: a phenomenon characterized by the formation of a thin layer of steam occuring between a hot wall and a fluid which is either a liquid, or a two-phase mixture of liquid and steam. In a liquid-cooled nuclear reactor film boiling takes place as a local vaporization of the fluid on contact with the fuel element clad, corresponding to the transition from saturated boiling to film boiling. This film induces a significant degradation in heat transfer, liable to lead to overheating in this area, and resulting damage of the fuel element clad (the so-called "burn-out"). See **Boiling crisis***.

Fissible (or **threshold fissioning**): see **Fissile***.

Fissile: refers to a **nuclide*** the **nuclei*** of which are capable of undergoing **fission*** under the effect of **neutrons*** of any energy, as low as it may be. Examples are uranium 233, uranium 235, and plutonium 239. Strictly speaking, it is not the so-called "fissile" nucleus that undergoes fission, but rather the compound nucleus formed after **neutron capture***. The adjective "fissile" covers a subcategory of the so-called "**fissible**" (or "**threshold fissioning**") nuclides, that are likely to undergo fission under the effect of neutrons of greater energy than a threshold value characteristic of those nuclides (the so-called "fission threshold") [*e.g.* uranium 238, thorium 232, curium 244, americium 241, americium 243, and californium 252]. **Fissile** is used in various phrases such as: **fissile nucleus**, **fissile core**, **fissile material**, **fissile unit**, **fissile system**, and **fissile height**. 8, 9, 13, 15, 31, 47, 59, 81, 96, 99, 100, 101, 107, 110, 115, 116, 118, 119, 173, 174, 188, 193, 194, 199-202, 204, 209, 210, 211, 219, 228, 229, 235, 236, 237, 238, 239, 240-245…

Fission: the splitting of a **heavy nucleus*** into two fragments of approximately equivalent masses, the so-called **fission products***. This transformation, that is a special case of **radioactive decay*** ("spontaneous fission") in some heavy nuclei, releases a large amount of energy, and is accompanied with the emission of neutrons and *gamma* radiation. The fission of the so-called "**fissile***" heavy nuclei can be induced by a collision with a neutron. 7-14, 19, 21-23, 25-32, 39-41, 45-47, 55, 56, 59, 63, 64, 89, 92, 93, 96-100, 104, 108, 111, 115, 116, 118, 120, 173, 175, 176, 180, 190, 193, 194, 197, 199, 210, 213, 219, 228, 235-238, 244.

Fission chamber: an ionization chamber used for **neutron*** detection, in which ionization is induced by the **fission products*** yielded by the nuclear reaction of neutrons on a **fissile*** material lining. 173, 174, 191, 233.

Fission products (**FPs**)**: nuclides*** yielded either directly, by **nuclear fission***, or indirectly, by the **disintegration*** of fission fragments. In the case of the binary fission induced by a thermal neutron on uranium 235, the atomic numbers of the nuclides range from Z = 28 (nickel) to Z = 66 (dysprosium), and their mass numbers from A = 72 to A = 193. 8, 9, 26, 27, 29-31, 39, 41, 46, 107, 108, 110, 129, 131, 141, 173, 176, 194, 195, 196, 198, 199, 202, 228, 229, 231, 232, 235, 237, 242.

Fission rate: see **Reaction rate***. 27, 59, 97, 98.

Fission yield (of a nuclide)**:** the probability of **nuclides*** being yielded by **fission***. See also **Cumulative fission Yield*** and **Primary fission yield***. 13, 19.

FLICA: a thermal-hydraulics simulation code developed at the CEA. 215, 217-219, 226.

FLOPS (or **Flops**)**:** Floating point Operations Per Second. 1 petaFlops = 10^{15} floating point operations per second. 1 exaFlops = 10^{18} floating point operations per second. 155-159.

Fluence: the integral of a particle flux density over a given time interval. Fluence is a dose unit used to quantify materials irradiation. This is the number of incoming particles (*e.g.* neutrons) per unit area during irradiation. 9, 13, 32, 103, 106, 110, 135, 136, 168, 180, 181, 185, 189, 196, 211, 213, 247, 250.

FP: see **Fission products***.

FR: Fast Reactor. See **Fast neutron reactor***.

Fuel: see **Nuclear fuel***.

Fuel assembly (or **fuel subassembly**, **assembly**)**:** in the **core*** of a water reactor, fuel **rods*** are grouped into clusters of suitable stiffness which are precisely positioned in the reactor core. The so-called "assembly" is that structure as a whole, gathering from 100 or so to a few hundred rods, that is loaded as a single unit into the reactor. 51, 52, 54, 63, 64, 70, 71, 76-81, 84, 89, 97, 127- 129, 134, 143, 144, 146, 147, 152, 153, 177, 185, 188, 196-199, 201- 209, 217- 221, 223, 224, 228, 229, 231, 247.

Fuel clad (or **clad** or **fuel cladding**)**:** a sealed envelope containing **nuclear fuel***, which ensures the containment of radioactive materials, and fuel protection against **coolant*** aggressions. 62, 63, 188, 190, 197, 200, 201, 205, 218, 221, 223, 225.

Fuel cycle: the whole series of steps which **nuclear fuel*** is to follow. The cycle especially includes ore extraction, concentration of **fissile*** material, conversion, **enrichment***, fuel element fabrication and use in reactors, **spent fuel treatment***, and **recycling***, if any, of fissile materials so recovered, as well as **radioactive waste*** conditioning and **disposal***. 29, 47, 96, 130, 134, 192, 193, 227-230, 235, 242, 253.

Fuel depletion (or **isotopic fuel depletion**)**:** the change over time in fuel composition, *i.e.* in fuel isotopic concentrations, as a function of irradiation. See also **Depletion code***. 32, 59, 132, 134, 145, 202, 206, 228.

Fuel rod: see **Rod***.

Fuel subassembly: see **Fuel assembly***.

Fukushima: a loss-of-coolant nuclear accident which took place at Fukushima (Japan), caused by an earthquake followed by a tsunami of exceptional amplitude (March 2001). 51.

Gamma**:** high-energy **photons***, emitted in particular during nuclear reactions or during the de-excitation of atomic **nuclei***. 8-10, 22, 27, 28-30, 32, 35, 105, 107, 137, 146, 172, 176, 181, 185, 186, 188-191, 196, 215, 227, 232-235, 247-249.

Gas-cooled fast reactor (**GFR**)**:** a **fast neutron reactor***, in which **coolant*** is gas, generally helium. 194, 208.

Gaussian quadrature: a quadrature formula exhibiting mathematical properties used in numerical methods for solving the **transport equation***. 34, 73, 74.

GCR: Gas-cooled reactor. 187.

GEN. I: first-generation reactors using natural uranium (natural uranium graphite gas [UNGG] reactors, MAGNOX reactors…). 28, 187.

GEN. II: second-generation reactors (1970's and 1980's decades): pressurized water reactors (PWR), boiling water reactors (BWR), sodium-cooled fast reactors (SFR), RBMK, CANDU, high-temperature reactors (HTR), molten salt reactors (MSR). 28, 187.

GEN. III: third-generation reactors (from 2005): advanced PWRs = EPR, AP-600, AP-1000… - advanced BWRs = ABWR-II, ESBWR, HC-BWR, SWR-1000 - advanced heavy water reactors = ACR-700 - pool reactors (small powers). 28, 187.

GEN. IV: fourth-generation reactors (from 2040) = GFR, SFR, VHTR, ASTRID prototype… 28, 187, 228.

Generation/depletion code: see **Depletion code***.

Generation time: the average time between a **fission*** and the following in the chain reaction. 175.

GFR: see **Gas-cooled fast reactor***.

Gray: a unit of **absorbed dose***, corresponding to the absorption of an energy of 1 joule per kilogram of matter.

Gray rod (**GB**)**:** see **Grey rod***.

Grey rod (or **gray rod**)**:** a **control rod*** absorbing fewer neutrons than a **black rod***, and allowing fine control of the nuclear reactor's power. 198.

Group (in neutronics): an energy interval within which average values are assigned to the various quantities characteristic of neutron interactions with their environment. 33-35, 40, 53, 62, 64-72, 75-77, 80, 81, 83, 84, 99, 136.

GT-MHR: Gas-Turbine Modular High Temperature Reactor. A gas-cooled reactor developed by General Atomics. 178, 187, 219, 220.

Half-life: see **Radioactive half-life***.

Heavy nuclei: isotopes* of the elements that exhibit a number of protons (atomic number) equal to or higher than 80. All the actinides and their daughter products belong to this group. 8, 40, 66, 107, 108, 110, 129, 131, 141, 177, 193, 195, 200, 204, 205, 219, 228, 234.

Heavy water (or **deuterium protoxide** [D_2O])**:** a natural form of water, in which hydrogen atoms are atoms of heavy hydrogen, or deuterium. It is approximately 10% heavier than light water, and occurs in nature in extremely small amounts (about one part of heavy water in 7,000 parts of water). Heavy water has a lower probability of neutron absorption than **light water***, which makes it attractive as a **moderator*** in some **nuclear reactors***. 7, 15, 16, 27, 180, 193, 194, 205, 258.

Heavy-water reactor (**HWR**)**:** a nuclear reactor in which the **moderator***, and usually the **coolant***, are heavy water. 16, 180.

High-Performance Computing: see **HPC***.

High temperature reactor (**HTR**)**:** a gas-cooled thermal neutron reactor, in which **coolant*** temperature at core outlet ranges from 600 °C to 900 °C. Generally coolant is helium. 129, 172, 194, 207, 208, 219-222.

Homogenization: an operation that consists in replacing a heterogeneous configuration (*e.g.* an assembly) by a homogeneous medium that is equivalent with respect to one or several predefined criteria (*e.g.* conservation of reaction rates). 16, 50, 52-54, 127, 129, 138, 143, 177, 198, 202, 217, 254.

HPC: High-Performance Computing based upon the use of supercomputers. 149, 152, 156-160, 169, 187, 255.

HTR: see **High Temperature Reactor***.

Hybrid system (or **accelerator-driven system**, **ADS**)**:** a hybrid reactor that couples a **subcritical*** reactor core with a high-energy proton accelerator. The latter uses **spallation*** reactions to provide the additional **neutrons*** required to sustain the **nuclear chain reaction***. 39, 40, 41, 107, 172, 186, 187.

Importance: this concept directly relates to the **adjoint flux*** used in neutronics for various purposes: perturbation calculation, calculation of effective quantities, Monte-Carlo simulation speedup through establishing an importance map. 58, 102, 104, 106, 140, 189, 202, 250.

Importance function: see **Importance***.

Importance map: see **Importance***.

Inelastic scattering: a scattering process in which the energy of the scattered particle changes in the center-of-mass system. 10, 11, 25, 28, 31, 45, 46, 52, 53, 55, 56, 57, 66, 68, 70, 76, 89, 90, 91, 92, 93, 95, 101, 120, 122, 193, 199, 236, 239.

INES scale: see **International Nuclear and radiological Event Scale***.

Infinite multiplication factor[+] (k_∞) [also called **infinite multiplication constant**]**:** see **Multiplication factor***.

Integral experiment: an experiment representative of a complex system, providing information on the global effect of several parameters or processes, rather than on their individual effects. 172, 180.

Integrated flux: see **Fluence***.

Integrated technology demonstrator: see **ASTRID***.

International Nuclear Event Scale: see **International Nuclear and radiological Event Scale***.

International Nuclear and radiological Event Scale (or **INES scale**)**:** the classification of nuclear events by increasing order of gravity, from the mere deviation, with no incidence regarding safety (level 0), to the major accident, with extended effects on health and the environment (level 7). Level 7 corresponds to an accident comparable with that of Tchernobyl. 244.

Irradiated fuel: see **Spent fuel***.

Irradiation cycle: the operating period of a reactor beween two successive refuelling operations. In France the irradiation cycles of nuclear power reactors are of 12-18 months. 135, 209.

Isotope: any nuclide of a given element. Isotopes are the forms of one same element, the nuclei of which display an identical proton number and a different neutron number. 22, 35, 41, 70, 85, 110-112, 205, 229, 236-238, 240, 241, 243-245.

Isotopic depletion code (or **isotope depletion code**)**:** see **Depletion code***. 134.

Isotopic fuel depletion: see **Fuel depletion***.

ITER: a reactor prototype for studying controlled thermonuclear fusion, which is based on an international collaboration. 190, 226, 249, 250, 251.

JEF (**JEF-2**), **JEFF** (**JEFF-3**)**:** a nuclear database centralized by the OECD/NEA. 11, 21, 23, 27-29, 31, 36, 64, 107, 111, 128, 130, 133, 143, 144, 181, 229, 230, 242, 253.

JHR: see **Jules Horowitz Reactor***.

Jules Horowitz reactor (**JHR**)**:** a research reactor dedicated to investigating materials and fuels under irradiation, studying some accidental situations, and producing radio-isotopes; currently under construction on the CEA Cadarache site. 15, 28, 29, 126, 128-132, 144, 145-147, 168, 205-208.

k_{∞}**:** see **Multiplication factor***.

k_{eff}**:** see **Multiplication factor***.

Lattice: in the **core*** of a nuclear reactor, array of **fuel assemblies***, **coolant*** and **moderator*** arranged according to a regular pattern. Each unit of this pattern is called a **cell***. 16, 52, 54, 73, 80, 81, 87, 127, 129, 130, 138, 139, 145, 154, 166, 171, 172, 204, 205, 206, 219.

Lattice calculation: see **Spectrum calculation***. 87, 127.

Leakage (**neutron**)**:** see **Neutron leakage***.

Lethargy: a nondimensional variable used in neutronics in order to characterize the energy loss of a neutron according to the relationship $u = \ln(E_0/E)$, where E_0 is a reference energy. 12, 65, 66, 67, 68.

Light water: ordinary water, as opposed to **heavy water***. 27, 154, 171, 180, 193, 204, 229.

Light water reactor (**LWR**)**:** a nuclear reactor in which **coolant*** and **moderator*** are light water. This reactor type gathers **pressurized water reactors*** and **boiling water reactors***. 138, 139, 143, 154, 160, 181, 204, 218.

LWR: see **Light Water Reactor***.

MA: see **Minor actinides***.

Macroscopic cross section: the product of the **microscopic cross section*** by the concentration of the nuclide of interest. In neutronics, the macroscopic cross section is usually expressed in cm^{-1}. It can also be interpreted as a probability density: probability of interaction (of the particle of interest moving through a given medium) per unit length. 46, 57, 58, 64, 66, 68, 76, 90, 92, 93, 96.

Magnox: an aluminium-magnesium alloy used as cladding material, particularly in certain British CO_2-cooled reactors (also referred to as Magnox reactors). 187.

Major actinides: see **Minor actinides***.

Material balance: the amounts of the various **nuclides*** occurring in a reactor's **core*** at a given time, resulting from each nuclide generated and lost due to nuclear reactions. 49, 59, 97, 131, 137, 195, 202, 217, 227-231.

MCNP: an American **Monte-Carlo* computer code*** for neutron and charged particle transport. 105, 137, 140, 151, 160, 226, 250, 25.

MENDEL (ModElisatioN code for DEpletion in nucLear systems)**:** a new-generation depletion (or "burnup") code shared by the **APOLLO3®*** and **TRIPOLI-4®*** transport codes. **MENDEL** computes the physical quantities of fuel cycle (see **DARWIN***). 127, 131, 132, 134-136.

Method Of Characteristics (**MOC**)**:** see especially p. 82. See also pp. 62, 77, 80-85, 87, 126, 127, 130, 143, 145, 146, 154, 197, 203, 205-207, 217, 218.

MeV: a mega electronvolt. This energy unit is generally used to express the energy released by nuclear reactions. 1 MeV corresponds to $1.6\ 10^{-13}$ Joule.

Microscopic cross section (or **cross section of a particle**)**:** the measure of the probability of interaction between an incident particle, or radiation, and a target nucleus, which makes it possible to assess the number of interactions between a particle or radiation flux (*e.g.* neutrons) and a system of target particles (*e.g.* uranium nuclei). Cross sections are generally expressed in **barns*** (1 barn = 10^{-24} cm^2). In neutronics, the main reactions of interest are those induced by neutrons: **fission***, **capture***, and **elastic scattering***. There is a microscopic cross section for each of these reactions. 11, 12, 23-26, 33, 34, 45-47, 49, 57, 58, 64-66, 68, 69, 76, 89, 90, 92, 93, 95, 96, 103, 111, 193, 195, 198, 210, 220, 230, 253.

Migration area: the area, usually expressed in cm^2, corresponding to the mean square of the distance traveled by neutrons in the reactor core, from their emission to their absorption. 213, 219.

Minor actinides (**MA**)**:** heavy nuclei produced in a reactor by successive **neutron*** captures from nuclei in the fuel. The **isotopes*** chiefly involved are neptunium 237, americium 241 and 243, and curium 243, 244, and 245. Uranium and **plutonium*** nuclei occurring or yielded in **nuclear fuel*** are referred to as **major actinides**. 22, 200.

Moderation: a process likely to help slow down neutrons in order to bring them progressively to a thermal equilibrium with the matter in which they are scattered. See also **Moderator***. 203, 204, 210, 218, 219, 237, 238, 240, 241, 243, 244.

Moderator: a material consisting of light **nuclei*** which slow down **fission neutrons*** through elastic collisions. Moderators are used to reduce the energy of neutrons emitted by uranium atoms during **fission***, so as to increase their probability to induce other fissions. The moderating material should have a low **capture*** capability to avoid "wasting" neutrons, and be sufficiently dense to ensure effective **moderation***. 22, 45, 52, 166, 171, 193-195, 197, 198, 203-205, 207, 208, 211, 215, 216, 218, 219, 224, 225, 237, 244.

Moderator-to-fuel ratio (or **ratio of moderator to fuel**, **degree of moderation**)**:** in a mixture of **fissile*** material and **moderator***, the ratio between the volume, or number of atoms, of the **moderator*** and the volume, or number of atoms, of **fissile*** material. This ratio governs average neutron energy. 204, 210, 218, 219, 243.

Monte-Carlo calculation: see **Monte-Carlo method***.

Monte-Carlo method (or **Monte-Carlo calculation**)**:** a statistical method to obtain an approximate integral value using a set of points randomly distributed according to a certain probability. It consists in repeating the assignment of a numerical value according to the various stages of a process involving randomness, and then calculating the average value and its statistical deviation (reflecting its accuracy) over all the values obtained. When applied to problems of particle transport in matter, it consists in simulating the traveling of a very large number of particles, strictly taking geometry and nuclear interactions into account, and then recording the results of interest. 11, 16, 34, 44, 52, 55, 62, 89-91, 97, 98, 100, 102, 104-106, 125, 131, 133, 134, 137, 140, 142, 160, 167, 196.

MORET: a multigroup and pointwise code for 3-D neutronics simulation that is based on the Monte-Carlo method for calculation of neutron transport under critical conditions. It is developed by the French Institute for radiation protection and nuclear safety (IRSN). 137, 140.

MOX fuel (also called **Mixed OXide fuel**)**:** a nuclear fuel containing mixed oxides of (natural or depleted) **uranium*** and **plutonium***. The use of MOX fuel makes it possible to recycle plutonium. (See also **Recycling***). 69-71, 79, 80, 110, 128, 171, 172, 176, 197, 223, 227-229, 231, 234.

Multigroup (or **groupwise**)**:** of a quantity put in a group, *i.e.* averaged over an energy interval or energy **group***.

Multigroup meshing: the partitioning of an energy domain by intervals called "**groups***", within which every energy-depending quantity is assumed to have a constant value. 33, 66-68, 70.

Multiphysics: of a computational approach and/or a software platform in which several computer codes relating to various disciplines are involved, *e.g.* neutronics, thermal-hydraulics, and thermal-mechanics. See also **SALOMÉ***. 149, 254.

Multiplication factor (**infinite** k_∞ and **effective** k_{eff})**:** in a neutron-multiplying medium, the average value of the number of new **fissions*** induced by the **neutrons*** generated by an initial fission. If **neutron leakage*** to the neighboring fuel assemblies or outside the reactor are not taken into account, this factor is known as the "infinite multiplication factor" and is noted k_∞. Otherwise, it is known as the "effective multiplication factor", and is noted k_{eff}. 7, 13, 15, 56, 59, 70, 89, 91, 99, 100, 115, 118, 119, 125, 174, 179, 185, 186, 202, 235.

Negative reactivity: a decrease in reactivity which can be induced by the insertion of a **neutron absorber*** (*e.g.* a control rod) in the reactor **core***. 110, 111, 194, 229.

NEPHTIS: a **code package*** dedicated to the study of high-temperature reactors, developed on the basis of **APOLLO2** and **CRONOS2** computer codes. 130, 220.

Neural network: a computational model inspired from brain biology. 104, 149.

Neutrino: an elementary particle of zero electric charge and very low mass, able to go through large thicknesses of material while carrying high energy, generated by the weak interaction in a number of nuclear reactions (*beta* disintegrations). 8, 10.

Neutron: an electrically neutral elementary particle of a 1.675 10^{-27} kg mass. The nature of this **nucleon*** was discovered in 1932 by the British physicist James Chadwick. Neutrons, together with protons, constitute atomic nuclei, and induce **fission reactions*** of **fissile*** nuclei, the energy of which is used in nuclear reactors. See especially p. 7.

Neutron absorber: a material likely to absorb **neutrons*** through a reaction of **neutron capture***. 15, 45, 52, 61, 71, 110, 128, 129, 143, 146, 171, 172, 174-176, 194, 195, 198, 199, 211, 216, 219.

Neutron balance: a detailed balance (by reaction type and isotope) of **neutrons*** generated and lost in a **fissile*** medium. Neutrons may disappear through absorption or **leakage***. 11, 12, 45, 51, 68, 78, 84, 115, 118, 197, 202, 211, 215, 217, 235, 236, 241.

Neutron capture: the capture of a **neutron*** by a nucleus. The capture is said to be "radiative" if it is immediately followed by emission of *gamma* radiation. It is said to be "**fertile***" if it induces the generation of a **fissile*** nucleus. 10, 11, 22, 23, 25, 28, 31, 40, 64, 66, 89, 91, 93, 95, 110, 111, 176, 193, 195, 197-199, 204, 219, 230, 232, 235-238.

Neutron flux: the number of neutrons that go through a unit area per unit time. 12, 22, 23, 28, 46, 54, 56, 77, 97, 99, 101, 102, 107, 110, 113, 115, 116, 136, 174, 211, 247, 248.

Neutron leakage: neutrons* escaping from the **core*** of a nuclear reactor. 41, 51, 54, 78, 115, 143, 154, 174, 177, 193, 197, 199-201, 205, 208, 211, 212, 219, 232, 236, 238.

Neutron physics: see **Neutronics***.

Neutron poison (or **poison**)**:** an element displaying a high potential for **neutron capture***, used to compensate, at least in part, excess **reactivity*** in **fissile*** media. Four natural elements are particularly neutron-absorbing: boron (due to its **isotope*** B 10), cadmium, hafnium, and gadolinium (due to its isotopes Gd 155 and Gd 157). Some poisons are referred to as "**burnable**" **poisons***, because they gradually disappear during in-pile burnup. Many **fission products*** are neutron poisons. See also **Poisoning***. 7, 110, 111, 128, 143, 144, 171, 174, 185, 194, 195, 197, 199, 203, 208, 229, 237, 238, 243, 245.

Neutron spectrometry: an experimental method giving access to the energy distribution of the **neutrons*** emitted by a source. The neutron spectrum so determined can be integrated over more or less broad energy bands, and the weight of each band, the so-called "**spectrum index***", can then be deduced.

Neutron spectrum: the energy distribution of the population of **neutrons*** occurring in the **core*** of a reactor. 34, 179, 188, 197, 199, 200, 203, 204, 207, 208, 210, 220.

Neutron transport: the neutron migration within the reactor, from their emission to their disappearance by absorption or leakage. 10-13, 16, 18, 33-35, 3-41, 44-46, 52-64, 66, 67, 70-77, 80-87, 89, 91, 97, 101, 102, 106, 107, 110, 115, 120-124, 127, 129-143, 146, 149, 152-154, 160, 161, 168, 171, 177, 178, 187, 191, 198, 202, 206, 208, 211, 217, 247, 250.

Neutron transport calculation: see **Neutron transport***.

Neutron transport equation: see **Neutron transport***.

Neutronics (or **neutron physics**)**:** the study of **neutrons*** travelling through **fissile*** and nonfissile media, and of the reactions they induce in matter, in particular in nuclear reactors with regard to their multiplication, and to the initiation and control of the **nuclear chain reaction***. See especially p. 7.

Nodal variational method: see p. 78.

Nominal power: for a nuclear reactor, the maximum operating power allowed in operation. 194, 221, 222.

Nordheim equation: an equation which governs the time evolution of a neutron population, in the approximation of point kinetics. 119.

Nuclear chain reaction (or **chain reaction**)**:** a series of nuclear **fissions*** during which released **neutrons*** generate new fissions, which, in turn, release new neutrons generating new fissions, and so on. 7-9, 11, 27, 58, 66, 120, 224, 228, 235-238.

Nuclear data evaluation: see **Evaluation of nuclear data***.

Nuclear fuel (or **fuel**)**:** the material involved in the **core*** of a nuclear reactor, containing the **fissile*** elements which maintain **nuclear chain reaction*** in it. The terms **nuclear fuel** may also refer to the structured elements which a reactor core is made of.

Nuclear fusion: a nuclear reaction during which two light **nuclei*** gather to form a heavier nucleus. 21, 29, 39, 141, 180, 186, 190, 226, 249-251.

Nuclear precursor: see **Radioactive filiation***.

Nuclear reactor: a device in which a **nuclear chain reaction*** can be initiated, sustained and controlled; by extension, the whole of this device and the related facilities. Its main components are **fissile* fuel***, **moderator***, shielding, **control rods***, and **coolant***. There exists a wide variety of nuclear reactors that may be distinguished mainly by their purpose, *i.e.* research reactors, irradiation reactors, experimental reactors, prototype reactors, and power reactors. 7, 9, 15, 16, 18, 28, 45, 51, 62, 63, 97, 103, 107, 113, 115, 116, 125, 153, 167, 180, 191, 196, 209, 210, 211, 213, 216, 229, 231, 247, 253.

Nuclear regulatory authority (**French**)**:** see **Regulatory authority for radiation protection and safety***.

Nuclear safety: all the technical dispositions and organizational measures applied to nuclear facilities or activities in order to prevent accidents, or limit their effects; by extension, the state resulting from these dispositions. Nuclear safety especially includes the design, building, operation, final shutdown, and dismantling of regulated nuclear facilities (INB: *Installations Nucléaires de Base*), as well as radioactive materials transport. 241, 245.

Nuclear safety authority (**French**)**:** see **Regulatory authority for radiation protection and safety***.

Nucleate boiling: a boiling characterized by the local generation of steam bubbles. 218.

Nucleons: particles the atomic **nucleus*** consists of, *i.e.* **protons*** and **neutrons***, interlinked by the strong interaction that ensures nuclear cohesion. See pp. 24 and 40.

Nucleus: the atomic core in which the major part of its mass and its whole positive charge are concentrated. Apart from hydrogen, it consists of **protons*** and **neutrons***. See the introduction, p. 8.

Nuclide: a nuclear species characterized by its mass number, its atomic number, and its nuclear energetic state. See the introduction, p. 12.

OSIRIS: a research reactor located at CEA/Saclay, dedicated to investigating materials and fuels under irradiation. 130, 166, 180-182, 187, 205, 206, 232, 234.

Pair creation: a process by which the energy of a *gamma* radiation, if sufficiently high, is turned into matter in the form of a particle-antiparticle pair. 32, 176.

Parent nucleus: see **Radioactive filiation***.

Payoff: see **Score***.

pcm: a **reactivity*** unit (an abbreviation for the French term *pour cent mille*, *i.e.* 10^{-5}).

Phase space: a six-dimensional space including three space dimensions, one energy dimension, and two angle dimensions (defining a direction). 12, 44, 45, 46, 51, 53, 55, 59, 62, 76, 89, 90, 92, 96, 101, 102, 117, 133.

Photon: an elementary particle with a mass equal to zero, accounting for a quantum of light. 9, 11, 12, 28, 31, 32, 33, 38, 40, 43, 45, 104, 133, 140, 144, 160, 196.

Pi meson: see **Pion***.

Pion (or **pi meson**)**:** a particle consisting of a quark u and an antiquark d, a vector of the strong interaction between two nucleons. 40.

Plenum: the free volume within a fuel **rod***, holding no fissile material. This volume is used to confine fission gases released by fuel, so that pressure is not increased too much in the rod. In a **nuclear reactor***, the term "plenum" refers to the free space within the vessel, beyond the space held by **fuel assemblies***. 200, 201, 222.

Plutonium: an element formed as a result of **neutron capture*** by uranium in the core of nuclear reactors. Odd plutonium **isotopes*** are **fissile***: so plutonium can be re-used as a nuclear fuel, *e.g.* as **MOX fuel***. 9, 31, 69, 70-72, 108, 110, 111, 160, 174, 200, 201, 204, 211, 219, 226-229, 235, 237, 242-244.

Point kinetics: the study of the neutronic behavior of **nuclear reactors*** as a function of time, assuming that this behavior is the same in every point of the reactor. 115-124, 175, 215, 224, 225.

Poison: see **Neutron poison***.

Poisoning: a phenomenon of **neutron capture*** by some **fission products*** which build up during irradiation (xenon 135, samarium 149…), thereby degrading the **neutron balance***. 51, 108, 110, 111, 198, 199, 203, 237, 241.

Potential radiotoxicity (or **radiotoxic inventory**)**:** for a material containing a certain amount of radionuclides, the value of the committed effective dose which would result from intake of all the occurring radionuclides. As the product of the radionuclide inventory by the "ingestion" dose coefficient for the above mentioned radionuclides, the potential radiotoxicity of a certain amount of radionuclides, *e.g.* in waste, is an indicator of the harmfulness of this amount in an accidental situation. 12, 131, 185, 186, 190, 248, 249.

Power coefficient: in a nuclear reactor, or any other multiplying medium, the ratio between the variation in **reactivity*** and the variation in power that induces it.

Power excursion: a very fast, transient increase in reactor power beyond operating power. This transient phenomenon may be induced in research nuclear reactors. 123.

ppm: a concentration unit (part per million, *i.e.* 10^{-6}).

Pressurized water reactor (**PWR**)**:** a light water-cooled and moderated nuclear reactor in which heat is transferred from the core to the heat exchanger by water kept at high pressure in the **primary coolant circuit***, in order to prevent its boiling. 23, 37, 63, 77, 89, 97, 98, 101, 110, 111, 129, 135, 152, 155, 166, 168, 171, 180, 181, 187-189, 194-198, 200, 203-208, 217-219, 223, 225, 227-229, 232, 234, 247, 248.

Primary coolant circuit (or **primary cooling system**, **primary system**)**:** a closed loop system, or a set of closed loops, that allows heat to be removed from **fuel elements*** in the reactor **core***, through circulation of a **coolant*** in direct contact with those fuel elements. 194, 195, 215, 216, 223, 225, 248.

Primary (**cooling**) **system:** see **Primary coolant circuit***.

Primary fission yield (of a fission product)**:** the output rate of a **fission product*** during a fission that is evaluated after the emission of **prompt neutrons***, and before all the other radioactive **decays*** through β^- transitions. The sum of these primary fission yields is normalized to 2 (neglecting ternary fission). 13, 27, 111, 242.

Probabilistic method (Monte-Carlo)**:** see **Monte-Carlo method***.

Prompt neutrons: neutrons* directly emitted at the very moment of **fission***. 8, 26, 27, 29, 30, 46, 55, 115, 116, 118-120, 223, 224.

Proton: one of the fundamental particles an atom consists of. The proton is located in the **nucleus***, and exhibits a positive electric charge equivalent to the negative charge of an **electron***, and a mass similar to that of a **neutron***. See the introduction, p. 7.

PWR: see **Pressurized water reactor***.

Qualification of a code package: all the processes allowing a computer code and its source data to be stated as good for service, within the limits of a defined validity area, and with controlled uncertainties. These processes include proofs of the quality of basic data, as well as **verification*** and **validation*** of the code. See also **Code package***. 17, 21, 126, 143, 144, 147, 163, 165, 166, 169, 170, 171, 172, 186, 187, 196, 212, 228, 229, 230, 231.

Radiation protection: all the rules, procedures and means of prevention and monitoring that are used to prevent or limit the harmful effects of **ionizing radiation*** on persons. The terms "radiation protection" relate to harmful effects produced on persons or on the environment. 8, 9, 12, 14, 15, 29, 35, 37, 39, 41, 47, 73, 104, 133, 137, 141, 185, 187, 188, 247, 253, 254.

Radioactive: see **Radioactivity***.

Radioactive daughter products: see **Radioactive filiation***.

Radioactive decay: see **Decay (radioactive)***.

Radioactive decay chain: see **Decay chain***.

Radioactive disintegration: see **Disintegration** (**radioactive**)*.

Radioactive filiation: the relationship between **nuclides*** arising from an initial nuclide, the so-called "father nuclide" (or radioactive precursor), after a series of **radioactive disintegrations***. These nuclei are referred to as "radioactive daughter products" or "daughter products".See also **Decay chain***. 113.

Radioactive half-life: the time it takes for half the initial number of atoms in a radioactive **nuclide*** sample to disappear by spontaneous **decay***. The radioactive half-life is a property characterizing each radioactive **isotope***. 10, 32, 35.

Radioactive precursor: see **Radioactive filiation***.

Radioactive waste (or **radwaste**)**:** any residue arising from the use of radioactive materials, for which no use is planned in the current state of knowledge, and that, due to its activity level, cannot be disposed of without control into the environment. Ultimate radioactive waste is radioactive waste that can no longer be treated under current technical and economic conditions, especially through extracting its valuable content, or reducing its polluting or hazardous character. 9, 28, 39, 141, 185-187, 190, 199, 200, 227, 231, 248.

Radioactive waste disposal: see **Disposal (of radioactive waste)***.

Radioactive waste storage: see **Storage (of radioactive waste)***.

Radioactivity: the property of some naturally-occurring or artificial elements displaying an unstable **nucleus*** to spontaneously emit particles or a radiation. This term most often refers to the emission of radiation during the **disintegration*** of an unstable element or during **fission***. 14, 41, 109, 112, 130, 187, 247, 249.

Radioisotope (or **Radioactive isotope**)**:** the atoms of chemical elements may have many isotopes (*i.e.* various forms) with different atomic numbers and atomic masses. If an isotope is radioactive, it is sometimes called a **radioisotope*** or **radionuclide***. See **Radionuclide***. 205.

Radiolysis: the dissociation of molecules by ionizing radiation. 186, 187, 190.

Radionuclide: an unstable **nuclide*** of an element that decays, or is spontaneously disintegrated emitting a radiation. 19, 32, 57, 107, 141, 229, 248.

Radiotoxic inventory: see **Potential radiotoxicity***.

Radwaste: see **Radioactive waste***.

Ratio of moderator to fuel: see **Moderator-to-fuel ratio***.

RBMK reactor: a graphite-moderated reactor cooled by water flowing in pressure tubes. This very type of reactor was involved in the Tchernobyl disaster. 187.

Reaction rate: the number of interactions of a given type between **neutrons*** and matter (capture, fission, scattering, generation, etc.) per unit time and volume, for a given reaction. 11-14, 46, 49, 52, 53, 65-70, 89, 97, 101, 107, 109, 125, 133, 136, 151, 172, 173, 176, 185, 186, 189, 194, 196, 202, 248.

Reactivity: a dimensionless quantity used to evaluate small variations in the **multiplication factor*** ***k*** around the critical value, and defined by the formula $\rho = (k - 1)/k$. Its value being very small, it is generally expressed in hundred thousandths, taking the **pcm*** *(pour cent mille)* as a unit. In a reactor, reactivity is equal to zero when the reactor is **critical***, positive when it is **supercritical***, and negative when it is **subcritical***. 13, 52, 58, 59. 110, 115, 117-120, 129, 143, 146, 147, 168, 171, 172, 174-176, 178, 180, 185, 188, 194, 195, 196, 199, 200-206, 211, 213, 215, 216, 218, 219, 221-225, 229, 242.

Reactivity coefficient: a variation in the **multiplication factor*** due to reactor operation, *i.e.* to changes in temperature and composition resulting from energy release and **neutron*** irradiation. 180, 176, 180, 215.

Reactivity feedback: the effects of variations in some parameters of a nuclear reactor, such as power, temperature, or void fraction, on its reactivity. See also **power coefficient***, **temperature coefficient***, and **void coefficient of reactivity***. 194, 200, 225.

Reactivity-Initiated Accident (also called **Reactivity Insertion Accident** or **RIA**)**:** an accident induced by an uncontrolled increase in **reactivity*** in a critical **nuclear reactor* core***. 188, 222, 223.

Reactor kinetics: the study of neutron flux variation over time in a reactor core that results from **reactivity*** variation; by extension, the variation itself, *i.e.* the rate at which changes in power take place. 8, 58, 59, 60, 75, 104, 115-124, 130, 144, 166, 174, 175, 180, 185, 191, 194, 215, 220, 223-225.

Reactor system (or **reactor type**)**:** a category of reactors which display common features relating to the nature and layout of fuel, moderator (if any), and coolant. This is a possible path for developing nuclear reactors capable of producing energy under cost-effective conditions. 16, 17, 45, 51, 127, 129, 130, 131, 132, 143, 166, 177, 178, 187, 199, 207, 213, 219, 225, 228, 249.

Reactor vessel (or **vessel**)**:** a vessel containing a reactor **core*** and its **coolant***. 9, 97, 103, 120, 135, 168, 171, 180, 181, 185, 189, 196, 211, 218, 223, 225, 247, 248.

Reference calculation: an "exact" calculation (very close to physical reality) with which other calculations carried out using approximations can be compared and validated. For example, **deterministic*** transport neutronics codes are validated by **Monte-Carlo*** probabilistic transport calculations. See also **Benchmark***. 71, 98, 125, 126, 166, 167, 169, 191.

Recycling (or **recycle**)**:** the re-use in a reactor of nuclear materials arising from **spent fuel treatment***. 130, 228.

Reflector: a reactor component placed on the boundary of the **core***, designed to send back **neutrons*** escaping from it. 28, 54, 66, 79, 129, 144-146, 178, 196, 198, 201, 202, 204, 205, 206,208, 210, 211, 219, 220, 239, 240, 245.

Regulatory authority for radiation protection and safety (French) (or **nuclear regulatory authority**, **French nuclear safety authority**)**:** an administrative authority that, on account of the State, ensures **nuclear safety*** and **radiation protection*** control in France in order to protect workers, patients, the public, and the environment from risks related to the use of nuclear energy. 232, 241, 245.

Relationship between radioactive nuclides: see **Radioactive filiation***.

Repository: the facility in which radioactive waste is placed, without scheduling further retrieval. See also **Disposal (of radioactive waste)***.

Reprocessing: see **Treatment (of spent fuel)*.**

RES *(Réacteur d'ESsais pour la propulsion navale)***:** a test reactor for naval propulsion, under construction on the CEA Cadarache site.

Residual power: the thermal power generated by a shutdown nuclear reactor, arising mainly from **fission products* activity***. 27, 130, 132, 137, 185, 188, 195, 196, 207, 220, 223, 227, 229, 230-234.

Resolved resonance: resonance* of the neutron-nucleus interaction for which the specific parameters (energy, widths) can be measured, as opposed to **unresolved resonances***, for which only statistical knowledge is possible. 21, 23, 24, 34, 85.

Resonance: in nuclear physics, the excited state of the compound **nucleus*** that results from coupling a target nucleus and an incident neutron. 11, 14, 18, 21-25, 31, 34, 37, 53, 54, 61, 62, 64, 66, 67, 68, 69, 71, 72, 85, 130, 177, 195, 197, 198, 202-205, 219, 242.

RIA: Reactivity Insertion Accident. See also **Reactivity-Initiated Accident***. 188, 222-224, 226.

Rod: a small-diameter tube closed at both ends, used as a component of the **core*** in a nuclear reactor and containing fissile, fertile or absorbing material. When containing fissile material, the rod is a fuel element. 52, 64, 66, 97, 98, 128, 135, 136, 174, 176, 178, 195, 198, 202, 206, 207, 209, 232, 233.

SALOMÉ: a platform developed at CEA, used as a coupling tool for data exchange and control of the various codes to be coupled for nuclear system simulation. 217, 218, 226.

Samarium: the fission product samarium 149 is particularly neutron-absorbing. Its presence in the core of a thermal neutron reactor has a significant impact on the neutron population. See also **Poisoning***. 51, 108, 110, 111, 198, 206.

Scattering: see **Elastic scattering*** and **Inelastic scattering***.

Schrödinger equation: an equation leading to a solution that provides the wave function of a nonrelativistic quantum system, governed by a hamiltonian, in which interactions between objects assumed to be elementary are described in terms of potentials. 24.

Score (or **payoff** or **tally**)**:** a value assigned to the estimator (random value) of a physical quantity during an event taking place in a **Monte-Carlo*** simulation. 91, 96, 133.

Secondary coolant circuit (or **secondary cooling system**)**:** a system designed for the flow of the **coolant*** that removes heat from the **primary coolant circuit***. 188, 203, 225.

Secondary cooling system: see **Secondary coolant circuit***.

Self-powered neutron detector (or **collectron**)**:** a **neutron*** or ***gamma**** radiation detector with no external power source that emits a signal resulting from electron emission by an electrode following **neutron capture*** or *gamma* photon absorption. 188, 233, 234.

Self-shielded: of a **cross section*** when it is reduced by applying a factor which takes into account the **self-shielding*** phenomenon. 53, 65, 66, 67, 69, 71, 77, 138, 139, 140.

Self-shielding: the depression of neutron flux in the vicinity of a resonance that results in a decrease in reaction rates. 14, 18, 34, 37, 53, 54, 65-72, 77, 85, 127, 130, 131, 138, 139, 146, 177, 197-199, 202-205.

SFR: see **Sodium-cooled fast reactor***.

Sievert (**Sv**)**:** a biological dose unit. 246.

Simulation: a set of methods that reproduce or predict the operation of complex systems through computing, especially in the various areas or nuclear research and development. After validation, these methods can be used for the design of new systems. 11, 26, 27, 29, 30, 39, 40, 41, 44, 51, 57, 58, 85, 89, 91-104, 106, 120, 123, 125, 133, 134, 136, 141, 142, 144, 149-153, 160, 165, 167, 175, 181, 191, 211, 212, 215, 216, 225, 226, 233, 247, 253-255.

S_N method: see p. 72.

Sodium-cooled fast reactor (**SFR**)**:** a **fast neutron reactor*** in which **coolant*** is liquid sodium. 130, 187, 199.

Socket: a software interface used for inter-process communication (computer term). 157, 158.

Source: a radioactive material that generates radiation for experimental or industrial purposes. 12, 107, 189, 190, 248.

Spallation: the splitting of a **heavy nucleus*** under the shock of a very highly energetic incident particle which is accompanied with a considerable emission of **neutrons***. This nuclear reaction involves a heavy target nucleus and a particle, most often a proton, accelerated up to an energy of a few hundred million **electronvolts***. Through successive collisions against the nucleons of the target nucleus, the incident particle ejects a high number of neutrons. For instance, a proton of 1 billion electronvolts projected onto a lead target can generate 25-30 neutrons. 39-41, 102, 131, 141, 142, 186.

Spallation target: a device involving a heavy material used to generate, through **spallation***, **neutrons*** that stand for the outer source of a **hybrid system***. 41, 186.

Specific burnup (also called **specific burnup**, or **burnup rate**, or **burnup**)**:** the total amount of energy released per unit mass in a nuclear fuel. Generally expressed in megawatts x days per ton (MW·d/t). See also **Burnup***. 13, 97, 107, 109, 110, 136, 143, 144, 188, 195, 198, 199, 201, 205, 206, 208, 211, 213, 215, 219, 223, 229-231, 233, 234.

Spectrum calculation (or **lattice calculation**)**:** the first step in the two-step computational scheme of a nuclear reactor, the second one being referred to as **core calculation***. The spectrum calculation relies on a lattice code used to determine space-homogenized, energy-condensed constants (cross sections…) required for core calculation. It is also referred to as **assembly calculation***. This step is achieved using for example the **APOLLO2*** code. 127

Spectrum index: see **Neutron spectrometry***. 166, 173.

Spent fuel: irradiated **nuclear fuel*** removed from a reactor, and whose **fissile*** material cannot be reused without undergoing appropriate **treatment***. 51, 107, 231.

Spent fuel treatment: see **Treatment** (**of spent fuel**)*.

Spin: the intrinsic angular momentum of a quantum object. Sometimes the use of the word "spin" is restricted to particles considered to be elementary. 24, 32.

Steam generator (**SG**)**:** in a nuclear reactor, an exchanger that allows transfer of heat from primary coolant to the water of the **secondary coolant circuit***, and turns it into steam to drive the turbogenerator. 123, 194, 218.

Storage (**of radioactive waste**) (or **radioactive waste storage**)**:** the action of placing radioactive waste temporarily in a specially designed facility. See also **Disposal** (**of radioactive waste**)*. 186, 187, 190, 227, 231.

Streaming: neutron leakage* in certain preferential directions due to heterogeneities in the reactor **core*** (*e.g.* gas channels). 209.

Subcritical: in neutronics, of a multiplying medium in which the number of **neutrons*** emitted by **fission*** is lower than the number of neutrons disappearing by absorption and leakage. In this case, the number of fissions observed during successive time intervals decreases, and the **chain reaction*** cannot be sustained in the medium without additional neutrons from an external source. For example, this is the case in planned subcritical reactors in which additional neutrons are brought to the reactor core by an accelerated particle beam. The interest of these reactors lies in their high capability for actinide **transmutation***. 7, 13, 55, 56, 58, 172, 179, 195, 202, 235, 236, 241.

Supercritical: of a multiplying medium in which the **effective multiplication factor*** is higher than 1. A system is said to be "supercritical" when the number of **neutrons*** emitted by **fission*** is higher than the number of neutrons disappearing by absorption and leakage. In this case, the number of fissions observed during sucessive time intervals increases. 7, 13, 55, 56, 58, 223, 235, 236.

Tally: see **Score***.

TALYS: a computer code dedicated to models of nuclear reactions. 23, 25.

Target uncertainty: the uncertainty aimed at in a calculation for utility purposes. 173, 203.

Temperature coefficient: a coefficient which expresses the variation in the neutron **multiplication factor*** in a reactor when its temperature changes. A negative temperature coefficient is an important criterion of **core*** stability. 166, 172, 176, 195, 211, 218, 219, 224.

TERA-100: one of the CEA's supercomputers. 153, 157.

Thermal neutrons (or **slow neutrons**)**:** neutrons in thermal equilibrium with the matter in which they move. In nuclear water reactors, thermal neutrons move at a rate of about 2 to 3 km/s, and their energy is neighboring one electronvolt fraction. 15, 18, 27, 31, 34, 66, 67, 110, 111, 115, 117, 179, 180, 193, 198, 199, 210, 211, 227.

Thermalization: the slowing-down of **neutrons*** in order to bring them gradually to thermal equilibrium with the matter in which they are scattered in the reactor. 16, 31, 37, 178, 193.

Tokamak: a toroidal axisymmetric machine allowing a thermonuclear plasma to be confined through the combination of two magnetic fields. The biggest tokamak in the world will be **ITER**, currently under construction on the CEA Cadarache site. 186, 190, 249, 250.

Transfer function (of a nuclear reactor)**:** a function that relates the frequency response of the neutron population in a reactor, to the frequency spectrum of a neutron source located within the reactor. 174.

Transfer cross section (**multigroup matrix**, **law**, **cross section**)**:** a **cross section*** that characterizes the transition of a neutron from one **energy group*** to another during an elastic or inelastic scattering reaction. 35, 46, 53, 63, 65, 67, 69, 89, 116, 117.

Transient: the slow or fast, scheduled or unscheduled evolution in the operating condition of a facility. In the case of a **nuclear reactor*** two classes are distinguished: normal transients, during which the values of physical parameters are kept within the technical specifications for operation, and accidental transients, that entail the operation of protection systems, and then of engineered safety systems. Some accidental transients are used as a reference for safety demonstrations, and are involved in reactor **design basis***. 9, 52, 121, 123, 135, 144, 185, 188, 195, 215, 218, 220, 221, 222, 223, 224, 254.

Transmutation: the transformation of a **nuclide*** into another through a nuclear reaction. 141, 199, 200, 232.

Transuranic elements: all the elements with higher atomic number than uranium. These **heavy nuclei*** are generated in nuclear reactors through **neutron capture***. They are classified into seven **nuclide*** families: uranium, neptunium, plutonium, americium, curium, berkelium, and californium.

Treatment (**of spent fuel**) (or **spent fuel treatment**) or **reprocessing:** all the operations performed on **spent fuel*** arising from nuclear reactors, in order to separate valuable materials such as uranium and plutonium, and condition the remaining waste. The term "(spent fuel) treatment" tends to replace "**reprocessing**" (see also **Recycling***). 186, 187, 227-229, 231.

TRIPOLI, TRIPOLI3, TRIPOLI-4®: Monte-Carlo-type neutronics computer codes used for simulation of neutron and *gamma* transport. 16, 37, 71, 94, 95, 97, 103-106, 126-128, 131-137, 142-146, 150, 151, 160, 168, 177, 178, 180-182, 217, 218, 226, 233, 242, 247-251, 254.

Uncertainty (**propagation**)**:** 21, 23, 25-28, 31, 33, 52, 58, 104, 126, 130, 132, 136, 143, 144, 147, 149, 152, 158, 165-170, 172, 173, 175, 177- 179, 188, 189, 191, 203, 230-232, 254.

UNGG *(Uranium Naturel-Graphite-Gaz)***:** the natural-uranium, graphite-moderated and (CO_2) gas-cooled reactor system. 187, 189, 249.

Unresolved resonance: see **Resolved resonance***.

UOX: the standard **light-water reactor*** fuel, consisting of uranium 235-**enriched*** uranium oxide. 71, 79, 80, 108, 110, 128, 172, 197, 210, 223, 228, 229, 230- 232, 234.

Uranium oxide fuel: see **UOX***.

Validation (**of a computer code**)**:** an approach designed to ensure that the results of a numerical simulation based on a given code reproduce the experiment. 40, 54, 70, 85, 95, 111, 126, 128, 136, 141, 143, 147, 165-170, 179-181, 191, 217, 226, 233, 234, 254.

Verification (**of a computer code**)**:** an approach designed to ensure that the equations of the physical model used in a code are solved correctly from the mathematical, computational, and computer viewpoint. Verification can include confrontation with calculation cases that can be solved analytically, or are solved by an assumed reference code. 95, 126, 165, 170, 191.

Very high temperature reactor (**VHTR**)**:** a thermal neutron reactor in which coolant is helium with a core outlet temperature over 900 °C. 187, 208, 220, 222.

Vessel: see **Reactor vessel***.

VHTR: see **Very high temperature reactor***. 177, 187, 208, 220, 222, 226.

Void coefficient of reactivity (or **void coefficient**)**:** a coefficient that expresses the variation in the **multiplication factor*** of a reactor when a larger volume of voids (*i.e.* areas of lower density, such as bubbles) is formed in **coolant*** than in normal conditions. If this coefficient is positive, a larger volume of voids will result in increased **reactivity*** and, so, increased power. In contrast, if it is negative, a larger volume of voids will tend to bring the reactor to shutdown. 153, 172, 176, 195, 200, 201, 218.

VVER: a Russian-design pressurized water power reactor. 104, 129, 179, 187.

WKB (**approximation**)**:** a Wentzel-Kramers-Brillouin approximation for solving a certain type of differential equations (*e.g.* the **Schrödinger equation*** describing the crossing of a potential barrier by a particle). 25.

Xenon: xenon 135, a powerful neutron absorber whose generation in a reactor core as the disintegration product of another fission product (iodine) upsets the neutronic behavior of the core with delay during a power transient. 9, 51, 108, 110, 111, 198, 199, 206, 221.

Xenon effect: see **Xenon***.

ZOÉ (1948-1976)**:** the first French atomic pile built at Fontenay-aux-Roses, designed for experiments on a self-sustained **nuclear chain reaction***. 15, 180.

Table of contents

Contributors to this Monograph:

Catherine Andrieux,
Pascal Archier,
Anne-Marie Baudron,
David Bernard,
Patrick Blaise,
Patrick Blanc-Tranchant,
Bernard Bonin,
Olivier Bouland,
Stéphane Bourganel,
Christophe Calvin,
Maurice Chiron,
Mireille Coste-Delclaux (Topic Editor),
Frédéric Damian,
Cheikh Diop (Topic Editor),
Éric Dumonteil,
Clément Fausser,
Philippe Fougeras,
Franck Gabriel,
Emmanuel Gagnier,
Danièle Gallo,
Jean-Pascal Hudelot,
François-Xavier Hugot,
Tan Dat Huynh,
Cédric Jouanne,
Jean-Jacques Lautard,
Frédéric Laye,
Yi-Kang Lee,
Richard Lenain,
Sylvie Leray,
Olivier Litaize,
Christine Magnaud,
Fausto Malvagi (Topic Editor),
Dominique Mijuin,
Claude Mounier,
Sylvie Naury,
Anne Nicolas (Topic Editor),
Gilles Noguère,
Jean-Marc Palau,
Jean-Charles le Pallec,
Yannick Pénéliau,
Odile Petit,
Christine Poinot-Salanon,
Xavier Raepsaet,
Paul Reuss,
Edwige Richebois,
Bénédicte Roque,
Éric Royer,
Cyrille de Saint Jean,
Richard Sanchez,
Alain Santamarina,
Simone Santandrea,
Olivier Sérot,
Michel Soldevila,
Jean Tommasi,
Jean-Christophe Trama,
Aimé Tsilanizara,

… along with, of course, all the members of the DEN Monographs Scientific Committee:

Bernard Bonin (Editor in chief):
Georges Berthoud, Gérard Ducros,
Damien Féron, Yannick Guérin,
Christian Latgé, Yves Limoge,
Gérard Santarini, Jean-Marie Seiler,
Étienne Vernaz (Research Directors).